DTMB

62 Series

Model	Lpx		Lwl		Bpx		Dep		βχ	βτχ	Centroid	Lcg aft of Centroid	Lcg from Transom		Lcg/Lpx	Centerline angle	Ap		Twisted angle	Lpx/Bpx	Ap/Vol	Lpx/Ap	Lpx/Vol	Cv	Vcg/Lpx	Shaft Angle	Lce Transom	
DTMB	Model-62																											
4665	3.912	ft	3.783	ft	1.956	ft	129.080	Lb	13.00	12.50	47.50	-12.00	1.389	ft	0.355	0.00	6.469	ft^2	0.50	2.00	3.979	2.366	3.104	0.269	------------	19.41	2.150	inç
	1.192	m	1.153	m	0.596	m	58.551	kg					0.423	m			0.6010	m^2									54.61	mm
	3.912	ft	3.783	ft	1.956	ft	129.080	Lb	13.00	12.50	47.50	-8.00	1.545	ft	0.395	0.00	6.469	ft^2	0.50	2.00	3.979	2.366	3.104	0.269	------------	19.41	2.150	inç
	1.192	m	1.153	m	0.596	m	58.551	kg					0.471	m			0.6010	m^2									54.61	mm
	3.912	ft	3.783	ft	1.956	ft	129.080	Lb	13.00	12.50	47.50	-4.00	1.702	ft	0.435	0.00	6.469	ft^2	0.50	2.00	3.979	2.366	3.104	0.269	------------	19.41	2.150	inç
	1.192	m	1.153	m	0.596	m	58.551	kg					0.519	m			0.6010	m^2									54.61	mm
	3.912	ft	3.783	ft	1.956	ft	129.080	Lb	13.00	12.50	47.50	0.00	1.858	ft	0.475	0.00	6.469	ft^2	0.50	2.00	3.979	2.366	3.104	0.269	------------	19.41	2.150	inç
	1.192	m	1.153	m	0.596	m	58.551	kg					0.566	m			0.6010	m^2									54.61	mm
	3.912	ft	3.783	ft	1.956	ft	80.070	Lb	13.00	12.50	47.50	-12.00	1.389	ft	0.355	0.00	6.469	ft^2	0.50	2.00	5.471	2.366	3.639	0.167	------------	19.41	2.150	inç
	1.192	m	1.153	m	0.596	m	36.320	kg					0.423	m			0.6010	m^2									54.61	mm
	3.912	ft	3.783	ft	1.956	ft	80.070	Lb	13.00	12.50	47.50	-8.00	1.545	ft	0.395	0.00	6.469	ft^2	0.50	2.00	5.471	2.366	3.639	0.167	------------	19.41	2.150	inç
	1.192	m	1.153	m	0.596	m	36.320	kg					0.471	m			0.6010	m^2									54.61	mm
	3.912	ft	3.783	ft	1.956	ft	80.070	Lb	13.00	12.50	47.50	-4.00	1.702	ft	0.435	0.00	6.469	ft^2	0.50	2.00	5.471	2.366	3.639	0.167	------------	19.41	2.150	inç
	1.192	m	1.153	m	0.596	m	36.320	kg					0.519	m			0.6010	m^2									54.61	mm
	3.912	ft	3.783	ft	1.956	ft	80.070	Lb	13.00	12.50	47.50	0.00	1.858	ft	0.475	0.00	6.469	ft^2	0.50	2.00	5.471	2.366	3.639	0.167	------------	19.41	2.150	inç
	1.192	m	1.153	m	0.596	m	36.320	kg					0.566	m			0.6010	m^2									54.61	mm
	3.912	ft	3.783	ft	1.956	ft	54.500	Lb	13.00	12.50	47.50	-12.00	1.389	ft	0.355	0.00	6.469	ft^2	0.50	2.00	7.071	2.366	4.137	0.114	------------	19.41	2.150	inç
	1.192	m	1.153	m	0.596	m	24.721	kg					0.423	m			0.6010	m^2									54.61	mm
	3.912	ft	3.783	ft	1.956	ft	54.500	Lb	13.00	12.50	47.50	-8.00	1.545	ft	0.395	0.00	6.469	ft^2	0.50	2.00	7.071	2.366	4.137	0.114	------------	19.41	2.150	inç
	1.192	m	1.153	m	0.596	m	24.721	kg					0.471	m			0.6010	m^2									54.61	mm
	3.912	ft	3.783	ft	1.956	ft	54.500	Lb	13.00	12.50	47.50	-4.00	1.702	ft	0.435	0.00	6.469	ft^2	0.50	2.00	7.071	2.366	4.137	0.114	------------	19.41	2.150	inç
	1.192	m	1.153	m	0.596	m	24.721	kg					0.519	m			0.6010	m^2									54.61	mm
	3.912	ft	3.783	ft	1.956	ft	54.500	Lb	13.00	12.50	47.50	0.00	1.858	ft	0.475	0.00	6.469	ft^2	0.50	2.00	7.071	2.366	4.137	0.114	------------	19.41	2.150	inç
	1.192	m	1.153	m	0.596	m	24.721	kg					0.566	m			0.6010	m^2									54.61	mm
	3.912	ft	3.783	ft	1.956	ft	55.700	Lb	13.00	12.50	47.50	0.00	1.858	ft	0.475	0.00	6.469	ft^2	0.50	2.00	6.969	2.366	4.107	0.116	------------	19.41	2.150	inç
	1.192	m	1.153	m	0.596	m	25.266	kg					0.566	m			0.6010	m^2									54.61	mm
	3.912	ft	3.783	ft	1.956	ft	41.350	Lb	13.00	12.50	47.50	-12.00	1.389	ft	0.355	0.00	6.469	ft^2	0.50	2.00	8.500	2.366	4.536	0.086	------------	19.41	2.150	inç
	1.192	m	1.153	m	0.596	m	18.756	kg					0.423	m			0.6010	m^2									54.61	mm
	3.912	ft	3.783	ft	1.956	ft	41.350	Lb	13.00	12.50	47.50	-8.00	1.545	ft	0.395	0.00	6.469	ft^2	0.50	2.00	8.500	2.366	4.536	0.086	------------	19.41	2.150	inç
	1.192	m	1.153	m	0.596	m	18.756	kg					0.471	m			0.6010	m^2									54.61	mm
	3.912	ft	3.783	ft	1.956	ft	41.350	Lb	13.00	12.50	47.50	-4.00	1.702	ft	0.435	0.00	6.469	ft^2	0.50	2.00	8.500	2.366	4.536	0.086	------------	19.41	2.150	inç
	1.192	m	1.153	m	0.596	m	18.756	kg					0.519	m			0.6010	m^2									54.61	mm
	3.912	ft	3.783	ft	1.956	ft	41.350	Lb	13.00	12.50	47.50	0.00	1.858	ft	0.475	0.00	6.469	ft^2	0.50	2.00	8.500	2.366	4.536	0.086	------------	19.41	2.150	inç
	1.192	m	1.153	m	0.596	m	18.756	kg					0.566	m			0.6010	m^2									54.61	mm

DTMB	Model-62																																						
Model	**Lpx**		**Lwl**		**Bpx**		**Dep**		**βχ**	**βτχ**	**Centroid**	**Lcg aft of Centroid**	**Lcg from Transom**		**Lcg/Lpx**	**Centerline angle**	**Ap**		**Twisted angle**	**Lpx/Bpx**	**Ap/Vol**	**Lpx/Ap**	**Lpx/Vol**	**Cv**	**Vcg/Lpx**	**Shaft Angle**	**Lce Transom**	
4666	**5.987**	**ft**	**5.836**	**ft**	**1.957**	**ft**	**235.700**	**Lb**	**13.00**	**12.50**	**48.20**	**-12.00**	**2.167**	**ft**	**0.362**	**0.00**	**9.715**	**ft^2**	**0.50**	**3.06**	**4.000**	**3.690**	**3.886**	**0.491**	----------	**12.97**	**2.150**	**inç**
	1.825	m	1.779	m	0.596	m	106.914	kg					0.661	m			0.9026	m^2									54.61	mm
	5.987	**ft**	**5.836**	**ft**	**1.957**	**ft**	**235.700**	**Lb**	**13.00**	**12.50**	**48.20**	**-8.00**	**2.407**	**ft**	**0.402**	**0.00**	**9.715**	**ft^2**	**0.50**	**3.06**	**4.000**	**3.690**	**3.886**	**0.491**	----------	**12.97**	**2.150**	**inç**
	1.825	m	1.779	m	0.596	m	106.914	kg					0.734	m			0.9026	m^2									54.61	mm
	5.987	**ft**	**5.836**	**ft**	**1.957**	**ft**	**235.700**	**Lb**	**13.00**	**12.50**	**48.20**	**-4.00**	**2.646**	**ft**	**0.442**	**0.00**	**9.715**	**ft^2**	**0.50**	**3.06**	**4.000**	**3.690**	**3.886**	**0.491**	----------	**12.97**	**2.150**	**inç**
	1.825	m	1.779	m	0.596	m	106.914	kg					0.807	m			0.9026	m^2									54.61	mm
	5.987	**ft**	**5.836**	**ft**	**1.957**	**ft**	**235.700**	**Lb**	**13.00**	**12.50**	**48.20**	**0.00**	**2.886**	**ft**	**0.482**	**0.00**	**9.714**	**ft^2**	**0.50**	**3.06**	**4.000**	**3.690**	**3.886**	**0.491**	----------	**12.97**	**2.150**	**inç**
	1.825	m	1.779	m	0.596	m	106.914	kg					0.880	m			0.9025	m^2									54.61	mm
	5.987	**ft**	**5.836**	**ft**	**1.957**	**ft**	**146.200**	**Lb**	**13.00**	**12.50**	**48.20**	**-12.00**	**2.167**	**ft**	**0.362**	**0.00**	**9.715**	**ft^2**	**0.50**	**3.06**	**5.500**	**3.690**	**4.557**	**0.305**	----------	**12.97**	**2.150**	**inç**
	1.825	m	1.779	m	0.596	m	66.316	kg					0.661	m			0.9026	m^2									54.61	mm
	5.987	**ft**	**5.836**	**ft**	**1.957**	**ft**	**146.200**	**Lb**	**13.00**	**12.50**	**48.20**	**-8.00**	**2.407**	**ft**	**0.402**	**0.00**	**9.715**	**ft^2**	**0.50**	**3.06**	**5.500**	**3.690**	**4.557**	**0.305**	----------	**12.97**	**2.150**	**inç**
	1.825	m	1.779	m	0.596	m	66.316	kg					0.734	m			0.9026	m^2									54.61	mm
	5.987	**ft**	**5.836**	**ft**	**1.957**	**ft**	**146.200**	**Lb**	**13.00**	**12.50**	**48.20**	**-4.00**	**2.646**	**ft**	**0.442**	**0.00**	**9.715**	**ft^2**	**0.50**	**3.06**	**5.500**	**3.690**	**4.557**	**0.305**	----------	**12.97**	**2.150**	**inç**
	1.825	m	1.779	m	0.596	m	66.316	kg					0.807	m			0.9026	m^2									54.61	mm
	5.987	**ft**	**5.836**	**ft**	**1.957**	**ft**	**146.200**	**Lb**	**13.00**	**12.50**	**48.20**	**0.00**	**2.886**	**ft**	**0.482**	**0.00**	**9.714**	**ft^2**	**0.50**	**3.06**	**5.499**	**3.690**	**4.557**	**0.305**	----------	**12.97**	**2.150**	**inç**
	1.825	m	1.779	m	0.596	m	66.316	kg					0.880	m			0.9025	m^2									54.61	mm
	5.987	**ft**	**5.836**	**ft**	**1.957**	**ft**	**101.800**	**Lb**	**13.00**	**12.50**	**48.20**	**-12.00**	**2.167**	**ft**	**0.362**	**0.00**	**9.715**	**ft^2**	**0.50**	**3.06**	**7.001**	**3.690**	**5.141**	**0.212**	----------	**12.97**	**2.150**	**inç**
	1.825	m	1.779	m	0.596	m	46.176	kg					0.661	m			0.9026	m^2									54.61	mm
	5.987	**ft**	**5.836**	**ft**	**1.957**	**ft**	**101.800**	**Lb**	**13.00**	**12.50**	**48.20**	**-8.00**	**2.407**	**ft**	**0.402**	**0.00**	**9.715**	**ft^2**	**0.50**	**3.06**	**7.001**	**3.690**	**5.141**	**0.212**	----------	**12.97**	**2.150**	**inç**
	1.825	m	1.779	m	0.596	m	46.176	kg					0.734	m			0.9026	m^2									54.61	mm
	5.987	**ft**	**5.836**	**ft**	**1.957**	**ft**	**101.800**	**Lb**	**13.00**	**12.50**	**48.20**	**-4.00**	**2.646**	**ft**	**0.442**	**0.00**	**9.715**	**ft^2**	**0.50**	**3.06**	**7.001**	**3.690**	**5.141**	**0.212**	----------	**12.97**	**2.150**	**inç**
	1.825	m	1.779	m	0.596	m	46.176	kg					0.807	m			0.9026	m^2									54.61	mm
	5.987	**ft**	**5.836**	**ft**	**1.957**	**ft**	**101.800**	**Lb**	**13.00**	**12.50**	**48.20**	**0.00**	**2.886**	**ft**	**0.482**	**0.00**	**9.714**	**ft^2**	**0.50**	**3.06**	**7.000**	**3.690**	**5.141**	**0.212**	----------	**12.97**	**2.150**	**inç**
	1.825	m	1.779	m	0.596	m	46.176	kg					0.880	m			0.9025	m^2									54.61	mm
	5.987	**ft**	**5.836**	**ft**	**1.957**	**ft**	**76.100**	**Lb**	**13.00**	**12.50**	**48.20**	**-12.00**	**2.167**	**ft**	**0.362**	**0.00**	**9.715**	**ft^2**	**0.50**	**3.06**	**8.500**	**3.690**	**5.665**	**0.159**	----------	**12.97**	**2.150**	**inç**
	1.825	m	1.779	m	0.596	m	34.519	kg					0.661	m			0.9026	m^2									54.61	mm
	5.987	**ft**	**5.836**	**ft**	**1.957**	**ft**	**76.100**	**Lb**	**13.00**	**12.50**	**48.20**	**-8.00**	**2.407**	**ft**	**0.402**	**0.00**	**9.715**	**ft^2**	**0.50**	**3.06**	**8.500**	**3.690**	**5.665**	**0.159**	----------	**12.97**	**2.150**	**inç**
	1.825	m	1.779	m	0.596	m	34.519	kg					0.734	m			0.9026	m^2									54.61	mm
	5.987	**ft**	**5.836**	**ft**	**1.957**	**ft**	**76.100**	**Lb**	**13.00**	**12.50**	**48.20**	**-4.00**	**2.646**	**ft**	**0.442**	**0.00**	**9.715**	**ft^2**	**0.50**	**3.06**	**8.500**	**3.690**	**5.665**	**0.159**	----------	**12.97**	**2.150**	**inç**
	1.825	m	1.779	m	0.596	m	34.519	kg					0.807	m			0.9026	m^2									54.61	mm
	5.987	**ft**	**5.836**	**ft**	**1.957**	**ft**	**76.100**	**Lb**	**13.00**	**12.50**	**48.20**	**0.00**	**2.886**	**ft**	**0.482**	**0.00**	**9.714**	**ft^2**	**0.50**	**3.06**	**8.499**	**3.690**	**5.665**	**0.159**	----------	**12.97**	**2.150**	**inç**
	1.825	m	1.779	m	0.596	m	34.519	kg					0.880	m			0.9025	m^2									54.61	mm
Webb-Sc1	**2.500**	**ft**	**2.388**	**ft**	**0.794**	**ft**	**22.000**	**Lb**	**11.00**	**5.00**	**57.30**	**-2.00**	**1.383**	**ft**	**0.553**	**0.00**	**4.000**	**ft^2**	**6.00**	**3.15**	**8.005**	**1.563**	**3.577**	**0.687**	----------	**12.00**	**0.000**	**inç**
	0.762	m	0.728	m	0.242	m	9.979	kg					0.421	m			0.3716	m^2									0.00	mm

DTMB		Model-62																												
	Wedge	Wedge																												
Model	Angle	Length	Lpx		Lwl		Bpx		Dep		βχ	βτχ	Centroid	Lcg aft	Lcg from		Lcg/Lpx	Centerline	Ap		Twisted	Lpx/Bpx	Ap/Vol	Lpx/Ap	Lpx/Vol	Cv	Vcg/Lpx	Shaft	Lce	
														of Centroid	Transom			angle			angle							Angle	Transom	
4666	2.00	0.10	5.987	ft	5.836	ft	1.957	ft	235.700	Lb	13.00	12.50	48.20	-8.00	2.407	ft	0.402	0.00	9.715	ft^2	0.50	3.06	4.000	3.690	3.886	0.491	-------------	12.97	2.150	inç
			1.825	m	1.779	m	0.596	m	106.914	kg					0.734	m			0.9026	m^2									54.61	mm
	5.00	0.10	5.987	ft	5.836	ft	1.957	ft	235.700	Lb	13.00	12.50	48.20	-8.00	2.407	ft	0.402	0.00	9.715	ft^2	0.50	3.06	4.000	3.690	3.886	0.491	-------------	12.97	2.150	inç
			1.825	m	1.779	m	0.596	m	106.914	kg					0.734	m			0.9026	m^2									54.61	mm
	10.00	0.10	5.987	ft	5.836	ft	1.957	ft	235.700	Lb	13.00	12.50	48.20	-8.00	2.407	ft	0.402	0.00	9.715	ft^2	0.50	3.06	4.000	3.690	3.886	0.491	-------------	12.97	2.150	inç
			1.825	m	1.779	m	0.596	m	106.914	kg					0.734	m			0.9026	m^2									54.61	mm
	2.00	0.10	5.987	ft	5.836	ft	1.957	ft	146.200	Lb	13.00	12.50	48.20	-8.00	2.407	ft	0.402	0.00	9.715	ft^2	0.50	3.06	5.500	3.690	4.557	0.305	-------------	12.97	2.150	inç
			1.825	m	1.779	m	0.596	m	66.316	kg					0.734	m			0.9026	m^2									54.61	mm
	5.00	0.10	5.987	ft	5.836	ft	1.957	ft	146.200	Lb	13.00	12.50	48.20	-8.00	2.407	ft	0.402	0.00	9.715	ft^2	0.50	3.06	5.500	3.690	4.557	0.305	-------------	12.97	2.150	inç
			1.825	m	1.779	m	0.596	m	66.316	kg					0.734	m			0.9026	m^2									54.61	mm
	10.00	0.10	5.987	ft	5.836	ft	1.957	ft	146.200	Lb	13.00	12.50	48.20	-8.00	2.407	ft	0.402	0.00	9.715	ft^2	0.50	3.06	5.500	3.690	4.557	0.305	-------------	12.97	2.150	inç
			1.825	m	1.779	m	0.596	m	66.316	kg					0.734	m			0.9026	m^2									54.61	mm
	2.00	0.10	5.987	ft	5.836	ft	1.957	ft	146.200	Lb	13.00	12.50	48.20	-4.00	2.646	ft	0.442	0.00	9.715	ft^2	0.50	3.06	5.500	3.690	4.557	0.305	-------------	12.97	2.150	inç
			1.825	m	1.779	m	0.596	m	66.316	kg					0.807	m			0.9026	m^2									54.61	mm
	5.00	0.10	5.987	ft	5.836	ft	1.957	ft	146.200	Lb	13.00	12.50	48.20	-4.00	2.646	ft	0.442	0.00	9.715	ft^2	0.50	3.06	5.500	3.690	4.557	0.305	-------------	12.97	2.150	inç

DTMB	Model-62																											
Model	**Lpx**		**Lwl**		**Bpx**		**Dep**		βχ	βτχ	**Centroid**	**Lcg aft of Centroid**	**Lcg from Transom**		**Lcg/Lpx**	**Centerline angle**	**Ap**		**Twisted angle**	**Lpx/Bpx**	**Ap/Vol**	**Lpx/Ap**	**Lpx/Vol**	**Cv**	**Vcg/Lpx**	**Shaft Angle**	**Lce Transom**	
4667	**8.000**	**ft**	**7.880**	**ft**	**1.955**	**ft**	**153.900**	**Lb**	**13.00**	**12.50**	**48.80**	**-6.00**	**3.424**	**ft**	**0.428**	**0.00**	**12.800**	**ft^2**	**0.50**	**4.09**	**7.005**	**5.000**	**5.918**	**0.322**	**-------------**	**10.00**	**2.150**	**inç**
	2.438	m	2.402	m	0.596	m	69.809	kg					1.044	m			1.1892	m^2									54.61	mm

DTMB	Model-62																											
Model	Lpx		Lwl		Bpx		Dep		βχ	βτχ	Centroid	Lcg aft	Lcg from		Lcg/Lpx	Centerline	Ap		Twisted	Lpx/Bpx	Ap/Vol	Lpx/Ap	Lpx/Vol	Cv	Vcg/Lpx	Shaft	Lce	
												of Centroid	Transom			angle			angle							Angle	Transom	
4667	8.000	ft	7.885	ft	1.955	ft	155.300	Lb	13.00	12.50	48.80	-6.00	3.424	ft	0.428	0.00	12.800	ft^2	0.50	4.09	7.000	5.000	5.916	0.325	-------------	10.00	2.150	inç
	2.438	m	2.403	m	0.596	m	70.444	kg					1.044	m			1.1892	m^2									54.61	mm

DTMB	Model-62																											
Model	**Lpx**		**Lwl**		**Bpx**		**Dep**		βχ	βτχ	**Centroid**	**Lcg aft of Centroid**	**Lcg from Transom**		**Lcg/Lpx**	**Centerline angle**	**Ap**		**Twisted angle**	**Lpx/Bpx**	**Ap/Vol**	**Lpx/Ap**	**Lpx/Vol**	**Cv**	**Vcg/Lpx**	**Shaft Angle**	Lce Transom	
4667-1	**8.000**	ft	**7.800**	ft	**1.956**	ft	**356.500**	Lb	**13.00**	**12.50**	**48.80**	**-12.00**	**2.944**	ft	**0.368**	**0.00**	**12.800**	ft^2	**0.50**	**4.09**	**4.000**	**5.000**	**4.524**	**0.744**	-------------	**10.00**	**2.150**	inç
	2.438	m	2.377	m	0.596	m	161.708	kg					0.897	m			1.1892	m^2									54.61	mm
	8.000	ft	**7.800**	ft	**1.956**	ft	**356.500**	Lb	**13.00**	**12.50**	**48.80**	**-8.00**	**3.264**	ft	**0.408**	**0.00**	**12.800**	ft^2	**0.50**	**4.09**	**4.000**	**5.000**	**4.524**	**0.744**	-------------	**10.00**	**2.150**	inç
	2.438	m	2.377	m	0.596	m	161.708	kg					0.995	m			1.1892	m^2									54.61	mm
	8.000	ft	**7.800**	ft	**1.956**	ft	**356.500**	Lb	**13.00**	**12.50**	**48.80**	**-4.00**	**3.584**	ft	**0.448**	**0.00**	**12.800**	ft^2	**0.50**	**4.09**	**4.000**	**5.000**	**4.524**	**0.744**	-------------	**10.00**	**2.150**	inç
	2.438	m	2.377	m	0.596	m	161.708	kg					1.092	m			1.1892	m^2									54.61	mm
	8.000	ft	**7.800**	ft	**1.956**	ft	**221.100**	Lb	**13.00**	**12.50**	**48.80**	**-12.00**	**2.944**	ft	**0.368**	**0.00**	**12.800**	ft^2	**0.50**	**4.09**	**5.500**	**5.000**	**5.305**	**0.461**	-------------	**10.00**	**2.150**	inç
	2.438	m	2.377	m	0.596	m	100.291	kg					0.897	m			1.1892	m^2									54.61	mm
	8.000	ft	**7.800**	ft	**1.956**	ft	**221.100**	Lb	**13.00**	**12.50**	**48.80**	**-8.00**	**3.264**	ft	**0.408**	**0.00**	**12.800**	ft^2	**0.50**	**4.09**	**5.500**	**5.000**	**5.305**	**0.461**	-------------	**10.00**	**2.150**	inç
	2.438	m	2.377	m	0.596	m	100.291	kg					0.995	m			1.1892	m^2									54.61	mm
	8.000	ft	**7.800**	ft	**1.956**	ft	**221.100**	Lb	**13.00**	**12.50**	**48.80**	**-4.00**	**3.584**	ft	**0.448**	**0.00**	**12.800**	ft^2	**0.50**	**4.09**	**5.500**	**5.000**	**5.305**	**0.461**	-------------	**10.00**	**2.150**	inç
	2.438	m	2.377	m	0.596	m	100.291	kg					1.092	m			1.1892	m^2									54.61	mm
	8.000	ft	**7.800**	ft	**1.956**	ft	**221.100**	Lb	**13.00**	**12.50**	**48.80**	**0.00**	**3.904**	ft	**0.488**	**0.00**	**12.800**	ft^2	**0.50**	**4.09**	**5.500**	**5.000**	**5.305**	**0.461**	-------------	**10.00**	**2.150**	inç
	2.438	m	2.377	m	0.596	m	100.291	kg					1.190	m			1.1892	m^2									54.61	mm
	8.000	ft	**7.800**	ft	**1.956**	ft	**154.000**	Lb	**13.00**	**12.50**	**48.80**	**-12.00**	**2.944**	ft	**0.368**	**0.00**	**12.800**	ft^2	**0.50**	**4.09**	**7.000**	**5.000**	**5.984**	**0.321**	-------------	**10.00**	**2.150**	inç
	2.438	m	2.377	m	0.596	m	69.854	kg					0.897	m			1.1892	m^2									54.61	mm
	8.000	ft	**7.800**	ft	**1.956**	ft	**154.000**	Lb	**13.00**	**12.50**	**48.80**	**-8.00**	**3.264**	ft	**0.408**	**0.00**	**12.800**	ft^2	**0.50**	**4.09**	**7.000**	**5.000**	**5.984**	**0.321**	-------------	**10.00**	**2.150**	inç
	2.438	m	2.377	m	0.596	m	69.854	kg					0.995	m			1.1892	m^2									54.61	mm
	8.000	ft	**7.800**	ft	**1.956**	ft	**154.000**	Lb	**13.00**	**12.50**	**48.80**	**-4.00**	**3.584**	ft	**0.448**	**0.00**	**12.800**	ft^2	**0.50**	**4.09**	**7.000**	**5.000**	**5.984**	**0.321**	-------------	**10.00**	**2.150**	inç
	2.438	m	2.377	m	0.596	m	69.854	kg					1.092	m			1.1892	m^2									54.61	mm
	8.000	ft	**7.800**	ft	**1.956**	ft	**154.000**	Lb	**13.00**	**12.50**	**48.80**	**0.00**	**3.904**	ft	**0.488**	**0.00**	**12.800**	ft^2	**0.50**	**4.09**	**7.000**	**5.000**	**5.984**	**0.321**	-------------	**10.00**	**2.150**	inç
	2.438	m	2.377	m	0.596	m	69.854	kg					1.190	m			1.1892	m^2									54.61	mm
	8.000	ft	**7.800**	ft	**1.956**	ft	**115.100**	Lb	**13.00**	**12.50**	**48.80**	**-12.00**	**2.944**	ft	**0.368**	**0.00**	**12.800**	ft^2	**0.50**	**4.09**	**8.499**	**5.000**	**6.594**	**0.240**	-------------	**10.00**	**2.150**	inç
	2.438	m	2.377	m	0.596	m	52.209	kg					0.897	m			1.1892	m^2									54.61	mm
	8.000	ft	**7.800**	ft	**1.956**	ft	**115.100**	Lb	**13.00**	**12.50**	**48.80**	**-8.00**	**3.264**	ft	**0.408**	**0.00**	**12.800**	ft^2	**0.50**	**4.09**	**8.499**	**5.000**	**6.594**	**0.240**	-------------	**10.00**	**2.150**	inç
	2.438	m	2.377	m	0.596	m	52.209	kg					0.995	m			1.1892	m^2									54.61	mm
	8.000	ft	**7.800**	ft	**1.956**	ft	**115.100**	Lb	**13.00**	**12.50**	**48.80**	**-4.00**	**3.584**	ft	**0.448**	**0.00**	**12.800**	ft^2	**0.50**	**4.09**	**8.499**	**5.000**	**6.594**	**0.240**	-------------	**10.00**	**2.150**	inç
	2.438	m	2.377	m	0.596	m	52.209	kg					1.092	m			1.1892	m^2									54.61	mm
	8.000	ft	**7.800**	ft	**1.956**	ft	**115.100**	Lb	**13.00**	**12.50**	**48.80**	**0.00**	**3.904**	ft	**0.488**	**0.00**	**12.800**	ft^2	**0.50**	**4.09**	**8.499**	**5.000**	**6.594**	**0.240**	-------------	**10.00**	**2.150**	inç
	2.438	m	2.377	m	0.596	m	52.209	kg					1.190	m			1.1892	m^2									54.61	mm
IUTT	**2.625**	ft	**2.559**	ft	**0.642**	ft	**5.307**	Lb	**13.00**	**12.50**	**48.80**	**0.00**	**1.281**	ft	**0.488**	**0.00**	**0.000**	ft^2	**0.50**	**4.09**	**0.000**	**ERR**	**6.033**	**0.314**	-------------	**10.00**	**2.150**	inç
	0.800	m	0.780	m	0.196	m	2.407	kg					0.390	m			0.0000	m^2									54.61	mm

DTMB Model		Wedge Angle	Model-62 Wedge Length	Lpx	Lwl	Bpx	Dep	βχ	βτχ	Centroid	Lcg aft of Centroid	Lcg from Transom	Lcg/Lpx	Centerline angle	Ap	Twisted angle	Lpx/Bpx	Ap/Vol	Lpx/Ap	Lpx/Vol	Cv	Vcg/Lpx	Shaft Angle	Lce Transom
4667-1	A	0.00	0.00	4.000 ft	3.900 ft	0.978 ft	14.374 Lb	13.00	12.50	48.80	-12.00	1.472 ft	0.368	0.00	3.200 ft^2	0.50	4.09	8.505	5.000	6.596	0.240	-------------	10.00	2.150 inç
				1.219 m	1.189 m	0.298 m	6.520 kg					0.449 m			0.2973 m^2									54.61 mm
	B	2.00	0.05	4.000 ft	3.900 ft	0.978 ft	14.374 Lb	13.00	12.50	48.80	-12.00	1.472 ft	0.368	0.00	3.200 ft^2	0.50	4.09	8.505	5.000	6.596	0.240	-------------	10.00	2.150 inç
				1.219 m	1.189 m	0.298 m	6.520 kg					0.449 m			0.2973 m^2									54.61 mm
	A	0.00	0.00	4.000 ft	3.900 ft	0.978 ft	19.290 Lb	13.00	12.50	48.80	-6.00	1.712 ft	0.428	0.00	3.200 ft^2	0.50	4.09	6.991	5.000	5.980	0.322	-------------	10.00	2.150 inç
				1.219 m	1.189 m	0.298 m	8.750 kg					0.522 m			0.2973 m^2									54.61 mm
	B	2.00	0.05	4.000 ft	3.900 ft	0.978 ft	19.290 Lb	13.00	12.50	48.80	-6.00	1.712 ft	0.428	0.00	3.200 ft^2	0.50	4.09	6.991	5.000	5.980	0.322	-------------	10.00	2.150 inç
				1.219 m	1.189 m	0.298 m	8.750 kg					0.522 m			0.2973 m^2									54.61 mm
	C	2.00	0.15	4.000 ft	3.900 ft	0.978 ft	19.290 Lb	13.00	12.50	48.80	-6.00	1.712 ft	0.428	0.00	3.200 ft^2	0.50	4.09	6.991	5.000	5.980	0.322	-------------	10.00	2.150 inç
				1.219 m	1.189 m	0.298 m	8.750 kg					0.522 m			0.2973 m^2									54.61 mm
	D	0.00	0.00	4.000 ft	3.900 ft	0.978 ft	19.290 Lb	13.00	12.50	48.80	-12.00	1.472 ft	0.368	0.00	3.200 ft^2	0.50	4.09	6.991	5.000	5.980	0.322	-------------	10.00	2.150 inç
				1.219 m	1.189 m	0.298 m	8.750 kg					0.449 m			0.2973 m^2									54.61 mm
	E	2.00	0.15	4.000 ft	3.900 ft	0.978 ft	19.290 Lb	13.00	12.50	48.80	-12.00	1.472 ft	0.368	0.00	3.200 ft^2	0.50	4.09	6.991	5.000	5.980	0.322	-------------	10.00	2.150 inç
				1.219 m	1.189 m	0.298 m	8.750 kg					0.449 m			0.2973 m^2									54.61 mm
	A	0.00	0.00	4.000 ft	3.900 ft	0.978 ft	27.623 Lb	13.00	12.50	48.80	-4.00	1.792 ft	0.448	0.00	3.200 ft^2	0.50	4.09	5.502	5.000	5.305	0.461	-------------	10.00	2.150 inç
				1.219 m	1.189 m	0.298 m	12.530 kg					0.546 m			0.2973 m^2									54.61 mm
	B	2.00	0.05	4.000 ft	3.900 ft	0.978 ft	27.623 Lb	13.00	12.50	48.80	-4.00	1.792 ft	0.448	0.00	3.200 ft^2	0.50	4.09	5.502	5.000	5.305	0.461	-------------	10.00	2.150 inç
				1.219 m	1.189 m	0.298 m	12.530 kg					0.546 m			0.2973 m^2									54.61 mm
	C	0.00	0.00	4.000 ft	3.900 ft	0.978 ft	27.623 Lb	13.00	12.50	48.80	-8.00	1.632 ft	0.408	0.00	3.200 ft^2	0.50	4.09	5.502	5.000	5.305	0.461	-------------	10.00	2.150 inç
				1.219 m	1.189 m	0.298 m	12.530 kg					0.497 m			0.2973 m^2									54.61 mm
	D	2.00	0.05	4.000 ft	3.900 ft	0.978 ft	27.623 Lb	13.00	12.50	48.80	-8.00	1.632 ft	0.408	0.00	3.200 ft^2	0.50	4.09	5.502	5.000	5.305	0.461	-------------	10.00	2.150 inç
				1.219 m	1.189 m	0.298 m	12.530 kg					0.497 m			0.2973 m^2									54.61 mm
	E	5.00	0.05	4.000 ft	3.900 ft	0.978 ft	27.623 Lb	13.00	12.50	48.80	-8.00	1.632 ft	0.408	0.00	3.200 ft^2	0.50	4.09	5.502	5.000	5.305	0.461	-------------	10.00	2.150 inç
				1.219 m	1.189 m	0.298 m	12.530 kg					0.497 m			0.2973 m^2									54.61 mm
	F	10.00	0.05	4.000 ft	3.900 ft	0.978 ft	27.623 Lb	13.00	12.50	48.80	-8.00	1.632 ft	0.408	0.00	3.200 ft^2	0.50	4.09	5.502	5.000	5.305	0.461	-------------	10.00	2.150 inç
				1.219 m	1.189 m	0.298 m	12.530 kg					0.497 m			0.2973 m^2									54.61 mm
	G	2.00	0.10	4.000 ft	3.900 ft	0.978 ft	27.623 Lb	13.00	12.50	48.80	-8.00	1.632 ft	0.408	0.00	3.200 ft^2	0.50	4.09	5.502	5.000	5.305	0.461	-------------	10.00	2.150 inç
				1.219 m	1.189 m	0.298 m	12.530 kg					0.497 m			0.2973 m^2									54.61 mm
	H	5.00	0.10	4.000 ft	3.900 ft	0.978 ft	27.623 Lb	13.00	12.50	48.80	-8.00	1.632 ft	0.408	0.00	3.200 ft^2	0.50	4.09	5.502	5.000	5.305	0.461	-------------	10.00	2.150 inç
				1.219 m	1.189 m	0.298 m	12.530 kg					0.497 m			0.2973 m^2									54.61 mm
	I	10.00	0.10	4.000 ft	3.900 ft	0.978 ft	27.623 Lb	13.00	12.50	48.80	-8.00	1.632 ft	0.408	0.00	3.200 ft^2	0.50	4.09	5.502	5.000	5.305	0.461	-------------	10.00	2.150 inç
				1.219 m	1.189 m	0.298 m	12.530 kg					0.497 m			0.2973 m^2									54.61 mm
	J	2.00	0.15	4.000 ft	3.900 ft	0.978 ft	27.623 Lb	13.00	12.50	48.80	-8.00	1.632 ft	0.408	0.00	3.200 ft^2	0.50	4.09	5.502	5.000	5.305	0.461	-------------	10.00	2.150 inç
				1.219 m	1.189 m	0.298 m	12.530 kg					0.497 m			0.2973 m^2									54.61 mm
	K	5.00	0.15	4.000 ft	3.900 ft	0.978 ft	27.623 Lb	13.00	12.50	48.80	-8.00	1.632 ft	0.408	0.00	3.200 ft^2	0.50	4.09	5.502	5.000	5.305	0.461	-------------	10.00	2.150 inç
				1.219 m	1.189 m	0.298 m	12.530 kg					0.497 m			0.2973 m^2									54.61 mm
	L	10.00	0.15	4.000 ft	3.900 ft	0.978 ft	27.623 Lb	13.00	12.50	48.80	-8.00	1.632 ft	0.408	0.00	3.200 ft^2	0.50	4.09	5.502	5.000	5.305	0.461	-------------	10.00	2.150 inç
				1.219 m	1.189 m	0.298 m	12.530 kg					0.497 m			0.2973 m^2									54.61 mm
	M	0.00	0.00	4.000 ft	3.900 ft	0.978 ft	27.623 Lb	13.00	12.50	48.80	-12.00	1.472 ft	0.368	0.00	3.200 ft^2	0.50	4.09	5.502	5.000	5.305	0.461	-------------	10.00	2.150 inç
				1.219 m	1.189 m	0.298 m	12.530 kg					0.449 m			0.2973 m^2									54.61 mm
	N	2.00	0.05	4.000 ft	3.900 ft	0.978 ft	27.623 Lb	13.00	12.50	48.80	-12.00	1.472 ft	0.368	0.00	3.200 ft^2	0.50	4.09	5.502	5.000	5.305	0.461	-------------	10.00	2.150 inç
				1.219 m	1.189 m	0.298 m	12.530 kg					0.449 m			0.2973 m^2									54.61 mm

DTMB	Model-62																				
Model	**Lpx**	**Lwl**	**Bpx**	**Dep**	βχ	βτχ	**Centroid**	**Lcg aft of Centroid**	**Lcg from Transom**	**Lcg/Lpx**	**Centerline angle**	**Ap**	**Twisted angle**	**Lpx/Bpx**	**Ap/Vol**	**Lpx/Ap**	**Lpx/Vol**	**Cv**	**Vcg/Lpx**	**Shaft Angle**	Lce Transom
4668	**8.000** ft	**7.862** ft	**1.455** ft	**228.600** Lb	**13.00**	**12.50**	**48.80**	**4.00**	**4.224** ft	**0.528**	**0.00**	**9.518** ft^2	**0.50**	**5.50**	**4.000**	**6.724**	**5.246**	**1.160**	-------------	**7.30**	**1.600** inç
	2.438 m	2.396 m	0.443 m	103.693 kg					1.287 m			0.8843 m^2									40.64 mm
	8.000 ft	**7.862** ft	**1.455** ft	**228.600** Lb	**13.00**	**12.50**	**48.80**	**0.00**	**3.904** ft	**0.488**	**0.00**	**9.518** ft^2	**0.50**	**5.50**	**4.000**	**6.724**	**5.246**	**1.160**	-------------	**7.30**	**1.600** inç
	2.438 m	2.396 m	0.443 m	103.693 kg					1.190 m			0.8843 m^2									40.64 mm
	8.000 ft	**7.862** ft	**1.455** ft	**141.800** Lb	**13.00**	**12.50**	**48.80**	**-12.00**	**2.944** ft	**0.368**	**0.00**	**9.518** ft^2	**0.50**	**5.50**	**5.499**	**6.724**	**6.151**	**0.720**	-------------	**7.30**	**1.600** inç
	2.438 m	2.396 m	0.443 m	64.320 kg					0.897 m			0.8843 m^2									40.64 mm
	8.000 ft	**7.862** ft	**1.455** ft	**141.800** Lb	**13.00**	**12.50**	**48.80**	**-8.00**	**3.264** ft	**0.408**	**0.00**	**9.518** ft^2	**0.50**	**5.50**	**5.499**	**6.724**	**6.151**	**0.720**	-------------	**7.30**	**1.600** inç
	2.438 m	2.396 m	0.443 m	64.320 kg					0.995 m			0.8843 m^2									40.64 mm
	8.000 ft	**7.862** ft	**1.455** ft	**141.800** Lb	**13.00**	**12.50**	**48.80**	**-4.00**	**3.584** ft	**0.448**	**0.00**	**9.518** ft^2	**0.50**	**5.50**	**5.499**	**6.724**	**6.151**	**0.720**	-------------	**7.30**	**1.600** inç
	2.438 m	2.396 m	0.443 m	64.320 kg					1.092 m			0.8843 m^2									40.64 mm
	8.000 ft	**7.800** ft	**1.455** ft	**141.800** Lb	**13.00**	**12.50**	**48.80**	**0.00**	**3.904** ft	**0.488**	**0.00**	**9.518** ft^2	**0.50**	**5.50**	**5.499**	**6.724**	**6.151**	**0.720**	-------------	**7.30**	**1.600** inç
	2.438 m	2.377 m	0.443 m	64.320 kg					1.190 m			0.8843 m^2									40.64 mm
	8.000 ft	**7.862** ft	**1.455** ft	**98.700** Lb	**13.00**	**12.50**	**48.80**	**-12.00**	**2.944** ft	**0.368**	**0.00**	**9.518** ft^2	**0.50**	**5.50**	**7.002**	**6.724**	**6.941**	**0.501**	-------------	**7.30**	**1.600** inç
	2.438 m	2.396 m	0.443 m	44.770 kg					0.897 m			0.8843 m^2									40.64 mm
	8.000 ft	**7.862** ft	**1.455** ft	**98.700** Lb	**13.00**	**12.50**	**48.80**	**-8.00**	**3.264** ft	**0.408**	**0.00**	**9.518** ft^2	**0.50**	**5.50**	**7.002**	**6.724**	**6.941**	**0.501**	-------------	**7.30**	**1.600** inç
	2.438 m	2.396 m	0.443 m	44.770 kg					0.995 m			0.8843 m^2									40.64 mm
	8.000 ft	**7.862** ft	**1.455** ft	**98.700** Lb	**13.00**	**12.50**	**48.80**	**-5.00**	**3.504** ft	**0.438**	**0.00**	**9.518** ft^2	**0.50**	**5.50**	**7.002**	**6.724**	**6.941**	**0.501**	-------------	**7.30**	**1.600** inç
	2.438 m	2.396 m	0.443 m	44.770 kg					1.068 m			0.8843 m^2									40.64 mm
	8.000 ft	**7.862** ft	**1.455** ft	**98.700** Lb	**13.00**	**12.50**	**48.80**	**-4.00**	**3.584** ft	**0.448**	**0.00**	**9.518** ft^2	**0.50**	**5.50**	**7.002**	**6.724**	**6.941**	**0.501**	-------------	**7.30**	**1.600** inç
	2.438 m	2.396 m	0.443 m	44.770 kg					1.092 m			0.8843 m^2									40.64 mm
	8.000 ft	**7.862** ft	**1.455** ft	**98.700** Lb	**13.00**	**12.50**	**48.80**	**0.00**	**3.904** ft	**0.488**	**0.00**	**9.518** ft^2	**0.50**	**5.50**	**7.002**	**6.724**	**6.941**	**0.501**	-------------	**7.30**	**1.600** inç
	2.438 m	2.396 m	0.443 m	44.770 kg					1.190 m			0.8843 m^2									40.64 mm
	8.000 ft	**7.862** ft	**1.455** ft	**73.800** Lb	**13.00**	**12.50**	**48.80**	**-12.00**	**2.944** ft	**0.368**	**0.00**	**9.518** ft^2	**0.50**	**5.50**	**8.500**	**6.724**	**7.647**	**0.374**	-------------	**7.30**	**1.600** inç
	2.438 m	2.396 m	0.443 m	33.476 kg					0.897 m			0.8843 m^2									40.64 mm
	8.000 ft	**7.862** ft	**1.455** ft	**73.800** Lb	**13.00**	**12.50**	**48.80**	**-8.00**	**3.264** ft	**0.408**	**0.00**	**9.518** ft^2	**0.50**	**5.50**	**8.500**	**6.724**	**7.647**	**0.374**	-------------	**7.30**	**1.600** inç
	2.438 m	2.396 m	0.443 m	33.476 kg					0.995 m			0.8843 m^2									40.64 mm
	8.000 ft	**7.862** ft	**1.455** ft	**73.800** Lb	**13.00**	**12.50**	**48.80**	**-4.00**	**3.584** ft	**0.448**	**0.00**	**9.518** ft^2	**0.50**	**5.50**	**8.500**	**6.724**	**7.647**	**0.374**	-------------	**7.30**	**1.600** inç
	2.438 m	2.396 m	0.443 m	33.476 kg					1.092 m			0.8843 m^2									40.64 mm
	8.000 ft	**7.862** ft	**1.455** ft	**73.800** Lb	**13.00**	**12.50**	**48.80**	**0.00**	**3.904** ft	**0.488**	**0.00**	**9.518** ft^2	**0.50**	**5.50**	**8.500**	**6.724**	**7.647**	**0.374**	-------------	**7.30**	**1.600** inç
	2.438 m	2.396 m	0.443 m	33.476 kg					1.190 m			0.8843 m^2									40.64 mm

DTMB Model-62

Model	Lpx		Lwl		Bpx		Dep		$\beta\chi$	$\beta\tau\chi$	Centroid	Lcg aft of Centroid	Lcg from Transom		Lcg/Lpx	Centerline angle	Ap		Twisted angle	Lpx/Bpx	Ap/Vol	Lpx/Ap	Lpx/Vol	Cv	Vcg/Lpx	Shaft Angle	Lce Transom	
4669	8.000	ft	7.862	ft	1.143	ft	159.200	Lb	13.00	12.50	48.80	4.00	4.224	ft	0.528	0.00	7.479	ft^2	0.50	7.00	4.000	8.557	5.919	1.665	-------------	7.30	1.600	inç
	2.438	m	2.396	m	0.348	m	72.213	kg					1.287	m			0.6948	m^2									40.64	mm
	8.000	ft	7.862	ft	1.143	ft	159.200	Lb	13.00	12.50	48.80	0.00	3.904	ft	0.488	0.00	7.479	ft^2	0.50	7.00	4.000	8.557	5.919	1.665	-------------	7.30	1.600	inç
	2.438	m	2.396	m	0.348	m	72.213	kg					1.190	m			0.6948	m^2									40.64	mm
	8.000	ft	7.862	ft	1.143	ft	101.800	Lb	13.00	12.50	48.80	-12.00	2.944	ft	0.368	0.00	7.479	ft^2	0.50	7.00	5.390	8.557	6.870	1.065	-------------	7.30	1.600	inç
	2.438	m	2.396	m	0.348	m	46.176	kg					0.897	m			0.6948	m^2									40.64	mm
	8.000	ft	7.862	ft	1.143	ft	101.800	Lb	13.00	12.50	48.80	-8.00	3.264	ft	0.408	0.00	7.479	ft^2	0.50	7.00	5.390	8.557	6.870	1.065	-------------	7.30	1.600	inç
	2.438	m	2.396	m	0.348	m	46.176	kg					0.995	m			0.6948	m^2									40.64	mm
	8.000	ft	7.862	ft	1.143	ft	101.800	Lb	13.00	12.50	48.80	-4.00	3.584	ft	0.448	0.00	7.479	ft^2	0.50	7.00	5.390	8.557	6.870	1.065	-------------	7.30	1.600	inç
	2.438	m	2.396	m	0.348	m	46.176	kg					1.092	m			0.6948	m^2									40.64	mm
	8.000	ft	7.800	ft	1.143	ft	101.800	Lb	13.00	12.50	48.80	0.00	3.904	ft	0.488	0.00	7.479	ft^2	0.50	7.00	5.390	8.557	6.870	1.065	-------------	7.30	1.600	inç
	2.438	m	2.377	m	0.348	m	46.176	kg					1.190	m			0.6948	m^2									40.64	mm
	8.000	ft	7.862	ft	1.143	ft	68.800	Lb	13.00	12.50	48.80	-12.00	2.944	ft	0.368	0.00	7.479	ft^2	0.50	7.00	6.999	8.557	7.828	0.720	-------------	7.30	1.600	inç
	2.438	m	2.396	m	0.348	m	31.208	kg					0.897	m			0.6948	m^2									40.64	mm
	8.000	ft	7.862	ft	1.143	ft	68.800	Lb	13.00	12.50	48.80	-8.00	3.264	ft	0.408	0.00	7.479	ft^2	0.50	7.00	6.999	8.557	7.828	0.720	-------------	7.30	1.600	inç
	2.438	m	2.396	m	0.348	m	31.208	kg					0.995	m			0.6948	m^2									40.64	mm
	8.000	ft	7.862	ft	1.143	ft	68.800	Lb	13.00	12.50	48.80	-6.00	3.424	ft	0.428	0.00	7.479	ft^2	0.50	7.00	6.999	8.557	7.828	0.720	-------------	7.30	1.600	inç
	2.438	m	2.396	m	0.348	m	31.208	kg					1.044	m			0.6948	m^2									40.64	mm
	8.000	ft	7.862	ft	1.143	ft	68.800	Lb	13.00	12.50	48.80	-4.00	3.584	ft	0.448	0.00	7.479	ft^2	0.50	7.00	6.999	8.557	7.828	0.720	-------------	7.30	1.600	inç
	2.438	m	2.396	m	0.348	m	31.208	kg					1.092	m			0.6948	m^2									40.64	mm
	8.000	ft	7.862	ft	1.143	ft	68.800	Lb	13.00	12.50	48.80	0.00	3.904	ft	0.488	0.00	7.479	ft^2	0.50	7.00	6.999	8.557	7.828	0.720	-------------	7.30	1.600	inç
	2.438	m	2.396	m	0.348	m	31.208	kg					1.190	m			0.6948	m^2									40.64	mm
	8.000	ft	7.862	ft	1.143	ft	51.400	Lb	13.00	12.50	48.80	-12.00	2.944	ft	0.368	0.00	7.479	ft^2	0.50	7.00	8.500	8.557	8.627	0.538	-------------	7.30	1.600	inç
	2.438	m	2.396	m	0.348	m	23.315	kg					0.897	m			0.6948	m^2									40.64	mm
	8.000	ft	7.862	ft	1.143	ft	51.400	Lb	13.00	12.50	48.80	-8.00	3.264	ft	0.408	0.00	7.479	ft^2	0.50	7.00	8.500	8.557	8.627	0.538	-------------	7.30	1.600	inç
	2.438	m	2.396	m	0.348	m	23.315	kg					0.995	m			0.6948	m^2									40.64	mm
	8.000	ft	7.862	ft	1.143	ft	51.400	Lb	13.00	12.50	48.80	-4.00	3.584	ft	0.448	0.00	7.479	ft^2	0.50	7.00	8.500	8.557	8.627	0.538	-------------	7.30	1.600	inç
	2.438	m	2.396	m	0.348	m	23.315	kg					1.092	m			0.6948	m^2									40.64	mm
	8.000	ft	7.862	ft	1.143	ft	51.400	Lb	13.00	12.50	48.80	0.00	3.904	ft	0.488	0.00	7.479	ft^2	0.50	7.00	8.500	8.557	8.627	0.538	-------------	7.30	1.600	inç
	2.438	m	2.396	m	0.348	m	23.315	kg					1.190	m			0.6948	m^2									40.64	mm

REPORTS

Resistance Tests of a Systematic Series of Planing Hull Forms

By Eugene P. Clement,[1] *Associate Member* and Donald L. Blount,[2] *Associate Member*

This paper presents the results of resistance tests of five planing boat models of different length-beam ratio. Each model was tested at a number of loads and LCG locations. The results are presented as curves of angle of attack and resistance-weight ratio versus Froude number. The resistance data have been corrected to boat weights of 10,000 and 100,000 lb. The measured values of wetted lengths, wetted surface, and rise of CG are also presented in tabular form. The conditions at which the models porpoised at high speed were determined and a graph defining the stable and unstable regions is included. A method was ascertained of collapsing the high-speed resistance data from the tests of the series into a single graph. A simplified prediction method was then developed which can be used to determine the high-speed resistance of planing hulls of a wide range of proportions, and of any gross weight from 1000 to 100,000 lb.

THE testing of a systematic series of ship or boat hull forms serves a number of useful purposes. The results show the effects on performance of changes in the design variables tested and also indicate optimum or desirable values for those variables. The data obtained can be used to predict the performance of projected new designs. Finally, the performance of the series can be used as a yardstick to gage the efficiency of new designs for which model tests have been made.

Several systematic series of hull forms for ships and boats of the displacement type have been tested, but only one series of hull forms for planing boats has been tested previously. This planing boat series was designated EMB Series 50; the test results were reported in Reference [1].[3] Series 50 was designed at the United States Experimental Model Basin (the predecessor of the David Taylor Model Basin) and the tests were run on 40-in. models at the Experimental Towing Tank of Stevens Institute of Technology. Although the results have been of some interest and use, they do have a number of drawbacks. The chief shortcoming is that the boundary flow of the models during the tests was evidently not fully turbulent. This is indicated by the fact that for some of the data points in the planing range the values of the total resistance coefficient are less than the values of frictional resistance coefficient for fully turbulent flow; i.e., the indicated result is that the wave-making resistance is negative. Another drawback of Series 50 concerns the parameters treated in the series. They have been found suitable for analysis and design of displacement ships, but they are not well suited for the analysis and design of planing craft. Finally, time has brought improvements in the design of planing hulls and, accordingly, the hull form of Series 50 has become somewhat old fashioned.

To fill an evident need a more up-to-date hull form has been developed at the David Taylor Model Basin to be the parent form for a systematic series of planing boat models. Five models of different length-beam ratio have been built and each has been tested for resistance at a number of loads and longitudinal center-of-gravity locations. The results of the tests of this series, designated TMB Series 62, are presented in this paper.

[1] Supervisory Naval Architect, David Taylor Model Basin, Navy Department, Washington, D. C.

[2] Naval Architect, David Taylor Model Basin, Navy Department, Washington, D. C.

[3] Numbers in brackets designate References at end of paper.

Presented at the Annual Meeting, New York, N. Y., November 14–15, 1963, of THE SOCIETY OF NAVAL ARCHITECTS AND MARINE ENGINEERS.

Development of the Parent

The background work leading to the design of the hull form utilized as the parent for this series is reported in [2]. Briefly, this work involved an analysis of the results of resistance tests of a number of previous designs and also of the features desirable for good steering qualities and good rough-water performance. As a result of these analyses, it was concluded that it would be desirable to depart from the hull form of Series 50 in the following particulars:

(*a*) The deadrise angle at the transom should be fairly high (12½ deg was selected).

(*b*) The after portion of the hull bottom should have a constant deadrise angle so that the high-speed planing area would be untwisted.

(*c*) The stern should be narrow, with the transom width equal to about 65 percent of the maximum chine width.

(*d*) The bow sections should be convex.

The lines of the hull form developed on the basis of these particulars and the results of model tests of the design are reported in [2].

The tests showed that the design had less resistance than any of the conventional stepless planing boat designs tested previously at the Model Basin, and from this point of view it seemed to be a satisfactory parent form for a systematic series. However, one change was made. The hull form as initially designed was quite close to being a form consisting entirely of developed surfaces. Accordingly, the keel, chine, and sheer lines of the design were maintained (in both plan and profile views) and the necessary changes were made to obtain a hull form which would consist entirely of developed surfaces. When a model of the new design was built and tested, the resistance was found to be essentially unchanged. Therefore, the new model was utilized as the parent model for the series.

Fig. 1 shows the body plans of both the original and the modified design. This figure indicates that the convexity of the bow sections (a desirable feature) was reduced by the change to developed surfaces. However, the developed-surface feature offers important advantages in regard to ease and economy of construction when the skin material is to be plywood or sheet metal. Also, the forward ends of the buttocks of the revised design are less steep, a feature which will tend to diminish pounding in rough water.

The Model Basin has developed a method of presenting the important features of a planing-hull form by three dimensionless "form-characteristics" curves. These curves, for the parent model of the Series, are presented in Fig. 2.

Plan and Scope of Series

It has been explained in previous reports (reference [3], for example) that three of the most important parameters affecting the performance of planing hulls are the ratio of length to beam, the relationship between hull size and gross weight, and the longitudinal location of the center of gravity. For most purposes in this paper, length-beam ratio is defined as the ratio of the projected chine length L_P to the maximum breadth over the chines B_{PX}. For those cases where it is desired to be more precise, it is defined (in a manner analagous to the definition of aspect ratio for a wing or hydrofoil) as the ratio of L_P to the mean breadth over the chines B_{PA}. The relationship between hull size and gross weight is ex-

Nomenclature

A_P = projected planing bottom area, excluding area of external spray strips
B_P = beam or breadth over chines, excluding external spray strips
B_{PA} = mean breadth over chines, A_P/L_P
B_{PT} = breadth over chines at transom, excluding external spray strips
B_{PX} = maximum breadth over chines, excluding external spray strips
BL = baseline
b = breadth over spray strips at longitudinal location of center of gravity
CL = centerline
CG = center of gravity
C_{Lb} = lift coefficient, $W/\frac{1}{2}\rho u^2 b^2$
F_∇ = Froude number based on volume, $v/(g\nabla^{1/3})^{1/2}$
g = acceleration due to gravity
L_P = projected chine length
LCG = longitudinal center of gravity location
l_{cp} = distance of center of pressure forward of transom
R = total resistance, lb
S = wetted surface area (this is actual wetted surface underway including area of sides which is wetted at low speeds and wetted bottom area of external spray strips; however, area wetted by spray is excluded)
v = speed, fps
V = speed, knots
W = displacement at rest, weight of
w = density of water (weight per unit volume)
λ = linear ratio, ship to model
α = angle of attack of after portion of planing bottom, deg (models as they appear in Fig. 4 are at an angle of attack, α, of zero deg)
β = dead rise angle of planing bottom in degrees. This angle is obtained by approximating each body plan section by a straight line
ν = kinematic viscosity, sq ft/sec
ρ = mass density of water, slugs/cu ft
∇ = displacement at rest, volume of

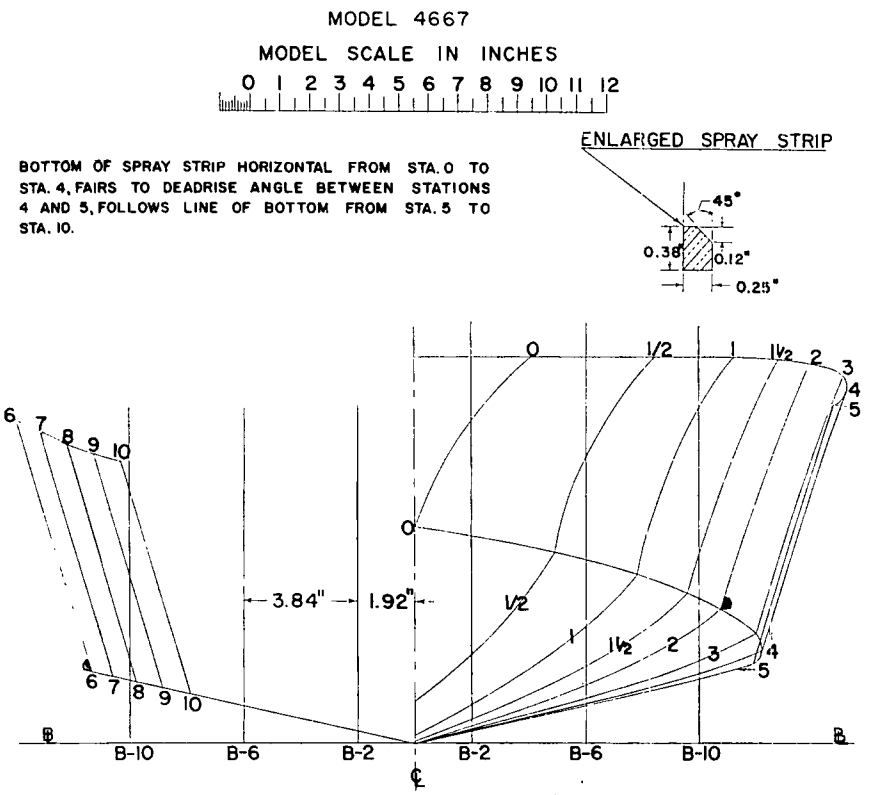

(a) Tentative Parent (Model 4667)

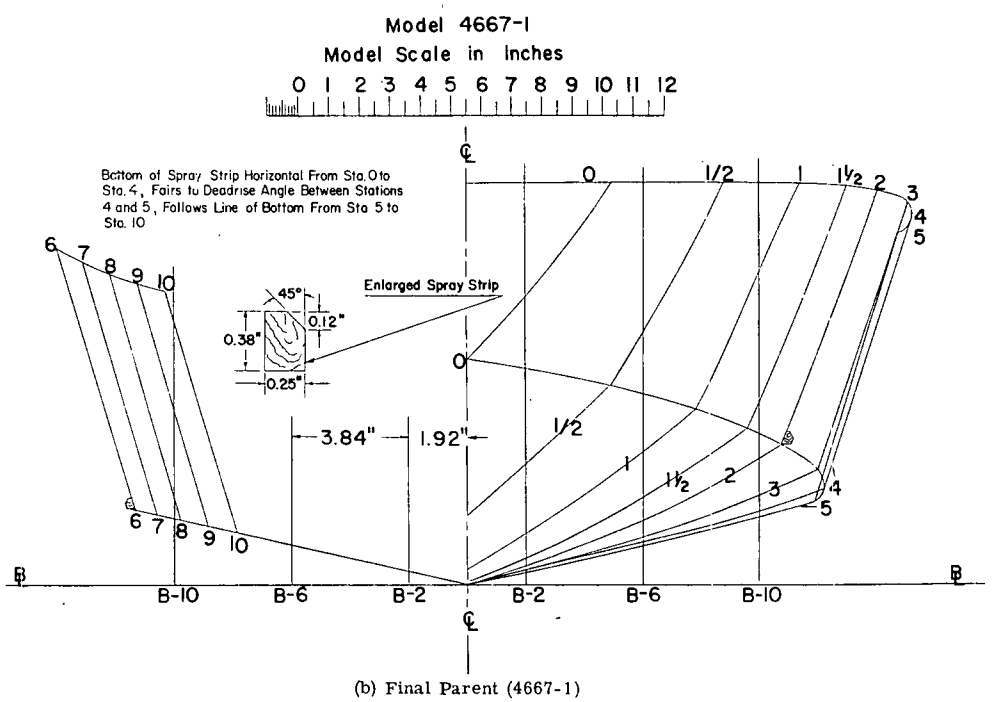

(b) Final Parent (4667-1)

Fig. 1 Body plans of tentative and final parent models

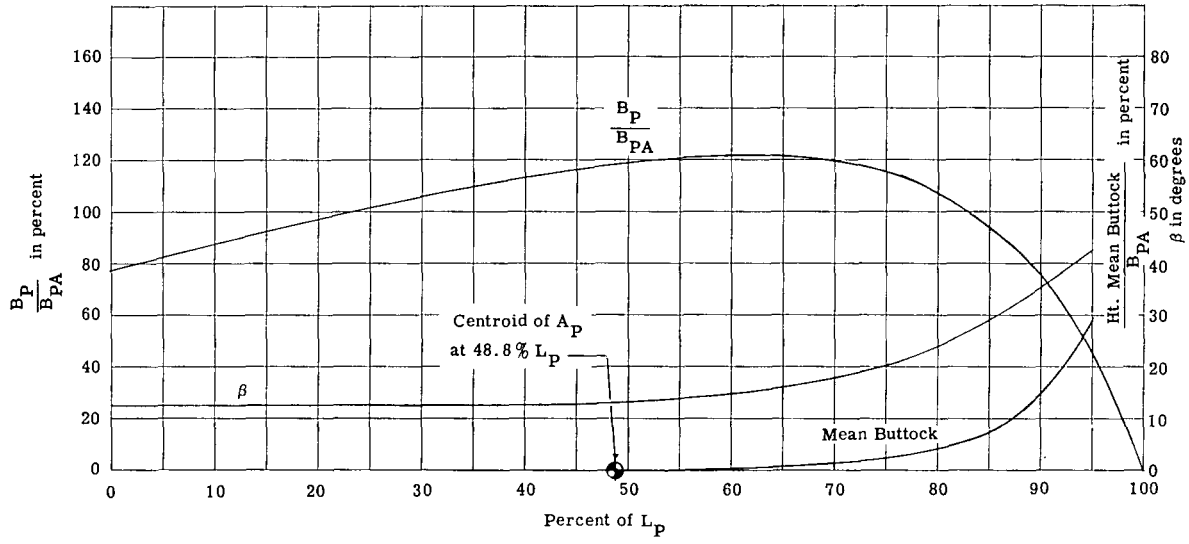

Fig. 2 Form characteristics curves for parent model

Table 1 Particulars of the Models of DTMB Series No. 62

Particulars	Model 4665	4666	4667-1	4668	4669
A_P, ft²	6.469	9.715	12.800	9.518	7.479
L_P, ft	3.912	5.987	8.000	8.000	8.000
B_{PA}, ft	1.654	1.623	1.600	1.190	0.935
B_{PX}, ft	1.956	1.956	1.956	1.455	1.143
B_{PT}, ft	1.565	1.386	1.250	0.934	0.734
L_P/B_{PA}	2.365	3.69	5.00	6.72	8.56
L_P/B_{PX}	2.00	3.06	4.09	5.50	7.00
B_{PX}/B_{PA}	1.18	1.21	1.22	1.22	1.22
B_{PT}/B_{PX}	0.80	0.71	0.64	0.64	0.64
Centroid of A_P, % L_P fwd of transom	47.5	48.2	48.8	48.8	48.8
Angle of a-b chine in plan view, deg	5.0	5.0	5.0	3.7	2.9
Half-angle of waterline entrance, deg	58	49	46	39	37

pressed by the dimensionless ratio $A_P/\nabla^{2/3}$, where A_P is the projected planing bottom area and ∇ is the volume of water displaced at rest. As pointed out in [3], if hulls with different length-beam ratios are compared on the basis of equal $A_P/\nabla^{2/3}$, then the comparison will be on the sound basis of very nearly equal values of hull area, hull volume, and hull structural weight. Longitudinal CG location is defined as the distance of the LCG from the centroid of the area A_P, expressed as a percentage of the length L_P.

The present series was planned so as to explore in a systematic way the effects of a wide variation in the three variables just mentioned. This can be done relatively economically when compared with the method used for systematic investigations of displacement-hull forms. This is possible because it is feasible to explore the effects of variation of loading and LCG location with a single model. Thus, different models are required only for exploration of the effect of length-beam ratio.

Five models, Models 4665, 4666, 4667-1, 4668, and 4669, were tested to explore the influence of length-beam ratio. They are shown in plan view in Fig. 3. Additional particulars of the models are given in Table 1. As can be seen, the values of length-beam ratio tested in the series correspond to values of L_P/B_{PX} of 2, 3.06, 4.09, 5.5 and 7. The extreme models are outside the generally accepted range of boat proportions, but one of the purposes of systematic-series work is to explore new and unfamiliar ground. The body plans for the five models are identical except for some slight

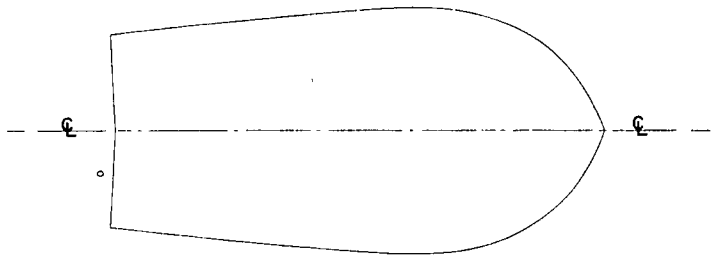

Model 4665 $L_P/B_{PX} = 2.00$

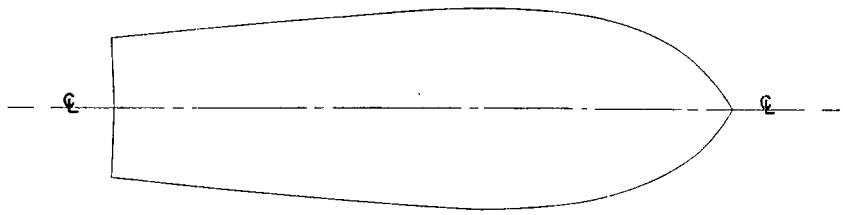

Model 4666 $L_P/B_{PX} = 3.06$

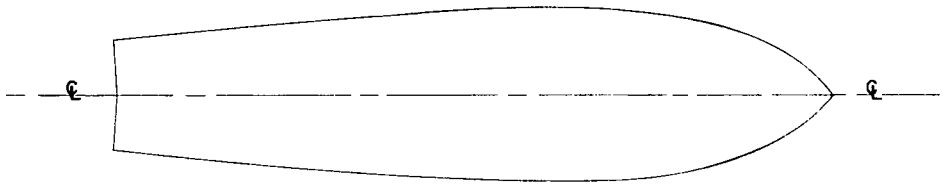

Model 4667-1 $L_P/B_{PX} = 4.09$

Model 4668 $L_P/B_{PX} = 5.50$

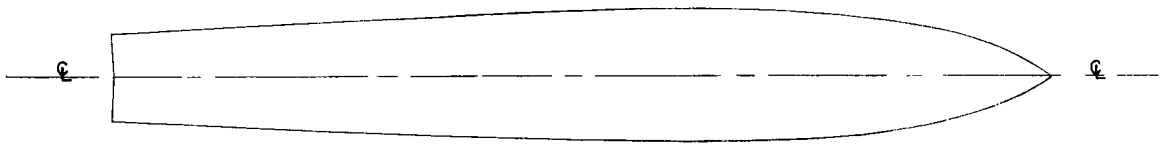

Model 4669 $L_P/B_{PX} = 7.00$

Fig. 3 Chine lines in plan view of five models of series

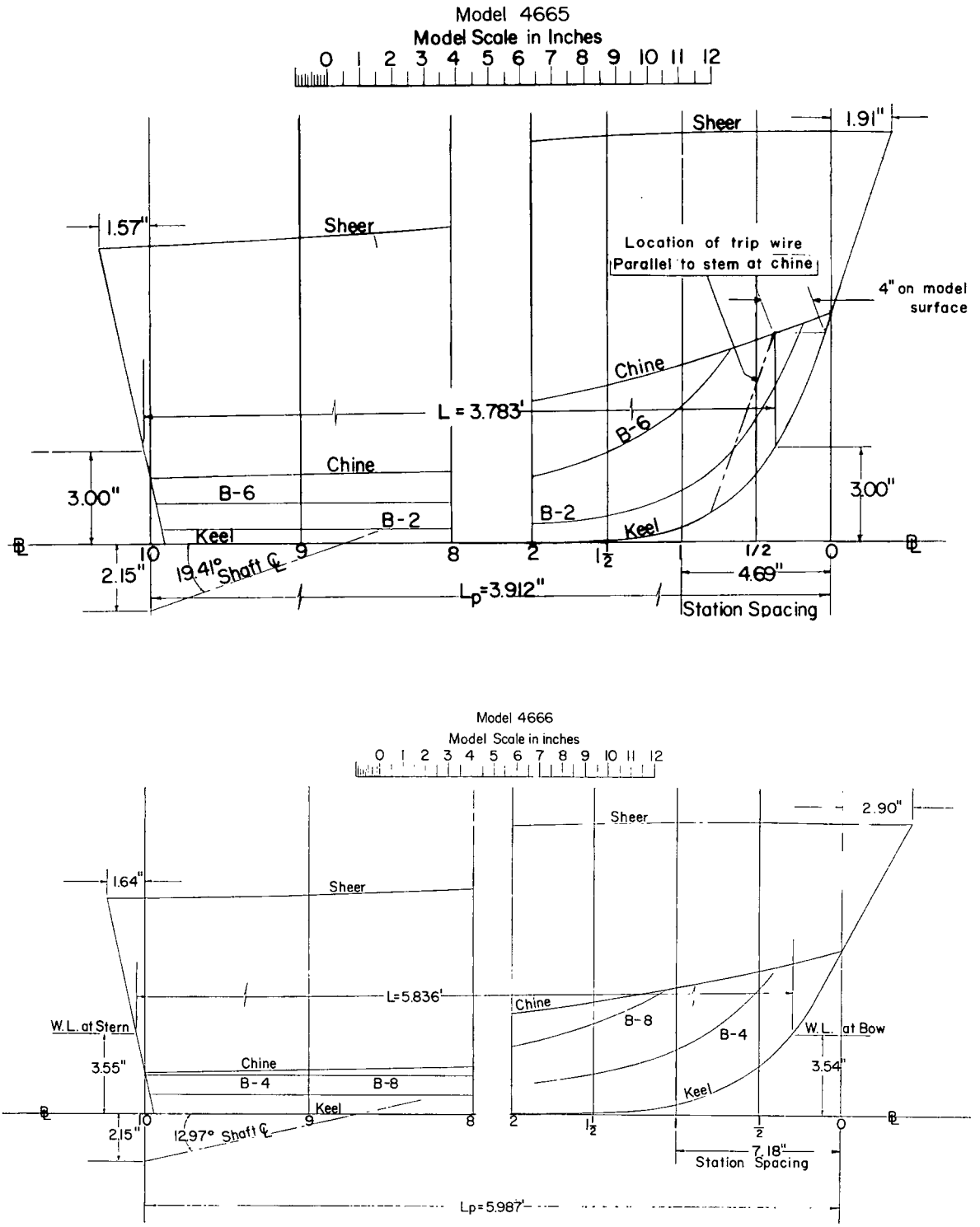

(a) Models 4665 and 4666

Fig. 4 Bow and stern endings of five models of series

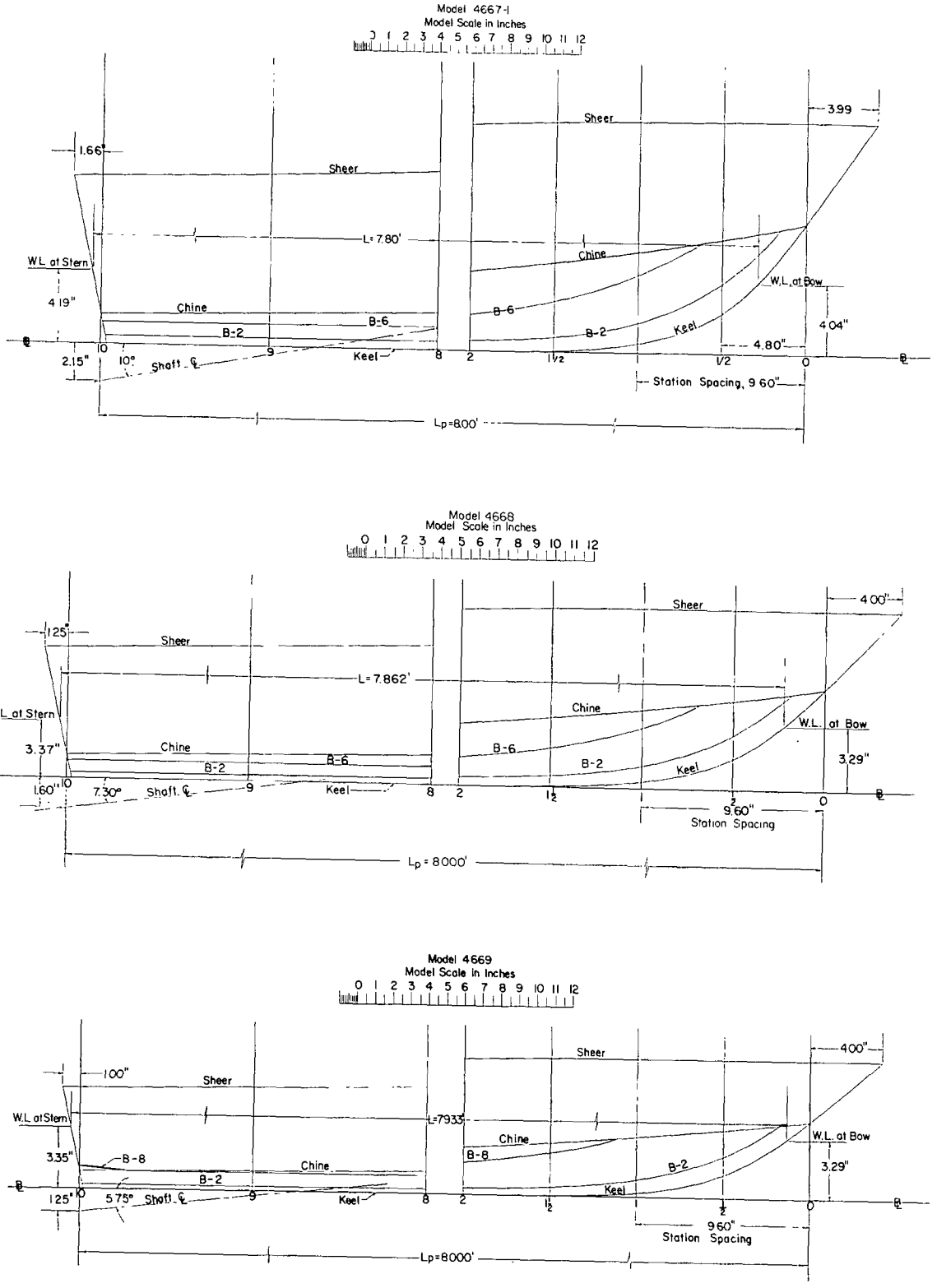

(b) Models 4667-1, 4668, and 4669

Fig. 4 Concluded

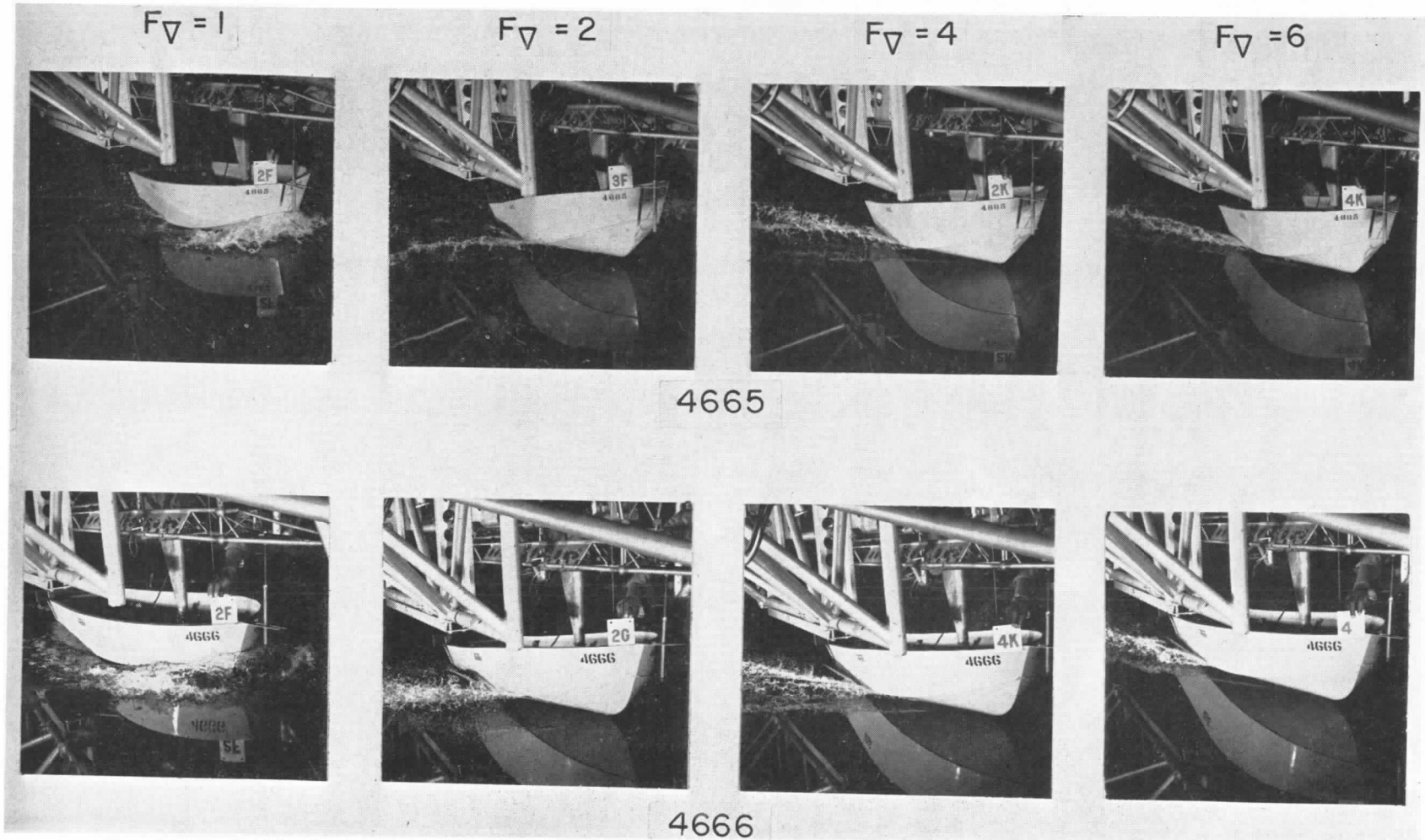

Fig. 5 Photographs of models at DTMB standard test condition ($A_P/\nabla^{2/3} = 7$, LCG at 6 percent L_P aft of certroid of A_P)

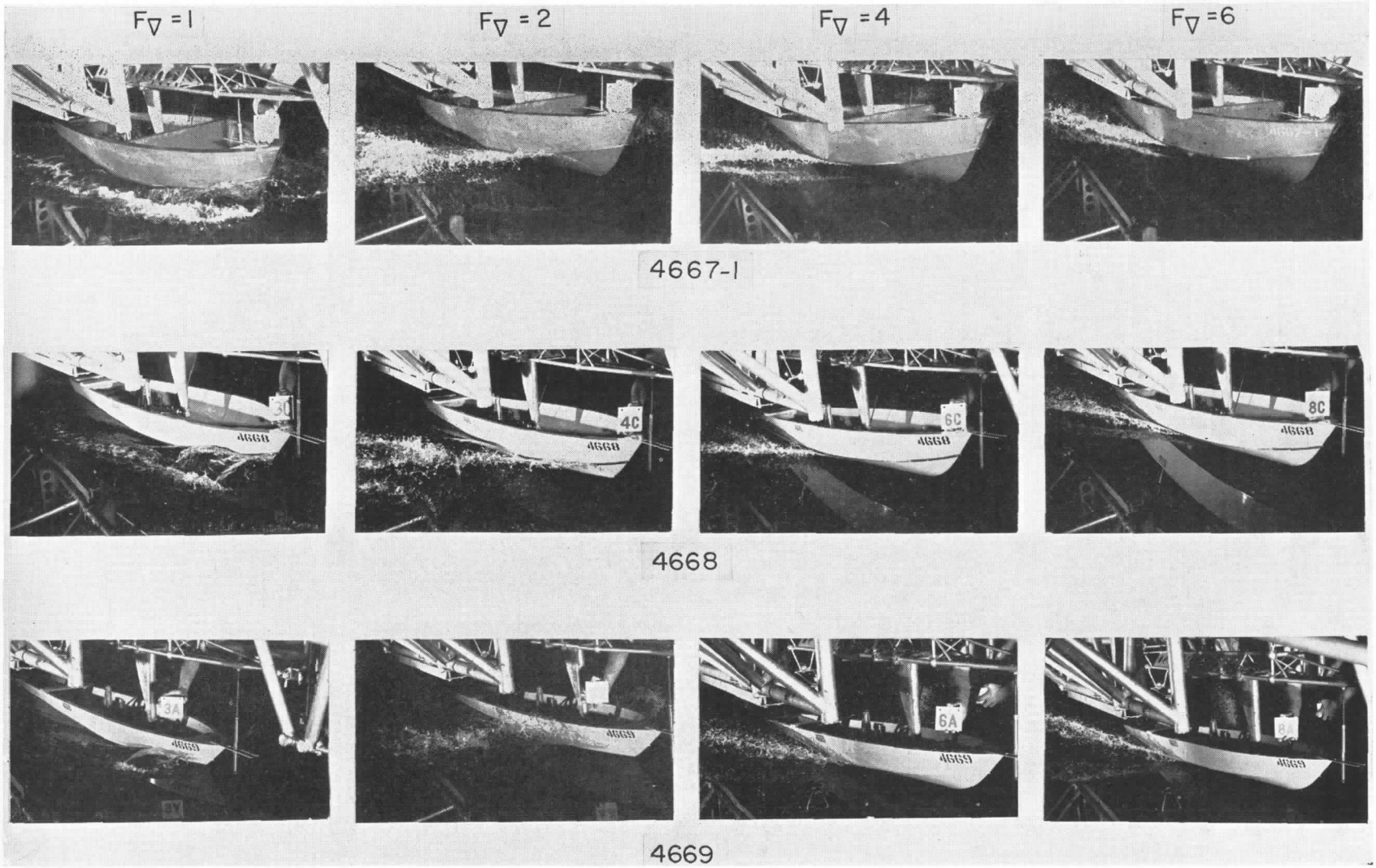

Fig. 5 Concluded

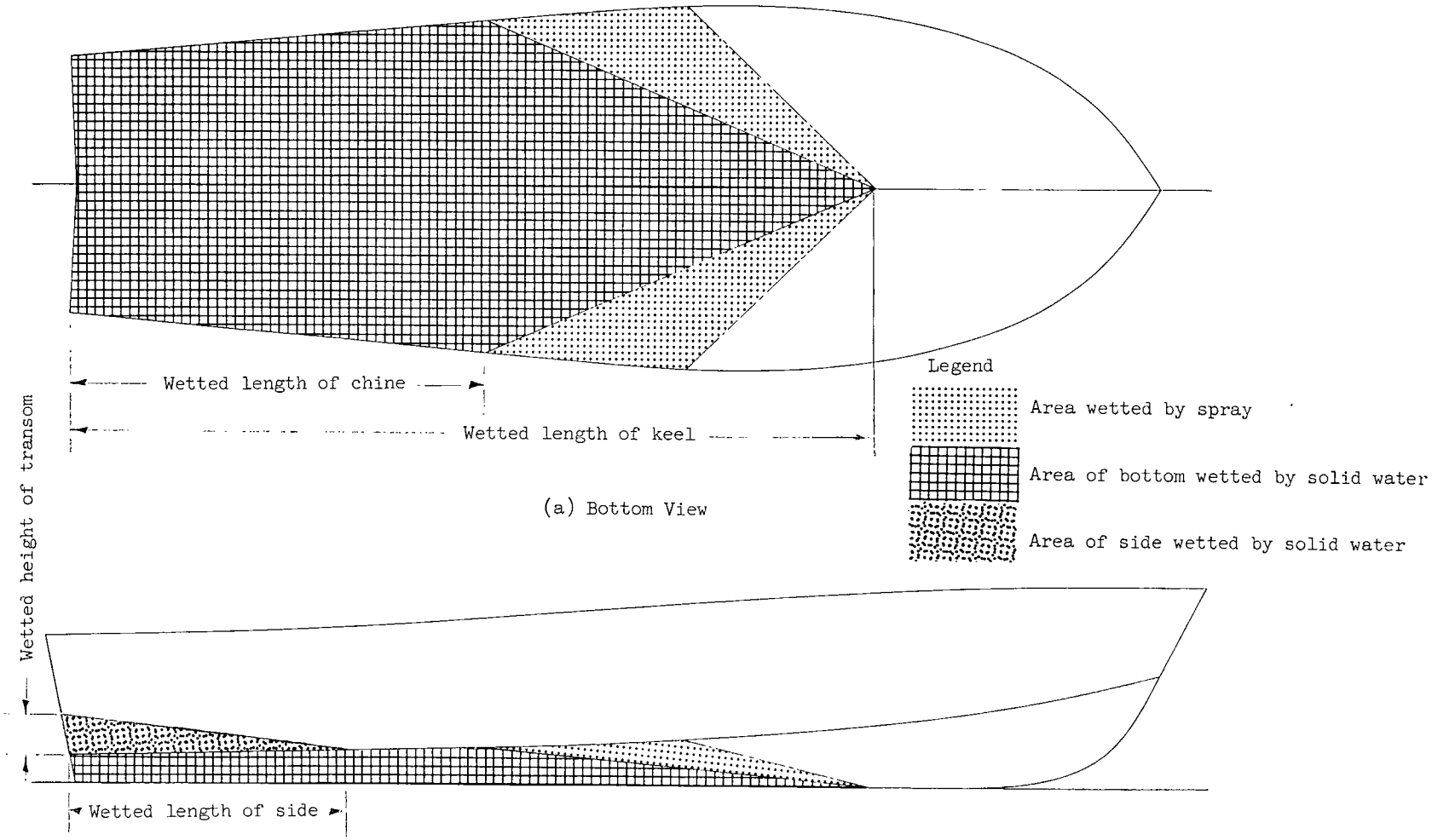

Fig. 6 Wetted lengths and wetted areas of a typical planing-boat mode

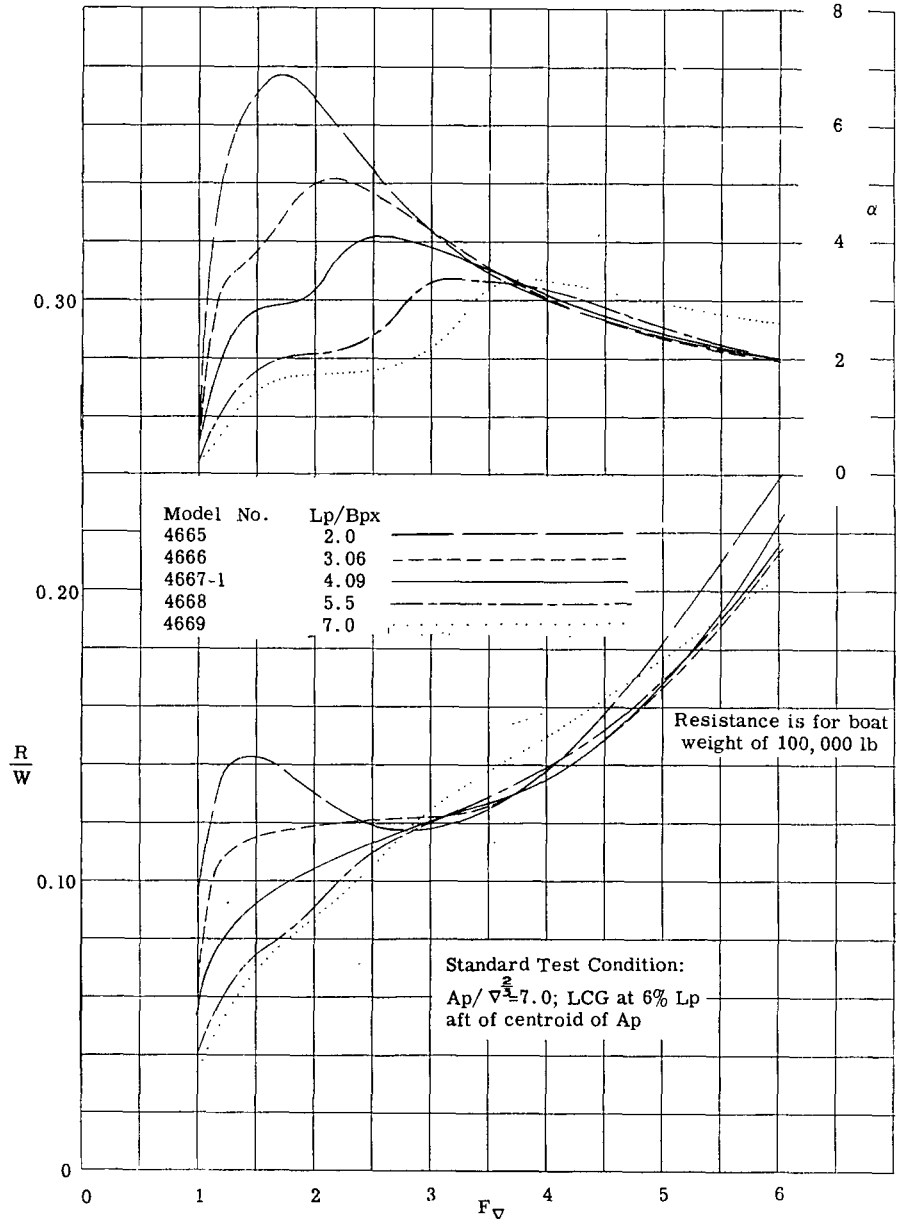

Fig. 7 Resistance/weight ratio and angle of attack versus speed coefficient for five models of series

after body variations in the models having length-beam ratios of 2 and 3.06. Essentially, the four additional models of the series were derived from the parent by maintaining the same shape of body plan but adjusting the station spacing and the size of the body plan to give the different length-beam ratios desired. However, this scheme was deviated from for the two models with the lowest values of length-beam ratio. The model with a length-beam ratio of 3.06 has proportions similar to those for the smaller sizes of pleasure craft, which are propelled either by outboard motors attached to the transom or by the inboard-outboard type of drive with the engine in the extreme stern. For such craft, with their centers of gravity quite far aft, the narrow transom width dictated by the original scheme of variation provides insufficient buoyancy at the stern. The transom widths were therefore arbitrarily widened for the two models having the lowest ratios of

Model No.	Symbol	Hull Designantion
3592-1	△	80 ft. PT 8
3626	□	70 ft. Elco PT Boat
3720	▽	79 ft. Higgins PT Boat
3722	⌂	80 ft. Elco PT Boat
3941	◇	77 ft. PT Boat
4300	○	Aircraft Rescue Boat
4309	◿	43 ft. Aircraft Rescue Boat (Sea Sled)
4310	⌓	43 ft. Aircraft Rescue Boat
4375	◁	90 ft. Aircraft Rescue Boat
4618-1	◇	40 ft. LCP(L)
4708	◇	45 ft. Steel Utility Boat
4665	▼	Series 62 L_P/B_{PX}= 2.00
4666	▲	Series 62 L_P/B_{PX}= 3.06
4667-1	●	Series 62 L_P/B_{PX}= 4.09
4668	■	Series 62 L_P/B_{PX}= 5.50
4669	◆	Series 62 L_P/B_{PX}= 7.00

Resistance corrected to 100, 000 lb displacement and salt water at 59° F using 1947 A.T.T.C. Model-Ship Correlation Line with zero roughness allowance.

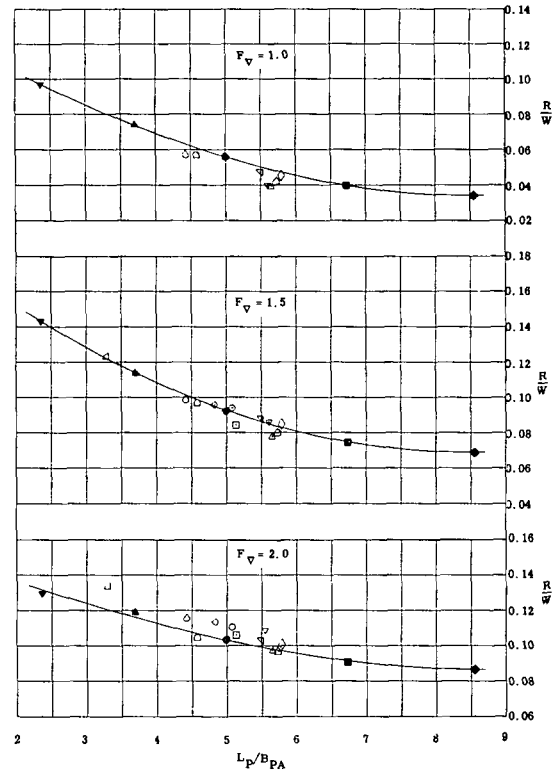

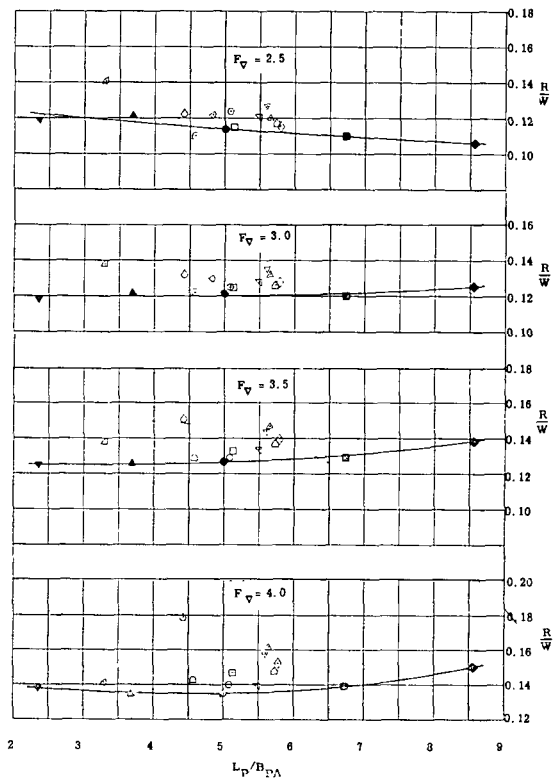

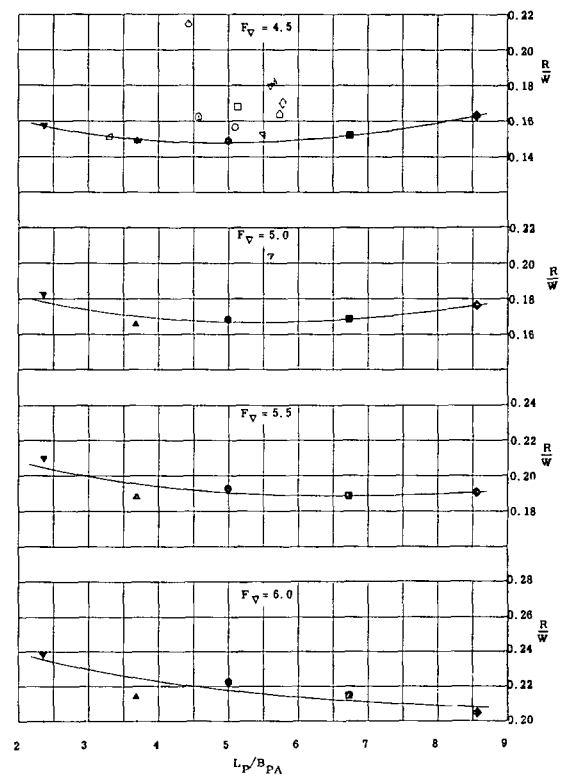

Fig. 8 Resistance/weight ratio for models of series and for other representative planing-boat designs

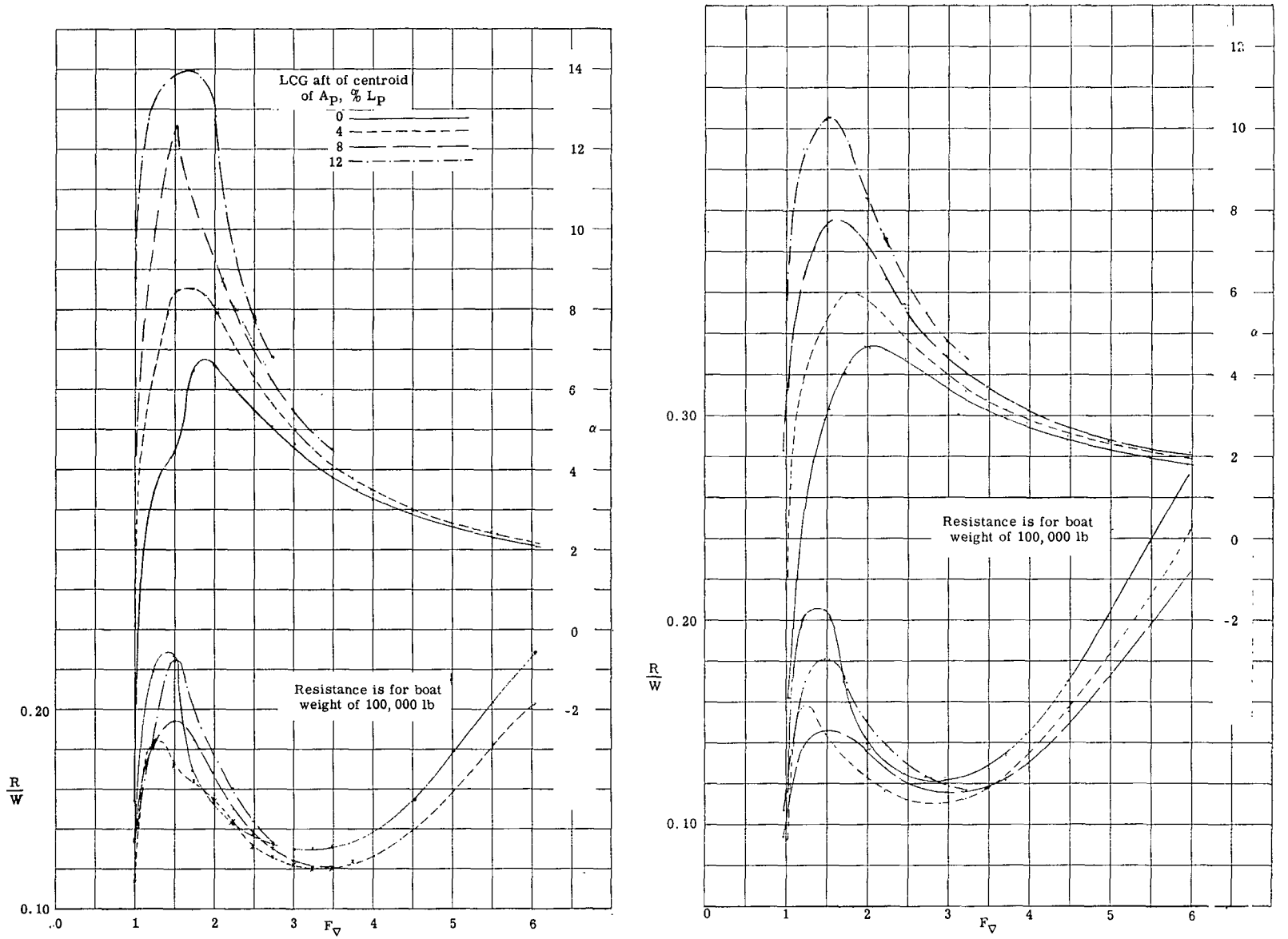

(a) $A_P/\nabla^{\frac{2}{3}} = 5.5$

(b) $A_P/\nabla^{\frac{2}{3}} = 7.0$

Fig. 9 Resistance/weight ratio and angle of attack versus speed coefficient, $L_P/B_{PX} = 2.00$

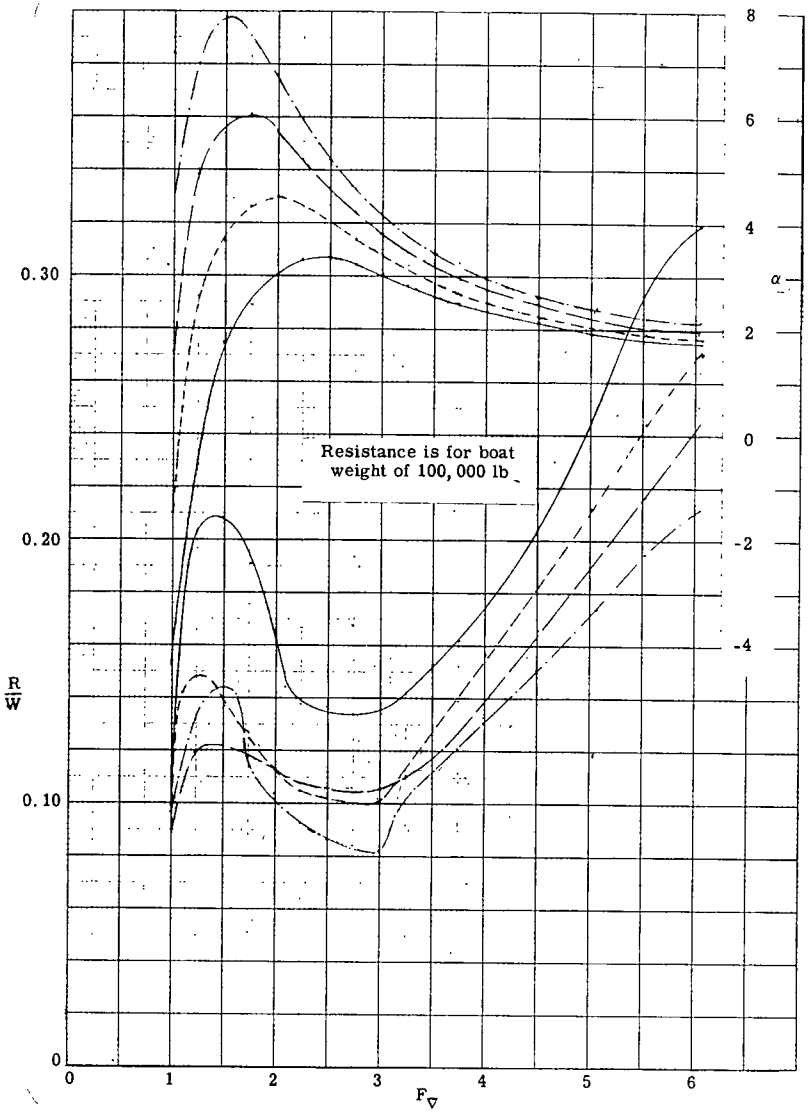

(c) $Ap/\nabla^{\frac{2}{3}} = 8.5$

Fig. 9 Continued

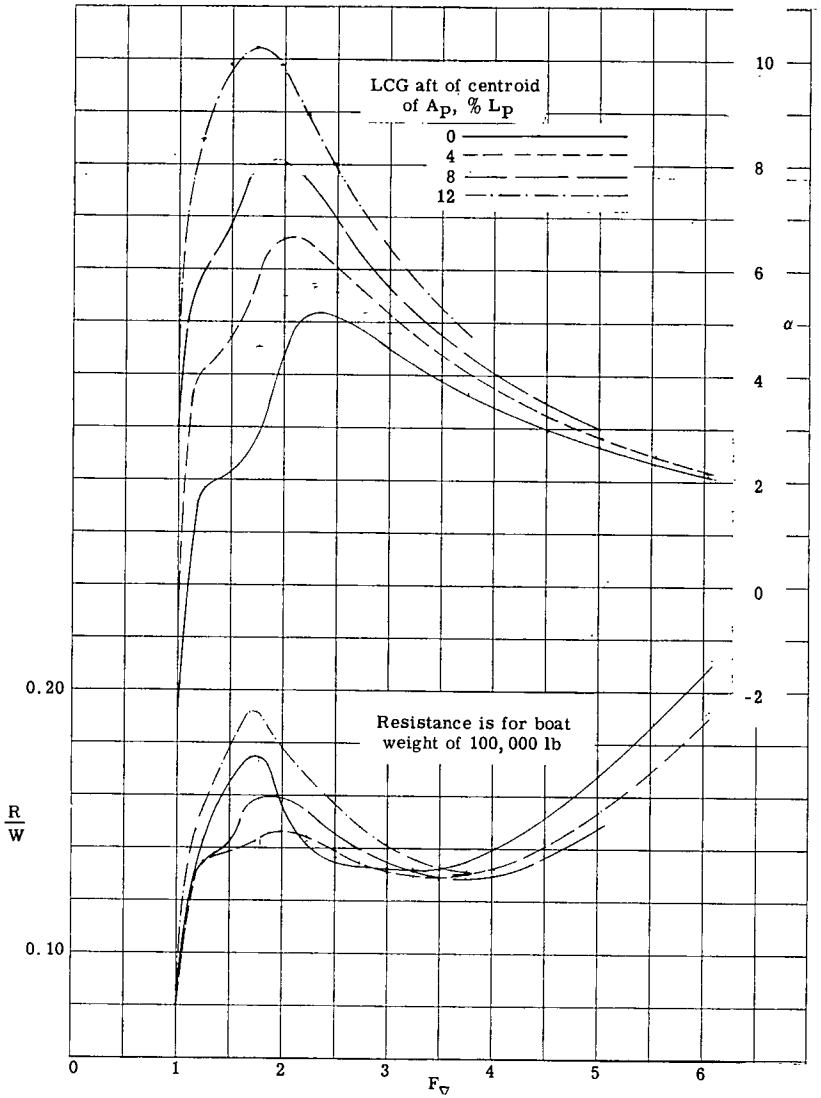

(a) $Ap/\nabla^{\frac{2}{3}} = 5.5$

Fig. 10 Resistance/weight ratio and angle of attack versus speed coefficient $L_P/B_{PX} = 3.06$

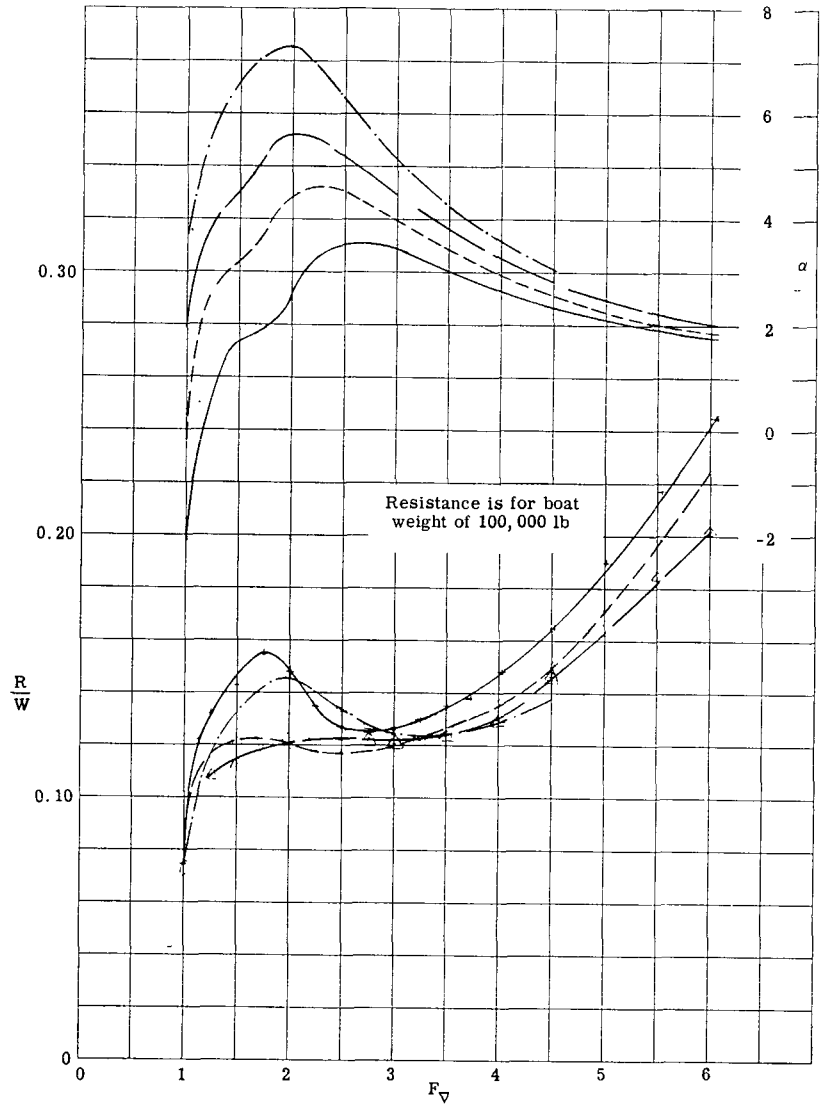

(b) $A_p/\nabla^{\frac{2}{3}} = 7.0$

Fig. 10 Continued

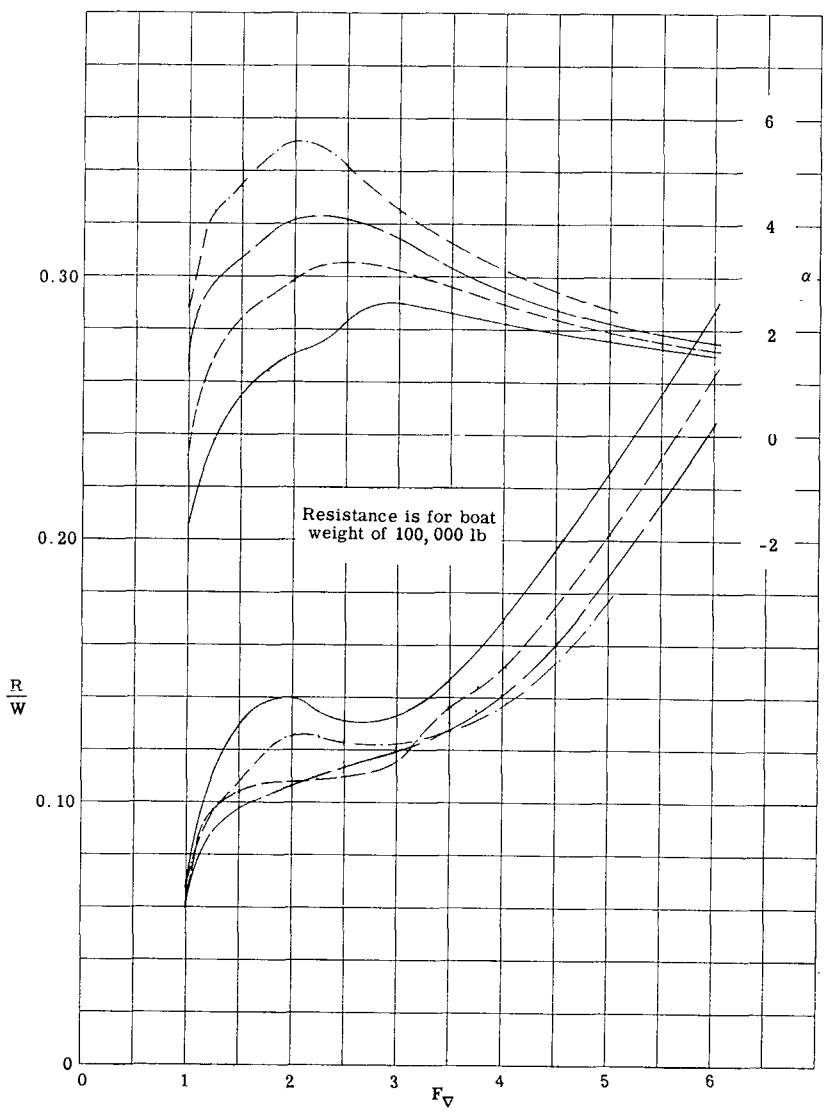

(c) $A_p/\nabla^{\frac{2}{3}} = 8.5$

Fig. 10 Concluded

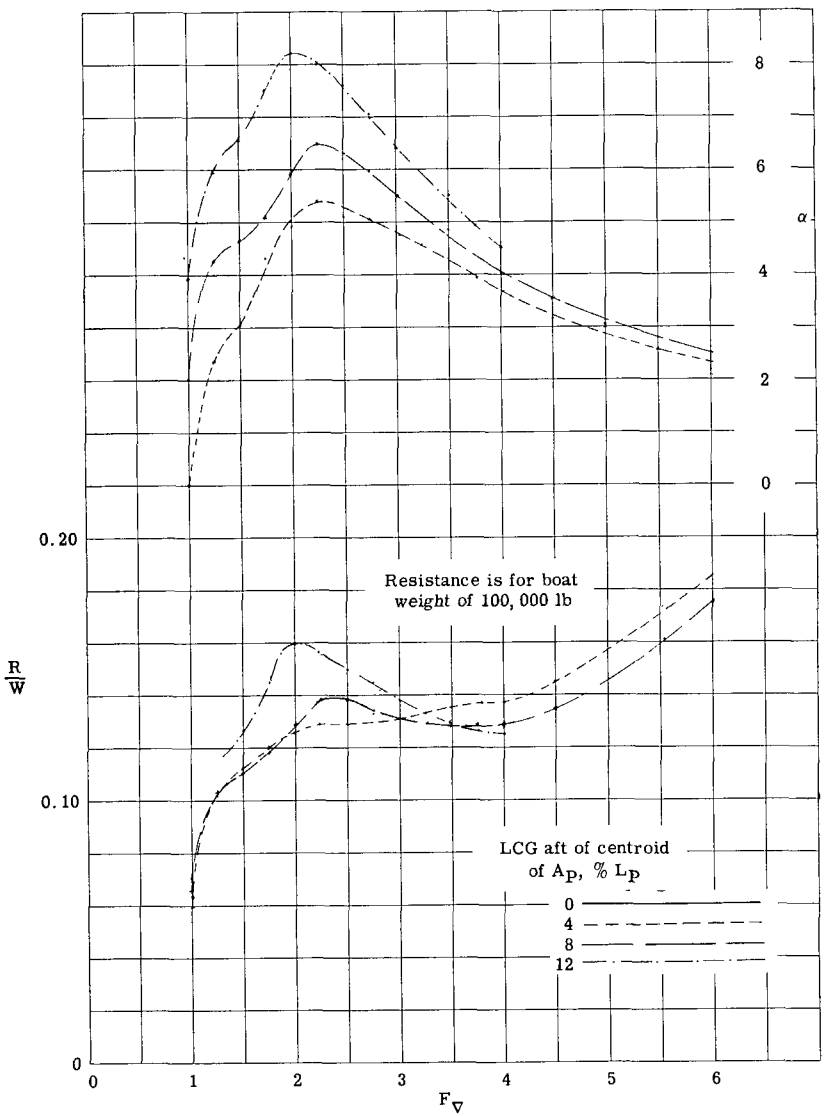

(a) $A_p/\nabla^{\frac{2}{3}} = 5.5$

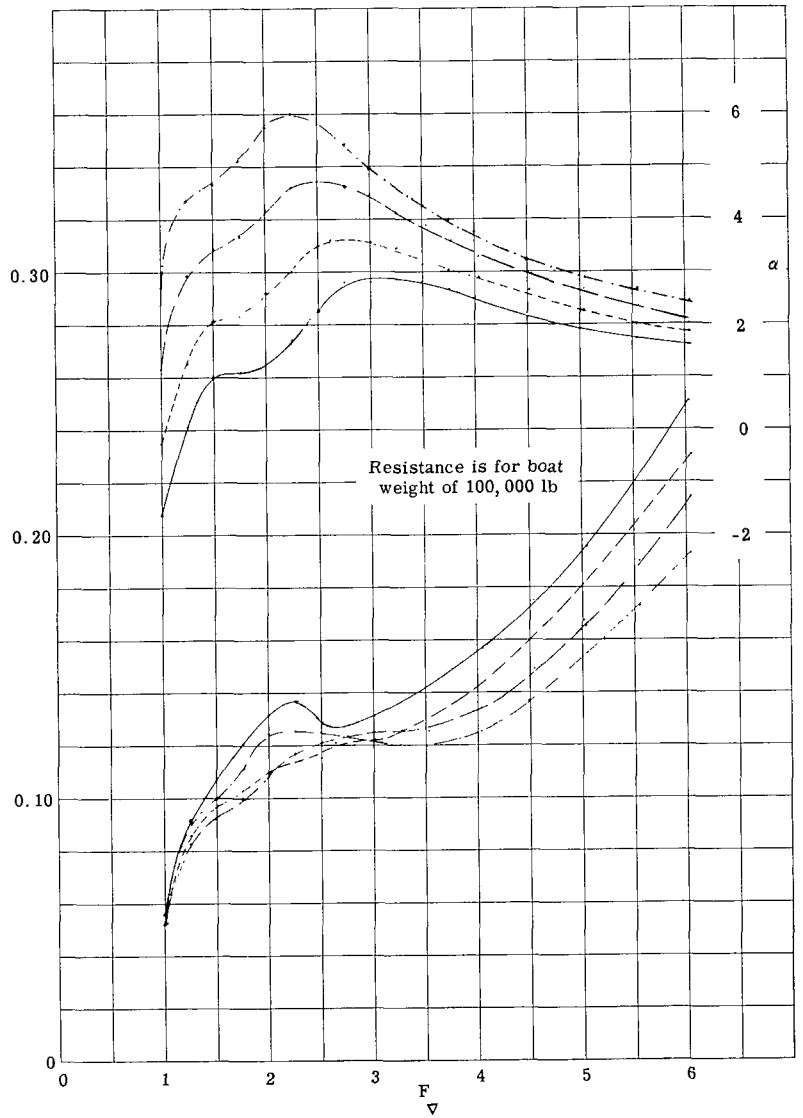

(b) $Ap/\nabla^{\frac{2}{3}} = 7.0$

Fig. 11 Resistance/weight ratio and angle of attack versus speed coefficient $L_P/B_{PX} = 4.09$

Fig. 11 Continued

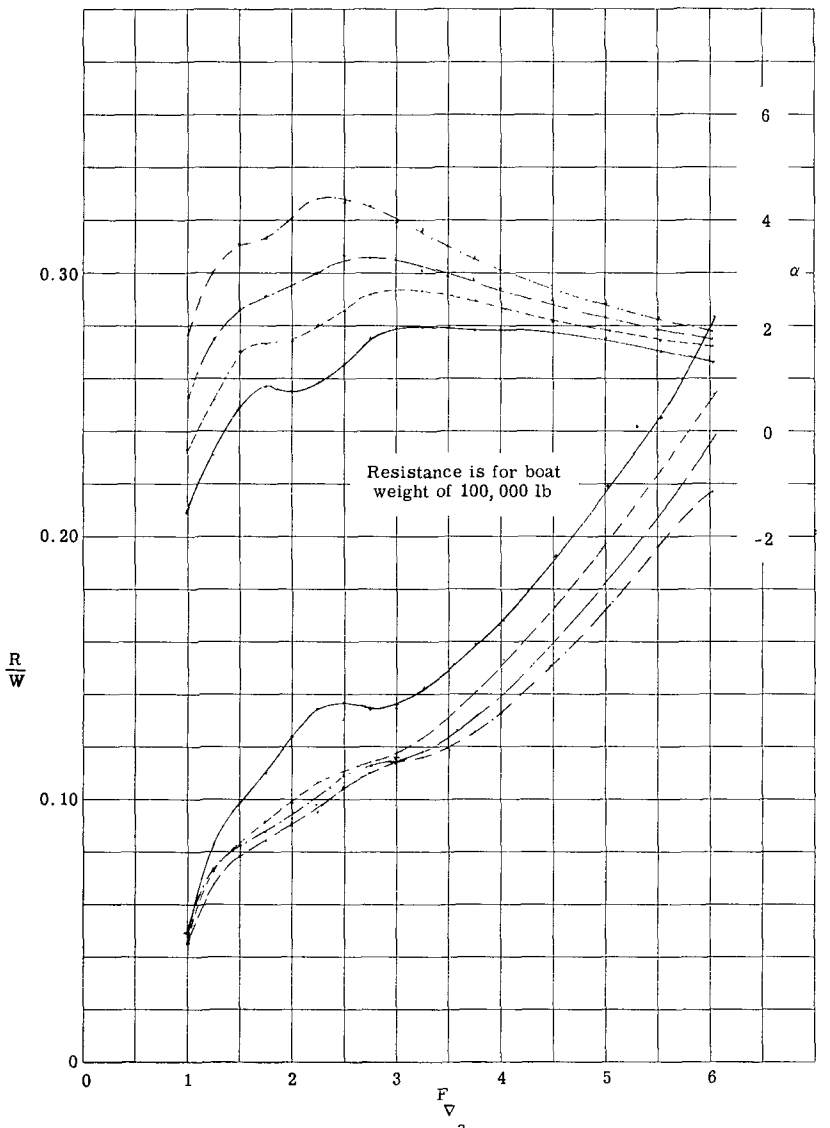

(c) $Ap/\nabla^{\frac{2}{3}} = 8.5$

Fig. 11 Concluded

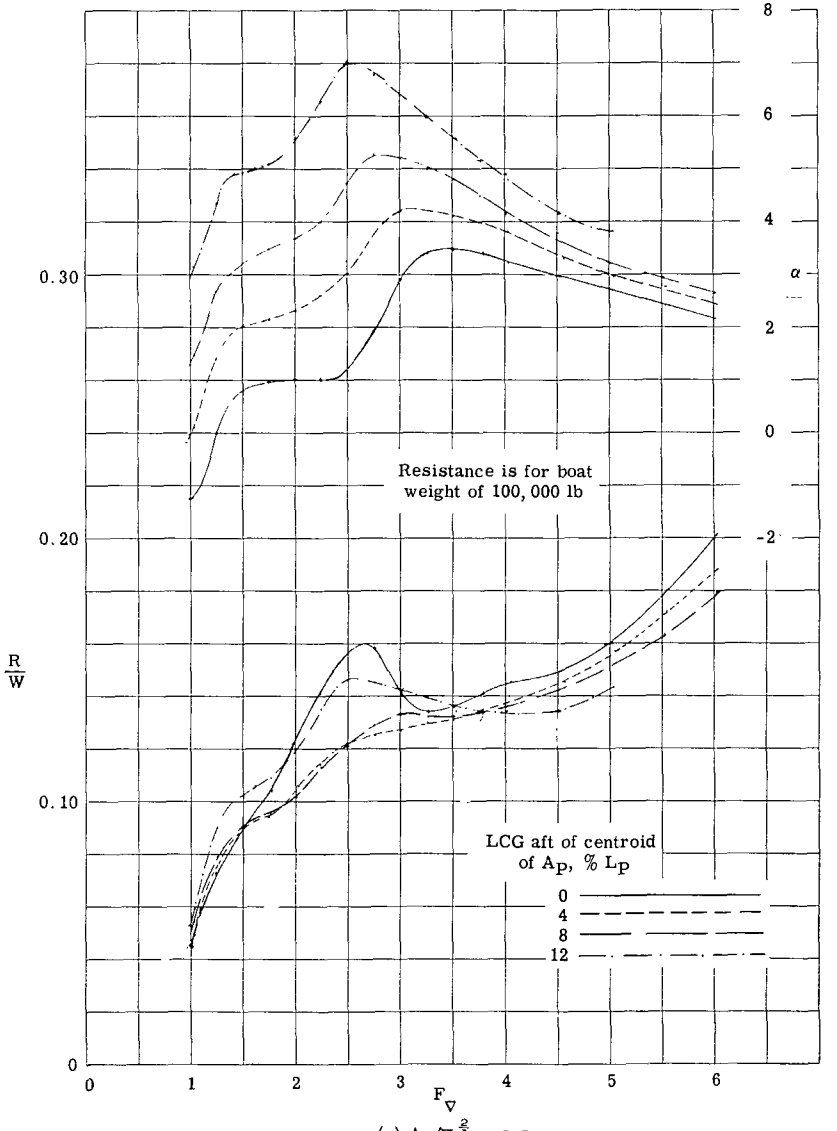

(a) $Ap/\nabla^{\frac{2}{3}} = 5.5$

Fig. 12 Resistance/weight ratio and angle of attack versus speed coefficient $L_P/B_{PX} = 5.50$

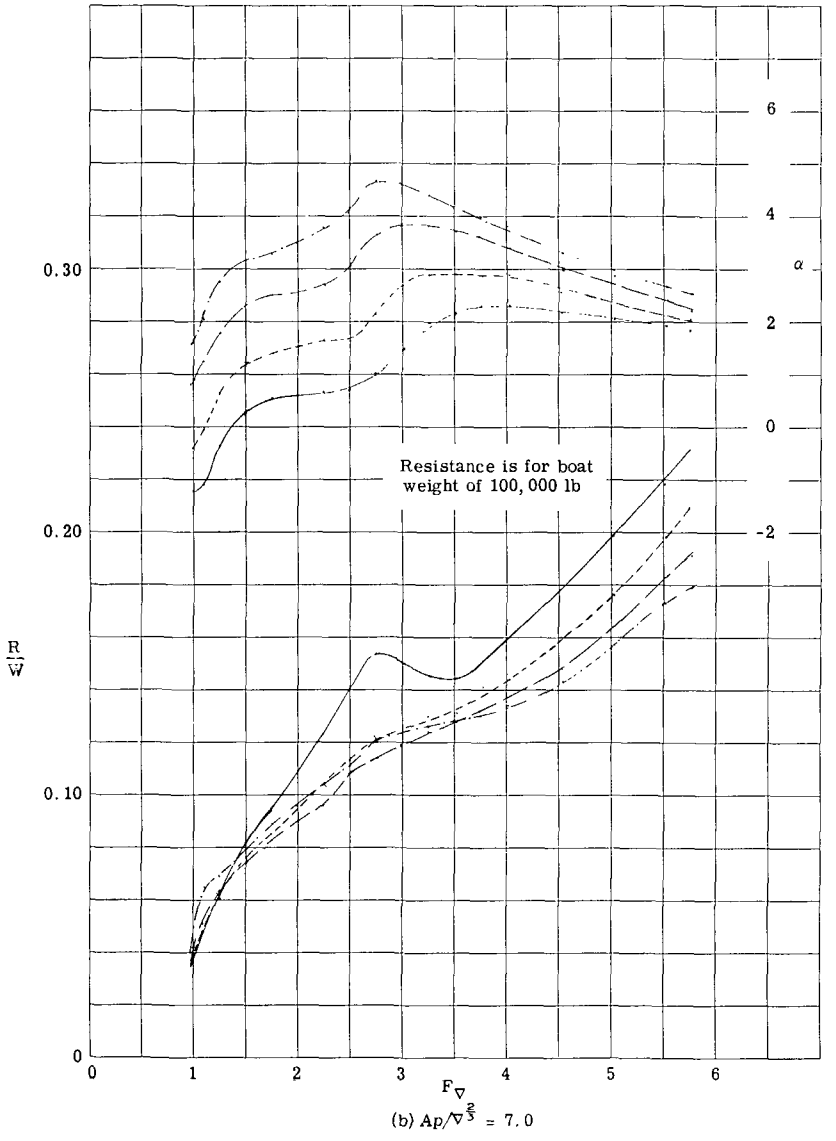

(b) $Ap/\nabla^{\frac{2}{3}} = 7.0$

Fig. 12 Continued

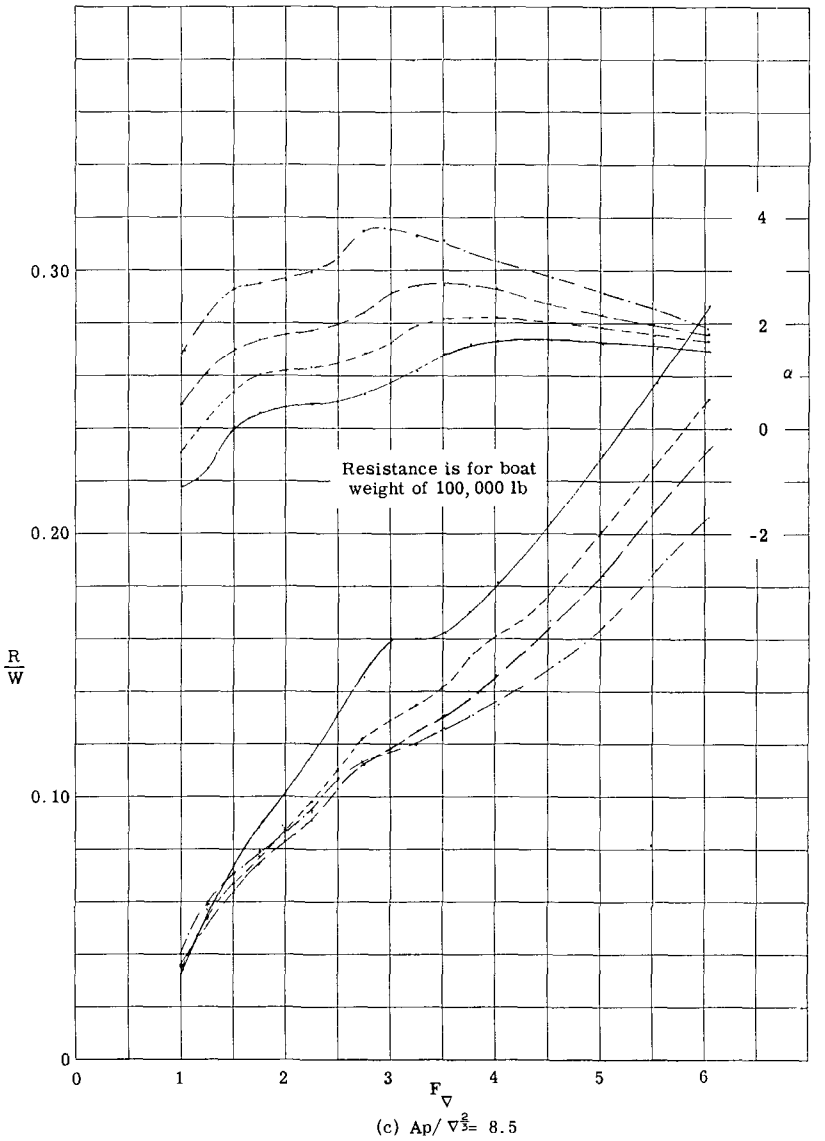

(c) $Ap/\nabla^{\frac{2}{3}} = 8.5$

Fig. 12 Concluded

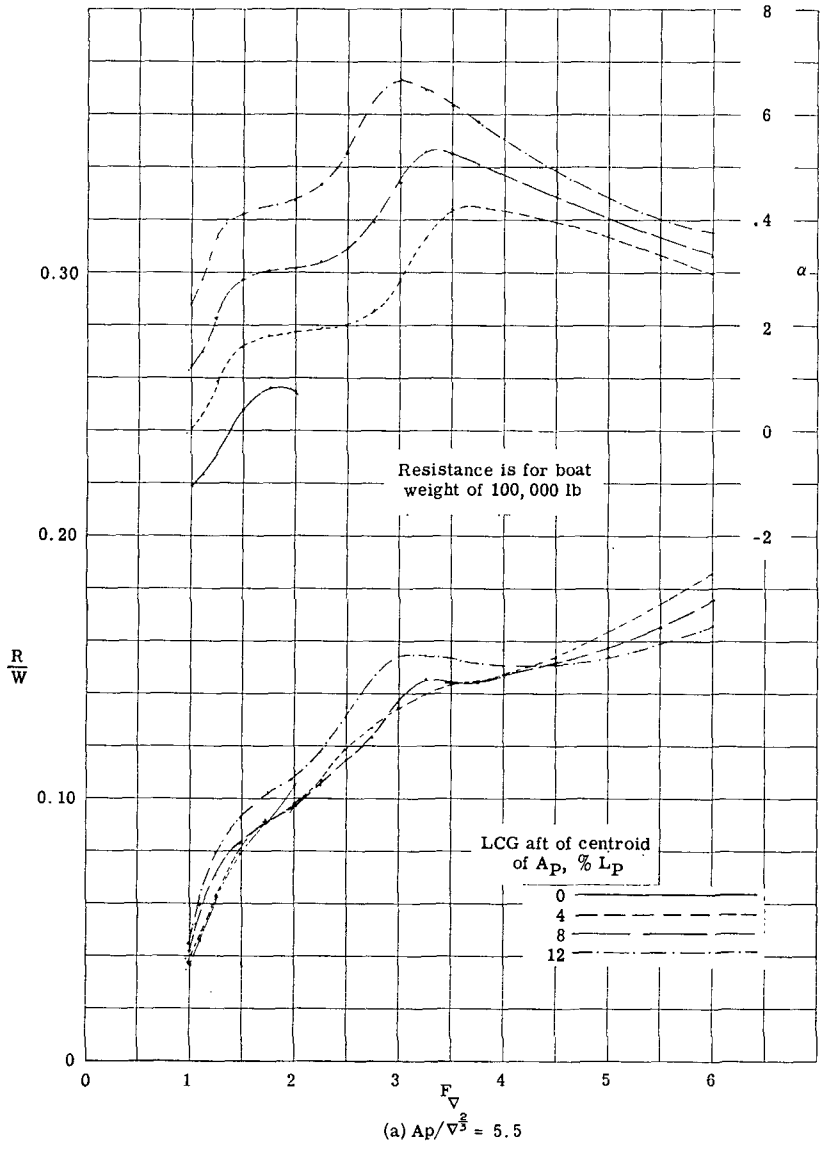

(a) $Ap/\nabla^{\frac{2}{3}} = 5.5$

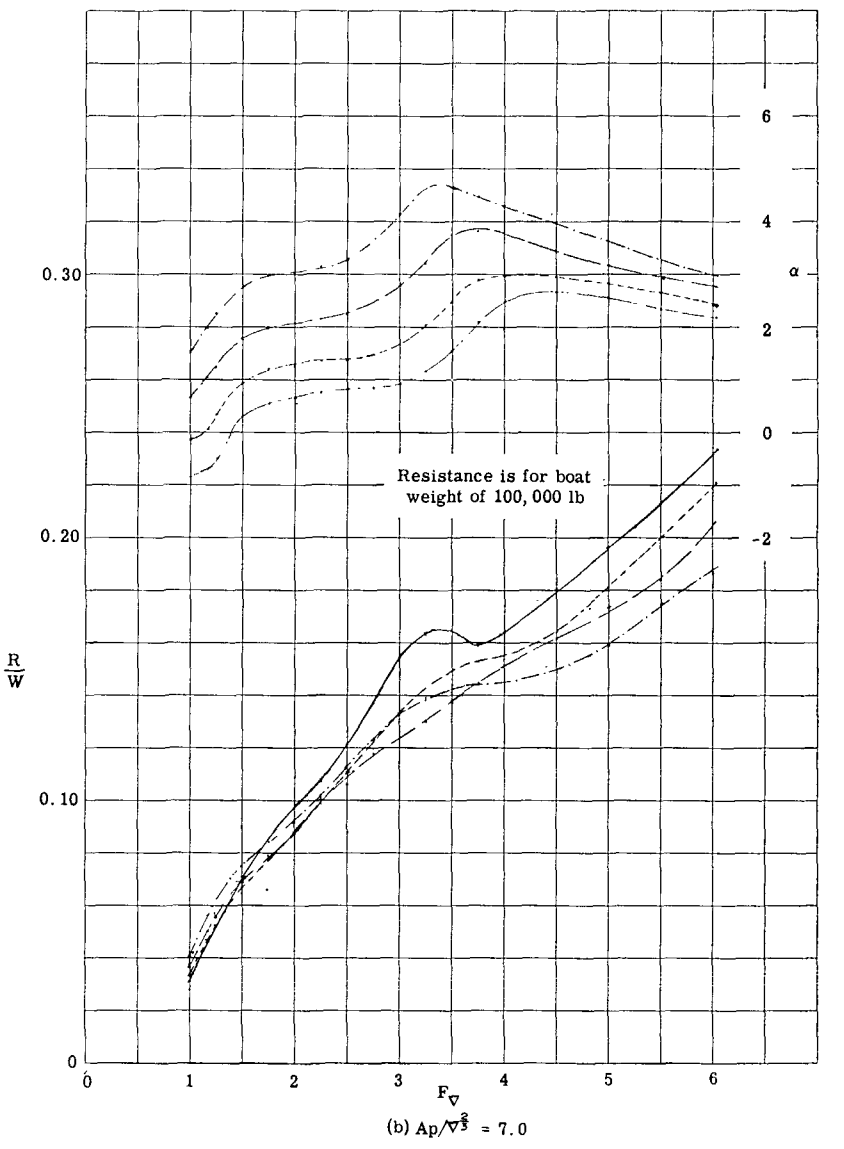

(b) $Ap/\nabla^{\frac{2}{3}} = 7.0$

Fig. 13 Resistance/weight ratio and angle of attack versus speed coefficient $L_P/B_{PX} = 7.00$

Fig. 13 Continued

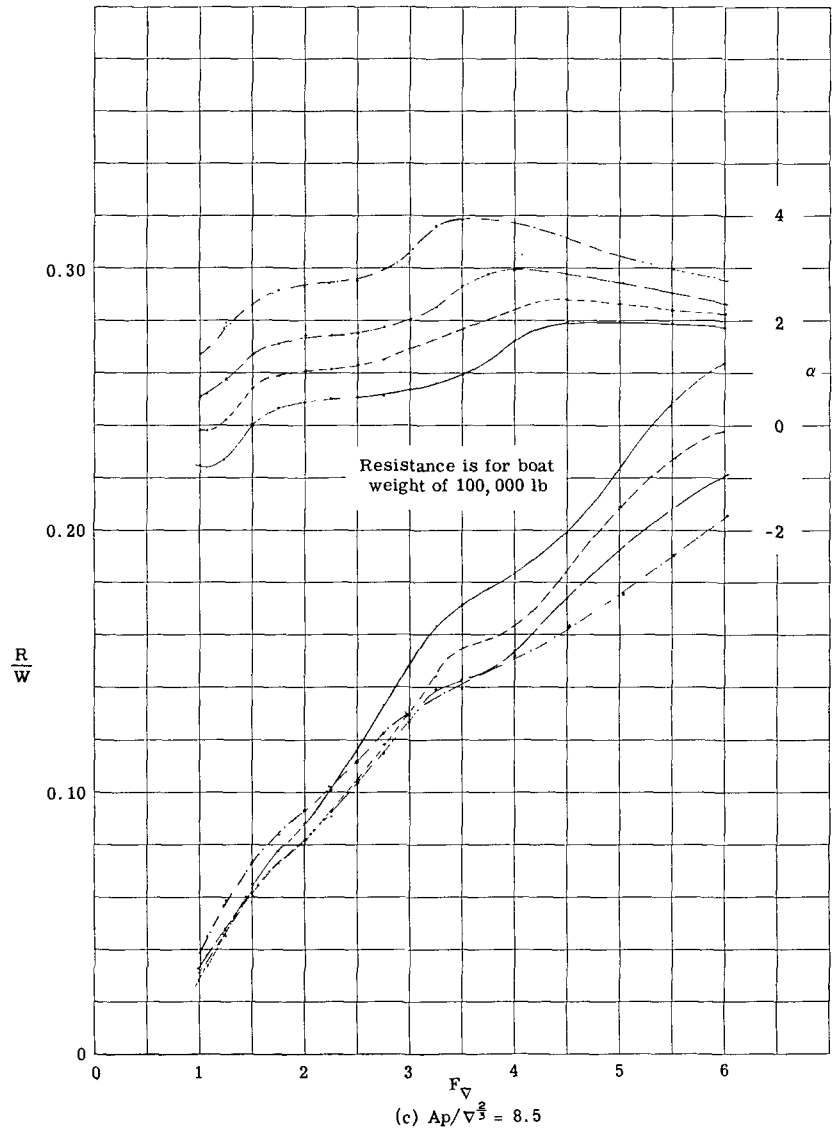

Fig. 13 Concluded

length to beam. The ratio of transom width to maximum chine width for the five models is given in Table 1. Table 1 also shows that the transom widths for Models 4665 and 4666 were selected so that the angle of the afterbody chine line in plan view would be the same as for the parent model (5 deg in each case). A check of the models of the series showed that the method of derivation had the desired effect of producing hull forms with developed surfaces.

Profiles of the bow and stern endings of the five models are shown in Fig. 4. The waterline shown for each model corresponds to the TMB standard test condition for planing hulls. Models 4667-1, 4668, and 4669 were each 8 ft long. However, Models 4665 and 4666 were made 4 ft and 6 ft long, respectively, to keep the model widths within the limits imposed by the carriage bay used for the tests. Spray strips were the only appendages fitted to the models. The shape of these strips is shown in Fig. 1. The ratio between spray-strip width and hull width was kept the same for all models of the series.

The values of $A_P/\nabla^{2/3}$ tested were 5.5, 7 and 8.5. The speed range was from F_∇ equals about 0.2 up to F_∇ equals 6.0. In addition, tests were made in the lower part of this speed range with an area coefficient $A_P/\nabla^{2/3}$ of 4. The LCG locations

were 0, 4, 8 and 12 percent L_P aft of the centroid. In general, all possible combinations were tested (a few conditions were found to be impractical) so that the planned program consisted of tests of each of the five models at sixteen different conditions for a total of 80 tests.

In order to provide a link with earlier work, each model was also tested at the TMB standard condition for planing craft. This condition corresponds to an area coefficient of 7 and to an LCG location at 6 percent L_P aft of the centroid. (This "standard condition" is discussed at some length in [3]).

Model Construction and Test Procedure

The parent model of the series was made of fiberglass and plastic so that it would be light enough for the self-propelled testing planned for the future. The remaining models were of wood. On each model, scales were marked along the keel, along one chine, and on one side of the transom for reading the solid-water wetted lengths on the bottom and the dimensions of the side area which was wetted at low speeds.

The models were tested in the high-speed basin at DTMB using Carriage 3. The high-speed basin is 20 ft wide and 2968 ft long, with a depth of 16 ft for the first 1800 ft (in the direction of travel for Carriage 3) and 10 ft for the remaining 1168 ft. Tests were made with one of the models of the series to determine the effect of the change in depth; this was found to be negligible.

Models 4666 through 4669 were considered to be of a size large enough to give accurate test results without the use of a device for stimulating turbulence. For Model 4665, the 4-ft model, trip wires 0.035 in. dia were fitted on each side of the stem as is shown in Fig. 4(*a*). Fig. 22 of reference [4] was used as a guide for the proper location of the turbulence-stimulation device.

The models were towed in the respective shaft lines indicated in Fig. 4. The shaft line for the parent model was located to correspond to a twin-shaft propulsion arrangement. For the other models, the depths of the shaft line at the various stations followed the same pattern of variation as the other body-plan dimensions and the shaft angle, accordingly, changed with change in length-beam ratio. The resistance recorded was the horizontal component of the towing force. Heave (rise) and pitch (change in trim angle) were recorded at each test speed. The intersections of the solid water with keel and chine and, at low speeds, the boundaries (at chine and transom) of the side wetted area were also recorded.

Results of Tests

The conditions at which the models were tested and the tabulated results of all the tests are given in the Appendix. The complete model test results are presented so that the user can extrapolate the data to any desired boat size. Photographs of the models underway are shown in Fig. 5.

The measured bottom wetted lengths are illustrated in Fig. 6 and tabulated in the Appendix. The principal wetted area to be taken into consideration in making the frictional-resistance correction for a planing boat is, of course, that part of the bottom area which is wetted by solid water, Fig. 6(*a*). The part of the bottom area which is wetted by spray is customarily neglected in making this correction. In the lower end of the speed range, a portion of the sides of a planing hull is also wetted and this area is illustrated in Fig. 6(*b*). This side wetted area is nearly triangular and, therefore, its magnitude can be approximated closely from the readings of the length and height of the wetted area on the scales marked on the side of the model. The values of the lengths and heights of the side wetted area have not been included in the tables in the Appendix, but in all cases this area has been added to the bottom area wetted by solid water to give the values of total wetted surface S which are shown in the tables. These total values are the ones used in making the frictional-resistance correction. The wetted length used for the calculation of Reynolds number is the arithmetic mean of the keel and chine wetted lengths given in the tables.

The resistance data of the series have been expanded to boat weights of 10,000 and 100,000 lb. The Schoenherr friction coefficients were used with zero roughness allowance. The heavier weight is representative of military planing craft, the lighter weight, of a medium-sized motor yacht. The resistance data for a boat weight of 100,000 lb are presented in Figs. 7 through 13 in the form of R/W versus F_∇. The angle of attack α of the planing bottom is also presented in each figure. Graphs of R/W versus F_∇ for a 10,000-lb boat weight are presented in Figs. 14 through 18.

Fig. 7 compares values of resistance and angle of attack for the five models of the series. The data are taken from tests at the Model Basin's standard condition for planing craft. It is interesting to note that the model with the next to the highest value of length-beam ratio has quite a low drag not only in the range of F_∇ below 3.0, but also in the high-speed region above a F_∇ of 5.0. At high speed less drag would be

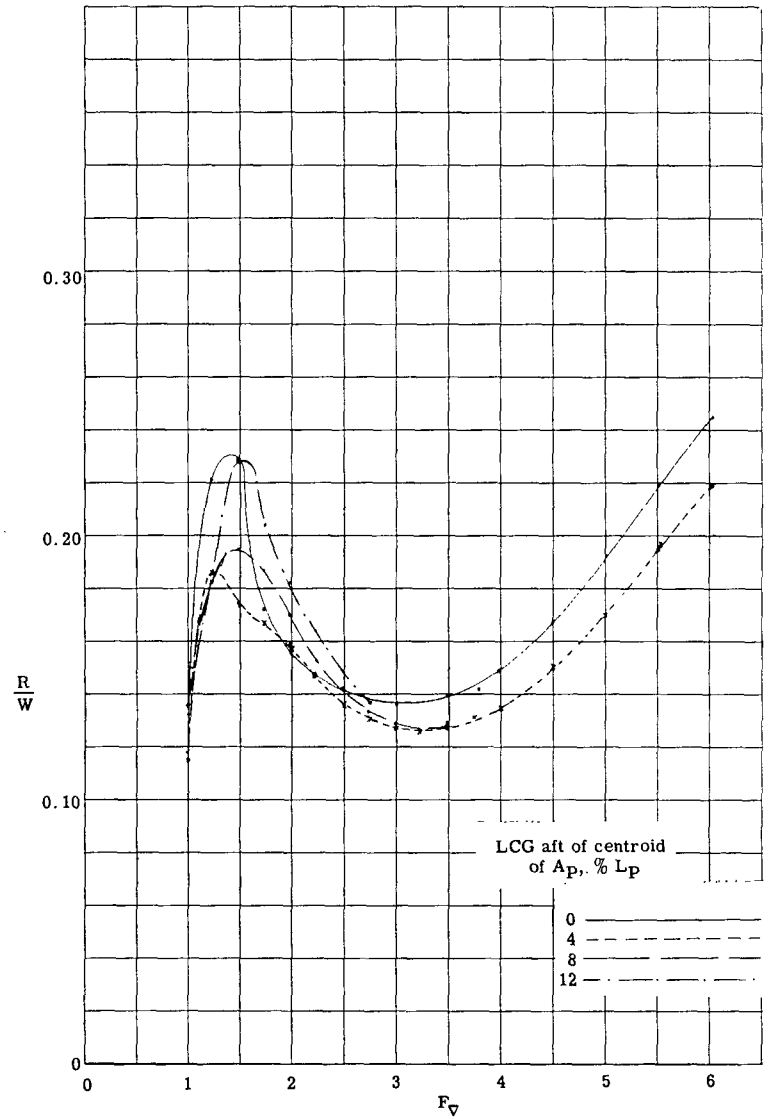

(a) $A_P/\nabla^{\frac{2}{3}} = 5.5$

Fig. 14 Resistance/weight ratio versus speed coefficient for a boat weight of 10,000 lb. $L_P/B_{PX} = 2.00$

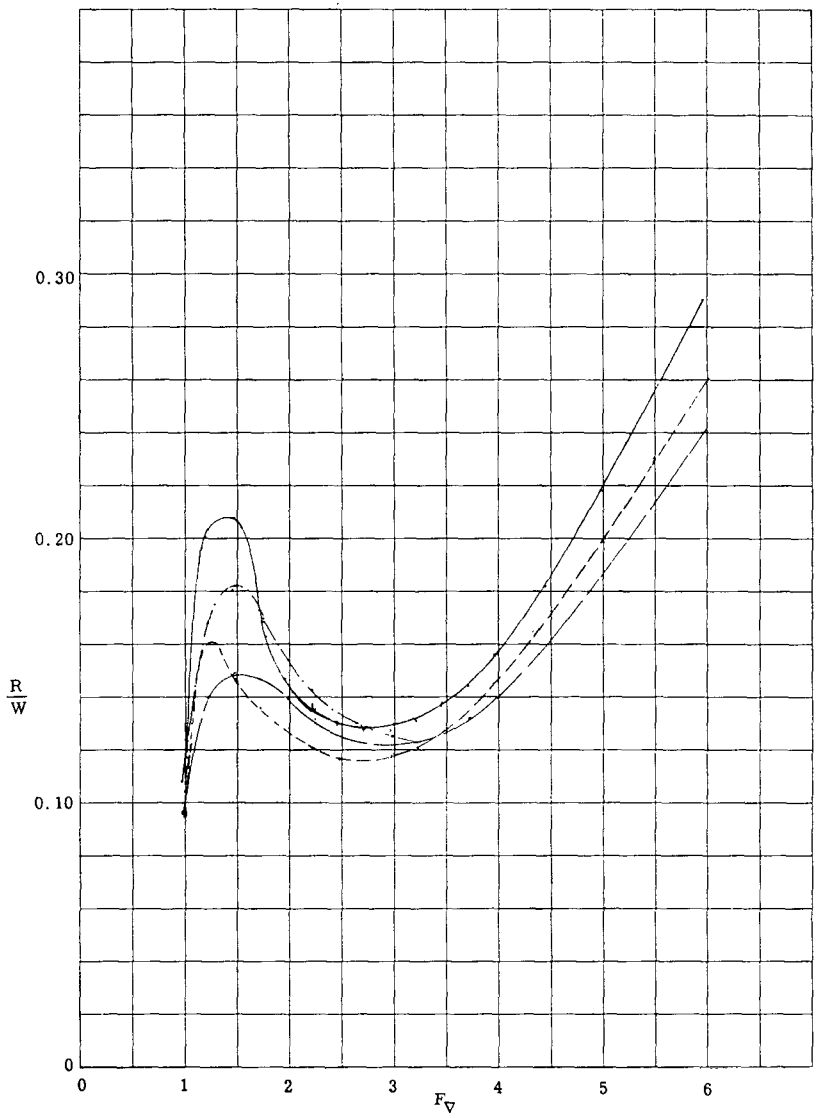

(b) $A_P/\nabla^{\frac{2}{3}} = 7.0$

Fig. 14 Continued

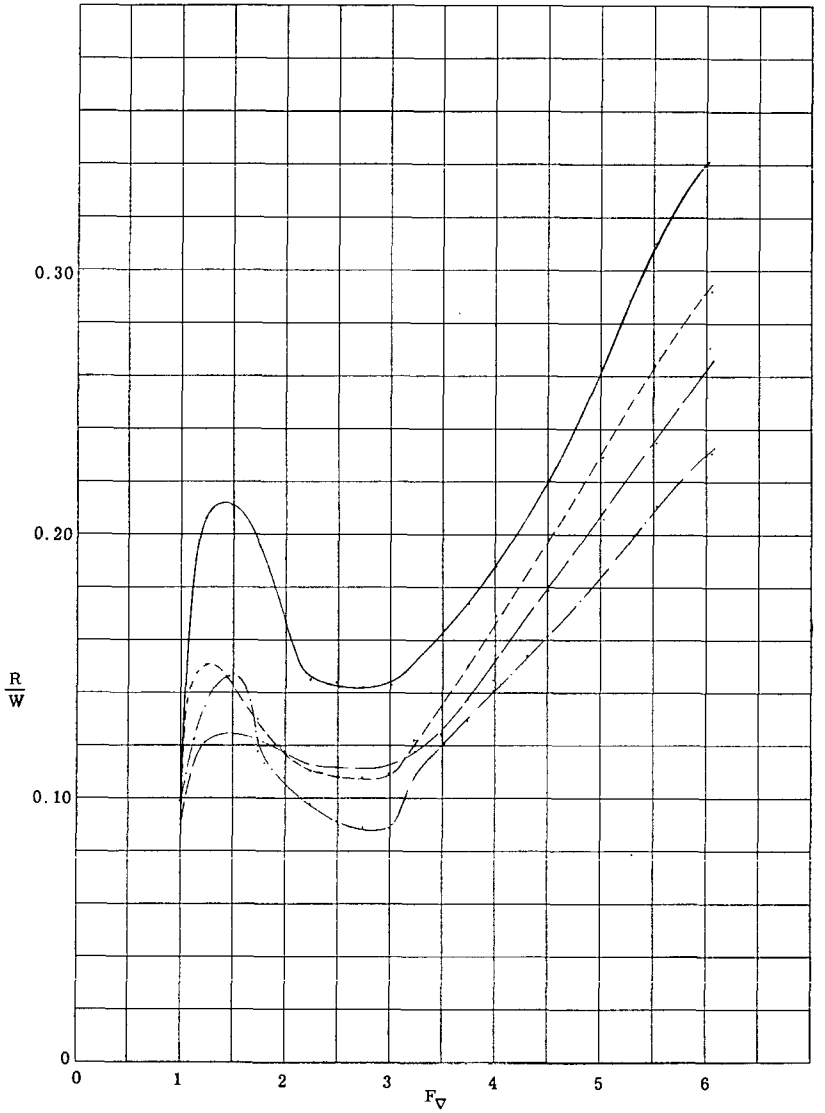

(c) $A_P/\nabla^{\frac{2}{3}} = 8.5$

Fig. 14 Concluded

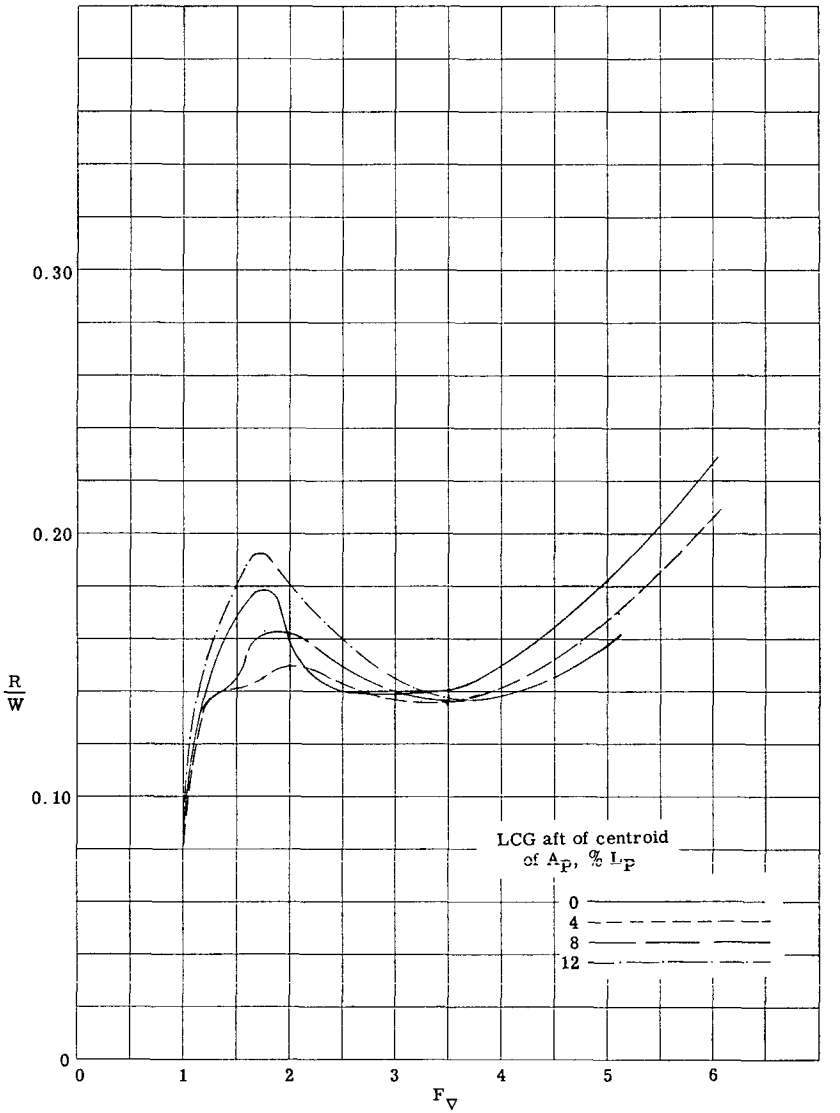

(a) $A_P/\nabla^{\frac{2}{3}} = 5.5$

Fig. 15 Resistance/weight ratio versus speed coefficient for a boat weight of 10,000 lb. $L_P/B_{PX} = 3.06$

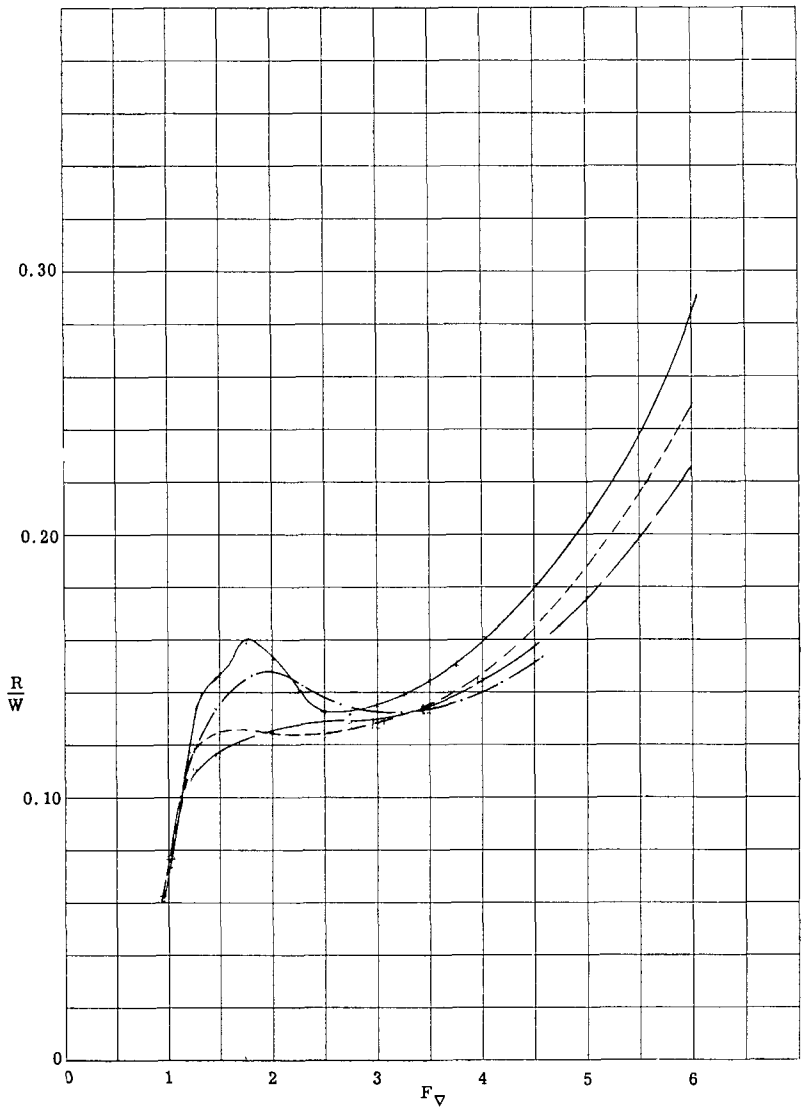

(b) $A_p/\nabla^{\frac{2}{3}} = 7.0$

Fig. 15 Continued

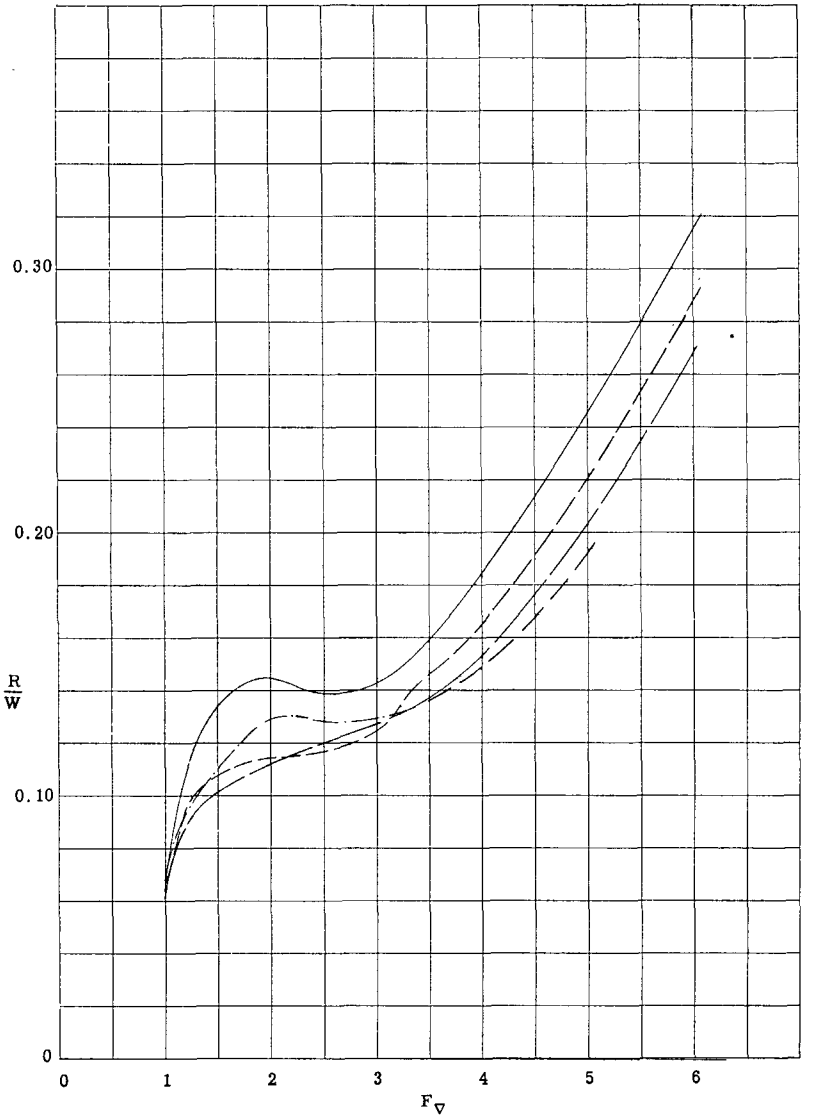

(c) $A_p/\nabla^{\frac{2}{3}} = 8.5$

Fig. 15 Concluded

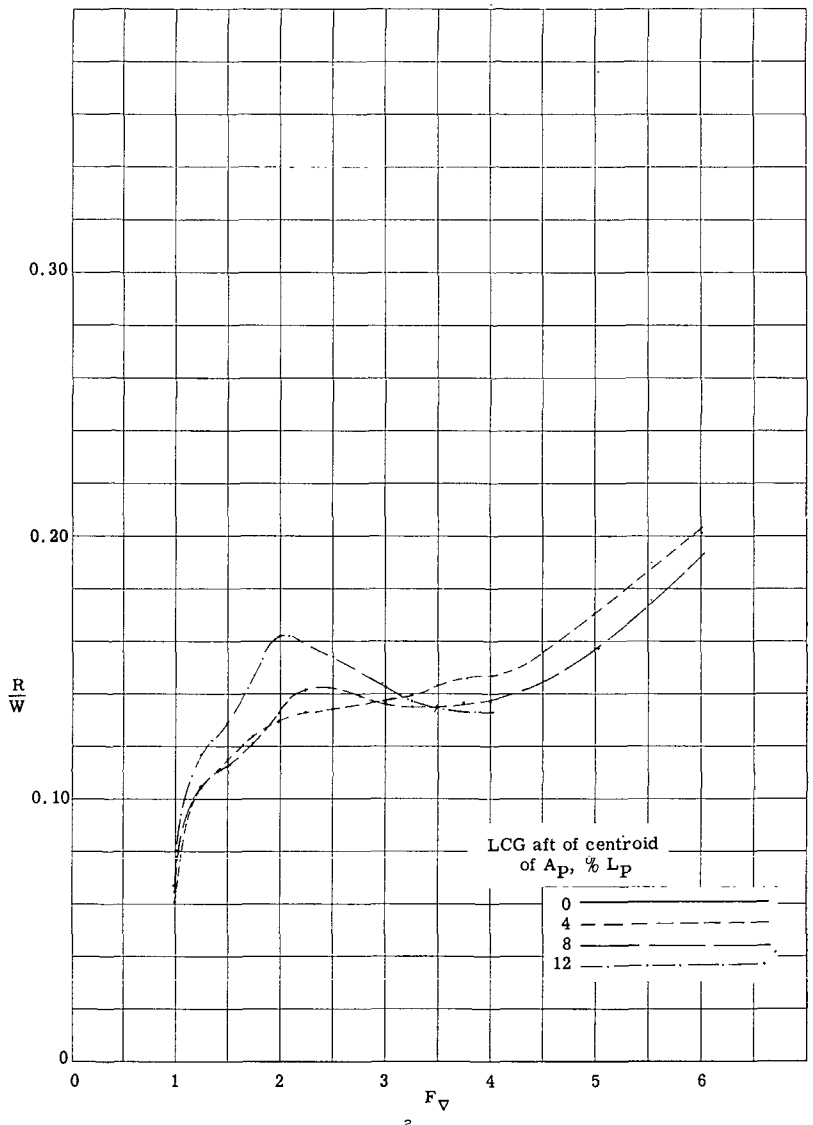

(a) $A_P/\nabla^{\frac{2}{3}} = 5.5$

Fig. 16 Resistance/weight ratio versus speed coefficient for a boat weight of 10,000 lb. $L_P/B_{PX} = 4.09$

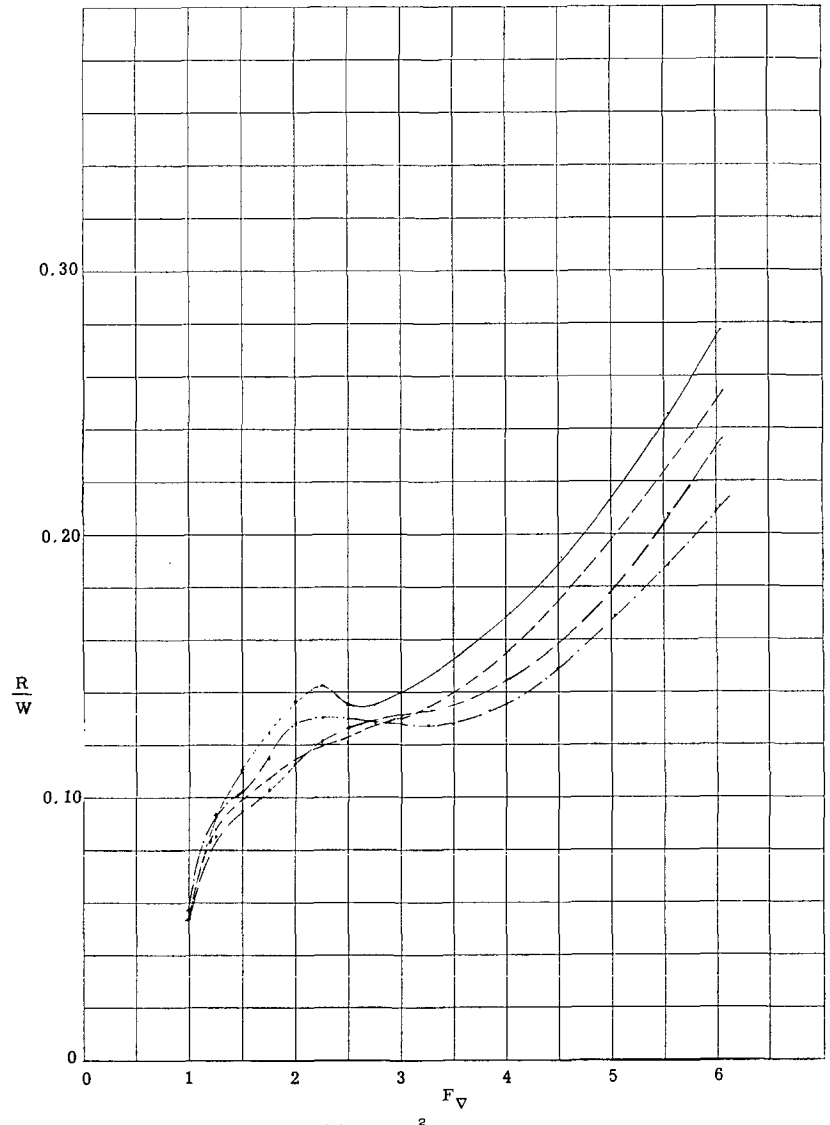

(b) $A_P/\nabla^{\frac{2}{3}} = 7.0$

Fig. 16 Continued

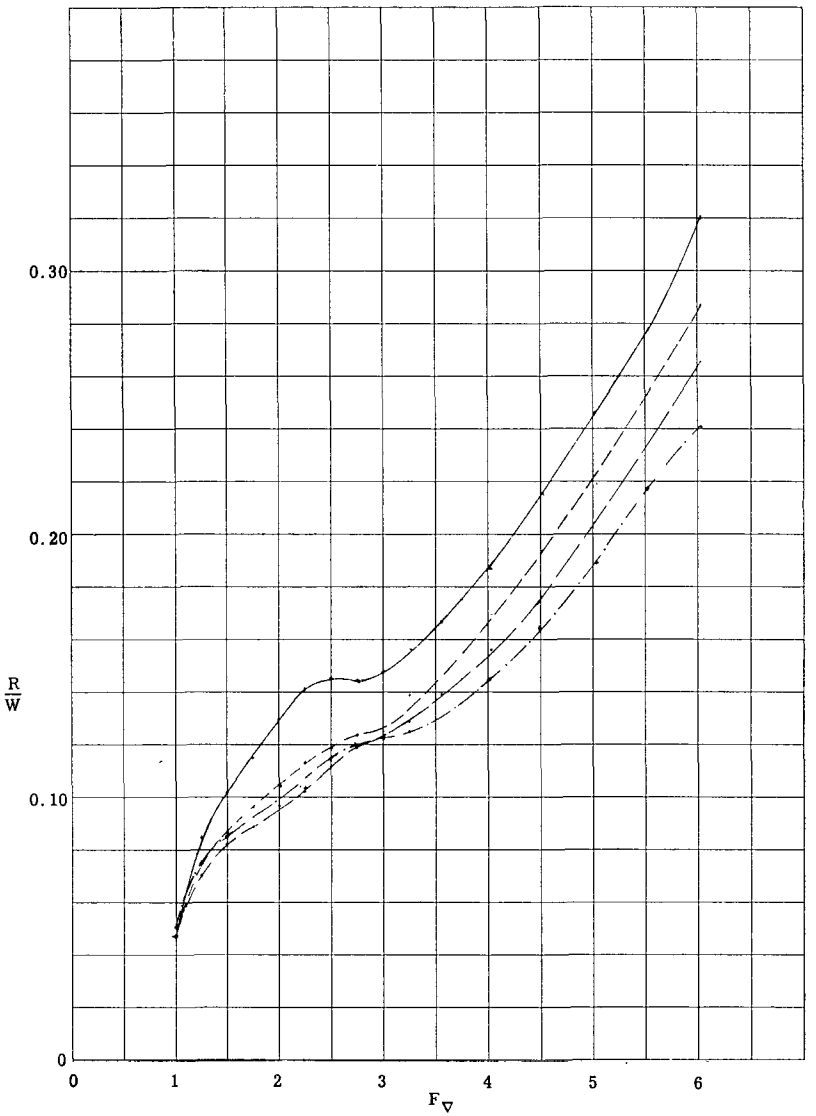

(c) $A_P/\nabla^{\frac{2}{3}} = 8.5$

Fig. 16 Concluded

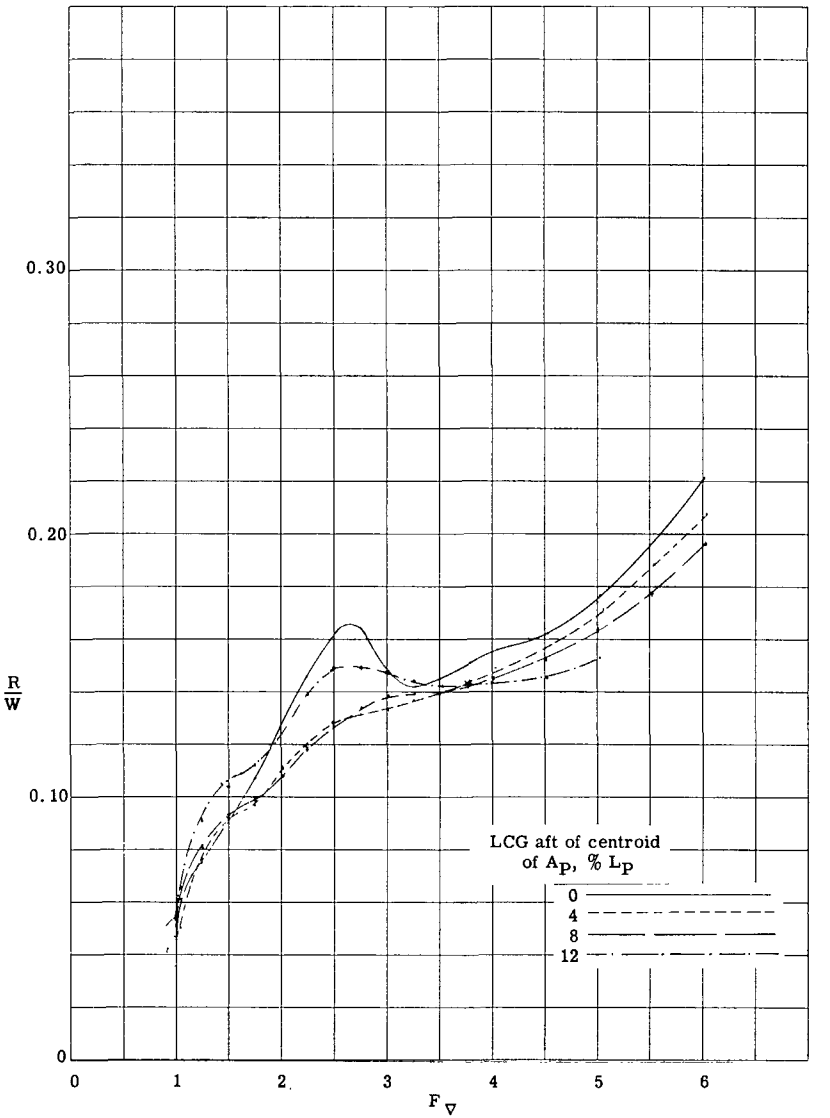

(a) $A_P/\nabla^{\frac{2}{3}} = 5.5$

Fig. 17 Resistance/weight ratio versus speed coefficient for a boat weight of 10,000 lb. $L_P/B_{PX} = 5.50$

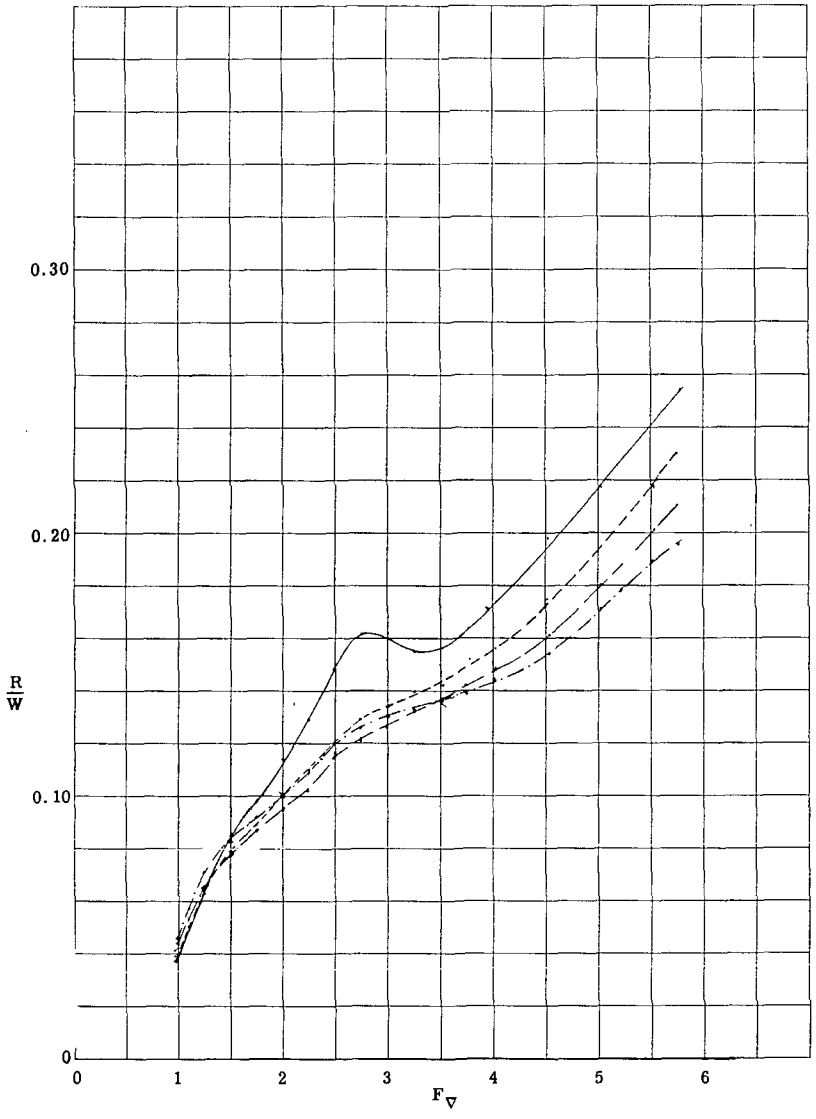

(b) $A_p/\nabla^{\frac{2}{3}} = 7.0$

Fig. 17 Continued

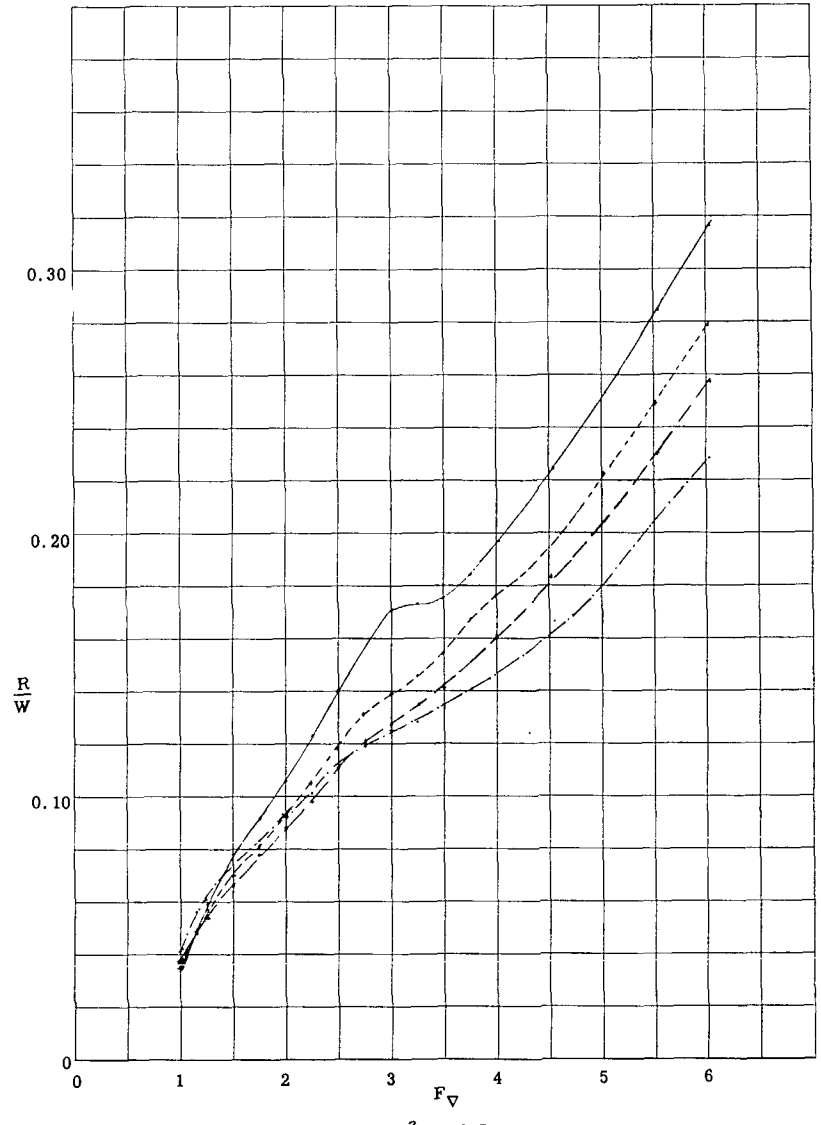

(c) $A_p/\nabla^{\frac{2}{3}} = 8.5$

Fig. 17 Concluded

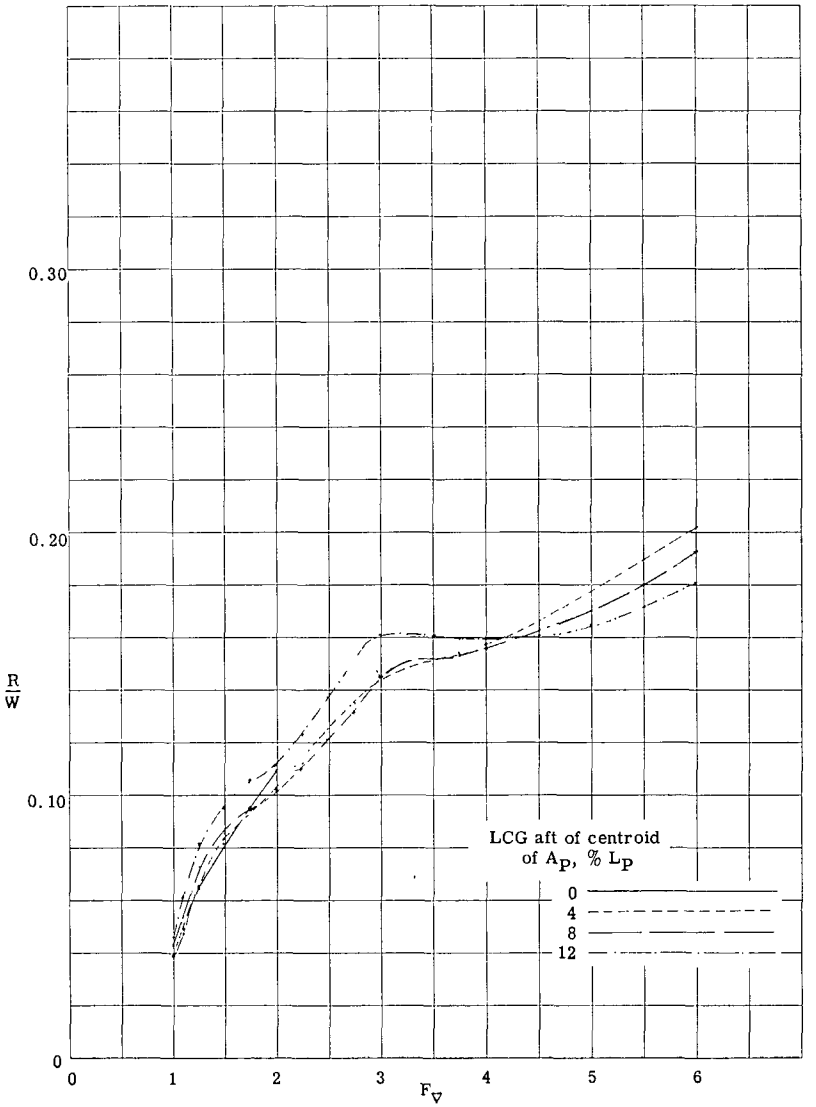

(a) $A_P/\nabla^{\frac{2}{3}} = 5.5$

Fig. 18 Resistance/weight ratio versus speed coefficient for a boat weight of 10,000 lb. $L_P/B_{PX} = 7.00$

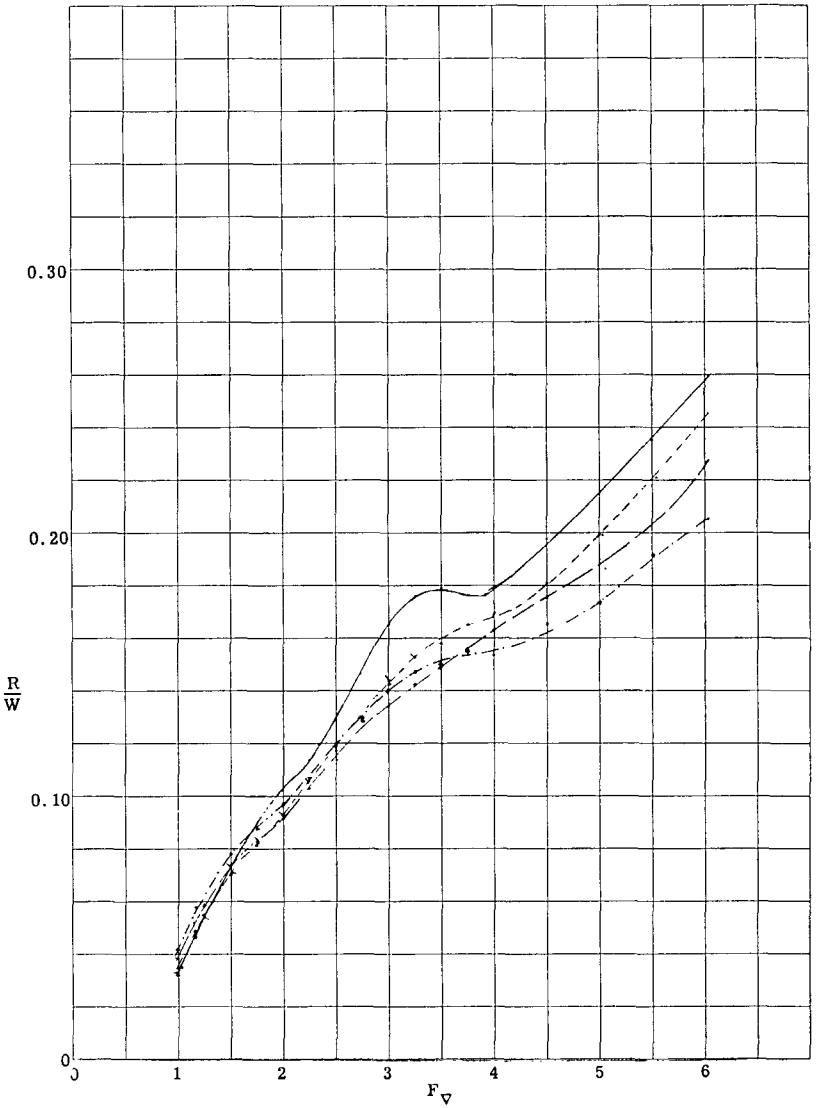

(b) $A_P/\nabla^{\frac{2}{3}} = 7.0$

Fig. 18 Continued

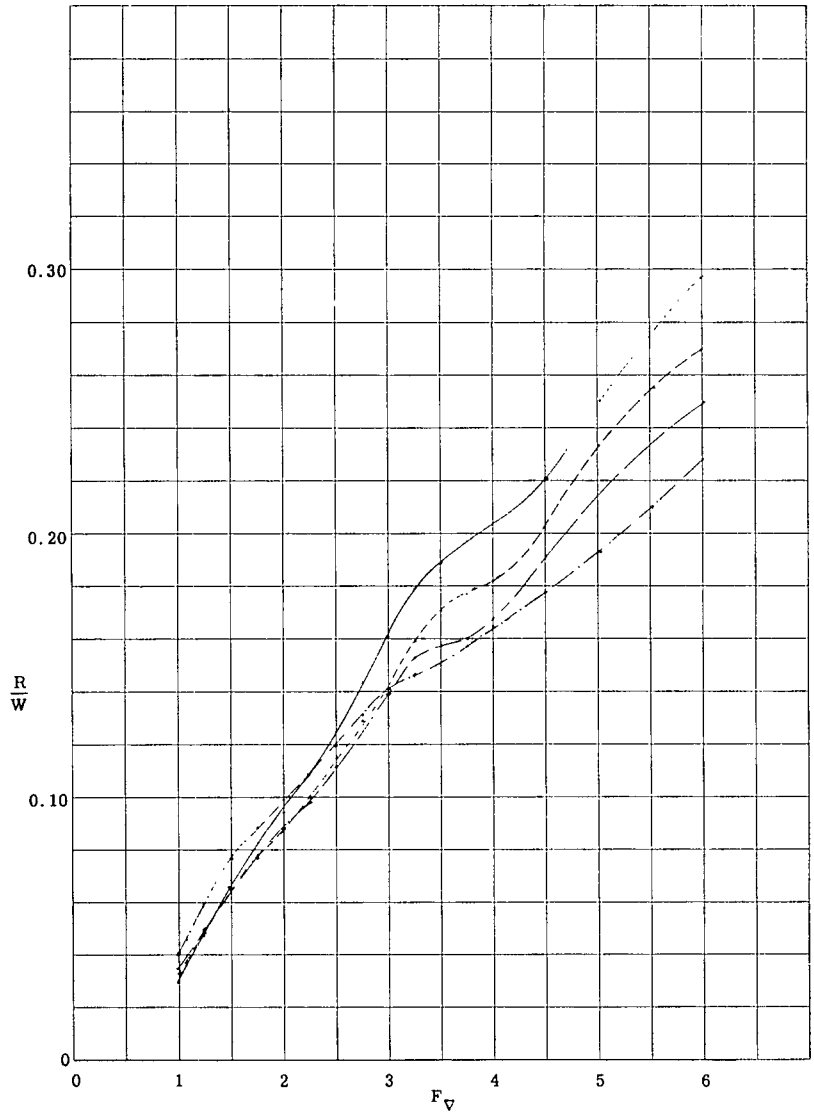

(c) $A_p/\nabla^{\frac{2}{3}} = 8.5$

Fig. 18 Concluded

expected for a short, wide hull than for a long, narrow hull because of the higher aspect ratio of the former. The fact that some contrary results were obtained is believed to be attributable to the lower aerodynamic drag of the narrow hulls.

In Fig. 8 the data in Fig. 7 have been cross-plotted against length-beam ratio. Resistance values from model tests of other representative planing-boat designs are also included in Fig. 8 in order to compare their performance with that of the series. At low speeds (below a F_∇ of 1.5), the hull forms of the series have slightly more drag than the other designs. At values of F_∇ of 2.0 and 2.5, the forms of the series have less drag than most of the other designs, and at values of F_∇ of 3.0 and above, the hull forms of the series have less drag than any of the other designs.

Figs. 9 through 13, and also Figs. 14 through 18, are arranged in order of increasing length-beam ratio, so that the data for Model 4665 appear first. Three graphs, which correspond to three values of area coefficient, are shown for each model. The four sets of curves on each graph correspond to the four values of LCG location which were investigated.

A number of facts are evident from Figs. 9 through 13 (or from Figs. 14 through 18): A length-beam ratio of 2 is impracticably low be-

$A_P/\nabla^{2/3}$	Symbol
5.5	
7.0	
8.5	

Model No.	L_P/B_{PA}
4665	2.365
4666	3.69
4667-1	5.00
4668	6.72
4669	8.56

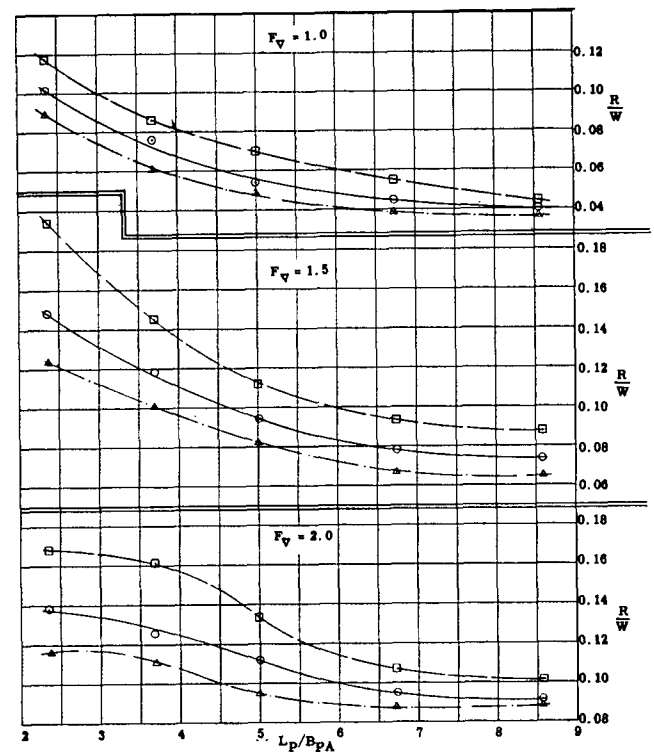

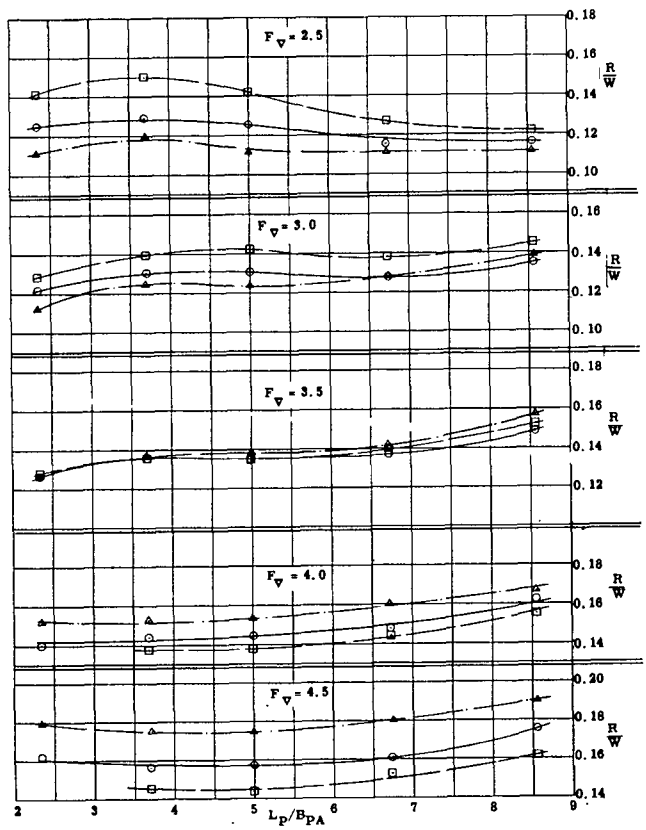

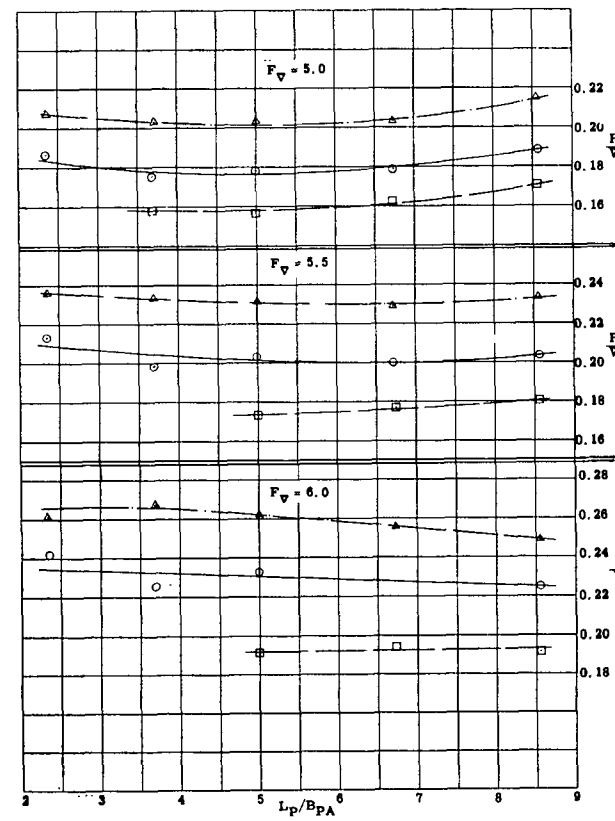

Fig. 19 Resistance/weight ratio versus length/beam (L_P/B_{PX}). 10,000 lb boat weight. LCG at 8 percent L_P aft of centroid of A_P

cause of the extreme hump in the drag curve. An LCG location at the centroid of the projected chine area (0 percent L_P aft of the centroid) is too far forward because the drag is consistently high throughout the speed range. At an area coefficient of 5.5 (which corresponds to a heavily loaded condition), an LCG location at 12 percent L_P aft of the centroid produces a pronounced hump in both the drag and trim curves and, therefore, this LCG location is too far aft. The graphs also indicate that for most of the range covered by the tests of this series, an LCG location between 4 and 8 percent L_P aft of the centroid will give good performance. However, the aftermost LCG location tested (12 percent) will always give the least drag at high speeds.

Resistance data from the tests of the different models, for one of the LCG locations investigated (8 percent L_P aft of the centroid), are cross-plotted against length-beam ratio in Fig. 19. This figure indicates a satisfactory consistency for the data from the different models. The figure also shows that for values of F_∇ below 3.5, a large hull (high value of area coefficient) will carry a given gross weight with the least resistance, whereas at values of F_∇ above 3.5, a small hull (low value of area coefficient) will give the least resistance for a boat of given gross weight.

For some of the tests of the series the models porpoised before the maximum intended speed ($F_\nabla = 6$) was obtained. Porpoising is defined here to be the combined oscillation in pitch and heave which increases in amplitude with time at a constant speed of the model. For those tests in which porpoising occurred the recording of resistance, and so on, was necessarily confined to speeds below that at which porpoising began. Since the conditions which produce porpoising are of interest, an attempt was made to define the porpoising limit for the various models and test conditions. Accordingly, the speeds for inception of porpoising were determined for the various conditions of loading and LCG location by towing each model at gradually increasing small increments of speed until the model was observed to become unstable. For the most part, this work was done with Models 4665 and 4666, since these were the models which exhibited most of the porpoising instability for the test conditions of the series. Since porpoising is a dynamic phenomenon, it was considered at first that the moment of inertia of the models was a factor to be considered. Reference [5] indicates, however, that the moment of inertia does not affect the speed for the inception of porpoising of a planing hull, although it does affect the amplitude and frequency of the oscillation. Therefore the moment of inertia was not determined or closely controlled for the tests at the different weights and LCG locations.

The experimental values of the conditions corresponding to the inception of porpoising tended to collapse into a single curve when plotted in the form of $C_{Lb}/(l_{cp}/b)$ versus F_∇. This plot is shown in Fig. 20, where the solid symbols correspond to the conditions at inception of porpoising. Some of the scatter is a result of the judgment involved in determining the point of porpoising inception. In order to obtain additional verification of the reliability of this line as a stability limit, selected points corresponding to stable operation at high speed for all five models were plotted on this figure using open symbols. These stable data points generally fell below the line defined by the porpoising-inception points and therefore, they tend to verify the validity of the line as a stability limit. The curve of the stability limit can be represented by the equation

$$\frac{C_{Lb}}{l_{cp}/b} = \frac{1.80}{(F_\nabla)^{2.5}}$$

A need has been expressed for additional data on the resistance of hydrofoil boat hulls in the low-speed hullborne condition. Data on the resistance of heavily loaded amphibious craft are also needed. These additional data are necessary because previous tests of planing-boat models usually have not included measurements of test data at low speeds. Therefore, during the tests of this series, data were recorded at closely spaced increments of speed below a value of $F_\nabla = 1.0$ in order to define carefully the low-speed drag. Resistance and angle-of-attack data for this low-speed range are presented in Figs. 21 through 25. The resistance data have been corrected to a boat weight of 100,000 lb.

Simplified Prediction Method

The complete model test results are presented in the Appendix so that the resistance of a boat of any size can be calculated from the results of any test. Accordingly, in those cases for which a projected new design corresponds closely enough to one of the tests of this series, the tabulated data can be used to predict the resistance of that particular boat. However, the spacing of the parameters investigated in the present study was quite wide, and therefore it will more generally be found that the values of length-beam ratio, area coefficient, and LCG location for a projected new design fall in between the values investigated.

Let us assume, for example, that the values selected for a projected new design are a weight of

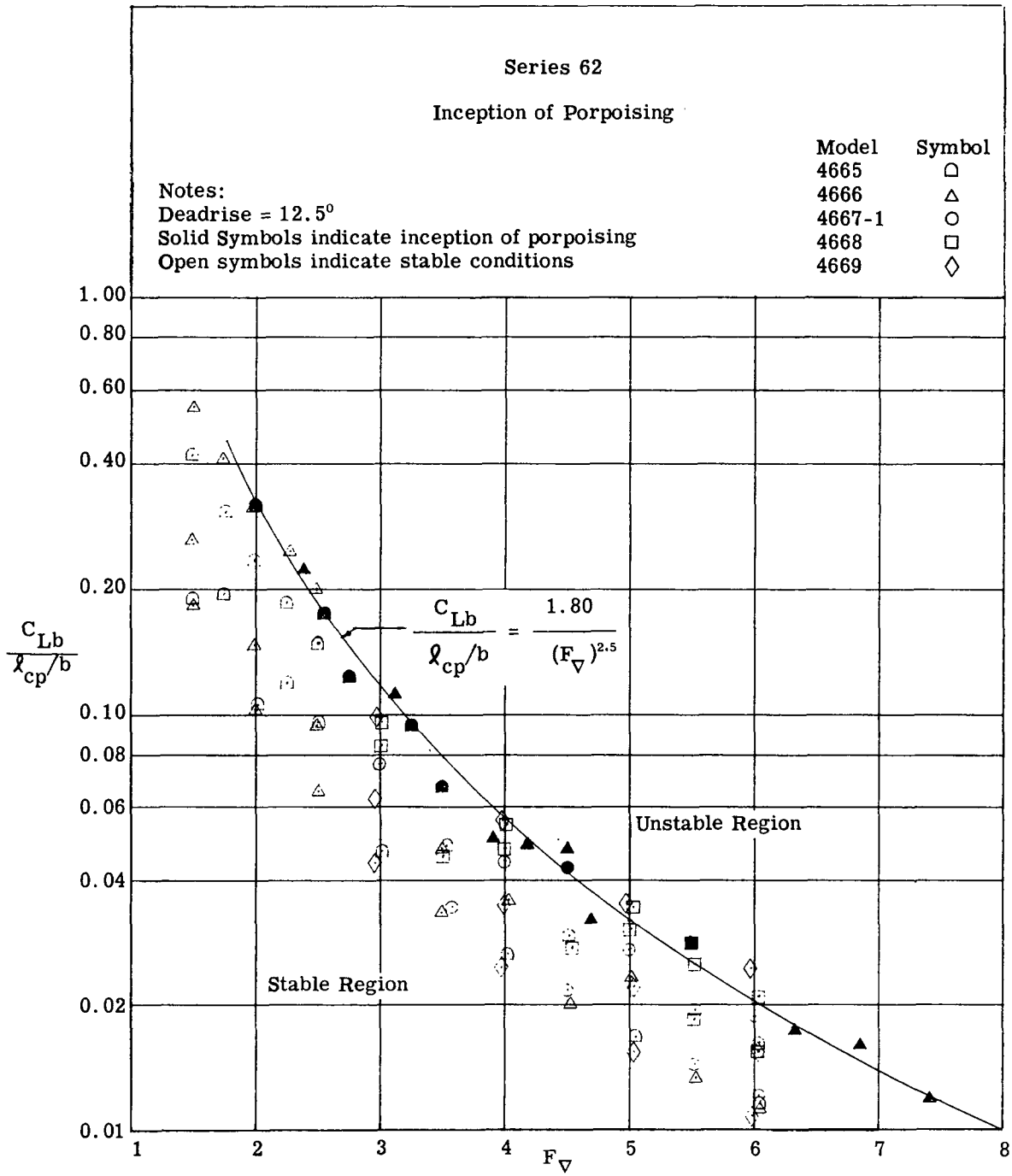

Fig. 20 Inception of porpoising for models of series 62

15,000 lb, a ratio of chine length to maximum chine beam of 3.5, and an area coefficient of 6.5. The data from the series have indicated that for most purposes the LCG location should fall into the relatively narrow range of from 4 to 8 percent L_P aft of the centroid. Therefore it seems reasonable to simplify the present hypothetical design problem by assuming that the LCG location is to be at 8 percent L_P aft of the centroid (this LCG location was one of those investigated extensively during this series). Even with this simplifying assumption, the process of developing an accurate

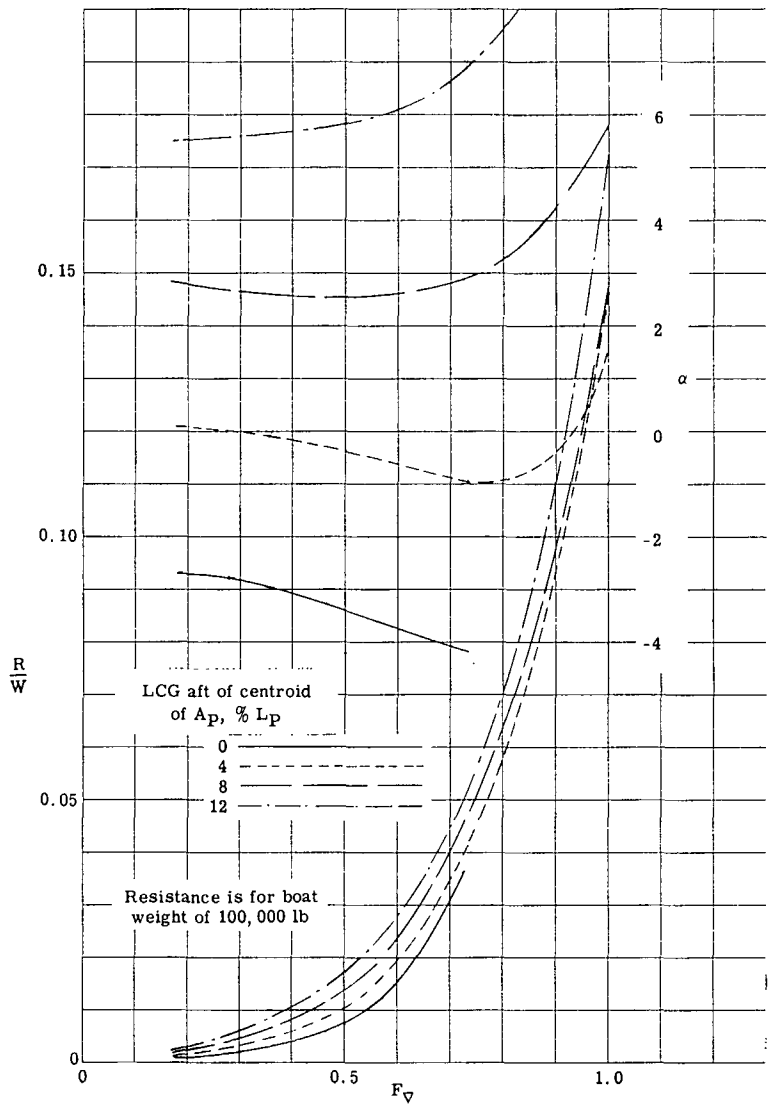

(a) $A_P/\nabla^{\frac{2}{3}} = 4.0$

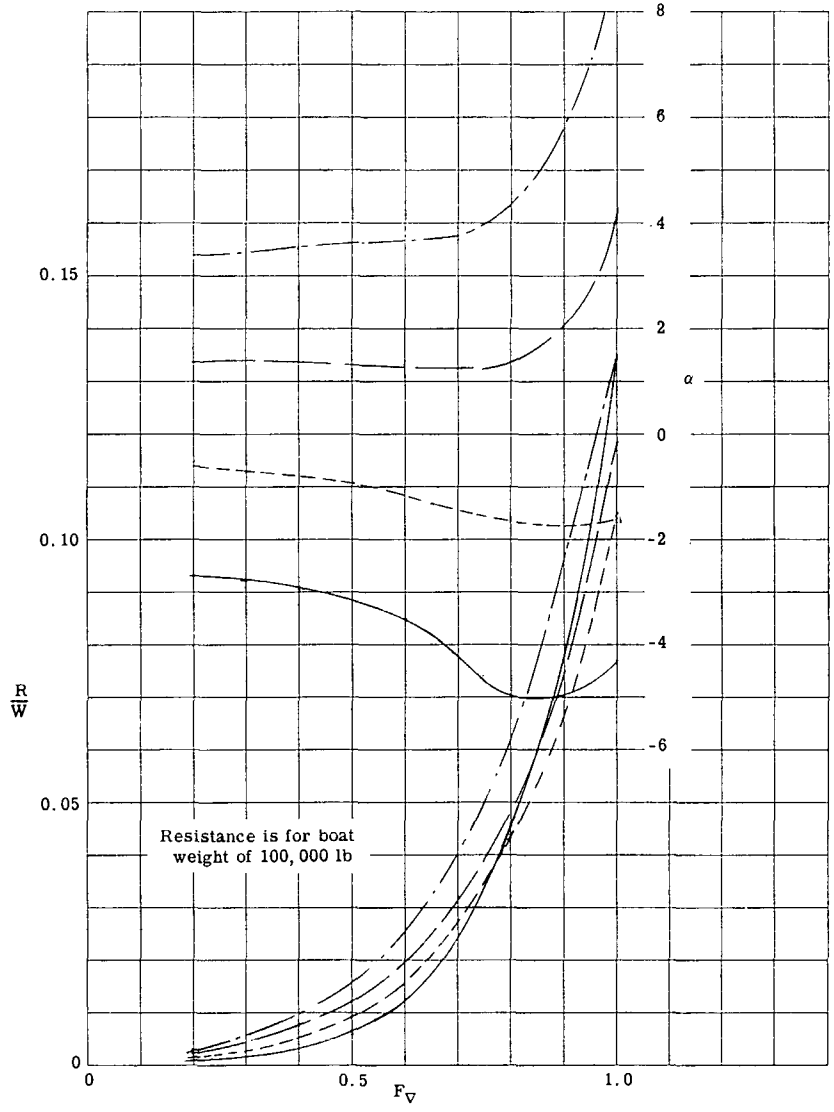

(b) $A_P/\nabla^{\frac{2}{3}} = 5.5$

Fig. 21 Resistance/weight ratio and angle of attack at low speeds. $L_P/B_{PX} = 2.00$

Fig. 21 Continued

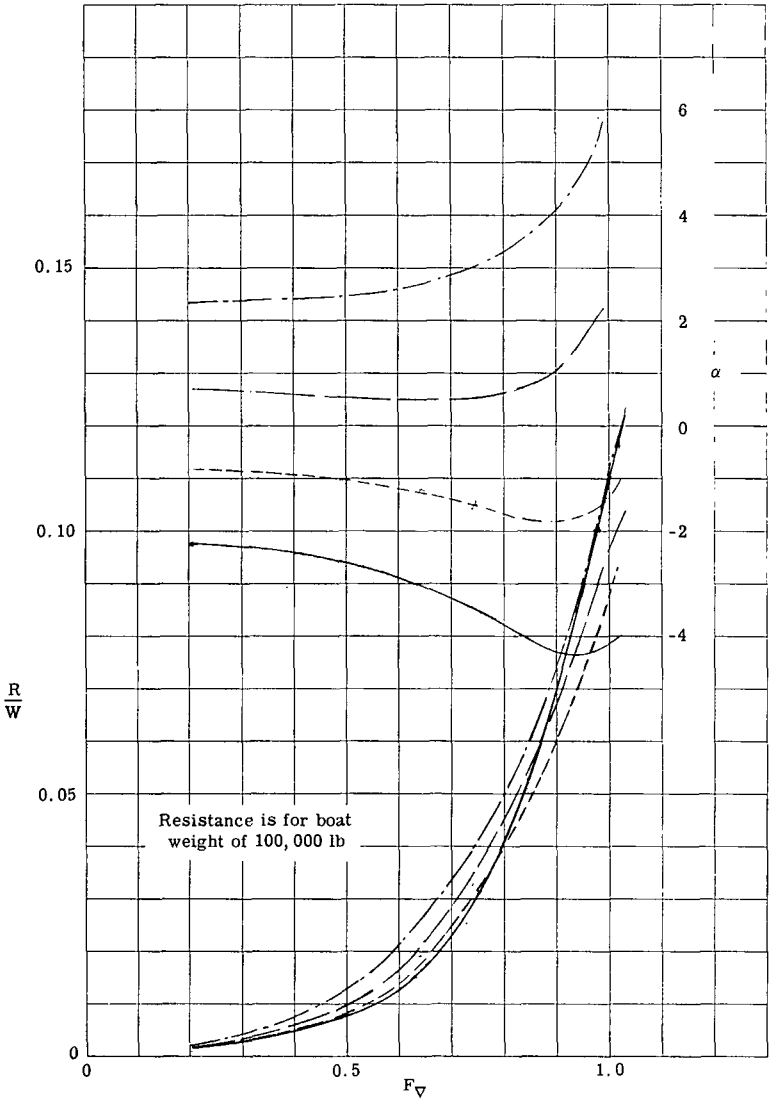

(c) $A_P/\nabla^{\frac{2}{3}} = 7.0$

Fig. 21 Continued

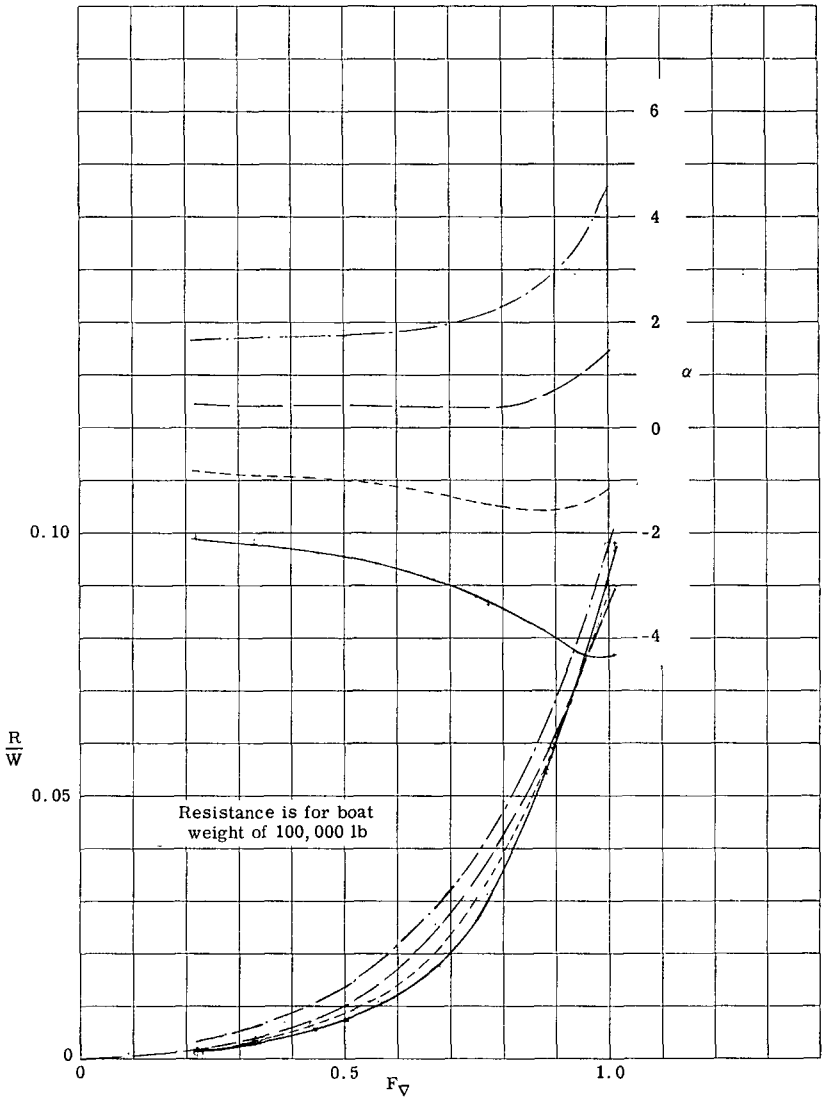

(d) $A_P/\nabla^{\frac{2}{3}} = 8.5$

Fig. 21 Concluded

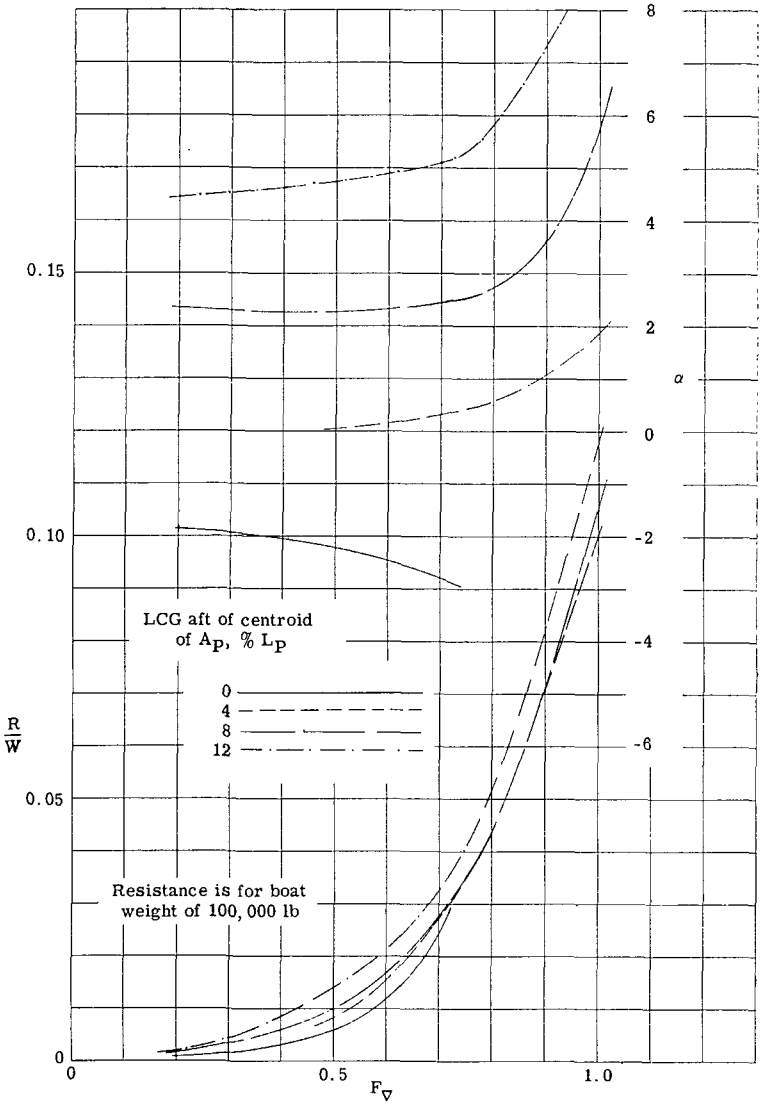

(a) $A_P/\nabla^{\frac{2}{3}} = 4.0$

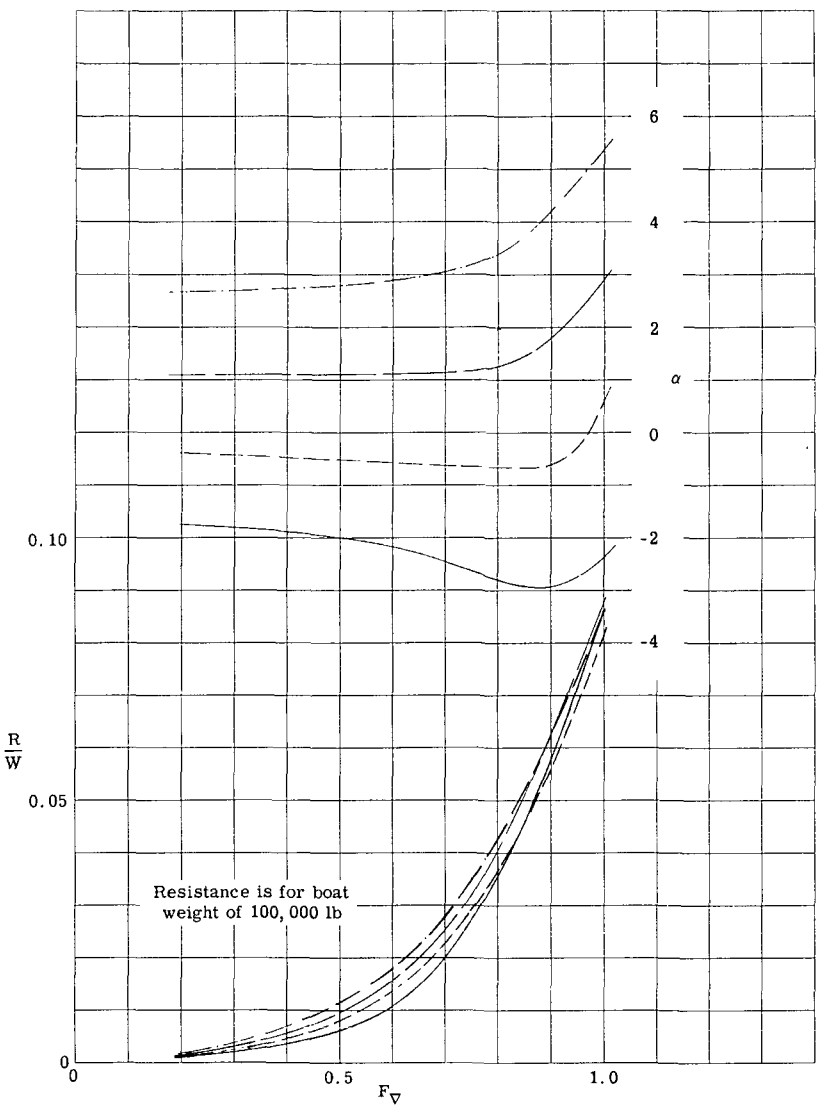

(b) $A_P/\nabla^{\frac{2}{3}} = 5.5$

Fig. 22 Resistance/weight ratio and angle of attack at low speeds. $L_P/B_{PX} = 3.06$

Fig. 22 Continued

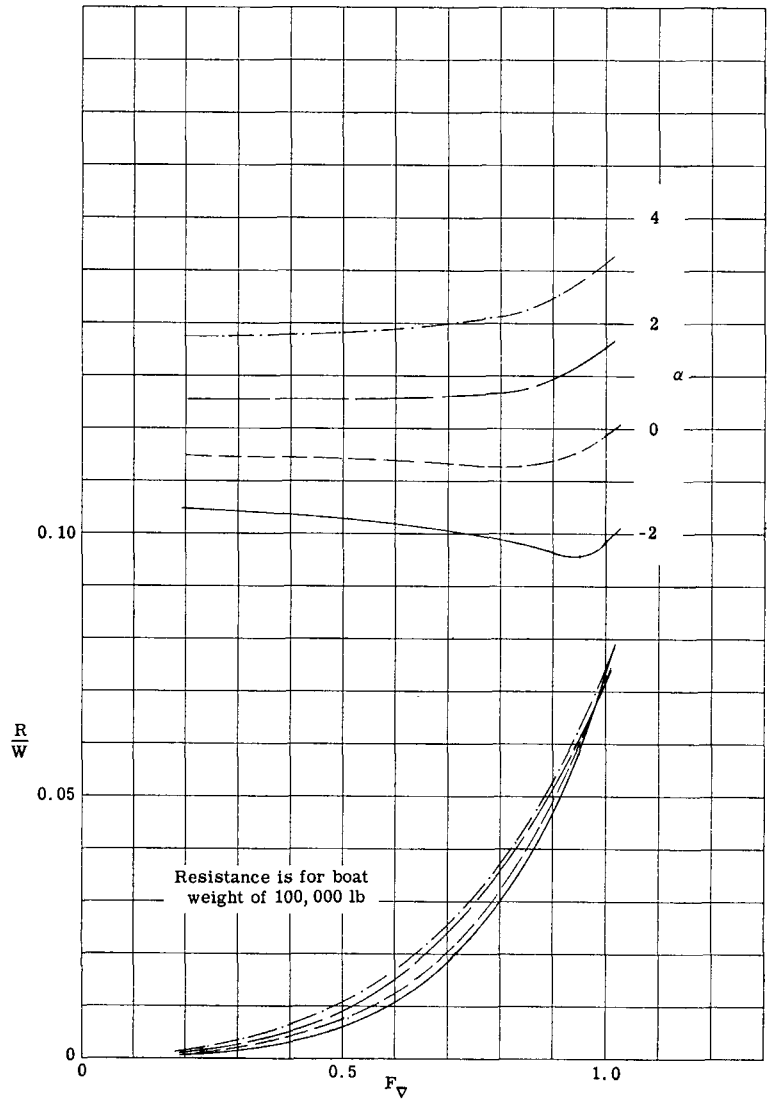

(c) $A_p/\nabla^{\frac{2}{3}} = 7.0$

Fig. 22 Continued

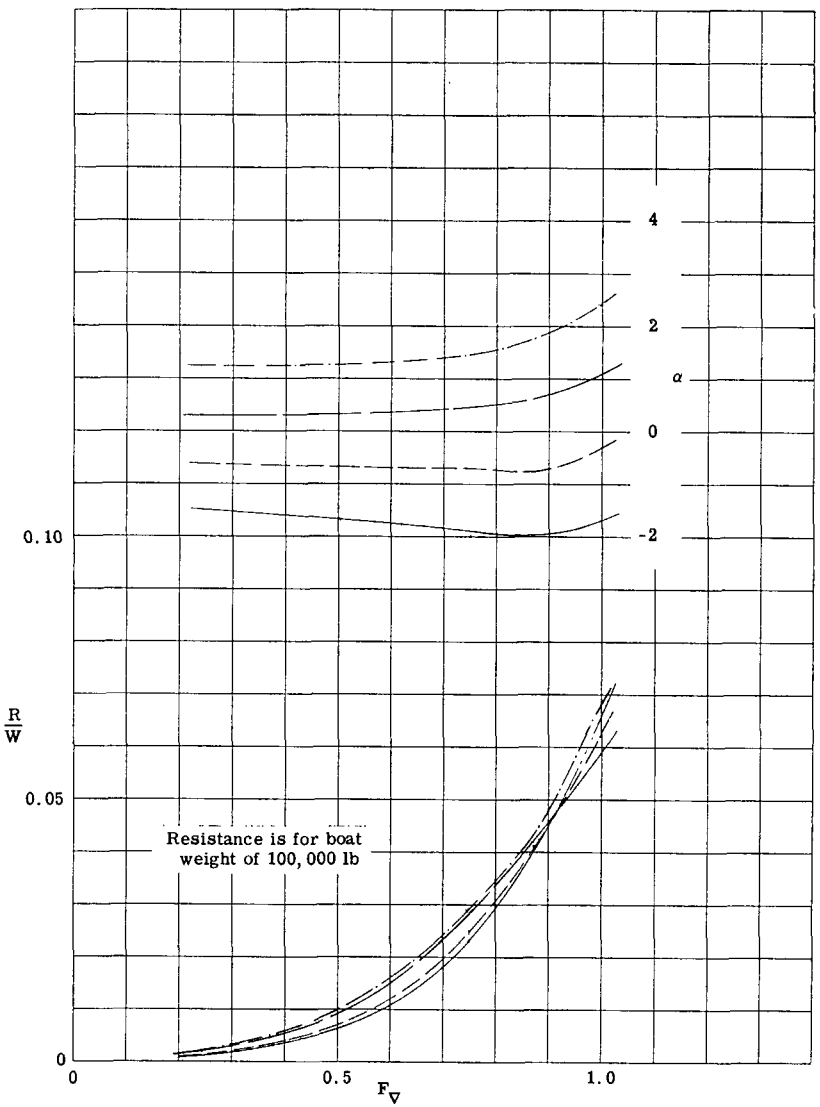

(d) $A_p/\nabla^{\frac{2}{3}} = 8.5$

Fig. 22 Concluded

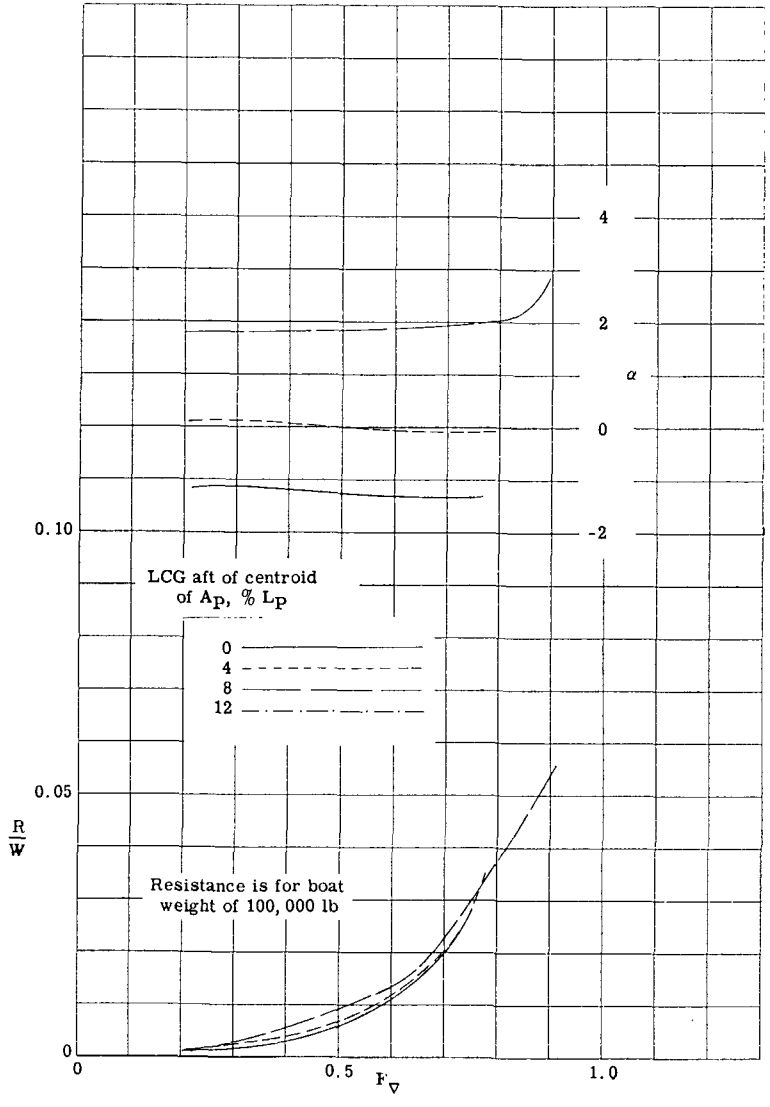

(a) $A_P/\nabla^{\frac{2}{3}} = 4.0$

Fig. 23 Resistance/weight ratio and angle of attack at low speeds. $L_P/B_{PX} = 4.09$

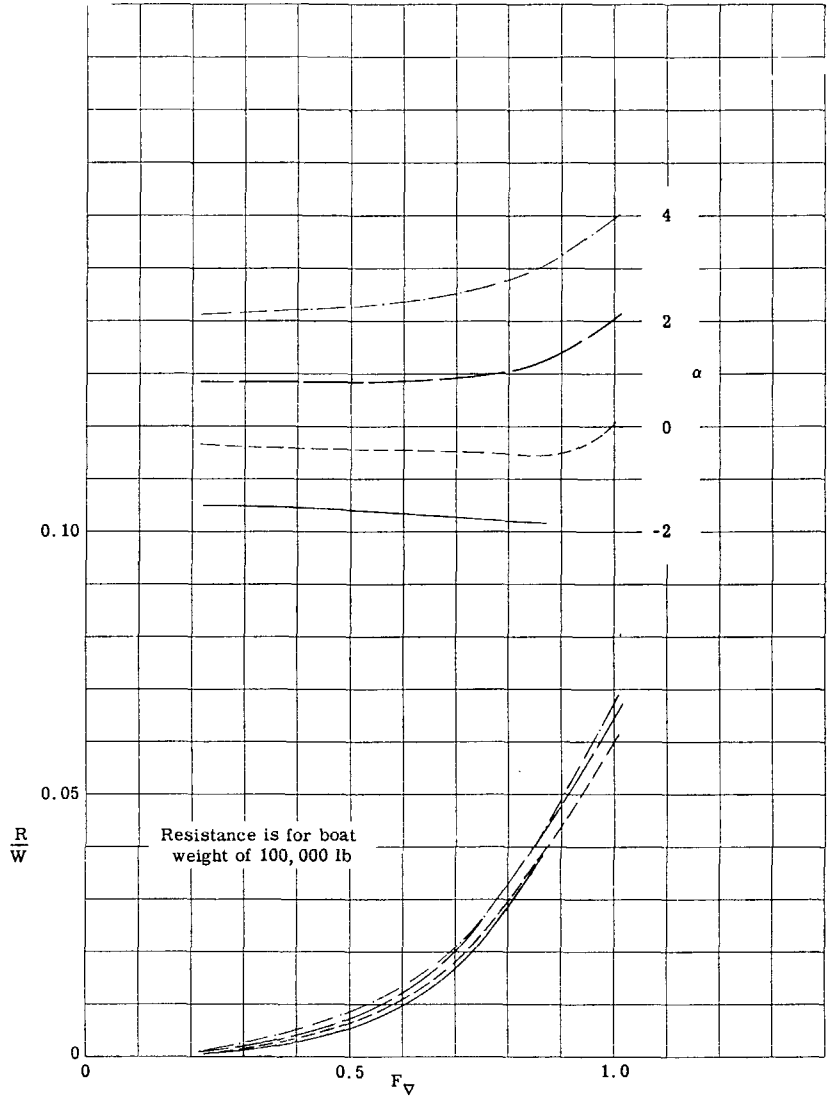

(b) $A_P/\nabla^{\frac{2}{3}} = 5.5$

Fig. 23 Continued

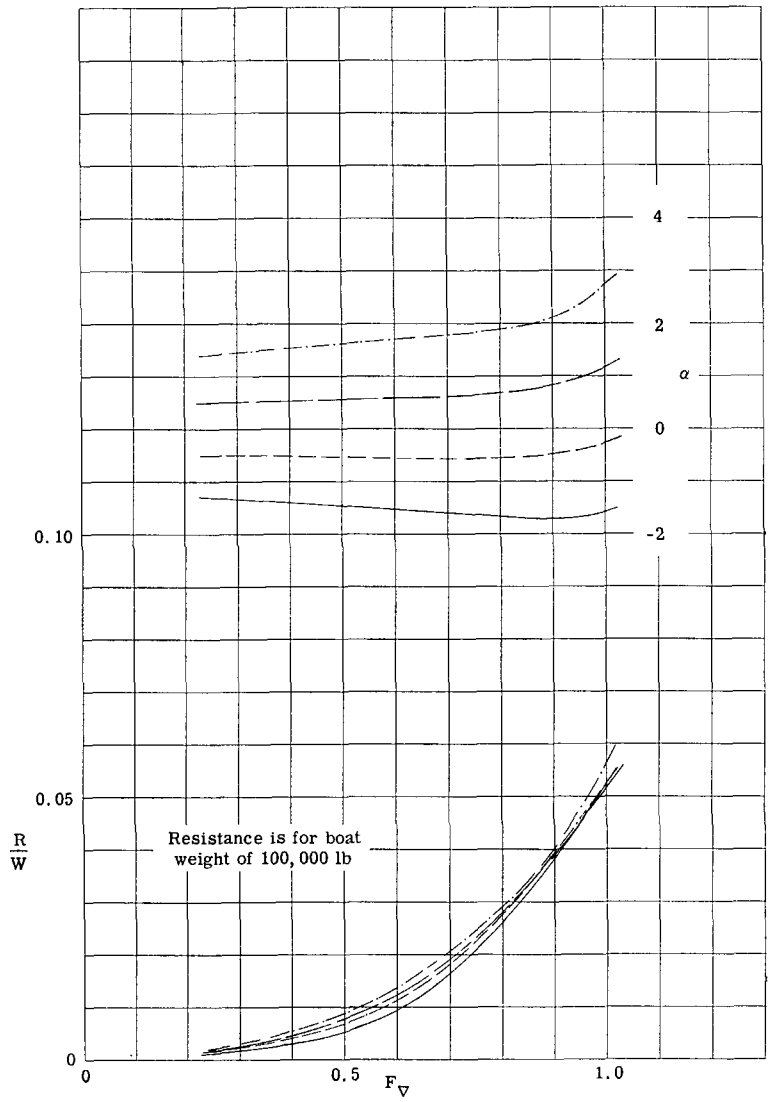

(c) $A_P/\nabla^{\frac{2}{3}} = 7.0$

Fig. 23 Continued

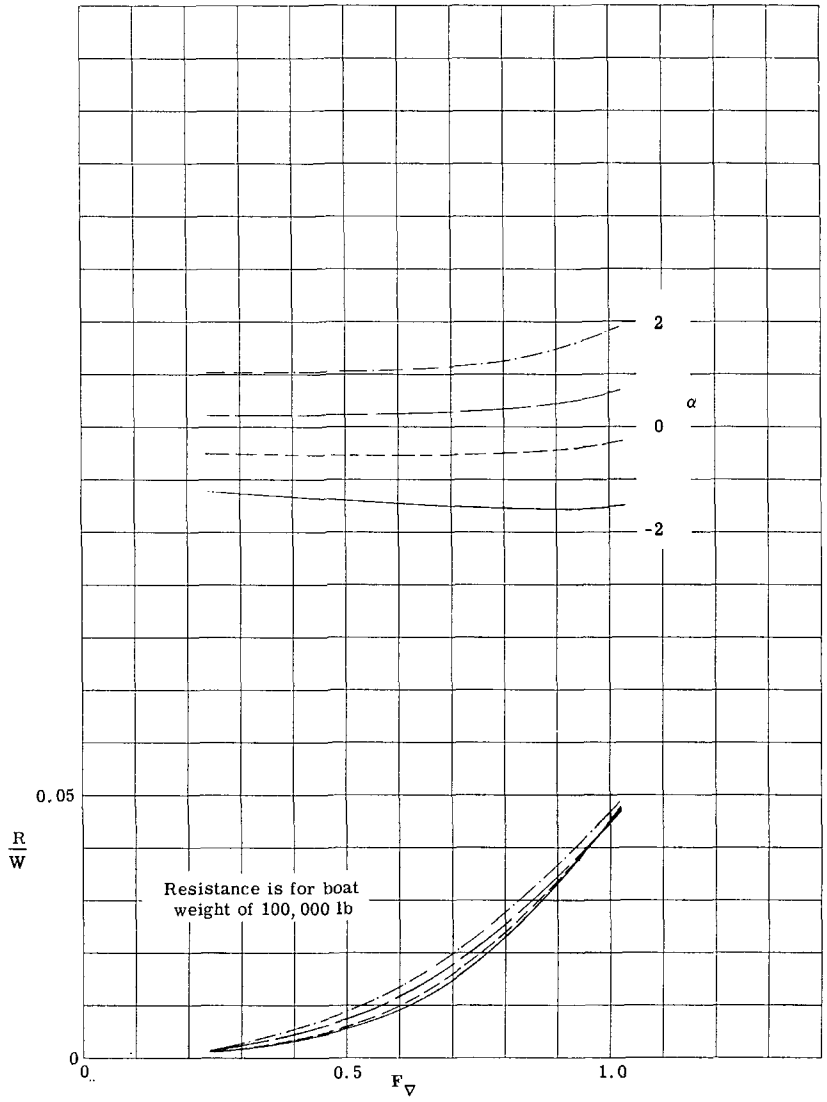

(d) $A_P/\nabla^{\frac{2}{3}} = 8.5$

Fig. 23 Concluded

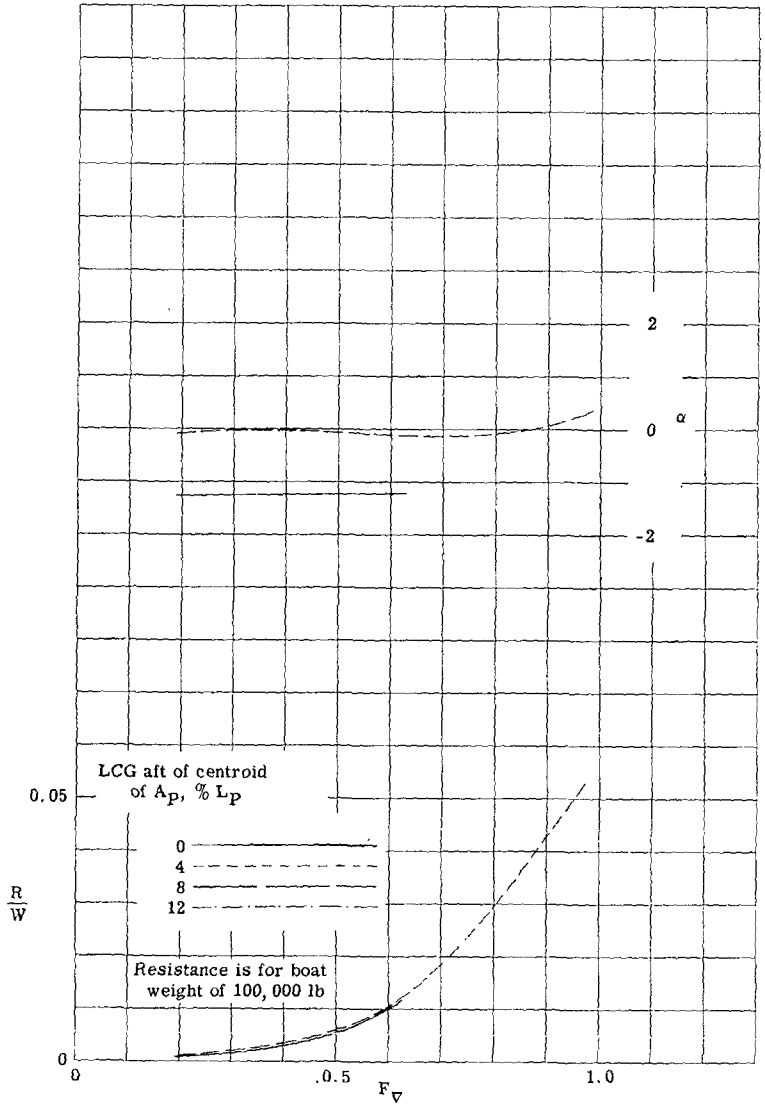

(a) $A_P/\nabla^{\frac{2}{3}} = 4.0$

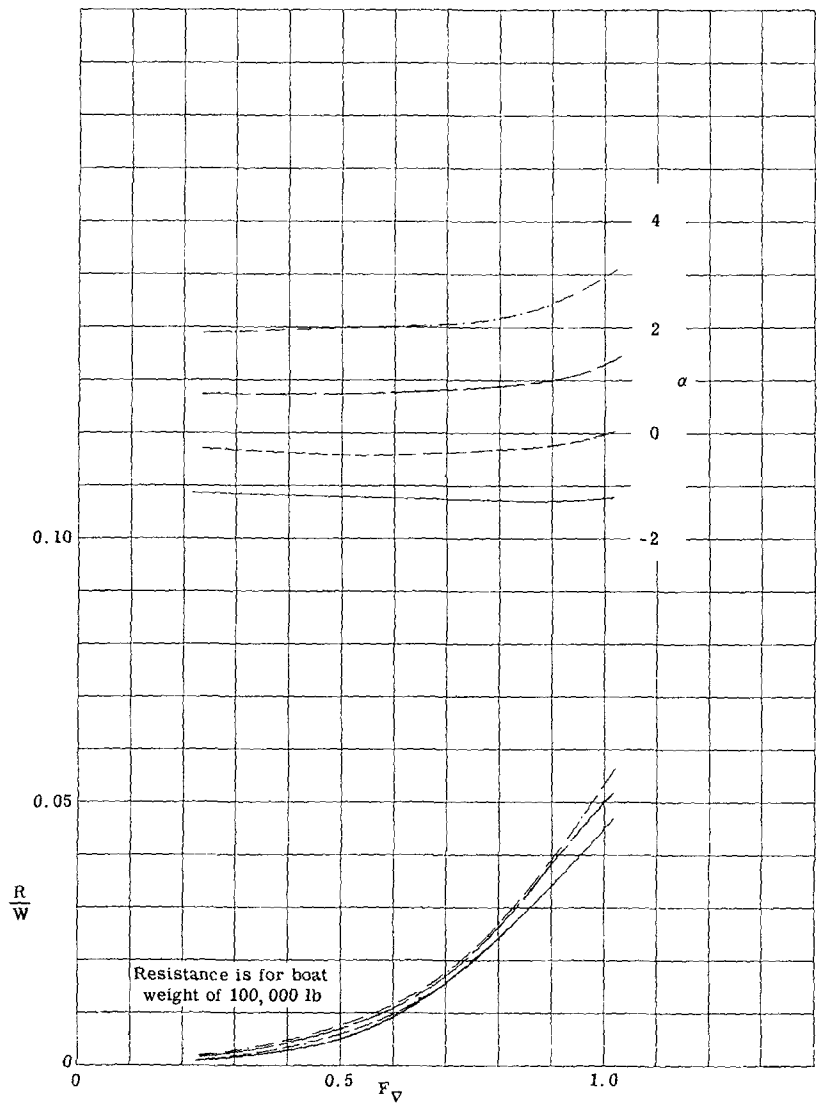

(b) $Ap/\nabla^{\frac{2}{3}} = 5.5$

Fig. 24 Resistance/weight ratio and angle of attack at low speeds. $L_P/B_{PX} = 5.50$

Fig. 24 Continued

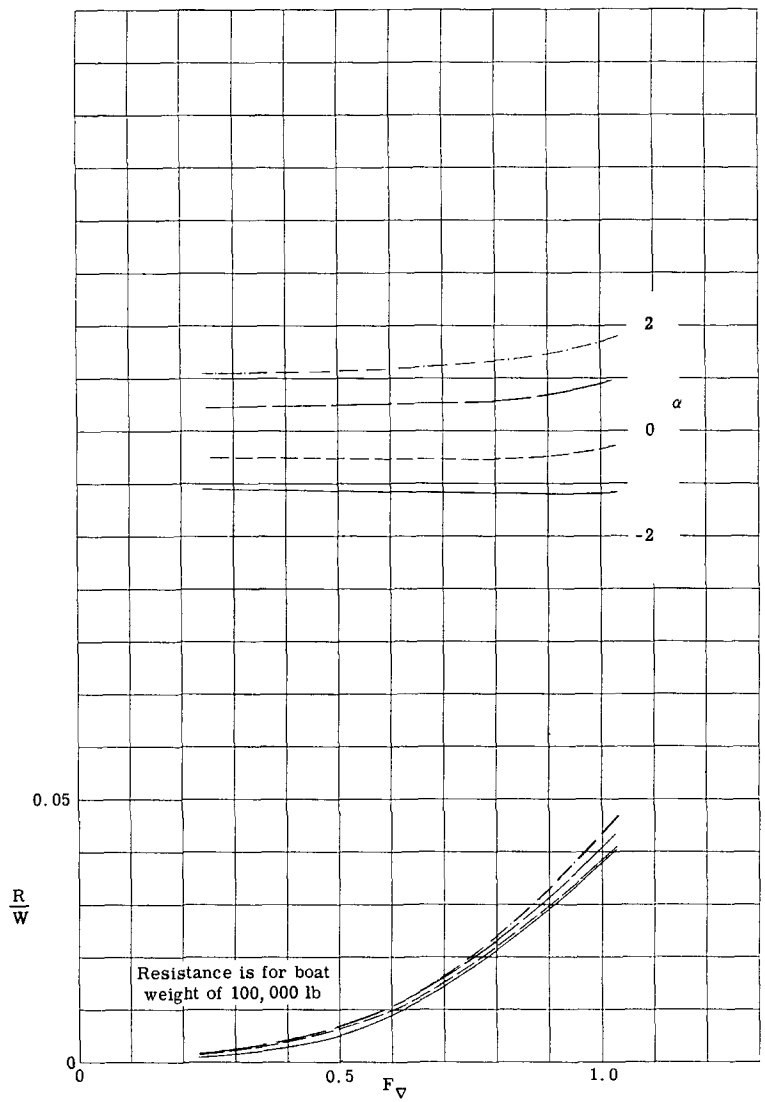

(c) $Ap/\nabla^{\frac{2}{3}} = 7.0$

Fig. 24 Continued

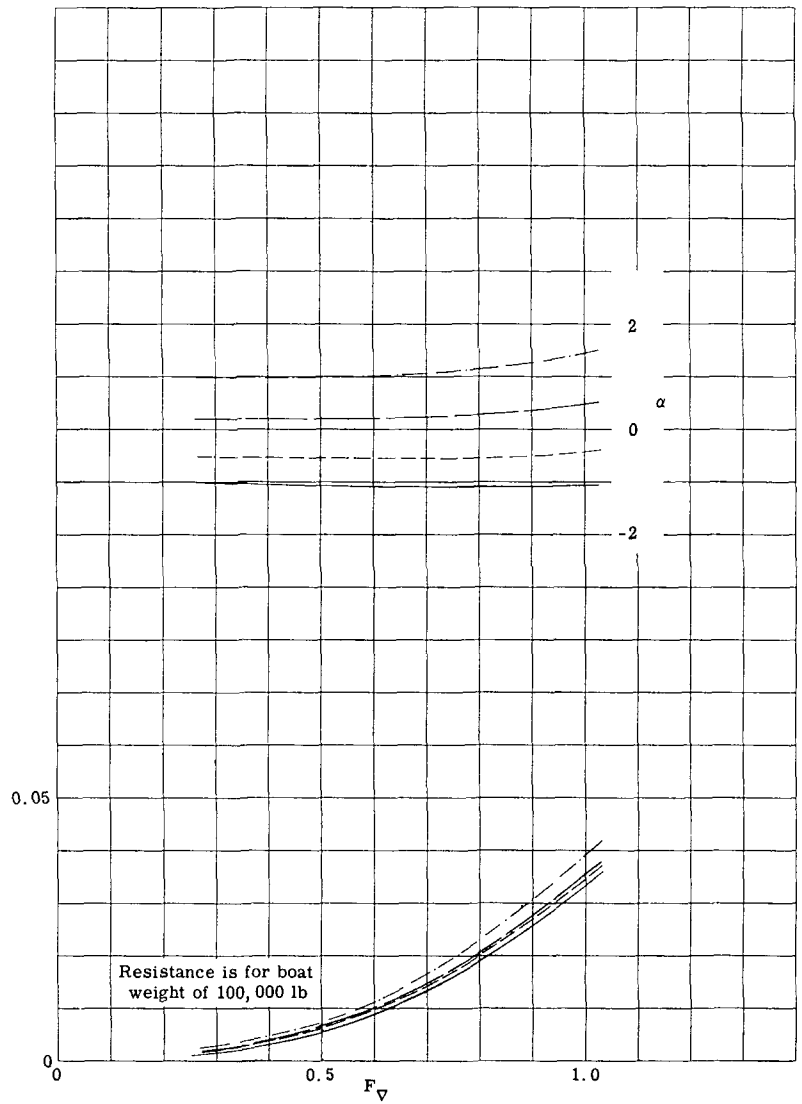

(d) $Ap/\nabla^{\frac{2}{3}} = 8.5$

Fig. 24 Concluded

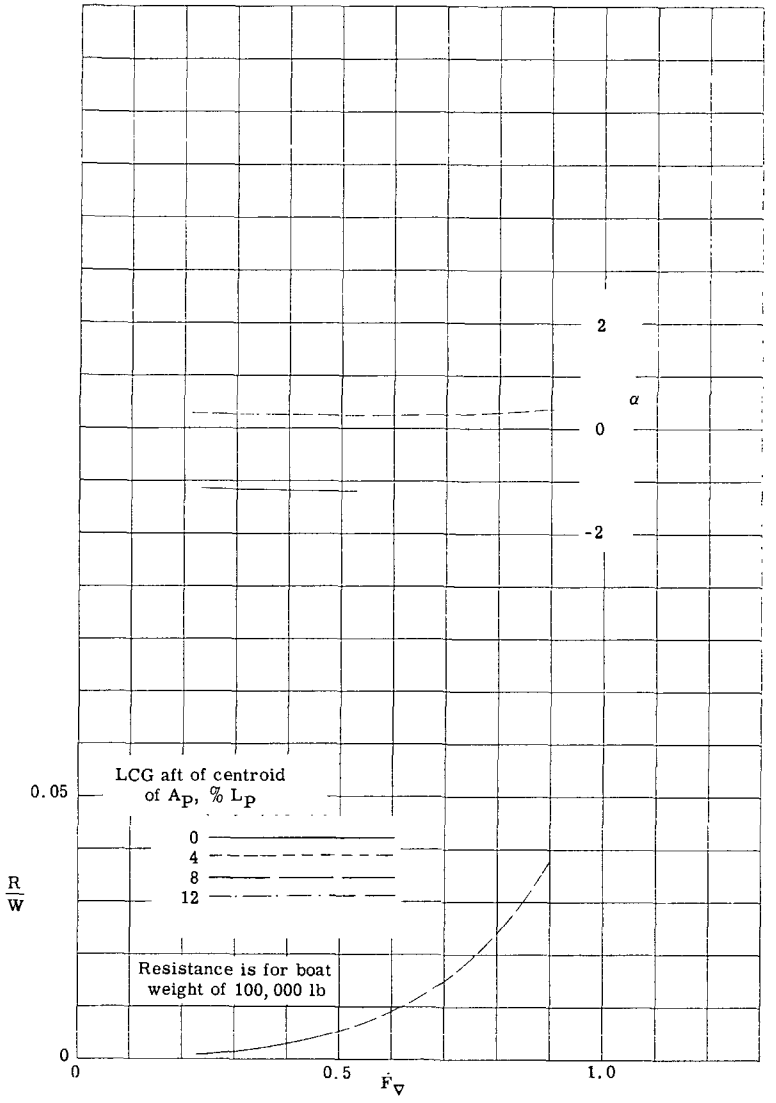

(a) $A_P/\nabla^{\frac{2}{3}} = 4.0$

Fig. 25 Resistance/weight ratio and angle of attack at low speeds. $L_P/B_{PX} = 7.00$

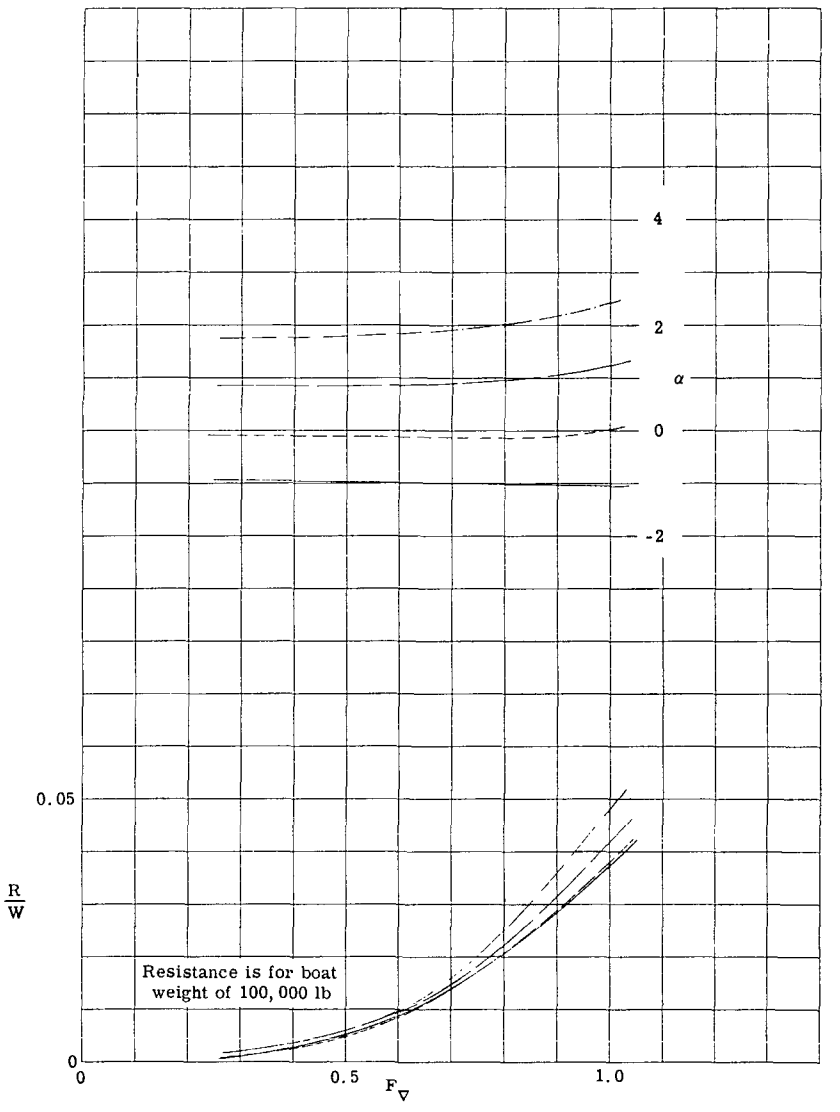

(b) $Ap/\nabla^{\frac{2}{3}} = 5.5$

Fig. 25 Continued

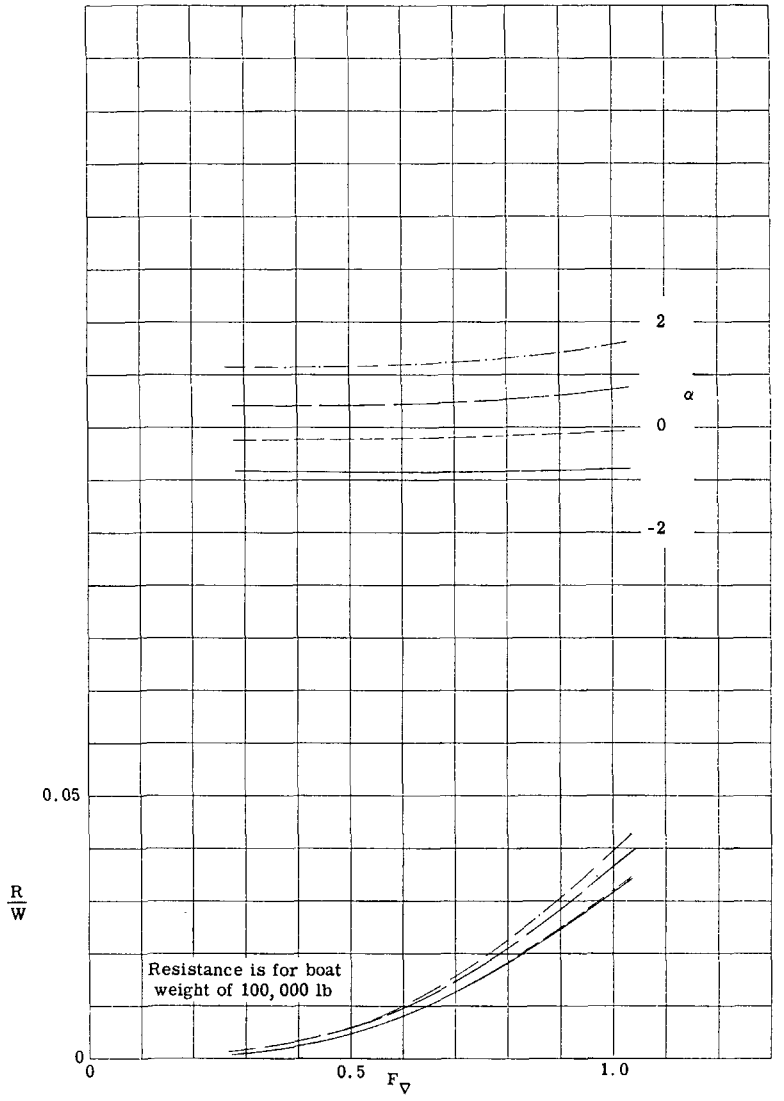

(c) $Ap/\nabla^{\frac{2}{3}} = 7.0$

Fig. 25 Continued

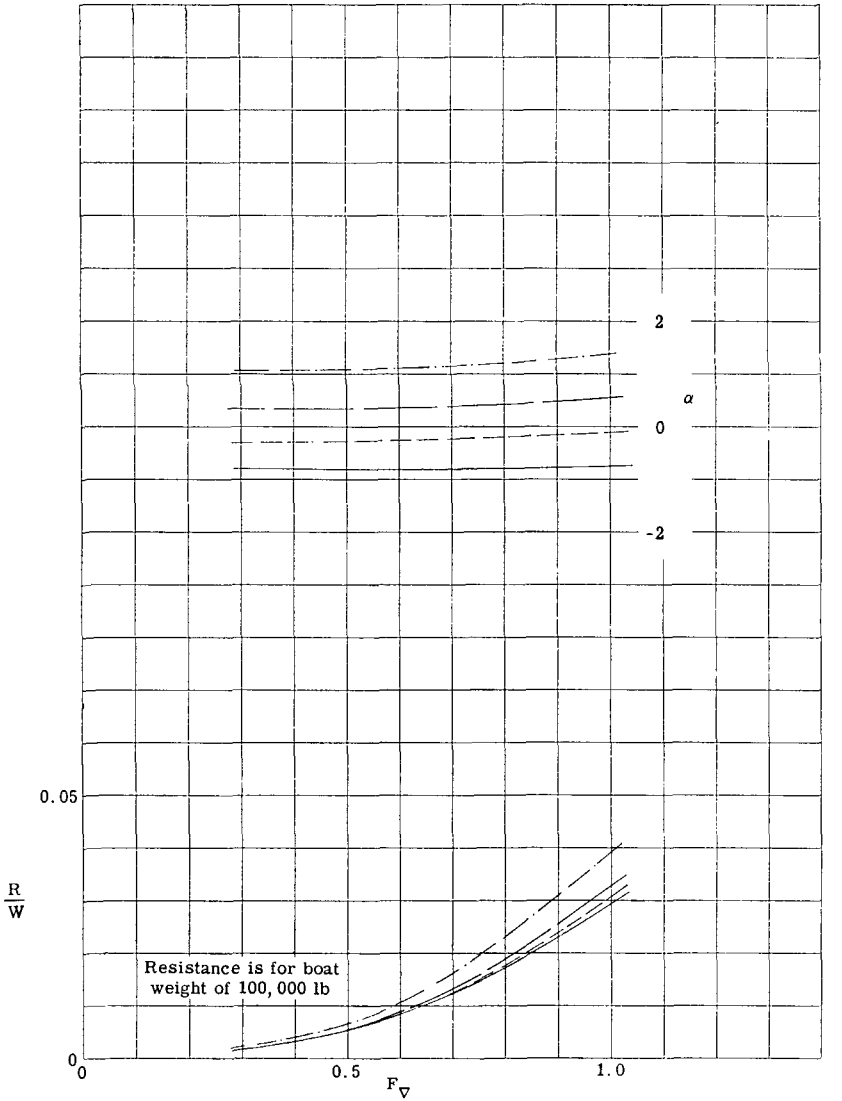

(d) $Ap/\nabla^{\frac{2}{3}} = 8.5$

Fig. 25 Concluded

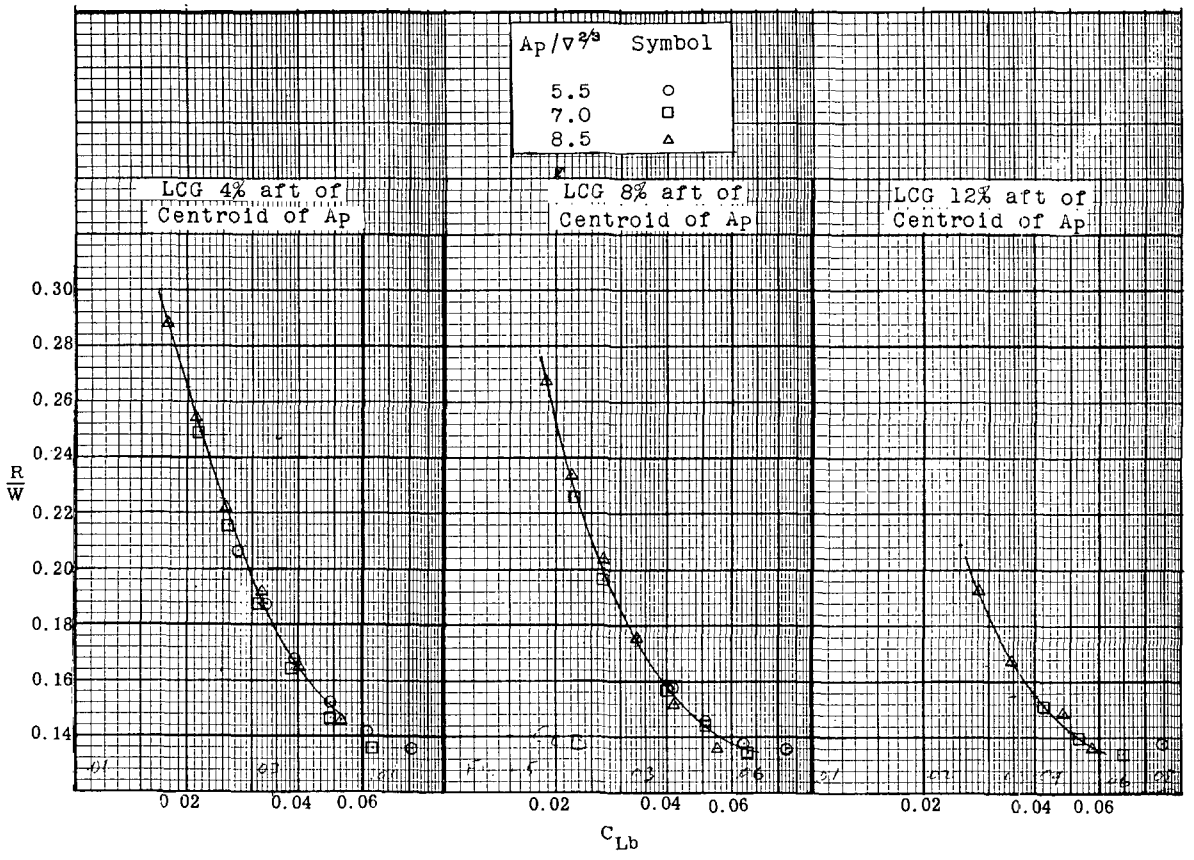

Fig. 26 Resistance/weight ratio versus lift coefficient (C_{Lb}), at high speed, from the tests of Model 4666. 10,000 lb boat weight

resistance curve for this arbitrary boat is a laborious task. Of the necessary steps, the first one would be to calculate the resistance of a boat of 15,000-lb displacement from each of those four tests which, in terms of length-beam ratio and area coefficient, bracket the assumed design values. After the four resistance curves for 15,000-lb displacement are obtained, the second step would be to interpolate between a pair of the curves (say between the curves for $L_P/B_{PX} = 3.06$ and $A_P/\nabla^{2/3} = 5.5$ and 7) to obtain a resistance curve for $L_P/B_{PX} = 3.06$ and $A_P/\nabla^{2/3} = 6.5$. The next step would be to interpolate between the two resistance curves for $L_P/B_{PX} = 4.1$ to obtain a curve for $L_P/B_{PX} = 4.1$ and $A_P/\nabla^{2/3} = 6.5$. The final step would be to interpolate between the two resistance curves for $A_P/\nabla^{2/3} = 6.5$ to obtain a curve for the assumed design values of $L_P/B_{PX} = 3.5$ and $A_P/\nabla^{2/3} = 6.5$.

A means of avoiding this laborious process is suggested by previous work at the Model Basin with equations for the high-speed performance of planing hulls. This work has shown that at high speed the resistance of a planing hull of given weight can be presented as a function of only the three variables, deadrise angle, aspect ratio, and lift coefficient. The deadrise angle of the portion of the hull which is wetted at high speed is constant for the models of the present series (12½ deg); as a result, the possibility is suggested that resistance for a given boat weight can be presented as a function of only two variables. The resistance as presented in Figs. 7 through 18 is a function of the three variables, F_∇, area coefficient, and LCG location. In this case, if the number of variables determining the high-speed resistance can be reduced from three to two, the number of curves required to present the high-speed resistance data can be reduced by a factor of about three or four.

The first step in establishing the validity of the suggested approach was to read off values of R/W for Model 4666 (at high speed) from the curves in Fig. 15 and then to plot them against the corresponding values of lift coefficient. Lift coefficient is defined here as $W/(\rho/2)v^2b^2$, where b is the breadth over the spray strips at the

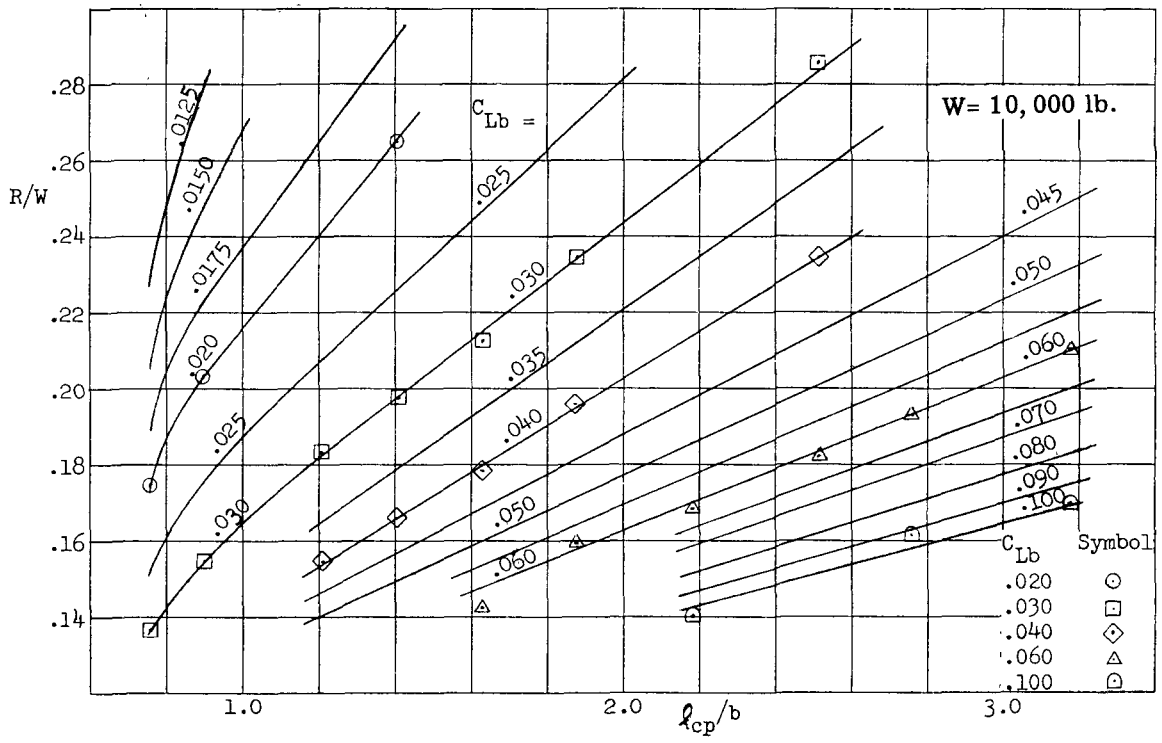

Fig. 27 Resistance/weight ratio versus l_{cp}/b with C_{Lb} as parameter

longitudinal location of the center of gravity. The resulting graph, Fig. 26, shows that the experimental results do, in fact, conform to what was indicated by the equations of resistance referred to previously. The resistance data from the tests at different loads, i.e., different area coefficients, collapse onto a single curve so that the resistance can be presented as a function of only two variables; that is, lift coefficient and LCG location. The data from the tests at the forwardmost LCG location (0 percent L_P aft of the centroid) did not collapse when plotted against lift coefficient. The assumption is that this is because the curved bow portion of the hull is wetted with this CG location. It was pointed out previously that this LCG location is outside the useful range because of the poor resistance characteristics.

The high-speed resistance data from the tests of the other models (except the 0 percent LCG data) were also plotted against lift coefficient. Values of R/W at suitable intervals of lift coefficient were then read off the resulting graphs (all were similar to Fig. 26), and plotted against l_{cp}/b, where l_{cp} is the distance of the center of pressure (or center of gravity) forward of the transom.

Fig. 27 is the graph obtained from this plotting. It can be seen that for any one value of lift coefficient, a single curve can be drawn through the R/W-values from the tests of all five models.

From Fig. 27, it is possible to determine accurate values of resistance at high speed for a 10,000-lb planing boat with the same body plan as that of the series, but with any arbitrary value of the ratio l_{cp}/b (therefore any arbitrary length-beam ratio) and any arbitrary condition of loading. Since Fig. 26 is limited to one particular boat weight, the procedure just explained was repeated for boat weights of 1000, 3000, 30,000 and 100,000 lb. Thus a graph similar to Fig. 27 was obtained for each of the boat weights treated.

Because of the way in which the data from the tests at the different loads had been found to collapse onto a single curve, Fig. 26, and the way in which the data from the tests of the different models then fell into line when plotted against l_{cp}/b, Fig. 27, it was necessary to utilize only a small number of the available tests in order to prepare the graphs for the different boat weights. More specifically, only the data for LCG locations of 4 and 12 percent L_P aft of the centroid were used, and at each LCG location the data for only load, i.e., one area coefficient, were used. Therefore, only ten tests were utilized, rather than the forty-five tests which were available.

After a graph had been prepared for each of the various boat weights, the cross curves shown in

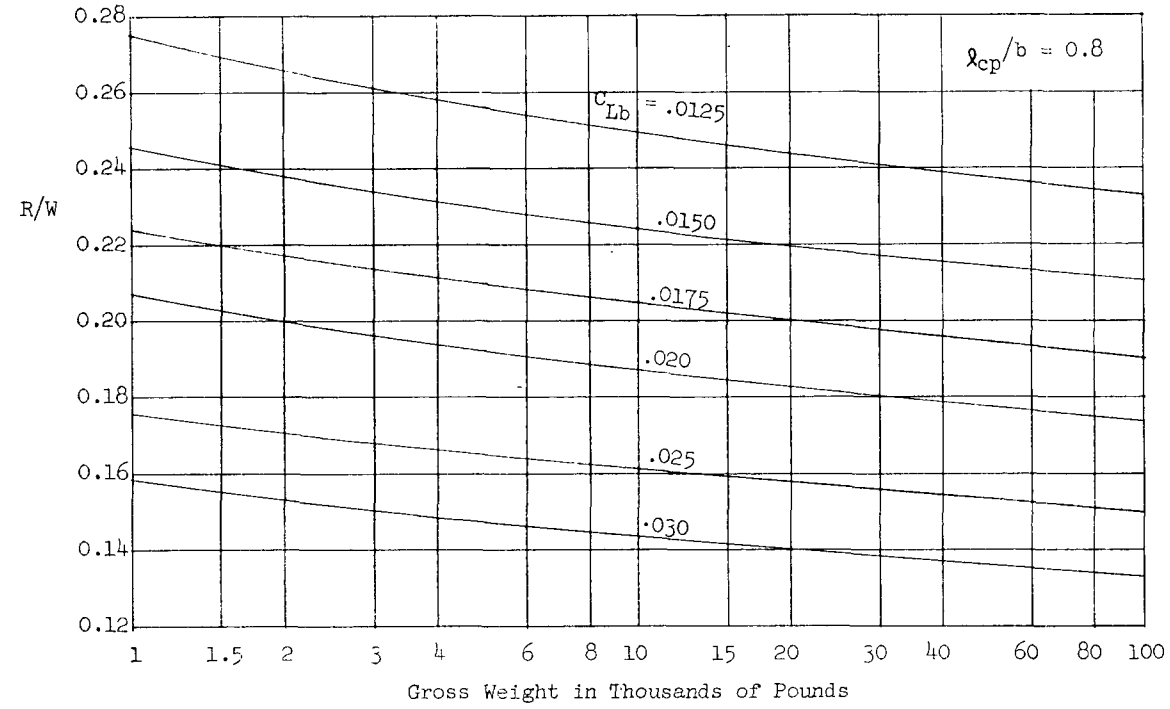

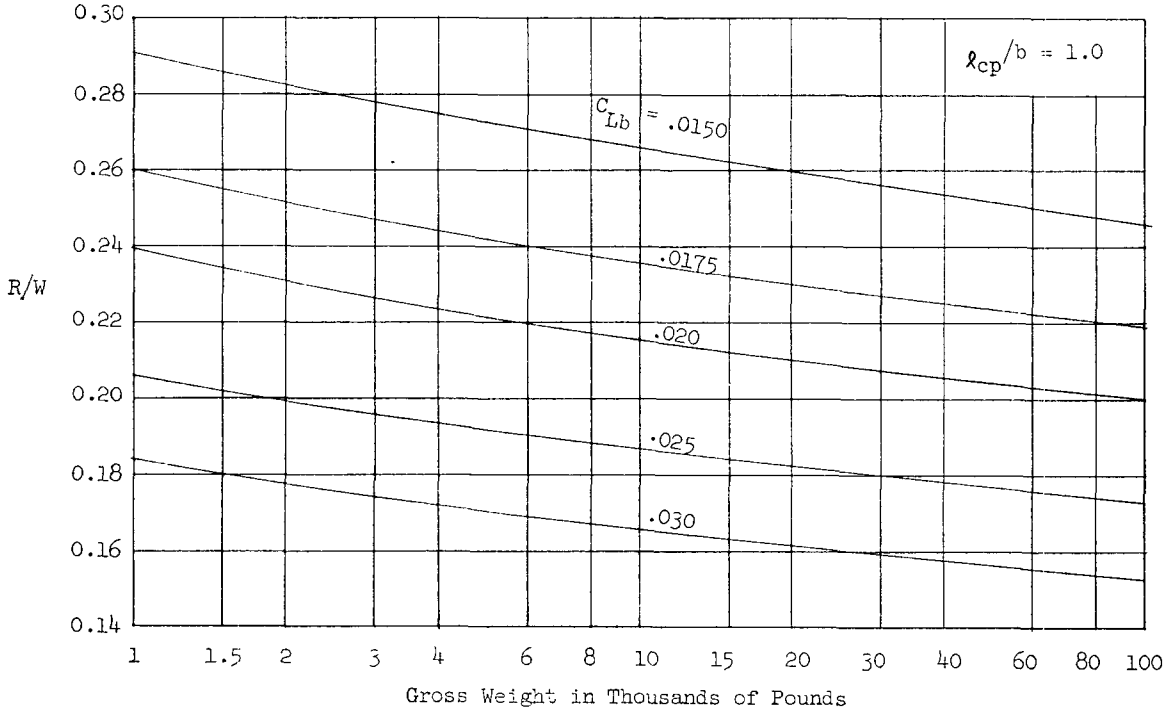

Fig. 28 Resistance/weight ratio versus gross weight of boat, with C_{Lb} as parameter

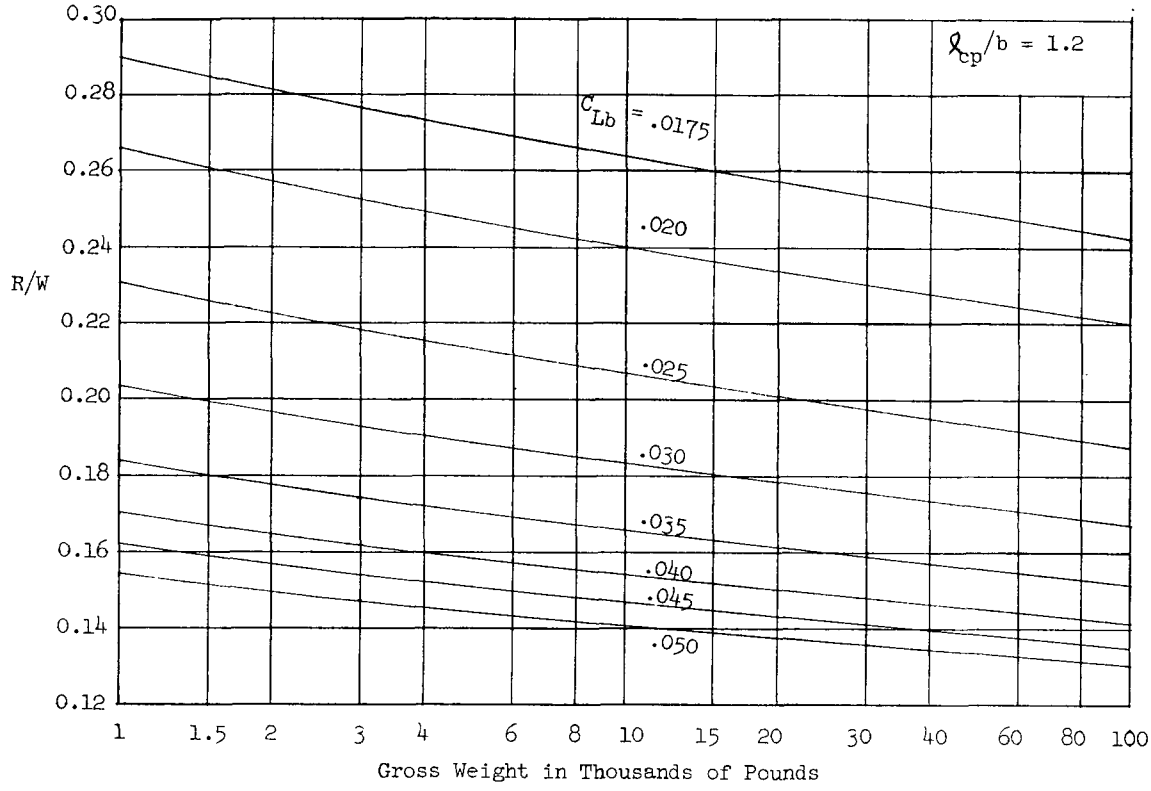

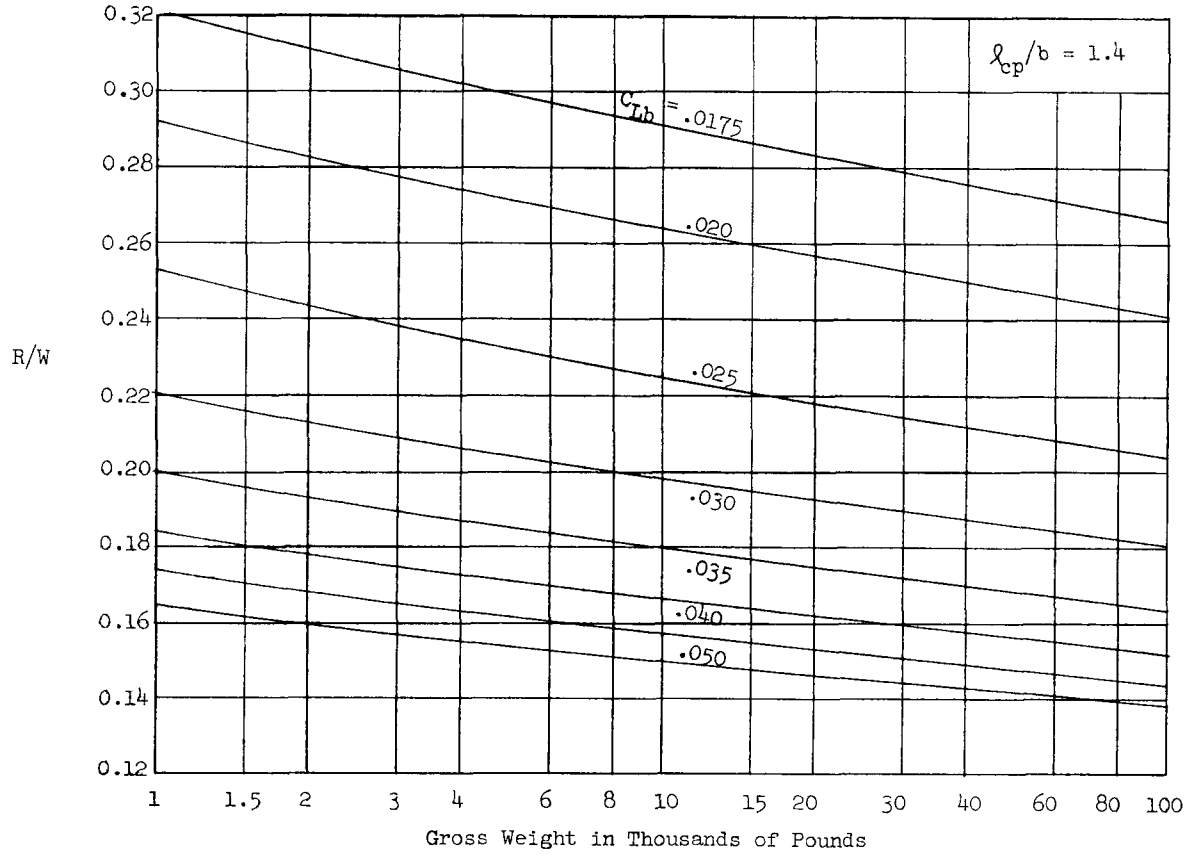

Fig. 28 Continued

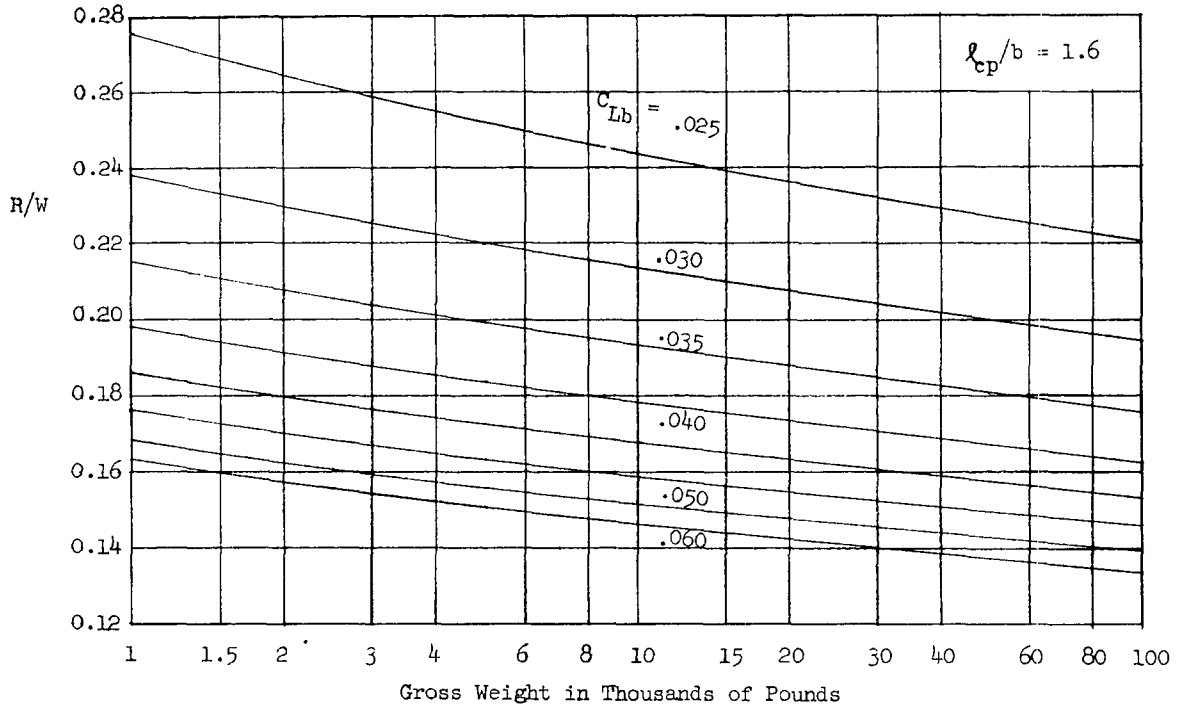

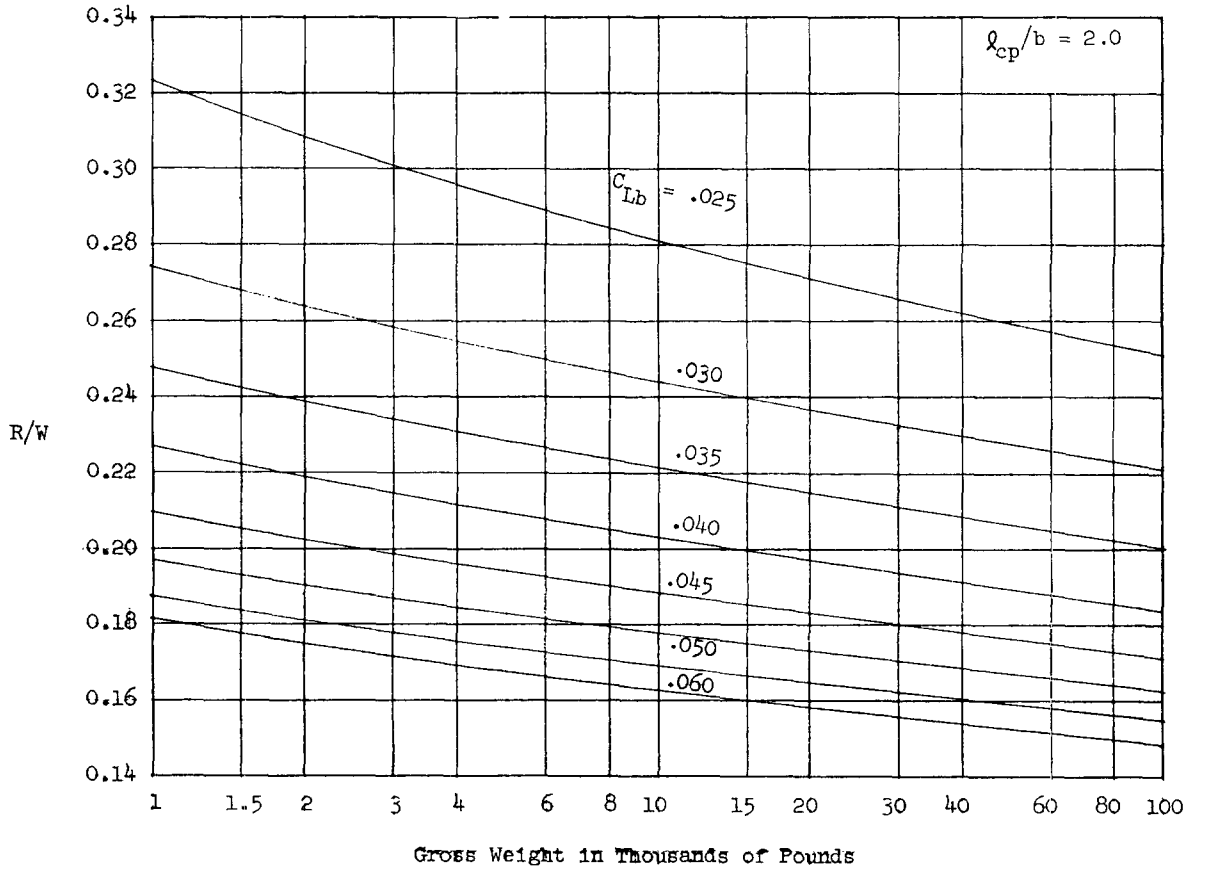

Fig. 28 Continued

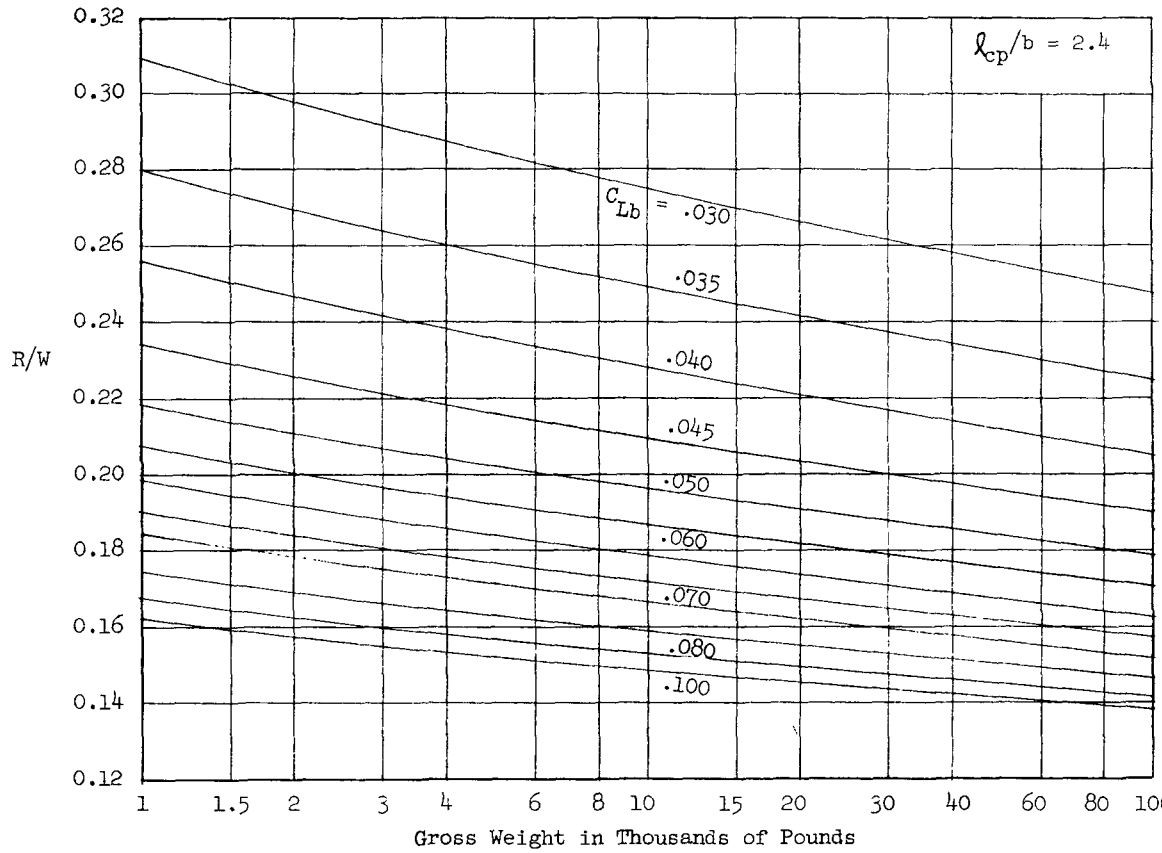

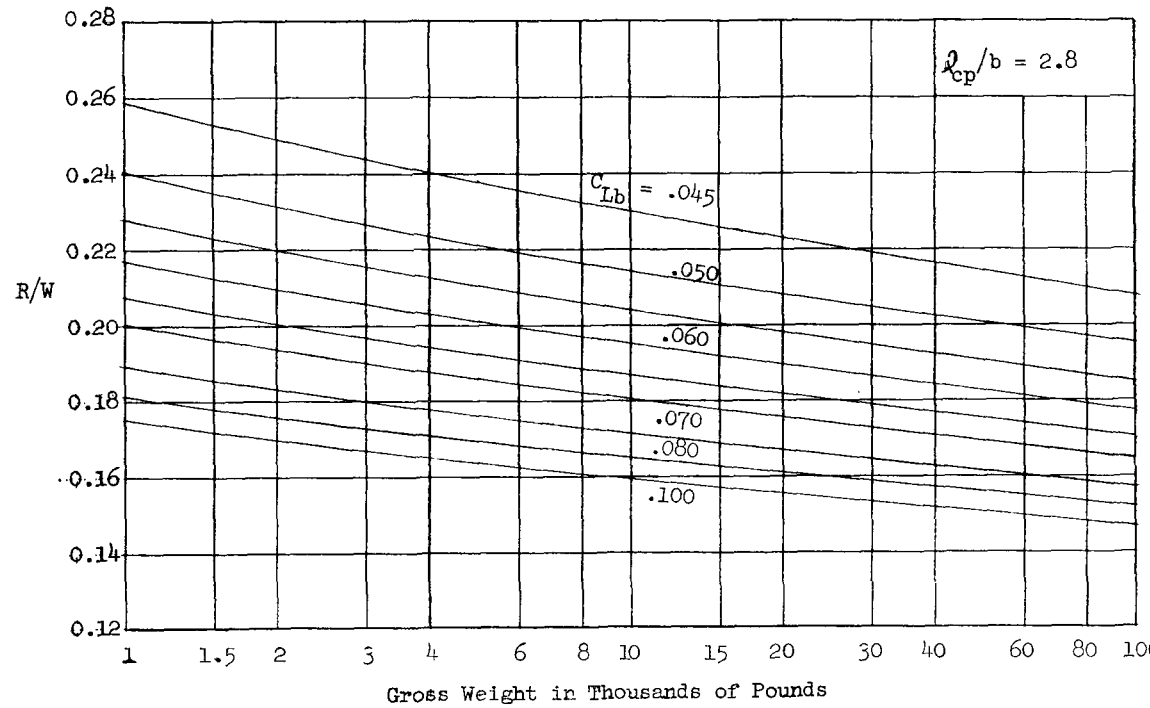

Fig. 28 Continued

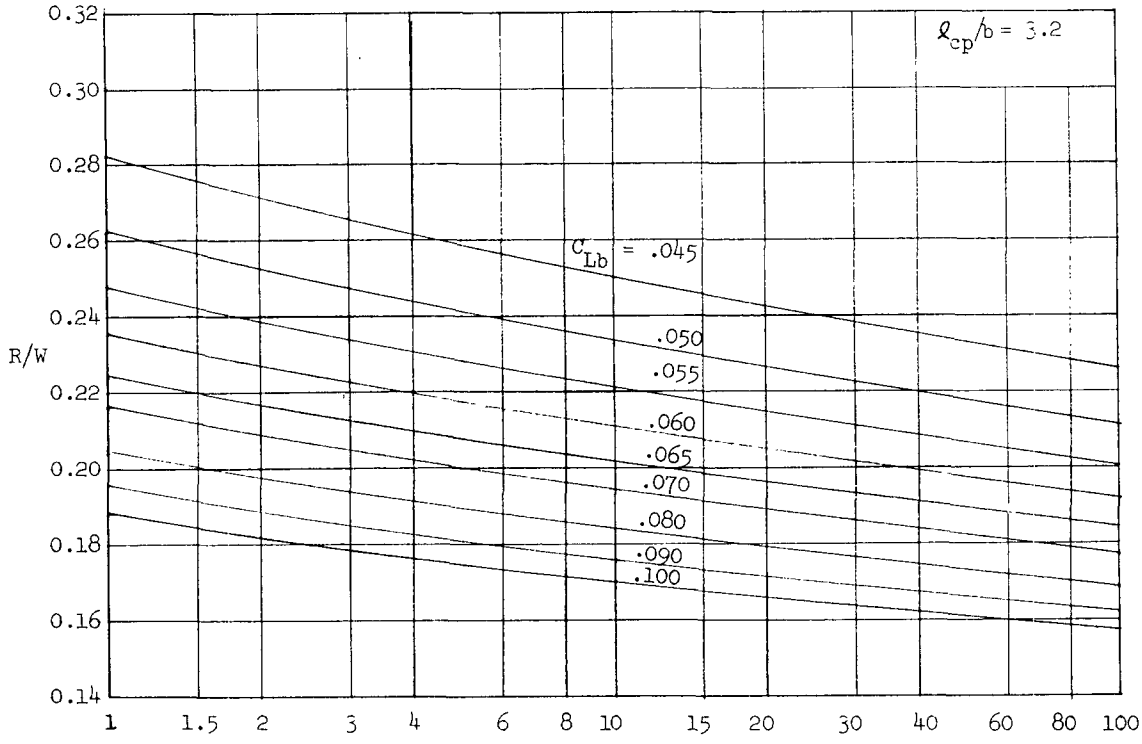

(e) $\ell_{cp}/b = 3.2$

Fig. 28 Concluded

Table 2

A	B	C	D	E	F	G
C_{Lb}	$\frac{R}{W}$	R	$\frac{1}{C_{Lb}}$	$\left(\frac{1}{C_{Lb}}\right)^{1/2}$	$v = \frac{W^{1/2}}{b}\left(\frac{1}{C_{Lb}}\right)^{1/2}$	V, knots
0.020	0.260	3900	50.00	7.071	79.53	47.12
0.025	0.221	3315	40.00	6.324	71.12	42.14
0.030	0.195	2925	33.33	5.773	64.93	38.47
0.035	0.177	2655	28.57	5.345	60.12	35.62
0.040	0.164	2460	25.00	5.000	56.24	33.32
0.045	0.155	2325	22.22	4.714	53.01	31.41
0.050	0.148	2220	20.00	4.472	50.26	29.78

Fig. 28 were prepared. These curves can be used to calculate the high-speed resistance of boats related to the present series in regard to shape of body plan, but of any size from 1000 to 100,000 lb, and for any ratio of l_{cp}/b from 0.8 to 3.2.

The procedure for carrying out this calculation is as follows: Assume that the resistance in the high-speed range is to be determined for a boat having a gross weight of 15,000 lb, a width over the spray strips of 10.9 ft, and a center of gravity located 15.3 ft forward of the transom. Then

$$l_{cp}/b = 15.3/10.9 = 1.4$$

Fig. 28(*b*) is then utilized since this figure applies to the particular LCG location of the present case. The succeeding steps are shown in the table of calculations, Table 2. First, the values of C_{Lb} for which the curves in Fig. 27 were prepared are entered in Column A. Next, Fig. 28 is entered with the given boat weight of 15,000 lb and a value of R/W is read off at each value of C_{Lb}. These values are entered in Column B. Next, multiplying the values of R/W by the boat weight, which is 15,000 lb, gives the values of boat resistance in pounds. These values are in Column C. The remaining step is to solve for the corresponding values of boat speed in the relationship

$$C_{Lb} = \frac{W}{\frac{1}{2}\rho v^2 b^2}$$

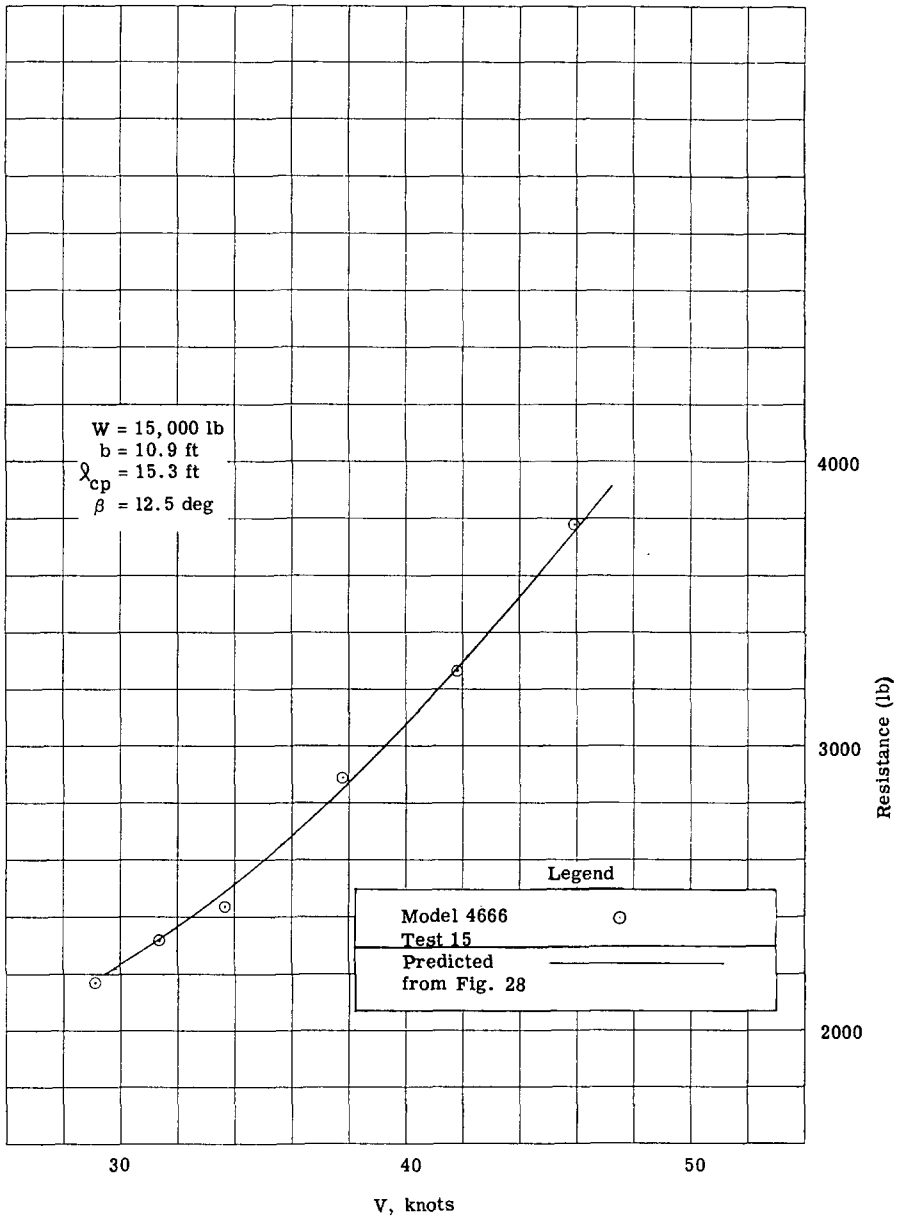

Fig. 29 Comparison of resistance of boat at high speed as predicted from Fig. 28, and as obtained from a model test of the series

Since $\frac{1}{2}\rho$ equals 1.00 for salt water, this simplifies to

$$C_{Lb} = \frac{W}{v^2 b^2}$$

Then

$$v = \frac{1}{b}\left(\frac{W}{C_{Lb}}\right)^{1/2}$$

Values of v are entered in Column F (intermediate steps are given in Columns D and E) and V in knots is put into Column G.

The hypothetical case selected for this sample calculation was chosen to correspond to one of the tests of the series, Test 15 of Model 4666. This was done, of course, to compare a prediction of performance from the curves in Fig. 28 with the prediction from an actual model test. Fig. 29 shows this comparison. The curve in the figure represents values from Table 2 and the symbols are test spots from Test 15 of Model 4666 (these have been corrected by the usual method to a boat weight of 15,000 lb). From the close agreement, it is concluded that the simple method

proposed will give accurate predictions of the high-speed resistance of planing boats of a wide ranges of sizes and proportions.

Acknowledgments

This work had been carried out as part of the Fundamental Hydromechanics Research Program of the Bureau of Ships, which is directed and administered for the Bureau by the Taylor Model Basin. The authors would like at this time to express their particular thanks to Mr. Jacques B. Hadler for his support and encouragement during the carrying out of this project.

This paper represents the work of numerous people besides the authors. Special mention should be made of the contribution of Mr. Charles W. Tate, who did a large part of the work of testing, calculating, and preparing figures. The assistance of Mr. John Pothier and Mr. John Gonnerman in this work is also very much appreciated. The authors are also indebted to Morris Engineering for assistance in the preparation of graphs and tables, and to Mrs. Shirley Childers for preparation of the manuscript.

References

1 K. S. M. Davidson and A. Suarez, "Tests of Twenty Related Models of V-Bottom Motor Boats—EMB Series 50," DTMB Report R-47, March 1949.

2 E. P. Clement, "Development and Model Tests of an Efficient Planing Hull Design," DTMB Report 1314, April 1959.

3 E. P. Clement, "How to use the SNAME Small Craft Data Sheets for Design and for Resistance Prediction," SNAME Technical and Research Bulletin No. 1–23.

4 C. Ridgley-Nevitt, "The Resistance of Trawler Hull Forms of 0.65 Prismatic Coefficient," TRANS. SNAME, vol. 64, 1956, pp. 433–468.

5 W. Sottorf, "Systematic Model Researches on the Stability Limits of the DVL Series of Float Designs," NACA Technical Memorandum 1254, December 1949.

Tables of Test Conditions and Data follow

Model 4665 - Test Conditions

Test No.	Model Weight, lb	$A_P/\nabla^{2/3}$	α_o, deg.	LCG Fwd of Sta. 10, ft	LCG Aft of Centroid of A_P, $\%L_P$	Draft above ℄ at Sta. 10, in.	Water temp., deg F
1	54.50	7.1	0.00	1.62	6	3.09	65.5
2	129.08	4.0	-2.60	1.86	0	4.17	64.5
3	129.08	4.0	0.10	1.70	4	5.37	64.5
4	129.08	4.0	2.77	1.55	8	6.45	64.5
5	129.08	4.0	5.45	1.39	12	7.65	64.5
6	80.07	5.5	-2.65	1.86	0	3.09	64.5
7	80.07	5.5	-0.63	1.70	4	3.69	64.5
8	80.07	5.5	1.35	1.55	8	4.53	64.5
9	80.07	5.5	3.30	1.39	12	5.25	64.5
10	55.77	7.0	-2.19	1.86	0	2.49	64.5
11	54.50	7.1	-0.76	1.70	4	2.97	65.5
12	54.50	7.1	0.80	1.55	8	3.57	65.5
13	54.50	7.1	2.38	1.39	12	4.05	65.5
14	41.35	8.5	-2.05	1.86	0	2.25	65.5
15	41.35	8.5	-0.82	1.70	4	2.49	65.5
16	41.35	8.5	0.42	1.55	8	2.97	65.5
17	41.35	8.5	0.64	1.39	12	3.45	65.5

Model 4666 - Test Conditions

Test No.	Model Weight, lb	$A_P/\nabla^{2/3}$	α_o, deg.	LCG Fwd of Sta. 10, ft	LCG Aft of Centroid of A_P, $\%L_P$	Draft above ℄ at Sta. 10, in.	Water temp., deg F
1	101.80	7.0	0.02	2.53	6	3.68	70.0
2	235.70	4.0	-1.85	2.89	0	5.12	67.0
3	235.70	4.0	0.25	2.65	4	6.44	67.0
4	235.70	4.0	2.30	2.41	8	7.52	67.0
5	235.70	4.0	4.40	2.17	12	8.60	67.0
6	146.20	5.5	-1.70	2.89	0	3.56	67 0
7	146.20	5.5	-0.30	2.65	4	4.40	67.0
8	146.20	5.5	1.12	2.41	8	5.24	67.0
9	146.20	5.5	2.68	2.17	12	6.18	67.0
10	101.80	7.0	-1.53	2.89	0	2.72	70.0
11	101.80	7.0	-0.53	2.65	4	3.32	70.0
12	101.80	7.0	0.55	2.41	8	3.92	67.0
12R	101.80	7.0	0.55	2.41	8	3.92	70.0
13	101.80	7.0	1.75	2.17	12	4.64	67.0
14	76.10	8.5	-1.47	2.89	0	2.48	67.0
15	76.10	8.5	-0.62	2.65	4	2.84	67.0
16	76.10	8.5	0.28	2.41	8	3.20	67.0
17	76.10	8.5	1.23	2.17	12	3.80	67.0

Model 4667-1 - Test Conditions

Test No.	Model Weight, lb	$A_P/\nabla^{2/3}$	α_o, deg.	LCG Fwd of Sta. 10, ft	LCG Aft of Centroid of A_P, $\%L_P$	Draft above ℄ at Sta. 10, in.	Water temp., deg F
1	154.00	7.0	0.10	3.43	6	3.98	67.0
1A	154.00	7.0	0.10	3.43	6	3.98	74 0
2	356.50	4.0	-1.10	3.91	0	5.06	74.0
3	356.50	4.0	0.17	3.59	4	7.22	74.0
4	356.50	4.0	1.80	3.27	8	8.30	74.0
6	221.10	5.5	-1.45	3.91	0	3.74	74.0
7	221.10	5.5	-0.32	3.59	4	4.46	74.0
8	221.10	5.5	0.85	3.27	8	5.54	74.0
9	221.10	5.5	2.16	2.95	12	6.62	74.0
10	154.00	7.0	-1.42	3.91	0	3.02	74.0
11	154.00	7.0	-0.50	3.59	4	3.62	74.0
12	154.00	7.0	0.50	3.27	8	4.22	74.0
13	154.00	7.0	1.50	3.59	12	5.06	74.0
14	115.10	8.5	-1.18	3.91	0	2.42	74.0
15	115.10	8.5	-0.50	3.59	4	3.02	75.0
16	115.10	8.5	0.22	3.27	8	3.50	75.0
17	115.10	8.5	1.00	2.95	12	4.22	75.0

Model 4668 - Test Conditions

Test No.	Model Weight, lb	$A_P/\nabla^{2/3}$	α_o, deg.	LCG Fwd of Sta. 10, ft	LCG Aft of Centroid of A_P, $\%L_P$	Draft above ℄ at Sta. 10, in.	Water temp., deg F
1	98.70	7.0	-0.15	3.47	5	3.25	74.0
2	228.60	4.0	-1.25	3.91	0	4.70	74.0
3	228.60	4.0	-0.05	3.59	4	5.78	74.0
6	141.80	5.5	-1.15	3.91	0	3.14	74.0
7	141.80	5.5	-0.30	3.59	4	3.90	74.0
8	141.80	5.5	0.70	3.27	8	4.70	74.0
9	141.80	5.5	1.87	2.95	12	5.54	74.0
10	98.70	7.0	-1.10	3.91	0	2.54	74.0
11	98.70	7.0	-0.48	3.59	4	3.14	74.0
12	98.70	7.0	0.44	3.27	8	3.74	74.0
13	98.70	7.0	1.09	2.95	12	4.22	74.0
14	73.80	8.5	-1.00	3.91	0	2.06	74.0
15	73.80	8.5	-0.52	3.59	4	2.54	74.0
16	73.80	8.5	0.17	3.27	8	3.02	74.0
17	73.80	8.5	0.95	2.95	12	3.62	74.0

Model 4669 - Test Conditions

Test No.	Model Weight, lb	$A_P/\nabla^{2/3}$	α_o, deg.	LCG Fwd of Sta. 10, ft	LCG Aft of Centroid of A_P, $\%L_P$	Draft above ℄ at Sta. 10, in.	Water temp., deg F
1	68.80	7.0	0.05	3.43	6	3.10	75.0
2	159.20	4.0	-1.13	3.91	0	4.18	75.0
3	159.20	4.0	0.30	3.59	4	5.38	75.0
6	101.80	5.5	-0.93	3.91	0	3.10	75.0
7	101.80	5.5	-0.10	3.59	4	3.58	75.0
8	101.80	5.5	0.82	3.27	8	4.42	75.0
9	101.80	5.5	1.75	2.95	12	5.26	75.0
10	68.80	7.0	-0.82	3.91	0	2.38	75.0
11	68.80	7.0	-0.25	3.59	4	2.74	75.0
12	68.80	7.0	0.42	3.27	8	3.34	75.0
13	68.80	7.0	1.15	2.95	12	3.82	75.0
14	51.40	8.5	-0.80	3.91	0	2.02	75.0
15	51.40	8.5	-0.35	3.59	4	2.38	75.0
16	51.40	8.5	0.33	3.27	8	2.74	75.0
17	51.40	8.5	1.06	2.95	12	3.34	75.0

Model 4665 Test No. 1

V, knots	R_t, lb	Wetted length of keel, ft	Wetted length of chine, ft	Re x 10^{-6}	S, ft^2	10^3 C_t	Change of trim, deg	CG rise, in	F_∇
0.69	0.10	3.75	2.30	0.315	5.89	12.793	0.00	0.00	0.21
1.06	0.20	3.75	2.30	0.483	5.89	10.809	-0.05	-0.08	0.32
1.39	0.40	3.75	2.30	0.634	5.88	12.604	-0.10	-0.12	0.42
1.63	0.59	3.75	2.30	0.743	5.84	13 857	-0.10	-0.07	0.50
1.76	0.74	3.80	2.60	0.849	6.18	14.046	-0.15	-0.15	0.54
2.10	1.21	3.80	2.40	0.981	5.98	16.587	-0.30	-0.20	0.64
2.43	1.99	3.85	2.20	1.108	5.84	20.849	-0.40	-0.32	0.74
2.43	1.99	3.85	2.40	1.144	6.02	20.205	-0.40	-0.27	0.74
2.78	3.06	3.85	2.00	1.225	5.69	25.188	-0.45	-0.40	0.85
3.23	5.37	3.80	3.20	1.704	6.60	28.257	0.70	-0.53	0.98
4.08	8.21	3.60	2.60	1.906	5.98	29.863	5.40	-0.14	1.24
4.92	8.24	3.40	2.20	2.076	5.33	23.094	6.55	0.39	1.50
5.54	8.32	3.15	2.00	2.150	4.78	20.526	6.90	0.87	1.69
6.54	8.04	3.00	1.80	2.365	4.38	15.539	6.50	1.20	1.99
7.32	7.76	2.90	1.60	2.482	4.03	13.011	5.90	1.39	2.23
8.14	7.63	2.90	1.50	2.699	3.91	10.648	5.30	1.54	2.48
8.98	7.64	2.90	1.40	2.909	3.80	9.030	4.70	1.68	2.73
9.72	7.86	2.90	1.20	3.003	3.57	8.431	4.25	1.83	2.96
10.56	8.21	2.90	1.10	3.183	3.46	7.711	3.85	1.76	3.22
11.42	8.66	3.00	1.00	3.442	3.46	6.955	3.50	1.87	3.48
12.22	9.16	3.10	0.90	3.683	3.46	6.426	3.28	1.84	3.72
13.11	9.85	3.15	0.80	3.902	3.40	6.103	3.00	1.83	3.99
14.74	11.44	3.20	0.60	4.220	3.23	5.890	2.65	1.94	4.49
16.38	13.12	3.20	0.40	4.443	3.02	5.864	2.33	2.05	4.99
18.02	15.06	3.25	0.20	4.684	2.86	5.863	2.14	2.06	5.49
19.64	16.90	3.30	0.00	4.883	2.71	5.848	2.00	2.05	5.98

Model 4665 Test No. 2

V, knots	R_t, lb	Wetted length of keel, ft	Wetted length of chine, ft	Re x 10^{-6}	S, ft^2	10^3 C_t	Change of trim, deg	CG rise, in	F_∇
0.69	0.18	3.90	3.60	0.385	7.36	18.507	-0.05	0.01	0.18
1.06	0.30	3.95	3.60	0.595	7.39	12.970	-0.15	-0.06	0.28
1.35	0.52	4.00	3.95	0.797	7.46	13.728	-0.35	-0.10	0.36
1.76	0.89	4.00	4.00	1.046	7.46	13.985	-0.65	-0.22	0.46
1.90	1.15	4.00	4.00	1.129	7.46	15.478	-1.60	-0.15	0.50
2.10	1.53	4.05	4.00	1.256	7.42	16.919	-1.00	-0.42	0.55
2.42	3.09	4.10	4.05	1.466	7.38	25.836	-1.55	1.54	0.64
2.76	4.93	4.10	4.10	1.682	7.59	30.875	-1.55	-0.96	0.73
2.77	4.98	3.90	4.10	1.647	7.64	30.760	-1.25	-1.15	0.73

Model 4665 Test No. 3

V, knots	R_t, lb	Wetted length of keel, ft	Wetted length of chine, ft	Re x 10^{-6}	S, ft^2	10^3 C_t	Change of trim, deg	CG rise in	F_∇
0.69	0.20	3.85	3.30	0.367	7.47	20.622	-0.02	0.01	0.18
1.06	0.45	3.85	3.30	0.563	7.43	19.616	-0.10	-0.07	0.28
1.39	0.72	3.90	3.40	0.754	7.48	18.082	-0.15	-0.16	0.37
1.76	1.25	3.90	3.60	0.981	7.55	19.349	-0.38	-0.29	0.46
1.90	1.60	3.90	3.60	1.059	7.60	21.099	-0.45	-0.22	0.50
2.09	2.05	3.90	3.90	1.211	7.78	21.828	-0.55	-0.44	0.55
2.43	3.60	4.00	4.00	1.444	7.82	28.187	-0.85	-0.55	0.64
2.75	5.29	4.00	4.00	1.635	8.02	31.586	-1.10	-0.67	0.73
2.78	5.59	4.00	4.00	1.653	8.02	32.658	-1.10	-0.82	0.73
3.80	18.63	4.10	4.10	2.315	8.04	58.070	1.40	-1.12	1.00
4.77	30.01	3.80	3.40	2.552	7.08	67.412	7.50	-0.09	1.26
5.70	29.88	3.40	2.60	2.541	5.74	58.011	12.95	1.76	1.50
6.63	28.18	3.20	2.30	2.709	5.17	44.870	12.20	2.68	1.75
7.60	25.86	3.00	2.10	2.880	4.72	34.299	10.90	3.26	2.00
8.54	23.72	2.60	1.90	2.856	4.03	29.204	9.55	3.51	2.25
9.69	21.76	2.50	1.80	3.096	3.80	22.078	9.15	3.48	2.56
10.42	20.74	2.70	1.70	3.407	3.91	17.659	7.30	3.82	2.75
11.36	19.84	2.70	1.60	3.630	3.80	14.645	6.55	4.00	3.00
12.30	19.37	2.70	1.50	3.839	3.68	12.580	5.80	4.17	3.24

Model 4665 Test No. 4

V, knots	R_t, lb	Wetted length of keel, ft	Wetted length of chine, ft	Re x 10^{-6}	S, ft^2	10^3 C_t	Change of trim, deg	CG rise, in	F_∇
0.69	0.30	3.80	3.00	0.349	7.41	30.677	0.03	-0.01	0.18
1.06	0.55	3.80	3.00	0.536	7.38	23.911	-0.07	0.02	0.28
1.39	1.00	3.80	3.10	0.713	7.48	24.939	-0.07	-0.08	0.37
1.73	1.64	3.85	3.20	0.906	7.57	26.247	-0.17	-0.14	0.46
1.90	1.99	3.85	3.10	0.981	7.51	26.596	0.13	-0.24	0.50
2.10	2.42	3.90	3.20	1.108	7.60	26.120	-0.27	-0.26	0.55
2.44	4.09	3.90	3.40	1.324	7.49	33.170	-0.07	-0.38	0.64
2.74	5.98	3.90	3.60	1.527	7.66	37.634	-0.01	-0.40	0.72
2.78	6.08	3.90	3.60	1.549	7.66	37.167	0.13	-0.54	0.73
3.81	19.46	3.80	3.60	2.095	7.80	62.218	3.01	0.03	1.00
4.75	33.14	3.30	2.60	2.082	5.95	89.365	4.45	3.49	1.25
5.70	33.47	3.00	2.20	2.202	4.84	77.057	13.05	2.00	1.50
6.60	30.04	2.80	2.00	2.354	4.38	56.992	11.35	2.92	1.74
7.60	27.10	2.60	1.80	2.485	3.91	43.383	9.38	3.48	2.00
8.50	24.51	2.40	1.70	2.589	3.57	34.399	6.15	4.41	2.24
9.64	22.46	2.40	1.60	2.865	3.46	25.305	6.13	4.32	2.54

Model 4665 Test No. 5

V, knots	R_t, lb	Wetted length of keel, ft	Wetted length of chine, ft	Re x 10^{-6}	S, ft^2	10^3 C_t	Change of trim, deg	CG rise, in	F_∇
0.69	0.38	3.70	2.70	0.328	7.20	40.041	0.10	-0.04	0.18
1.05	0.70	3.70	2.80	0.507	7.35	31.154	0.15	-0.05	0.28
1.36	1.30	3.75	2.70	0.652	7.26	34.902	0.25	-0.14	0.36
1.83	2.09	3.75	2.80	0.891	7.44	30.406	0.35	-0.17	0.48
1.89	2.79	3.75	2.80	0.920	7.32	38.639	0.45	-0.16	0.50
2.09	3.19	3.80	2.80	1.025	7.33	36.038	0.45	-0.11	0.55
2.43	4.54	3.80	2.80	1.192	7.38	37.643	0.75	-0.37	0.64
2.75	7.03	3.80	2.80	1.349	7.46	45.090	1.55	-0.45	0.73
2.78	6.98	3.80	2.80	1.363	7.17	45.564	1.50	-0.43	0.73
3.79	22.64	3.40	2.80	1.746	6.51	87.686	8.21	0.00	1.00
4.73	38.39	2.80	2.20	1.757	4.85	128.050	14.45	1.53	1.25
5.69	37.04	2.40	1.90	1.818	3.80	108.990	13.30	2.83	1.50
6.60	33.67	2.20	1.70	1.913	3.34	83.631	10.85	3.58	1.74
7.59	28.85	2.00	1.60	2.030	3.02	60.044	9.30	4.22	2.00

Model 4665 Test No. 6

V, knots	R_t, lb	Wetted length of keel, ft	Wetted length of chine, ft	Re x 10^{-6}	S, ft^2	10^3 C_t	Change of trim, deg	CG rise, in	F_∇
0.70	0.20	3.85	3.10	0.361	6.60	22.260	-0.05	-0.09	0.20
1.06	0.20	3.85	3.10	0.547	6.60	9.635	-0.15	-0.06	0.30
1.39	0.40	3.85	3.20	0.728	6.70	11.061	-0.30	-0.11	0.40
1.77	0.59	3.90	3.20	0.934	6.70	10.222	-0.55	-0.24	0.51
2.05	0.67	3.90	3.20	1.082	6.73	8.576	-0.55	-0.24	0.59
2.10	1.19	3.95	3.95	1.233	6.92	14.113	-0.85	-0.36	0.60
2.42	2.14	4.00	4.00	1.439	6.92	19.067	-1.50	-0.57	0.69
2.62	2.88	4.00	4.00	1.557	7.06	21.537	-1.95	-0.65	0.75
2.78	3.68	4.05	4.05	1.673	7.10	24.276	-2.30	-0.75	0.79
3.51	11.12	4.10	4.10	2.139	7.38	44.240	-1.65	-1.43	1.00
4.36	18.15	4.00	4.00	2.592	7.02	49.242	6.05	-0.21	1.25
5.23	18.93	3.80	3.20	2.720	6.74	37.151	7.10	0.09	1.49
6.12	14.51	3.70	2.50	2.819	5.91	23.729	9.15	1.02	1.75
7.00	13.58	3.40	2.30	2.965	5.38	18.622	9.26	1.44	2.00
7.86	12.79	3.30	2.10	3.154	5.06	14.805	8.65	1.86	2.24
8.76	12.48	3.30	1.90	3.385	4.84	12.168	8.15	2.10	2.50
9.64	12.26	3.20	1.80	3.581	4.61	10.357	7.75	2.11	2.75
10.54	12.38	3.20	1.70	3.837	4.49	8.975	7.25	2.25	3.01
11.38	12.77	3.30	1.60	4.143	4.49	7.937	6.85	2.36	3.25
12.24	13.06	3.30	1.50	4.365	4.38	7.206	6.50	2.46	3.50
13.32	13.49	3.30	1.40	4.652	4.26	6.455	6.15	2.56	3.80
14.00	14.29	3.35	1.30	4.837	4.20	6.276	5.90	2.63	4.00
15.84	16.15	3.35	1.10	5.237	3.97	5.864	5.75	2.67	4.52
17.62	18.49	3.40	0.80	5.499	3.68	5.852	5.20	2.73	5.03
19.34	21.08	3.40	0.70	5.892	3.57	5.713	4.95	2.60	5.52
21.18	23.63	3.40	0.50	6.138	3.34	5.700	4.75	2.65	6.05

Model 4665 Test No. 7

V, knots	R_t, lb	Wetted length of keel, ft	Wetted length of chine, ft	Re x 10^{-6}	S, ft^2	10^3 C_t	Change of trim, deg	CG rise, in	F_∇
0.69	0.11	3.75	2.80	0.336	6.51	12.730	0.03	-0.11	0.20
1.07	0.34	3.80	2.90	0.533	6.63	16.097	-0.02	-0.09	0.31
1.39	0.50	3.80	2.90	0.692	6.63	14.006	-0.17	-0.15	0.40
1.75	0.87	3.85	2.90	0.878	6.63	15.566	-0.27	-0.22	0.50
1.76	1.89	3.85	2.90	0.883	6.64	33.313	-0.32	-0.20	0.50
2.09	1.49	3.85	2.70	1.017	6.43	19.206	-0.52	-0.34	0.60
2.42	2.38	3.90	3.90	1.403	7.05	20.825	-0.87	-0.44	0.69
2.64	3.13	3.90	3.90	1.530	7.11	22.875	-0.97	-0.51	0.75
2.79	3.68	3.95	3.95	1.638	7.12	24.022	-0.97	-0.66	0.80
3.54	9.57	4.00	4.00	2.104	7.46	37.053	0.73	-1.02	1.01
4.37	15.35	3.70	3.10	2.208	6.63	43.901	7.08	-0.11	1.25
5.22	14.51	3.45	2.50	2.308	5.78	33.353	9.03	0.71	1.49
6.14	13.98	3.10	2.20	2.418	4.95	27.118	9.23	1.45	1.75
6.98	13.33	3.00	2.00	2.593	4.61	21.472	8.63	1.83	1.99
7.84	12.64	2.90	1.90	2.796	4.38	16.999	7.78	2.08	2.24
8.72	11.90	2.90	1.70	2.980	4.15	13.664	6.98	2.32	2.49
9.58	11.61	2.90	1.60	3.203	4.03	11.363	6.23	2.44	2.74
10.52	11.51	2.90	1.50	3.439	3.91	9.619	5.63	2.52	3.00
11.34	11.57	2.90	1.40	3.623	3.80	8.570	5.18	2.55	3.24
12.24	11.88	2.90	1.30	3.820	3.68	7.792	4.63	2.47	3.50
13.16	12.40	3.00	1.20	4.107	3.68	7.035	4.43	2.58	3.76
14.06	12.89	3.10	1.10	4.388	3.68	6.405	4.13	2.63	4.02
15.82	14.80	3.20	0.90	4.819	3.57	5.995	3.63	2.82	4.52
17.58	16.60	3.20	0.70	5.094	3.34	5.810	3.28	2.82	5.02
19.32	18.93	3.30	0.50	5.455	3.23	5.674	3.08	2.78	5.52
19.34	18.98	3.20	0.50	5.317	3.13	5.874	3.08	2.68	5.52
21.18	21.26	3.30	0.40	5.823	3.13	5.488	2.60	2.72	6.05

Model 4665 Test No. 8

V, knots	R_t, lb	Wetted length of keel, ft	Wetted length of chine, ft	Re x 10^{-6}	S, ft^2	10^3 C_t	Change of trim, deg	CG rise, in	F_∇
0.69	0.20	3.70	2.60	0.323	6.42	23.564	0.00	0.00	0.20
1.04	0.40	3.75	2.60	0.491	6.47	20.579	0.00	-0.10	0.30
1.38	0.67	3.75	2.70	0.661	6.53	19.382	0.00	-0.10	0.39
1.75	1.09	3.80	2.70	0.845	6.57	19.663	-0.05	-0.18	0.50
1.77	1.09	3.80	2.70	0.855	6.59	19.148	-0.05	-0.18	0.51
2.08	1.79	3.85	2.60	0.997	6.50	23.022	-0.05	-0.28	0.59
2.43	2.79	3.85	2.50	1.147	6.42	26.577	-0.15	-0.35	0.69
2.62	3.48	3.85	2.40	1.217	6.34	28.967	-0.15	-0.35	0.75
2.78	3.98	3.90	3.90	1.611	7.24	25.749	0.00	-0.50	0.79
3.50	9.82	3.80	3.40	1.872	6.98	41.574	2.95	-0.70	1.00
4.34	14.98	3.40	2.50	1.903	5.94	48.473	8.55	0.10	1.24
5.20	16.13	3.00	2.20	2.009	4.84	44.628	11.22	0.41	1.49
6.11	15.49	2.60	1.90	2.043	4.03	37.246	9.13	1.61	1.75
6.96	14.26	2.40	1.80	2.172	3.68	28.912	7.95	2.01	1.99
7.86	13.06	2.50	1.70	2.453	3.68	20.771	6.75	2.31	2.24
8.74	12.30	2.60	1.50	2.663	3.57	16.329	5.75	2.45	2.50
9.58	11.71	2.60	1.40	2.847	3.46	13.363	4.85	2.55	2.74
10.52	11.46	2.70	1.30	3.127	3.46	10.846	4.15	2.69	3.00
11.42	11.46	2.70	1.20	3.309	3.34	9.510	3.55	2.59	3.26
12.26	11.71	2.80	1.10	3.553	3.34	8.430	3.15	2.63	3.50

Model 4665 Test No. 9

V, knots	R_t, lb	Wetted length of keel, ft	Wetted length of chine, ft	Re x 10^3	S, ft^2	10^3 C_t	Change of trim, deg	CG rise, in	F_∇
0.69	0.22	3.70	2.30	0.308	6.22	26.794	0.10	-0.04	0.20
1.06	0.50	3.70	2.30	0.473	6.22	25.784	0.15	-0.05	0.30
1.39	0.88	3.75	2.30	0.625	6.28	26.109	0.20	-0.07	0.40
1.75	1.37	3.75	2.30	0.787	6.26	25.899	0.25	-0.09	0.50
1.76	1.49	3.75	2.30	0.791	6.26	27.842	0.30	-0.11	0.50
2.09	2.19	3.75	2.40	0.955	6.34	28.630	0.40	-0.14	0.60
2.42	3.29	3.80	2.40	1.115	6.43	31.596	0.60	-0.31	0.69
2.61	4.48	3.80	2.30	1.183	6.31	37.757	1.00	-0.25	0.75
2.78	4.83	3.75	2.30	1.250	6.26	36.163	1.20	-0.33	0.79
3.50	11.17	3.55	2.20	1.495	5.81	56.785	5.50	-0.25	1.00
4.38	15.01	2.90	2.20	1.660	4.93	57.391	10.00	0.67	1.25
5.22	18.31	2.50	1.90	1.707	3.91	62.132	10.35	1.65	1.49
6.10	16.86	2.40	1.70	1.858	3.57	45.924	10.72	1.62	1.74
6.98	15.14	2.20	1.50	1.919	3.13	35.970	9.28	1.93	1.99
7.84	13.78	2.20	1.40	2.097	3.02	26.882	5.70	2.78	2.24
8.74	12.65	2.20	1.30	2.273	2.91	20.574	4.50	2.91	2.50
9.60	11.86	2.30	1.20	2.497	2.91	15.987	3.50	2.96	2.74

Model 4665 Test No. 10

V, knots	R_t, lb	Wetted length of keel, ft	Wetted length of chine, ft	Re x 10^{-6}	S, ft^2	10^3 C_t	Change of trim, deg	CG rise, in	F_∇
0.68	0.00	3.75	2.70	0.326	6.09	-0.114	-0.06	0.02	0.21
0.69	0.12	3.75	2.60	0.326	6.01	15.062	-0.06	0.02	0.21
1.05	0.30	3.75	2.60	0.495	6.01	16.256	-0.11	-0.17	0.32
1.40	0.35	3.80	2.70	0.676	6.14	10.398	-0.26	-0.13	0.42
1.62	0.49	3.80	2.70	0.782	6.14	11.100	-0.41	-0.19	0.49
1.75	0.51	3.80	2.70	0.845	6.14	9.877	-0.51	-0.26	0.53
2.09	0.99	3.85	2.50	0.986	6.01	13.642	-0.81	-0.27	0.63
2.11	1.24	3.90	3.90	1.223	6.86	14.694	0.99	-0.08	0.64
2.40	1.64	3.90	3.90	1.391	6.80	15.117	-1.31	-0.43	0.73
2.42	1.69	3.90	3.90	1.403	6.80	15.320	-1.26	-0.44	0.73
2.50	1.96	3.90	3.90	1.449	6.80	16.731	-1.36	-0.41	0.76
2.78	2.78	3.90	3.90	1.611	6.80	19.152	-1.86	-0.57	0.84
3.22	5.97	3.95	3.95	1.890	6.90	30.212	-2.06	-0.92	0.98
3.38	6.85	3.95	3.95	1.984	6.90	31.473	-1.71	-1.02	1.03
4.06	11.76	3.90	3.90	2.353	6.88	37.503	2.79	-0.89	1.23
4.88	12.14	3.70	3.00	2.429	6.35	29.035	5.09	0.01	1.48
5.07	11.94	3.70	2.80	2.449	6.18	27.209	5.34	0.09	1.54
5.66	10.32	3.60	2.50	2.565	5.80	20.086	6.24	0.58	1.72
5.91	9.81	3.60	2.40	2.635	5.69	17.874	5.49	0.95	1.79
6.50	9.01	3.55	2.20	2.777	5.44	14.201	6.89	1.05	1.97
6.72	8.73	3.50	2.20	2.846	5.38	13.001	7.34	0.92	2.04
7.34	8.56	3.45	2.00	2.972	5.12	11.242	6.79	1.28	2.23
8.14	8.38	3.40	1.90	3.206	4.95	9.246	6.59	1.44	2.47
8.96	8.29	3.40	1.70	3.395	4.72	7.913	6.19	1.65	2.72
9.76	8.65	3.40	1.50	3.554	4.49	7.315	5.89	1.83	2.96
10.60	9.01	3.40	1.40	3.781	4.38	6.627	5.59	1.82	3.22
11.42	9.41	3.40	1.30	3.988	4.26	6.128	5.34	1.89	3.46
12.24	9.93	3.40	1.20	4.184	4.15	5.786	5.11	1.85	3.71
13.04	10.78	3.40	1.10	4.360	4.03	5.692	5.04	1.87	3.96
14.70	12.59	3.40	0.90	4.697	3.80	5.550	4.59	2.00	4.46
16.40	15.00	3.40	0.70	4.996	3.57	5.655	4.39	2.06	4.98
18.04	17.43	3.40	0.50	5.228	3.34	5.796	4.19	2.11	5.47
19.64	19.68	3.40	0.30	5.399	3.13	5.906	3.99	2.07	5.96

Model 4665 Test No. 11

V, knots	R_t, lb	Wetted length of keel, ft	Wetted length of chine, ft	Re x 10^{-6}	S, ft^2	10^3 C_t	Change of trim, deg	CG rise, in	F_∇
0.69	0.10	3.75	2.40	0.320	5.95	12.659	-0.04	0.01	0.21
1.05	0.25	3.75	2.40	0.486	5.95	13.661	-0.09	-0.02	0.32
1.62	0.39	3.80	2.40	0.757	5.97	9.105	-0.19	-0.04	0.49
1.62	0.59	3.80	2.40	0.757	5.98	13.705	-0.34	0.00	0.49
1.77	0.64	3.80	2.50	0.840	6.04	12.295	-0.39	-0.08	0.54
2.11	1.17	3.85	2.40	0.993	5.99	15.860	-0.49	-0.26	0.64
2.44	1.99	3.85	2.20	1.112	5.82	20.737	-0.74	-0.28	0.74
2.45	1.93	3.85	2.30	1.135	5.89	19.697	-0.74	-0.38	0.75
2.79	3.02	3.85	2.40	1.314	6.02	23.342	-1.04	-0.50	0.85
3.34	5.47	3.85	3.20	1.774	6.62	26.839	-0.19	0.36	1.02
4.07	9.11	3.70	3.00	2.054	6.37	31.243	4.66	0.81	1.24
4.90	8.49	3.60	2.40	2.215	5.77	22.196	5.96	0.52	1.49
5.72	8.02	3.45	2.10	2.391	5.22	16.974	6.76	0.98	1.74
6.58	7.69	3.25	1.90	2.553	4.78	13.444	6.56	1.34	2.00
7.34	7.44	3.15	1.80	2.737	4.55	10.982	6.16	1.56	2.24
8.14	7.35	3.10	1.60	2.882	4.26	9.418	5.66	1.81	2.48
8.94	7.24	3.10	1.40	3.031	4.03	8.140	5.16	1.76	2.72
9.78	7.65	3.10	1.30	3.242	3.91	7.399	4.81	1.76	2.98
10.62	8.01	3.20	1.20	3.520	3.91	6.566	4.36	1.80	3.23
11.42	8.46	3.20	1.10	3.699	3.80	6.183	4.06	1.89	3.48
12.22	8.91	3.25	1.00	3.912	3.74	5.775	3.91	1.83	3.72
13.00	9.81	3.25	0.90	4.064	3.63	5.795	3.66	1.91	3.96
14.70	11.51	3.30	0.70	4.429	3.46	5.577	3.26	2.03	4.48
16.42	13.45	3.30	0.50	4.700	3.23	5.582	3.06	2.09	5.00
18.04	15.45	3.35	0.30	4.960	3.07	5.595	2.86	2.05	5.49
19.66	17.54	3.35	0.10	5.109	2.86	5.740	2.71	2.09	5.99

Model 4665 Test No. 12

V, knots	R_t, lb	Wetted length of keel, ft	Wetted length of chine, ft	Re x 10^{-6}	S, ft^2	10^3 C_t	Change of trim, deg	CG rise, in	F_∇
0.69	0.10	3.70	2.30	0.312	5.54	13.609	-0.10	-0.07	0.21
1.06	0.20	3.70	2.30	0.479	5.54	11.498	-0.15	-0.05	0.32
1.39	0.45	3.75	2.30	0.633	5.59	14.926	-0.20	-0.03	0.42
1.62	0.69	3.75	2.30	0.738	5.59	17.111	0.00	-0.05	0.49
1.77	0.79	3.75	2.40	0.820	5.71	16.045	-0.25	-0.07	0.54
2.09	1.34	3.80	2.40	0.976	5.75	19.290	-0.25	-0.12	0.64
2.41	2.14	3.80	2.20	1.089	5.52	24.135	0.00	-0.25	0.73
2.42	2.09	3.80	2.40	1.130	5.79	22.264	-0.25	-0.27	0.74
2.78	3.08	3.85	2.60	1.351	6.09	23.686	-0.10	-0.37	0.85
3.23	5.50	3.75	3.00	1.642	6.46	29.568	1.35	-0.46	0.98
4.06	8.01	3.50	2.50	1.835	5.47	32.143	5.55	-0.08	1.24
4.92	8.54	3.20	2.10	1.964	4.40	29.012	6.80	0.49	1.50
5.70	8.52	2.90	1.90	2.061	3.58	26.507	6.90	1.06	1.74
6.52	8.19	2.70	1.70	2.161	3.01	23.183	6.35	1.35	1.99
7.36	7.86	2.70	1.50	2.329	2.74	19.158	5.50	1.63	2.24
8.10	7.65	2.70	1.40	2.502	2.61	16.143	4.80	1.77	2.47
8.96	7.59	2.70	1.30	2.700	2.49	13.735	4.15	1.79	2.73
9.78	7.73	2.80	1.20	2.947	2.49	11.741	3.65	1.86	2.98
10.62	8.01	2.80	1.10	3.120	2.38	10.820	3.25	1.90	3.23
11.42	8.26	2.85	1.00	3.312	2.32	9.889	2.90	1.91	3.48
12.22	8.71	2.90	0.90	3.498	2.26	9.329	2.60	1.97	3.72
13.10	9.31	3.00	0.70	3.651	2.16	9.093	2.35	1.95	3.99
14.74	10.74	3.65	0.50	4.608	2.68	6.679	1.90	2.05	4.49
16.38	12.58	3.20	0.40	4.442	2.06	8.242	1.60	2.16	4.99
18.04	14.37	3.20	0.20	4.620	1.88	8.489	1.40	2.17	5.49
19.64	16.10	3.20	0.00	4.734	1.74	8.690	1.30	2.21	5.98

Model 4665 Test No. 13

V, knots	R_t, lb	Wetted length of keel, ft	Wetted length of chine, ft	Re x 10^{-6}	S, ft^2	10^3 C_t	Change of trim, deg	CG rise, in	F_∇
0.69	0.05	3.70	2.10	0.301	5.74	6.496	0.02	-0.01	0.21
1.04	0.25	3.70	2.10	0.454	5.73	14.475	0.07	-0.02	0.32
1.39	0.55	3.70	2.10	0.607	5.73	17.851	0.12	-0.04	0.42
1.66	0.79	3.70	2.20	0.738	5.86	17.791	0.02	-0.01	0.51
1.76	1.04	3.75	2.20	0.789	5.86	20.782	0.22	-0.08	0.54
2.09	1.64	3.75	2.20	0.937	5.86	23.173	0.42	-0.25	0.64
2.42	2.34	3.75	2.10	1.066	5.76	25.051	0.62	-0.22	0.74
2.43	2.49	3.75	2.20	1.089	5.85	26.051	0.62	-0.22	0.74
2.79	3.58	3.70	2.10	1.219	5.71	29.147	1.27	-0.35	0.85
3.25	6.17	3.60	2.40	1.469	5.88	35.982	3.42	-0.26	0.99
4.07	9.51	3.10	2.10	1.594	5.00	41.569	7.12	0.18	1.24
4.91	10.29	2.40	1.80	1.554	3.68	41.933	7.90	0.91	1.50
5.80	9.61	2.30	1.60	1.704	3.34	30.927	7.22	1.45	1.77
6.55	8.89	2.30	1.40	1.826	3.13	23.996	5.92	1.81	1.99
7.33	8.36	2.30	1.30	1.988	3.02	18.661	4.92	1.91	2.23
8.98	7.79	2.30	1.10	2.300	2.81	12.442	3.12	2.10	2.73
9.76	7.75	2.40	1.00	2.500	2.81	10.481	2.42	2.14	2.97
10.62	7.76	2.40	0.90	2.640	2.71	9.185	2.02	2.18	3.23

Model 4665 Test No. 14

V, knots	R_t, lb	Wetted length of keel, ft	Wetted length of chine, ft	Re x 10^{-6}	S, ft^2	10^3 C_t	Change of trim, deg	CG rise, in	F_∇
0.69	0.10	3.70	2.20	0.307	5.59	13.478	-0.06	-0.03	0.22
1.04	0.20	3.75	2.20	0.466	5.64	11.731	-0.16	-0.05	0.33
1.40	0.30	3.80	2.30	0.643	5.78	9.436	-0.33	-0.11	0.45
1.59	0.39	3.80	2.40	0.743	5.88	9.602	-0.40	-0.09	0.51
1.76	0.49	3.85	2.40	0.829	5.92	9.722	-0.50	-0.16	0.56
2.10	0.89	3.85	2.30	0.973	5.83	12.520	-0.83	-0.26	0.67
2.35	1.29	3.85	2.20	1.071	5.74	14.701	-1.16	-0.32	0.75
2.42	1.49	3.85	2.10	1.085	5.64	16.285	-1.33	-0.32	0.77
2.78	2.48	3.90	3.40	1.529	6.65	17.480	-1.78	-0.50	0.89
3.16	4.38	3.90	3.20	1.690	6.55	24.222	-2.29	-0.10	1.01
3.94	8.91	3.80	3.00	2.018	6.37	32.621	1.47	0.13	1.26
4.70	9.24	3.70	2.80	2.301	6.14	24.686	3.80	-0.18	1.50
5.52	8.72	3.65	2.40	2.516	5.76	17.989	4.50	0.23	1.76
6.30	7.70	3.60	2.10	2.705	5.42	12.963	5.07	0.56	2.01
7.04	6.87	3.55	1.90	2.890	5.12	9.811	5.37	0.83	2.24
7.84	6.99	3.50	1.70	3.071	4.84	8.511	5.39	1.02	2.50
8.62	7.06	3.50	1.50	3.247	4.61	7.459	5.27	1.16	2.75
9.44	7.25	3.50	1.40	3.485	4.49	6.552	5.07	1.26	3.01
10.20	7.73	3.40	1.20	3.535	4.15	6.487	4.87	1.37	3.25
11.00	8.39	3.40	1.10	3.729	4.03	6.225	4.67	1.38	3.51
11.82	8.99	3.40	1.00	3.918	3.91	5.949	4.52	1.42	3.77
12.58	9.69	3.45	0.80	4.028	3.74	5.924	4.37	1.46	4.01
14.18	11.38	3.45	0.60	4.326	3.51	5.830	4.17	1.52	4.52
15.82	13.45	3.45	0.40	4.588	3.29	5.913	3.97	1.63	5.04
17.36	15.67	3.45	0.10	4.642	2.97	6.344	3.82	1.62	5.54
18.98	17.26	3.45	0.00	4.933	2.86	6.060	3.77	1.63	6.05

Model 4665 Test No. 15

V, knots	R_t, lb	Wetted length of keel, ft	Wetted length of chine, ft	Re x 10^{-6}	S, ft^2	10^3 C_t	Change of trim, deg	CG rise, in	F_∇
0.68	0.10	3.70	2.10	0.297	5.50	14.107	0.00	0.00	0.22
1.04	0.20	3.75	2.10	0.458	5.54	11.930	-0.08	0.02	0.33
1.38	0.35	3.75	2.10	0.608	5.55	11.844	-0.13	-0.01	0.44
1.59	0.49	3.75	2.10	0.701	5.55	12.750	-0.18	-0.05	0.51
1.78	0.59	3.80	2.30	0.818	5.79	11.688	-0.18	-0.15	0.57
2.08	1.19	3.80	2.40	0.971	5.88	16.936	-0.43	-0.17	0.66
2.33	1.39	3.85	2.10	1.044	5.64	16.398	-0.63	-0.21	0.74
2.40	1.54	3.85	2.30	1.112	5.84	16.521	-0.63	-0.26	0.77
2.76	2.48	3.85	1.90	1.196	5.51	21.404	-0.78	-0.42	0.88
3.14	4.08	3.80	3.40	1.703	6.70	22.344	-0.33	-0.50	1.00
3.94	6.61	3.70	2.80	1.929	6.18	24.960	3.42	-0.32	1.26
4.72	6.24	3.60	2.30	2.098	5.63	18.021	4.47	0.17	1.51
5.50	6.02	3.50	2.10	2.320	5.29	13.617	5.12	0.57	1.75
6.26	5.60	3.45	1.90	2.523	5.01	10.332	5.32	0.81	2.00
7.04	5.42	3.35	1.70	2.678	4.67	8.486	5.12	1.02	2.24
7.86	5.44	3.30	1.50	2.842	4.38	7.280	4.82	1.16	2.51
8.62	5.56	3.30	1.40	3.052	4.26	6.352	4.52	1.35	2.75
9.42	5.77	3.30	1.20	3.193	4.03	5.841	4.22	1.39	3.00
10.20	6.33	3.30	1.10	3.381	3.91	5.627	4.02	1.50	3.25
11.00	7.24	3.30	0.90	3.480	3.68	5.877	3.67	1.50	3.51
11.76	7.84	3.30	0.80	3.632	3.57	5.750	3.47	1.56	3.75
12.58	8.79	3.30	0.70	3.791	3.46	5.816	3.32	1.51	4.01
14.19	10.33	3.35	0.50	4.115	3.29	5.644	3.07	1.53	4.52
15.78	11.90	3.35	0.30	4.339	3.07	5.632	2.87	1.69	5.03
17.40	13.61	3.35	0.10	4.522	2.86	5.686	2.72	1.69	5.55
18.98	15.16	3.35	0.00	4.790	2.76	5.518	2.62	1.72	6.05

Model 4665 Test No. 16

V, knots	R_t, lb	Wetted length of keel, ft	Wetted length of chine, ft	Re x 10^{-6}	S, ft^2	10^3 C_t	Change of trim, deg	CG rise, in	F_∇
0.68	0.10	3.70	1.90	0.287	5.34	14.533	0.00	0.00	0.22
1.04	0.20	3.70	1.90	0.439	5.34	12.391	-0.02	0.06	0.33
1.39	0.40	3.75	1.90	0.592	5.38	13.776	-0.02	0.01	0.44
1.69	0.54	3.75	1.90	0.719	5.39	12.771	0.00	0.00	0.54
1.76	0.69	3.75	2.10	0.776	5.60	14.457	-0.07	0.02	0.56
2.08	1.17	3.75	2.10	0.917	5.59	17.490	-0.02	-0.04	0.66
2.34	1.64	3.80	2.00	1.022	5.56	19.467	-0.02	-0.14	0.75
2.42	1.71	3.80	2.00	1.057	5.57	18.935	-0.07	-0.13	0.77
2.78	2.64	3.80	1.80	1.173	5.36	23.066	0.18	-0.26	0.89
3.16	3.98	3.70	1.80	1.309	5.28	27.276	1.13	-0.38	1.01
3.90	5.36	3.60	2.30	1.733	5.70	22.382	4.48	-2.92	1.24
4.72	5.64	3.45	2.10	1.973	5.28	17.366	5.28	0.31	1.51
5.50	5.57	3.15	1.80	2.051	4.55	14.648	5.63	0.69	1.75
6.24	5.45	2.95	1.60	2.139	4.09	12.393	5.28	0.91	1.99
7.02	5.37	2.85	1.50	2.300	3.86	10.235	4.78	1.18	2.24
7.83	5.44	2.85	1.30	2.448	3.63	8.860	4.23	1.31	2.50
8.62	5.61	2.85	1.20	2.630	3.51	7.777	3.78	1.42	2.75
9.40	5.59	2.90	1.10	2.832	3.46	6.627	3.38	1.45	3.00
10.18	6.23	3.00	0.90	2.991	3.34	6.508	3.03	1.57	3.25
11.00	6.49	3.00	0.80	3.149	3.23	6.000	2.83	1.54	3.51
11.78	7.19	3.05	0.70	3.328	3.18	5.898	2.53	1.59	3.76
12.51	7.61	3.10	0.60	3.487	3.13	5.634	2.33	1.56	3.99
14.16	9.33	3.10	0.40	3.733	2.91	5.780	2.03	1.61	4.52
15.78	10.75	3.15	0.20	3.982	2.76	5.662	1.92	1.70	5.03
17.37	12.22	3.20	0.00	4.187	2.61	5.607	1.58	1.81	5.54
18.92	14.15	3.20	0.00	4.561	2.61	5.474	1.53	1.78	6.03

Model 4665 Test No. 17

V, knots	R_t, lb	Wetted length of keel, ft	Wetted length of chine, ft	Re x 10^{-6}	S, ft^2	10^3 C_t	Change of trim, deg	CG rise, in	F_∇
0.69	0.15	3.65	1.80	0.283	5.26	21.546	0.01	0.00	0.22
1.06	0.30	3.70	1.80	0.439	5.30	18.090	0.06	0.02	0.34
1.39	0.55	3.70	1.80	0.576	5.28	19.348	0.06	-0.02	0.44
1.59	0.69	3.70	1.80	0.659	5.30	18.762	0.16	-0.06	0.51
1.76	0.94	3.70	1.80	0.729	5.30	20.789	0.16	-0.06	0.56
2.10	1.34	3.70	2.00	0.902	5.50	20.002	0.31	-0.11	0.67
2.36	1.84	3.65	2.00	1.005	5.46	21.860	0.51	-0.18	0.75
2.44	2.01	3.65	1.90	1.020	5.35	22.786	0.51	-0.18	0.78
2.98	2.98	3.65	1.90	1.246	5.36	22.626	1.16	-0.26	0.95
3.15	4.33	3.60	2.00	1.329	5.44	29.012	2.91	-0.28	1.00
3.94	5.91	3.20	2.00	1.543	4.94	27.888	5.36	0.10	1.26
4.72	6.44	2.80	1.80	1.636	4.15	25.247	6.21	0.65	1.51
5.50	5.32	2.60	1.70	1.782	3.80	16.767	5.91	1.11	1.75
6.26	4.97	2.40	1.40	1.792	3.23	14.193	5.16	1.37	2.00
7.06	4.62	2.40	1.20	1.915	3.02	11.119	4.31	1.47	2.25
7.84	4.44	2.40	1.10	2.067	2.91	8.977	3.56	1.59	2.50
8.64	4.51	2.50	1.00	2.278	2.91	7.501	3.01	1.63	2.76
9.38	4.57	2.50	0.90	2.402	2.81	6.692	2.56	1.64	2.99
10.20	5.93	2.60	0.80	2.612	2.81	7.340	2.11	1.75	3.25
11.06	6.18	2.60	0.70	2.749	2.71	6.750	1.79	1.67	3.53
11.76	6.69	2.70	0.60	2.923	2.71	6.461	1.61	1.73	3.75
12.57	7.27	2.70	0.50	3.030	2.61	6.373	1.31	1.74	4.01
14.13	8.38	2.80	0.30	3.300	2.52	6.033	0.96	1.71	4.51
15.87	9.65	2.80	0.00	3.347	2.25	6.152	0.71	1.85	5.06
17.37	10.97	2.80	0.00	3.664	2.25	5.838	0.56	1.95	5.54
18.98	12.16	2.80	0.00	4.003	2.25	5.423	0.51	1.87	6.05

Model 4666 Test No. 1

V, knots	R_t, lb	Wetted length of keel, ft	Wetted length of chine, ft	Re x 10^{-6}	S, ft^2	10^3 C_t	Change of trim, deg	CG rise, in.	F_∇
0.86	0.26	5.80	4.00	0.674	9.530	13.252	0.00	0.00	0.24
1.31	0.51	5.80	4.00	1.027	9.530	11.292	-0.02	-0.01	0.36
1.75	1.01	5.85	4.10	1.394	9.530	12.541	-0.05	-0.04	0.48
1.85	1.13	5.80	4.10	1.466	9.490	12.613	-0.07	-0.08	0.51
2.18	1.86	5.85	4.30	1.771	9.740	14.552	-0.09	-0.15	0.60
2.62	3.11	5.85	4.00	2.065	9.420	17.407	-0.12	-0.25	0.72
2.78	3.51	5.85	4.00	2.191	9.450	17.383	-0.10	-0.23	0.76
3.08	4.90	5.80	5.20	2.711	10.360	18.064	-0.04	-0.32	0.84
3.48	7.30	5.80	5.20	3.064	10.420	20.941	0.38	-0.56	0.95
3.68	8.32	5.80	5.40	3.298	10.660	20.875	0.80	-0.39	1.01
4.61	11.98	5.60	4.50	3.726	9.750	20.949	3.40	-0.06	1.26
5.52	12.78	5.55	4.20	4.307	9.300	16.342	3.78	0.22	1.51
6.39	13.31	5.45	3.90	4.781	8.840	13.348	4.33	0.51	1.75
7.31	13.60	5.10	3.50	5.031	7.870	11.714	4.93	0.96	2.01
8.21	13.97	4.80	3.20	5.256	7.220	10.394	5.01	0.13	2.25
9.08	14.18	4.60	3.00	5.522	6.800	9.153	4.88	0.16	2.49
10.04	14.72	4.40	2.90	5.865	6.490	8.151	4.45	0.18	2.76
10.98	14.82	4.40	2.70	6.239	6.280	7.085	4.17	0.19	3.01
11.86	16.01	4.40	2.60	6.644	6.180	6.670	3.91	0.20	3.25
12.80	15.91	4.40	2.50	7.068	6.080	5.787	3.63	0.22	3.51
13.66	16.87	4.40	2.30	7.324	5.870	5.576	3.41	0.20	3.75
14.62	17.64	4.45	2.20	7.780	5.820	5.134	3.21	0.21	4.01
16.46	19.91	4.50	2.00	8.562	5.670	4.694	2.75	0.22	4.52
18.30	23.06	4.60	1.80	9.373	5.570	4.477	2.43	0.25	5.02
20.20	26.44	4.70	1.60	10.184	5.470	4.288	2.11	0.26	5.54
22.00	29.74	4.80	1.40	10.916	5.370	4.142	1.96	0.26	6.04

Model 4666 Test No. 2

V, knots	R_t, lb	Wetted length of keel, ft	Wetted length of chine, ft	Re x 10^{-6}	S, ft^2	10^3 C_t	Change of trim, deg	CG rise, in	F_∇
0.85	0.27	6.00	5.80	0.770	11.91	11.394	0.00	1.13	0.20
1.35	0.54	6.00	6.00	1.244	11.98	8.971	-0.10	1.08	0.32
1.72	1.09	6.00	6.00	1.585	11.92	11.209	-0.20	1.01	0.41
2.15	1.80	6.00	6.00	1.982	11.92	11.844	-0.45	0.87	0.51
2.61	3.45	6.00	6.00	2.406	11.86	15.479	-0.70	0.72	0.62
3.02	7.17	6.00	6.00	2.784	11.68	24.399	-1.00	0.55	0.72

Model 4666 Test No. 3

V, knots	R_t, lb	Wetted length of keel, ft	Wetted length of chine, ft	Re x 10^{-6}	S, ft^2	10^3 C_t	Change of trim, deg	CG rise, in	F_∇
2.10	2.19	6.00	6.00	1.936	12.52	14.379	-0.23	-0.22	0.50
3.16	8.88	6.00	6.00	2.913	12.52	25.749	-0.70	-0.67	0.75
4.18	24.15	6.00	6.00	3.854	13.32	37.616	1.60	-1.13	1.00
5.22	41.72	5.80	5.40	4.492	11.75	47.236	6.20	-0.39	1.25
6.28	43.50	5.60	4.90	5.066	10.94	36.547	7.40	0.54	1.50
7.30	46.39	5.00	4.10	5.104	8.75	36.064	9.70	1.55	1.74
8.32	46.74	4.50	3.70	5.242	7.45	32.854	10.00	2.48	1.99
9.38	45.14	4.30	3.50	5.621	7.00	26.568	9.10	3.01	2.24
10.48	42.63	4.20	3.30	6.039	6.70	21.000	8.13	3.40	2.50
11.52	40.56	4.10	3.20	6.461	6.50	17.044	7.50	3.76	2.75
12.56	38.64	4.10	3.00	6.851	6.30	14.093	6.78	4.07	3.00
13.56	37.36	4.10	2.90	7.293	6.20	11.879	6.02	4.41	3.24
14.74	36.56	4.10	2.80	7.814	6.10	9.999	5.85	5.10	3.52
15.80	36.27	4.10	2.70	8.255	6.00	8.778	5.40	5.26	3.77
16.80	36.47	4.10	2.70	8.777	6.00	7.807	5.05	5.18	4.01

Model 4666 Test No. 4

V, knots	R_t, lb	Wetted length of keel, ft	Wetted length of chine, ft	Re x 10^{-6}	S, ft^2	10^3 C_t	Change of trim, deg	CG rise, in	F_∇
0.86	0.45	5.85	4.90	0.710	12.06	18.307	0.03	0.01	0.21
1.29	1.00	5.85	5.00	1.074	12.17	17.901	0.00	0.00	0.31
1.72	1.69	5.90	5.00	1.440	12.20	16.979	0.00	-0.10	0.41
2.10	2.59	5.90	5.00	1.758	12.16	17.509	0.00	-0.10	0.50
2.14	2.79	5.95	5.00	1.802	12.21	18.092	-0.04	-0.22	0.51
2.60	4.78	6.00	6.00	2.397	12.72	20.152	0.05	-0.27	0.62
3.04	8.18	6.00	6.00	2.802	12.58	25.507	0.13	-0.43	0.73
3.12	8.78	6.00	6.00	2.876	12.58	25.991	0.23	-0.38	0.74
3.44	12.07	6.00	6.00	3.171	12.56	28.439	0.55	-0.63	0.82
4.19	25.45	5.80	5.60	3.670	12.79	41.085	3.50	-0.60	1.00
5.21	43.52	5.40	4.60	4.003	11.06	52.548	7.25	0.10	1.24
6.29	49.38	4.90	4.00	4.301	8.15	55.513	9.31	0.99	1.50
7.29	53.34	4.40	3.50	4.425	7.10	51.243	10.65	2.23	1.74
8.32	50.19	4.00	3.30	4.666	6.50	40.435	9.53	3.09	1.99
9.38	46.94	3.80	3.10	4.973	6.10	31.703	8.40	3.65	2.24
10.44	43.88	3.60	2.90	5.214	5.70	25.603	7.25	4.06	2.49
11.54	40.96	3.60	2.80	5.674	5.58	19.981	6.35	4.52	2.75
12.54	38.79	3.60	2.70	6.070	5.50	16.258	5.43	4.78	2.99

Model 4666 Test No. 5

V, knots	R_t, lb	Wetted length of keel, ft	Wetted length of chine, ft	Re x 10^{-6}	S, ft^2	10^3 C_t	Change of trim, deg	CG rise, in	F_∇
0.85	0.60	5.75	4.60	0.666	11.86	25.408	0.05	0.02	0.20
1.30	1.30	5.80	4.70	1.048	12.15	22.953	0.15	-0.03	0.31
1.72	2.29	5.80	4.70	1.387	12.15	23.103	0.25	0.01	0.41
2.09	3.59	5.85	4.60	1.676	11.87	25.103	0.31	-0.06	0.50
2.15	3.99	5.85	4.70	1.744	12.07	25.929	0.35	-0.15	0.51
2.59	5.98	5.90	4.60	2.089	12.01	26.908	0.53	-0.17	0.62
3.03	8.88	5.80	5.00	2.514	12.55	27.942	0.75	-0.37	0.72
3.13	10.08	5.80	5.20	2.645	12.66	29.464	0.95	-0.28	0.75
3.43	13.97	5.80	6.40	3.215	13.30	32.366	1.75	-0.44	0.82
4.18	28.35	5.55	4.80	3.327	12.43	47.320	4.70	-0.46	1.00
5.21	50.72	4.80	4.00	3.522	9.47	71.524	8.33	-0.28	1.24
6.28	60.08	4.20	3.40	3.667	6.80	81.210	11.00	0.84	1.50
7.28	59.34	3.60	3.10	3.747	6.00	67.646	11.00	2.13	1.74
8.32	55.34	3.60	2.90	4.155	5.70	50.842	10.20	3.35	1.99
9.38	50.36	3.60	2.70	4.540	5.50	37.724	8.68	3.10	2.24

Model 4666 Test No. 6

V, knots	R_t, lb	Wetted length of keel, ft	Wetted length of chine, ft	Re x 10^{-6}	S, ft^2	10^3 C_t	Change of trim, deg	CG rise, in	F_∇
0.84	0.21	5.90	5.20	0.716	10.75	10.056	-0.05	-0.03	0.22
1.26	0.45	5.90	5.00	1.055	10.62	9.681	-0.10	-0.06	0.33
1.72	0.81	6.00	5.20	1.480	10.77	9.219	-0.25	-0.14	0.44
1.92	1.14	6.00	5.00	1.622	10.60	10.577	-0.33	-0.17	0.50
2.12	1.49	6.00	4.60	0.615	10.25	11.726	-0.35	-0.20	0.55
2.61	2.78	6.10	6.10	2.446	10.88	13.598	-0.68	-0.44	0.67
2.89	4.14	6.10	6.10	2.709	10.86	16.546	-0.90	-0.47	0.75
3.03	5.38	6.10	6.10	2.840	10.84	19.598	-0.95	-0.53	0.78
3.43	8.37	6.20	6.20	3.268	10.96	23.532	-1.25	-0.77	0.89
3.88	13.16	6.00	6.00	3.577	10.99	28.834	-0.68	-0.99	1.00
4.82	21.84	6.00	6.00	4.296	11.40	29.892	3.55	-0.57	1.25
5.78	24.95	6.00	5.60	5.151	11.04	24.522	3.83	-0.18	1.49
6.72	27.41	5.60	5.20	5.576	10.51	20.935	4.48	0.34	1.74
7.72	24.72	5.60	4.40	5.931	9.45	15.910	6.00	0.94	2.00
8.62	22.68	5.40	3.90	6.159	8.55	12.941	6.82	1.52	2.23
9.61	22.18	5.20	3.60	6.497	8.05	10.815	6.78	1.94	2.48
10.61	22.22	5.10	3.40	6.929	7.73	9.256	6.53	2.19	2.74
11.58	22.50	5.00	3.30	7.385	7.52	8.088	6.18	2.50	2.99
12.54	22.88	4.90	3.10	7.708	7.21	7.315	5.90	2.52	3.24
13.56	23.26	4.90	3.00	8.231	7.12	6.440	5.60	2.60	3.51
14.56	24.18	4.90	2.90	8.726	7.01	5.898	5.35	2.75	3.76
15.60	25.54	4.90	2.80	9.229	6.98	5.450	5.05	2.95	4.03
17.44	28.50	4.90	2.50	9.916	6.60	5.146	4.65	2.94	4.51
19.42	31.69	5.00	2.40	11.042	6.60	4.615	4.35	2.99	5.02
21.38	35.95	5.10	2.20	11.992	6.50	4.386	4.00	3.01	5.53
23.36	40.30	5.20	2.00	12.923	6.40	4.183	3.78	2.98	6.04

Model 4666 Test No. 7

V, knots	R_t, lb	Wetted length of keel, ft	Wetted length of chine, ft	Re x 10^{-6}	S, ft^2	10^3 C_t	Change of trim, deg	CG rise, in	F_∇
0.86	0.30	5.85	4.60	0.689	10.48	14.050	-0.10	-0.10	0.22
1.29	0.60	5.90	4.80	1.060	10.72	12.198	-0.15	-0.13	0.33
1.72	1.04	5.90	4.80	1.414	10.67	11.945	-0.20	-0.06	0.44
1.92	1.37	5.90	4.70	1.563	10.48	12.859	-0.22	-0.12	0.50
2.12	1.79	6.00	4.60	1.726	10.56	13.674	-0.25	-0.11	0.55
2.61	3.18	6.00	4.40	2.085	10.30	16.430	-0.32	-0.27	0.67
2.89	4.64	6.00	4.20	2.264	10.14	19.862	-0.33	-0.27	0.75
3.03	5.33	6.00	4.00	2.328	9.96	21.132	-0.40	-0.41	0.78
3.44	8.07	6.00	3.80	2.590	9.83	25.151	-0.38	-0.58	0.89
3.86	12.46	6.00	6.00	3.559	11.92	25.433	-0.30	-1.15	1.00
4.85	20.64	5.70	5.00	3.987	10.66	29.839	4.37	-0.31	1.25
5.78	21.50	5.60	4.70	4.574	10.08	23.143	5.00	0.27	1.49
6.72	22.16	5.40	4.20	4.956	9.25	19.230	6.00	0.75	1.74
7.70	23.02	5.00	3.80	5.206	8.04	17.505	6.88	1.36	1.99
8.69	22.98	4.70	3.40	5.408	7.32	15.069	6.78	1.90	2.25
9.60	22.38	4.50	3.20	5.679	6.90	12.757	6.35	2.17	2.48
10.60	22.12	4.45	3.10	6.157	6.75	10.572	5.90	2.38	2.74
11.60	21.90	4.40	2.90	6.506	6.50	9.076	5.45	2.59	3.00
12.58	21.93	4.30	2.80	6.862	6.30	7.973	5.08	2.69	3.25
13.50	22.26	4.30	2.70	7.261	6.20	7.141	4.60	2.93	3.49
14.58	23.18	4.30	2.60	7.729	6.10	6.480	4.30	2.97	3.77
15.60	23.84	4.40	2.50	8.270	6.10	5.821	4.05	3.11	4.03
17.94	26.30	4.40	2.30	9.235	5.88	5.038	3.45	3.11	4.51
19.44	29.09	4.50	2.10	9.858	5.75	4.853	3.10	3.13	5.02
21.44	32.66	4.60	1.90	10.707	5.70	4.518	2.77	3.05	5.54
23.32	36.40	4.70	1.80	11.646	5.70	4.257	2.45	2.95	6.03

Model 4666 Test No. 8

V, knots	R_t, lb	Wetted length of keel, ft	Wetted length of chine, ft	Re x 10^{-6}	S, ft^2	10^3 C_t	Change of trim, deg	CG rise, in	F_∇
0.86	0.33	5.78	4.40	0.672	10.50	15.435	-0.02	-0.01	0.22
1.29	0.65	5.82	4.35	1.007	10.46	13.541	-0.02	-0.01	0.33
1.71	1.20	5.87	4.50	1.361	11.10	13.405	-0.02	-0.01	0.44
1.93	1.64	5.85	4.45	1.527	10.48	15.235	-0.02	-0.02	0.50
2.15	2.09	5.90	4.40	1.701	10.46	15.672	-0.02	-0.02	0.56
2.60	3.58	5.95	4.20	2.029	10.27	18.694	0.03	-0.01	0.67
2.90	4.99	5.90	4.00	2.205	10.00	21.508	0.03	-0.02	0.75
3.02	5.78	6.00	3.90	2.297	10.06	22.838	0.08	0.00	0.78
3.42	9.02	6.00	3.70	2.548	9.86	28.353	0.53	0.19	0.88
3.88	13.26	6.00	6.00	3.577	11.38	28.058	1.83	0.73	1.00
4.82	20.47	5.50	4.40	3.666	9.93	32.165	4.88	2.08	1.25
5.80	21.90	5.30	4.00	4.144	9.27	25.457	5.68	2.48	1.50
6.72	24.39	4.80	3.60	4.337	7.82	25.036	6.88	3.07	1.74
7.82	24.65	4.40	3.30	4.626	6.90	21.177	6.98	3.17	2.02
8.65	24.05	4.20	3.10	4.851	6.50	17.925	6.53	3.03	2.24
9.60	23.43	4.00	2.90	5.089	6.10	15.108	5.88	2.77	2.48
10.60	22.50	3.80	2.75	5.342	5.75	12.624	5.18	2.50	2.74
11.60	21.97	3.60	2.60	5.526	5.40	10.960	4.58	2.26	3.00
12.58	21.83	3.60	2.50	5.896	5.28	9.470	4.13	2.06	3.25
13.53	21.81	3.50	2.40	6.133	5.08	8.501	3.68	1.87	3.50
14.58	22.28	3.50	2.30	6.497	5.00	7.598	3.18	1.67	3.77
15.58	22.74	3.60	2.20	6.943	5.00	6.792	2.88	1.56	4.03
17.40	24.80	3.80	2.00	7.754	5.00	5.938	2.38	1.35	4.50
19.36	27.19	4.00	1.87	8.746	5.08	5.176	1.88	1.13	5.00

Model 4666 Test No. 9

V, knots	R_t, lb	Wetted length of keel, ft	Wetted length of chine, ft	Re x 10^{-6}	S, ft^2	10^3 C_t	Change of trim, deg	CG rise, in	F_∇
0.86	0.35	5.70	4.10	0.647	10.30	16.672	0.02	0.01	0.22
1.30	0.80	5.75	4.10	0.984	10.33	16.618	0.07	0.03	0.34
1.84	1.43	5.77	4.20	1.408	10.37	14.768	0.07	0.03	0.48
1.94	1.87	5.78	4.20	1.487	10.35	17.408	1.12	0.47	0.50
2.15	2.39	5.80	4.20	1.651	10.46	17.922	0.17	0.06	0.56
2.60	3.98	5.85	4.10	1.989	10.39	20.542	0.32	0.11	0.67
2.90	5.49	5.85	3.90	2.174	10.21	23.178	0.49	0.17	0.75
3.02	6.38	5.85	3.80	2.236	10.01	25.333	0.62	0.21	0.78
3.45	9.47	5.85	3.80	2.555	10.02	28.786	1.44	0.52	0.89
3.86	13.16	5.85	4.70	3.131	10.94	29.267	1.57	0.58	1.00
4.82	23.44	5.70	4.50	3.777	10.06	36.356	5.82	2.25	1.25
5.79	27.00	5.56	4.30	4.386	9.65	30.254	7.22	2.60	1.50
6.71	28.61	4.20	3.10	3.763	6.50	35.437	7.57	3.06	1.73
7.70	27.15	3.50	2.90	3.786	5.60	29.641	7.22	3.01	1.99
8.68	24.28	3.20	2.70	3.934	5.05	23.132	6.27	2.68	2.24
9.61	24.58	3.20	2.50	4.208	4.90	19.690	5.32	2.33	2.48
10.60	23.32	3.20	2.42	4.577	4.80	15.674	4.52	2.04	2.74
11.60	22.48	3.20	2.30	4.902	4.70	12.885	3.72	1.75	3.00
12.60	22.05	3.30	2.20	5.324	4.70	10.712	3.12	1.53	3.26
13.52	21.86	3.30	2.10	5.609	4.60	9.424	2.62	1.34	3.49
14.51	21.98	3.30	2.05	5.975	4.60	8.227	2.12	1.14	3.75

Model 4666 Test No. 10

V, knots	R_t, lb	Wetted length of keel, ft	Wetted length of chine, ft	Re x 10^{-6}	S, ft^2	$10^3 C_t$	Change of trim, deg	CG rise, in.	F_∇
0.88	0.16	5.85	4.50	0.730	9.720	7.610	0.00	0.10	0.24
1.30	0.36	5.85	4.50	1.077	9.680	7.974	0.10	0.14	0.36
1.74	0.71	5.90	4.60	1.462	9.800	8.677	0.17	0.10	0.48
1.85	0.71	5.90	4.60	1.554	9.800	7.676	0.21	-0.12	0.51
2.18	1.31	5.90	4.60	1.832	9.680	10.316	0.29	0.30	0.60
2.63	2.36	5.90	5.90	2.484	10.610	11.637	0.46	-0.12	0.72
2.78	2.87	5.90	5.90	2.625	10.620	12.653	0.51	-0.30	0.76
3.06	4.10	5.90	5.90	2.890	10.600	14.985	0.72	-0.37	0.84
3.49	6.75	5.90	5.90	3.296	10.710	18.694	0.82	-0.48	0.96
3.68	8.20	5.90	5.90	3.475	10.420	20.476	0.56	-0.63	1.01
4.60	14.26	5.80	5.60	4.197	10.080	23.423	0.30	-0.17	1.26
5.45	15.66	5.80	5.10	4.754	9.900	18.938	3.13	-0.03	1.50
6.39	17.24	5.75	4.80	5.395	9.390	15.437	3.38	0.33	1.75
7.24	17.08	5.60	4.30	5.736	8.440	12.571	4.08	0.68	1.99
7.32	16.80	5.60	4.30	5.799	8.440	12.101	4.08	0.68	2.01
8.20	15.84	5.30	3.90	6.037	8.240	10.110	4.83	1.02	2.25
8.21	15.67	5.30	3.90	6.045	8.240	9.977	4.83	1.02	2.25
9.10	15.38	5.40	3.60	6.554	7.840	8.159	5.03	1.34	2.50
9.11	15.22	5.40	3.60	6.562	7.890	8.061	5.03	1.34	2.50
10.00	15.58	5.30	3.30	6.882	7.740	7.196	5.01	1.43	2.74
10.04	15.37	5.35	3.30	6.950	7.740	7.001	5.01	1.43	2.76
10.94	15.87	5.30	3.20	7.442	7.430	6.206	4.93	1.58	3.00
10.96	15.65	5.30	3.20	7.455	7.740	6.098	4.93	1.58	3.01
11.88	16.64	5.20	3.00	7.796	7.320	5.747	4.74	1.67	3.26
12.74	17.52	5.20	2.90	8.258	7.220	5.336	4.63	1.91	3.50
13.64	18.32	5.20	2.80	8.733	7.010	4.940	5.46	2.59	3.74
14.64	19.76	5.20	2.60	9.139	6.800	4.761	4.33	2.08	4.02
16.48	22.46	5.20	2.40	10.023	6.590	4.403	3.98	2.23	4.52
18.24	25.97	5.20	2.20	10.802	6.390	4.287	3.76	2.30	5.01
20.18	29.84	5.20	2.00	11.628	6.180	4.155	3.56	2.38	5.54
20.18	29.44	5.20	2.00	11.628	6.386	4.099	3.56	2.38	5.54
22.02	33.79	5.20	1.80	12.335	6.179	4.084	3.38	3.78	6.04
22.04	33.79	5.20	1.80	12.347	6.179	4.077	3.38	2.43	6.05

Model 4666 Test No. 12

V, knots	R_t, lb	Wetted length of keel, ft	Wetted length of chine, ft	Re x 10^{-6}	S, ft^2	$10^3 C_t$	Change of trim, deg	CG rise, in.	F_∇
0.86	0.19	5.73	2.77	0.562	8.130	11.315	0.00	0.00	0.24
1.29	0.50	5.78	2.89	0.860	8.310	13.097	0.00	0.00	0.35
1.73	0.91	5.80	2.92	1.160	8.340	13.204	0.00	0.00	0.47
1.83	1.09	5.83	2.92	1.231	8.350	14.121	0.00	0.00	0.50
2.15	1.71	5.87	3.00	1.466	8.480	15.790	0.05	-0.08	0.59
2.60	2.79	5.90	2.89	1.760	8.400	17.771	0.10	-0.15	0.71
2.75	3.36	5.95	2.85	1.860	8.400	19.131	0.05	-0.18	0.75
3.04	4.55	6.00	4.50	2.790	9.930	17.937	0.17	-0.22	0.83
3.45	6.58	6.00	4.50	1.230	9.970	20.076	0.60	-0.41	0.95
3.65	7.92	6.00	4.50	2.947	9.960	21.597	0.05	-0.98	1.00
4.55	11.76	5.60	4.20	3.428	9.540	21.559	3.45	-0.33	1.25
5.45	12.61	5.50	4.00	3.981	9.270	16.591	4.00	0.24	1.50
5.46	12.61	5.45	4.00	3.967	9.040	16.949	3.85	-0.14	1.50
6.35	13.29	5.20	3.70	4.345	8.540	13.967	4.65	0.95	1.74
6.36	13.29	5.43	4.00	4.611	9.360	12.705	4.65	0.95	1.74
7.28	14.26	4.70	3.30	4.478	7.220	13.487	5.15	1.29	2.00
7.29	14.26	4.70	3.20	4.428	7.120	13.646	5.15	1.29	2.00
8.17	14.49	4.40	3.10	4.711	6.700	11.732	5.15	1.59	2.24
8.18	14.53	4.40	3.10	4.717	6.700	11.735	4.95	1.30	2.24
9.06	14.56	4.20	2.90	4.946	6.280	10.219	4.65	1.55	2.49
9.08	14.58	4.30	2.90	5.027	6.390	10.022	4.65	0.95	2.49
10.02	14.78	4.00	2.80	5.239	5.970	8.918	4.35	1.81	2.75
10.03	14.70	4.10	2.70	5.244	5.970	8.858	4.35	0.61	2.75
10.92	14.92	4.10	2.70	5.709	5.970	7.582	3.93	2.10	3.00
10.92	14.97	4.10	2.60	5.625	5.870	7.740	3.95	1.91	3.00
11.86	15.23	4.20	2.59	6.192	5.964	6.572	3.50	2.20	3.25
12.76	15.71	4.20	2.48	6.554	5.852	5.970	3.30	2.40	3.50
13.66	16.51	4.20	2.40	6.932	5.771	5.551	3.25	2.37	3.75
14.62	17.37	4.20	2.32	7.329	5.690	5.170	2.70	2.31	4.01

Model 4666 Test No. 11

V, knots	R_t, lb	Wetted length of keel, ft	Wetted length of chine, ft	Re x 10^{-6}	S, ft^2	$10^3 C_t$	Change of trim, deg	CG rise, in.	F_∇
0.86	0.20	5.80	4.20	0.688	9.600	10.612	0.00	0.00	0.24
1.29	0.46	5.80	4.20	1.032	9.580	10.456	-0.07	-0.09	0.35
1.74	0.86	5.85	4.20	1.399	9.580	10.745	-0.10	-0.10	0.48
1.84	0.94	5.85	4.20	1.480	9.580	10.502	-0.12	-0.06	0.50
2.15	1.46	5.85	4.40	1.764	9.750	11.729	-0.17	-0.19	0.59
2.62	2.61	5.85	4.00	2.065	9.330	14.742	-0.25	-0.23	0.72
2.78	3.06	5.85	3.80	2.147	9.170	15.622	-0.27	-0.19	0.76
3.06	4.31	5.85	5.85	2.865	10.720	15.532	-0.30	-0.36	0.84
3.45	6.60	5.85	5.85	3.230	10.770	18.642	-0.12	-0.46	0.95
3.67	8.10	5.80	5.80	3.407	10.680	20.382	0.21	-0.49	1.01
4.59	12.68	5.75	5.00	3.949	10.210	21.354	0.30	-0.40	1.26
5.48	13.36	5.60	4.50	4.429	9.530	16.915	0.36	0.05	1.50
6.39	13.99	5.55	4.20	4.986	9.290	13.350	0.40	0.32	1.75
7.31	13.70	5.40	3.80	5.382	8.480	10.951	0.47	0.76	2.01
8.20	13.87	5.20	3.50	5.709	7.940	9.406	0.49	1.03	2.25
9.10	14.02	5.05	3.20	6.008	7.480	8.200	0.49	1.36	2.50
10.04	14.67	4.90	3.00	6.348	7.120	7.409	0.47	1.53	2.76
10.94	15.02	4.70	2.90	6.654	6.800	6.681	0.45	1.80	3.00
11.82	15.68	4.70	2.70	7.000	6.590	6.164	0.42	1.97	3.24
12.76	16.34	4.60	2.60	7.352	6.390	5.692	0.40	1.90	3.50
13.64	17.24	4.70	2.50	7.859	6.390	5.256	0.38	1.99	3.74
14.64	18.24	4.80	2.40	8.436	6.390	4.825	0.36	2.12	4.02
14.64	18.16	4.80	2.40	8.436	6.390	4.804	0.36	2.10	4.02
16.48	20.58	4.80	2.10	9.100	6.070	4.517	0.32	2.23	4.52
18.34	23.59	4.80	1.90	9.834	5.870	4.325	0.29	2.32	5.03
20.16	27.41	4.90	1.80	10.809	5.870	4.159	0.28	2.40	5.53

Model 4666 Test No. 13

V, knots	R_t, lb	Wetted length of keel, ft	Wetted length of chine, ft	Re x 10^{-6}	S, ft^2	$10^3 C_t$	Change of trim, deg	CG rise, in	F_∇
0.85	0.27	5.70	3.60	0.607	9.25	14.674	0.00	0.00	0.23
1.30	0.58	5.70	3.60	0.928	9.23	13.486	0.00	0.00	0.36
1.72	1.09	5.73	3.60	1.231	9.18	14.553	0.05	-0.03	0.47
1.83	1.31	5.75	3.65	1.321	9.25	15.338	0.10	-0.06	0.50
2.14	1.92	5.80	3.80	1.578	9.42	16.137	0.15	-0.08	0.59
2.60	3.03	5.80	3.70	1.897	9.33	17.415	0.25	-0.19	0.71
2.74	3.65	5.80	3.60	1.978	9.28	18.993	0.35	-0.15	0.75
3.04	4.73	5.80	3.50	2.172	9.22	20.124	0.45	-0.30	0.83
3.47	6.82	5.80	3.60	2.506	9.45	21.729	0.65	-0.71	0.95
3.65	8.12	5.70	4.20	2.776	9.71	22.755	1.95	0.64	1.00
4.56	12.74	5.30	3.80	3.188	8.92	24.899	4.05	-0.34	1.25
5.45	14.32	4.80	3.50	3.475	7.94	22.011	4.85	0.20	1.50
6.70	15.74	4.15	3.10	3.727	6.54	19.434	5.45	0.66	1.84
7.28	15.94	3.90	2.90	3.803	5.99	18.201	5.55	1.20	2.00
8.18	15.53	3.70	2.60	3.959	5.50	15.297	5.05	1.48	2.25
9.08	15.12	3.60	2.50	4.255	5.29	12.567	4.45	1.81	2.49
10.02	14.89	3.60	2.40	4.619	5.19	10.358	3.95	1.99	2.75
10.93	14.88	3.60	2.20	4.870	5.00	9.030	3.35	2.03	3.00
11.87	14.85	3.60	2.10	5.198	4.90	7.797	2.95	2.26	3.26
12.76	15.35	3.60	2.00	5.490	4.80	7.120	2.45	2.14	3.50
13.64	15.77	3.60	1.90	5.764	4.70	6.537	2.15	2.21	3.75
14.60	16.35	3.60	1.80	6.057	4.60	6.044	1.90	2.30	4.01
16.49	18.18	3.70	1.60	6.715	4.50	5.386	1.25	2.32	4.53

Model 4666 Test 12R

V, knots	R_t, lb	Wetted length of keel, ft	Wetted length of chine, ft	Re x 10^{-6}	S, ft^2	$10^3 C_t$	Change of trim, deg	CG rise, in.	F_∇
4.58	11.88	5.60	4.30	3.629	9.530	21.520	3.48	-0.31	1.26
5.47	12.51	5.50	4.00	4.159	9.120	16.598	3.93	0.03	1.50
6.36	13.24	5.25	3.70	4.555	8.510	13.925	4.55	0.40	1.75
7.30	13.98	4.75	3.30	4.703	7.300	13.006	5.05	0.74	2.00
8.20	14.27	4.50	3.10	4.987	6.800	11.296	4.95	1.15	2.25
20.16	24.87	4.50	1.50	9.680	5.180	4.278	1.75	2.35	5.53
22.02	28.44	4.50	1.30	10.221	4.990	4.256	1.55	2.45	6.04

Model 4666 Test No. 14

V, knots	R_t, lb	Wetted length of keel, ft	Wetted length of chine, ft	Re x 10^{-6}	S, ft^2	10^3 C_t	Change of trim, deg	CG rise, in	F_∇
0.85	0.16	5.80	3.80	0.626	8.82	9.119	-0.03	1.24	0.25
1.30	0.32	5.80	3.80	0.958	8.82	7.785	-0.08	1.21	0.37
1.72	0.59	5.80	3.80	1.268	8.82	8.200	-0.13	1.18	0.50
1.75	0.61	5.80	4.00	1.317	9.02	8.009	-0.13	1.18	0.50
2.15	1.09	5.80	4.00	1.618	9.02	9.477	-0.18	1.05	0.62
2.60	2.00	6.00	3.80	1.957	9.02	11.891	-0.28	1.09	0.75
2.60	2.04	6.00	3.80	1.957	9.02	12.128	-0.33	1.07	0.75
3.03	3.46	6.00	3.50	2.211	8.73	15.650	-0.50	0.87	0.87
3.45	5.49	6.00	3.10	2.412	8.35	20.025	-0.33	0.79	0.99
3.50	5.57	6.00	4.80	2.904	9.89	16.666	-0.23	0.83	1.01
4.32	9.55	5.80	4.00	2.921	8.04	23.072	1.37	1.65	1.25
5.20	10.60	5.80	4.60	4.155	9.71	14.635	2.67	1.22	1.50
6.05	11.75	5.80	4.00	4.555	9.18	12.676	2.67	1.36	1.74
6.95	12.21	5.60	4.00	5.126	8.98	10.204	3.07	1.65	2.00
7.80	12.22	5.80	3.80	5.753	8.97	8.117	3.17	1.70	2.25
8.68	12.13	5.50	3.50	6.002	8.24	7.083	3.77	2.35	2.50
9.50	12.56	5.50	3.20	6.350	7.94	6.354	3.87	2.30	2.74
10.40	12.86	5.40	3.00	6.712	7.62	5.656	3.97	2.16	3.00
11.25	13.72	5.40	2.80	7.088	7.42	5.296	3.87	1.91	3.24
12.12	14.64	5.30	2.70	7.450	7.21	5.011	3.77	1.65	3.49
13.00	16.05	5.30	2.60	7.891	7.11	4.842	3.67	2.68	3.75
13.90	17.18	5.30	2.40	8.223	6.90	4.671	3.57	2.73	4.01
15.70	20.23	5.20	2.10	8.806	6.50	4.577	3.47	2.96	4.52
17.40	23.31	5.20	1.90	9.492	6.30	4.430	3.27	3.05	5.01
19.20	26.67	5.20	1.70	10.179	6.09	4.306	3.17	3.09	5.53
20.96	30.17	5.30	1.40	10.790	7.94	3.135	2.87	3.01	6.04

Model 4666 Test No. 15

V, knots	R_t, lb	Wetted length of keel, ft	Wetted length of chine, ft	Re x 10^{-6}	S, ft^2	10^3 C_t	Change of trim, deg	CG rise, in	F_∇
0.84	0.18	5.75	3.60	0.604	10.67	8.677	0.00	0.00	0.24
1.30	0.35	5.80	3.60	0.938	10.52	7.140	-0.03	-0.02	0.37
1.72	0.69	5.82	3.65	1.252	10.35	8.171	-0.06	-0.03	0.50
1.75	0.69	5.83	3.60	1.269	10.26	7.963	-0.06	-0.04	0.50
2.13	1.27	5.85	3.90	1.597	10.64	9.539	-0.08	-0.05	0.61
2.60	2.16	5.90	3.70	1.917	10.27	11.279	-0.08	-0.05	0.75
2.61	2.17	5.90	3.70	1.925	10.27	11.245	-0.08	-0.05	0.75
3.03	3.56	6.00	3.50	2.211	10.11	13.909	-0.16	-0.10	0.87
3.45	5.22	6.00	3.10	2.412	10.33	15.391	0.22	0.07	0.99
3.49	5.32	6.00	3.10	2.440	10.24	15.462	0.42	0.17	1.01
4.32	8.15	5.85	4.50	3.438	8.00	19.789	2.12	0.97	1.25
5.20	8.97	5.70	4.00	3.875	10.57	11.376	2.87	1.37	1.50
6.02	9.73	5.60	3.80	4.348	8.90	10.935	3.22	1.31	1.74
6.91	9.91	5.47	3.60	4.810	8.54	8.810	3.52	1.73	1.99
7.79	10.07	5.35	3.35	5.207	8.65	6.954	3.82	1.90	2.25
8.65	10.48	5.23	3.13	5.556	7.62	6.663	3.90	1.95	2.49
9.60	10.64	5.10	2.90	5.901	7.21	5.804	3.82	1.94	2.77
10.30	11.98	5.00	2.70	6.093	6.90	5.932	3.72	1.91	2.97
11.29	12.56	4.90	2.60	6.506	6.70	5.331	3.57	1.84	3.25
12.12	13.66	4.90	2.45	6.854	6.60	5.107	3.42	1.79	3.49
13.06	14.70	4.90	2.45	7.385	6.60	4.734	3.27	1.72	3.76
14.00	15.63	4.90	2.20	7.637	6.30	4.588	3.10	1.64	4.03
15.73	18.48	4.90	1.70	8.218	5.99	4.520	2.72	1.47	4.53
17.40	21.03	4.90	1.70	8.823	5.79	4.349	2.54	1.39	5.01
19.10	24.30	5.00	1.43	9.451	5.60	4.312	2.37	1.32	5.50
21.00	27.72	5.10	1.25	10.262	5.60	4.069	2.22	1.25	6.05

Model 4666 Test No. 16

V, knots	R_t, lb	Wetted length of keel, ft	Wetted length of chine, ft	Re x 10^{-6}	S, ft^2	10^3 C_t	Change of trim, deg	CG rise, in	F_∇
0.84	0.20	5.70	3.50	0.593	8.81	11.674	0.05	0.02	0.24
1.30	0.41	5.75	3.50	0.922	8.81	9.988	0.03	-0.08	0.37
1.72	0.80	5.80	3.40	1.215	8.76	11.192	0.05	-0.10	0.50
1.76	0.84	5.75	3.40	1.238	10.44	9.418	0.04	-0.08	0.51
2.14	1.44	5.80	3.70	1.562	9.01	12.654	0.17	-0.10	0.62
2.60	2.48	5.75	3.60	1.869	8.89	14.960	0.24	-0.21	0.75
2.60	2.43	5.70	3.30	1.797	8.51	15.314	0.12	-0.14	0.75
3.06	3.58	5.70	3.20	2.092	8.40	16.502	0.27	-0.32	0.88
3.44	4.97	5.70	4.40	2.722	9.78	15.568	0.77	-0.45	0.99
3.49	5.69	5.70	4.40	2.708	9.70	17.459	0.87	-0.37	1.01
4.35	7.55	5.60	4.10	3.242	9.28	15.586	2.65	-0.31	1.25
5.19	8.40	5.50	3.80	3.708	8.79	12.861	3.04	-0.03	1.50
6.08	8.78	5.40	3.60	4.204	8.40	10.250	3.49	0.29	1.75
6.94	9.36	5.10	3.30	4.479	7.66	9.197	3.82	0.54	2.00
7.78	9.99	4.80	3.00	4.662	7.01	8.535	3.87	0.77	2.24
8.64	10.40	4.60	2.80	4.912	6.60	7.652	3.77	1.02	2.49
9.52	10.84	4.45	2.60	5.295	6.40	6.774	3.62	1.24	2.74
10.40	11.38	4.40	2.50	5.513	6.09	6.263	3.46	1.36	3.00
11.24	11.79	4.40	2.30	5.786	5.89	5.743	3.15	1.51	3.24
12.16	12.61	4.40	2.20	6.166	5.79	5.339	2.87	1.48	3.75
13.00	13.55	4.40	2.10	8.490	5.69	5.108	2.67	1.48	3.75
13.90	14.33	4.40	1.90	6.728	5.50	4.888	2.50	1.59	4.01
15.72	16.73	4.50	1.70	7.488	5.39	4.553	2.07	1.78	4.53
17.42	19.31	4.50	1.50	8.298	5.39	4.279	1.87	1.79	5.02
19.16	22.30	4.60	1.30	8.685	5.09	4.326	1.62	1.87	5.52
20.96	25.52	4.70	1.10	9.340	5.00	4.211	1.47	1.79	6.04

Model 4666 Test No. 17

V, knots	R_t, lb	Wetted length of keel, ft	Wetted length of chine, ft	Re x 10^{-6}	S, ft^2	10^3 C_t	Change of trim, deg	CG rise, in	F_∇
0.86	0.20	5.65	3.30	0.592	8.69	11.292	0.02	0.01	0.25
1.29	0.45	5.70	3.30	0.892	8.69	11.281	0.02	0.01	0.37
1.71	0.84	5.70	3.30	1.182	8.69	11.988	0.04	-0.08	0.49
1.76	0.94	5.70	3.30	2.350	8.69	12.662	0.02	-0.09	0.51
2.13	1.54	5.70	3.40	1.489	8.74	14.082	0.12	-0.15	0.61
2.60	2.48	5.75	3.40	1.829	8.84	15.045	0.22	-0.20	0.75
2.60	2.48	5.70	3.50	1.837	8.88	14.978	0.22	-0.20	0.75
3.03	3.68	5.70	3.00	2.025	8.33	17.446	0.52	-0.27	0.87
3.43	5.27	5.60	2.80	2.213	7.99	20.325	1.12	-0.31	0.99
3.47	5.57	5.60	2.80	2.239	8.00	20.962	1.22	-0.37	1.00
4.31	8.15	5.40	3.70	3.013	8.65	18.386	3.02	-0.29	1.24
5.18	8.82	5.20	3.50	3.462	8.22	14.496	3.52	0.03	1.49
6.04	10.00	4.70	3.20	3.666	7.27	13.668	4.02	3.01	1.74
6.91	10.66	4.20	2.90	3.769	6.30	12.846	4.32	2.95	1.99
7.78	10.87	4.00	2.70	4.005	5.89	11.053	4.22	1.12	2.24
8.65	10.88	3.90	2.50	4.253	5.60	9.413	3.82	1.25	2.49
9.50	11.04	3.80	2.30	4.452	5.29	8.382	3.52	1.51	2.74
10.40	11.23	3.80	2.20	4.794	5.19	7.252	2.97	1.47	3.00
11.24	11.79	3.80	2.10	5.095	5.09	6.646	2.72	1.57	3.24
12.14	12.26	3.80	2.00	5.410	5.00	6.031	2.47	1.76	3.50
13.02	13.15	3.80	1.90	5.702	4.90	5.739	2.12	1.70	3.75
14.00	13.83	3.80	1.80	6.024	4.80	5.329	1.82	1.77	4.03
15.74	15.78	3.90	1.60	6.651	4.70	4.912	1.52	1.94	4.54
17.40	18.21	4.00	1.40	7.219	4.60	5.000	1.12	1.87	5.01

Model 4667-1 Test No. 1

V, knots	R_t, lb	Wetted length of keel, ft	Wetted length of chine, ft	Re x 10^{-6}	S, ft^2	10^3 C_t	Change of trim, deg	CG rise, in	F_∇
3.88	8.75	8.00	7.40	4.591	14.55	14.481	0.50	0.15	0.99
4.86	13.83	7.70	6.65	5.362	14.61	14.528	2.10	-0.38	1.25
5.83	15.66	7.55	6.10	6.110	13.55	12.326	2.75	-0.16	1.49
6.82	16.95	7.46	5.82	6.959	12.70	10.401	2.85	0.06	1.75
7.81	18.29	7.37	5.45	7.693	12.55	8.661	3.15	0.29	2.00
8.80	19.32	7.06	5.20	8.289	11.68	7.743	3.70	0.63	2.26
9.76	20.30	6.62	4.70	8.489	10.10	7.648	4.00	0.86	2.50
10.74	21.26	6.40	4.43	8.945	9.60	6.960	3.95	1.10	2.75
11.72	22.17	6.20	4.23	9.401	9.20	6.359	3.85	1.31	3.00
12.70	23.10	6.05	4.10	9.914	8.92	5.820	3.65	1.43	3.25
13.68	24.00	6.00	3.90	10.406	8.67	5.362	3.45	1.59	3.51
14.70	25.36	6.00	3.75	11.023	8.54	4.981	3.30	1.78	3.77
15.70	26.61	6.00	3.60	11.580	8.35	4.687	3.00	1.85	4.02
17.64	29.89	6.00	3.30	12.605	8.04	4.331	2.60	1.97	4.52
19.62	34.54	6.18	3.15	14.050	8.05	4.040	2.35	2.06	5.03
21.60	40.13	6.35	2.95	15.434	8.04	3.873	2.15	2.14	5.54
23.56	45.55	6.50	1.95	15.278	7.18	4.143	1.85	2.17	6.04

Model 4667-1 Test No. 2

V, knots	R_t, lb	Wetted length of keel, ft	Wetted length of chine, ft	Re x 10^{-6}	S, ft^2	10^3 C_t	Change of trim, deg	CG rise, in	F_∇
1.00	0.50	8.00	8.00	1.229	16.27	11.140	-0.04	-0.02	0.22
1.51	1.00	8.00	8.00	1.856	16.27	9.773	-0.09	-0.07	0.34
2.00	1.80	8.00	8.00	2.458	16.27	10.026	-0.13	-0.14	0.45
2.24	2.39	8.00	8.00	2.753	16.27	10.614	-0.15	0.00	0.50
2.49	3.59	8.00	8.00	3.061	16.27	12.901	-0.19	-0.28	0.55
2.98	6.18	8.00	8.00	3.663	16.27	15.506	-0.22	-0.28	0.66
3.23	8.68	8.00	8.00	3.970	16.27	18.539	-0.22	-0.28	0.72
3.35	9.97	8.00	8.00	4.118	16.27	19.794	-0.23	0.13	0.75

Model 4667-1 Test No. 4

V, knots	R_t, lb	Wetted length of keel, ft	Wetted length of chine, ft	Re x 10^{-6}	S, ft^2	10^3 C_t	Change of trim, deg	CG rise, in	F_∇
1.00	0.55	7.85	7.03	1.149	17.05	11.693	0.00	0.00	0.22
1.51	1.55	7.90	7.05	1.735	17.05	14.455	0.00	-0.01	0.34
1.98	2.75	7.95	7.05	2.275	17.05	14.916	0.02	0.10	0.44
2.51	4.54	8.00	8.00	2.885	17.05	15.322	0.02	-0.16	0.56
2.98	7.03	8.00	8.00	3.425	17.05	16.831	0.08	-0.23	0.66
3.52	13.22	8.00	8.00	4.046	17.05	22.685	0.20	-0.36	0.78
3.99	19.21	8.00	8.00	4.586	17.05	25.654	0.88	-0.45	0.89

Model 4667-1 Test No. 1A

V, knots	R_t, lb	Wetted length ft		Re x 10^{-6}	S, ft^2	10^3 C_t	Change of trim, deg	CG rise, in	F_∇
1.01	0.30	6.90		1.070	13.30	8.020	0.00	0.00	0.26
2.02	1.44	7.27		2.256	13.88	9.217	0.00	0.00	0.52
3.02	4.15	7.55		3.503	14.30	11.535	0.05	0.20	0.77
4.00	9.54	7.60		4.671	14.55	14.854	0.70	-0.31	1.03
6.97	17.16	6.58		7.047	12.68	10.098	2.90	0.21	1.79
7.98	18.66	6.38		7.823	12.50	8.497	3.25	0.42	2.04
11.00	21.85	5.30		8.959	9.40	6.964	3.95	1.44	2.82
12.01	22.48	5.15		9.504	9.11	6.201	3.85	1.61	3.08
15.12	25.83	4.90		11.385	8.42	4.864	3.15	1.92	3.87
16.05	27.04	4.80		11.839	8.28	4.595	2.90	2.02	4.11
19.08	33.15	4.67		13.692	8.00	4.126	2.40	2.13	4.89
20.10	35.51	4.72		14.579	8.08	3.943	2.20	2.08	5.15
23.08	44.20	4.40		15.605	7.55	3.984	1.95	2.30	5.91

Model 4667-1 Test No. 3

V, knots	R_t, lb	Wetted length of keel, ft	Wetted length of chine, ft	Re x 10^{-6}	S, ft^2	10^3 C_t	Change of trim, deg	CG rise, in	F_∇
1.00	0.37	7.95	7.40	1.229	16.79	7.988	-0.07	-0.04	0.22
1.51	1.23	8.00	7.60	1.856	16.79	11.647	-0.08	-0.03	0.34
1.99	2.00	8.00	8.00	2.446	16.79	10.905	-0.14	0.01	0.44
2.23	2.89	8.00	8.00	2.741	16.79	12.550	-0.17	0.00	0.50
2.52	3.64	8.00	8.00	3.098	16.79	12.376	-0.21	0.00	0.56
2.99	6.43	8.00	8.00	3.675	16.79	15.528	-0.26	0.05	0.67
3.37	10.67	8.00	8.00	4.143	16.79	20.286	-0.27	0.12	0.75
3.49	12.67	8.00	8.00	4.290	16.79	22.458	-0.27	0.13	0.78

Model 4667-1 Test No. 6

V, knots	R_t, lb	Wetted length of keel, ft	Wetted length of chine, ft	Re x 10^{-6}	S, ft^2	10^3 C_t	Change of trim, deg	CG rise, in	F_∇
1.00	0.35	7.95	7.20	1.229	14.99	8.464	-0.05	-0.03	0.24
1.51	0.70	8.00	7.20	1.856	14.99	7.426	-0.08	-0.04	0.36
2.00	1.38	8.00	8.00	2.458	14.99	8.343	-0.14	-0.07	0.48
2.08	1.49	8.00	8.00	2.557	14.99	8.330	-0.15	-0.10	0.50
2.50	2.59	8.00	8.00	3.073	14.99	10.022	-0.20	-0.09	0.60
3.00	4.58	8.00	8.00	3.688	14.99	12.306	-0.28	-0.33	0.72
3.08	5.28	8.00	8.00	3.786	14.99	13.460	-0.30	-0.30	0.74
3.23	6.28	8.00	8.00	3.970	14.99	14.558	-0.34	-0.38	0.78
3.51	8.37	8.00	8.00	4.315	14.99	16.429	-0.41	-0.32	0.85

Model 4667-1 Test No. 7

V, knots	R_t, lb	Wetted length of keel, ft	Wetted length of chine, ft	Re x 10^{-6}	S, ft^2	10^3 C_t	Change of trim, deg	CG rise, in	F_∇
1.00	0.35	7.90	6.70	1.121	14.74	8.607	-0.04	-0.04	0.24
1.51	0.75	7.90	6.70	1.693	14.67	8.130	-0.07	-0.08	0.36
1.99	1.52	7.90	6.70	2.232	14.67	9.485	-0.10	-0.12	0.48
2.07	1.70	7.85	6.70	2.315	14.55	9.887	-0.13	-0.82	0.50
2.50	2.87	7.90	6.70	2.804	14.60	11.400	-0.17	-0.24	0.60
3.00	4.78	7.90	6.70	3.365	14.54	13.241	-0.18	-0.27	0.72
3.07	5.58	8.00	6.60	3.443	14.58	14.721	-0.18	-0.27	0.74
3.25	6.58	8.00	7.00	3.745	14.87	15.187	-0.22	-0.35	0.78
3.50	8.67	8.00	7.30	4.114	15.16	16.923	-0.23	-0.40	0.84
4.12	13.96	8.00	8.00	5.065	15.71	18.977	0.32	-0.54	0.99
5.18	23.93	8.00	8.00	6.368	16.43	19.677	2.67	-0.56	1.25
6.20	26.49	8.00	6.60	6.955	14.91	16.754	3.34	-0.21	1.50
7.22	28.75	7.60	6.40	7.766	14.43	13.855	4.62	0.51	1.74
8.24	30.31	7.40	6.00	8.484	13.18	12.278	5.22	0.99	1.99
9.26	31.25	7.40	5.40	9.107	12.05	10.963	5.72	1.42	2.23
10.36	31.69	7.10	5.00	9.631	10.90	9.819	5.42	1.26	2.50
11.38	33.03	6.70	4.70	9.968	10.20	9.064	5.37	1.93	2.75
12.58	33.03	6.40	4.50	10.535	9.68	7.816	5.07	1.86	3.04
13.46	33.86	6.30	4.35	11.024	9.45	7.169	4.89	2.12	3.25
14.44	34.88	6.10	4.20	11.428	9.06	6.693	4.62	2.50	3.48
15.64	35.87	6.00	4.05	12.089	8.83	6.020	4.22	2.56	3.77
16.64	36.38	6.00	3.90	12.657	8.68	5.487	3.99	2.61	4.01
18.68	39.46	6.00	3.70	13.922	8.45	4.851	3.45	2.70	4.51
20.73	43.40	6.10	3.40	15.131	8.24	4.443	3.32	2.97	4.99
22.80	48.85	6.20	3.30	16.642	8.24	4.134	2.90	3.01	5.53
24.88	52.55	6.40	3.10	18.161	8.24	3.735	2.50	3.05	6.00

Model 4667-1 Test No. 8

V, knots	R_t, lb	Wetted length of keel, ft	Wetted length of chine, ft	Re x 10^{-6}	S, ft^2	10^3 C_t	Change of trim, deg	CG rise, in	F_∇
1.00	0.45	7.80	6.10	1.068	14.38	11.343	0.00	-0.04	0.24
1.51	0.97	7.80	6.10	1.612	14.38	10.726	0.00	-0.04	0.36
2.00	1.54	7.80	6.10	2.136	14.38	9.705	0.00	-0.04	0.48
2.07	2.00	7.85	6.20	2.233	14.59	11.600	-0.01	-0.08	0.50
2.51	3.11	7.87	6.40	2.754	14.86	12.043	0.05	-0.15	0.61
3.02	5.48	7.90	6.60	3.364	15.10	14.425	0.10	-0.21	0.73
3.09	6.13	7.90	6.60	3.442	15.03	15.485	0.15	-0.19	0.75
3.24	7.38	7.90	6.80	3.634	15.34	16.614	0.20	-0.26	0.78
3.51	9.32	7.90	7.00	3.964	15.61	17.567	0.25	-0.32	0.85
4.12	14.96	7.90	7.40	4.843	16.21	19.709	1.16	0.43	0.99
5.15	24.12	7.80	6.60	5.698	15.07	21.875	3.40	-0.34	1.24
6.19	25.99	7.40	6.10	6.420	13.54	18.160	3.81	-0.03	1.49
7.20	28.15	7.20	5.70	7.136	12.94	15.212	4.23	0.31	1.74
8.23	30.75	6.70	5.20	7.525	11.68	14.090	5.05	0.70	1.99
9.26	32.85	5.90	4.70	7.541	9.36	14.837	5.65	1.23	2.23
10.36	33.18	5.70	4.40	8.039	8.85	12.662	5.45	1.66	2.50
11.36	32.82	5.50	4.20	8.466	8.45	10.910	5.13	1.55	2.74
12.44	32.44	5.30	4.10	8.984	8.15	9.323	4.65	1.47	3.00
13.44	32.52	5.40	3.95	9.665	8.10	8.057	4.15	2.76	3.24
14.44	32.78	5.30	3.80	10.096	7.80	7.306	3.97	2.71	3.48
15.66	33.41	5.30	3.60	10.709	7.67	6.439	3.54	2.81	3.78
16.64	33.90	5.30	3.50	11.251	7.53	5.894	3.18	2.91	4.01
18.78	36.60	5.40	3.30	12.554	7.43	5.063	2.67	2.99	4.53
20.88	40.01	5.50	3.10	13.797	7.33	4.538	2.17	3.13	5.04
22.88	45.05	5.50	3.00	14.943	7.23	4.315	1.66	3.64	5.52
24.95	49.95	5.80	2.80	16.486	7.33	3.968	1.63	3.16	6.02

Model 4667-1 Test No. 9

V, knots	R_t, lb	Wetted length of keel, ft	Wetted length of chine, ft	Re x 10^{-6}	S, ft^2	10^3 C_t	Change of trim, deg	CG rise, in	F_∇
0.99	0.52	7.65	5.80	1.022	14.57	13.209	-0.01	0.04	0.24
1.51	1.10	7.65	5.80	1.559	14.57	12.006	0.04	0.02	0.36
2.00	2.05	7.65	5.80	2.065	14.57	12.750	0.09	-0.05	0.48
2.08	2.25	7.70	6.00	2.189	14.80	12.740	0.09	0.03	0.50
2.50	3.49	7.72	6.20	2.673	15.04	13.458	0.17	-0.15	0.60
3.00	5.65	7.75	6.40	3.264	15.35	14.824	0.44	-0.15	0.72
3.09	6.13	7.75	6.40	3.361	15.36	15.152	0.44	-0.17	0.75
3.23	7.28	7.70	6.50	3.524	15.45	16.373	0.57	-0.17	0.78
3.50	9.27	7.70	6.50	3.818	15.55	17.641	0.69	-0.27	0.84
4.13	15.46	7.60	6.60	4.506	15.77	20.835	1.76	-0.44	1.00
5.15	26.67	7.20	5.80	5.144	13.55	26.901	3.79	-0.39	1.24
6.20	29.39	6.80	5.40	5.811	12.35	22.441	4.39	0.09	1.50
7.21	33.40	5.50	4.40	5.484	8.65	26.925	5.34	0.52	1.74
8.29	36.89	5.00	4.10	5.796	7.80	24.946	6.04	1.30	2.00
9.29	36.35	4.80	3.90	6.210	7.42	20.576	5.84	2.78	2.24
10.30	35.58	4.70	3.70	6.647	7.15	17.003	5.44	2.11	2.49
11.40	34.51	--	--	7.217	6.97	13.810	4.89	2.59	2.75
12.48	33.44	4.60	3.50	7.767	6.80	11.445	4.24	2.59	3.01
13.50	32.76	4.60	3.40	8.298	6.75	9.653	3.64	2.75	3.26
14.40	32.38	4.60	3.30	8.740	6.65	8.512	3.34	2.94	3.47
15.64	32.32	4.70	3.20	9.493	6.65	7.202	2.74	3.13	3.77
16.68	32.62	4.70	3.10	9.996	6.55	6.489	2.34	3.24	4.02

Model 4667-1 Test No. 10

V, knots	R_t, lb	Wetted length of keel, ft	Wetted length of chine, ft	Re x 10^{-6}	S, ft^2	10^3 C_t	Change of trim, deg	CG rise, in	F_∇
1.00	0.25	7.83	6.00	1.063	13.10	6.918	0.12	0.07	0.26
1.50	0.60	7.83	6.00	1.595	13.10	7.380	0.02	0.01	0.38
1.97	1.13	7.90	6.40	2.164	13.54	7.798	-0.04	-0.02	0.50
2.00	1.12	7.83	6.00	2.126	13.10	7.748	-0.13	-0.12	0.51
2.50	2.15	7.83	6.00	2.658	13.10	9.519	-0.20	-0.20	0.64
2.91	3.66	7.95	7.95	3.555	14.50	10.806	-0.20	-0.16	0.75
3.00	3.83	7.83	6.00	3.190	13.10	11.775	-0.23	-0.22	0.77
3.22	4.94	7.83	6.00	3.424	13.10	13.184	-0.27	-0.28	0.83
3.50	5.32	7.83	6.00	3.721	13.10	12.017	-0.30	-0.30	0.90
3.90	8.81	8.00	8.00	4.794	14.50	14.480	-0.20	-0.39	1.00
4.88	15.02	7.80	7.00	5.549	14.21	16.090	1.47	-0.40	1.25
5.83	18.05	7.80	7.00	6.629	14.35	13.415	2.42	-0.15	1.49
6.84	20.45	7.60	6.60	7.462	13.79	11.490	2.52	0.09	1.75
7.82	22.74	7.60	6.60	8.532	13.79	9.775	2.57	0.23	2.00
8.80	24.05	7.60	6.20	9.331	13.69	8.223	3.12	0.54	2.26
9.80	23.29	7.50	5.60	9.864	13.03	6.746	3.67	3.35	2.51
10.78	23.42	7.35	5.20	10.403	11.48	6.364	4.22	3.49	2.76
11.74	24.30	7.20	4.90	10.914	10.90	4.752	4.22	1.20	3.01
12.68	26.11	7.15	4.70	11.594	10.70	5.501	4.27	1.40	3.25
13.64	26.63	7.05	4.50	12.157	10.40	4.989	4.22	1.76	3.50
14.68	28.86	7.00	4.35	12.858	10.20	4.759	4.07	1.89	3.76
15.78	30.69	7.00	4.20	13.579	10.00	4.468	3.92	2.03	4.04
17.64	34.78	7.00	3.90	14.773	9.68	4.186	3.52	2.06	4.52
19.71	39.47	7.00	3.65	16.144	9.45	3.897	3.32	2.16	5.05
21.60	45.19	7.00	3.40	17.260	9.15	3.837	3.12	2.22	5.54
23.56	51.06	7.00	3.20	18.464	8.99	3.709	3.02	2.38	6.04

Model 4667-1 Test No. 11

V, knots	R_t, lb	Wetted length of keel, ft	Wetted length of chine, ft	Re x 10^{-6}	S, ft^2	10^3 C_t	Change of trim, deg	CG rise, in	F_∇
1.00	0.40	7.80	5.80	1.044	12.30	11.788	0.00	0.00	0.26
1.51	0.70	7.80	5.80	1.577	12.30	9.049	-0.02	-0.03	0.39
1.92	1.30	7.85	5.60	1.991	12.22	10.463	0.00	-0.02	0.49
1.99	1.30	7.80	5.80	2.079	12.30	9.676	-0.05	-0.09	0.51
2.51	2.44	7.80	5.80	2.622	12.30	11.414	-0.10	-0.15	0.64
2.92	3.88	7.90	5.60	3.028	12.22	13.500	-0.04	-0.18	0.75
2.99	4.08	7.80	5.80	3.124	12.30	13.450	-0.05	-0.21	0.77
3.22	5.20	7.80	5.80	3.364	12.30	14.781	0.00	-0.23	0.83
3.52	6.49	7.80	5.80	3.678	12.30	15.438	0.00	-0.31	0.90
3.91	8.76	7.90	7.60	4.656	13.62	15.250	0.25	-0.34	1.00
4.87	14.26	7.85	7.20	5.650	13.45	16.205	1.75	-0.43	1.25
5.84	16.30	7.70	6.60	6.416	12.90	13.430	2.58	-0.18	1.50
6.84	17.97	7.60	6.20	7.252	14.86	9.370	2.66	0.05	1.75
7.80	19.43	7.50	6.00	8.090	13.78	8.401	3.10	0.31	2.00
8.78	20.33	7.40	5.40	8.635	12.36	7.734	3.50	0.55	2.25
9.78	20.77	7.10	5.00	9.092	10.90	7.222	4.00	0.75	2.51
10.76	21.78	6.90	4.70	9.590	10.40	6.557	4.10	1.07	2.63
11.76	22.69	6.70	4.50	10.120	10.00	5.947	4.06	1.21	3.01
12.72	23.72	6.60	4.30	10.653	9.67	5.496	3.93	1.44	3.26
13.64	24.95	6.40	4.15	11.067	9.35	5.199	3.62	1.49	3.50
14.72	26.74	6.40	4.00	11.762	9.15	4.889	3.52	1.79	3.77
15.74	28.07	6.40	3.85	12.384	9.02	4.553	3.39	1.86	4.03
17.66	32.79	6.45	3.60	13.623	8.82	4.321	3.15	2.03	4.53
19.62	36.58	6.50	3.30	14.773	8.55	4.029	2.76	2.08	5.03
21.64	42.83	6.60	3.10	16.128	8.45	3.923	2.50	2.12	5.55
23.60	47.01	6.70	2.90	17.408	8.25	3.709	2.35	2.19	6.05

Model 4667-1 Test No. 12

V. knots	R_t, lb	Wetted length of keel, ft	Wetted length of chine, ft	Re x 10^{-6}	S, ft^2	10^3 C_t	Change of trim, deg	CG rise, in	F_∇
1.01	0.39	7.70	5.50	1.024	12.95	10.710	0.01	0.00	0.26
1.52	0.75	7.70	5.50	1.541	12.95	9.089	0.01	-0.06	0.39
1.94	1.45	7.80	5.10	1.922	12.72	10.982	0.05	-0.11	0.50
2.00	1.48	7.70	5.50	2.028	12.92	10.381	0.03	-0.07	0.51
2.50	2.58	7.70	5.50	2.535	12.78	11.709	0.06	-0.21	0.64
2.93	4.18	7.70	5.20	2.904	12.59	14.021	0.14	-0.25	0.75
3.00	4.08	7.70	5.50	3.042	12.56	13.083	0.15	-0.18	0.77
3.24	5.27	7.70	5.50	3.286	12.41	14.665	0.20	-0.19	0.83
3.50	6.55	7.70	5.50	3.549	12.34	15.707	0.30	-0.29	0.90
3.91	8.76	7.60	6.30	4.175	13.74	15.117	0.67	-0.42	1.00
4.87	13.89	7.40	6.20	5.089	13.75	15.440	2.41	-0.41	1.25
5.86	15.62	7.40	5.60	5.853	12.65	13.035	2.91	-0.14	1.50
6.84	17.12	7.30	5.30	6.622	12.35	10.741	3.15	0.15	1.75
7.82	18.95	7.00	5.00	7.210	12.10	9.283	3.65	0.43	2.00
8.81	20.43	6.40	4.60	7.446	10.55	9.044	4.10	0.68	2.26
9.80	21.22	6.00	4.20	7.680	8.97	8.929	4.20	1.01	2.51
10.78	21.88	5.80	4.00	8.117	8.55	7.983	4.10	1.20	2.76
11.78	22.54	5.80	3.80	8.689	8.35	7.051	3.95	1.37	3.02
12.82	23.03	5.50	3.60	8.963	7.83	6.487	3.60	1.52	3.29
13.74	23.44	5.50	3.50	9.501	7.73	5.822	3.37	1.85	3.52
14.74	25.20	5.40	3.40	9.966	7.54	5.576	3.08	1.98	3.78
15.74	25.81	5.40	3.20	10.400	7.32	5.159	2.78	2.01	4.03
17.70	29.07	5.40	3.10	11.560	7.24	4.646	2.45	2.13	4.54
19.62	32.72	5.40	2.90	12.512	7.04	4.377	2.15	2.16	5.03
21.62	37.83	5.60	2.60	13.621	6.94	4.227	1.80	2.18	5.54
23.58	42.50	5.80	2.00	14.132	6.55	4.230	1.50	2.22	6.04

Model 4667-1 Test No. 13

V, knots	R_t, lb	Wetted length of keel, ft	Wetted length of chine, ft	Re x 10^{-6}	S, ft^2	10^3 C_t	Change of trim, deg	CG rise, in	F_∇
1.00	0.45	7.60	5.10	0.977	11.51	14.172	-0.03	-0.01	0.26
1.50	0.90	7.60	5.15	1.470	11.57	12.533	-0.03	-0.02	0.38
1.94	1.60	7.60	5.20	1.907	11.60	13.287	0.15	-0.03	0.50
1.99	1.60	7.60	5.20	1.957	11.60	12.627	0.13	0.00	0.51
2.49	2.81	7.60	5.15	2.441	11.57	14.200	0.20	-0.09	0.64
2.93	4.23	7.60	5.10	2.859	12.67	14.099	0.30	-0.19	0.75
3.00	4.48	7.60	5.15	2.941	11.57	15.595	0.33	-0.15	0.77
3.22	5.50	7.60	6.20	3.409	12.47	15.421	0.40	-0.19	0.83
3.50	6.57	7.60	6.50	3.791	12.73	15.272	0.59	-0.22	0.90
3.89	9.36	7.90	7.60	4.632	14.79	15.160	1.20	-0.31	1.00
4.51	13.47	7.45	7.15	5.128	13.30	18.049	2.35	-0.34	1.16
4.88	15.16	7.20	6.90	5.286	14.09	16.378	2.85	-0.32	1.25
4.89	15.19	7.30	6.80	5.297	14.09	16.343	2.85	-0.32	1.25
5.84	16.70	7.00	6.30	5.968	12.99	13.664	3.15	-0.06	1.50
6.89	18.71	6.50	5.80	6.511	11.10	12.871	3.60	0.34	1.77
7.81	21.01	5.50	5.60	6.661	9.90	12.612	4.25	0.59	2.00
8.80	21.58	5.50	5.20	7.234	9.48	10.655	4.50	1.05	2.26
9.72	21.73	5.20	4.90	7.543	8.85	9.421	4.30	1.32	2.49
10.78	21.76	4.90	4.70	7.951	8.35	8.129	3.90	1.51	2.76
11.74	22.00	4.70	4.50	8.298	7.93	7.296	3.45	1.72	3.01
12.72	22.12	4.60	4.40	8.796	7.73	6.411	3.30	2.05	3.26
13.64	22.40	4.40	4.20	9.013	7.35	5.938	2.75	2.14	3.50
14.68	23.41	4.30	4.10	9.474	7.14	5.515	2.50	2.22	3.76
15.72	24.17	4.20	4.00	9.904	6.94	5.109	2.25	1.86	4.03
17.52	26.74	4.05	3.85	10.634	6.65	4.749	1.70	2.38	4.49
19.64	30.52	3.90	3.70	11.468	6.35	4.517	1.35	2.46	5.03
21.62	34.13	3.70	3.50	11.960	5.96	4.441	1.15	2.60	5.54
23.60	38.33	3.60	3.40	12.693	5.80	4.301	0.90	2.59	6.05

Model 4667-1 Test No. 14

V. knots	R_t, lb	Wetted length of keel, ft	Wetted length of chine, ft	Re x 10^{-6}	S, ft^2	10^3 C_t	Change of trim, deg	CG rise, in	F_∇
1.00	0.25	7.85	4.80	0.971	11.66	7.772	-0.07	-0.08	0.27
1.50	0.50	7.90	5.50	1.544	11.33	7.110	-0.12	-0.11	0.40
1.86	0.85	7.85	4.80	1.809	11.69	7.621	-0.32	-0.18	0.50
2.00	0.95	7.90	5.90	2.120	12.70	6.779	-0.12	-0.08	0.54
2.50	1.84	7.95	5.80	2.643	12.72	8.390	-0.35	-0.29	0.67
2.80	2.55	8.00	5.80	2.968	12.73	9.262	-0.37	-0.22	0.75
3.00	3.13	8.00	5.50	3.111	12.45	10.126	-0.35	-0.33	0.81
3.50	4.94	8.00	4.90	3.469	11.90	12.284	-0.40	-0.40	0.94
3.72	6.02	8.00	8.00	4.573	13.92	11.329	-0.37	-0.22	1.00
4.00	7.03	8.05	4.20	3.761	11.25	14.157	-0.22	-0.68	1.08
4.66	10.44	8.00	5.60	4.869	12.64	13.788	0.73	-0.45	1.25
5.58	12.71	8.00	6.60	6.259	13.62	10.864	1.63	-0.34	1.50
6.49	14.48	7.90	7.20	7.210	13.03	9.564	2.03	-0.03	1.75
7.42	16.43	7.85	7.85	8.951	13.17	8.214	1.93	0.09	2.00
8.31	18.20	7.80	7.80	9.960	13.37	7.146	2.08	0.18	2.24
9.28	19.15	7.60	7.60	10.838	13.81	5.837	2.43	0.29	2.50
10.18	19.42	7.50	7.40	11.654	13.35	5.088	2.93	0.70	2.74
11.18	20.23	7.40	7.20	12.541	13.11	4.475	3.13	0.76	3.01
12.12	21.62	7.30	6.90	13.223	12.81	4.165	3.13	0.89	3.26
13.20	23.38	7.25	6.60	14.037	12.52	3.885	3.13	0.98	3.55
13.92	24.23	7.20	6.40	14.546	12.30	3.685	3.08	1.04	3.74
14.96	26.52	7.20	6.10	15.288	12.05	3.565	3.08	1.25	4.02
16.80	30.86	7.10	5.90	16.781	11.77	3.367	3.03	1.44	4.52
18.64	35.58	7.10	5.70	18.332	11.59	3.203	2.93	1.56	5.01
20.56	40.55	7.10	5.60	20.063	11.50	3.024	2.68	1.63	5.53
22.40	46.75	7.00	5.50	21.514	11.30	2.989	2.48	1.61	6.03

Model 4667-1 Test No. 15

V, knots	R_t, lb	Wetted length of keel, ft	Wetted length of chine, ft	Re x 10^{-6}	S, ft^2	10^3 C_t	Change of trim, deg	CG rise, in	F_∇
1.00	0.25	7.75	5.10	0.988	12.02	7.539	0.00	0.00	0.27
1.50	0.50	7.80	5.15	1.493	12.16	6.624	-0.02	-0.01	0.40
1.86	0.87	7.82	5.10	1.846	12.08	7.548	0.00	0.00	0.50
2.00	1.08	7.82	5.20	2.00	12.46	7.855	-0.05	-0.05	0.54
2.50	1.97	7.90	5.40	2.554	12.40	9.214	-0.05	-0.06	0.67
2.79	2.78	7.90	5.40	2.851	12.40	10.440	0.00	-0.04	0.75
3.00	3.23	7.90	5.30	3.042	12.82	10.148	0.00	-0.13	0.81
3.50	4.87	8.00	4.80	3.442	11.83	12.182	0.10	-0.16	0.94
3.72	5.87	8.00	4.40	3.544	11.55	13.314	0.15	-0.26	1.00
4.00	6.81	8.00	4.10	3.718	12.31	12.533	0.35	-0.24	1.08
4.63	9.16	7.90	3.20	3.948	10.30	15.039	1.10	-0.88	1.25
5.56	11.01	7.70	7.70	6.579	14.12	9.143	2.00	0.00	1.50
6.48	12.35	7.65	7.65	7.617	13.93	7.654	2.15	0.17	1.74
7.42	13.70	7.60	7.60	8.665	13.88	6.499	2.20	0.29	2.00
8.34	14.95	7.55	7.40	9.586	13.38	5.823	2.50	0.37	2.24
9.24	15.94	7.35	7.00	10.195	12.95	5.226	2.76	0.51	2.49
10.22	16.85	7.30	6.40	10.758	12.37	4.727	3.08	0.87	2.75
11.15	17.73	7.00	6.00	11.137	11.77	4.392	3.15	0.56	3.00
12.12	19.27	6.90	5.65	11.696	11.37	4.182	3.14	1.20	3.26
13.28	19.79	6.90	5.00	12.142	10.70	3.802	3.05	1.31	3.57
13.98	21.97	6.90	4.95	12.718	10.62	3.837	2.96	1.40	3.76
14.98	23.98	6.80	4.80	13.351	10.40	3.725	2.80	1.40	4.03
16.74	27.65	6.80	4.60	14.663	10.20	3.507	2.59	1.28	4.50
18.72	31.76	6.80	4.40	16.109	10.00	3.285	2.37	1.69	5.04
20.52	36.58	6.80	4.30	17.501	9.88	3.187	2.20	1.75	5.52
21.74	39.46	6.80	4.20	18.374	9.77	3.098	2.15	1.81	5.85
22.42	41.77	6.80	4.20	18.949	9.77	3.083	2.10	1.79	6.03

Model 4667-1 Test No. 16

V, knots	R_t, lb	Wetted length of keel, ft	Wetted length of chine, ft	Re x 10^{-6}	S, ft^2	10^3 C_t	Change of trim, deg	CG rise, in	F_∇
1.00	0.30	7.70	4.40	0.929	10.90	9.977	0.00	-0.02	0.27
1.50	0.60	7.70	4.20	1.371	11.32	8.539	0.00	-0.07	0.40
1.86	1.02	7.72	4.90	1.803	11.87	9.007	0.02	-0.08	0.50
2.00	1.25	7.75	4.90	1.942	12.01	9.432	0.04	-0.09	0.54
2.50	2.14	7.80	5.10	2.477	12.22	10.157	0.04	-0.15	0.67
2.80	2.83	7.80	5.10	2.775	12.19	10.735	0.06	-0.16	0.75
3.00	3.43	7.80	5.60	3.088	11.75	11.757	0.12	-0.21	0.81
3.50	4.87	7.80	4.60	3.334	11.70	12.317	0.25	-0.24	0.94
3.72	5.82	7.80	4.40	3.487	11.55	13.200	0.42	-0.16	1.00
4.00	6.66	7.83	3.70	3.540	10.87	13.881	0.66	-0.39	1.08
4.63	8.82	7.70	7.70	5.478	14.01	10.646	1.50	-0.37	1.25
5.57	10.43	7.50	7.40	6.376	13.91	8.761	2.08	-0.21	1.50
6.50	11.48	7.45	7.20	7.321	13.66	7.210	2.33	0.06	1.75
7.42	12.75	7.30	6.90	8.095	13.36	6.283	2.52	0.17	2.00
8.33	13.58	7.10	6.10	8.448	12.43	5.707	2.78	0.38	2.24
9.24	14.86	6.80	5.40	8.661	11.00	5.736	3.10	0.60	2.49
10.20	15.95	6.50	5.20	9.169	10.50	5.293	3.06	0.76	2.74
11.12	16.82	6.40	5.00	9.740	10.20	4.834	3.02	0.85	2.99
12.06	17.75	6.20	4.90	10.285	9.90	4.469	2.83	1.26	3.24
13.24	19.08	6.00	4.70	10.885	9.48	4.162	2.70	1.29	3.56
14.00	20.40	6.00	4.65	11.467	9.45	3.992	2.62	1.34	3.77
14.98	21.93	5.60	4.50	11.625	8.88	3.989	2.48	1.43	4.03
16.62	24.78	5.60	4.30	12.642	8.67	3.751	2.25	1.59	4.47
18.64	29.23	5.80	4.10	14.179	8.67	3.517	1.92	1.58	5.01
20.52	33.25	5.80	3.95	15.388	8.53	3.356	1.68	1.70	5.52
22.40	37.17	5.60	3.90	16.350	8.25	3.255	1.52	1.71	6.03

Model 4667-1 Test No. 17

V, knots	R_t, lb	Wetted length of keel, ft	Wetted length of chine, ft	Re x 10^{-6}	S, ft^2	10^3 C_t	Change of trim, deg	CG rise, in	F_∇
1.00	0.30	7.61	4.65	0.941	11.79	9.224	0.06	0.02	0.27
1.50	0.72	7.65	4.65	1.417	11.88	9.764	0.05	0.02	0.40
1.82	1.20	7.62	4.65	1.714	11.77	11.159	0.05	-0.08	0.49
1.99	1.35	7.65	4.70	1.889	11.89	10.394	0.06	0.02	0.54
2.50	2.39	7.67	4.90	2.412	12.05	11.504	0.12	-0.13	0.67
2.79	3.08	7.65	4.90	2.692	12.03	11.923	0.17	-0.18	0.75
2.98	3.63	7.70	4.80	2.862	11.97	12.380	0.23	-0.12	0.80
3.50	5.17	7.70	4.50	3.280	11.63	13.155	0.60	-0.17	0.94
3.72	6.27	7.65	4.20	3.384	11.41	14.395	0.84	-0.28	1.00
4.00	7.16	7.60	7.40	4.610	14.13	11.480	1.12	-0.26	1.08
4.62	9.39	7.42	7.00	5.118	13.58	11.743	2.00	-0.24	1.24
5.56	10.76	7.20	6.30	5.767	12.79	9.865	2.55	0.06	1.50
6.50	11.78	7.00	5.90	6.442	12.20	8.284	2.66	0.19	1.75
7.41	13.34	6.60	5.40	6.832	11.20	7.863	3.04	0.49	1.99
8.30	13.40	6.00	5.10	7.015	9.78	7.209	3.45	0.90	2.23
9.22	15.06	4.90	5.60	7.438	9.27	6.928	3.32	1.11	2.48
10.22	15.69	5.20	4.60	7.695	8.55	6.369	3.25	1.13	2.75
11.12	16.24	5.00	4.40	8.031	8.15	5.841	2.95	1.04	2.99
12.07	16.77	4.80	4.25	8.383	7.78	5.363	2.79	1.50	3.25
13.24	17.58	4.70	4.05	8.911	7.50	4.709	2.49	1.53	3.56
13.94	18.72	4.60	4.00	9.211	7.37	4.738	2.26	1.57	3.75
15.00	19.98	4.50	3.90	9.681	7.15	4.502	2.06	1.69	4.03
16.64	22.73	4.40	3.70	10.356	6.80	4.376	1.74	1.79	4.48
18.68	26.46	4.50	3.55	11.568	6.81	4.036	1.40	1.87	5.02
20.52	30.51	4.60	3.40	12.613	6.75	3.891	1.10	1.92	5.52
22.40	34.12	4.50	3.25	13.769	6.70	3.679	0.87	1.91	6.03

Model 4668 Test No. 1

V, knots	R_t, lb	Wetted length of keel, ft	Wetted length of chine, ft	Re x 10^{-6}	S, ft^2	10^3 C_t	Change of trim, deg	CG rise, in	F_∇
1.00	0.20	7.83	6.40	1.199	10.54	6.884	-0.03	-0.07	0.28
1.51	0.50	7.85	6.40	1.811	10.54	7.549	-0.14	-0.13	0.42
1.80	0.78	7.85	6.40	2.159	10.54	8.289	-0.16	-0.14	0.50
2.00	0.99	7.85	6.40	2.399	10.48	8.568	-0.18	-0.15	0.55
2.50	1.74	7.85	6.00	2.914	10.18	9.923	-0.11	-0.16	0.69
2.74	2.19	7.85	7.60	3.563	10.91	9.701	-0.01	-0.16	0.76
3.00	2.83	7.80	7.60	3.891	10.85	10.514	0.06	-0.17	0.83
3.51	4.02	7.75	7.60	4.541	10.81	10.952	0.12	-0.27	0.97
3.60	4.37	7.80	7.60	4.670	10.83	11.296	0.14	-0.27	0.99
4.00	5.43	7.70	7.60	5.155	10.70	11.507	0.46	-0.37	1.10
4.54	6.82	7.70	7.40	5.774	10.60	11.326	1.09	-0.35	1.25
5.42	8.49	7.70	7.00	6.711	10.67	9.827	1.64	-0.33	1.50
6.30	9.62	7.65	6.80	7.663	10.49	8.383	1.87	-0.16	1.74
7.22	10.85	7.60	6.50	8.575	10.26	7.360	1.91	-0.01	1.99
8.16	12.06	7.60	6.30	9.554	10.03	6.552	2.05	0.08	2.25
9.00	13.29	7.50	5.90	10.159	9.74	6.112	2.24	0.30	2.48
10.00	14.40	7.35	5.50	10.816	9.23	5.660	2.63	0.37	2.76
10.88	15.05	7.10	5.10	11.181	8.95	5.154	3.11	0.61	3.00
11.78	15.58	6.80	4.80	11.510	7.74	5.263	3.24	0.78	3.25
12.68	16.41	6.50	4.60	11.856	7.36	5.031	3.26	1.07	3.50
13.62	17.15	6.30	4.30	12.161	7.00	4.792	3.23	1.28	3.76
14.64	18.35	6.20	4.20	12.825	6.84	4.541	3.14	1.41	4.04
16.40	20.59	6.00	3.90	13.676	6.46	4.299	2.92	1.68	4.53
18.22	23.11	5.90	3.70	14.734	6.23	4.054	2.61	1.73	5.03
20.04	26.04	5.90	3.50	15.868	6.07	3.876	2.37	1.80	5.53
20.84	27.43	5.90	3.45	16.431	6.06	3.781	2.32	1.88	5.75

Model 4668 Test No. 2

V, knots	R_t, lb	Wetted length ft		Re x 10^{-6}	S, ft^2	10^3 C_t	Change of trim, deg	CG rise, in	F_∇
1.00	0.37	8.10		1.364	10.45	12.847	0.00	0.00	0.24
1.51	0.68	8.20		2.085	10.45	10.358	0.00	0.00	0.36
2.00	1.23	8.30		2.796	10.44	10.687	0.00	-0.02	0.48
2.51	2.51	8.78		3.712	10.45	13.835	0.00	-0.04	0.60

Model 4668 Test No. 7

V, knots	R_t, lb	Wetted length of keel, ft	Wetted length of chine, ft	Re x 10^{-6}	S, ft^2	10^3 C_t	Change of trim, deg	CG rise, in	F_∇
1.00	0.26	7.90	7.00	1.255	11.81	7.987	-0.01	-0.01	0.26
1.52	0.59	7.95	7.00	1.912	11.82	7.841	-0.10	-0.06	0.39
1.94	1.05	8.00	6.90	2.434	11.44	8.851	-0.15	-0.11	0.50
2.00	0.98	8.00	7.00	2.527	11.77	7.552	-0.12	-0.07	0.52
2.50	2.03	8.00	7.80	3.327	11.90	9.903	-0.16	-0.18	0.65
2.92	2.26	8.00	7.80	3.886	11.61	8.284	-0.05	-0.18	0.76
3.00	3.51	8.00	7.80	3.992	11.77	12.022	-0.02	-0.21	0.78
3.52	5.49	8.00	8.00	4.744	11.62	13.835	0.10	-0.22	0.91
3.86	7.06	8.00	7.80	5.137	11.33	15.174	0.28	-0.44	1.00
4.00	7.56	8.00	7.80	5.323	11.48	14.933	0.40	-0.42	1.04
4.78	11.54	7.80	7.40	6.120	11.47	15.976	1.70	-0.51	1.24
5.76	13.86	7.80	7.20	7.278	11.29	13.425	2.33	-0.34	1.50
6.74	14.87	7.70	7.10	8.402	11.27	10.538	2.43	-0.08	1.75
7.74	17.03	7.65	6.90	9.480	11.05	9.334	2.60	0.14	2.01
8.60	18.50	7.60	6.70	10.359	10.83	8.380	2.90	0.39	2.23
9.58	19.95	7.45	6.20	11.007	9.97	8.851	4.40	-0.11	2.49
10.62	20.57	7.15	5.60	11.399	9.07	8.156	4.15	0.92	2.76
11.58	20.96	6.60	5.10	11.413	7.81	7.261	4.50	1.14	3.01
12.54	21.66	6.20	4.90	11.725	7.36	6.790	4.49	1.51	3.26
13.50	22.18	6.50	4.70	12.168	7.12	6.201	4.38	1.77	3.51
14.54	23.14	5.90	4.50	12.738	6.84	5.806	4.28	2.10	3.78
15.50	24.20	5.80	4.30	13.187	6.60	5.537	4.10	2.29	4.03
17.57	25.91	5.70	4.10	14.504	6.38	4.773	3.58	2.47	4.56
19.38	28.49	5.65	3.90	15.574	6.27	4.389	3.28	2.65	5.04
21.30	31.52	5.65	3.70	16.758	6.03	4.180	3.06	2.83	5.53
23.22	35.02	5.70	3.60	18.190	6.00	3.927	2.70	2.81	6.03

Model 4668 Test No. 3

V, knots	R_t, lb	Wetted length ft		Re x 10^{-6}	S, ft^2	10^3 C_t	Change of trim, deg	CG rise, in	F_∇
1.00	0.35	8.03		1.352	10.52	12.072	0.01	0.01	0.24
1.52	0.79	8.05		2.061	10.51	11.811	0.02	0.00	0.36
2.00	1.42	8.10		2.729	10.51	12.256	0.00	-0.02	0.48
2.50	2.67	8.20		3.453	10.51	14.750	-0.05	-0.15	0.60
3.00	4.88	8.78		4.437	10.53	18.684	-0.05	-0.24	0.72
3.50	8.97	8.78		5.177	10.53	25.232	-0.08	-0.34	0.84
4.00	11.81	8.78		5.916	10.57	25.338	0.30	-0.53	0.96

Model 4668 Test No. 6

V, knots	R_t, lb	Wetted length ft		Re x 10^{-6}	S, ft^2	10^3 C_t	Change of trim deg	CG rise, in	F_∇
1.00	0.25	8.78		1.479	11.54	7.860	-0.01	-0.01	0.26
1.50	0.50	8.78		2.218	11.54	6.988	-0.04	-0.03	0.39
1.92	0.98	8.78		2.840	11.54	8.360	-0.07	-0.14	0.50
2.00	0.99	8.78		2.958	11.54	7.781	-0.09	-0.06	0.52
2.50	2.03	8.78		3.698	11.45	10.292	-0.11	-0.16	0.65
2.90	3.16	8.78		4.289	11.54	11.813	-0.13	-0.19	0.75
3.00	3.48	8.78		4.437	11.45	12.252	-0.10	-0.25	0.78
3.50	5.47	8.78		5.177	11.45	14.149	-0.13	-0.29	0.91
3.84	6.96	8.78		5.680	11.80	14.513	-0.10	-0.35	1.00
4.00	7.61	8.78		5.916	11.80	14.624	-0.07	-0.46	1.04
4.78	11.19	8.78		7.070	12.33	14.411	1.15	-0.68	1.24
5.76	13.91	8.78		8.520	12.15	12.520	1.95	-0.47	1.50
6.76	16.37	8.78		9.999	12.33	10.541	2.13	--	1.76
7.64	19.23	8.78		11.301	11.98	9.977	2.15	-0.10	1.98
8.62	22.38	8.78		12.750	11.50	9.502	2.15	0.03	2.24
10.60	25.37	7.30		13.036	9.77	8.385	3.05	0.28	2.75
11.58	23.31	6.77		13.207	9.08	6.946	4.03	0.84	3.01
12.58	22.64	6.35		13.458	8.55	6.071	4.55	1.36	3.27
13.54	23.38	6.10		13.915	8.17	5.663	4.60	1.67	3.51
14.58	24.54	5.90		14.492	7.88	5.315	4.53	1.85	3.79
15.54	25.50	5.72		14.975	7.62	5.028	4.35	2.02	4.04
17.40	26.96	5.50		16.123	7.28	4.438	4.13	2.37	4.52
19.34	29.50	5.35		17.432	7.08	4.042	3.83	2.49	5.02
21.30	33.92	5.25		18.839	6.92	3.920	3.55	2.56	5.53
23.14	37.62	5.15		20.077	6.75	3.776	3.29	2.59	6.01

Model 4668 Test No. 8

V, knots	R_t, lb	Wetted length of keel, ft	Wetted length of chine, ft	Re x 10^{-6}	S, ft^2	10^3 C_t	Change of trim, deg	CG rise, in	F_∇
1.00	0.30	7.83	6.40	1.197	11.36	9.581	0.02	0.01	0.26
1.50	0.65	7.85	6.40	1.799	11.37	9.219	0.00	-0.02	0.39
1.92	1.22	7.85	6.40	0.394	11.49	0.039	0.02	-0.04	0.50
2.00	1.32	7.87	6.60	2.436	11.56	10.357	0.04	-0.06	0.52
2.51	2.18	7.87	7.60	3.268	11.72	10.713	0.08	-0.10	0.65
2.92	3.53	7.85	7.60	3.797	11.78	12.752	0.13	-0.14	0.76
3.00	3.78	7.87	7.60	3.906	11.73	12.990	0.17	-0.19	0.78
3.50	6.17	7.85	7.60	4.552	11.61	15.740	0.30	-0.32	0.91
3.84	7.66	7.83	7.60	4.987	11.76	16.027	0.59	-0.38	1.00
4.00	8.31	7.80	7.60	5.189	11.67	16.147	0.78	-0.42	1.04
4.80	12.12	7.75	7.10	6.000	11.35	16.815	1.97	-0.52	1.25
5.74	13.96	7.60	6.70	6.914	11.40	13.485	2.49	-0.38	1.49
6.76	15.12	7.50	6.40	7.915	10.78	11.136	2.78	-0.05	1.76
7.72	16.53	7.40	6.20	8.844	10.38	9.694	2.99	0.22	2.01
8.64	18.20	7.20	5.80	9.461	9.84	8.989	3.30	0.38	2.24
9.60	19.63	6.83	5.30	9.801	9.07	8.520	4.00	0.73	2.49
10.62	20.77	5.90	4.80	9.574	7.80	8.566	4.55	1.14	2.76
11.58	21.41	5.60	4.50	9.852	6.60	8.777	4.50	1.40	3.01
12.58	21.64	5.40	4.30	10.279	6.30	7.875	4.30	1.72	3.27
13.50	21.96	5.40	4.20	10.917	6.23	7.017	4.10	2.04	3.51
14.50	22.64	5.30	4.10	11.481	6.07	6.436	3.79	2.28	3.77
15.44	23.30	5.20	3.90	11.705	5.88	6.031	3.45	2.31	4.01
17.37	24.81	5.10	3.70	12.876	5.63	5.299	3.08	2.59	4.51
19.24	26.94	5.10	3.60	14.100	5.55	4.757	2.50	2.64	5.00
21.24	29.67	5.20	3.40	15.387	5.47	4.362	2.22	2.80	5.52
23.22	32.85	5.20	3.30	16.626	5.24	4.218	1.95	2.83	6.03

Model 4668 Test No. 10

V, knots	R_t, lb	Wetted length of keel, ft	Wetted length of chine, ft	Re x 10^{-6}	S, ft^2	10^3 C_t	Change of trim, deg	CG rise, in	F_∇
1.00	0.18	7.90	7.00	1.255	10.54	6.196	-0.02	0.09	0.28
1.50	0.43	7.90	7.00	1.882	10.54	6.580	-0.02	0.07	0.41
1.80	0.65	8.00	7.00	2.274	10.58	6.881	-0.03	-0.06	0.50
2.00	0.82	7.90	7.00	2.510	10.54	7.056	-0.05	0.15	0.55
2.50	1.61	7.90	7.00	3.137	10.47	8.927	-0.09	0.03	0.69
2.73	2.06	7.80	7.20	3.449	10.58	9.480	-0.09	-0.26	0.75
3.00	2.66	7.90	7.00	3.765	10.47	10.242	-0.09	-0.06	0.83
3.53	3.97	7.90	7.00	4.430	10.47	11.041	-0.12	-0.18	0.97
4.00	5.29	7.90	7.00	5.020	10.61	11.306	0.00	-0.30	1.10
4.53	6.86	7.90	7.00	5.685	10.75	11.283	0.72	0.27	1.25
5.42	9.15	7.90	7.60	7.076	11.16	10.126	0.85	-0.55	1.50
6.32	10.71	7.90	7.30	8.092	10.98	8.860	1.65	-0.04	1.74
7.23	12.49	7.40	7.00	8.770	10.62	8.163	1.70	-0.09	2.00
8.13	14.31	7.60	7.20	10.135	10.78	7.287	1.77	0.05	2.24
9.04	16.41	7.80	7.20	11.422	10.55	6.906	1.80	0.08	2.49
9.98	18.11	7.60	6.80	12.106	10.12	6.519	2.10	0.28	2.75
10.90	18.15	7.60	6.40	12.854	9.70	5.714	2.57	0.47	3.01
11.80	17.94	7.50	5.60	13.021	9.15	5.109	3.09	0.56	3.26
12.72	18.13	7.30	5.20	13.393	8.40	4.840	3.24	0.81	3.51
13.64	19.25	7.20	5.00	14.017	8.17	4.595	3.38	0.90	3.76
14.60	20.53	6.86	4.80	14.340	7.90	4.423	3.38	1.23	4.03
16.38	23.51	6.80	4.40	15.453	7.43	4.274	3.24	1.51	4.52
18.20	26.01	6.60	4.10	16.404	7.07	4.030	3.13	1.74	5.02
20.00	28.72	6.20	3.90	17.016	6.62	3.113	3.00	1.80	5.52
20.80	30.56	6.40	3.80	17.871	6.68	3.836	2.91	1.79	5.74

Model 4668 Test No. 9

V, knots	R_t, lb	Wetted length of keel, ft	Wetted length of chine, ft	Re x 10^{-6}	S, ft^2	10^3 C_t	Change of trim, deg	CG rise, in	F_∇
1.00	0.39	7.65	6.00	1.148	11.32	12.499	0.03	-0.01	0.26
1.51	0.78	7.70	6.00	1.742	11.35	10.939	0.05	-0.06	0.39
1.90	1.28	7.75	6.00	2.199	11.37	11.316	0.11	-0.05	0.49
2.00	1.36	7.73	6.00	2.311	11.36	10.859	0.11	-0.05	0.52
2.50	2.28	7.75	6.00	2.893	11.37	11.641	0.15	-0.11	0.65
2.92	3.30	7.75	7.20	3.674	11.86	11.841	0.23	-0.20	0.76
3.00	3.78	7.75	7.20	3.775	11.86	12.848	0.26	-0.27	0.78
3.52	6.35	7.70	7.00	4.358	11.68	15.920	0.66	-0.30	0.91
3.84	8.08	7.65	6.80	4.670	11.64	17.080	1.08	-0.40	1.00
4.00	9.06	7.60	6.80	4.852	11.67	17.604	1.28	-0.40	1.04
4.80	13.54	7.40	6.20	5.337	10.95	19.472	1.47	-0.94	1.25
5.52	15.57	7.20	5.90	6.091	10.59	17.507	3.03	-0.22	1.43
5.78	15.51	7.10	5.80	6.280	10.04	16.777	3.03	-0.20	1.50
5.99	16.08	7.05	5.70	6.428	10.09	16.115	3.08	-0.12	1.56
6.22	16.32	7.00	5.70	6.654	9.99	15.320	3.13	-0.08	1.62
6.76	16.79	6.80	5.60	7.061	9.53	13.988	3.22	0.13	1.76
7.68	18.63	6.30	5.20	7.439	8.80	13.022	3.68	0.44	2.00
8.62	20.80	5.70	4.20	7.188	7.03	14.447	4.41	0.83	2.24
9.58	22.38	5.10	4.30	7.585	6.07	14.575	5.13	1.23	2.49
10.59	22.52	4.90	4.10	8.028	5.77	12.626	4.91	1.73	2.75
11.60	22.31	4.70	3.90	8.403	5.46	11.017	4.52	2.03	3.01
12.56	22.14	4.60	3.70	8.781	5.23	9.736	4.11	2.44	3.26
13.60	22.11	4.50	3.70	9.394	5.15	8.421	3.68	2.61	3.53
14.52	22.39	4.50	3.50	9.785	5.01	7.691	3.28	2.78	3.77
15.44	22.60	4.40	3.40	10.144	4.85	7.092	3.01	2.78	4.01
17.40	23.46	4.40	3.30	11.286	4.78	5.881	2.28	2.95	4.52
19.36	25.09	4.40	3.10	12.231	4.65	5.223	1.93	3.16	5.03

Model 4668 Test No. 11

V, knots	R_t, lb	Wetted length of keel, ft	Wetted length of chine, ft	Re x 10^{-6}	S, ft^2	10^3 C_t	Change of trim, deg	CG rise, in	F_∇
1.00	0.25	7.85	6.50	1.207	10.55	8.597	-0.02	-0.01	0.28
1.51	0.50	7.85	6.50	1.823	10.55	7.543	-0.04	-0.04	0.42
1.78	0.80	7.90	6.50	2.159	10.58	8.661	-0.03	-0.04	0.49
2.00	0.99	7.87	6.50	2.419	10.49	8.560	-0.06	-0.06	0.55
2.50	1.69	7.87	6.10	2.939	10.22	9.600	-0.06	-0.11	0.69
2.74	2.16	7.90	7.60	3.577	10.89	9.586	-0.06	-0.22	0.76
3.00	2.73	7.90	7.60	3.917	10.85	10.143	-0.02	-0.21	0.83
3.50	3.99	7.90	7.60	4.569	10.85	10.892	0.06	-0.27	0.97
4.00	5.36	7.85	7.60	5.202	10.89	11.161	0.43	-0.35	1.10
4.52	6.89	7.85	7.50	5.840	10.86	11.267	1.10	-0.36	1.25
4.52	6.79	7.80	7.40	5.787	10.70	11.269	1.08	-0.32	1.25
5.44	8.53	7.75	7.10	6.800	10.89	9.603	1.68	-0.27	1.50
6.32	9.79	7.70	6.80	7.719	10.67	8.334	1.88	-0.10	1.74
7.20	11.06	7.65	6.60	8.636	10.36	7.471	1.98	0.06	1.99
8.12	12.31	7.60	6.40	9.576	10.14	6.680	2.12	0.24	2.24
9.03	13.58	7.55	6.10	10.375	9.86	6.128	2.10	0.23	2.49
9.92	14.66	7.40	5.70	10.946	9.32	5.799	2.61	0.31	2.74
10.86	15.35	7.20	5.30	11.435	8.58	5.504	3.15	0.59	3.00
11.78	16.09	7.00	4.90	11.808	7.95	5.291	3.35	0.95	3.25
12.74	16.53	6.70	4.70	12.234	7.59	4.868	3.38	1.17	3.52
13.66	17.79	6.40	4.50	12.542	7.22	4.791	3.35	1.35	3.77
14.58	18.48	6.30	4.30	13.018	6.98	4.519	3.35	1.45	4.02
16.38	20.86	6.20	4.00	14.074	6.68	4.223	3.03	1.67	4.52
18.20	23.31	6.10	3.80	15.178	6.46	3.952	2.82	1.85	5.02
20.04	26.37	6.00	3.60	16.206	6.23	3.969	2.55	1.94	5.53
20.84	27.96	6.00	3.60	16.853	6.23	3.749	2.52	1.95	5.75

Model 4668 Test No. 12

V, knots	R_t, lb	Wetted length of keel, ft	Wetted length of chine, ft	Re x 10^{-6}	S, ft^2	10^3 C_t	Change of trim, deg	CG rise, in	F_∇
1.00	0.25	7.77	5.90	1.150	9.41	9.638	0.00	-0.10	0.28
1.50	0.50	7.80	5.90	1.731	9.43	8.553	0.03	-0.08	0.41
1.78	0.85	7.80	5.90	2.054	10.49	9.280	0.02	0.01	0.49
2.00	1.04	7.80	5.90	2.308	9.36	10.078	0.06	-0.10	0.55
2.50	1.84	7.80	5.80	2.864	10.24	10.431	0.09	-0.05	0.69
2.71	2.19	7.80	7.20	3.424	10.51	10.295	0.11	-0.14	0.75
3.00	2.80	7.80	7.20	3.790	10.89	10.365	0.21	-0.22	0.83
3.50	4.17	7.75	7.20	4.404	10.83	11.404	0.36	-0.10	0.97
3.62	4.65	7.75	7.20	4.555	10.53	12.227	0.45	-0.25	1.00
3.99	5.63	7.75	7.20	5.021	10.80	11.880	0.78	-0.30	1.10
4.52	6.99	7.67	6.80	5.505	10.56	11.755	1.35	-0.38	1.25
5.40	8.39	7.55	6.40	6.341	10.32	10.115	1.86	-0.29	1.49
6.32	9.52	7.47	6.10	7.219	10.14	8.528	2.06	0.06	1.74
7.20	10.49	7.40	6.00	8.127	9.84	7.461	1.16	-0.35	1.99
8.12	11.43	7.30	5.60	8.823	9.31	6.756	2.26	0.37	2.24
9.02	12.92	7.10	5.30	9.421	8.91	6.466	2.61	0.35	2.49
10.00	13.69	6.45	4.80	9.468	7.82	6.351	3.21	0.77	2.76
10.84	14.25	6.00	4.50	9.587	6.92	6.358	3.41	0.96	2.99
11.78	14.98	5.80	4.30	10.022	6.61	5.925	3.36	1.34	3.25
12.74	15.68	5.60	4.10	10.409	6.30	5.563	3.26	1.58	3.52
13.56	16.40	5.50	3.90	10.737	6.08	5.322	3.16	1.51	3.74
14.56	17.30	5.40	3.80	11.283	5.93	4.993	2.94	1.67	4.02
16.40	19.03	5.30	3.60	12.295	5.68	4.519	2.54	1.81	4.53
18.20	21.46	5.30	3.40	13.338	5.54	4.243	2.41	2.04	5.02
20.04	24.22	5.30	3.20	14.349	5.39	4.059	1.96	2.11	5.53
20.86	25.31	5.30	3.10	14.760	5.30	3.982	1.76	2.15	5.76

Model 4668 Test No. 13

V, knots	R_t, lb	Wetted length of keel, ft	Wetted length of chine, ft	Re x 10^{-6}	S, ft^2	10^3 C_t	Change of trim, deg	CG rise, in	F_∇
1.00	0.25	7.70	5.55	1.115	10.25	8.849	0.01	0.00	0.28
1.51	0.55	7.70	5.55	1.684	10.20	8.582	0.03	0.01	0.42
1.81	0.90	7.70	5.60	2.027	10.31	9.669	0.04	0.02	0.50
2.00	1.04	7.70	5.40	2.207	10.02	9.414	0.05	0.02	0.55
2.50	1.81	7.70	5.40	2.758	10.02	10.487	0.13	-0.04	0.69
2.72	2.29	7.70	5.50	3.024	10.11	11.109	0.21	-0.01	0.75
3.00	2.95	7.73	5.30	3.290	9.93	11.976	0.25	-0.10	0.83
3.51	4.39	7.67	6.60	4.216	9.75	13.259	0.48	-0.20	0.97
3.62	4.87	7.65	6.60	4.342	9.63	14.002	0.56	-0.25	1.00
4.00	6.01	7.60	6.40	4.649	10.41	13.091	0.94	-0.37	1.10
4.53	7.54	7.55	6.20	5.243	10.53	12.660	1.67	-0.33	1.25
5.43	8.93	7.35	5.80	6.010	10.23	10.741	2.06	-0.27	1.50
6.32	9.99	7.20	5.60	6.814	9.52	9.532	2.19	-0.01	1.74
7.22	10.95	7.00	5.30	7.480	9.00	8.468	2.39	0.27	1.99
8.16	12.06	6.70	5.00	8.042	8.46	7.767	2.69	0.41	2.25
9.02	12.86	6.10	4.70	8.206	7.48	7.667	2.98	0.53	2.49
9.98	13.89	5.50	4.20	8.154	6.30	8.031	3.56	0.86	2.75
10.88	14.45	5.20	4.00	8.431	5.93	7.469	3.51	1.18	3.00
11.76	14.94	5.10	3.90	8.915	5.77	6.793	3.30	1.38	3.25
12.72	15.38	4.95	3.70	9.257	5.50	6.270	3.01	1.45	3.51
13.60	15.90	4.90	3.60	9.737	5.40	5.776	2.89	1.70	3.75
14.54	16.57	4.80	3.45	10.092	5.16	5.511	2.71	2.02	4.01
16.40	18.11	4.75	3.30	11.107	5.02	4.866	2.21	2.14	4.53
18.18	20.21	4.75	3.10	12.006	4.87	4.555	1.89	2.23	5.02
19.98	22.52	4.75	2.90	12.858	4.73	4.327	1.56	2.35	5.51
20.86	23.48	4.80	2.80	13.354	4.71	4.156	1.43	2.34	5.76

Model 4668 Test No. 14

V, knots	R_t, lb	Wetted length of keel, ft	Wetted length of chine, ft	Re x 10^{-6}	S, ft^2	10^3 C_t	Change of trim, deg	CG rise, in	F_∇
0.99	0.20	7.85	6.30	1.179	9.91	7.473	-0.02	-0.01	0.29
1.51	0.36	7.85	6.30	1.798	9.85	5.818	-0.03	-0.02	0.44
1.72	0.57	7.85	6.30	2.048	9.85	7.099	-0.02	-0.01	0.50
1.99	0.74	7.88	6.30	2.376	9.82	6.905	-0.09	-0.06	0.58
2.50	1.34	7.88	6.30	2.986	9.87	7.882	-0.09	-0.06	0.72
2.61	1.54	7.85	5.90	3.020	9.57	8.571	-0.04	-0.16	0.76
2.99	2.08	7.90	5.40	3.349	9.24	9.136	-0.07	-0.25	0.87
3.42	2.87	7.85	5.27	3.779	9.12	9.762	-0.10	-0.57	0.99
3.52	2.92	7.90	5.00	3.825	8.93	9.575	-0.10	-0.25	1.02
4.00	4.01	7.90	4.60	4.211	8.68	10.476	0.01	-0.30	1.16
4.32	4.78	7.90	4.40	4.476	8.60	10.806	0.22	-0.37	1.25
5.18	6.43	7.80	7.20	6.545	10.39	8.368	1.02	-0.34	1.50
6.02	7.70	7.75	7.20	7.576	10.29	7.492	1.30	-0.15	1.74
6.89	8.97	7.75	7.00	8.555	10.26	6.682	1.39	-0.02	2.00
7.78	10.48	7.70	6.80	9.502	10.09	6.226	1.45	0.04	2.25
8.60	11.98	7.70	6.70	10.432	10.01	5.871	1.50	0.14	2.49
9.48	13.39	7.65	6.50	11.291	9.88	5.471	1.65	0.24	2.75
10.32	14.89	7.60	6.20	11.996	9.62	5.273	1.88	0.35	2.99
11.22	15.28	7.55	5.80	12.608	9.20	4.787	2.10	0.48	3.25
12.14	15.67	7.45	5.30	13.028	8.57	4.501	2.40	0.66	3.52
12.94	16.56	7.40	5.00	13.298	8.18	4.386	2.60	0.77	3.75
13.88	17.84	7.30	4.70	14.030	8.03	4.184	2.64	0.87	4.02
15.64	20.49	7.15	4.00	14.676	7.72	3.937	2.64	1.15	4.53
17.37	23.32	7.10	4.10	16.388	7.45	3.764	2.60	1.19	5.03
19.11	26.28	7.00	3.80	17.385	7.15	3.652	2.50	1.32	5.54
20.84	29.38	6.90	3.60	18.433	6.92	3.547	2.45	1.49	6.04

Model 4668 Test No. 15

V, knots	R_t, lb	Wetted length of keel, ft	Wetted length of chine, ft	Re x 10^{-6}	S, ft^2	10^3 C_t	Change of trim, deg	CG rise, in	F_∇
1.00	0.20	7.80	5.70	1.137	9.69	7.488	-0.01	-0.02	0.29
1.51	0.40	7.80	5.70	1.717	9.63	6.611	-0.01	-0.05	0.44
1.72	0.60	7.80	5.70	1.955	9.63	7.643	0.00	0.00	0.50
1.99	0.79	7.80	5.70	2.263	9.63	7.516	-0.02	-0.06	0.58
2.51	1.39	7.80	5.70	2.854	9.52	8.409	-0.02	-0.11	0.73
2.60	1.54	7.80	5.70	2.956	9.58	8.628	0.00	-0.11	0.75
2.99	2.18	7.80	5.30	3.299	9.20	9.617	0.04	-0.18	0.87
3.44	2.97	7.80	4.90	3.680	8.94	10.187	0.04	-0.26	1.00
3.52	3.07	7.80	4.90	3.765	8.94	10.056	0.12	-0.23	1.02
3.99	3.96	7.80	4.40	4.100	8.70	10.373	0.46	-0.21	1.16
4.32	4.60	7.75	4.20	4.345	8.35	10.710	0.70	0.10	1.25
5.14	5.88	7.70	6.90	6.321	10.20	7.917	1.20	-0.31	1.49
6.03	6.90	7.65	6.60	7.233	9.93	6.934	1.53	-0.11	1.75
6.88	7.97	7.60	6.40	8.113	9.76	6.259	1.61	0.08	1.99
7.72	9.08	7.60	6.10	8.909	9.63	5.740	1.66	0.18	2.24
8.58	10.28	7.55	5.90	9.713	9.43	5.373	1.75	0.28	2.49
9.44	11.54	7.50	5.60	10.496	9.26	5.074	1.92	0.37	2.74
10.36	12.39	7.40	5.20	10.996	8.76	4.781	2.18	0.47	3.00
11.22	13.05	7.25	4.90	11.474	8.13	4.626	2.48	0.61	3.25
12.06	13.89	7.15	4.70	12.028	7.92	4.375	2.57	0.85	3.49
12.98	15.11	7.00	4.40	12.464	7.60	4.281	2.61	0.87	3.76
13.86	16.05	6.80	4.20	12.842	7.28	4.423	2.62	1.01	4.02
15.66	18.09	6.60	3.90	13.851	6.92	3.867	2.52	1.23	4.54
17.31	20.60	6.50	3.70	14.873	6.68	3.734	2.43	1.42	5.01
19.02	23.23	6.40	3.50	15.861	6.45	3.612	2.28	1.48	5.51
20.80	26.21	6.30	3.30	16.820	6.30	3.489	2.16	1.61	6.03

Model 4668 Test No. 16

V, knots	R_t, lb	Wetted length of keel, ft	Wetted length of chine, ft	Re x 10^{-6}	S, ft^2	10^3 C_t	Change of trim, deg	CG rise, in	F_∇
1.00	0.20	7.73	5.40	1.105	9.61	7.551	0.01	-0.04	0.29
1.51	0.45	7.75	5.40	1.671	9.62	7.445	0.01	-0.04	0.44
1.72	0.66	7.75	5.40	1.903	9.62	8.417	0.02	-0.02	0.50
2.00	0.84	7.75	5.40	2.213	9.51	8.011	0.03	-0.08	0.58
2.51	1.45	7.75	5.40	2.778	9.51	8.781	0.08	-0.14	0.73
2.61	1.66	7.75	5.40	2.888	9.31	9.498	0.10	-0.05	0.76
3.00	2.18	7.75	5.20	3.270	9.29	9.460	0.19	-0.15	0.87
3.43	3.05	7.75	4.80	3.623	9.00	10.452	0.28	-0.19	0.99
3.51	3.10	7.75	4.80	3.707	9.04	10.099	0.30	-0.23	1.02
4.00	3.96	7.75	4.40	4.090	8.79	10.216	0.67	-0.29	1.16
4.31	4.45	7.65	6.60	5.170	10.15	8.563	0.86	-0.35	1.25
5.18	5.56	7.60	6.20	6.021	9.86	7.625	1.33	-0.29	1.50
6.02	6.65	7.50	5.90	6.795	9.56	6.964	1.51	-0.14	1.74
6.88	7.57	7.50	5.65	7.615	9.31	6.232	1.62	0.04	1.99
7.76	8.53	7.40	5.45	8.393	9.10	5.648	1.65	0.14	2.25
8.60	9.67	7.30	5.20	9.055	8.72	5.440	1.81	0.24	2.49
9.51	10.64	7.15	4.90	9.645	8.37	5.100	2.03	0.30	2.76
10.36	11.31	6.80	4.60	9.948	7.73	4.946	2.42	0.50	3.00
11.24	11.98	6.40	4.30	10.130	7.07	4.866	2.53	0.65	3.26
12.12	12.67	6.20	4.10	10.620	6.84	4.575	2.53	0.91	3.51
12.96	13.66	6.00	3.95	10.850	6.47	4.561	2.52	0.99	3.75
13.84	14.44	5.80	3.80	11.190	6.23	4.390	2.47	1.08	4.01
15.60	16.64	5.70	3.50	12.090	5.92	4.190	2.18	1.25	4.52
17.36	18.42	5.65	3.30	12.930	5.64	3.932	1.96	1.38	5.03
17.36	18.42	5.65	3.20	12.930	5.64	3.932	1.96	1.38	5.03
19.10	21.33	5.65	3.10	14.060	5.57	3.808	1.82	1.46	5.53
20.84	23.93	5.65	2.90	14.990	5.43	3.681	1.63	1.56	6.04

Model 4669 Test No. 1

V, knots	R_t, lb	Wetted length of keel, ft	Wetted length of chine, ft	Re x 10^{-6}	S, ft^2	10^3 C_t	Change of trim, deg	CG rise, in	F_∇
1.00	0.21	7.83	6.70	1.238	8.72	8.738	0.00	0.00	0.29
1.50	0.44	7.85	6.80	1.873	8.74	8.121	0.00	0.00	0.44
1.70	0.55	7.87	6.80	2.129	8.79	7.857	0.00	0.00	0.50
1.98	0.75	7.87	7.87	2.658	8.96	7.749	0.00	0.06	0.58
2.50	1.32	7.90	7.90	3.369	8.91	8.602	0.02	-0.04	0.73
2.57	1.37	7.90	7.90	3.464	8.91	8.448	0.05	-0.03	0.75
3.00	2.04	7.90	7.90	4.043	8.85	9.293	0.12	-0.07	0.88
3.38	2.80	7.90	7.90	4.556	8.81	10.095	0.20	-0.05	0.99
3.50	2.93	7.90	7.90	4.717	8.78	9.885	0.25	-0.07	1.03
4.00	3.79	7.85	7.85	5.357	8.77	9.800	0.52	-0.24	1.17
4.24	4.29	7.80	7.80	5.642	9.39	9.222	0.82	-0.34	1.24
5.09	5.49	7.75	7.75	6.730	9.36	8.215	1.35	-0.29	1.49
5.95	6.45	7.70	7.70	7.817	9.28	7.124	1.55	-0.05	1.74
6.78	7.31	7.65	7.60	8.815	9.20	6.272	1.65	0.07	1.99
7.65	8.29	7.60	7.50	9.854	9.12	5.636	1.70	0.04	2.24
8.54	9.33	7.55	7.45	10.928	9.05	5.129	1.75	0.18	2.50
9.35	10.40	7.50	7.35	11.837	9.07	4.759	1.88	0.32	2.74
10.22	11.39	7.40	7.00	12.555	9.05	4.372	2.12	0.30	3.00
11.05	12.22	7.20	6.50	12.915	8.84	4.108	2.65	0.52	3.24
11.96	12.78	6.70	5.80	12.754	8.50	3.814	3.08	0.78	3.51
12.80	12.89	6.20	5.50	12.776	6.10	4.680	3.23	0.93	3.75
13.64	13.63	5.90	5.30	13.033	5.83	4.560	3.28	1.08	4.00
15.35	15.15	5.50	4.90	13.619	5.35	4.361	3.10	1.64	4.50
17.10	16.57	5.50	4.80	15.026	5.29	3.887	2.90	1.69	5.01
18.80	18.22	5.30	4.60	15.878	5.05	3.704	2.73	1.92	5.51
20.50	19.44	5.00	4.40	16.439	4.75	3.534	2.55	2.09	6.01

Model 4668 Test No. 17

V, knots	R_t, lb	Wetted length of keel, ft	Wetted length of chine, ft	Re x 10^{-6}	S, ft^2	10^3 C_t	Change of trim, deg	CG rise, in	F_∇
1.00	0.25	7.63	4.95	1.059	9.39	9.659	0.03	0.01	0.29
1.50	0.55	7.63	4.95	1.589	9.34	9.498	0.05	0.02	0.43
1.72	0.70	7.63	4.95	1.822	9.35	9.185	0.05	-0.07	0.50
2.00	0.99	7.63	5.00	2.126	9.33	9.624	0.05	-0.07	0.58
2.51	1.54	7.63	5.10	2.689	9.38	9.455	0.13	-0.11	0.73
2.60	1.74	7.63	5.00	2.763	9.29	10.052	0.15	-0.11	0.75
3.00	2.43	7.60	4.90	3.158	9.28	10.556	0.27	-0.18	0.87
3.42	3.35	7.60	4.70	3.543	8.93	11.637	0.47	-0.25	0.99
3.52	3.42	7.60	4.70	3.647	9.05	11.067	0.52	-0.25	1.02
3.98	4.51	7.35	4.30	3.902	8.58	12.040	0.93	-0.35	1.15
4.30	4.97	7.47	5.50	4.694	9.45	10.320	1.18	-0.36	1.25
5.14	6.13	7.30	5.40	5.498	9.27	9.081	1.68	-0.18	1.49
6.02	6.92	7.15	5.10	6.207	8.82	7.855	1.80	0.03	1.74
6.92	7.79	7.00	4.95	6.960	8.44	6.993	1.85	0.13	2.01
7.76	8.63	6.75	4.70	7.478	8.04	6.467	2.00	0.30	2.25
8.62	9.63	6.10	4.40	7.624	7.15	6.576	2.30	0.43	2.50
9.46	10.12	5.60	4.10	7.729	6.30	6.512	2.79	0.72	2.74
10.36	10.74	5.40	3.90	8.116	6.00	6.051	2.80	0.87	3.00
11.20	11.13	5.10	3.70	8.302	5.62	5.728	2.70	1.11	3.24
12.10	11.87	4.90	3.50	8.561	5.40	5.447	2.61	1.19	3.51
12.94	12.43	4.80	3.40	8.938	5.16	5.220	2.35	1.18	3.75
13.90	13.06	4.80	3.25	9.414	5.03	4.876	2.19	1.32	4.03
15.66	14.97	4.80	3.00	10.289	4.85	4.566	1.89	1.55	4.54
17.38	16.57	4.80	2.80	11.126	4.71	4.225	1.62	1.70	5.04
19.06	18.78	4.80	2.65	11.945	4.60	4.077	1.28	1.73	5.52
20.82	21.08	7.55	4.30	12.978	4.55	3.878	0.93	1.77	6.03

Model 4669 Test No. 2

V, knots	R_t, lb	Wetted length ft		Re x 10^{-6}	S, ft^2	10^3 C_t	Change of trim, deg	CG rise, in	F_∇
1.00	0.24	8.03		1.393	13.06	6.668	-0.01	-0.01	0.25
1.52	0.53	8.03		2.118	12.96	6.425	-0.03	-0.02	0.39
1.93	0.90	8.03		2.687	12.79	6.858	-0.07	-0.05	0.49
2.00	0.93	8.03		2.784	12.79	6.596	-0.07	-0.16	0.51

Model 4669 Test No. 3

V, knots	R_t, lb	Wetted length ft		Re x 10^{-6}	S, ft^2	10^3 C_t	Change of trim, deg	CG rise, in	F_∇
1.00	0.30	8.05		1.373	13.04	8.348	0.00	0.11	0.25
1.52	0.57	8.06		2.090	13.04	6.867	-0.03	-0.02	0.39
1.98	1.04	8.06		2.722	13.04	7.383	-0.05	-0.03	0.50
2.00	1.10	8.06		2.750	13.04	7.652	-0.05	-0.03	0.51
2.54	2.18	8.06		3.493	13.04	9.403	-0.07	-0.16	0.65
2.96	3.56	8.01		4.045	12.53	11.767	0.00	-0.23	0.75
3.00	3.61	8.01		4.100	12.53	11.615	0.00	-0.28	0.76
3.50	6.32	8.01		4.783	12.53	14.940	0.05	-0.31	0.89

Model 4669 Test No. 6

V, knots	R_t, lb	Wetted length ft		Re x 10^{-6}	S, ft^2	10^3 C_t	Change of trim, deg	CG rise, in	F_∇
1.00	0.10	8.05		1.373	9.32	3.893	0.00	0.00	0.27
1.54	0.45	8.07		2.120	9.32	7.392	-0.02	-0.01	0.42
1.81	0.66	8.10		2.501	9.25	7.903	-0.05	-0.04	0.50
2.00	0.84	8.10		2.764	9.17	8.309	-0.05	-0.04	0.55
2.52	1.64	8.10		3.482	9.25	10.132	-0.09	-0.07	0.69
2.75	1.95	8.12		3.810	9.25	10.116	-0.10	-0.07	0.76
3.02	2.63	8.14		4.194	9.25	11.312	-0.07	-0.16	0.83
3.53	3.97	8.15		4.908	9.17	12.608	-0.12	-0.25	0.97
3.63	4.22	8.16		5.054	9.25	12.564	-0.10	-0.30	1.00
4.00	5.21	8.18		5.582	9.50	12.437	0.10	-0.37	1.10
4.54	7.02	8.20		6.352	9.60	12.874	--	--	1.25
5.40	8.96	8.30		7.647	9.85	11.319	1.33	--	1.48
6.32	10.49	8.30		8.950	9.77	9.754	1.73	-0.19	1.74
7.22	12.25	8.30		10.224	9.77	8.727	1.68	-0.12	1.98

Model 4669 Test No. 7

V, knots	R_t, lb	Wetted length of keel, ft	Wetted length of chine, ft	Re x 10^{-6}	S, ft^2	10^3 C_t	Change of trim, deg	CG rise, in	F_∇
1.00	0.18	7.96	--	1.358	9.50	6.875	0.00	0.00	0.27
1.50	0.41	8.00	7.95	2.039	9.61	6.881	0.00	0.00	0.41
1.80	0.61	8.00	8.00	2.456	9.57	7.140	-0.03	-0.02	0.49
2.00	0.78	8.00	8.00	2.730	9.48	7.464	-0.03	-0.08	0.55
2.50	1.67	8.02	8.02	3.421	9.33	10.392	-0.03	-0.13	0.69
2.75	2.00	8.02	8.02	3.763	9.37	10.243	-0.03	-0.13	0.76
3.00	2.69	8.02	8.02	4.105	9.27	11.699	0.01	-0.22	0.82
3.50	4.05	8.04	8.04	4.801	9.56	12.548	0.03	-0.32	0.96
3.65	4.27	8.04	8.04	5.007	9.72	11.966	0.05	-0.36	1.00
4.00	5.43	8.05	8.05	5.494	10.04	12.265	0.40	-0.24	1.10
4.50	7.15	8.10	8.10	6.219	10.22	12.536	1.03	-0.45	1.24
5.42	9.19	7.90	7.90	7.305	10.23	11.096	1.70	-0.57	1.49
6.35	10.51	7.90	7.90	8.559	10.15	9.318	1.90	-0.27	1.74
7.22	11.55	7.80	7.80	9.608	10.13	7.936	1.97	-0.11	1.98
8.12	12.82	7.80	7.70	10.737	9.85	7.163	2.03	-0.02	2.23
9.00	14.40	7.75	7.70	11.870	9.81	6.575	2.10	0.14	2.47
9.98	15.76	7.68	7.60	13.009	10.04	5.719	2.37	0.26	2.74
10.90	17.17	7.50	7.30	13.762	10.20	5.141	2.93	0.40	2.99
11.80	17.69	7.20	6.60	13.892	9.50	4.852	3.75	0.77	3.24
12.70	17.72	6.40	6.00	13.435	6.53	6.105	4.30	1.07	3.49
13.60	17.87	6.10	5.70	13.691	6.16	5.691	4.33	1.54	3.73
14.55	18.59	5.90	5.60	14.275	6.00	5.310	4.23	1.64	3.99
16.38	19.82	5.60	5.30	15.231	5.65	4.744	4.03	2.07	4.50
18.20	21.52	5.40	5.05	16.210	5.37	4.390	3.80	2.37	5.00
20.00	23.57	5.45	4.90	17.642	5.32	4.019	3.37	2.53	5.49
21.80	25.60	5.37	4.70	18.709	5.14	3.798	3.10	2.69	5.99

Model 4669 Test No. 8

V, knots	R_t, lb	Wetted length of keel, ft	Wetted length of chine, ft	Re x 10^{-6}	S, ft^2	10^3 C_t	Change of trim, deg	CG rise, in	F_∇
1.00	0.21	7.85	7.00	1.266	9.65	7.896	0.03	0.02	0.27
1.52	0.50	7.88	7.05	1.934	9.65	8.139	0.03	0.02	0.42
1.80	0.70	7.90	7.90	2.426	9.86	7.952	0.03	0.02	0.49
2.00	0.87	7.90	7.90	2.695	9.83	8.028	0.05	-0.08	0.55
2.51	1.69	7.92	7.92	3.391	9.72	10.015	0.05	-0.14	0.69
2.75	2.02	7.95	7.95	3.730	9.73	9.962	0.08	-0.12	0.76
3.00	2.78	7.95	7.95	4.069	10.25	10.934	0.15	-0.19	0.82
3.51	4.44	7.95	7.95	4.761	10.25	12.758	0.31	-0.27	0.96
3.65	4.77	7.93	7.93	4.938	10.24	12.688	0.40	-0.27	1.00
4.00	5.90	7.90	7.90	5.391	10.46	12.791	0.68	-0.45	1.10
4.52	7.95	7.86	7.80	6.038	10.45	13.512	1.31	-0.53	1.24
5.40	9.45	7.70	7.65	7.066	10.40	11.307	2.03	-0.45	1.48
6.32	10.54	7.62	7.50	8.152	10.05	9.527	2.20	-0.29	1.74
7.22	11.49	7.53	7.40	9.190	9.91	8.070	2.26	-0.09	1.98
8.15	12.61	7.45	7.20	10.179	9.75	7.065	2.38	0.26	2.24
9.03	14.07	6.20	7.35	10.430	9.76	6.415	2.61	0.39	2.48
9.97	15.33	7.05	6.55	11.567	9.38	5.966	3.13	0.58	2.74
10.92	16.58	6.40	6.00	11.552	7.65	6.595	3.88	0.95	3.00
11.78	17.25	5.88	5.55	11.476	5.95	7.581	4.48	1.08	3.23
12.70	17.30	5.63	5.30	11.831	5.66	6.876	4.41	1.43	3.49
13.68	17.79	5.63	5.15	12.581	5.58	6.181	4.23	1.66	3.76
14.55	18.20	5.33	5.00	12.810	5.30	5.886	4.11	2.04	3.99
16.40	19.35	5.30	4.75	14.047	5.13	5.089	3.56	2.33	4.50
18.10	20.53	5.23	4.60	15.163	5.01	4.539	3.18	2.56	4.97
20.00	21.94	4.87	4.40	15.799	4.66	4.265	2.93	2.98	5.49
21.84	23.67	5.30	4.30	17.887	4.50	3.996	2.48	2.77	6.00

Model 4669 Test No. 9

V, knots	R_t, lb	Wetted length of keel, ft	Wetted length of chine, ft	Re x 10^{-6}	S, ft^2	10^3 C_t	Change of trim, deg	CG rise, in	F_∇
1.00	0.22	7.73	6.40	1.204	9.60	8.315	0.02	0.01	0.27
1.50	0.52	7.75	6.50	1.822	9.56	8.772	0.02	0.01	0.41
1.79	0.80	7.76	6.50	2.177	9.55	9.489	0.05	0.03	0.49
2.00	0.97	7.76	6.50	2.433	9.55	9.214	0.05	-0.03	0.55
2.50	1.73	7.76	7.73	3.301	9.91	10.136	0.15	-0.09	0.69
2.70	2.29	7.77	7.77	3.579	9.91	11.502	0.22	-0.11	0.74
2.98	3.08	7.77	7.77	3.950	9.91	12.699	0.30	-0.18	0.82
3.44	4.73	7.75	7.70	4.531	9.89	14.666	0.52	-0.24	0.94
3.62	5.03	7.75	7.70	4.768	10.72	12.993	0.65	-0.34	0.99
4.00	6.66	7.70	7.60	5.221	10.80	13.985	1.12	-0.33	1.10
4.52	8.85	7.55	7.40	5.761	10.24	15.350	1.90	-0.39	1.24
5.40	10.37	7.35	7.00	6.606	9.88	13.060	2.35	-0.38	1.48
6.33	11.67	7.20	6.70	7.506	9.63	10.974	2.50	-0.14	1.74
7.20	12.45	7.00	6.50	8.292	9.37	9.300	2.62	0.20	1.98
8.13	13.82	6.75	6.20	8.975	8.96	8.467	2.92	0.35	2.23
9.00	15.37	6.20	5.90	9.290	8.36	8.236	3.50	0.64	2.47
10.83	17.66	5.00	5.10	9.331	5.17	10.567	4.88	1.33	2.97
11.78	17.79	4.80	4.90	9.748	4.93	9.435	4.70	1.69	3.23
12.70	17.92	4.60	4.70	10.076	4.68	8.614	4.40	2.04	3.49
13.64	17.95	4.50	4.60	10.589	4.57	7.660	4.10	2.34	3.75
14.50	18.67	4.40	4.50	11.009	4.45	7.240	--	--	5.56
16.35	18.70	4.20	4.30	11.856	4.23	6.000	3.22	2.85	4.49
18.20	19.52	4.10	4.10	12.732	4.05	5.280	2.72	3.04	5.00
20.00	20.54	3.90	3.90	13.308	3.82	4.877	2.25	3.48	5.49
21.80	21.90	4.00	3.85	14.395	3.77	4.435	1.98	3.38	5.96

Model 4669 Test No. 10

V, knots	R_t, lb	Wetted length of keel, ft	Wetted length of chine, ft	Re x 10^{-6}	S, ft^2	10^3 C_t	Change of trim, deg	CG rise, in	F_∇
1.00	0.10	7.93	7.30	1.300	8.67	4.185	0.00	0.00	0.29
1.51	0.33	7.96	7.96	2.050	8.79	5.975	0.00	0.11	0.44
1.70	0.45	7.98	7.98	2.314	8.78	6.436	0.00	0.00	0.50
2.00	0.69	8.00	8.00	2.730	8.70	7.194	-0.03	-0.19	0.59
2.48	1.21	8.00	8.00	3.385	8.67	8.234	-0.05	-0.04	0.73
2.57	1.29	8.00	8.00	3.508	8.68	8.165	-0.05	-0.04	0.75
3.00	1.93	8.05	8.05	4.120	8.56	9.090	0.00	-0.23	0.88
3.40	2.49	8.05	8.05	4.669	8.48	9.217	-0.01	-0.18	1.00
3.52	2.73	8.06	8.06	4.840	8.51	9.395	-0.01	-26.34	1.03
4.00	3.66	8.10	8.10	5.528	8.65	9.595	0.12	-27.14	1.17
4.25	4.12	8.15	8.15	5.910	8.62	9.602	0.32	-29.41	1.25
5.12	5.66	8.00	8.00	6.988	9.15	8.562	1.12	-33.08	1.49
5.96	6.86	7.90	7.90	8.033	9.12	7.684	1.37	-31.99	1.75
6.80	8.04	7.90	7.90	9.165	9.19	6.865	1.47	-31.22	1.99
7.68	9.06	7.85	7.85	10.286	9.08	6.138	1.57	-31.00	2.25
8.57	10.39	7.85	7.85	11.478	9.06	5.666	1.62	-29.81	2.51
9.33	11.80	7.80	7.80	12.417	9.03	5.447	1.65	-30.28	2.73
10.22	13.43	7.80	7.70	13.514	9.14	5.104	1.72	-29.04	3.00
11.11	14.56	7.70	7.60	14.501	9.35	4.578	1.99	-31.16	3.26
11.90	15.09	7.60	7.45	15.268	9.30	4.157	2.37	-31.41	3.49
12.81	15.34	7.40	7.05	15.780	9.33	3.636	2.91	-31.85	3.75
13.65	15.17	7.15	6.40	15.767	7.27	4.064	3.29	-30.47	4.00
15.40	16.86	6.80	5.80	16.554	6.65	3.879	3.45	-27.40	4.51
17.09	18.53	6.40	5.45	17.262	6.18	3.725	3.35	-24.37	5.01
18.75	20.43	6.20	5.20	18.235	5.95	3.544	3.12	-22.16	5.50
20.60	22.69	6.00	5.00	19.331	5.70	3.404	2.99	-20.28	6.04

Model 4669 Test No. 11

V, knots	R_t, lb	Wetted length of keel, ft	Wetted length of chine, ft	Re x 10^{-6}	S, ft^2	10^3 C_t	Change of trim, deg	CG rise, in	F_∇
0.99	0.10	7.90	6.60	1.224	8.57	4.325	-0.05	-0.03	0.29
1.51	0.33	7.90	7.00	1.919	8.71	6.032	-0.10	-0.07	0.44
1.68	0.43	7.90	6.95	2.126	8.68	6.371	-0.10	-0.18	0.49
2.00	0.70	7.90	7.90	2.695	8.85	7.175	-0.10	-0.07	0.59
2.48	1.31	7.95	7.95	3.364	8.75	8.833	-0.05	-0.20	0.73
2.57	1.31	7.95	7.95	3.486	8.75	8.226	-0.05	-0.20	0.75
2.98	1.99	8.00	8.00	4.067	8.74	9.304	0.05	-0.19	0.87
3.40	2.68	8.00	8.00	4.640	8.70	9.669	0.10	-0.16	1.00
3.54	2.77	8.00	8.00	4.832	8.70	9.220	0.10	-0.16	1.04
4.00	3.71	8.00	8.00	5.460	8.77	9.593	0.30	-0.37	1.17
4.29	4.18	7.95	7.95	5.819	8.89	9.270	0.57	-0.41	1.26
5.15	5.45	7.80	7.80	6.854	9.38	7.949	1.18	-0.46	1.51
6.00	6.42	7.80	7.70	7.934	9.26	6.988	1.45	-0.17	1.76
6.81	7.40	7.75	7.70	8.970	9.23	6.273	1.50	-0.14	2.00
7.64	8.52	7.70	7.65	9.998	9.19	5.763	1.58	0.03	2.24
8.55	9.69	7.70	7.65	11.189	9.24	5.205	1.62	0.11	2.51
9.38	10.67	7.65	7.50	12.275	9.20	4.783	1.72	0.06	2.75
10.23	12.00	7.58	7.42	13.091	9.17	4.537	1.93	0.20	3.00
11.10	12.94	7.48	7.10	13.806	9.30	4.098	2.28	0.26	3.25
11.90	13.59	7.25	6.60	14.050	9.12	3.818	2.73	0.39	3.49
12.80	13.74	6.80	5.90	13.868	6.70	4.542	3.15	0.55	3.75
13.60	14.10	6.40	5.70	14.039	6.35	4.356	3.22	0.93	3.99
15.40	15.43	6.10	5.30	15.108	6.00	3.935	3.18	1.30	4.51
17.10	17.03	5.50	5.00	15.317	5.42	3.899	3.05	1.56	5.01
18.84	19.05	5.40	4.80	16.394	5.23	3.723	2.88	1.78	5.52
20.55	21.17	5.20	4.60	17.181	5.00	3.638	2.65	1.91	6.02

Model 4669 Test No. 12

V, knots	R_t, lb	Wetted length of keel, ft	Wetted length of chine, ft	Re x 10^{-6}	S, ft^2	10^3 C_t	Change of trim, deg	CG rise, in	F_∇
0.99	0.14	7.80	6.45	1.202	8.64	6.004	0.00	0.00	0.29
1.50	0.44	7.80	6.40	1.817	8.63	8.225	0.00	0.00	0.44
1.68	0.55	7.82	6.60	2.066	8.68	7.408	0.00	0.10	0.49
2.00	0.75	7.82	6.40	2.426	8.60	7.911	0.00	0.00	0.59
2.51	1.36	7.84	7.84	3.357	9.08	8.627	0.05	0.03	0.74
2.55	1.39	7.85	7.85	3.415	9.09	8.534	0.08	0.04	0.75
3.00	2.18	7.86	7.86	4.023	8.95	9.820	0.18	0.04	0.88
3.40	2.90	7.86	7.86	4.559	8.96	10.160	0.25	-0.12	1.00
3.50	3.07	7.86	7.86	4.693	8.94	10.172	0.30	-0.10	1.03
4.00	3.96	7.83	7.80	5.337	9.05	9.923	0.61	-0.24	1.17
4.25	4.43	7.80	7.80	5.656	9.62	9.251	0.83	-0.27	1.25
5.14	5.62	7.70	7.65	6.726	9.44	8.177	1.36	-0.25	1.51
5.98	6.57	7.60	7.50	7.703	9.32	7.153	1.58	-0.13	1.75
6.80	7.38	7.55	7.40	8.667	9.23	6.274	1.65	0.05	1.99
7.63	8.47	7.50	7.25	9.594	9.09	5.808	1.71	0.08	2.24
8.51	9.33	7.45	7.10	10.556	8.99	5.200	1.80	0.13	2.49
9.52	10.65	7.30	6.80	11.451	9.01	4.732	2.10	0.29	2.79
10.25	11.34	7.15	6.40	11.840	8.86	4.420	2.36	0.42	3.00
11.10	12.14	6.60	5.80	11.742	8.47	4.221	2.78	0.54	3.25
12.00	12.21	5.90	5.40	11.568	5.90	5.214	3.33	0.87	3.52
12.80	12.71	5.55	5.20	11.684	5.53	5.090	3.38	0.90	3.75
13.65	13.42	5.40	5.00	12.111	5.35	4.885	3.43	1.17	4.00
15.40	14.69	5.20	4.75	13.059	5.07	4.433	3.03	1.47	4.51
17.10	16.08	4.90	4.60	13.859	4.80	4.157	2.73	1.66	5.01
18.90	17.44	4.80	4.40	14.834	4.63	3.826	2.48	1.78	5.54
20.60	19.50	4.50	4.20	15.289	4.34	3.812	2.31	1.94	6.04

Model 4669 Test No. 13

V, knots	R_t, lb	Wetted length of keel, ft	Wetted length of chine, ft	Re x 10^{-6}	S, ft^2	10^3 C_t	Change of trim, deg	CG rise, in	F_∇
0.99	0.15	7.70	5.60	1.123	8.30	6.695	0.00	0.00	0.29
1.50	0.41	7.70	5.70	1.714	8.36	7.909	0.03	0.02	0.44
1.70	0.56	7.70	5.90	1.972	8.44	8.331	0.03	0.02	0.50
2.00	0.77	7.70	6.00	2.337	8.51	8.208	0.05	-0.09	0.59
2.50	1.41	7.70	5.85	2.887	8.36	9.792	0.10	-0.01	0.73
2.57	1.42	7.70	7.50	3.332	9.09	8.583	0.10	-0.06	0.75
3.00	2.32	7.70	7.60	3.915	9.11	10.267	0.22	-0.17	0.88
3.40	3.17	7.70	7.60	4.437	9.09	10.946	0.40	-0.08	1.00
3.52	3.31	7.70	7.60	4.594	9.14	10.606	0.45	-0.17	1.03
3.99	4.38	7.65	7.55	5.174	9.12	10.946	0.85	-0.30	1.17
4.24	4.44	7.58	7.45	5.433	9.08	9.870	1.10	-0.46	1.24
5.10	6.00	7.45	7.10	6.326	9.07	9.228	1.63	-0.24	1.49
5.98	6.81	7.30	6.80	7.193	8.61	8.025	1.82	-0.09	1.75
6.80	7.62	7.20	6.50	7.947	8.34	7.170	1.88	-0.12	1.99
7.65	8.52	7.10	6.40	8.810	8.18	6.458	1.98	0.16	2.24
8.50	9.49	6.80	6.00	9.282	7.62	6.255	2.10	0.16	2.49
9.35	10.45	6.60	5.70	9.811	7.19	6.032	2.55	0.28	2.74
10.20	11.17	5.70	5.35	9.606	6.10	6.386	2.97	0.60	2.99
11.10	11.59	5.10	4.90	9.469	5.12	6.666	3.55	1.01	3.25
11.95	11.97	5.00	4.80	9.991	5.00	6.083	3.48	1.20	3.50
12.75	12.42	4.80	4.60	10.224	4.75	5.836	3.32	1.29	3.74
13.65	12.53	4.70	4.50	10.713	4.63	5.270	3.13	1.53	4.00
15.38	13.69	4.50	4.25	11.467	4.36	4.816	2.80	1.98	4.51
17.10	14.63	4.30	4.10	12.254	4.15	4.374	2.53	2.19	5.01
18.80	16.27	4.20	3.90	12.991	4.00	4.176	2.08	2.30	5.51
20.58	17.57	3.94	3.80	13.589	3.77	3.993	1.83	2.39	6.03

Model 4669 Test No. 14

V, knots	R_t, lb	Wetted length of keel, ft	Wetted length of chine, ft	Re x 10^{-6}	S, ft^2	10^3 C_t	Change of trim, deg	CG rise, in	F_∇
1.00	0.11	7.90	6.30	1.211	7.50	5.322	0.00	0.00	0.31
1.50	0.32	7.90	6.90	1.893	8.24	6.263	0.00	0.00	0.46
1.60	0.36	7.90	7.80	2.143	8.48	6.020	-0.03	-0.02	0.49
2.00	0.56	7.90	7.90	2.695	8.51	5.969	0.00	-0.06	0.62
2.40	0.94	7.95	7.95	3.255	8.46	7.001	0.00	-0.11	0.74
2.46	1.01	7.95	7.95	3.336	8.45	7.167	0.00	-0.09	0.76
3.00	1.59	7.95	7.95	4.069	8.48	7.559	0.02	-0.12	0.92
3.24	1.79	8.00	8.00	4.422	8.47	7.306	0.02	-0.10	1.00
3.48	2.16	8.00	8.00	4.750	8.46	7.650	0.00	-0.15	1.07
4.00	2.83	8.00	8.00	5.460	8.49	7.559	0.12	-0.19	1.23
4.04	2.96	8.00	8.00	5.514	8.52	7.724	0.15	-0.17	1.24
4.88	4.05	7.90	7.90	6.577	8.50	7.260	0.80	-0.20	1.50
5.70	4.99	7.85	7.85	7.634	8.94	6.233	1.13	0.04	1.75
6.50	5.79	7.80	7.80	8.650	8.92	5.574	1.23	0.06	2.00
7.28	6.74	7.80	7.80	9.688	8.92	5.173	1.30	0.00	2.24
8.10	7.80	7.75	7.70	10.669	8.80	4.902	1.35	0.20	2.49
8.96	9.05	7.75	7.70	11.802	8.87	4.611	1.37	0.27	2.76
9.64	10.13	7.70	7.65	12.615	8.85	4.469	1.47	0.23	2.97
10.58	11.42	7.70	7.65	13.846	8.85	4.183	1.60	0.38	3.26
11.36	12.24	7.65	7.50	14.673	8.90	3.867	1.75	0.44	3.50
12.20	13.05	7.53	7.40	15.528	8.90	3.575	2.03	0.42	3.75
12.90	14.01	7.40	7.00	15.847	8.69	3.511	2.40	0.52	3.97
14.70	14.64	7.10	6.20	16.679	7.04	3.492	2.75	0.89	4.52
16.34	16.59	6.83	5.50	17.174	6.48	3.479	2.77	1.19	5.03
17.80	18.28	6.60	5.20	17.919	6.16	3.398	2.72	1.38	5.48
19.48	20.18	6.40	4.90	20.441	6.25	3.087	2.63	1.48	5.99

Model 4669 Test No. 15

V, knots	R_t, lb	Wetted length of keel, ft	Wetted length of chine, ft	Re x 10^{-6}	S, ft^2	10^3 C_t	Change of trim, deg	CG rise, in	F_∇
1.00	0.10	7.82	5.70	1.153	7.79	4.658	0.05	0.09	0.31
1.50	0.35	7.83	5.70	1.730	7.79	7.249	0.05	0.03	0.46
1.62	0.38	7.84	6.40	1.968	8.12	6.473	0.05	0.03	0.50
2.00	0.60	7.85	6.50	2.446	8.20	6.637	0.10	0.01	0.62
2.00	0.62	7.65	7.65	2.610	8.20	6.859	0.10	0.01	0.62
2.42	0.99	7.87	7.87	3.249	8.68	7.067	0.15	0.04	0.74
2.52	1.04	7.88	7.88	3.388	8.74	6.800	0.15	-0.01	0.78
3.00	1.66	7.88	7.88	4.033	8.66	7.728	0.20	0.08	0.92
3.24	1.96	7.90	7.90	4.367	8.64	7.842	0.25	-0.06	1.00
3.50	2.22	7.90	7.90	4.717	8.66	7.593	0.25	-0.17	1.08
4.00	2.86	7.90	7.90	5.391	8.58	7.559	0.45	-0.15	1.23
4.06	2.93	7.80	7.85	5.417	8.51	7.579	0.50	-0.23	1.25
4.86	3.94	7.80	7.80	6.468	9.07	6.674	1.05	-0.10	1.50
5.68	4.75	7.75	7.70	7.481	8.87	6.023	1.28	-0.06	1.75
6.50	5.49	7.70	7.68	8.528	9.02	5.227	1.38	0.01	2.00
7.26	6.37	7.65	7.60	9.439	8.99	4.878	1.45	0.05	2.23
7.28	6.34	7.68	7.65	9.527	8.99	4.828	1.42	0.15	2.24
8.14	7.33	7.63	7.60	10.583	8.87	4.525	1.50	0.25	2.50
8.14	7.31	7.60	7.50	10.486	8.87	4.513	1.55	0.12	2.50
8.94	8.29	7.60	7.55	11.547	8.82	4.267	1.58	0.36	2.75
9.68	9.16	7.55	7.45	12.387	8.84	4.012	1.80	0.28	2.98
10.58	10.41	7.50	7.30	13.358	8.77	3.848	2.08	0.52	3.26
11.36	11.34	7.40	6.95	13.897	8.69	3.669	2.08	0.35	3.50
12.20	11.91	7.20	6.30	14.051	8.42	3.448	2.38	0.44	3.75
13.00	12.30	6.90	5.70	13.974	7.68	3.438	2.48	0.50	4.00
14.70	13.40	6.40	5.30	14.672	6.10	3.689	2.72	1.11	4.52
16.30	15.76	6.00	5.00	15.296	5.70	3.772	2.65	1.18	5.02
18.00	17.34	5.64	4.70	16.984	5.30	3.659	2.52	1.43	5.54
19.45	18.48	5.33	4.60	15.664	5.05	3.505	2.45	1.61	5.98

Model 4669 Test No. 16

V, knots	R_t, lb	Wetted length of keel, ft	Wetted length of chine, ft	Re x 10^{-6}	S, ft^2	10^3 C_t	Change of trim, deg	CG rise, in	F_∇
1.00	0.10	7.75	5.40	1.120	7.78	4.664	0.00	0.00	0.31
1.50	0.30	7.75	5.80	1.732	7.80	6.202	0.00	-0.11	0.46
1.63	0.40	7.76	5.80	1.885	7.91	6.911	0.00	-0.11	0.50
2.00	0.63	7.77	6.00	2.347	7.90	7.234	0.02	-0.16	0.62
2.42	1.02	7.79	5.80	2.803	7.81	8.093	0.05	-0.14	0.74
2.50	1.08	7.80	5.80	2.900	8.32	7.536	0.07	-0.13	0.77
3.00	1.71	7.80	7.80	3.992	8.58	8.035	0.15	-0.14	0.92
3.24	2.06	7.80	7.80	4.311	8.58	8.300	0.19	-0.17	1.00
3.50	2.36	7.80	7.80	4.658	8.63	8.101	0.27	-0.29	1.08
4.00	2.97	7.73	7.70	5.268	8.64	7.795	0.54	-0.36	1.23
4.06	3.02	7.73	7.70	5.347	8.63	7.704	0.60	-0.27	1.25
4.86	3.92	7.66	7.60	6.327	8.85	6.805	1.02	-0.31	1.50
5.68	4.73	7.58	7.45	7.278	8.69	6.122	1.22	-0.30	1.75
6.50	5.47	7.54	7.25	8.196	8.54	5.501	1.37	-0.10	2.00
7.28	6.16	7.50	7.30	9.191	8.44	4.997	1.37	0.07	2.24
8.08	7.11	7.45	7.20	10.091	8.31	4.755	1.42	0.04	2.49
8.96	8.01	7.40	7.00	11.007	8.19	4.420	1.52	0.15	2.76
9.68	9.02	7.30	6.70	11.561	8.46	4.129	1.67	0.24	2.98
10.54	9.97	7.10	6.10	11.869	8.07	4.035	1.90	0.32	3.24
11.36	10.42	6.70	5.60	11.920	7.69	3.810	2.32	0.51	3.50
12.18	10.28	6.10	5.25	11.783	5.92	4.247	2.54	0.69	3.75
13.00	10.81	5.80	5.05	12.022	5.60	4.144	2.62	0.74	4.00
14.68	12.38	5.40	4.70	12.649	5.17	4.032	2.52	1.13	4.52
16.32	13.71	5.50	4.50	13.923	5.12	3.648	2.37	1.38	5.02
17.88	15.83	5.52	4.30	14.979	5.01	3.586	2.27	1.44	5.50
19.56	17.07	5.80	4.20	16.687	5.12	3.162	1.97	1.49	6.02

Model 4669 Test No. 17

V, knots	R_t, lb	Wetted length of keel, ft	Wetted length of chine, ft	Re x 10^{-6}	S, ft^2	10^3 C_t	Change of trim, deg	CG rise, in	F_∇
1.00	0.18	7.63	5.40	1.110	7.79	8.384	0.00	0.00	0.31
1.51	0.39	7.65	5.40	1.679	7.75	8.008	0.04	-0.04	0.46
1.62	0.45	7.65	5.40	1.802	7.75	8.031	0.04	-0.04	0.50
2.00	0.75	7.65	5.45	2.235	7.78	8.745	0.07	-0.13	0.62
2.42	1.16	7.65	5.50	2.712	7.84	9.168	0.11	-0.11	0.74
2.51	1.29	7.65	5.43	2.800	7.78	9.550	0.14	-0.10	0.77
3.00	1.97	7.65	5.30	3.311	7.62	10.423	0.24	-0.14	0.92
3.24	2.32	7.63	5.20	3.549	7.52	10.665	0.31	-0.12	1.00
3.50	2.68	7.62	5.05	3.780	7.47	10.628	0.42	-0.27	1.08
3.99	3.41	7.55	7.30	5.051	8.61	9.027	0.79	-0.33	1.23
4.07	3.56	7.52	7.25	5.124	8.55	9.121	0.89	-0.28	1.25
4.87	4.48	7.40	6.90	5.941	8.41	8.150	1.24	-0.22	1.50
5.68	5.26	7.25	6.50	6.658	8.31	7.119	1.52	-0.13	1.75
6.50	5.98	7.15	6.20	7.397	8.11	6.333	1.59	-0.04	2.00
7.28	6.59	7.00	6.00	8.073	7.56	5.968	1.64	0.10	2.24
8.12	7.35	6.85	5.75	8.728	7.32	5.526	1.69	0.24	2.50
8.96	8.17	6.50	5.60	9.249	7.09	5.208	1.89	0.39	2.76
9.68	8.68	6.10	5.30	9.414	6.60	5.093	2.19	0.43	2.98
10.58	9.10	5.40	4.90	9.296	5.77	5.112	2.74	0.71	3.26
11.40	9.27	5.00	4.70	9.433	4.93	5.250	2.84	0.88	3.51
12.16	9.78	4.80	4.50	9.647	4.68	5.128	2.79	1.08	3.74
13.00	10.32	4.75	4.40	10.136	4.58	4.838	2.79	1.19	4.00
14.66	11.36	4.60	4.10	10.880	4.34	4.419	2.54	2.47	4.51
16.36	12.49	4.40	3.92	11.612	4.11	4.120	2.14	1.76	5.03
17.94	13.77	4.30	3.80	12.397	4.00	3.881	1.89	1.86	5.52
19.60	15.07	4.20	3.65	13.109	3.83	3.716	1.67	1.98	6.03

Discussion

Capt. Francis X. Forest, USN (Ret), *Member:* This paper and the author's preceding works in this field provide information which is almost indispensable for the design of some types of high-speed craft, where the predicted speeds under unusual and sometimes rigid requirements and the choice of engines and propellers are limited and critical. The author presents information directly applicable to the selection of a form, the estimate of resistance, and the shape of the resistance curves. The information is specific and enables the designer to identify critical problem areas and factors. Information relating to the resistance at "hump" speeds under various conditions of loading may be of particular importance. The planing-type hull must be able to surmount the hump resistance before it may proceed to maximum speed. The thrust at maximum speed may well be less than the thrust required to surmount the hump.

The resistance data are presented in a very usable form. From a design standpoint it would be of considerable interest to know to what degree these data may correlate with corresponding model tests of this type of craft in other model basins and in particular whether any relationship with full-scale performance has been attempted or planned.

In this connection, although the resistance data have been presented in considerable detail, it may be pointed out that in using these data the designer is faced ultimately with an evaluation of thrust and wake factors in order to obtain the delivered horsepower or the shaft horsepower. This is a matter of considerable concern, since some test data of model self-propelled craft of this type have indicated that wake and thrust factors as high as 0.20 and 0.30, respectively, may be encountered. That these factors may not be attributable to any deficiency in instrumentation seems to be borne out in at least two instances where the full-scale craft with propellers designed on the basis of factors of this magnitude have performed essentially as predicted from model tests. It might be hoped that the resistance data of this paper may later be supplemented by some information concerning the propulsion factors to be expected.

The simplified interpolation method suggested by the author, for example, Fig. 28, might well be extended to a greater range of C_{Lb}. For example values of 0.037 have been encountered for some of the charts and of 0.092 others. With reference to these curves and to the precise method of interpolation described by the author, it is to be noted that many other uncertainties are involved in the final determination of power requirements. The differences in R/W involved in interpolation are relatively small. Interpolation between the 100,000 and the 10,000 points on the resistance contours might be made with satisfactory accuracy by a direct interpolation in terms of displacement or, since the difference is largely due to Reynolds number, an interpolation proportional to the cube roots of the displacement might be a reasonable basis.

The resistance data covers area load factors as low as 5.5. It would be desirable for some of the work for which this paper is particularly valuable to have data for craft planing at load factors as low as 4.3 and volumetric Froude numbers of the order of 4.0.

In previous papers the author has included a plot showing the relationship of Froude numbers, speed, and displacement. It would be desirable that such a plot be added to the present paper.

The resistance data are supported by model tests and the variables are well selected for design purposes. Some comparisons of the curves are of considerable interest. For example Fig. 15 and following text indicate the following.

$A_p\nabla^{2/3}$	5.5	8.5
Maximum hump R/W.....	0.19+	0.145
Minimum hump.....	0.15	No "hump"
R/W at $F_\nabla = 4.5$.....	0.165	0.19

These results appear to indicate that care in the arrangement and balance of heavily loaded craft can reduce the hump resistance to values which are of the same order as those of lighter loaded craft. The further implication that at high Froude numbers heavily loaded craft might be designed with less total resistance for a given speed than the lighter loaded craft is a far cry from the conventional design concept.

Further, in these two cases it is of interest to note that the maximum hump at an area load factor of 5.5 occurs with the center of gravity 12 percent aft of the centroid, while with an area load factor of 8.5, the maximum hump is considerably reduced and occurs with the center of gravity at the centroid.

Fig. 15 indicates that with a load factor of 5.5, moving the center of gravity forward from the 12 percent to the 4 percent point reduces the hump resistance (and the corresponding engine

torque) by approximately 17 percent. Fig. 14 indicates that by moving the center of gravity from the centroid to a position 8 percent aft of the centroid the reduction in hump resistance is of the order of 40 percent.

Such information is obviously of the greatest value to the designer, particularly when the engine, even though of extremely high powers such as are available in the modern gas turbine may be pressed to its limit to meet extreme performance demands. It need not be pointed out that under such widely varying conditions of thrust the need for special considerations such as controllable-pitch propellers may well be brought out by study of these data.

Some comment will no doubt be made concerning the lines of the hull. The narrowed transom probably improves performance in quartering seas and reduces the tendency to broach. At the same time it also limits the space which may be needed for multiple engine and shaft installations. Heavily loaded craft such as amphibians are more often than not restricted in overall dimensions. It may be preferable to continue the maximum beam to the stern in order to obtain every possible square foot of planing area. This does not necessarily incur a penalty since the area-load coefficient is increased. In one case it appears from model tests that the attendant increase in load coefficient resulted in decrease in resistance coefficient at the hump.

The convex bow sections may not meet the approval of many who are familiar with the excellent performance of some craft using concave sections. The convex sections have several advantages, however, and are perhaps an essential for surf performance in the amphibian craft to which the author refers. They have been doing well in a heavily loaded planing hull at speeds of about 40 knots.

Cdr. Peter Du Cane, RN (Ret), *Member:* We are familiar with the Series 50 methodical series but the present series is of greater value for the reasons set forth in this paper.

It is true that the Davidson Laboratory of the Stevens Institute, through Korvin-Kroukovsky, Savitsky, and others, has developed a very elegant method whereby the performance of any given hull form may be approximated and remarkably consistent results can be obtained. It is, however, the unexpected or nonlinear behavior which is difficult to predict in this way.

An example given in the paper is the difficulty to account for the fact that over a considerable range the form with greater length/beam ratio will represent the optimum.

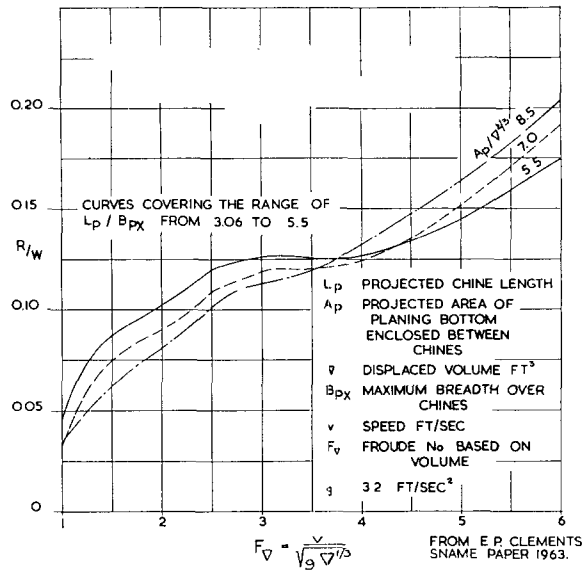

Fig. 30

Of course in any of these methods it is remarkably difficult to predict hump and propulsion characteristics which can be critical.

The practical designer, on the whole, does not find any readily and simply used method of deciding upon optimum form and dimensions.

If this work has a fault so far as the ordinary worker in the field is concerned it is that it is a bit complicated owing to the necessity for deciding upon the various nondimensional parameters, some of which are unfamiliar to us as an every day criterion. This refers perhaps particularly to the Froude relationship used here. No one will question its validity, which is based upon the two-thirds power of the volume of displaced water. However, compared to the normal speed-length relationship in terms of which most of us probably think it is abstruse and requires a bit of arithmetic before we know where we are

With a view to making all this excellent information even more readily available—in other words to make it unnecessary to go right through the many pages of this work in order to obtain a first-order answer—I have had prepared what may be termed a distillation or envelope consisting of three curves, which can be used quite readily by the designer to give him at least a quick idea of possibilities by glancing at one graph only.

The three curves shown here, Fig. 30, make quite clear the tendency so far as L/B is concerned as well as the influence of loading on planing efficiency.

Of course, from the practical designer's point of view, these tables are best considered as a use-

ful aid in the preliminary design stage, but it has to be clearly understood in this light.

To start with these are maxima. The curves depict the best that can be expected. I will make no secret of the fact that they represent a better hull form resistance-wise than any we have so far used in craft we have produced to order for seagoing.

While the author mentions this point in his text it is still necessary to point out that the utilization of this hull must be very dependent upon the performance in a seaway and at speed.

It is here we might cast some slight doubt, based on simple towing trials carried out from the end of an outrigger and towed by a speedboat at scale speed in the upper reaches of Portsmouth Harbour. Here we found in comparison with two of our forms which are known to be good all round performers there seemed an element of slamming as well as propensity for covering the decks with spray. The latter can probably be dealt with by suitable spray suppressor.

The slamming tendency, which we suspect to be there can, we believe, be eliminated to a considerable extent by raising the run of the chine forward thereby presenting a deeper vee to the oncoming wave system.

The results postulated here, which show among other things that the greatest beam-to-length ratio is by no means synonymous with efficiency are most interesting and in marked contrast to one work on the naval architecture of planing hulls published in this country where the most dogmatic statements on this subject are made.

Strangely enough this work has received considerable popularity among the semi-technical and at least one type of fast patrol boat has been designed based on these principles, where resistance qualities are by no means outstanding and comparatively speaking the slamming is considerable.

That there is no such simple solution as to say, for instance, that beam always leads us to an optimum is very pleasant but quite misleading as our authors' results show. Many factors other than resistance qualities come into this consideration, not least of which is the tendency to slam, a probably increased structural problem leading to greater weight per cubic number and the tendency towards a nasty resistance hump early in the speed range.

It is here we should mention the use of adjustable transom flaps which, besides helping a hull through a hump speed range, can do quite a lot to improve performance in a head sea. Some forms can even be improved in their resistance qualities by what is virtually an approach to the "Sottorf" concave buttocks effect as set out in "High Speed Small Craft," 2nd edition, page 48.

Finally there is one feature of our distillate or envelope curves which is worth mentioning. This is the fact that if we make use of a planing form running in the range below $F_\nabla = 3.0$ it will be seen R/W becomes quite favorable, in fact more so than most practical hydrofoils, and I suspect this applies also to the hovercraft as so far developed. What is required here is, of course, a long craft which in turn requires the very high power now available from gas-turbine units such as the Bristol-Siddeley Olympus.

Nevertheless if the real operating efficiency taking into account L/D and propulsive efficiency is known it is quite remarkable how well such forms compare even so far as real seakeeping is concerned. The price advantage and lack of complication are impressive.

Russell F. Colton,[4] ***Visitor:*** The authors' comments about the 62 Series shape being designed for "good steering qualities and good rough-water performance" brought to mind the tests which our laboratory had performed on a full-scale 25-ft Bertram hull. This boat is considered to be the ultimate in handling and riding qualities by the open water racing enthusiasts. Our experience with this boat has further verified these qualities, but at the expense of a considerable amount of performance.

Fig. 31 of this discussion has been prepared to illustrate the performance discrepancy between the Bertram and the 62 Series hulls both converted to a 10,000-lb boat. While the Bertram boat would have considerably more air drag (because of

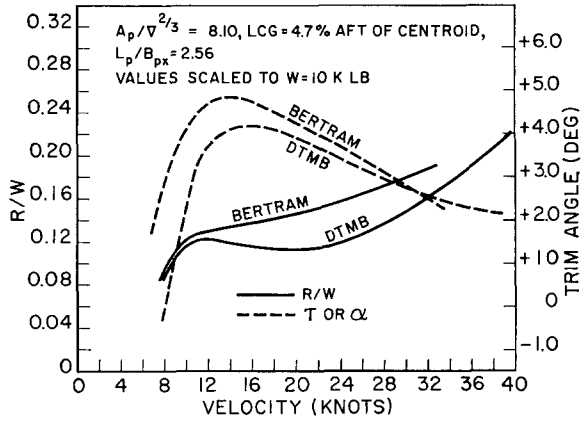

Fig. 31 Comparison of V-25 Bertram with DTMB Series 62

[4] Marine Laboratory, Collins Radio Company, Cedar Rapids, Iowa.

the additional superstructure) than the 62 Series, there can be no doubt which boat would win a race—everything else being equal. I think this graph indicates that the authors do indeed have a high-performance planing vessel, while the riding and handling characteristics must certainly be better than the so-called "pounding" hull of the 50 Series.

I note with interest the fact that the narrower hulls tend to show a marked improvement in performance at the higher Froude numbers. Since this is contrary to experience, I made a few checks of the data to determine the cause for this seeming contradiction. From my rather hurried calculations it appears that air drag may indeed account for most of this difference, as the authors suggest, but there still seems to be an additional element which defies explanation. The fact that the drag decreases with the narrower boats regardless of its origin would point to the use of this shape as a high-speed hull, providing roll stability is not overcompromised. It appears that further study of the causes for this drag reduction may be in order.

The authors' presentation of the stability limits encountered in their research is refreshing in view of the simple method in which they were able to present the results. This should prove to be a valuable asset to those using these charts for further design work.

After having gone through the set of calculations presented earlier in this discussion, I fully appreciate the authors' remark about the "laborious process" necessary to extrapolate a boat design from the original sets of curves. The final set of design curves, in terms of C_{Lb}, R/W, l_{cp}/b, and weight should greatly facilitate this process.

Finally, I would like to suggest to Taylor Model Basin generally, and the authors specifically, that this excellent work be extended. As many readers know, there is a conspicuous absence of good data on prismatic planing surfaces. It is true that there have been a number of reports written on this topic, but they all seem to lack in one way or another; insufficient range of variables, too much scatter, too small a Reynolds number, model data not available, certain measurements missing, and so on. My suggestion would be to conduct tests with the range of variables and model size used here, but on a series of simple unwarped, straight, prismatic surfaces in deadrises of 5, 10, 15, 20 and 25 deg. Particular attention should be paid to the very low and intermediate Froude-number range. These data are necessary before we can establish a complete understanding of the mechanics involved in planing-hull performance.

James L. Moss, *Associate Member:* The authors present R/W curves for the models tested expanded to two different full-scale displacements; viz., 10,000 and 100,000 lb. Differences in specific resistance in each case, at identical volume Froude numbers, are obviously owing to the different methods by which the frictional and residual-resistance components are scaled. Also presented are curves of angle of attack, or trim, but for only one full-scale displacement with the assumption that angle of attack for the model and any full-size hull should be the same at corresponding Froude numbers. By dimensional analysis there is no reason to suspect otherwise. However, for the same reason that R/W decreases with increasing size, it would seem that there ought to be a scale effect involved regarding trim. A free body diagram for the wetted portion of the bottom of a planing surface is shown in Fig. 32, herewith.

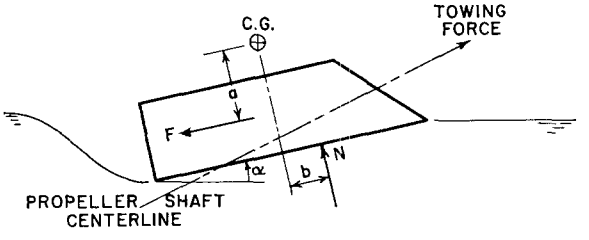

Fig. 32 Free-body diagram of towed planing surface

The horizontal drag is

$$R = F \cos \alpha + N \sin \alpha \qquad (1)$$

In equation (1), the first term on the right-hand side represents the horizontal friction drag (the total friction drag component is assumed to act parallel to the keel) and the second term is the induced or residual drag. The trimming moment, taken positive counterclockwise about the center of gravity, which is not to be interpreted as meaning the boat trims about the center of gravity, is

$$M = Nb - Fa \qquad (2)$$

Assuming for constant Froude number that the distances a and b scale in the ordinary fashion, then M scales according to the relative magnitudes of F and N which differ as the size of hull changes. Owing to the increasing proportion of total drag of the induced-drag component with increasing size, the positive contribution to trimming moment in equation (2) becomes proportionately greater when going from model to full scale. Therefore, model tests would tend to

underpredict trim angle. One would expect that as trim changes the distances a and b, as well as the drag components, would also change with further complications resulting. The addition of propellers under the boat might also tend to increase the trim by a decrease in bottom pressure loading near the transom owing to the increased water velocity caused by the propellers.

In that the authors have presented data which, in many cases, exhibit rather small changes in resistance resulting from relatively major changes in LCG position, loading, and length-beam ratio, the possibility exists that scale effect on trim and the resulting changes in the force components, though perhaps small, might have important consequences. Their comments on this matter would be appreciated.

Peter M. Kimon, *Member:* It is felt that the variation in the deadrise angle should form a part of TMB Series 62. The effect of deadrise angle on resistance at high speeds is at least as important as the L_P/B_{PA} ratio.

Approximate resistance values for deadrise angles of 0 and 20 deg at an L_P/B_{PA} ratio of 4.6 have been superimposed on the author's Fig. 8 and are shown here in Fig. 33. The data were obtained from Clement.[5] At the high speeds, $F_\nabla = 5.5$, $F_\nabla = 6.0$, the R/W values were adjusted to show approximate differences above and below the resistance line which represents the 12.5-deg deadrise angle of TMB Series 62. In order to establish the applicability of these values, a comparison was made between the resistance of the prismatic surfaces of the earlier report[5] and the TMB Series 62.

The similarity of loading between a prismatic surface and the TMB Series 62 models could be established by a load coefficient based on projected wetted area and it is defined here as $W/\rho\, g\, P_A^{3/2}$. The symbols W, ρ, and g have already been defined by the authors and P_A is the principal wetted area projected on a plane parallel to the keel. An approximate mean wetted length could be assumed equal to $l_{cp}/0.70$. Accordingly, the area P_A has been defined as the projected area aft of the $l_{cp}/0.70$ length.

The load coefficient $W/\rho\, g\, P_A^{3/2}$ for the standard test condition of the Series 62, at $L_P/B_{PA} = 4.6$, is approximately equal to 0.100. Similarly the prismatic surface of the previous report[5] has

[5] E. P. Clement, "Analyzing the Stepless Planing Boat," DTMB Report 1093, April 1956.

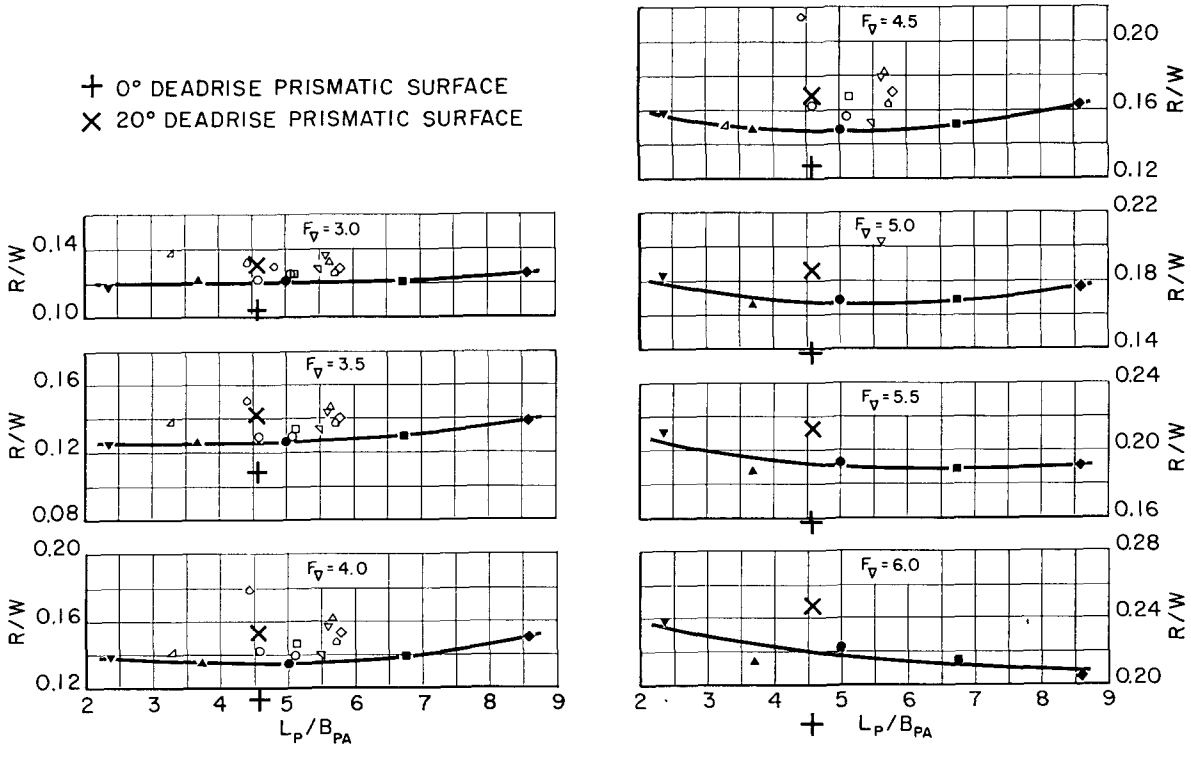

Fig. 33 Resistance/weight ratio for models of TMB Series 62, 0 and 20-deg deadrise, prismatic surfaces, and other representative planing-boat designs

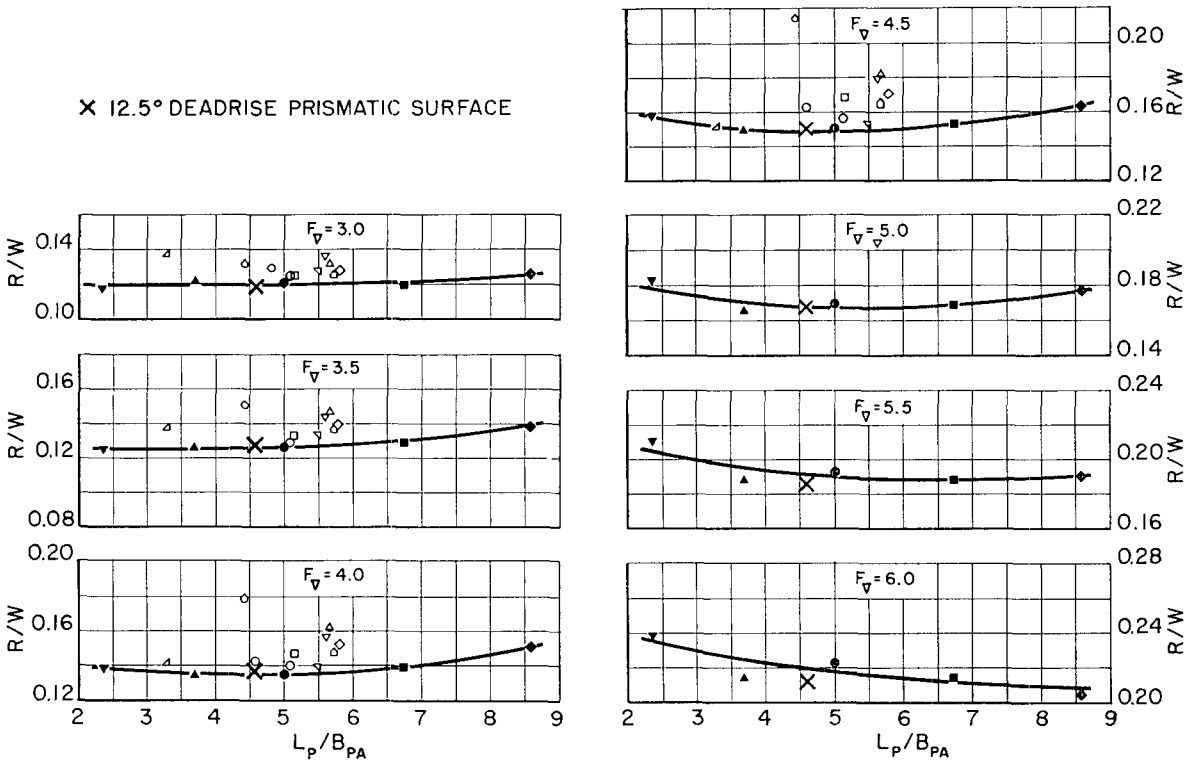

Fig. 34 Resistance/weight ratio for models of TMB Series 62, a 12.5-deg deadrise prismatic surface and other representative planing-boat designs

a load coefficient of

$$W/(bl_{cp}/0.70)^{3/2}\rho\, g = 0.098$$

The difference between these two values is sufficiently small to permit direct comparison without additional corrections.

From Fig. 15,[5] the R/W values of a prismatic surface, having a deadrise angle of 12.5 deg and an l_{cp}/b ratio of 1.69, were obtained by cross fairing. It can be shown that the l_{cp}/b ratio of 1.69, when compared with the TMB Series 62 at standard conditions, corresponds approximately to $L_P/B_{PA} = 4.6$. Accordingly, the R/W values of a 12.5-deg deadrise prismatic surface have been superimposed on Fig. 8 of the paper at $L_P/B_{PA} = 4.6$. The results, shown in Fig. 34, herewith are interesting in that they indicate almost perfect agreement with the experimental results of TMB Series 62.

The data for the prismatic surface do not include air drag. This would partly explain the small discrepancy in resistance at the very high speeds of $F_\nabla = 5.5$ and $F_\nabla = 6.0$.

In general, the results suggest that resistance at high speeds, for quite a range in L_P/b ratios and with variations in the shape of the projected planing bottom area, can be accurately estimated from planing characteristics of prismatic surfaces.

It is suggested that the authors, by the use of available data and data from a limited number of new tests of prismatic surfaces, could extend the usefulness of TMB Series 62 results by including a method for obtaining resistance values at other deadrise angles.

Young H. Chey, *Associate Member:* The writer recently tested, in smooth water and in irregular waves, three hard-chine models and three round-bottom models, with length-beam ratios of 3, 4 and 5 in each model group. The work was performed under a contract with the Bureau of Ships, U.S. Navy.

The characteristics of the models tested by the writer are shown in Tables 3 and 4 of this discussion.

The specific resistances and the angles of attack of the after portions of the planing bottoms are shown in Fig. 35; the resistances are for a displacement of 100,000 lb. In expanding the model-resistance data for the full-size boat, the Schoenherr friction coefficients were used, with zero roughness allowance. The wetted areas of

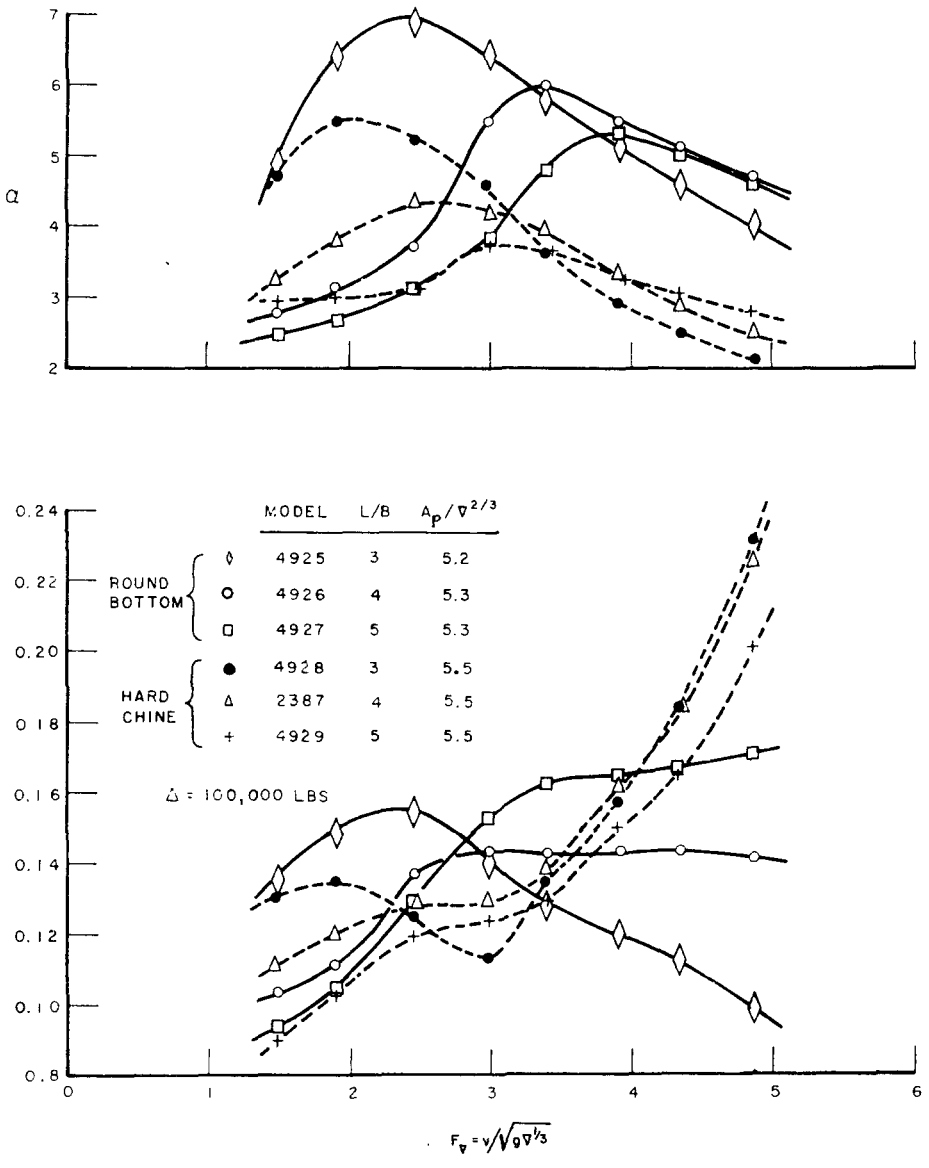

Fig. 35 Specific resistance and α of three round-bottom hulls and three hard-chine hulls

Table 3 Characteristics of Round-Bottom Models

	Model 4925	Model 4926	Model 4927
LWL, in.	31.2	36.05	40.45
Beam at WL, in.	10.5	9.035	8.0
LWL/B_{WL}	2.97	4.0	5.05
LCG abaft amidships in percent of LWL	9.9	7.8	9.4

Table 4 Characteristics of Hard-Chine Models

	Model 4928	Model 2387	Model 4929
LWL, in.	31.6	36.0	40.45
Beam at WL, in.	10.5	9.15	8.25
LWL/B_{WL}	3.0	3.94	4.90
LCG abaft amidships in percent of LWL	6.6	6.1	5.9

the models were obtained by using a method identical with that described in the paper.

The pattern, with respect to speed, of the hard-chine trim angles of the hull and specific resistances in smooth water, as tested by the writer, appears to be very like that of the models tested by the authors. However, the figure indicates that the round-bottom hulls maintained trim

angles consistently larger than those of the hard-chine hulls–particularly at Froude numbers above 3.5.

It may be noted, also, that the round-bottom hulls had less resistance than the hard-chine hulls, in the same Froude-number range. In comparing Fig. 35 with Fig. 7 of the paper, one finds that the round-bottom hulls are better as far as resistance in smooth water is concerned.

The point the writer would like to bring out in making the comparison, is that the hull having a trim angle closest to an optimum angle will have the least resistance. The optimum angle of trim, in terms of angle of attack of mean stern buttock lines with respect to resistance in smooth water, was discussed in great detail by A. B. Murray in a paper presented at the February 1950 meeting of the New England Section of the Society. This angle ranges from 4 to $5^1/_2$ deg, the exact angle depending upon dead rise. Therefore, from a purely hydrodynamic point of view, the most important consideration is how to maintain this angle throughout the speed-range of interest. It appears to be almost impossible to solve this problem in design of the main hull alone. A possible solution may be a moment control device, such as a small hydrofoil near the stern, either incorporated with rudders, or separated from rudders. With the latter arrangement, a retractable device would be preferable.

Following a study of the results of the resistances and seakeeping qualities of the six models tested in rough water, it was felt, also, that attention should be directed to the desirability of controlling trim moment. It was found that the superior resistance characteristics of the round-bottom models, in smooth water, disappeared almost completely when they were tested in waves. These round-bottom models, which maintained higher mean trim angle than the hard-chine hulls, had, also, relatively large heave amplitudes and acceleration amplitudes in waves.

The primary cause of this poor performance of the round-bottom hulls in a seaway is believed to be the large attack angle of the stern bottoms. Therefore one cannot guarantee, always, that a hull having superior resistance characteristics in smooth water will be the best performer in a seaway also.

It has been the general practice of the Davidson Laboratory to use the wetted keel lengths of planing-boat models for the calculation of Reynolds numbers. The authors used the arithmetic mean of the keel and chine wetted lengths, in their calculation of Reynolds numbers. For the sake of easy comparison, it would be desirable to settle on one method.

In their nomenclature, the authors define l_{cp} as the distance of the center of pressure forward of the transom; but for computing l_{cp}/b, the distance between the transom and the center of gravity was substituted for l_{cp}, on page 539 of the paper. It would be desirable to clarify this point.

Daniel Savitsky, *Member:* The present paper on the TMB Series 62 hard-chine planing hulls is of extreme interest to the Davidson Laboratory, since, for the past 15 years, we have conducted continuous fundamental studies on hard-chine prismatic planing forms under the sponsorship of the Office of Naval Research. The results of some of these studies are contained in the available literature[6,7,8] and are presented in such a form as to define the significance of hull geometric and operating parameters on planing performance and further are presented in a form intended for rapid prediction of the power requirements and stability of planing hulls such as the present TMB Series 62.

These methods have been used with great success by the Davidson Laboratory in analyzing planing-hull forms tested at our laboratory. As will be shown, we were equally successful in predicting the high-speed test results contained in the present paper.

Time does not permit a presentation of the Stevens' method for prediction of planing performance—but these are readily found in the literature. In summary the prediction method is based on use of the following equations for the lift, drag, and wetted areas of prismatic planing surfaces:

Lift

$$C_L = \frac{\Delta}{\frac{1}{2}\ \rho\ V^2 b^2} = \tau^{1.1}\left[0.0120\,\lambda^{1/2} + \frac{0.0055\,\lambda^{5/2}}{C_V{}^2}\right]$$

Center of Pressure

$$C_p = 0.75 - \frac{1}{5.21\ (C_V{}^2/\lambda^2) + 2.39}$$

Drag

$$R = \Delta \tan\tau + \tfrac{1}{2}\ \rho\ V^2 \lambda b^2\ C_f$$

---

[6] Daniel Savitsky and Joseph Neidinger, "Wetted Area and Center of Pressure of Planing Surfaces at Very Low Speeds," Davidson Laboratory, Stevens Institute of Technology Report 493, July 1954 (published by IAS).

[7] B. V. Korvin-Kroukovsky, Daniel Savitsky, and W. F. Lehman, "Wetted Area and Center of Pressure of Planing Surfaces," Davidson Laboratory, Stevens Institute of Technology Report 360, August 1949 (published by IAS).

[8] A. B. Murray, "The Hydrodynamics of Planing Hulls," paper presented at Feb. 1950 meeting of New England Section of SNAME.

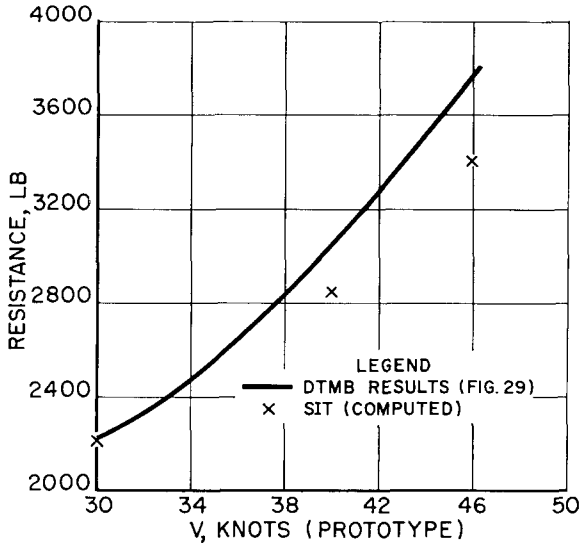

Fig. 36 Comparison of high-speed planing resistance. Computed by Davidson Laboratory; measured by DTMB. (TMB Model 4666-Test 15)

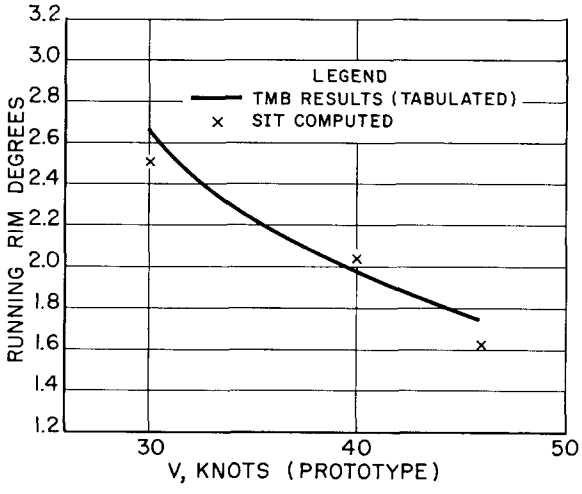

Fig. 37 Comparison of high speed planing trim. Computed by Davidson Laboratory; measured by TMB. (TMB Model 4666-Test 15)

where

Δ = weight of planing boat
λ = mean wetted length-beam ratio of planing area
τ = trim angle of after portion of planing area, deg
b = beam of planing boat, ft
C_V = speed coefficient = $V/\sqrt{gb}$
V = speed, fps
C_p = distance from transom to center of pressure divided by beam
C_f = Schoenherr friction coefficient

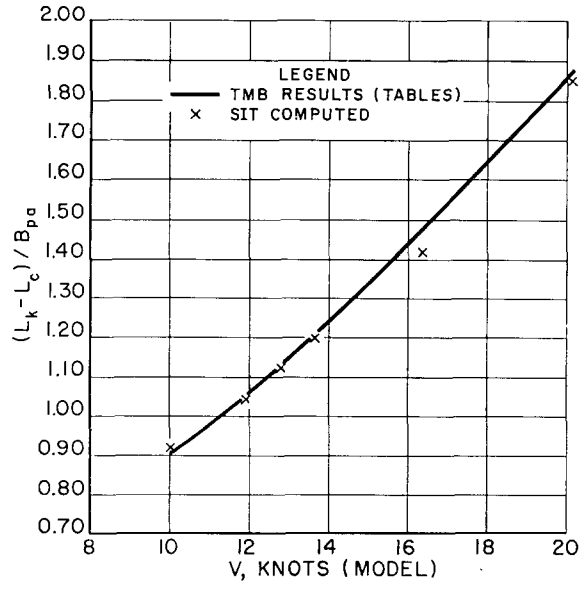

Fig. 38 Comparison of high speed wetted areas. Computed by Davidson Laboratory; measured by TMB. (TMB Model 4666-Test No. 1)

For any deadrise hull, center of gravity position, thrust-line location, speed, and weight of boat the foregoing equations can be used to predict the wetted bottom area, running trim, resistance, and porpoising stability. The accompanying illustrations show a comparison of measured TMB results and those predicted by the SIT method.

Fig. 36 of this discussion compares the resistance contained in Fig. 29 of the paper with those calculated by SIT. (Allowance is made for the air tare of the DTMB test results.) It is seen that the calculated results at low speed are in agreement with the DTMB results. At the higher speeds (40 and 46 knots) the computed values are approximately 7 percent lower than the DTMB values. This difference may be attributed to the spray drag which has not been accounted for in SIT computation.

A comparison was made of the computed and measured high-speed running trim for TMB model 4666, Test No. 15. These results are given in Fig. 37 for full-scale speeds of 30, 40 and 46 knots. It is seen that the agreement between Stevens' computed and TMB measured trim angle is within 10 percent.

The high-speed wetted-bottom areas (designated pressure area by the authors) were also computed by the Stevens' method and compared with those measured by TMB. As an example, TMB model 4666—Test No. 1 is used and comparisons made between measured and calculated values of the difference in wetted keel and chine

length as given in the tabulation of data. The calculated values are given by the equation

$$L_K - L_c = \frac{B_{PA}}{\pi} \frac{\tan\beta}{\tan\tau}$$

The comparison in Fig. 38 shows excellent agreement between computed and measured values of wetted lengths.

Porpoising limits can be predicted similarly but the writer has not had the opportunity to make the calculations for the TMB models. He would like to discuss these results with the authors at some future time.

In summary then, it appears that analytical methods for predicting the high-speed performance of prismatic planing surfaces are well in hand. These latest data again confirm the adequacy of the existing procedure. It appears to me that further planing research should be directed to the problems of loads on typical bow forms where the deadrise and buttock lines are not of constant angle. The low-speed data of the paper are particularly useful in this regard.

Joseph G. Koelbel, Jr., *Associate Member:* One impressive feature of the paper is the care with which the work has been done and with which the data have been presented. The fact that the method of turbulence stimulation is detailed and discussed, that the water temperature for each run is given, and that all data have been carefully reported, gives the reader great confidence in the tests. A specific benefit of the Series 62 tests, in addition to those mentioned by the authors, is that they give resistance, wetted area and trim angle measurements for forward CG locations at low speeds. For these conditions the existing seaplane material (based on tests of prismatic surfaces) gives wetted lengths in excess of the normal boat length, and consequently neither the wetted area nor the trim-angle prediction is strictly applicable.

The following opinions are based on considerable successful experience with rough-water planing hulls, but any critical remarks among them are not intended as a general criticism of the Series 62 parent form, which is an excellent hull design.

The 12½-deg deadrise at the transom is good. A few degrees more would not have hurt, but twice that amount, for example, would have been excessive. An advantage of greater deadrise is that the hull can run with the chines dry at the higher speeds, especially if spray rails are fitted properly. This reduces the wetted area at high speeds, as though the hull were narrower, but still provides the beam required to get over the hump without too much resistance. However, excessive deadrise causes tenderness in roll at planing speeds, even with spray rails.

The bottom could perhaps have been warped some in the afterbody to give more deadrise amidships and at the bow. To more closely represent the best in modern practice, the chine planform should not have been so full forward. These changes would produce a better sea boat without hurting the planing performance. The narrow stern is in general very good. However, for a boat designed to operate at the low end of the planing range, or for any boat where getting over the hump without excessive trim is a problem, a wide transom is better. At hump speeds, when a large percentage of the lift is buoyant, a broad stern moves the center of buoyancy aft thereby producing a lower trim angle and less resistance. Convex bow sections are definitely very good. The convexity could have been carried farther aft in conjunction with increasing the deadrise.

The authors state that making the buttocks less steep in the forebody will reduce pounding. While this is true in some cases, as in changing the forebody shape by increasing the station spacing, it is the writer's opinion that stating the matter in this way may lead to wrong conclusions. For example, it is easy to picture a forebody with rather flat easy buttocks which also has flat sections and will therefore pound badly. In the case of the parent form of this series, it does not seem appropriate to say that the increased pounding due to straightening the sections will be ameliorated because the buttocks have incidentally been flattened, especially when the convexity of the sections was near the chine where it is much more effective than when near the keel.

The coefficients used at DTMB are, of course, dimensionally correct and useful for comparing the boats of this series. However, it is felt that they do not give a valid comparison among boats with differing hull forms and are inconvenient for data-reduction purposes. The reason for this is that the length and area measurements are made on parts of the boat which are out of water at all speeds, particularly at planing speeds. Because of this, the length, shape, and area of the chine planform (and hence the values of $A_p/\nabla^{2/3}$, L/B, and l_{cg} aft of the centroid of A_p) can be varied without affecting the planing performance of the boat. Conversely, it is possible to hold these parameters constant while radically changing the planing performance. While no system of coefficients is perfect, the seaplane coefficients, based on beam and l_{cg} measured from the transom, seem to be better in this respect. The authors apparently bear this out since they have found their

data to correlate better when the seaplane coefficients are used.

In Fig. 7, for Froude number 6, which is high speed, the narrowest hull is shown to have less resistance than the widest one. As the authors point out, this is the opposite of what would be expected. It is stated in the paper that air resistance may account for this. Using the information in the paper and a guess at the drag coefficient, the air resistance was calculated to be, at most, 3.4 lb for the wide model and 1.3 lb for the narrow model. Subtracting these values from the measured total resistances does not reverse their relative positions.

However, it was noted that the wetted area tabulated in the Appendix does not include the area wetted by spray. The measured total resistance, of course, includes the contribution of the spray wetted area. If the resistance of the spray wetted area is eliminated by calculating the frictional resistance due only to the solid wetted area, and adding the wave-making resistance (which is equal to the displacement multiplied by the tangent of the trim angle) the resistances of the wide and narrow models become 11.8 lb and 18.5 lb respectively. Dividing each by the appropriate displacement gives R/W values of 0.216 and 0.269 which have the relative magnitudes one would expect. It appears that the spray wetted area puts a definite limit on the advantage that may be gained by a high aspect ratio in a deadrise surface.

The matter of spray wetted area has important implications in the expansion of model data to full size. The standard procedure is to calculate the frictional resistance of the model, subtract this from the total measured resistance, and assume that the residual resistance is mostly wave making. For the fully planing model, the wave-making resistance can be calculated directly, as noted. Spot checks were made on a number of the runs tabulated in the Appendix, calculating the wave making from the trim angle and the frictional resistance from the tabulated wetted area. In each case, this was considerably less than the tabulated total resistance, sometimes by as much as 16 percent. The calculations were repeated increasing the wetted area to include the spray wetted area, according to an earlier report,[9] and in each case then the total calculated resistance agreed well with the total tabulated resistance. If this analysis is correct, use of the tabulated wetted area when expanding to full size results in Froude scaling an appreciable percentage of the frictional resistance. Therefore, it would seem that the spray wetted area should have been included in the tables of the Appendix. At low speeds, where the wave-making resistance cannot be calculated directly, the standard procedure can be used to good advantage but again the correct wetted area should be used.

On the other hand, simply including the spray wetted area with the solid wetted area in the frictional-resistance calculation does not produce the accuracy this discussion may seem to imply. Differences in Reynolds number, in the amount of air entrained, and in the direction of flow make the calculations only approximate. The authors are aware of these and other considerations and it would therefore be helpful to know more of the background of their decision to present the wetted area as they did.

The prediction method shown in Fig. 28 is excellent and very simple to use, but is confined to a narrow range of high speeds. The unique feature of this paper is that it presents accurate data on boat shaped models extending well into the displacement speed range and it will be a great help to naval architects when these data have been reduced to a prediction method which will cover the complete range of speeds. The prediction must also include the trim angle because proper running attitude is often more important than low resistance. The authors have probably given some thought to this and it would be of interest to know if development of such a prediction method is planned at DTMB.

J. F. Stoltz,[10] *Visitor:* In discussing Fig. 7, the authors have made one statement which I do not understand: "At high speed less drag would be expected for a short, wide hull than for a long, narrow hull because of the higher aspect ratio of the former." I am sure the authors will agree that, based on our present knowledge of the mathematics of planing surfaces and on actual observation, the optimum length-beam ratio from the standpoint of minimum drag at high speeds is not that of the short, wide hull with maximum aspect ratio. On the contrary, strictly from the standpoint of minimum drag alone, the optimum beam becomes narrower with higher speed. Minimum drag for the planing surface is achieved when the combination of parameters is such that it produces an optimum angle of attack. For a flat (zero deadrise) surface this angle is very close to $4.75/b^{1/3}$ deg (where b is the beam, in feet).

[9] Daniel Savitsky and E. W. Ross, "Turbulence Stimulation in the Boundary Layer of Planing Surfaces—Part II —Preliminary Experimental Investigation," Davidson Laboratory, Stevens Institute of Technology, Experimental Towing Tank Report No. 444, August 1952.

[10] Address: 448 S. Kensington Ave., La Grange, Ill.

For the deadrise surface, this value is slightly greater (obtained by dividing the foregoing expression by the 2.1 root of a fraction representing the ratio of lift for the deadrise surface to the lift for an equivalent flat surface).

It is not surprising, therefore, that the long narrow hull may have less resistance at the low, subplaning speeds and again at higher speeds where the narrow beam results in a more favorable angle of attack.

While it cannot be denied that the proposed definition of the porpoising limit for the series in question seems to be supported by the data, I would like to question the use of a plot of the lift coefficient divided by LCG in beams, versus the Froude number (based on volume) for this purpose.

To illustrate the basis for my question, this type of relationship implies (*a*) progressively less porpoising stability with increasing speed, and (*b*) progressively greater porpoising stability with increasing beam (other parameters remaining the same). Speed-trim curves developed at Davidson Laboratory as well as an empirical relationship based on wetted-area dimensions which I developed separately and actual observations on prototype hulls all indicate that (*a*) deadrise surfaces which are not deep into the porpoising range often regain stability at higher speeds and (*b*) under no circumstances is porpoising stability improved with a higher aspect ratio (wider beam). The absence of data deep in the unstable region indicates that the phenomenon of regained stability was not explored.

From the standpoint of almost idle curiosity I compared the authors' prediction of resistance for a 15,000-lb boat of 10.9 ft beam and 12½-deg deadrise with an approximation equation which I formulated and presented for laymen (in slightly different form) in *Motor Boating* in 1961–1962. The equation is

$$R = 0.0175W\left[\frac{25W}{V_M{}^2b^2} + \frac{B}{15}\right] + \frac{V_M{}^2b^2}{100}$$

where

R = resistance, lb
W = gross weight, lb
B = deadrise angle, deg
V_M = speed, statute miles per hr
b = beam, ft

The expression in the brackets is an approximation of the angle of attack, T, (in degrees) the first term, $0.0175WT$, is the wave-making resistance, and the second term is an approximation of the skin-friction resistance. I thought the authors might be interested in seeing this equation, Fig. 39, as plotted and superimposed on their Fig. 29. Obviously, the close agreement is more coincidence than science since the equation is based on (*a*) a relatively small and constant buoyant component of lift, (*b*) frictional resistance based on a considerably smaller hull, and (*c*) an LCG location farther aft (1¼ beams forward of the transom). The two latter deviations are compensating in this instance.

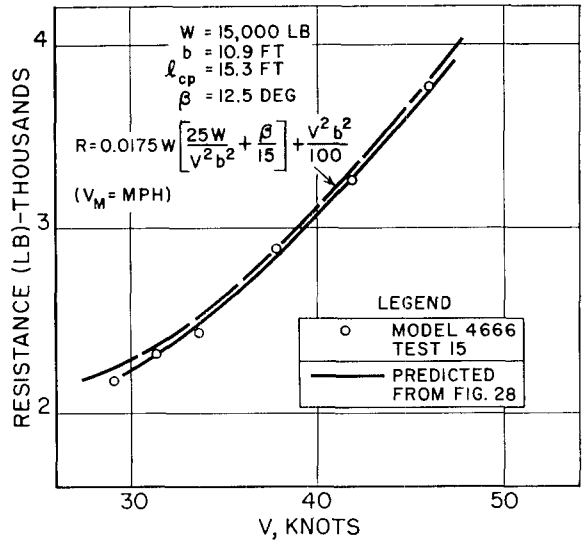

Fig. 39

By more classical methods of calculating resistance, I found reasonably close agreement with Fig. 29, the degree of variance being within the range of accuracy for the aerodynamic drag.

John H. Nachtsheim, Member: In Fig. 29 of the paper the authors prove the validity of their method by sampling some of the data used to derive the method against the method derived. It seems that if the method is a good method it should also stand the test of data other than that upon which it was derived. In order to test it in that way and actually to try the method suggested, I selected a recent model test of a similar hull, the 52-ft LCSR, for comparison. From the LCSR dimensions I used the method in the paper to predict the resistance for the conditions of 34,000 lb and for the standard 100,000-lb condition. Then, from the actual model tests of the LCSR, I plotted the resistance predictions for both conditions. Fig. 40 of this discussion shows the corresponding curves for the 100,000-lb condition. The model test prediction is about 20 percent higher than the prediction

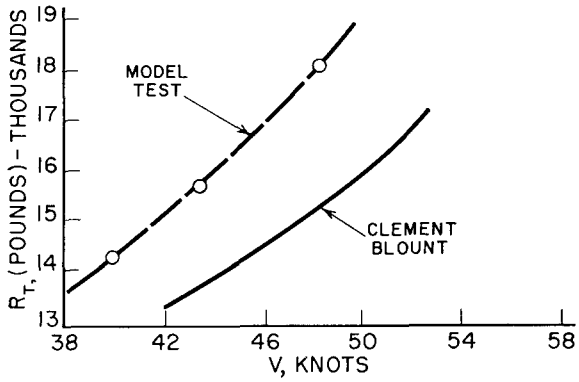

Fig. 40

based on the author's method. Can the authors explain this rather wide discrepancy?

If there are features designed into boats which takes them this far from the resistance predicted utilizing the paper, should not some precautions be suggested by the authors for potential users of the paper? Otherwise the impression is made that this paper is all that's needed to predict accurately the resistance of a planing hull form.

David D. Beach, *Member:* The writer has used the basic design philosophy presented by the first author in reference [2] of the paper, and is most gratified to see that that basic hull form, of proven suitability for runabouts and high-performance express cruisers, has been further developed in this paper.

As to the parent form and the final form of DTMB 4667-1, the only comment seems to be to areas other than hull efficiency. First, the topsides, while fine for plywood and wrapped-on metal plates, is a little less than esthetic. While this has no bearing at all on the bottom, in boats and yachts we do get involved with appearance, and some slight concavity to the topsides forward produces the fuller deckline demanded in boats nowadays, and this is important in the yacht market. Also, the narrow transom with increasing beam at amidships will play considerable havoc with the problems of suitable accommodations aft. This is not important except in larger craft where the length-beam ratio is highest. We all like to have full-width berths, port and starboard, and space between them, and it is a considerable chore to do this with the rapidly tucking in of the chine.

The authors have modified the basic transom beam to maximum beam ratio to provide for bouyancy aft in the case of outboard powered boats and larger craft with stern installations of their propulsive machinery and tanks. This is an appreciated concession to the pleasure boat design problem, but it remains to be seen if the concession is adequate. Appreciating the basic design premise, as stated in [2], as to the need, or lack thereof, for transom beam and planing area aft, this designer feels that, in yachts and pleasure craft, the arrangement requirements will continue to outweigh the power requirements.

The writer feels that this narrow beam at the transom is responsible for the extreme range of trim attitudes which several of the tests indicate. While conventional, parallel chine craft may not, as is indicated in Fig. 8, be as efficient, these craft—or at least some of them—do not exhibit the extreme "bow-up" attitude during acceleration or part throttle cruising. It appears that the data establish another dilemma in small-boat design, i.e., "if you want to run flat out when wide open, you'll never be able to see over the bow when you ease up on the throttle."

However, as a final comment, we in the small pleasure boat and yacht field have only meager model test and full-scale trial data to use as a check against the academic approach. However, I have assured myself, through checking against the trial data and model test results, of three essentially prismatic afterbody craft, that the procedure outlined and illustrated in the concluding paragraphs of the paper does, indeed, produce a highly satisfactory result. The correlation is good.

If a gracious management and a proper budget allotment can be obtained, it is not unlikely that a full-scale evaluation of this form will be undertaken later this winter or early in the spring in Baltimore and I will look forward to the results to be obtained therefrom.

Charles Garland, *Associate Member:* In 1958, a model entitled SC-1 was constructed and tested at the Robinson Model Basin at Webb Institute. This model was similar in many respects to model 4666 of the paper. However, the expanded resistance of SC-1 for a 10,000-lb displacement (salt water) was about 10 percent lower than that of model 4666. Table 5 gives a comparison of these two models.

Would the authors comment on the difference in resistance? Has there been any work done on the effect of chine area distribution to resistance? Could the difference in resistance be partially due to deadrise?

The writer has compared different hull forms on the basis of equal loading factor $A_p/\nabla^{2/3}$ and believes this to be a sound basis of comparison.

Table 5

	Model 4666	Model SC-1
L_p/B_{pa}	3.69	3.96
L_p/B_{px}	3.06	3.15
B_{px}/B_{pa}	1.21	1.26
B_{pt}/B_{px}	.71	.877
Centroid of A_p % L_p fwd	48.2	57.3
B_{px} fwd % L_p	60	38
Deadrise midships/ transom	13°/12½°	11°/5°
Shaft angle, deg	12.97	12
Model WL length, ft	5.987	2.3875
Extrapolation to 10,000 lb	Schoenherr ΔCf = 0(?)	1957ITTC ΔCf = 0.0001
Turbulence stimulation	None	Strut before model
Hull lines	Developable surface	Developable surface

RESISTANCE DATA

	Model 4666 $A_p/\nabla^{2/3} = 8.0$ LCG 8% aft centroid AP	Model SC-1 $A_p/\nabla^{2/3} = 8.0$ LCG 2% aft centroid AP
F_∇	R/W	R/W
1.5	0.107	0.095
2	0.116	0.108
2.5	0.123	0.112
3	0.128	0.120
3.5	0.136	0.123
4	0.148	0.138
4.5	0.172	0.153
5	0.196	
5.5	0.224	
6	0 258	

As revealed by the test data of this series, the loading factor really relates to the actual wetted surface measurement. At F_∇ values above 3.5, high hull loading factors show larger model wetted-surface areas than lower hull loading factors. Since frictional resistance is the governing measure at these high speeds, the hull loading factor, which is a still water measurement, does relate to actual measured wetted surface at high speeds.

The writer has compared different models of similar L_p/B_{pa} at the same loading factor in regular wave trains. These tests were run at the MIT model basin on an equal power basis. In waves the wetted surface is, of course, a variable coupled with ship motions. However, these tests revealed roughly equal speed losses in waves for hulls with similar loading factors.

Although the dimensionless variables presented appear to describe adequately planing-hull resistance in still water, the designer is still faced with several problems. Take the 10,000-lb boat for instance. This corresponds roughly to a 30-ft-long pleasure craft. A practical speed range for this craft is, say 25 to 35 knots. This would correspond to F_∇ values of 3.2 to 4.5. The parent hull at 35 knots has an EHP of 170. To propel a 30-ft boat at 35 knots, this would roughly require 350 to 400 shp on two screws. This engine and fuel installation would weigh roughly 4000 lb. Therefore, the practical power limits are rapidly reached. To further complicate the design issue, at $F_\nabla = 3.2$ to 4.5 resistance differences of less than 7 percent are noted for L_p/B_{px} from 2.00 to 5.50. For this size pleasure craft, this generally important variable does not appear to be a strong design variable for this hull series. Of course, all tests are run in still water and a type of rough-water criterion needs to be applied. The authors' comments would be appreciated on this subject.

Paul R. Van Mater, Jr., *Associate Member:* The authors have made a straightforward presentation of data together with an extremely simple and convenient method for resistance prediction. For the most part the reader is left to form his own conclusions as to the effect of form and proportion. In particular the authors do not emphasize the importance of trim angle in planing-boat performance. To illustrate the trim-dependent nature of the planing boat, cross plots of angle of attack, α versus R/W have been prepared for one loading condition and two LCG locations, using values picked from Figs. 9 through 12. The curves are presented only for the case of fully developed planing, the inception of which is indicated by I on the plots, Figs. 41 and 42. Inspection of these curves leads to the following observations:

(*a*) The lowest R/W values occur at an angle of attack of about 4¼. This optimum angle of attack appears to be largely independent of LCG location and L/B, except that as the models become longer and narrower the angle of attack never becomes large enough to approach the optimum.

(*b*) There is a serious resistance penalty associated with small angles of trim. In reducing the trim from 4 to 2 deg resistance increases of 80–100 percent are noted.

(*c*) It is well known that planing efficiency is increased as aspect ratio is increased. The plots confirm this and indicate that one reason is that the higher aspect ratios (lower L/B ratios) permit the model to operate in the optimum trim range.

It is anticipated that further cross plotting will confirm the foregoing trends for the remainder of the series. The existence of an optimum angle of attack that is largely independent of form variations has been known for some time, but has not received popular acceptance. It does, however, suggest some interesting possibilities. Form changes such as an increase of deadrise or round-

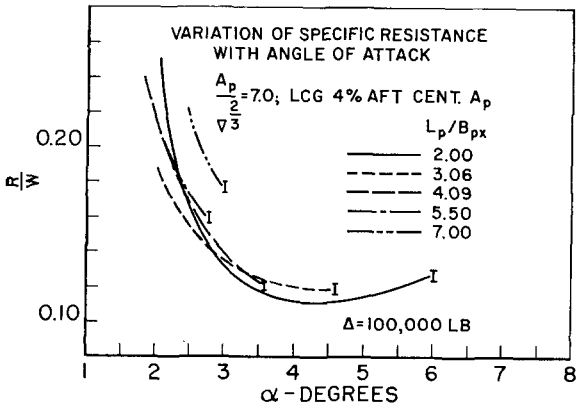

Fig. 41 Variation of specific resistance with angle of attack

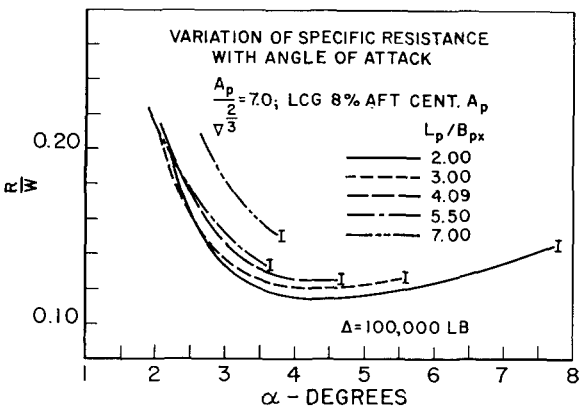

Fig. 42 Variation of specific resistance with angle of attack

Table 6 Comparison of Model Test With Semi-Empirical Method

Based on Test No. 12 DTMB Model 4667-1

MODEL CHARACTERISTICS

L_P/B_{PX} = 4.09 $A_P/\nabla^{2/3}$ = 7.00 LCG = 8 percent aft centroid of A_P

	Model test	Semi-empirical	Model test	Semi-empirical
Displacement, lb	154.00		100,000	
Speed, knots	12.82		37.56	
F_∇	3.29		3.29	
R_t, lb	23.03	22.41	12,500	12,000
α, deg	4.10	4.00	4.10	4.08

ing of bilges which result in loss of lift but an increase in running trim angle may actually produce a net gain in resistance by permitting the boat to operate nearer the optimum trim angle. On the other hand the addition of wedges or the presence of a hook in the after buttocks tending to reduce the trim can be expected to be uniformly detrimental in the fully developed planing region. These features will show an advantage only in the transitional region where trim angles may be excessive.

In a discussion of this paper Moss has questioned the possibilities of scale effects in trim predictions based on model tests. In light of the foregoing discussion it is clear that if the model does not accurately reflect the full-size trim behavior then the validity of the entire model test procedure is in doubt. In order to check this possibility a prediction method was employed in which the trim angle is determined explicitly for any scale ratio. In this method frictional and pressure forces are calculated as a function of trim angle using the semi-empirical equations of Savitsky and Neidinger.[6] Two simultaneous equations representing the center of pressure as a function of trim angle are solved graphically. One equation locates the center pressure based on the character of the pressure distribution over the bottom. The other equation is simply a statement of force and moment balance. Four forces—thrust, weight, normal pressure force, and frictional resistance—appear in this later equation. Any change in the magnitude of the frictional force relative to the other forces will affect the final solution for trim angle.

A data point in Test 12 of Model 4667-1 was selected as representative and the foregoing calculation procedure applied for both model size and the 100,000-lb expansion. Results are given in Table 6 herewith. The calculated value of R_t and α for model size are within about 2½ percent of the model test data point. The prediction of trim angle increases from 4.00 deg for the model to 4.08 deg for the 100,000-lb boat, the difference being due to the differing proportion of frictional resistance present in full size. In short, it appears that scale effects are present in trim predictions, but they will not seriously affect the prediction unless the scale ratio becomes very large.

The implication by the authors that the center of gravity and the center of pressure are at the same location is not fully understood. If this were the case then as speed increases a planing boat would not undergo the large changes of trim that are characteristic of its behavior. As a matter of fact, for the 100,000-lb example calculated in the foregoing the separation between weight and pressure forces is 0.134 ft.

In closing, the authors' comments on the following questions regarding scale effects are invited:

(*a*) Is there any consistent trend when comparing model test trim predictions with trial results?

(*b*) Side wetting often appears in model tests. Does this also appear on the full-size boat?

(*c*) Will the absence of propeller suction in a towed model test seriously affect the trim?

Guiseppe Scarpa, *Life Associate Member:* The present paper should be of great interest to naval architects owing to the few studies on this subject leading to useful conclusions. In this brief note I shall limit myself to a consideration of the variables in function of which the resistance is expressed. Essentially they are A_P; B_{PX}; $\mathbf{F}_\nabla$; L_P; $\nabla^{2/3}$ and X_G, horizontal length from LCG to after end of L_P.

I believe that it is possible to do without the variable L_P, as this length does not matter in planing, while what matters is the actual length, a function of the fore-and-aft position of LCG. Similarly it is possible to do without A_P since it is substituted by functions of X_G and B_{PX}. Consequently, there would be only four variables and with these, the three ratios

$$\frac{X_G}{\nabla^{1/3}}; \quad \frac{B_{PX}}{\nabla^{1/3}}; \quad \mathbf{F}_\nabla$$

thus greatly simplifying the procedure.

Authors' Closure

In replying to the numerous stimulating comments on their paper, the authors would like first of all to acknowledge that there are more interesting points about the hydrodynamics of planing hulls in the comments than in the paper itself.

In this connection, Captain Forest's commentary on the important hump region is particularly appreciated since it fills a noticeable gap in the text of the original paper. A graph, Fig. 43, of volume Froude number ($\mathbf{F}_\nabla$) as a function of boat speed and weight has been added in accordance with Captain Forest's suggestion.

The performance data on the Bertram boat which were included in Mr. Colton's discussion, and the performance data on the high-speed designs tested at the Davidson Laboratory, which were presented by Mr. Young Chey, will obviously be of considerable interest to the readers of the paper.

The authors acknowledge with appreciation the numerous valuable suggestions for future research on planing hulls. In this connection, Mr. Kimon's points in regard to extending the work to include other deadrise angles seem particularly well taken. Mr. Kimon's proposed scheme for extending the series to include other deadrise angles seems extremely good.

Mr. Moss has raised an interesting question in regard to trim angle. The Model Basin has examined the question of scale effect on both resistance and trim by testing a geometric series of planing hull forms. One of the surprising results obtained was that the trim angle was consistently lower for a large model than for a smaller model. This is contrary to the result indicated by Mr. Moss's analysis, which seems to us to be correct. We are not able to explain the anomaly.

Mr. Young Chey and also Mr. Van Mater asked about center-of-pressure location versus center-of-gravity location. The authors believe that no significant error will result from the assumption that the pressure force on the bottom of the hull passes through the hull center of gravity, and therefore that the above two dimensions can be used interchangeably.

Mr. Koelbel has offered an interesting and well-informed commentary, and the authors agree with most, though not all, of the opinions which he has expressed. Mr. Koelbel stresses the importance of spray-wetted area. During the time which has elapsed since the graphs and tables of this paper were prepared, the Model Basin has also devoted some attention to this subject. One result of this work is David Taylor Model Basin Report 1818, which shows how spray drag of planing boats can largely be eliminated by an appropriate arrangement of longitudinal spray strips. Also, it is now our standard practice to include tabulated values of spray-wetted lengths in the Model Basin data sheets for planing craft. In answer to Mr. Koelbel's question as to why the authors treated the wetted area as they did, the answer is simply that they followed the well-trodden path of conventional past practice. Furthermore, as Mr. Koelbel's comments indicate, it is not clear even at this considerably later date, that a better or more accurate method is known.

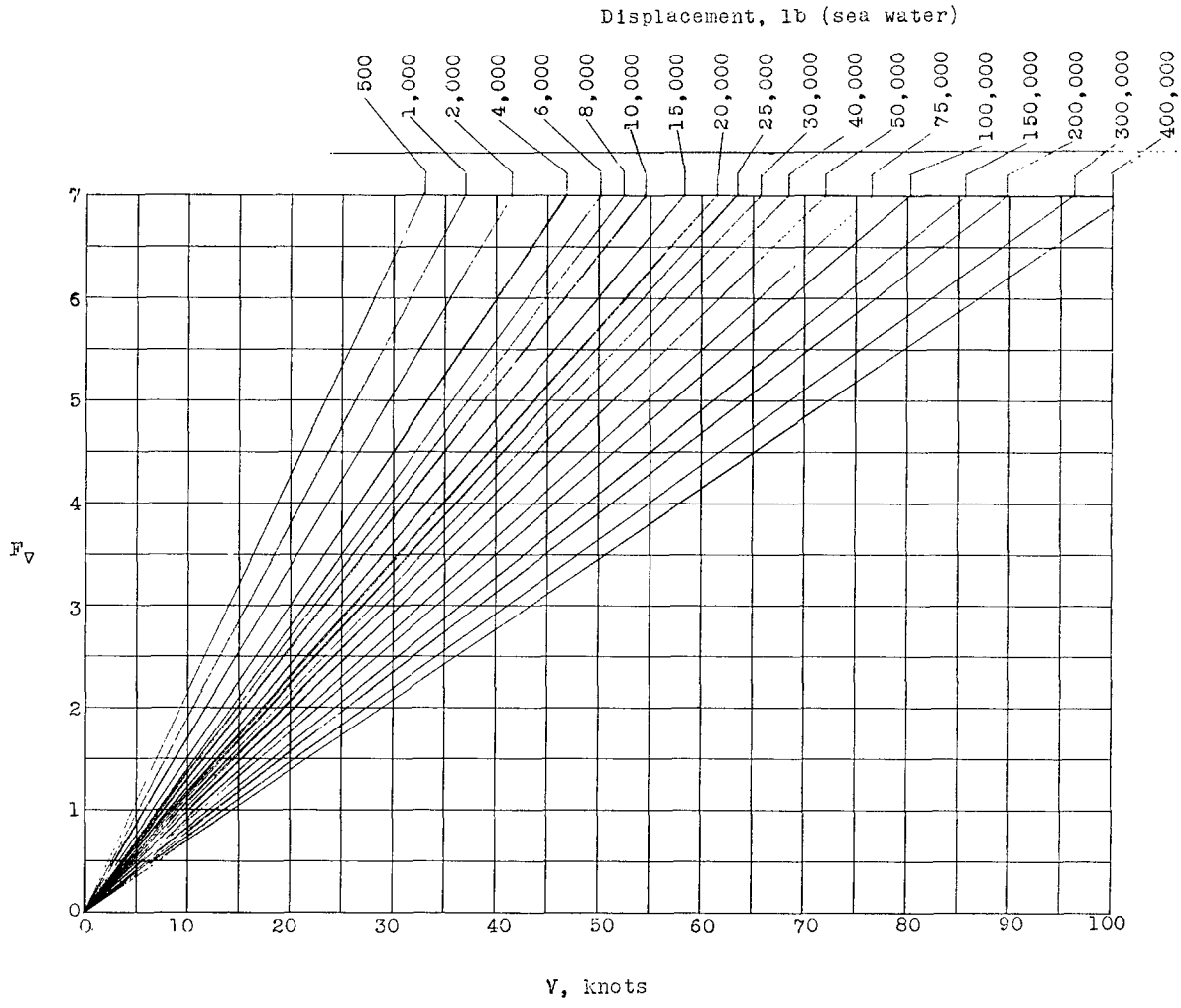

Fig. 43 Variation of volume Froude number with speed and displacement

Mr. Stoltz is puzzled as to why we expected less drag at high speed for a short wide hull than for a long narrow hull. An important point here is that the comparisons in this paper between hulls having different length-beam ratios were made on the basis of equal planform area. Therefore, when we visualize a short wide hull being altered in the direction of a higher length-beam ratio, we consider that if the width is reduced by dividing it by a number greater than one, the length is to be multiplied by the same number in order to keep the planform area unchanged. Mr. Stoltz in raising his question evidently considers change in length-beam ratio as a change in width with the length held constant. When the length-beam ratio is varied in this manner, we entirely agree with Mr. Stoltz that increase in length-beam ratio would lead to less drag at high speed.

Mr. Stoltz's remark that a porpoising deadrise surface will often regain stability at a higher speed is an interesting one. He is correct in his assumption that this phenomenon of regained stability was not explored during the tests of this planing-boat series.

Mr. Nachtsheim's point is clearly a valid one. The hull form of Series 62 was the result of a considerable amount of time and effort directed toward the development of a design having low drag at planing speeds. The hull forms for which the series test results can be used to predict performance would necessarily be similar to the design of the series and would therefore also have the features giving low drag at planing speeds. With that restriction, the data can be used as stated to predict the resistance of boats of a wide range of sizes and proportions.

Planing hull studies at the Model Basin have

shown that for low drag at high speeds the planing bottom should have a narrow stern and straight parallel buttocks: i.e., no twist or hook. The LCSR design which Mr. Nachtsheim has utilized for his comparison has, on the other hand, a wide stern, and both twist and buttock hook in the planing area. These are evidently the reasons why the high-speed drag of the LCSR design is considerably greater than that of the corresponding Series 62 design.

The resistance of Mr. Garland's planing boat design, as predicted from tests of a model 2.4 ft long, seems remarkably low. The authors strongly suspect that the reason is either laminar flow or experimental error. If the resistance data were valid the design would be a very remarkable one.

Mr. Van Mater has contributed interesting discussions of optimum angle of attack for planing hulls and of the influence of scale effect on trim angle. To the best of the authors' knowledge data are not available on which to base satisfactory answers to the questions raised by Mr. Van Mater at the conclusion of his comments.

In reply to Professor Savitsky, the authors would like first of all to acknowledge their indebtedness to Professor Savitsky and his colleagues at the Davidson Laboratory for the many fundamental studies of the hydrodynamics of planing forms which they have made available. Their work is, of course, well known, and is of invaluable aid to all serious students of the subject. The authors are also familiar with Professor Savitsky's equation for predicting the resistance of planing hulls, but have found it to be less accurate for high speeds than an equation developed at the Taylor Model Basin. The DTMB equation has the important advantage of including a term for spray drag. A significant difference between the two equations is that Professor Savitsky's takes account of buoyancy and Froude-number effects and accordingly is meaningful down to quite low speeds. The DTMB resistance equation is applicable only for high speeds where buoyancy and Froude-number effects become negligible. However, since a smaller number of variables is involved, it lends itself readily to the development of design charts for the optimization of planing hull performance. The DTMB resistance equation for planing hulls and some design guides which have been developed from it can be found in DTMB Report 1490.

SMALL CRAFT
DATA SHEET NO. 1

S.N.A.M.E. Small Craft Data Sheet No. 1

Hard-chine boat, L_P/B_{PX}=4.09

Model No. TMB-4667

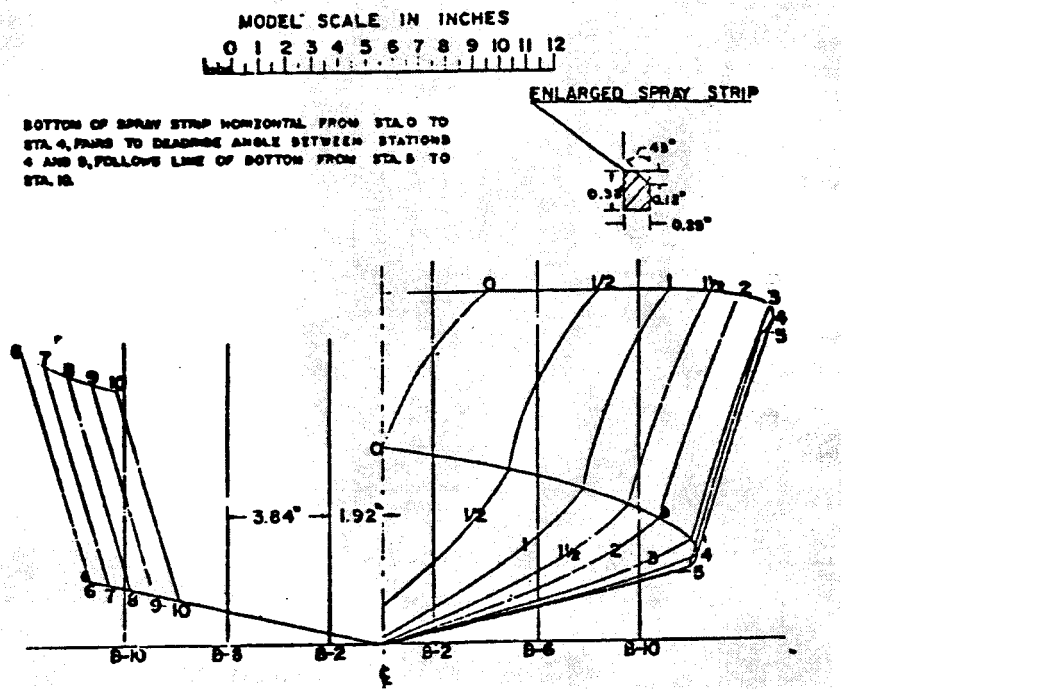

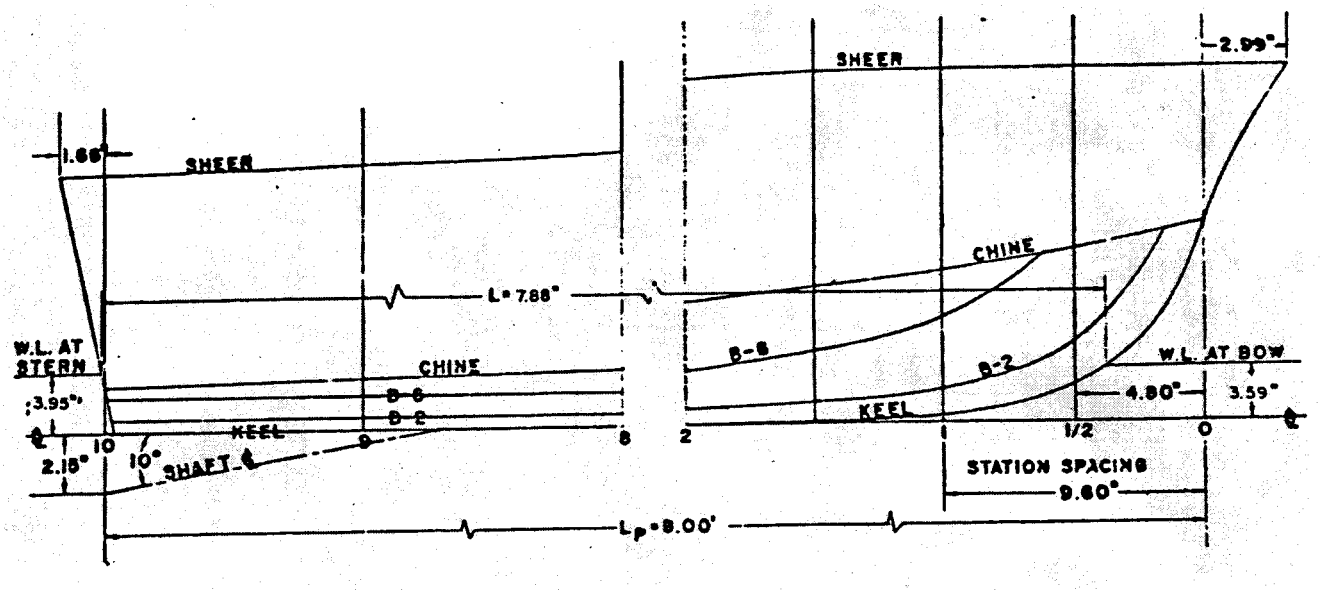

MODEL PARTICULARS, TEST CONDITIONS, AND RESULTS

Boat: Parent Model for Planing Boat Series
Model Number: 4667
Appendages: Spray Strips
Laboratory: Datmobas
Basin: High-Speed
Basin Size: 2698' x 21' x (10'8 16')
Model Length: 8.00 ft
Test: 0 Date: 4 Nov. 57
Water Temperature: 72° F
Specific Weight: 62.3 lb/ft^3
Model Material: Wood
Model Finish: Paint
Turbulence Stimul.: None

Remarks: Model was towed in the shaft line shown in the profile drawing

Planing Bottom Dimensions and Coefficients

L_P 8.00 ft
B_{PX} 1.955 ft
B_{PA} 1.600 ft
A_P 12.80 ft^2
$A_P/\nabla^{2/3}$ 7.00
$L_P/\nabla^{1/3}$ 5.917
L_P/B_{PA} 5.000

LWL Dimensions and Coefficients

L
B_X
H
L/B_X
$L/\nabla^{1/3}$
C_B
C_P
C_W

Model Test Condition

Δ, lb 153.9 τ_0 0.20 deg x stern α_0 0.20 deg
LCG location 3.42 ft forward of station 10
(LCG location 6 percent L_P aft of centroid of A_P)

Model Test Results

V, knots	R_t, lb	Wetted length of keel, ft	Wetted length of chine, ft	Rex10^{-6}	S, ft^2	10^3 C_t	Change of trim, deg	CG rise, in.	F_∇
0	—	7.80	5.40	—	—	—	0.00	0.00	0.00
3.90	8.57	7.80	7.50	4.966	14.52	14.056	0.48	-0.38	1.00
4.88	13.33	7.80	6.60	5.774	14.36	14.122	2.00	-0.55	1.25
5.85	15.12	7.70	6.10	6.632	13.42	11.926	2.62	-0.23	1.50
6.84	16.40	7.60	5.80	7.531	12.95	9.803	2.77	0.04	1.75
7.83	17.79	7.40	5.40	8.234	12.44	8.448	3.07	0.29	2.01
8.81	19.19	7.10	5.00	8.758	11.45	7.821	3.57	0.58	2.26
9.77	20.31	6.60	4.60	8.893	9.93	7.761	3.78	1.01	2.50
10.75	21.26	6.20	4.40	9.363	9.28	7.173	3.80	1.31	2.76
11.74	22.11	6.00	4.20	9.837	8.85	6.565	3.67	1.55	3.01
12.70	22.96	5.80	4.00	10.25	8.43	6.123	3.53	1.68	3.25
13.64	23.95	5.80	3.80	10.76	8.23	5.672	3.32	1.98	3.50
14.66	25.17	5.70	3.60	11.20	7.93	5.356	3.12	2.09	3.76
15.66	26.17	5.70	3.40	11.71	7.73	5.013	3.97	2.17	4.01
16.60	27.54	5.70	3.30	12.27	7.62	4.757	2.73	2.26	4.25
17.60	29.43	5.70	3.20	12.87	7.53	4.582	2.65	2.30	4.51
18.55	31.23	5.70	3.10	13.41	7.42	4.436	2.53	2.35	4.75

PERFORMANCE CHARACTERISTICS

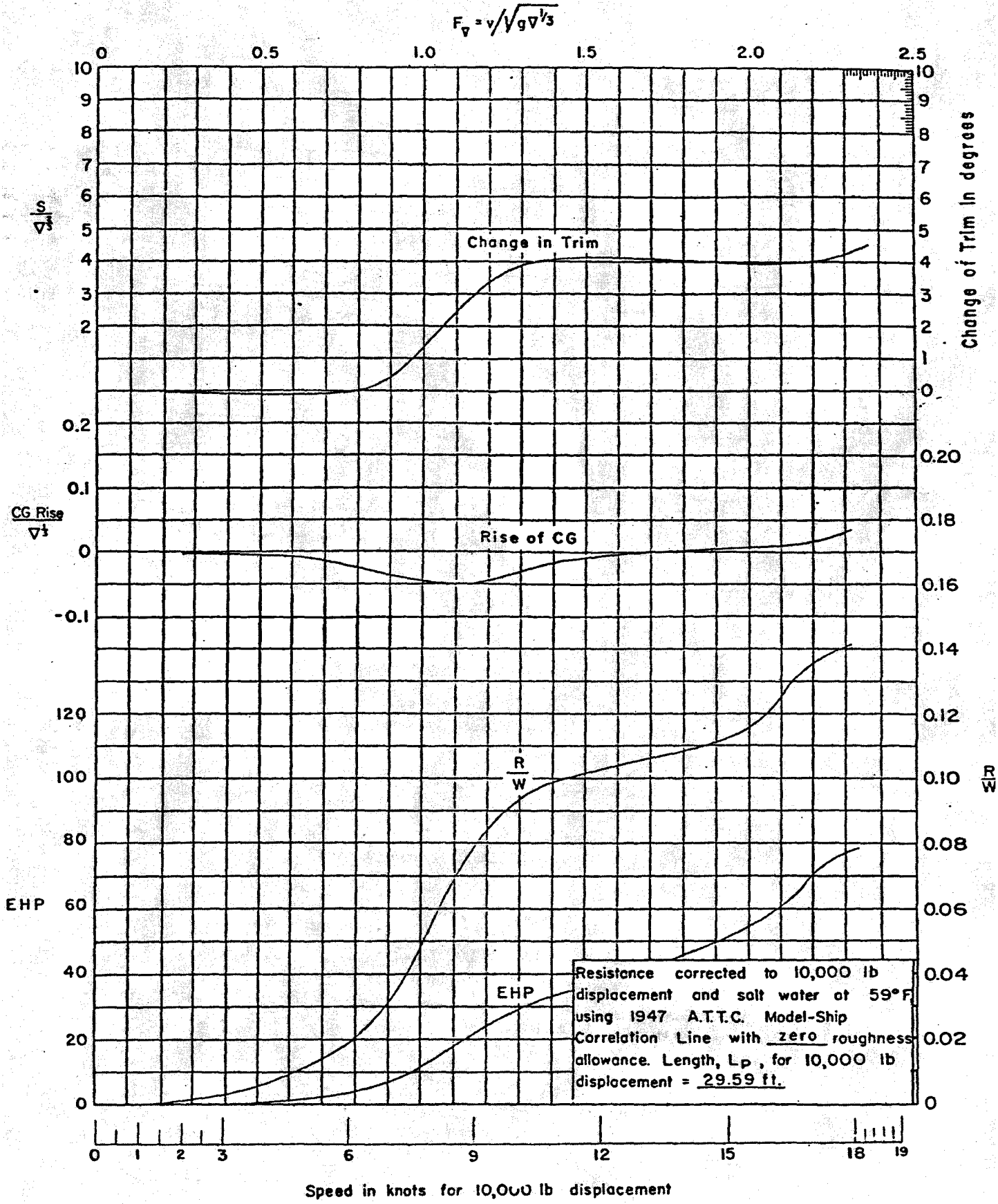

FORM CHARACTERISTICS

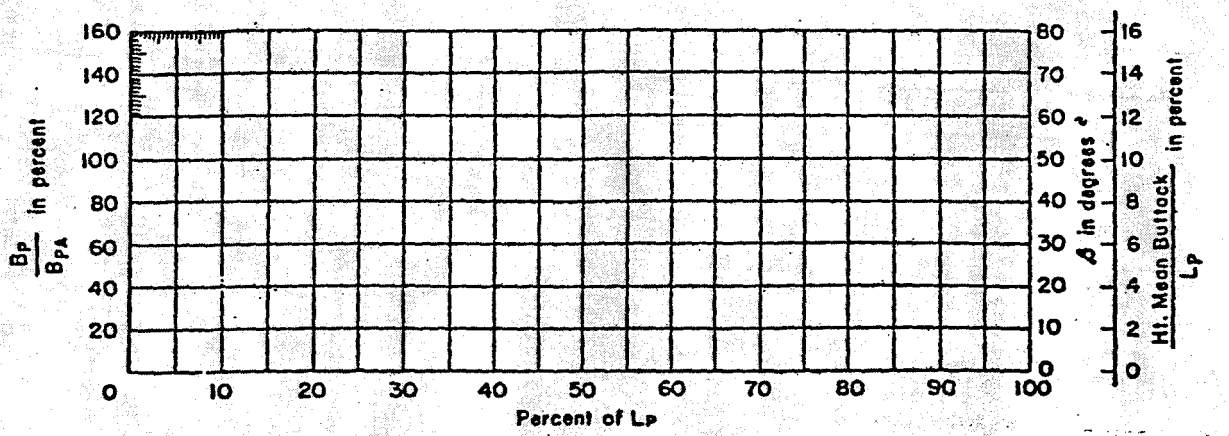

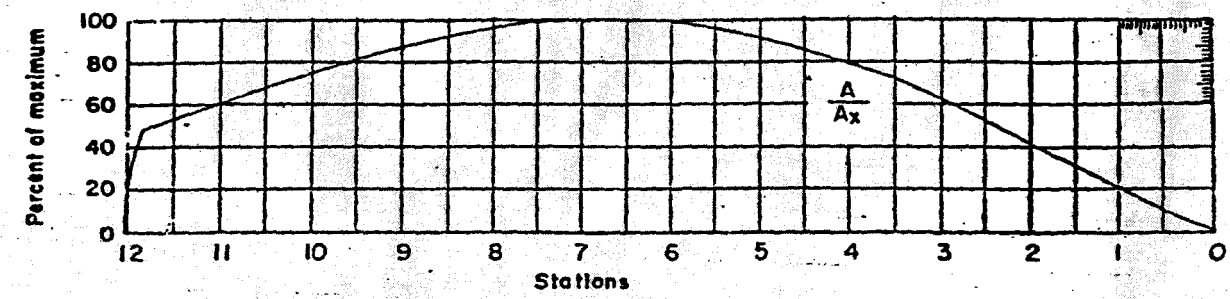

Notation

As far as possible the notation used is consistent with the Society's "Explanatory Notes for Resistance and Propulsion Data Sheets" (Technical and Research Bulletin No. 1-13). Exceptions and additions are listed below. The subscript P designates the planing bottom which is the portion of the bottom bounded by the chines and transom.

A_P	Projected planing bottom area, excluding area of external spray strips
B_P	Beam or breadth over chines, excluding external spray strips
B_{PA}	Mean breadth over chines, A_P/L_P
B_{PX}	Maximum breadth over chines, excluding external spray strips
L_P	Projected chine length
S	Area of wetted surface (This is the actual wetted surface underway including the area of the sides which is wetted at low speeds and the wetted bottom area of external spray strips; however, the area wetted by spray is excluded).
α	Angle of attack of stern portion of planing bottom in degrees
β	Dead rise angle of planing bottom in degrees. This angle is obtained by approximating each body plan section by a straight line.
Δ	Displacement at rest, weight of
τ	Trim angle of hull with respect to attitude as drawn in degrees
∇	Displacement at rest, volume of

Subscript o indicates value when hull is at rest in water.

DEPARTMENT OF THE NAVY

HYDROMECHANICS

AERODYNAMICS

STRUCTURAL MECHANICS

APPLIED MATHEMATICS

ACOUSTICS AND VIBRATION

GENERAL RESISTANCE TEST OF A STEPLESS PLANING HULL WITH APPLICATION TO A HYDROFOIL CONFIGURATION

by

Lawrence Benen

HYDROMECHANICS LABORATORY
RESEARCH AND DEVELOPMENT REPORT

July 1965

Report 2006

GENERAL RESISTANCE TEST OF A STEPLESS PLANING HULL WITH APPLICATION TO A HYDROFOIL CONFIGURATION

by

Lawrence Benen

July 1965

Report 2006
SS 600-000
Task 1707

TABLE OF CONTENTS

LIST OF FIGURES

LIST OF TABLES

NOTATION

A_P	Projected planing bottom area, excluding area of external spray strips, in feet^2
B_P	Beam or breadth over chines, excluding external spray strips, in feet
B_{PA}	Mean breadth over chines, A_P/L_P
B_{PX}	Maximum breadth over chines, excluding external spray strips, in feet
b	Mean breadth over chines, $b = B_{PA} = A_P/L_P$, in feet
C_d	Draft coefficient d/b
C_f	Friction coefficient
CG	Center of gravity
C_{La}	Lift coefficient of aft foil $L_a/\frac{1}{2}\rho S_a V^2$
C_{Lf}	Lift coefficient of forward foil $L_f/\frac{1}{2}\rho S_f V^2$
C_{lm}	Mean wetted length coefficient l_m/b
C_M	Trimming moment coefficient M/wb^4
C_R	Resistance coefficient R/wb^3
C_S	Wetted surface coefficient S/b^2
C_V	Speed coefficient $V/\sqrt{gb}$
C_Δ	Load coefficient Δ/wb^3
D	Drag in pounds
D_a	Drag of aft foil in pounds
D_f	Drag of forward foil in pounds
d	Draft, feet
g	Acceleration due to gravity, 32.174 feet per second^2
H	Depth of foil below water surface in feet

L	Hydrofoil lift in pounds
L_a	Lift on aft foil in pounds
LCG	Longitudinal center of gravity (see Figure 1)
$(L/D)_a$	Lift-drag ratio of aft foil
$(L/D)_f$	Lift-drag ratio of forward foil
L_f	Lift on forward foil in pounds
L_P	Projected chine length of model in feet
l_m	Mean wetted length in feet
M	Trimming moment of the hull about LCG in pound feet
M_{cg}	Moment about CG of boat in pound feet
q	Dynamic pressure, $\rho V^2/2$ in pounds per foot^2
R	Hull resistance in pounds
Re	Reynolds Number, Vl/υ
S	Area of wetted surface in square feet (This is the actual wetted surface of the bottom area including spray strips; however, the area wetted by spray is not included.)
S_a	Projected area of aft foil in feet^2
S_f	Projected area of forward foil in feet^2
T	Propeller thrust in pounds
V	Speed of boat in feet/second
V_o	Takeoff velocity in feet/second
w	Density of water in pound/feet^3
X_a	Distance along X-axis from CG to lift force on aft foil in feet
X_f	Distance along X-axis from CG to lift force on forward foil in feet
X,Y,Z	Coordinate axis system fixed in the boat
Z_a	Distance along Z-axis from CG to drag force on aft foil in feet
Z_f	Distance along Z-axis from CG to drag force on forward foil in feet

Z_T	Distance along Z-axis from CG to thrust axis in feet
α_a	Total angle of attack of aft foil with respect to the horizontal in degrees
α_f	Total angle of attack of forward foil with respect to the horizontal in degrees
α_o	Angle of foil incidence in degrees
β	Angle of change in foil incidence (trim control forward foil) in degrees
Δ	Load on hull in pounds
Δ_o	Displacement at rest in pounds
ν	Kinematic viscosity of water in feet^2/second
ρ	Density of water in slugs per feet^3
τ	Trim angle of hull (angle between water surface and the reference line of hull) in degrees

ABSTRACT

General resistance tests of TMB Model 4567 were conducted in the Langley Field facility of the David Taylor Model Basin to determine the performance characteristics of one of a series of hulls which might be adaptable for use with hydrofoils. Resistance, trimming moment, and wetted length were measured for several load, trim, and speed conditions. All data are presented in nondimensional form for use in comparing hull forms and calculating take-off performance.

ADMINISTRATIVE INFORMATION

This study was authorized as part of the Hydrofoil Accelerated Program by Bureau of Ships letter S-F013 02 01, Serial 420-228 of 30 August 1960. The scope of the program was delineated in Bureau of Ships letter 3900, Serial 341B-125 of 13 August 1963. Funding was under SS 600-000, Task 1707.

INTRODUCTION

With the recent development of hydrofoil craft as a means of commercial and military transport, theoretical and experimental effort has been concentrated on the hydrofoil. Such concentration of effort is proper inasmuch as the hydrofoils make this craft different from a planing or displacement boat. This difference must be exploited in order to realize possible advantages, such as increase in speed or improvement of behavior in rough water, which can be obtained by the use of hydrofoils.

Along with the development of hydrofoil systems, however, the design of the hull is also of importance. Experience with hull designs for other types of boats has provided the basis for most of the hydrofoil hull designs. The designers of various hydrofoil craft have pursued policies of independent development that have given rise to striking differences in the hull lines. Although it is quite possible that there is little difference in the performance of good examples of the various types of hulls, direct comparisons are not possible at present because of the scarcity of published test results. Moreover, much of the data have

been obtained at only a few loads and trims. Little data are directly applicable to hydrofoil use, where the trim change during takeoff may be large and the load on the hull varies from full load to zero.

In order to provide data on hydrofoil hulls which might be used in performance calculations for preliminary designs, the Bureau of Ships initiated a program under which a number of hulls at representative unloading conditions were to be tested at a range of speeds and trims. The object of this program was to obtain data and to develop a method of presenting the results in the form of nondimensional lift, drag, and trimming moment coefficients for use in comparing hull forms and calculating takeoff performance. The end result is to establish criteria on which the design of efficient and optimized hulls can be based.

The High Speed Phenomena Division of the David Taylor Model Basin tested three hull models: Models 4667, 4335-2, and 4776. Model 4667 is a stepless planing hull; Models 4335-2 and 4776 are stepped planing hulls. This report presents the results of the tests of Model 4667 in nondimensional form together with a sample calculation for a takeoff performance computation.

DESCRIPTION OF MODEL

Figure 1 presents the line and form characteristics of the 8-foot model designated as Model 4667. Previous data[1] have indicated that this hull has less resistance than most stepless planing hull designs tested to date; accordingly Model 4667 was chosen as representative of an efficient planing hull used as a hydrofoil craft. The ratio of length to average beam (L_p/b) is 5. The model has a constant deadrise of 12 1/2 deg which continues from the transom to 40 percent of the length. The deadrise increases from this point to 36 deg at 90 percent length. The model was made of laminated mahogany, painted with gray enamel, and rubbed to a smooth finish. Scales were marked on keel, chine, and transom to facilitate the reading of wetted lengths.

---

[1]References are listed on page 39.

APPARATUS AND PROCEDURE

Langley Tank 1, in which the model was tested, is described in Reference 2. The towing gear used during the tests is shown in Figure 2. It consists primarily of a drag dynamometer incorporating a load cell to measure drag and a counterbalancing arrangement which includes two lift load cells to measure the tension in the tapes which support the towing gate and the model. By counterbalancing the model to zero displacement and then removing weight from the balance pan equal to the desired load, a range of model displacements may be obtained. Likewise, for a given displacement, the lift of a hydrofoil may be simulated by adding weights to the balance pan. The readings of the load cells were recorded on strip charts.

The model was fixed in trim at the towing point. The trim was set at zero when the baseline was parallel to the undisturbed water surface. The hydrodynamic trimming moments were calculated from the distribution of the load as determined from changes in tensions in the supporting tapes. The trimming moments are referred to the LCG. Positive moments tend to raise the bow.

Wetted lengths were read visually and from underwater and overwater photographs. Wetted areas were computed from these data.

The draft of the model was determined by use of a sonic surface-wave transducer. The transducer, as shown in Figure 2, was attached to the towing gate, ahead of the model. The draft was set at zero with the keel at the transom just touching the water. The output from the transducer was recorded on an oscillograph recorder.

In a general fixed-trim test, data are obtained for a number of constant loads, speeds, and trims through a range which is considered practicable. This procedure is similar to that used for tests of seaplane hulls.[3] Resistance, wetted length, draft, and trimming moment are measured. A wide range of trim angles is investigated so that, in general, the trim angle for minimum resistance and for zero trimming moment can be established. The unloading curves which set the boundaries for the range of speed and load conditions used in these tests are shown in Figure 3.

RESULTS AND DISCUSSION

Various methods were considered for the presentation of data. The primary consideration in selecting a method is that it should lend itself to computation of the hydrofoil craft takeoff resistance and should be suitable for comparing the resistance characteristics of different hull designs for various sizes of boats.

The takeoff of a hydrofoil boat is similar to that of a seaplane in that an auxiliary lifting device unloads the hull as the speed increases. Consequently coefficients were chosen which had been found satisfactory for presenting results of force tests of seaplane hulls. These coefficients are usually based upon the maximum beam; however the mean beam B_{PA}, indicated in Figure 1, is probably a more familiar dimension in working with boats and is therefore used. For simplicity, the symbol b is henceforth substituted for B_{PA}. The nondimensional coefficients are defined as follows:

C_Δ	load coefficient (Δ/wb^3)
C_R	resistance coefficient (R/wb^3)
C_V	speed coefficient $(V/\sqrt{gb})$
C_M	trimming-moment coefficient (M/wb^4)
C_{lm}	mean wetted length coefficient (l_m/b)
C_S	wetted-surface coefficient (S/b^2)
C_d	draft coefficient (d/b)

Any consistent system of units may be used.

The basic data are presented in coefficient form in Table 1. The resistance coefficients include the air drag of the model, but the air tare of the towing gear has been deducted. Crossplots at specific speed coefficients have been prepared from plots of the basic data against speed coefficient. These crossplots are presented in Figure 4 where resistance coefficient is plotted against trim with load coefficient as a parameter (solid lines). Selection of speed coefficient included in Figure 4 was such that, in the vicinity of the hump resistance, the speed coefficients

are closely spaced. Curves of constant trimming moment coefficient (dashed lines) are included so that the resistance coefficient and the trimming moment coefficient required to maintain the trim may be readily determined for any given load coefficient and trim. The resistance corresponding to zero trimming moment coefficient (free to trim) or any other assumed trimming moment coefficient may be obtained with equal facility.

The static data are presented in Figure 5; trimming moment coefficient and draft coefficient are plotted against trim with load coefficient as the parameter. The trimming moment coefficients may be used to compute the trim at rest for other positions of the center of gravity than that used in these tests.

The wetted area coefficients C_S plotted against trim with load coefficient as the parameter are presented in Figure 6. The mean wetted length coefficients C_{lm} versus trim with load coefficient as the parameter are presented in Figure 7. The curves for C_{lm} are used for the calculation of Reynolds number. C_{lm} and C_S are used to make friction corrections that are required in calculation of the total resistance of the full size craft.

USE OF DATA

To illustrate the use of the hull data for determining the resistance in preliminary design studies, a sample calculation will be made for a hypothetical hydrofoil boat having a gross load Δ_o of 100,000 lb and a cruising speed of 50 knots when foilborne. The hydrofoil characteristics will be assumed, and results of tests of Model 4667 will be used to determine the contribution of the hull to the total resistance.

HULL DIMENSIONS

In order to determine the factor for scaling the model to the full-size craft, it will be assumed that Δ_o of 100,000 corresponds to a gross load coefficient C_Δ of 0.6, which is the design gross load coefficient for the hull without hydrofoils. The model gross load then becomes

$$wb^3 \times C_\Delta = 63.2(1.6)^3 \times 0.6 = 155.3 \text{ lb}$$

The linear ratio is given by

$$\lambda = \left(\frac{\text{ship } \Delta_o}{\text{model } \Delta_o} \times \frac{\text{density of water in which model was tested}}{\text{density of sea water}} \right)^{1/3}$$

$$= \left(\frac{100{,}000}{155.3} \times \frac{1.964}{1.9905} \right)^{1/3}$$

$$\lambda = 8.597$$

The full-size dimensions of the hull are

length - $\lambda\ L_p$ (model) = $8.597 \times 8.00 = 68.78$ ft

mean beam - $\lambda\ B_{PA}$ (model) = $8.597 \times 1.600 = 13.76$ ft

LCG - λ LCG (model) = $8.597 \times 3.47 = 29.83$ ft distance forward of Station 10 where L_p, B_p, and LCG are obtained from Figure 1.

The following numerical relationships can be established, knowing the mean beam of the hull

$$C_\Delta = \frac{\Delta}{64.04 \times (13.76)^3} = \frac{\Delta}{166{,}800}$$

$$C_R = \frac{R}{166{,}800}$$

$$C_V = \frac{V}{\sqrt{32.174 \times 13.76}} = \frac{V}{21.04}$$

$$C_M = \frac{M}{64.04 \times (13.76)^4} = \frac{M}{2{,}296{,}000}$$

HYDROFOIL CONFIGURATION

The foil configuration (Figure 8) is a Canard system, consisting of a submerged small control foil ahead of the LCG and a submerged large main foil just aft of the LCG. At cruising speed, the forward foil carries 25 percent of the gross load (25,000 lb) and the main foil carries 75 percent (75,000 lb). The spacing between the foils is 38 ft.

The selection of a Canard system is not an arbitrary choice but one that, at the outset, appears to be adaptable to a stepless planing hull. At high speed coefficients, an acceptable hull lift-drag ratio is obtained only with large negative (bow down) hull trimming moments. To overcome this negative moment, the Canard system produces an opposite moment by virtue of a positive lift force on the control surface. If a more conventional hydrofoil system with the control foil behind the CG were used, the moment opposing the negative hull moment would be produced by a negative lift by the control foil.

For simplicity, the main and the bow foils are considered to have the same geometry. No mention is made of form characteristics such as aspect ratio, span of the foil, spray interference effect, etc., as they are not considered essential to the scope of this report. The foil as designed is considered satisfactory for the problem at hand, i.e., to illustrate the takeoff computations. The assumed curves for the lift and drag coefficients are presented in Figure 9 and apply to both foils. These curves are for complete foil assemblies, including strut, pod, and foil. To further simplify the illustration, the lift and drag coefficients are considered to be independent of speed.

If the foil loading is taken at 1100 lb/ft^2, the areas of the bow and the main foils become 22.7 and 68.2 ft^2, respectively. At a cruise speed of 50 knots, the lift coefficient is determined from

$$C_L = L/1/2\rho\ SV^2$$

and

$$C_L = 0.1550$$

for both foils. From Figure 9, the corresponding angle of attack α_o while in the cruising condition is 1.7 deg and the lift-drag ratio L/D of the foil system is 8.1.

Assuming the boat trim to be zero and the thrust axis coincident with the drag vector, the relative locations of the foils and the LCG must be such that the sum of the pitching moments due to the lift of the foils is zero. Since the distance between foils is 38 ft, the distance of the main foil behind the LCG is found to be 9.5 ft and the forward foil is 28.5 ft forward of the LCG.

COMPUTATION OF TAKEOFF RESISTANCE

At any given speed, the following conditions must be satisfied:

a. The sum of the lift forces must equal the gross load

$$\Delta + L_f + L_a = \Delta_o \qquad [1]$$

b. The sum of the moments must equal zero

$$\Sigma M_{CG} = TZ_T + M + L_f X_f - L_a X_a - D_f Z_f - D_a Z_a = 0 \qquad [2]$$

Equation [2] is the static moment equation for the Canard configuration shown in Figure 8. The moments are taken about the LCG and the assumption is made that the trim angles will be small and that the thrust vector is parallel to the X-axis.

In order to determine the resistance coefficient C_R, the load coefficient C_Δ must be known for each speed. The load Δ and, consequently, C_Δ depend upon the bow and main foil lift, which, in turn, depends upon the angle of attack of the foils, hence on the trim τ of the hull. Because the angle of incidence of the bow foil will vary throughout the speed range, the following method has been devised to make possible a good first approximation for the bow foil angle of attack. Using the numerical relationships previously established, at a $C_V = 2.0$

$$V = 2.0 \times 21.04 = 42.08 \text{ fps}$$

Entering the curves of Figure 4g, it can be seen that the trim for the hull at this speed must be a compromise between drag and moment. The minimum values of C_R occur between approximately 2.3 and 4.4 deg, whereas C_M equal to zero corresponds to a trim variation from 1.4 to 3.4 deg for the values of C_Δ expected at this C_V. Choosing the hull trim τ equal to 2.5 deg, the angle of attack of the rear foil is

$$\tau + \alpha_o = \alpha_a$$

$$2.5 + 1.7 = 4.2 \text{ deg}$$

The dynamic pressure

$$q = 1/2\ \rho\ V^2 = 1/2(1.9905)\ (42.08)^2 = 1762$$

The lift coefficient and the lift drag ratio of the rear foil from Figure 9 are

$$C_{La} = 0.26$$

$$(L/D)_a = 9.2$$

and the lift and drag are

$$L_a = q\, S_a\, C_{La} = 1762 \times 68.2 \times 0.26 = 31{,}240 \text{ lb}$$

$$D_a = \frac{31{,}240}{9.2} = 3396 \text{ lb}$$

Assuming that $Z_a = Z_f = Z_T = 8$ ft and putting this value and the thrust T = 16,000 lb obtained from the assumed thrust curve (Figure 10) into the moment Equation [2]

$$M_{CG} = 16{,}000 \times 8 + 2{,}296{,}000\, C_M + 28.5\, L_f - 31{,}240 \times 9.5$$

$$- 8\, D_f - 3396 \times 8 = 0$$

which reduces to

$$28.5\, L_f - 8\, D_f = 195{,}948 - 2{,}296{,}000\, C_M$$

The moment due to the drag of the front foil is evidently small compared to that due to its lift. Therefore the assumption of a value of 10 for its lift-drag ratio is reasonable. This substitution will further simplify the moment equation by eliminating D_f. With some rearranging, the equation becomes

$$L_f = 7{,}074 - 82{,}888\, C_M$$

The total load is sustained by the sum of the hull lift and foil lift; therefore, referring to Equation [1]

$$100{,}000 = L_f + 31{,}240 + 166{,}800\, C_\Delta$$

Eliminating L_f from this and the preceding equation

$$C_M = 2.012\, C_\Delta - 0.7442$$

A few trial values of C_Δ with some interpolation in Figure 4g are required to determine that

$$C_\Delta = 0.345$$

and

$$C_M = -0.050$$

and

$$C_R = 0.042$$

and the hull resistance

$$R = 0.042 \times 166,800 = 7,006 \text{ lb}$$

The lift required of the front foil is

$$L_f = 100,000 - 31,240 - 166,800 \times 0.345 = 11,214 \text{ lb}$$

The lift coefficient of the front foil is

$$C_{Lf} = \frac{11,214}{1762 \times 22.7} = 0.2804$$

which, by referring to Figure 9, can be obtained with $\alpha_f = 4.7$ deg. The control angle

$$\beta = \alpha_f - \tau - \alpha_o =$$

$$4.7 - 2.5 - 1.7 =$$

$$\beta = 0.5 \text{ deg}$$

From Figure 9

$$(L/D) = 9.2$$

$$D_f = \frac{11,214}{9.2} = 1,219 \text{ lb}$$

The error introduced into the moment equation by the assumption of an L/D of 10 (whereas the actual L/D is 9.2) is 784 ft lb. This error is small. The practicable accuracy is mainly dependent upon the precision of taking values from the plots. It should be possible to interpolate C_M to $\pm$ .005.

The resulting variation in moment would therefore be

$$(2{,}296{,}000)\ .005 = 11{,}480 \text{ ft lb}$$

This moment corresponds to a shift in the LCG for the full-size craft of approximately 0.11 ft, or a change in the angle of attack of the control foil of approximately 0.2 deg.

A complete takeoff computation sheet is shown as Table 2. The columns are headed with the values of C_V covering the speed range to foil-borne operation. Results of the takeoff computation are presented in Figure 10. The curves show the variation of thrust, hull resistance, hull trim, and change of foil incidence with speed coefficient.

FRICTION CORRECTION

An accurate preliminary analysis of the data for the 100,000-lb craft requires that the drag data should be corrected for the difference between the frictional resistance coeffficients of the model and the full-scale craft. The following equations are used to determine this friction correction:

$$Re = \frac{C_V \sqrt{gb}\ C_{lm}\ b}{\upsilon} \qquad [3]$$

$$C_{R\ corr} = C_R + 1/2(C_V)^2\ C_S\ \left[-C_{f\ (model)} + C_{f\ (full\ size)}\right] \qquad [4]$$

Equation [3] has been derived from the standard form of Reynolds number so that the coefficients from Figure 7 for the desired speed coefficient and trim may be substituted directly. Equation [4] has been derived so that C_R and C_S from Figures 4 and 6, respectively, can be substituted with the friction coefficients corresponding to the model and full-size Reynolds numbers obtained from Equation [3] to obtain the corrected resistance coefficient.

The correction for hull friction drag is computed in the following manner. Referring to Figure 7b, for a C_V of 2, enter the curves at τ of 2.5 deg. At a C_Δ of 0.345, C_{lm} is found to be 3.47. Substituting this value and the model mean beam into Equation [3], for the model:

$$Re = \frac{2.0 \times 1.600 \times 3.47 \sqrt{32.174 \times 1.600}}{1.028 \times 10^{-5}}$$

$$Re = 7.750 \times 10^{6}$$

$$C_f = 3.059 \times 10^{-3}$$

for the full-size craft and salt water at 59F:

$$Re = \frac{2.0 \times 13.76 \times 3.47 \sqrt{32.174 \times 13.76}}{1.282 \times 10^{-5}}$$

$$Re = 1.567 \times 10^{8}$$

$$C_f = 1.947 \times 10^{-3}$$

Using Equation [4] and C_S from Figure 6

$$C_{R\ corr} = 0.042 + 1/2(2.0)^2 \times 3.90 \left[(-3.059 + 1.947)\ 10^{-3}\right]$$

$$C_{R\ corr} = 0.0333$$

$$R_{corr} = 166,800 \times 0.0333 = 5,554\ lb$$

It can be seen from this result that at a $C_V = 2.0$, the correction for friction drag is 21 percent of the total hull drag and should definitely be taken into consideration when making a detailed design analysis of the hull.

Total correct drag = 5,554 + 1,219 + 3,396 = 10,169

CONCLUDING REMARKS

This report is the first of a series under the Bureau of Ships Accelerated Hydrofoil Program which deals with methods of testing and presentation of data specifically for the application of the hull to a

hydrofoil configuration. Hulls of different design have been and will be tested and the data presented in a similar manner.

After the completion of this phase of the program, a correlation of the data and characteristics of the various hull designs can be made. An outcome of the correlation should be design criteria utilizing the best characteristics of those tested.

The results of the test program for Model 4667 indicate that because of the high negative trimming moments (bow down), a Canard foil system with controlled incidence on the forward foil is a practical configuration. If a conventional or tandem foil system is used, a controlled negative angle of incidence with negative lift would have to be used for the aft foil to oppose the high lift on the aft portion of the hull planing surface.

In order to avoid the high negative trimming moments found in the tests of Model 4667, it would seem that a good hydrofoil hull might possibly have a step or the hull should have narrow sections aft with the CG located forward. A combination of these might be preferable.

It is noted here, however, that the tests made and those to be made are indicative only of trends in the design of hydrofoil hulls and should not be considered applicable for specific design purposes. For a specific design, it would be necessary to test the model in combination with a foil system.

David Taylor Model Basin Small Craft Data Sheet

Hard chine boat, $L_p/B_{px} = 4.09$

TMB Model No. 4667

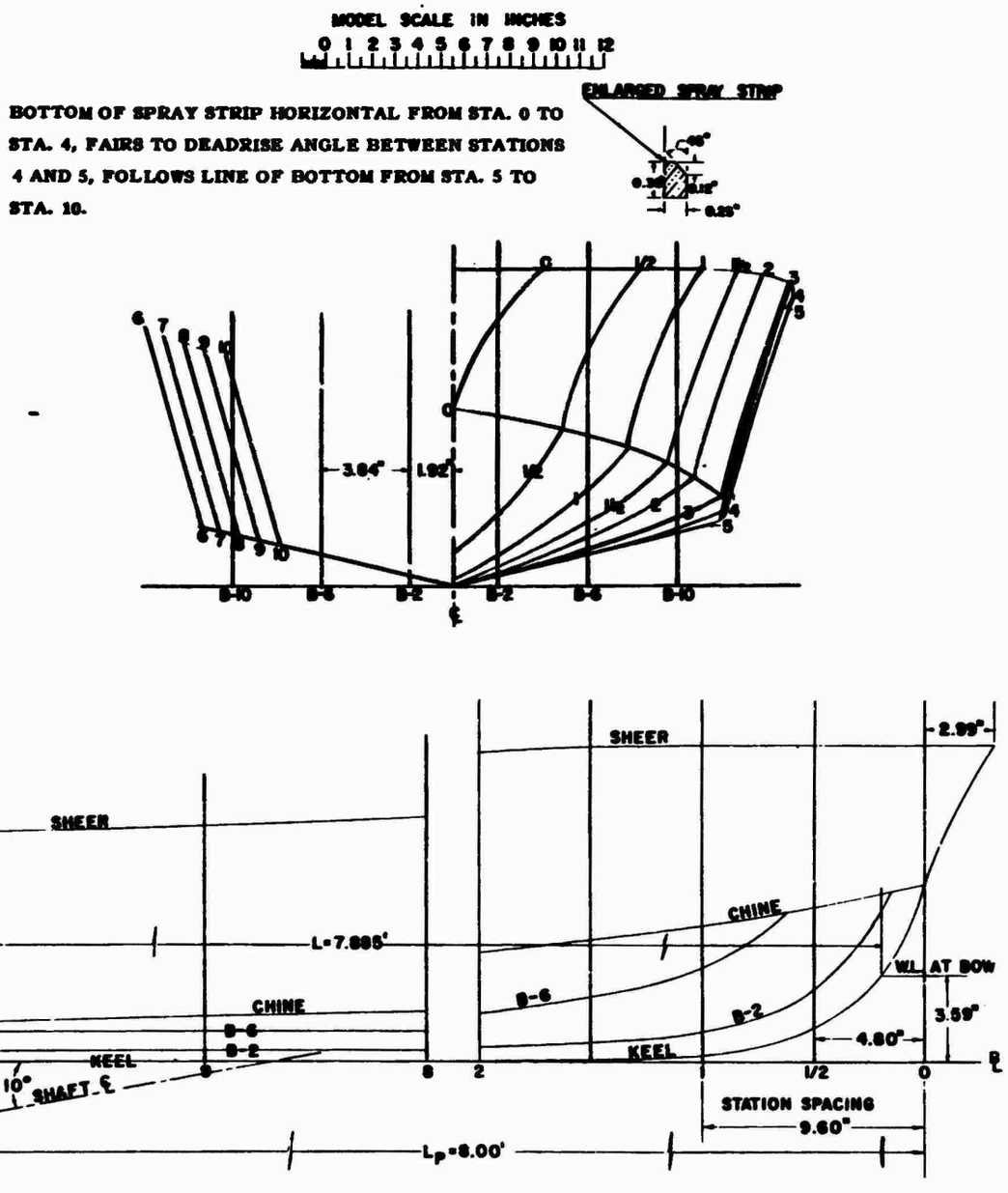

Figure 1 - Design Data Sheet

MODEL PARTICULARS, TEST CONDITIONS, AND RESULTS

Boat Research Model for Hydrofoil Hull Series
Model Number 4667
Appendages Spray Strips
Laboratory DATMOBAS
Basin Langley Tank 1

Basin Size 2920' X 24' X 12'
Model Length 8.00 ft
Water Temperature 72°F
Specific Weight 63.2 lb/ft^3
Model Material Wood
Model Finish Paint
Turbulence Stimul. None

Planing Bottom Dimensions and Coefficients		LWL Dimensions and Coefficients	
L_p	8.00 ft	L	
B_{PX}	1.955 ft	B_X	
B_{PA}	1.600 ft	H	
A_p	12.80 ft^2	L/B_X	
$A_p/\nabla^{2/3}$	7.00	$L/\nabla^{1/3}$	
$L_p/\nabla^{1/3}$	5.917	C_B	
L_p/B_{PA}	5.000	C_p	
		C_W	

LCG location 3.42 ft forward of station 10
(LCG location 6 percent L_p aft of centroid of A_p)

FORM CHARACTERISTICS

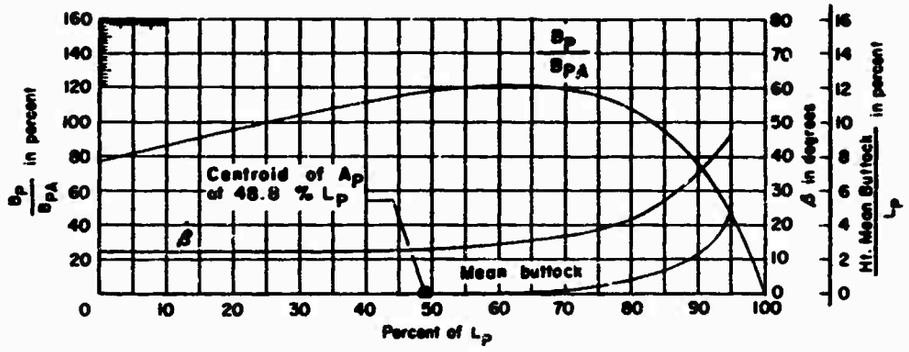

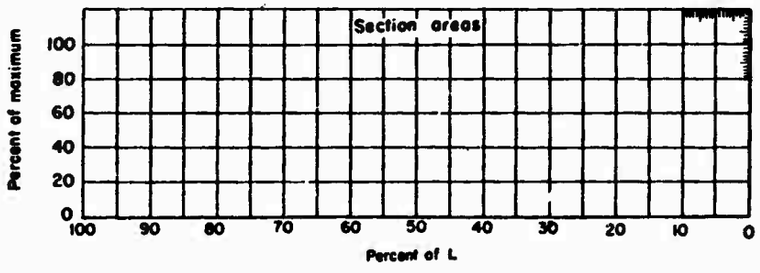

Figure 1 - Continued

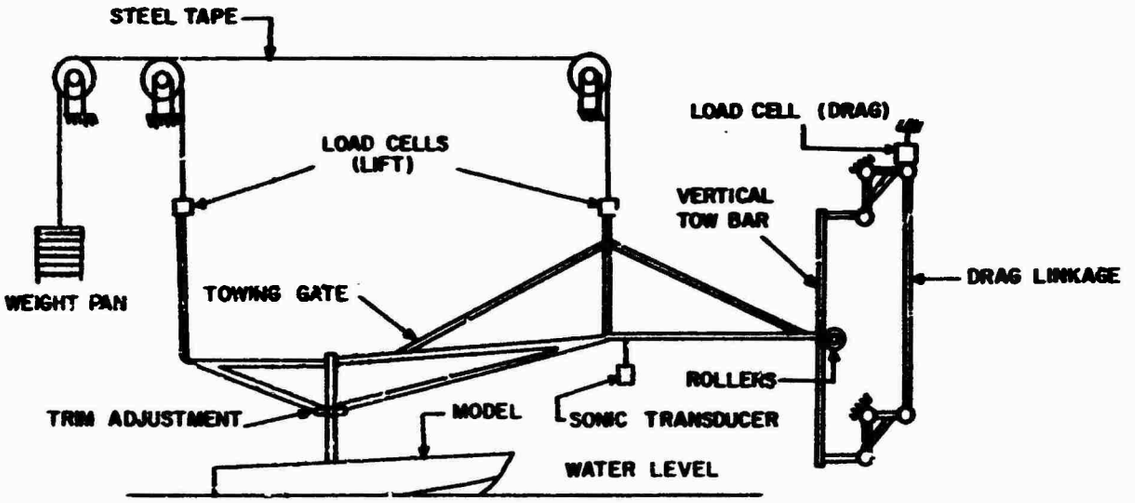

Figure 2 - Small Boat Towing Gear

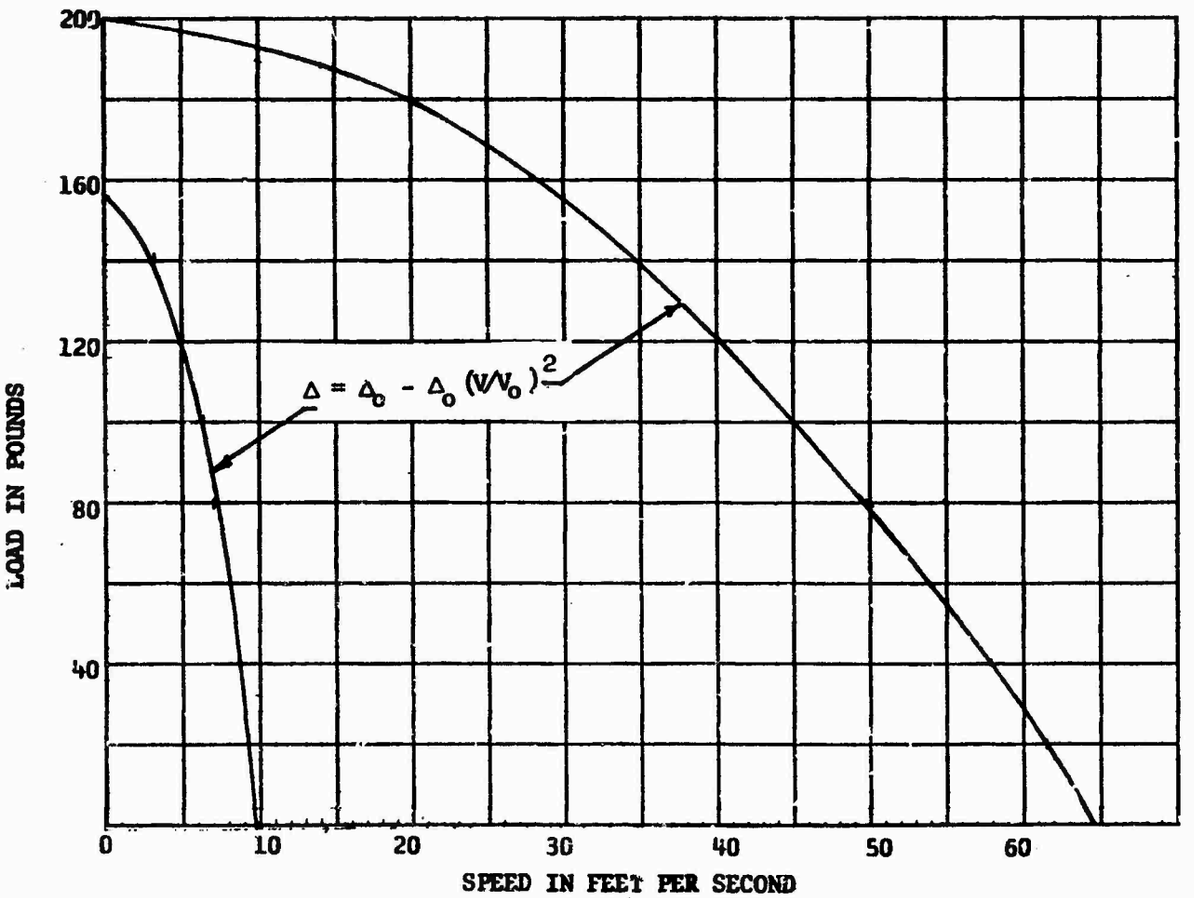

Figure 3 - Unloading Boundaries

Figure 4 - Variation of Resistance and Pitching Moment Coefficients with Trim and Load Coefficients

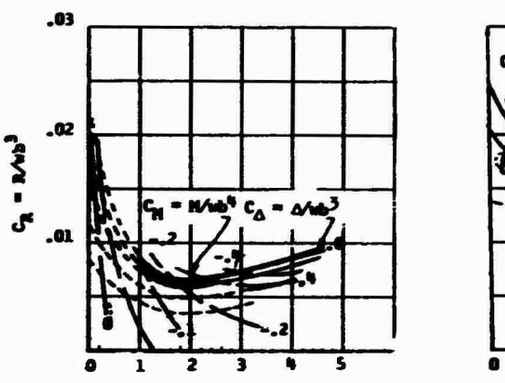

Figure 4a - $C_V = 0.5$

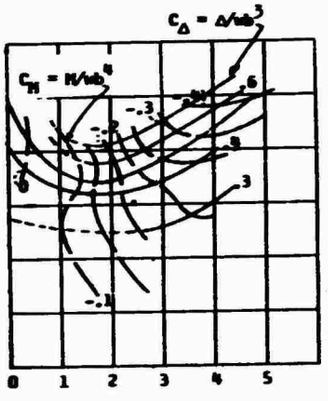

Figure 4b - $C_V = 0.75$

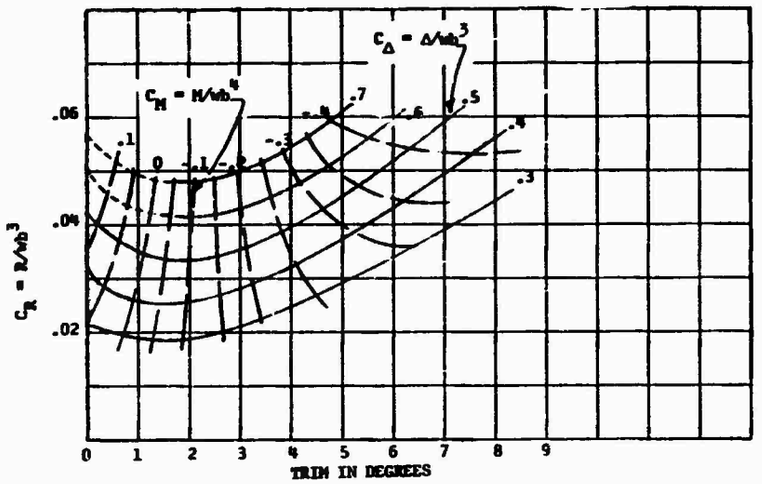

Figure 4c - $C_V = 1.0$

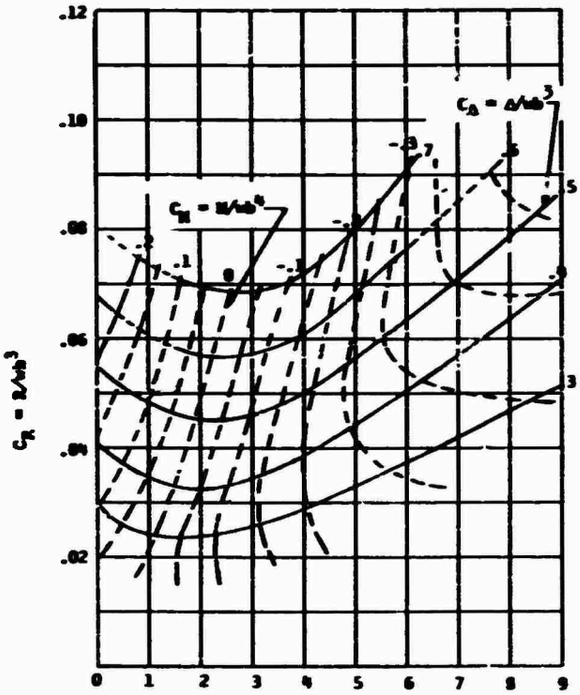

Figure 4d - C_V = 1.25

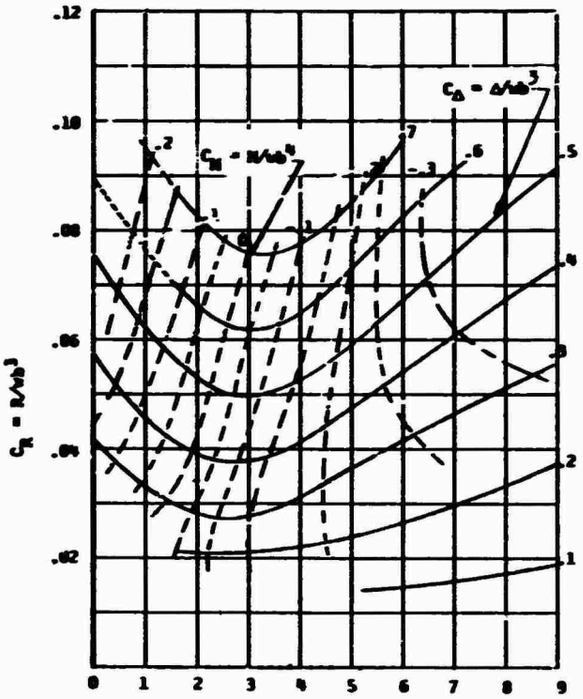

Figure 4e - C_V = 1.5

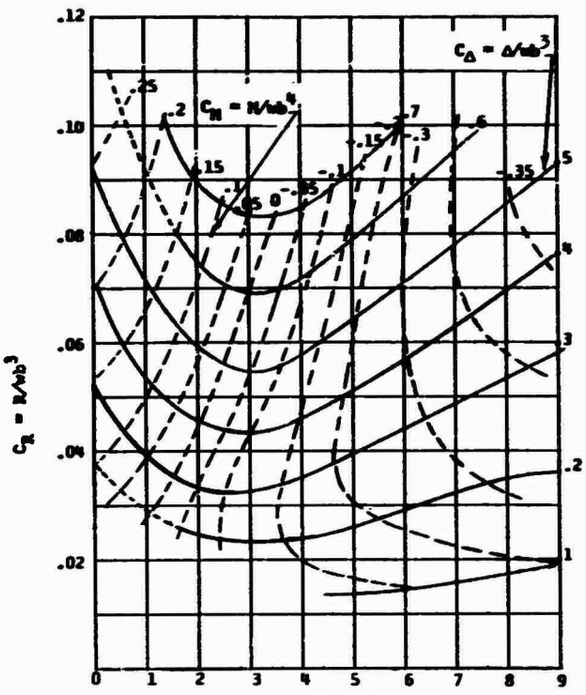

Figure 4f - C_V = 1.75

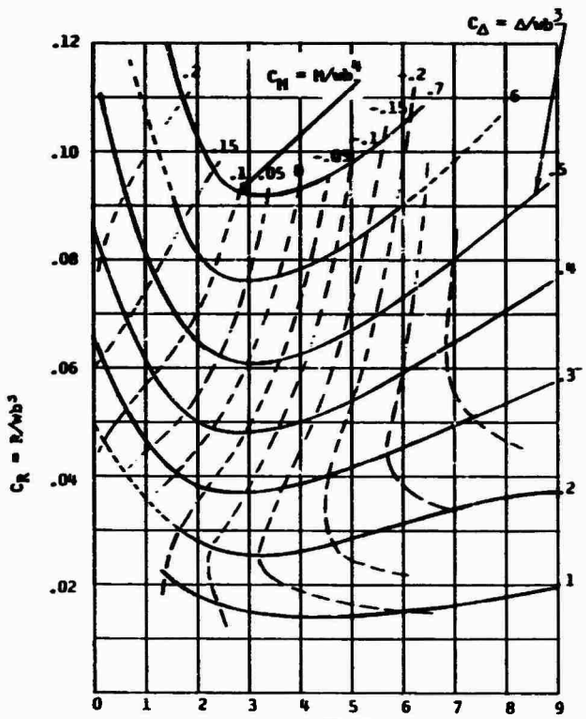

Figure 4g - C_V = 2.0

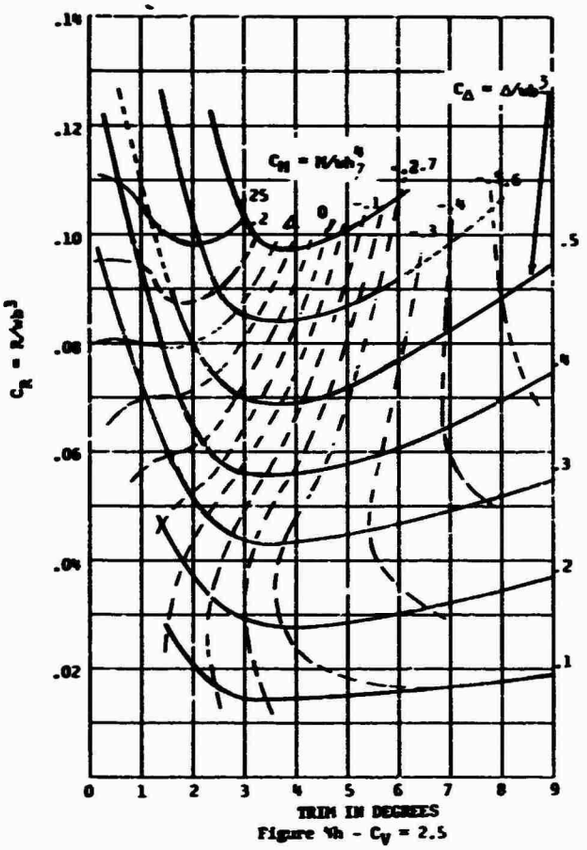

Figure 4h - $C_V = 2.5$

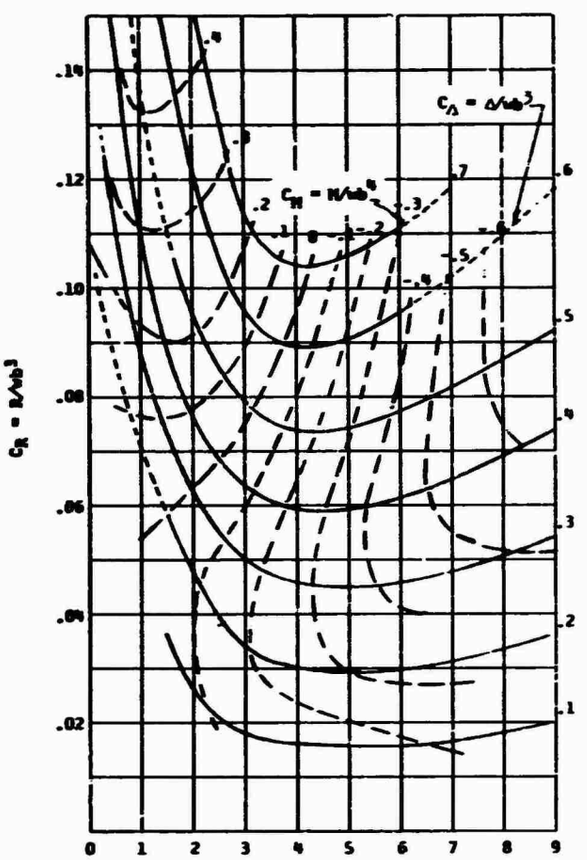

Figure 4i - $C_V = 3.0$

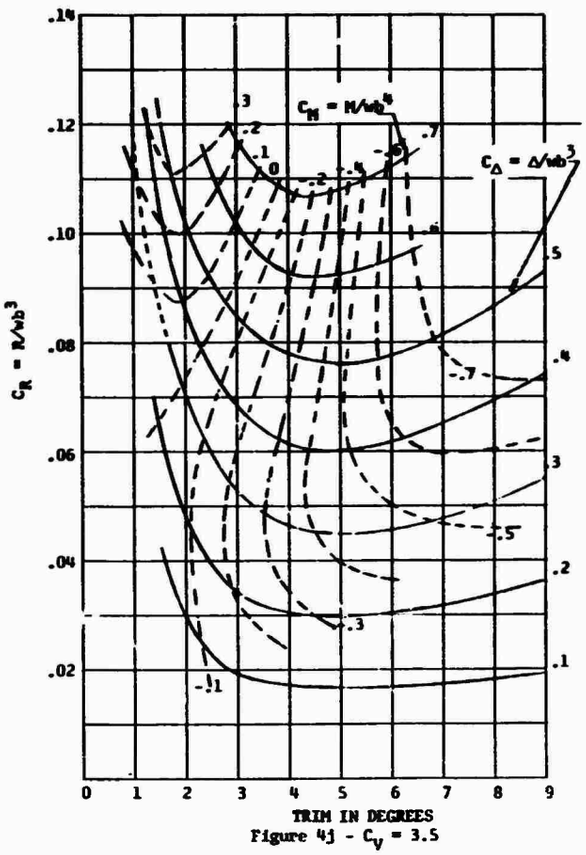

Figure 4j - $C_V = 3.5$

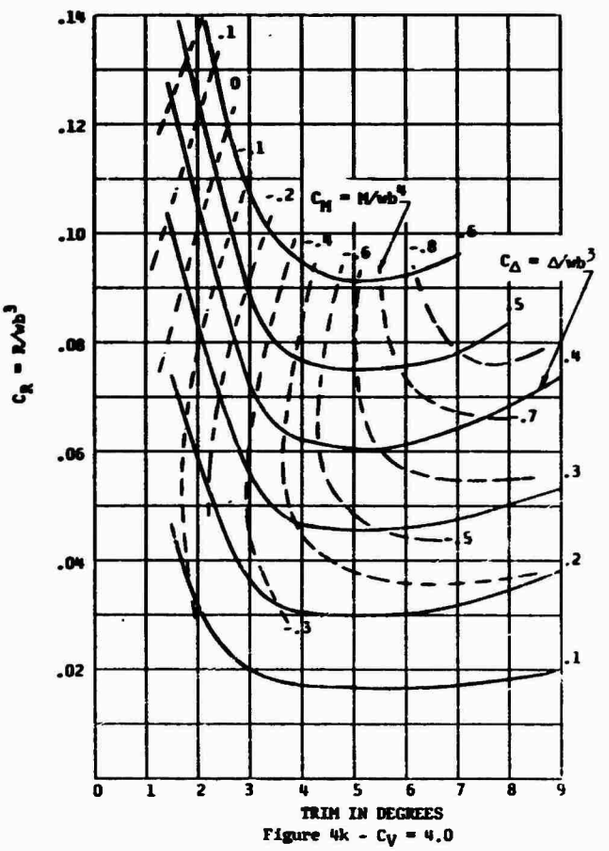

Figure 4k - $C_V = 4.0$

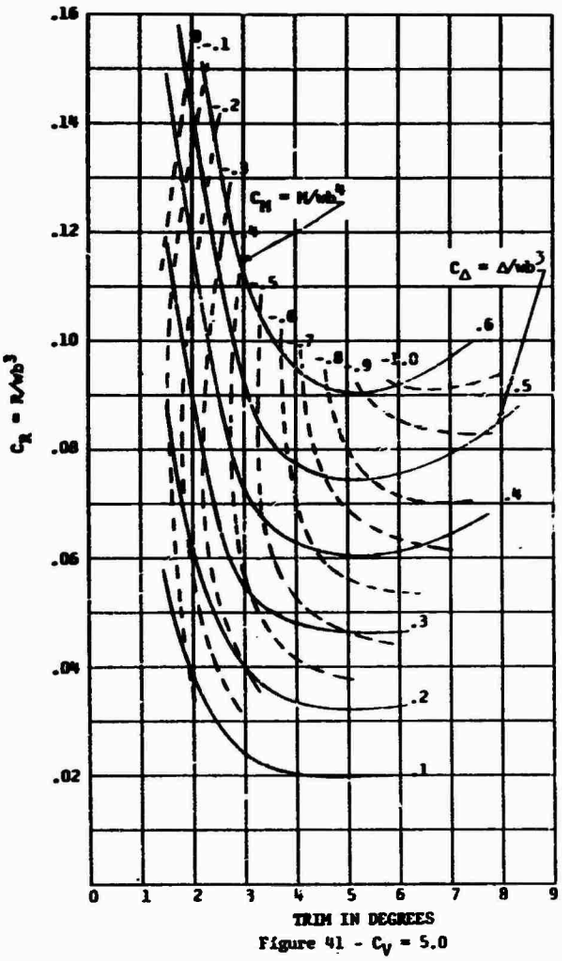

Figure 41 - C_V = 5.0

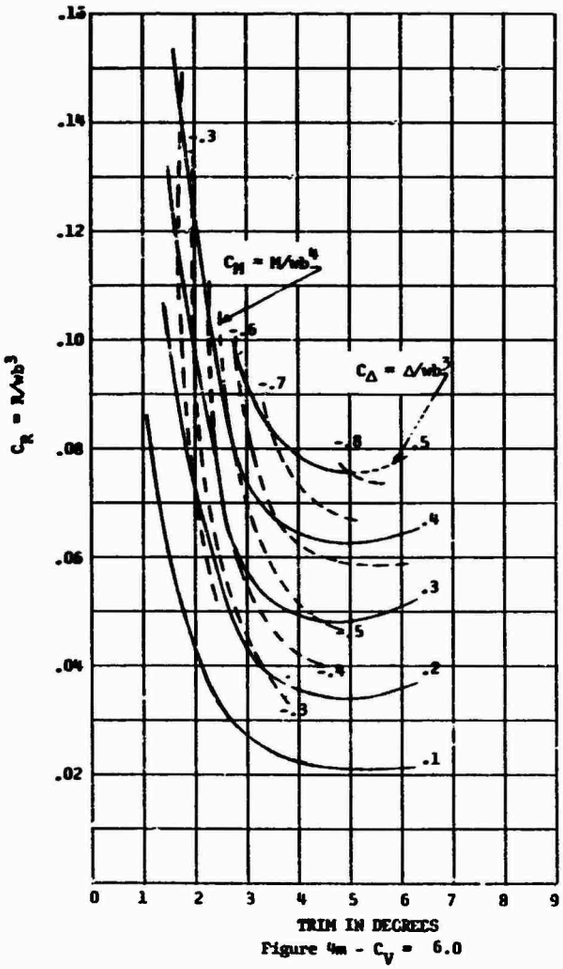

Figure 4m - C_V = 6.0

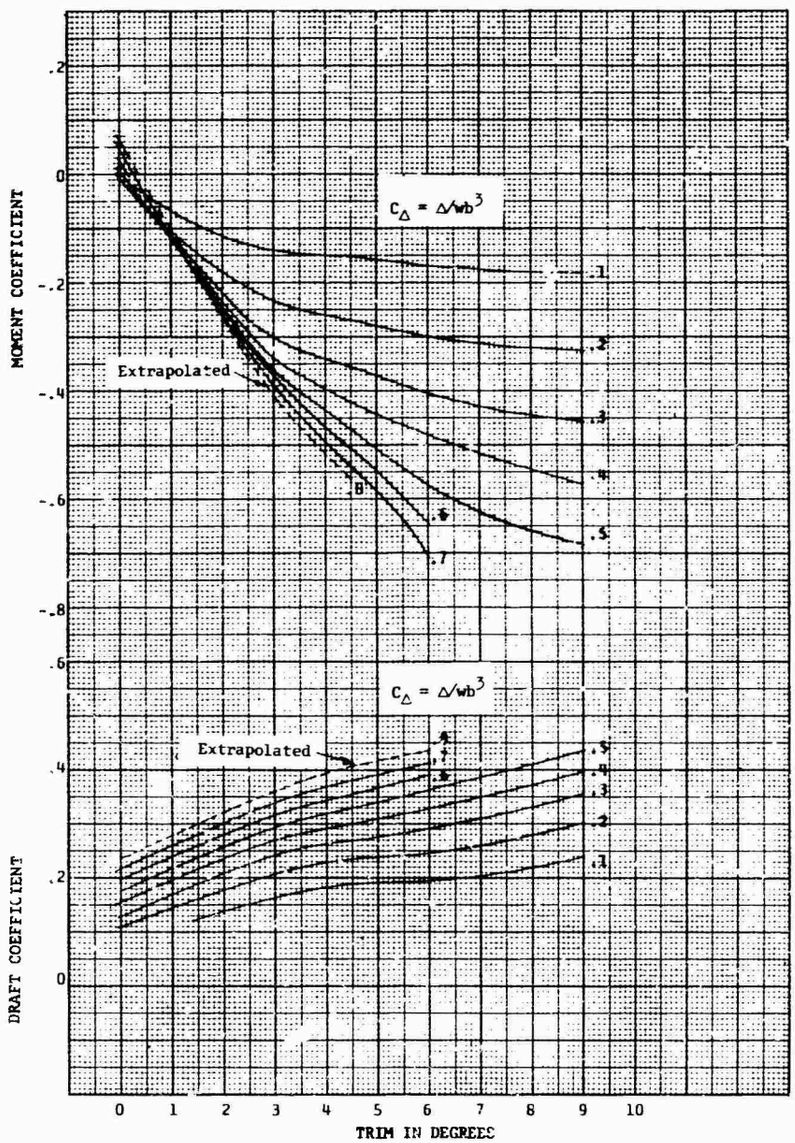

Figure 5 - Model 4667 Static Properties

Figure 6 - Variation of Wetted Surface Coefficient with Trim and Load Coefficient

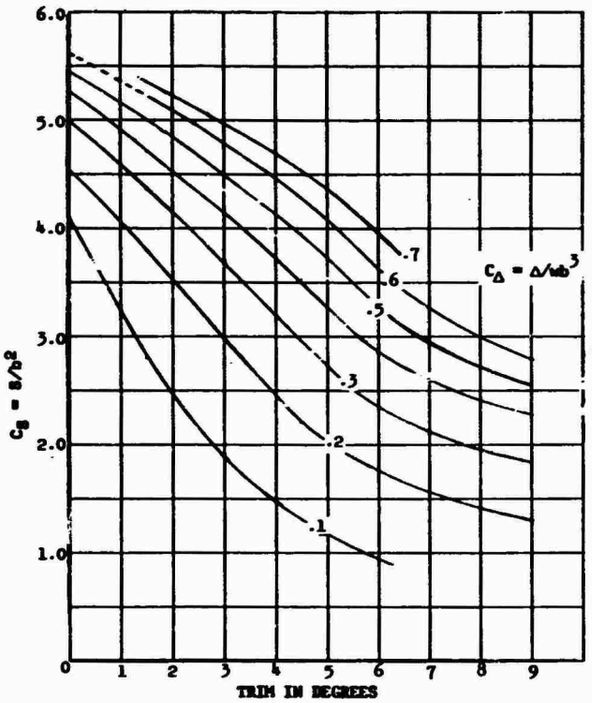

Figure 6a - $C_V = 1.5$

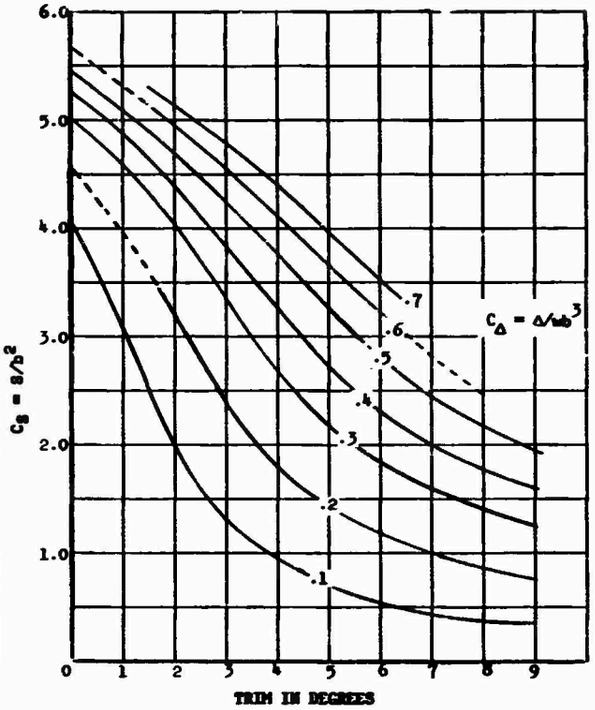

Figure 6b - $C_V = 2.0$

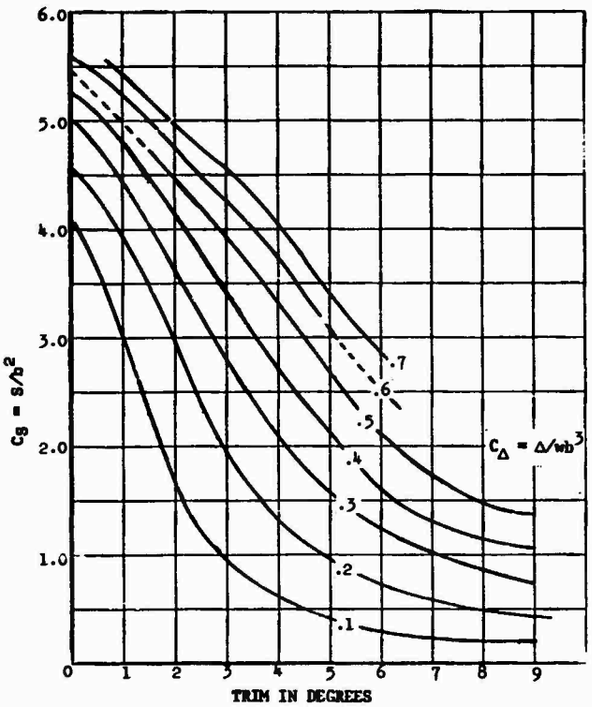

Figure 6c - $C_V = 2.5$

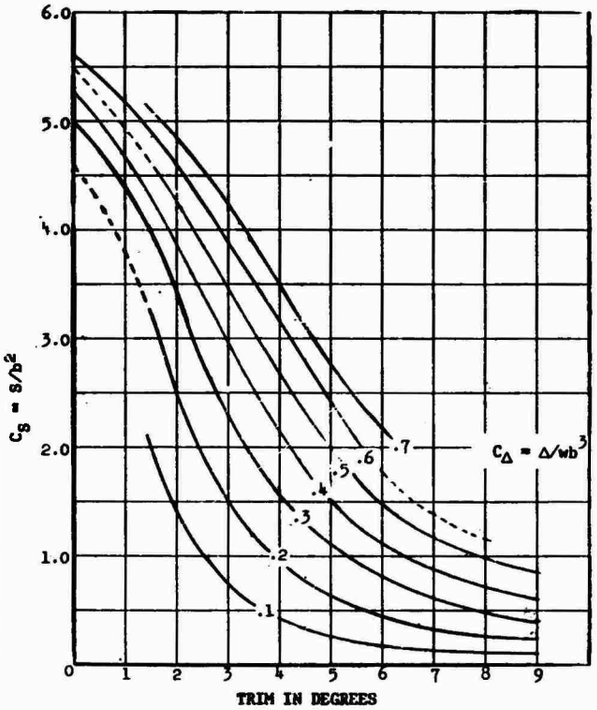

Figure 6d - $C_V = 3.0$

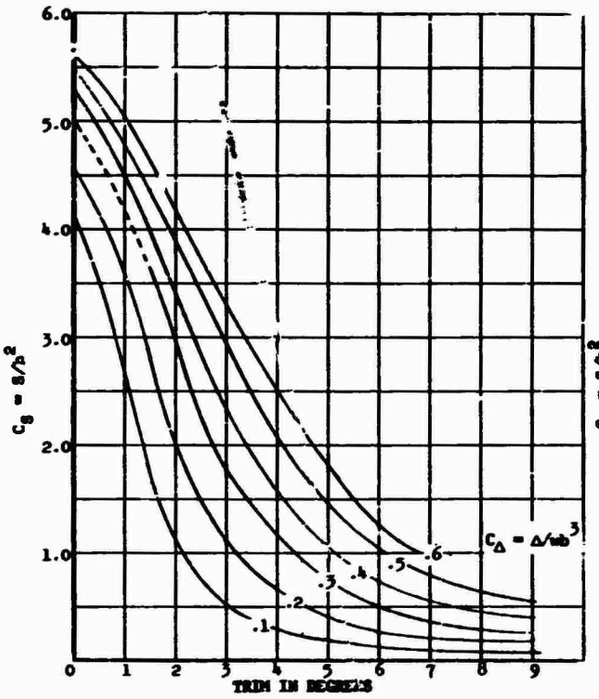

Figure 6e - C_V - 3.5

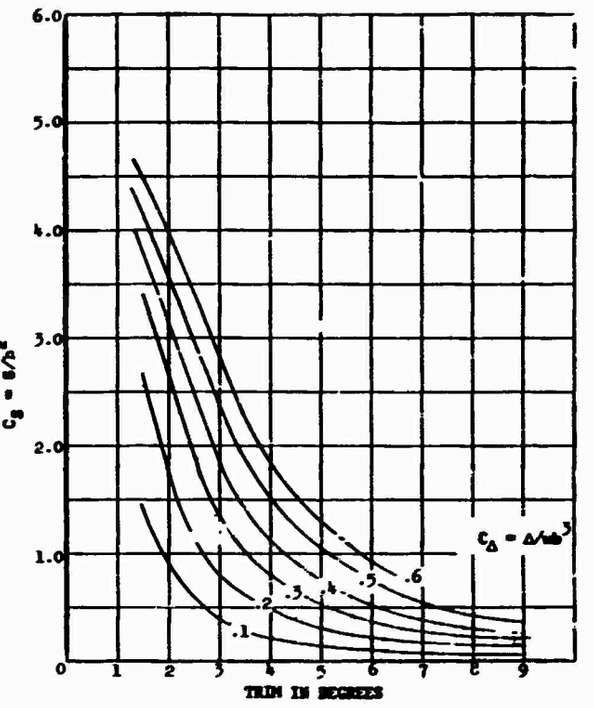

Figure 6f - C_V = 4.0

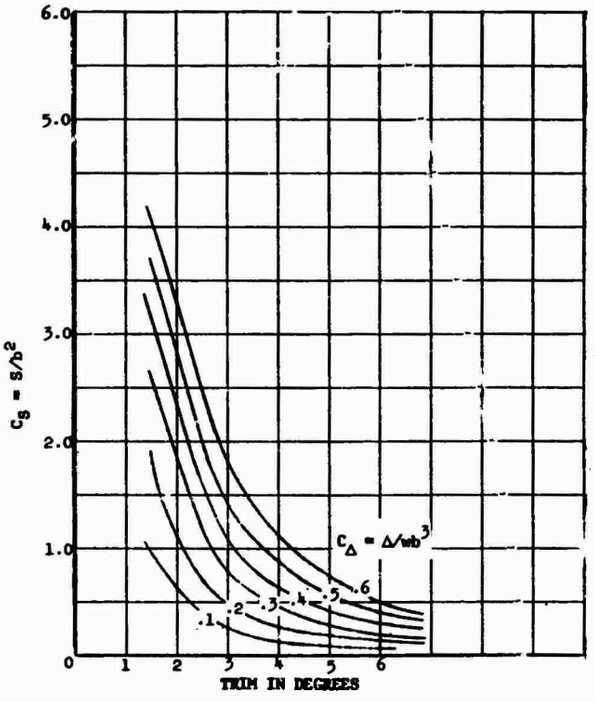

Figure 6g - C_V - 5.0

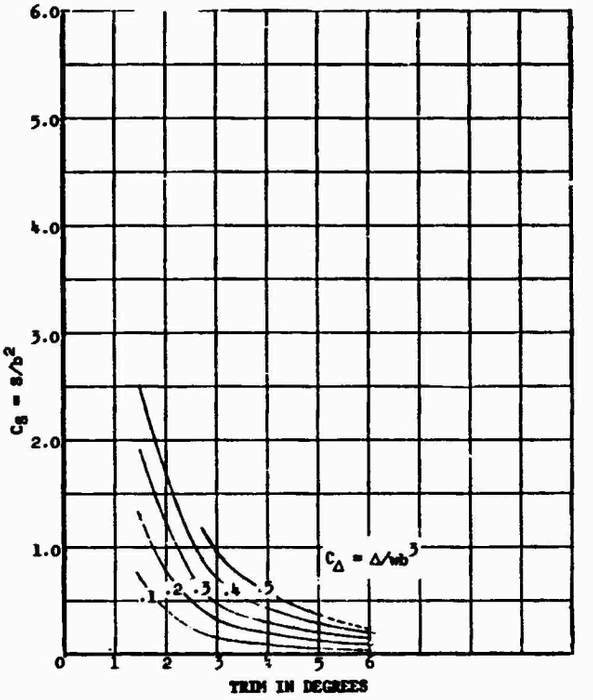

Figure 6h - C_V = 6.0

Figure 7 - Variation of Mean Wetted Length Coefficient with Trim and Load Coefficients

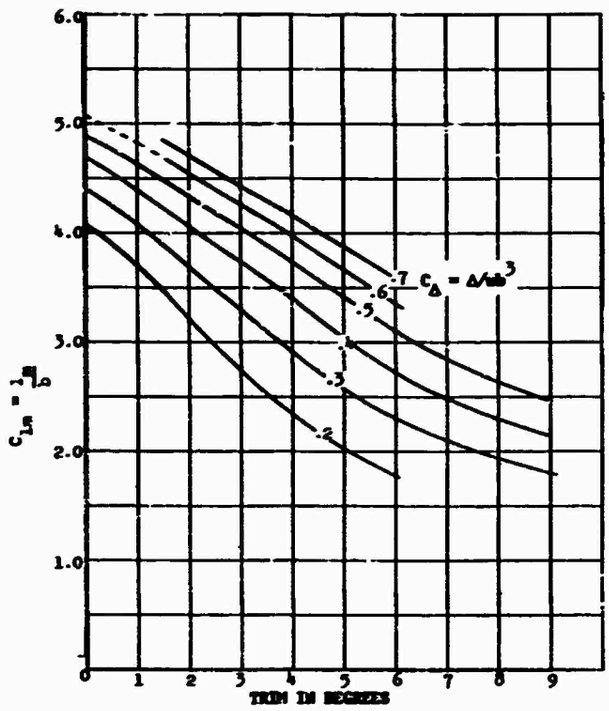

Figure 7a - $C_V = 1.5$

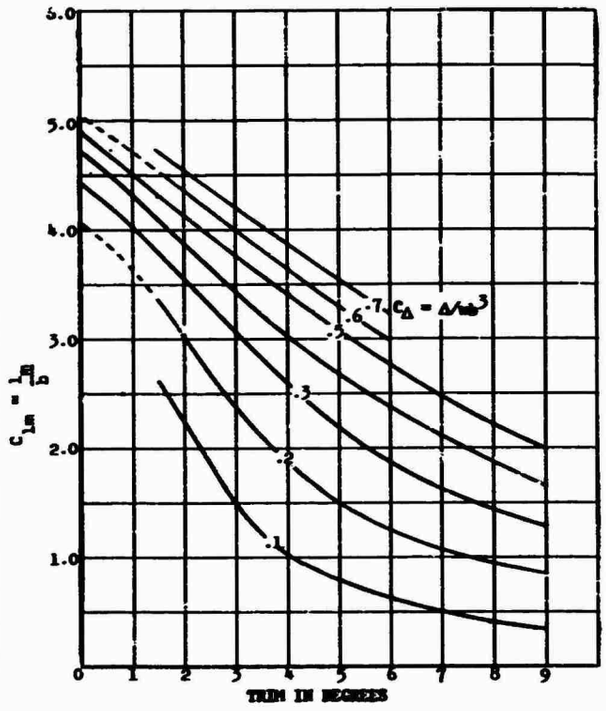

Figure 7b - $C_V = 2.0$

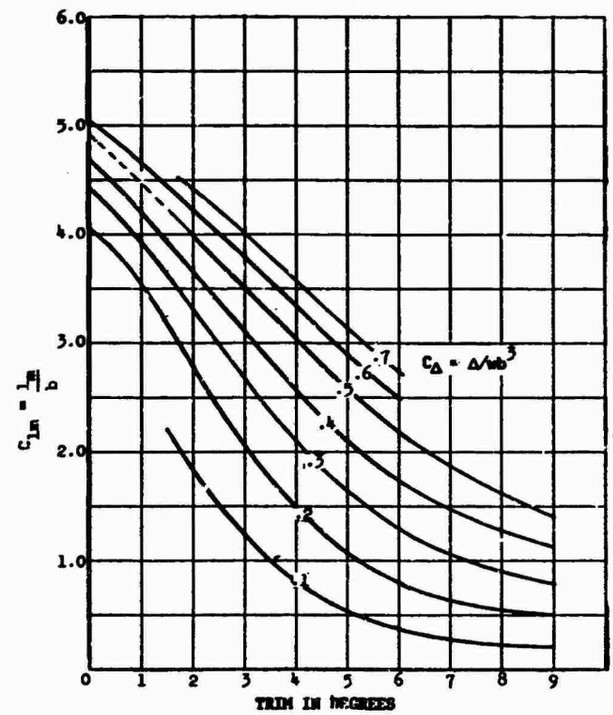

Figure 7c - $C_V = 2.5$

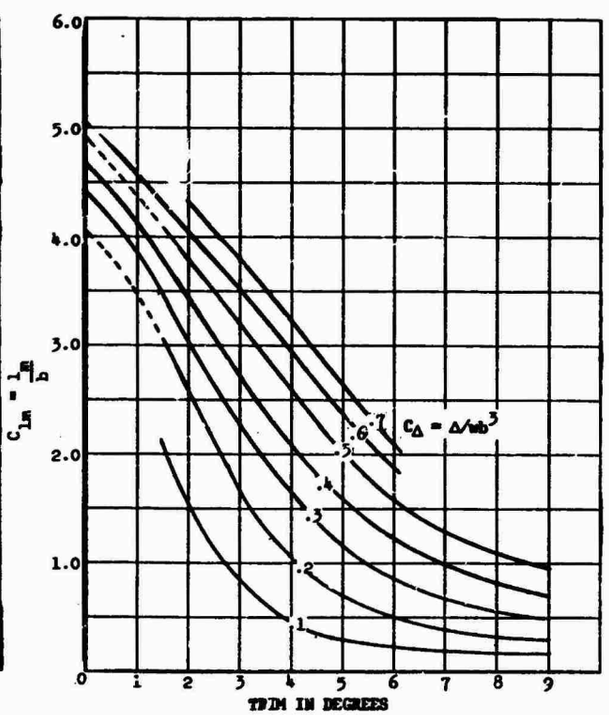

Figure 7d - $C_V = 3.0$

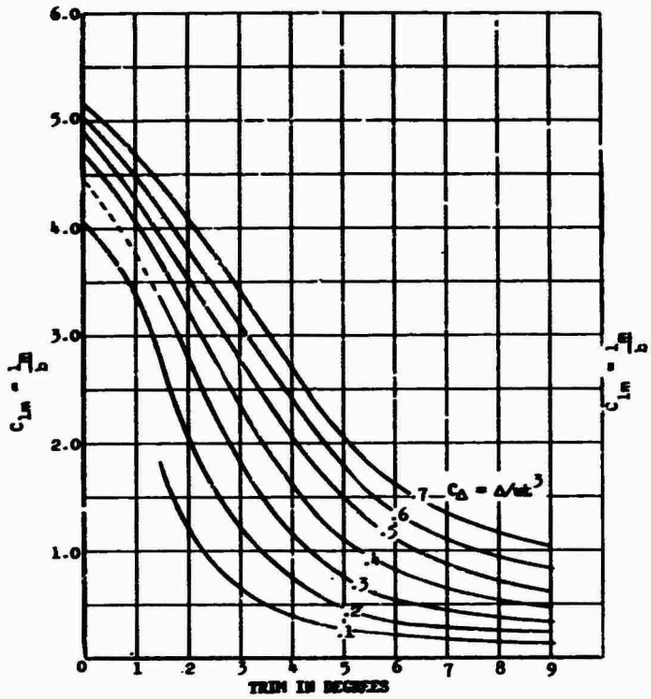

Figure 7e - $C_V = 3.5$

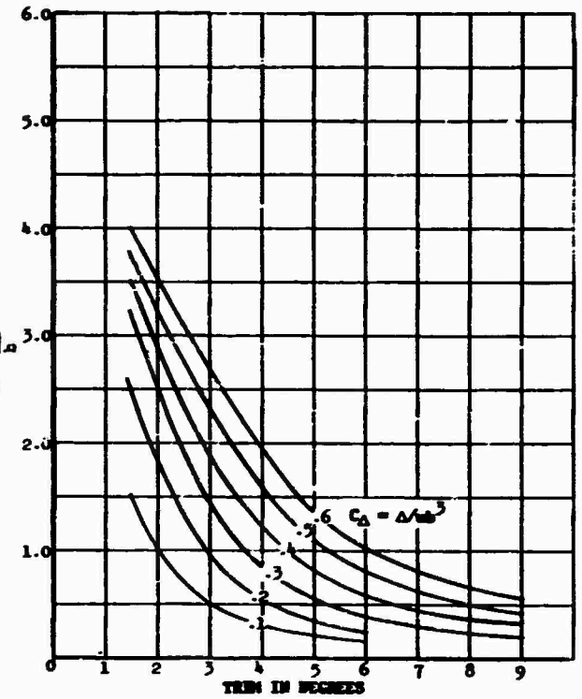

Figure 7f - $C_V = 4.0$

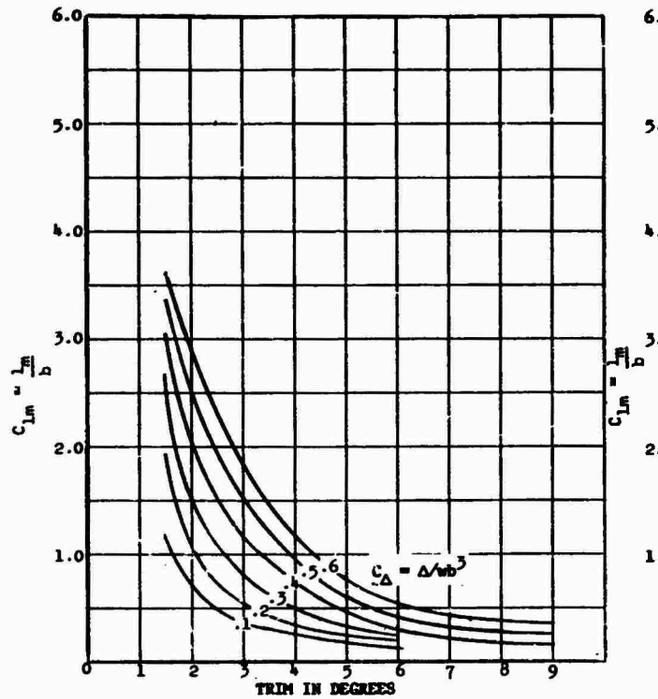

Figure 7g - $C_V = 5.0$

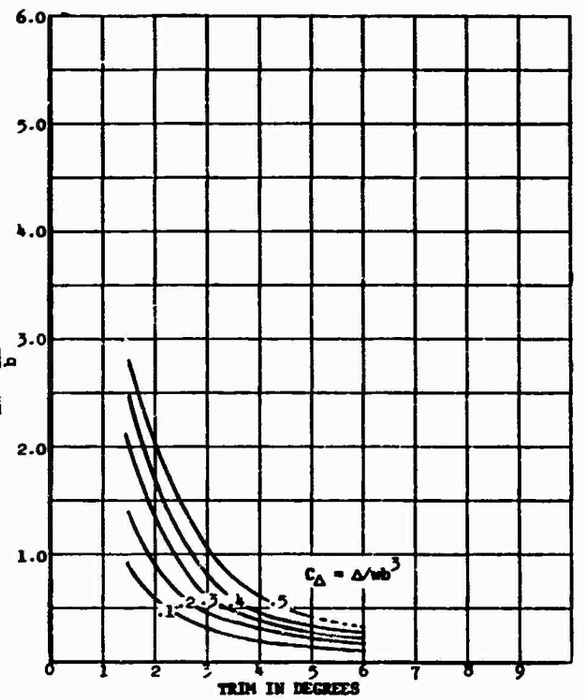

Figure 7h - $C_V = 6.0$

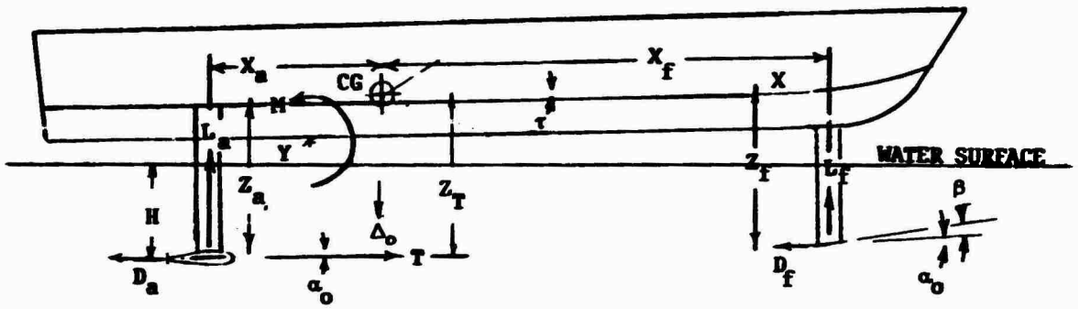

Figure 8 - Geometry and Forces of a Canard Configuration during Takeoff

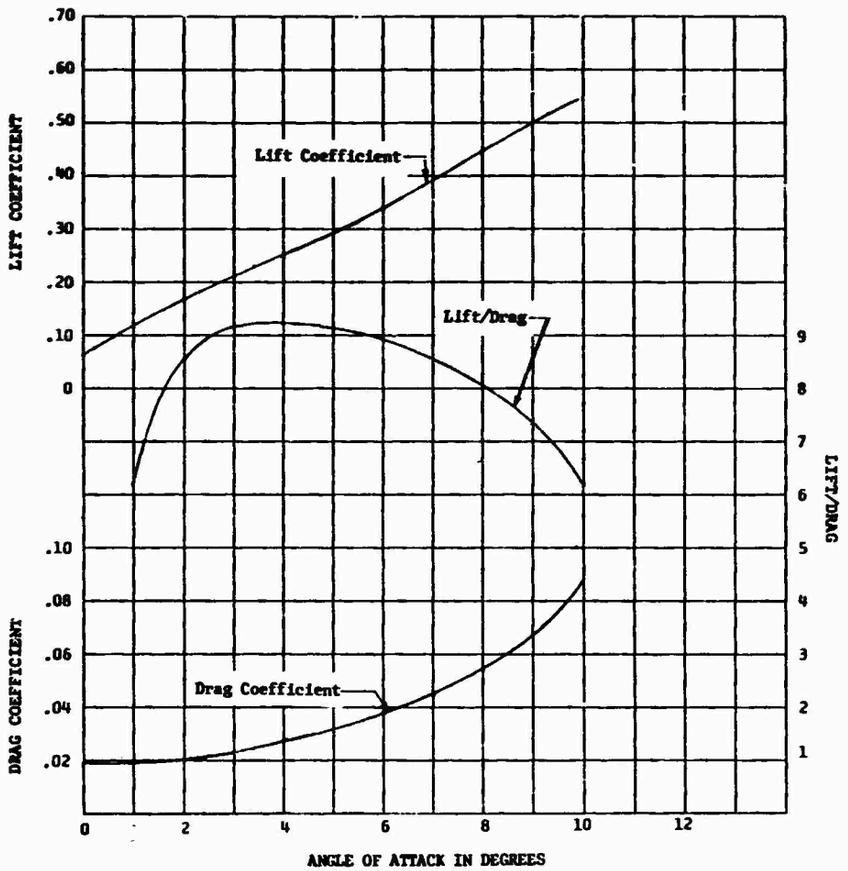

Figure 9 - Lift and Drag Coefficients for Foil Assemblies

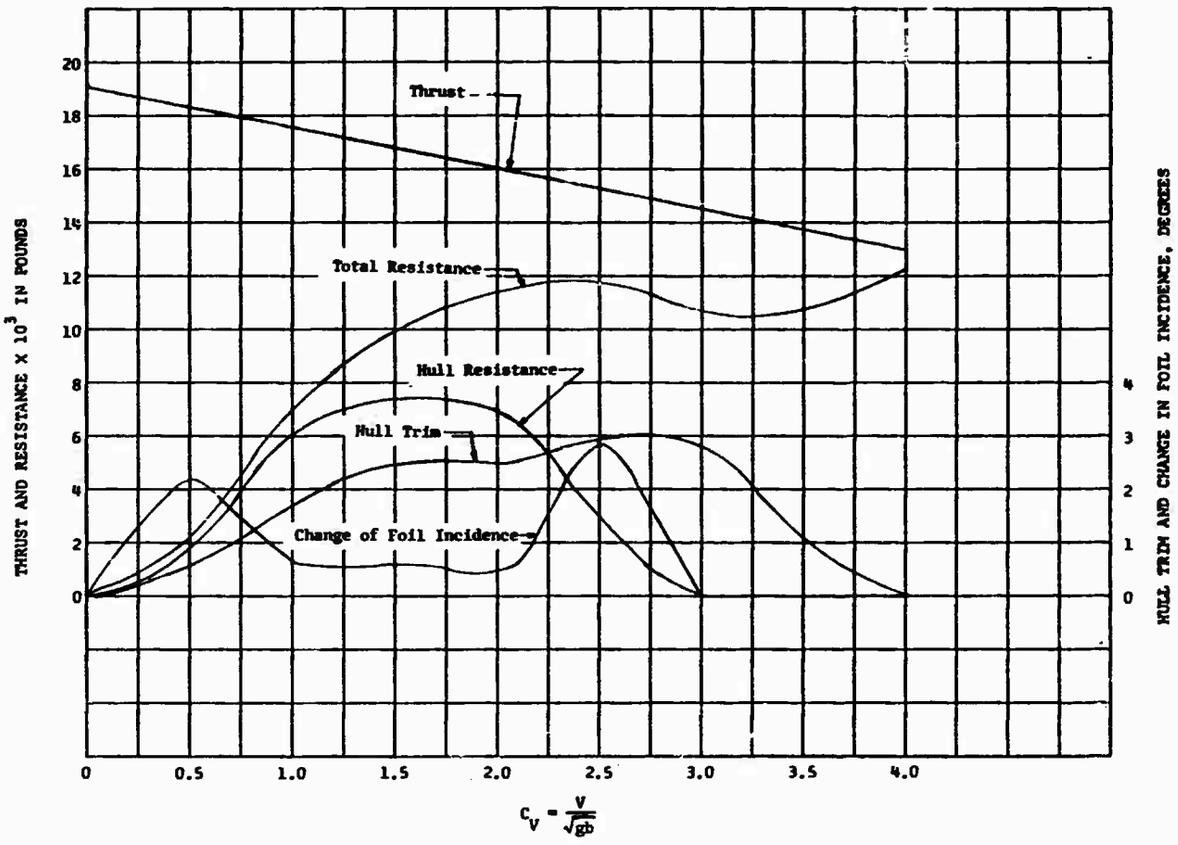

Figure 10 - Variation of Thrust, Hull Resistance, Total Resistance, Hull Trim, and Change of Foil Incidence with Speed Coefficient

TABLE 1

Test Data for Model 4667

Trim, τ deg	C_Δ	C_V	C_R	C_M	C_S	C_{lm}	C_d
0	0.232	1.10	0.0208	0.063	4.69	4.11	-0.008
0	.232	1.64	.0367	.114	4.69	4.11	-.010
0	.232	1.99	.0575	.137	4.69	4.04	-.018
0	.232	2.39	.0733	.155	4.69	4.04	-.010
0	.232	2.78	.1007	.206	4.69	4.04	-.016
0	.232	3.31	.1393	.282	4.69	4.04	-.016
0	.232	3.87	.1783	.355	4.69	4.04	-.021
0	.309	1.12	.0259	.076	5.00	4.50	.018
0	.309	1.60	.0479	.157	5.00	4.50	.016
0	.309	1.99	.0675	.173	5.00	4.44	.010
0	.309	2.41	.0953	.219	5.00	4.44	.005
0	.309	2.87	.1355	.297	5.00	4.44	.005
0	.309	3.38	.1857	.406	5.00	4.44	.008
0	.386	.89	.0200	.037	5.24	4.69	.031
0	.386	1.15	.0363	.123	5.24	4.69	.042
0	.386	1.61	.0598	.194	5.24	4.69	.039
0	.386	1.99	.0853	.219	5.24	4.69	.021
0	.386	2.42	.1212	.268	5.24	4.69	.016
0	.386	2.78	.1664	.349	5.24	4.69	.034
0	.386	3.37	.2582	.495	5.24	4.69	.039
0	.463	.56	.0058	.008	5.40	4.12	.036
0	.463	.86	.0208	.030	5.40	4.12	.050
0	.463	1.13	.0455	.154	5.40	4.84	.068
0	.463	1.59	.0722	.233	5.40	4.84	.060
0	.463	2.02	.1061	.244	5.40	4.84	.047
0	.463	2.39	.1474	.285	5.40	4.84	.042
0	.463	2.84	.2185	.359	5.40	4.84	.060
0	.541	.56	.0089	.007	5.40	4.25	.060
0	.541	.84	.0247	.032	5.40	--	.070
0	.541	1.11	.0517	.167	5.40	4.91	.068
0	.541	1.53	.0845	.259	5.40	4.91	.078
0	.541	1.95	.1258	.264	5.40	4.91	.070
0	.541	2.37	.1748	.282	5.40	4.91	.070
1.5	.077	1.97	.0181	-.050	2.13	2.25	.022
1.5	.077	2.41	.0228	-.055	1.92	2.00	.031
1.5	.077	2.71	.0278	-.049	1.74	1.83	.032
1.5	.077	3.33	.0347	-.049	1.37	1.56	.041
1.5	.077	3.87	.0386	-.051	1.12	1.25	.052
1.5	.077	4.52	.0440	-.056	.86	1.03	.057
1.5	.077	5.45	.0498	-.044	.63	.88	.065
1.5	.077	6.22	.0544	-.049	.50	.78	.069
1.5	.077	6.99	.0590	-.042	.42	.72	.073
1.5	.077	7.52	.0629	-.042	.38	.66	.077
1.5	.077	8.38	.0676	-.037	.28	.59	.078
1.5	.154	1.60	.0201	-.060	3.41	3.20	-.003
1.5	.154	1.99	.0274	-.050	3.28	3.13	.012
1.5	.154	2.48	.0378	-.040	3.09	2.94	.023
1.5	.154	2.78	.0455	-.029	2.91	2.81	.026
1.5	.154	3.35	.0540	-.029	2.50	2.50	.036
1.5	.154	3.91	.0618	-.047	2.11	2.13	.047
1.5	.154	4.63	.0702	-.074	1.60	1.75	.062
1.5	.154	5.40	.0780	-.094	1.20	1.38	.073
1.5	.154	6.18	.0849	-.108	.94	1.08	.078
1.5	.154	6.93	.0922	-.108	.75	.94	.086
1.5	.154	7.66	.0984	-.095	.64	.89	.094
1.5	.154	8.35	.1042	-.096	.63	.82	.096

Table 1 - Continued

Trim, τ deg	C_A	C_V	C_R	C_M	C_S	C_{lm}	C_d
1.5	0.232	1.15	0.0164	-0.058	3.99	3.29	-0.016
1.5	.232	1.52	.0239	-.032	4.00	3.63	0
1.5	.232	1.99	.0340	-.016	3.91	3.50	.016
1.5	.232	2.38	.0448	-.005	3.77	3.38	.026
1.5	.232	2.78	.0579	.016	3.60	3.31	.032
1.5	.232	3.35	.0699	.012	3.27	3.11	.043
1.5	.232	3.91	.0818	.014	2.85	2.81	.055
1.5	.232	4.56	.0934	-.028	2.39	2.38	.073
1.5	.232	5.47	.1034	-.076	1.78	1.86	.088
1.5	.232	6.33	.1127	-.116	1.33	1.50	.099
1.5	.232	6.96	.1189	-.144	1.09	1.31	.104
1.5	.232	7.66	.1262	-.156	.91	1.06	.117
1.5	.309	1.15	.0232	-.037	4.40	3.88	-.021
1.5	.309	1.59	.0316	0	4.43	3.94	0
1.5	.309	1.99	.0417	.015	4.32	3.78	.012
1.5	.309	2.45	.0533	.050	4.20	3.71	.023
1.5	.309	2.83	.0670	.079	4.07	3.53	.033
1.5	.309	3.27	.0822	.095	3.87	3.48	.047
1.5	.309	3.91	.1000	.100	3.46	3.25	.052
1.5	.309	4.63	.1162	.041	2.94	2.91	.068
1.5	.309	5.47	.1289	-.018	2.33	2.34	.091
1.5	.309	6.25	.1366	-.106	1.82	1.94	.104
1.5	.309	6.96	.1440	-.159	1.49	1.63	.115
1.5	.386	.84	.0193	-.112	4.07	3.69	-.020
1.5	.386	1.15	.0289	-.013	4.69	4.19	-.020
1.5	.386	1.54	.0405	.043	4.65	4.13	-.003
1.5	.386	1.99	.0521	.070	4.54	4.00	.016
1.5	.386	2.46	.0645	.115	4.42	3.93	.026
1.5	.386	2.74	.0791	.163	4.34	3.84	.034
1.5	.386	3.37	.0984	.192	4.08	3.70	.050
1.5	.386	3.87	.1185	.194	3.85	3.48	.060
1.5	.386	4.63	.1374	.154	3.37	3.23	.077
1.5	.386	5.47	.1548	.057	2.78	2.78	.099
1.5	.386	6.33	.1633	.048	2.17	2.25	.117
1.5	.386	6.96	.1737	-.119	1.80	1.94	.125
1.5	.463	.58	.0077	-.169	4.42	3.91	-.004
1.5	.463	.86	.0224	-.106	4.32	3.81	-.013
1.5	.463	1.11	.0351	-.001	5.16	4.44	-.018
1.5	.463	1.54	.0502	.078	4.85	4.31	-.003
1.5	.463	1.99	.0652	.116	4.73	4.21	.016
1.5	.463	2.32	.0776	.170	4.65	4.14	.026
1.5	.463	2.78	.0934	.241	4.54	4.03	.036
1.5	.463	3.31	.1115	.301	4.36	3.86	.050
1.5	.463	3.87	.1312	.315	4.11	3.71	.064
1.5	.463	4.55	.1552	.282	3.78	3.44	.083
1.5	.463	5.47	.1768	.168	3.21	3.08	.104
1.5	.541	.28	.0010	-.185	4.50	3.98	-.008
1.5	.541	.56	.0077	-.173	4.69	4.03	-.009
1.5	.541	.86	.0243	.044	4.38	3.88	-.018
1.5	.541	1.15	.0452	.036	5.40	4.63	-.026
1.5	.541	1.60	.0652	.123	5.10	4.49	-.008
1.5	.541	1.99	.0791	.161	4.99	4.39	.008
1.5	.541	2.32	.0961	.244	4.86	4.25	.018
1.5	.541	2.78	.1139	.361	4.71	4.21	.034
1.5	.541	3.31	.1305	.424	4.54	4.00	.050
1.5	.541	3.87	.1455	.436	4.34	3.86	.068
1.5	.541	4.63	.1714	.419	4.03	3.63	.088
1.5	.541	5.41	.1953	.317	3.61	3.31	.109

Table 1 - Continued

Trim, τ deg	C_f	C_V	C_R	C_M	C_S	C_{l_m}	C_d
1.5	0.618	0.28	0.0011	-0.193	4.54	4.06	-0.005
1.5	.618	.56	.0085	-.182	4.69	4.13	-.008
1.5	.618	.86	.0282	-.120	--	--	-.026
1.5	.618	1.15	.0552	.056	5.40	4.69	-.036
1.5	.618	1.57	.0760	.149	5.26	4.63	-.021
1.5	.618	1.99	.0965	.196	5.16	4.46	0
1.5	.618	2.38	.1208	.290	5.04	4.45	.010
1.5	.618	2.78	.1420	.182	4.13	4.38	.123
1.5	.618	3.33	.1583	.545	4.77	4.19	.042
1.5	.618	3.94	.1698	.585	4.60	4.00	.062
1.5	.695	.28	.0019	-.210	4.69	4.16	-.005
1.5	.695	.56	.0089	-.199	4.77	4.19	-.016
1.5	.695	.86	.0309	-.141	--	--	-.016
1.5	.695	1.15	.0641	.053	5.40	4.81	-.026
1.5	.695	1.59	.0911	.165	5.36	4.75	-.016
1.5	.695	1.99	.1150	.202	5.32	4.69	0
1.5	.695	2.32	.1440	.311	5.24	4.56	.013
1.5	.695	2.84	.1795	.494	5.16	4.56	.031
1.5	.695	3.31	.1980	.638	5.00	4.43	.047
1.5	.772	.28	.0010	-.215	4.85	4.25	.010
1.5	.772	.57	.0096	-.203	4.85	4.28	.003
1.5	.772	.86	.0336	-.142	--	--	-.008
1.5	.772	1.15	.0714	.066	5.40	4.88	-.013
1.5	.772	1.54	.1034	.196	5.40	4.81	-.005
1.5	.772	1.99	.1316	.245	5.40	4.78	.008
1.5	.772	2.32	.1710	.347	5.40	4.75	.021
3.0	.077	1.97	.0112	.106	.89	1.13	.055
3.0	.077	2.32	.0108	.121	.80	.88	.072
3.0	.077	2.80	.0131	.133	.56	.62	.083
3.0	.077	3.51	.0154	.131	.37	.45	.099
3.0	.077	4.25	.0170	.102	.27	.38	.108
3.0	.077	4.87	.0181	.102	.20	.33	.113
3.0	.077	5.56	.0197	.107	.16	.29	.119
3.0	.077	6.76	.0212	.085	.12	.25	.121
3.0	.077	6.96	.0239	.067	.10	.22	.125
3.0	.077	7.65	.0255	.059	.09	.21	.127
3.0	.077	8.35	.0290	.053	.08	.19	.129
3.0	.154	1.57	.0181	.148	2.39	2.33	.021
3.0	.154	1.95	.0220	.147	2.03	2.03	.042
3.0	.154	2.38	.0235	.159	1.66	1.71	.068
3.0	.154	2.78	.0251	.172	1.25	1.36	.087
3.0	.154	3.54	.0278	.215	.77	.88	.116
3.0	.154	4.18	.0285	.227	.53	.62	.133
3.0	.154	4.83	.0320	.235	.40	.47	.140
3.0	.154	5.56	.0351	.228	.30	.41	.145
3.0	.154	6.26	.0367	.204	.25	.38	.149
3.0	.154	6.96	.0390	.205	.20	.34	.152
3.0	.154	7.65	.0413	.188	.17	.31	.156
3.0	.154	8.35	.0452	.189	.15	.29	.157
3.0	.232	1.12	.0201	.155	3.52	3.25	-.005
3.0	.232	1.52	.0243	-.148	3.13	2.91	.016
3.0	.232	1.96	.0297	-.139	2.70	2.60	.036
3.0	.232	2.34	.0332	.147	2.35	2.32	.057
3.0	.232	2.81	.0378	.174	1.92	1.94	.080
3.0	.232	3.45	.0405	.237	1.35	1.44	.112
3.0	.232	4.15	.0421	.304	.86	.98	.141
3.0	.232	4.83	.0425	.336	.59	.68	.155

Table 1 - Continued

Trim, τ deg	C_Δ	C_V	C_R	C_M	C_S	C_{lm}	C_d
3.0	0.232	5.57	0.0460	0.344	0.45	0.51	0.165
3.0	.232	6.26	.0483	.348	.35	.45	.171
3.0	.232	6.96	.0540	.338	.29	.41	.174
3.0	.232	7.72	.0568	.355	.25	.38	.177
3.0	.309	.87	.0224	-.220	3.83	3.50	-.006
3.0	.309	1.12	.0305	-.152	4.07	3.66	-.009
3.0	.309	1.56	.0378	-.152	3.76	3.41	.014
3.0	.309	1.96	.0463	.111	3.38	3.13	.026
3.0	.309	2.37	.0518	.099	2.98	2.83	.053
3.0	.309	2.80	.0590	.101	2.56	2.47	.073
3.0	.309	3.41	.0668	.222	1.92	1.96	.111
3.0	.309	4.17	.0691	.325	1.21	1.38	.146
3.0	.309	4.85	.0695	.399	.85	.95	.167
3.0	.309	5.56	.0710	.435	.61	.70	.181
3.0	.309	6.26	.0722	.425	.48	.55	.189
3.0	.309	6.96	.0784	.440	.40	.47	.194
3.0	.386	.87	.0224	.244	4.08	3.63	-.018
3.0	.386	1.12	.0305	.147	4.30	3.88	-.016
3.0	.386	1.56	.0378	.126	4.14	3.73	.005
3.0	.386	1.96	.0463	.082	3.83	3.50	.026
3.0	.386	2.37	.0518	.076	3.52	3.22	.047
3.0	.386	2.80	.0590	.072	3.07	2.88	.067
3.0	.386	3.41	.0668	.164	2.42	2.36	.099
3.0	.386	4.17	.0691	.318	1.56	1.66	.144
3.0	.386	4.85	.0695	.428	1.11	1.21	.169
3.0	.386	5.56	.0710	.488	.80	.91	.188
3.0	.386	6.26	.0722	.548	.63	.72	.199
3.0	.386	6.96	.0784	.544	.49	.56	.206
3.0	.463	.53	.0070	.338	4.09	3.73	-.013
3.0	.463	.86	.0251	.265	4.22	3.81	-.023
3.0	.463	1.12	.0375	.130	4.42	4.06	-.021
3.0	.463	1.51	.0455	.094	4.38	3.94	.004
3.0	.463	1.95	.0548	.053	4.17	3.75	.018
3.0	.463	2.35	.0620	.010	3.91	3.54	.043
3.0	.463	2.77	.0700	.012	3.52	3.23	.064
3.0	.463	3.45	.0780	.101	2.75	2.64	.104
3.0	.463	4.18	.0826	.263	1.96	2.00	.142
3.0	.463	4.81	.0840	.408	1.45	1.48	.159
3.0	.463	5.56	.0854	.522	1.03	1.13	.194
3.0	.463	6.26	.0854	.616	.80	.91	.207
3.0	.541	.28	.0019	.292	4.29	3.79	-.002
3.0	.541	.55	.0085	.350	4.32	3.87	-.008
3.0	.541	.87	.0289	.266	4.39	3.87	-.016
3.0	.541	1.13	.0460	.111	4.54	4.22	-.023
3.0	.541	1.57	.0560	.064	4.61	4.08	.004
3.0	.541	1.99	.0668	.007	4.43	3.94	.026
3.0	.541	2.39	.0738	.052	4.22	3.77	.045
3.0	.541	2.81	.0819	.070	3.91	3.50	.068
3.0	.541	3.45	.0922	-.015	3.21	2.99	.107
3.0	.541	4.15	.0962	-.185	2.36	2.35	.146
3.0	.541	4.84	.0984	-.129	1.72	1.77	.179
3.0	.541	5.56	.0992	-.522	1.25	1.34	.203
3.0	.618	.31	.0031	-.390	4.36	3.88	-.003
3.0	.618	.59	.0108	-.362	4.42	3.97	-.009
3.0	.618	.88	.0309	-.283	4.50	4.00	-.019
3.0	.618	1.12	.0544	-.099	4.61	4.36	-.031
3.0	.618	1.57	.0668	-.028	4.81	4.22	0

Table 1 - Continued

Trim, τ deg	C_Δ	C_V	C_R	C_M	C_S	C_{lm}	C_d
3.0	0.618	1.98	0.0780	0.048	4.65	4.09	0.020
3.0	.618	2.39	.0864	.139	4.42	3.95	.042
3.0	.618	2.79	.0946	.167	4.22	3.78	.065
3.0	.618	3.45	.1042	.096	3.54	3.25	.105
3.0	.618	4.18	.1115	.010	2.66	2.59	.148
3.0	.618	4.86	.1146	.343	2.02	2.08	.183
3.0	.695	.28	.0027	.401	4.46	3.98	-.002
3.0	.695	.59	.0116	.370	4.50	4.04	-.009
3.0	.695	.88	.0359	.275	4.56	3.99	-.022
3.0	.695	1.12	.0633	.086	4.85	4.48	-.031
3.0	.695	1.53	.0776	.011	4.97	4.38	-.005
3.0	.695	1.96	.0907	.053	4.82	4.23	.011
3.0	.695	2.41	.1015	--	4.61	4.08	.040
3.0	.695	2.78	.1081	--	4.38	3.91	.062
3.0	.695	3.48	.1173	--	3.75	3.50	.107
3.0	.772	.28	.0019	.152	4.54	4.03	-.005
3.0	.772	.56	.0096	.369	4.55	4.13	-.013
3.0	.772	.84	.0328	.288	4.61	4.06	-.029
3.0	.772	1.12	.0706	.064	5.08	4.59	-.039
3.0	.772	1.49	.0880	.065	5.06	4.53	-.015
3.0	.772	1.98	.1042	.152	4.90	4.34	.018
4.5	.077	1.99	.0104	-.121	.63	.72	.086
4.5	.077	2.38	.0112	-.134	.35	.41	.109
4.5	.077	2.78	.0120	-.132	.28	.34	.112
4.5	.077	3.30	.0127	-.130	.21	.29	.117
4.5	.077	3.91	.0139	-.128	.15	.25	.127
4.5	.077	4.56	.0150	-.118	.09	.20	.130
4.5	.077	5.42	.0174	-.107	.06	.19	.135
4.5	.077	6.26	.0189	-.089	.05	.16	.140
4.5	.077	6.96	.0212	-.070	.04	.12	.143
4.5	.077	7.66	.0228	-.046	.03	.11	.148
4.5	.077	8.35	.0250	-.027	.02	.09	.152
4.5	.154	1.60	.0189	-.157	1.64	1.81	.042
4.5	.154	1.95	.0204	-.172	1.27	1.48	.073
4.5	.154	2.32	.0212	-.196	.94	1.04	.104
4.5	.154	2.78	.0224	-.230	.67	.75	.131
4.5	.154	3.36	.0235	-.252	.41	.46	.150
4.5	.154	3.98	.0247	-.250	.27	.34	.163
4.5	.154	4.64	.0243	-.256	.19	.29	.170
4.5	.154	5.41	.0266	-.253	.14	.25	.176
4.5	.154	6.26	.0313	-.226	.11	.22	.181
4.5	.154	6.79	.0336	-.220	.09	.20	.185
4.5	.154	7.66	.0343	-.195	.07	.19	.190
4.5	.154	8.35	.0374	-.176	.06	.16	.193
4.5	.232	1.16	.0235	-.214	2.78	2.66	0
4.5	.232	1.54	.0266	-.184	2.39	2.34	.031
4.5	.232	1.94	.0301	-.188	1.92	2.01	.050
4.5	.232	2.32	.0324	-.217	1.49	1.61	.094
4.5	.232	2.78	.0332	-.272	1.13	1.22	.122
4.5	.232	3.36	.0324	-.340	.77	.79	.156
4.5	.232	3.87	.0336	-.363	.48	.56	.180
4.5	.232	4.55	.0355	-.379	.31	.36	.195
4.5	.232	5.42	.0382	-.374	.23	.31	.202
4.5	.232	6.26	.0397	-.372	.17	.27	.209
4.5	.232	6.96	.0425	-.368	.14	.25	.214
4.5	.232	7.66	.0459	-.323	.11	.22	.216

Table 1 - Continued

Trim, τ deg	C_{ℓ}	C_V	C_R	C_M	C_{ξ}	C_{lm}	C_d
4.5	0.309	1.16	0.0316	-0.221	3.28	3.03	0.005
4.5	.309	1.54	.0370	-.205	2.90	2.76	.026
4.5	.309	1.93	.0401	-.183	2.49	2.47	.057
4.5	.309	2.31	.0440	-.221	2.03	2.03	.083
4.5	.309	2.78	.0467	-.267	1.56	1.66	.125
4.5	.309	3.27	.0486	-.364	1.09	1.13	.159
4.5	.309	3.87	.0475	-.442	.73	.78	.190
4.5	.309	4.55	.0471	-.485	.47	.52	.214
4.5	.309	5.42	.0490	-.503	.31	.36	.229
4.5	.309	6.26	.0517	-.484	.24	.31	.237
4.5	.309	6.96	.0529	-.490	.19	.28	.241
4.5	.386	.87	.0278	-.316	3.75	3.38	-.016
4.5	.386	1.12	.0370	-.240	3.75	3.38	-.008
4.5	.386	1.55	.0448	-.199	3.44	3.18	.018
4.5	.386	1.99	.0506	-.165	2.97	2.84	.050
4.5	.386	2.38	.0540	-.191	2.44	2.41	.083
4.5	.386	2.78	.0575	-.250	1.99	1.97	.117
4.5	.386	3.33	.0583	-.366	1.41	1.47	.159
4.5	.386	3.91	.0582	-.484	.95	1.03	.195
4.5	.386	4.64	.0587	-.568	.61	.70	.225
4.5	.386	5.40	.0587	-.621	.41	.47	.242
4.5	.386	6.22	.0618	-.624	.30	.34	.250
4.5	.386	6.96	.0637	-.621	.25	.31	.254
4.5	.463	.53	.0085	-.440	3.52	3.25	-.008
4.5	.463	.88	.0316	-.329	4.27	3.66	-.010
4.5	.463	1.13	.0452	-.229	4.22	3.66	-.009
4.5	.463	1.59	.0536	-.185	3.73	3.34	.021
4.5	.463	1.99	.0602	-.129	3.36	3.13	.046
4.5	.463	2.39	.0644	-.146	2.90	2.75	.073
4.5	.463	2.78	.0679	-.201	2.42	2.38	.109
4.5	.463	3.36	.0706	-.339	1.74	1.81	.156
4.5	.463	3.91	.0702	-.494	1.25	1.38	.198
4.5	.463	4.57	.0690	-.627	.85	.88	.227
4.5	.463	5.37	.0690	-.720	.56	.59	.251
4.5	.463	6.26	.0714	-.748	.39	.44	.263
4.5	.541	.56	.0096	-.462	3.97	3.56	-.005
4.5	.541	.89	.0355	-.353	4.38	3.81	-.009
4.5	.541	1.16	.0544	-.223	4.38	3.88	-.005
4.5	.541	1.57	.0629	-.172	4.09	3.63	.016
4.5	.541	1.99	.0706	-.098	3.74	3.44	.042
4.5	.541	2.38	.0753	-.099	3.32	3.00	.070
4.5	.541	2.82	.0795	-.149	2.82	2.66	.102
4.5	.541	3.31	.0822	-.291	2.11	2.09	.146
4.5	.541	3.87	.0830	-.468	1.52	1.53	.190
4.5	.541	4.64	.0811	-.652	1.02	1.09	.232
4.5	.541	5.42	.0811	-.802	.66	.72	.260
4.5	.541	6.22	.0818	-.874	.45	.50	.276
4.5	.618	.54	.0108	-.485	4.14	3.72	0
4.5	.618	.86	.0324	-.403	4.38	3.91	-.009
4.5	.618	1.16	.0614	-.216	4.54	4.06	-.010
4.5	.618	1.54	.0726	-.153	4.34	3.88	.016
4.5	.618	1.99	.0811	-.076	3.99	3.59	.042
4.5	.618	2.37	.0857	-.038	3.60	3.28	.068
4.5	.618	2.78	.0903	-.074	3.09	2.88	.099
4.5	.618	3.36	.0938	-.243	2.42	2.31	.138
4.5	.618	3.91	.0953	-.446	1.80	1.81	.190
4.5	.618	4.64	.0934	-.693	1.17	1.25	.242
4.5	.618	5.36	.0934	-.861	.78	.84	.271

Table 1 - Continued

Trim, τ deg	C_Δ	C_V	C_R	C_M	C_S	C_{lm}	C_d
4.5	0.695	0.28	0.0038	-0.538	4.14	3.69	-.005
4.5	.695	.58	.0135	-.513	4.38	3.88	-.010
4.5	.695	.86	.0355	-.402	4.69	4.16	-.010
4.5	.695	1.16	.0710	-.223	4.73	4.19	-.008
4.5	.695	1.59	.0822	-.131	4.57	4.00	.010
4.5	.695	1.94	.0899	-.042	4.22	3.78	.026
4.5	.695	2.41	.0973	-.032	3.83	3.56	.060
4.5	.695	2.78	.1027	-.007	3.44	3.13	.073
4.5	.695	3.38	.1054	-.181	2.66	2.47	.141
4.5	.772	.23	.0035	-.576	4.38	3.86	-.003
4.5	.772	.28	.0038	-.572	4.38	3.86	-.003
4.5	.772	.56	.0127	-.546	4.54	3.96	-.005
4.5	.772	.86	.0316	-.470	4.69	3.93	-.010
4.5	.772	1.11	.0768	-.220	4.85	4.30	-.010
4.5	.772	1.60	.0930	-.084	4.69	4.13	0
4.5	.772	1.99	.1042	-.020	4.34	3.98	.023
6.0	.077	1.54	.0112	-.124	.72	.82	.078
6.0	.077	1.99	.0116	-.130	.37	.42	.115
6.0	.077	2.37	.0112	-.122	.24	.28	.130
6.0	.077	2.78	.0123	-.126	.18	.24	.130
6.0	.077	3.48	.0131	-.125	.11	.19	.142
6.0	.077	4.18	.0150	-.116	.08	.16	.148
6.0	.077	4.87	.0162	-.111	.05	.12	.151
6.0	.077	5.57	.0174	-.084	.04	.12	.154
6.0	.077	6.33	.0197	-.073	.03	.09	.156
6.0	.077	6.96	.0220	-.056	.02	.08	.157
6.0	.077	8.28	.0247	-.003	.02	.06	.159
6.0	.154	1.13	.0201	-.180	1.80	1.81	.021
6.0	.154	1.59	.0228	-.176	1.41	1.44	.065
6.0	.154	1.99	.0235	-.200	.94	.94	.117
6.0	.154	2.27	.0235	-.238	.58	.66	.146
6.0	.154	2.74	.0235	-.259	.37	.42	.172
6.0	.154	3.44	.0239	-.268	.23	.27	.186
5.0	.154	4.18	.0247	-.261	.15	.22	.194
6.0	.154	4.87	.0270	-.251	.11	.19	.200
6.0	.154	5.57	.0282	-.242	.08	.17	.204
6.0	.154	6.26	.0305	-.221	.06	.14	.208
6.0	.154	7.66	.0343	-.188	.03	.10	.211
6.0	.154	8.35	.0367	-.159	.02	.09	.211
6.0	.232	.85	.0251	-.272	2.50	2.38	-.005
6.0	.232	1.13	.0289	-.242	2.27	2.25	.016
6.0	.232	1.53	.0328	-.223	1.96	1.94	.052
6.0	.232	1.95	.0343	-.244	1.49	1.56	.104
6.0	.232	2.39	.0355	-.303	.94	1.13	.156
6.0	.232	2.78	.0359	-.343	.67	.75	.183
6.0	.232	3.48	.0347	-.385	.39	.38	.214
6.0	.232	4.18	.0351	-.404	.24	.28	.227
6.0	.232	4.84	.0367	-.398	.17	.23	.234
6.0	.232	5.47	.0397	-.390	.13	.20	.238
6.0	.232	6.17	.0428	-.364	.11	.19	.242
6.0	.232	6.85	.0452	-.362	.08	.16	.246
6.0	.232	7.52	.0463	-.352	.06	.14	.247
6.0	.309	.87	.0320	--	--	2.69	-.009
6.0	.309	1.08	.0374	-.281	2.82	2.63	.003
6.0	.309	1.69	.0452	-.243	2.27	2.19	.055
6.0	.309	1.96	.0471	-.258	1.92	1.94	.083
6.0	.309	2.25	.0479	-.297	1.56	1.63	.255

Table 1 - Continued

Trim. α deg	C_A	C_V	C_R	C_M	C_S	C_{lm}	C_d
6.0	0.309	2.37	0.0479	-0.318	1.47	1.50	0.138
6.0	.309	2.76	.0475	-.389	1.02	1.09	.180
6.0	.309	3.06	.0471	-.437	.77	.84	.202
6.0	.309	3.48	.0463	-.486	.55	.62	.227
6.0	.309	4.12	.0471	-.524	.33	.38	.245
6.0	.309	4.80	.0475	-.537	.24	.28	.255
6.0	.309	5.61	.0502	-.512	.17	.24	.260
6.0	.309	6.22	.0517	-.516	.13	.20	.265
6.0	.309	6.96	.0540	-.488	.11	.19	.267
6.0	.309	7.60	.0552	--	--	.17	.270
6.0	.385	.56	.0116	-.458	2.82	2.69	-.026
6.0	.386	.88	.0374	-.374	3.21	2.98	-.008
6.0	.386	1.18	.0482	-.305	3.13	2.91	0
6.0	.386	1.58	.0536	-.256	2.77	2.61	.036
6.0	.386	1.99	.0571	-.251	2.35	2.25	.078
6.0	.386	2.39	.0587	-.321	1.72	1.75	.128
6.0	.386	2.78	.0598	-.419	1.25	1.34	.169
6.0	.386	3.48	.0598	-.559	.72	.78	.229
6.0	.386	3.86	.0598	-.606	.55	.62	.250
6.0	.386	4.63	.0594	-.653	.35	.40	.268
6.0	.386	5.41	.0606	-.655	.21	.27	.279
6.0	.386	6.18	.0625	-.652	.18	.24	.284
6.0	.386	6.96	.0648	-.648	.13	.20	.289
6.0	.463	.60	.0127	-.506	3.21	2.97	-.010
6.0	.463	.88	.0413	-.414	3.44	3.19	-.016
6.0	.463	1.15	.0571	-.315	3.36	3.13	-.005
6.0	.463	1.55	.0641	-.268	3.07	2.88	.029
6.0	.463	2.00	.0679	-.237	2.61	2.56	.068
6.0	.463	2.41	.0710	-.299	2.11	2.06	.120
6.0	.463	2.78	.0726	-.404	1.64	1.69	.162
6.0	.463	3.34	.0718	-.553	1.06	1.16	.221
6.0	.463	3.87	.0714	-.670	.74	.78	.255
6.0	.463	4.52	.0695	-.765	.51	.50	.281
6.0	.463	5.47	.0718	-.796	.27	.28	.300
6.0	.463	6.18	.0733	-.794	.20	.25	.305
6.0	.541	.28	.0027	-.606	3.28	3.06	0
6.0	.541	.60	.0143	-.580	3.40	3.13	-.026
6.0	.541	.86	.0386	-.480	3.75	3.38	-.008
6.0	.541	1.18	.0660	-.342	3.75	3.38	.001
6.0	.541	1.59	.0745	-.281	3.44	3.13	.031
6.0	.541	2.07	.0803	-.237	2.97	2.78	.083
6.0	.541	2.38	.0814	-.300	2.42	2.38	.115
6.0	.541	2.78	.0841	-.400	1.92	1.91	.164
6.0	.541	3.34	.0849	-.583	1.29	1.38	.227
6.0	.541	3.94	.0826	-.744	.86	.95	.271
6.0	.541	4.73	.0822	-.881	.48	.56	.302
6.0	.541	5.57	.0830	-.934	.32	.38	.320
6.0	.618	.28	.0031	-.654	3.60	3.25	--
6.0	.618	.56	.0154	-.619	3.60	3.25	--
6.0	.618	.85	.0374	-.524	3.91	3.54	--
6.0	.618	1.17	.0756	-.338	4.07	3.65	--
6.0	.618	1.56	.0865	-.277	3.75	3.31	.026
6.0	.618	1.99	.0915	-.198	3.30	3.06	.065
6.0	.618	2.32	.0946	-.229	2.74	2.69	.094
6.0	.618	2.78	.0965	-.377	2.21	2.16	.159
6.0	.618	3.33	.0984	-.558	1.50	1.59	.224
6.0	.618	3.90	.0961	-.763	1.03	1.13	.271
6.0	.618	4.73	.0946	-.958	.63	.69	.318

Table 1 - Continued

Trim, τ deg	C_Δ	C_V	C_R	C_M	C_S	C_{lm}	C_d
6.0	0.618	5.57	0.0949	-1.048	0.39	0.44	0.340
6.0	.695	.28	.0038	-.699	3.75	3.38	.001
6.0	.695	.56	.0193	-.648	3.83	3.44	-.003
6.0	.695	.84	.0386	-.561	4.14	3.69	-.005
6.0	.695	1.11	.0845	-.356	4.22	3.75	-.005
6.0	.695	1.53	.0973	-.260	3.91	3.50	.021
6.0	.695	1.95	.1038	-.166	3.52	3.25	.052
6.0	.695	2.37	.1065	-.190	2.99	2.81	.094
6.0	.695	2.78	.1081	-.300	2.50	2.38	.141
6.0	.695	3.34	.1112	-.535	1.76	1.78	.208
6.0	.695	3.90	.1081	-.764	1.68	1.28	.260
6.0	.772	.28	.0046	-.730	3.91	3.50	.005
6.0	.772	.56	.0193	-.693	3.99	3.56	.003
6.0	.772	.84	.0459	-.569	4.38	3.88	0
6.0	.772	1.11	.0930	-.348	4.46	3.94	0
6.0	.772	1.53	.1085	-.231	4.14	3.69	.021
6.0	.772	1.95	.1169	-.125	3.79	3.44	.050
9.0	.077	1.60	.0143	-.140	.44	.50	.120
9.0	.077	1.99	.0147	-.147	.24	.26	.151
9.0	.077	2.35	.0147	-.147	.17	.19	.162
9.0	.077	2.78	.0154	-.148	.12	.15	.162
9.0	.077	3.36	.0162	-.137	.08	.12	.168
9.0	.077	3.91	.0158	-.130	.06	.10	.174
9.0	.154	1.54	.0278	-.218	1.02	1.08	.094
9.0	.154	1.99	.0282	-.257	.57	.62	.167
9.0	.154	2.39	.0278	-.281	.31	.40	.208
9.0	.154	2.78	.0282	-.281	.22	.25	.220
9.0	.154	3.36	.0282	-.282	.15	.17	.224
9.0	.154	3.91	.0289	-.281	.12	.15	.234
9.0	.232	1.16	.0386	-.254	1.84	1.84	.018
9.0	.232	1.55	.0428	-.248	1.41	1.47	.031
9.0	.232	2.01	.0432	-.303	.90	.97	.172
9.0	.232	2.32	.0432	-.350	.60	.62	.211
9.0	.232	2.78	.0425	-.380	.36	.44	.247
9.0	.232	3.34	.0425	-.406	.22	.25	.263
9.0	.232	3.87	.0432	-.379	.16	.19	.268
9.0	.309	1.15	.0529	-.316	2.21	2.16	.021
9.0	.309	1.58	.0575	-.318	1.83	1.84	.073
9.0	.309	1.99	.0583	-.352	1.31	1.38	.146
9.0	.309	2.32	.0579	-.443	.86	.94	.208
9.0	.309	2.74	.0556	-.510	.55	.61	.255
9.0	.309	3.31	.0560	-.556	.34	.41	.292
9.0	.309	3.87	.0556	-.566	.23	.25	.305
9.0	.309	4.80	.0590	-.561	.14	.17	.315
9.0	.386	.88	.0444	-.452	2.58	2.47	-.007
9.0	.386	1.11	.0664	-.353	2.50	2.41	.003
9.0	.386	1.54	.0722	-.336	2.19	2.16	.055
9.0	.386	1.99	.0733	-.381	1.64	1.69	.130
9.0	.386	2.36	.0722	-.475	1.19	1.26	.203
9.0	.386	2.78	.0718	-.588	.74	.81	.260
9.0	.386	3.35	.0714	-.664	.45	.51	.307
9.0	.386	3.98	.0714	-.705	.27	.32	.328
9.0	.386	4.73	.0733	-.698	.17	.21	.343
9.0	.463	.56	.0185	-.608	2.66	2.53	-.010

Table 1 - Continued

Trim, τ deg	C_{Δ}	C_V	C_R	C_M	C_S	C_{lm}	C_d
9.0	0.463	0.84	0.0490	-0.520	2.82	2.66	-0.013
9.0	.463	1.11	.0787	-.417	2.78	2.63	-.003
9.0	.463	1.53	.0845	-.355	2.42	2.34	.042
9.0	.463	1.94	.0880	-.386	1.91	1.91	.112
9.0	.463	2.36	.0884	-.507	1.33	1.41	.198
9.0	.463	2.78	.0876	-.630	.94	1.00	.258
9.0	.463	3.34	.0857	-.758	.56	.62	.315
9.0	.463	3.89	.0845	-.820	.36	.41	.341
9.0	.463	4.73	.0872	-.850	.22	.25	.362
9.0	.463	5.56	.0892	-.848	.16	.19	.372
9.0	.541	.28	.0038	-.755	2.74	2.56	-.003
9.0	.541	.56	.0193	-.676	2.82	2.63	-.010
9.0	.541	.84	.0475	-.590	3.13	2.84	-.016
9.0	.541	1.11	.0895	-.455	3.09	2.81	-.008
9.0	.541	1.53	.0961	-.384	2.66	2.53	.034
9.0	.541	1.94	.1004	-.393	2.19	2.16	.099
9.0	.541	2.36	.1023	-.566	1.56	1.68	.190
9.0	.541	2.78	.1011	-.665	1.16	1.28	.250
9.0	.541	3.34	.1011	-.815	.74	.81	.312
9.0	.541	3.89	.0992	--	.47	.53	.354
9.0	.541	4.73	.0996	--	.27	.32	.383
9.0	.541	5.56	.1027	--	.17	.25	.396

TABLE 2

Calculated Take-off Data

C_V	0.5	1.0	1.5	2.0	2.5	3.0	3.5	4.0
Velocity	10.52	21.04	31.56	42.08	52.60	63.12	73.64	84.16
Trim	0.60	1.70	2.50	2.50	3.00	2.90	1.10	0
α_a	2.30	3.40	4.20	4.20	4.70	4.60	2.80	1.70
C'_{La}	0.180	0.230	0.260	0.260	0.280	0.277	0.204	0.156
$(L/D)_a$	8.50	9.20	9.20	9.20	9.20	9.20	9.10	8.10
q	110	441	991	1,762	2,753	3,964	5,396	7,050
L_a	1,350	6,918	17,572	31,240	52,571	75,000	75,000	75,000
D_a	159	752	1,910	3,396	5,714	8,152	8,242	9,259
C_Δ	0.592	0.547	0.464	0.345	0.127			
C_M	-0.066	-0.061	-0.0476	-0.050	-0.136	FOILBORNE		
C_R	0.012	0.0375	0.045	0.042	0.018			
R	1,986	6,206	7,448	7,006	2,979	0	0	0
M	-150,117	-138,744	-108,266	-114,800	-309,332			
L_f	680	2,491	5,630	11,214	26,411	25,000	25,000	25,000
C_{Lf}	0.272	0.249	0.250	0.280	0.422	0.277	0.204	0.156
$(L/D)_f$	9.2	9.2	9.2	9.2	8.3	9.2	9.1	8.1
α_f	4.5	4.0	4.0	4.7	7.6	4.6	2.8	1.7
D_f	74	270	612	1,219	3,182	2,717	2,743	3,086
$D_f + D_a$	233	1,022	2,522	4,615	8,896	10,869	10,985	12,345
$R + D_f + D_a$	2,219	7,228	9,970	11,621	11,875	10,869	10,985	12,345
T	18,100	17,700	16,800	16,000	15,300	14,500	13,800	13,000
H	8.0	8.0	8.0	8.0	8.0	2.0	2.0	2.0
β	2.2	0.6	0.6	0.5	2.9	0	0	0

NOTE: Where the hull is foilborne, the air drag of the hull has not been added.

REFERENCES

1. Clement, E. P., "Development and Model Tests of an Efficient Planing Hull Design," David Taylor Model Basin Report 1314 (Apr 1959).

2. Olson, R. E. and Brownell, W. F., "Facilities and Research Capabilities, High Speed Phenomena Division, David Taylor Model Basin, Langley Field, Va.," David Taylor Model Basin Report 1809 (Apr 1964).

3. Parkinson, J. B. et al., "Aerodynamic and Hydrodynamic Tests of a Family of Models of Flying-Boat Hulls Derived from a Streamline Body, NACA Model 84 Series," National Advisory Committee for Aeronautics Report 766 (1943).

ERRATA SHEET

for

David Taylor Model Basin Report 2006, July 1965

Report 2006 – General Resistance Test of a Stepless Planing Hull with Application to a Hydrofoil Configuration:

The values of C_M and C_d are erroneous and the data required to compute correct values are not available.

DESIGNING FOR OPTIMUM PLANING PERFORMANCE

by

E.P. Clement

The wetted portion of most planing hulls at high speed consists of a nearly prismatic shape – i.e., a shape with approximately constant beam and deadrise, with straight buttock lines. The planing performance of such a configuration is a function of only a few variables, and can now be predicted by utilizing the results of previous model testing and analytical work. The high speed performance of the five planing hull models making up the DTMB Series 62 can, for example, be represented in a single graph (see Figure 1). The body plan used for the models of this series is shown in Figure 2. The chine lines in plan view for three of the hull forms tested are shown in Figure 3, and the resistance and trim for one condition of weight and LCG location are shown in Figure 4. Each of the five models was tested at ten different conditions of weight and LCG location – making a total of fifty tests in all. And, the high-speed results from all fifty tests have been successfully collapsed onto the single graph of Figure 1. This figure accordingly presents the high-speed performance of planing hulls having a wide range of values of length-beam ratio, weight, and center of gravity location, and the resistance curves for this variety of planing configurations can readily be reconstructed by means of that graph. The planing hulls of Series 62 each had a deadrise angle of 12½ degrees, so that Figure 1 is accordingly restricted to that value of deadrise. However, graphs like Figure 1 could be constructed (by model test or by calculation) for other values of deadrise. A relatively limited number of model tests of a particular configuration of a deep-Vee hull with spray strakes could be utilized, for example, to construct a graph like Figure 1, and it could then be used to solve a variety of design problems for that configuration.

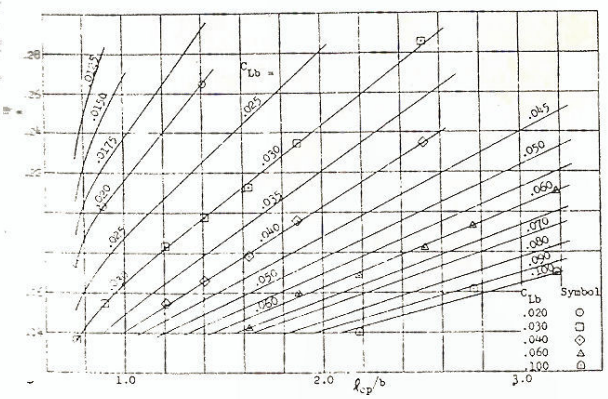

Figure 1. Resistance/weight ratio versus l_{cp}/b with C_{Lb} as parameter – from the high-speed test results for DTMB Series 62.

The use to which Figure 1 can be put can readily be shown by an example. Assume it is wished to determine, for a speed of 40 knots and a gross weight of 10,000 pounds, the resistance of the hull configuration shown in Figures 2 and 3 which has a length/beam ratio of 3.1. The beam dimension to be used in connection with Figure 1 is the width over the spray strips at the longitudinal location of the center of gravity, and this dimension, for the hull being considered, is 8.54 feet. The ratio of the distance of the center of pressure forward of the transom to the beam is then:

$$l_{cp}/b = l_{cg}/b = 11.6/8.54 = 1.36$$

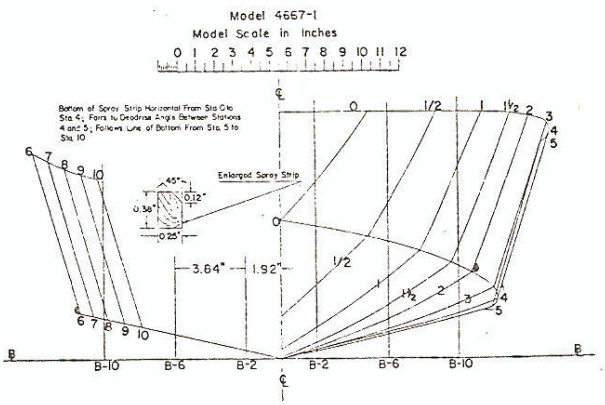

Figure 2. Body plan of the model used as the parent for DTMB Series 62.

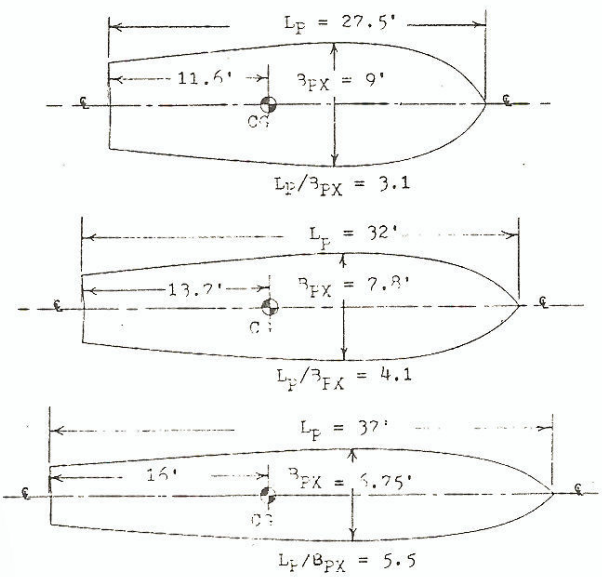

Figure 3. Chine lines in plan view for three of the hulls of DTMB Series 62 (The dimensions given are full-scale for a gross weight of 10,000 pounds).

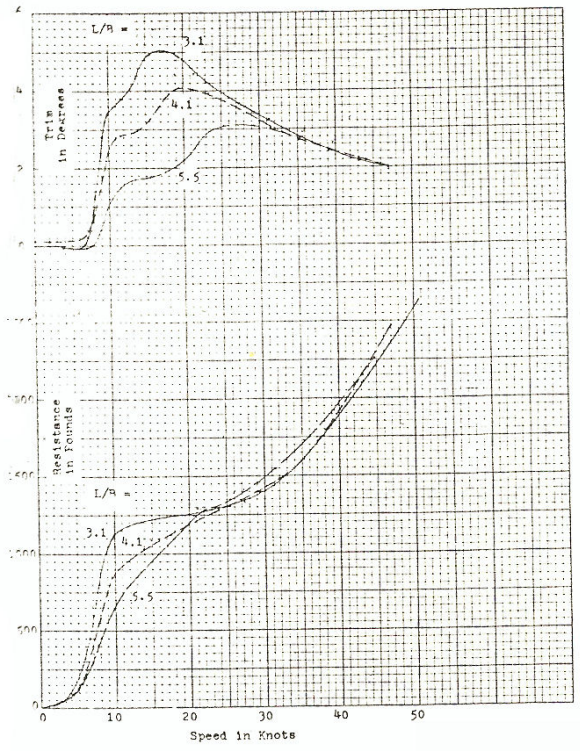

Figure 4. Resistance and trim for three planing hulls of different length/beam ratio. Gross weight equals 10,000 pounds.

Also, the lift coefficient,

$$C_{Lb} = \frac{W}{\rho/2\, v^2 b^2} = \frac{10{,}000}{(67.5)^2 \cdot (8.54)^2} = 0.03$$

(since $\rho/2$ is 1.00 for salt water, and 40 knots = 67.5 fps).

Accordingly, entering Figure 1 with a value of l_{cp}/b of 1.36, and a value of C_{Lb} of 0.03, the value of the resistance/weight ratio, R/W, is found to be 0.19. Then, multiplying this ratio by the weight of the boat (10,000 pounds), a resistance value of 1900 pounds is obtained -- which agrees very satisfactorily with the value shown in Figure 4.

Figure 1 also shows, for a wide variety of planing hulls, the effect on resistance of changing the longitudinal position of the center of gravity. Assume, for the case just given, that the weight, beam, and speed are to remain the same, and that it is wished to determine the effects on resistance of different longitudinal positions of the center of gravity. The value of the lift coefficient, C_{Lb}, then remains equal to 0.03 and Figure 1 shows immediately that if the center of gravity is moved forward so that the value of l_{cg}/b (and therefore of l_{cp}/b) becomes 1.6, the resistance will increase to 2100 pounds, and if it is moved aft so that the value of l_{cg}/b is 1.1, the resistance will decrease to approximately 1700 pounds. This relationship between resistance and center of gravity position at high speed explains the emphasis in the design of many fast planing boats on positioning the major weights (engines, etc.) close to the transom, so that the *CG* will be as far aft as possible. If this process is carried too far, however, the boat will be likely to propoise at high speed.

Figure 1 also indicates the effect on resistance of altering the beam of a projected new design. Reducing the beam causes the value of the lift coefficient, C_{Lb}, to increase, and this in turn will produce a significant reduction in resistance. This relationship between beam and resistance is, of course, the reason for the emphasis in the design of many recent offshore racing powerboats on reducing the beam. It also explains the beneficial effect of the spray strakes of a deep-Vee hull in causing the boat to run on a reduced beam at high speed.

The foregoing discussion has explained that the high-speed resistance of a typical planing boat can be lowered either by moving the center of gravity aft or by decreasing the beam. A major effect of either of these changes is to reduce the size of the planing area (i.e., the area supporting the weight of the boat in the planing condition). It is evidently of interest to determine how far this process can be advantageously carried – or, in other words, what the optimum planing area is for supporting a given weight of boat at a given speed. The trend of the curves in Figure 1 is of interest in this connection. The curve for C_{Lb} equals 0.03, for example (which corresponds to a weight of 10,000 pounds, a beam of 8.54 feet, and a speed of 40 knots), indicates that the resistance will continue to decrease if the center of gravity is moved closer to the transom than the minimum distance represented in the graph (i.e., is moved close enough to the transom to give a value of l_{cp}/b less than 0.75). However, practical considerations will limit the extent to which planing area can be reduced by moving the *CG* towards the transom. For one thing, the practical utility of a boat will be severely restricted if the emphasis is on such a far-aft center of gravity that no significant items of weight (i.e., machinery, outfit, or payload) can be carried in the forward part of the boat. Also, the lower limiting value of l_{cp}/b of Figure 1, which was obtained from tests of models of unstepped hulls, corresponds to the minimum value which could be tested without causing the models to porpoise.

The practical result of the foregoing considerations is that it is necessary to resort to the stepped type of hull in order to be able to design for optimum lifting area and minimum resistance. When it is assumed that the hull type being designed is a stepped hull (with a

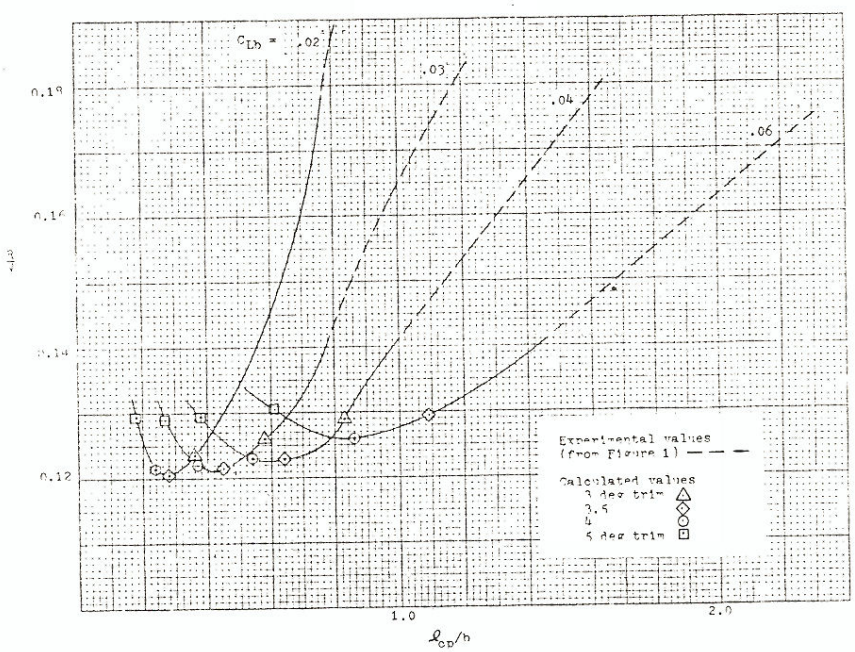

Figure 5. Resistance/weight ratio versus l_{cp}/b with C_{Lb} as parameter. Extended to low values of l_{cp}/b by calculation.

main forebody planing surface carrying most of the load), then the center of pressure location is measured forward of the step rather than forward of the transom. By positioning the step appropriately in relation to the *LCG* of the boat it is possible to design on the basis of the optimum value of l_{cp}/b – corresponding to the condition for minimum resistance. Furthermore, the permissible latitude in fore and aft positioning of the step means that the *LCG* can be located near the midpoint of the boat, and therefore the full length of the boat can be utilized for carrying useful items of weight.

In Figure 5, some of the curves of Figure 1 have been extended to the low values of l_{cp}/b corresponding to the points of minimum resistance. This was done by calculation – utilizing equations developed from the results of systematic tests of planing surfaces. The planing surfaces tested included the feature of sweptback trailing edges – a necessary characteristic in order to obtain the low values of l_{cp}/b corresponding to the points of minimum resistance. The calculations were made for 12½ degrees deadrise angle (i.e., the same deadrise as for the experimental results given in Figure 1). Trailing edge sweepback angle for the calculations was 55 degrees (corresponding to a step included angle of 70 degrees).

Each of the curves of Figure 5 has a point of minimum resistance, and the values of l_{cp}/b and trim corresponding to these points can be used to guide the development of designs having optimum efficiency. The curves show that optimum trim for the various loading conditions represented will generally be between 3.5 and 4 degrees, and that values of resistance/weight ratio as low as 0.121 can be attained. For the design example considered previously, corresponding to a value of C_{Lb} of 0.03, minimum resistance will be achieved with a ratio of l_{cp}/b of about 0.4. Hull resistance for the optimum stepped hull will accordingly be 1210 pounds (i.e., $0.121 \cdot 10{,}000$) – compared with resistance values ranging between 1700 and 2100 pounds for the various unstepped cases considered previously.

The results of some further studies, made to determine the optimum planing configurations for two different design conditions, are shown in Figure 6.

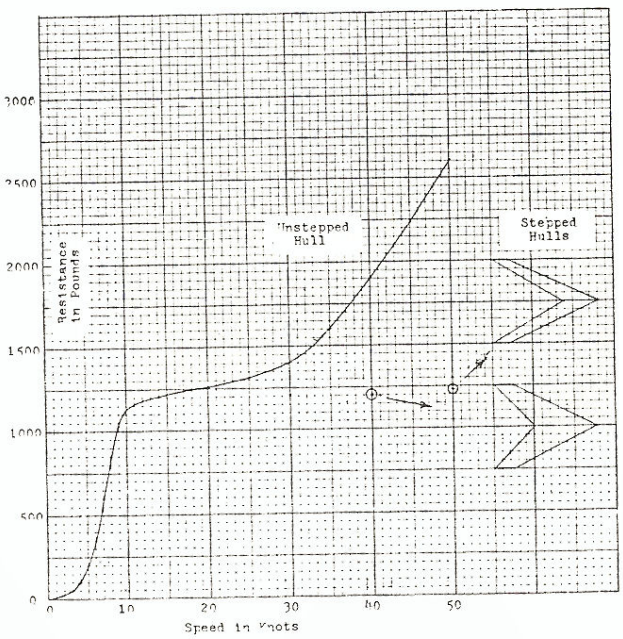

Figure 6. Resistance of two optimum planing configurations (stepped hull case) – compared with the resistance of a conventional unstepped hull. Boat weight in each case is 10,000 pounds, and deadrise is 12½ degrees.

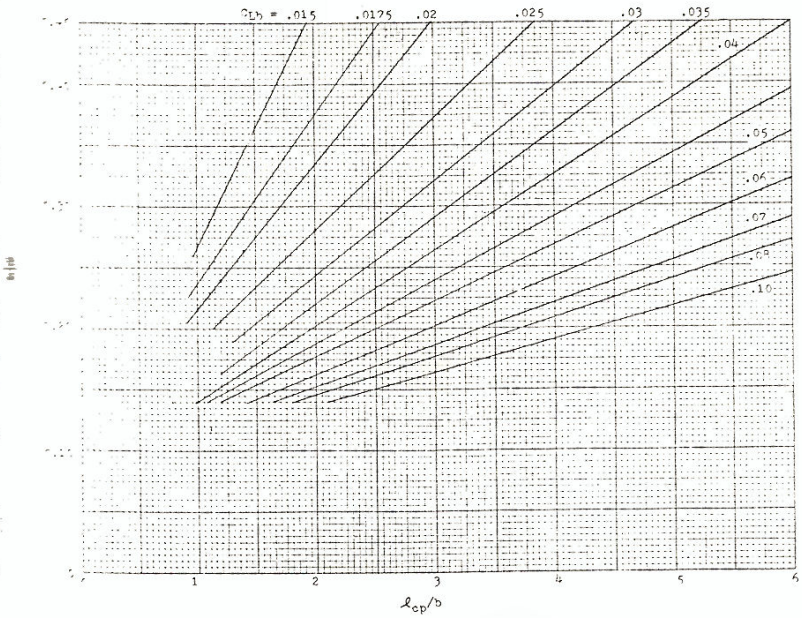

Figure 7. Resistance/weight ratio versus l_{cp}/b with C_{Lb} as parameter. Extended to high values of l_{cp}/b by straight-line extrapolation.

The planform configurations and resistance values are indicated for planing surfaces designed to carry a weight of 10,000 pounds at speeds of 40 and 50 knots. For both cases the deadrise angle has been taken as 12½ degrees, and the beam as 8.33 feet. Also shown, for comparison, is the resistance curve for a conventional unstepped planing hull having the same values of weight and deadrise angle, and approximately the same beam (this resistance curve is the same as that given in Figure 4 for a hull with $L/B = 3.1$).

In Figure 7, the upper (straight) portions of the curves of Figure 1 have been extrapolated to cover a wider range of design values. thereby extending into the range of values of C_{Lb} and l_{cp}/b corresponding to the case of high-speed offshore racers. Some checking by calculation has verified that reasonably accurate performance values would result from this extrapolation. An example will indicate how Figure 7 can be used to illuminate some aspects of the performance of these craft.

Assume the case of a boat weighing 4 tons, with *LCG* 12 feet forward of the transom, a design speed of 85 *mph*, a chine width of 6 feet, and a wetted bottom width at high speed of 3 feet. Assume, furthermore, that the basic deadrise angle of the hull bottom is 25 degrees, and that one-half of the hull bottom is covered by spray strakes having horizontal (zero deadrise angle) lower surfaces. For this admittedly somewhat extreme example the average bottom deadrise angle is 12½ degrees, and therefore Figure 7 can be assumed to be applicable. Figure 7 can now be utilized as follows:

Since $V = 85$ *mph*, then $v = 125$ *fps*, and since $\rho/2 = 1.00$ for salt water,

$$C_{Lb} = \frac{W}{\rho/2 \cdot v^2 \cdot b^2} = \frac{4 \cdot 2240}{(125)^2 \cdot (3)^2} = 0.064$$

Also, $l_{cp}/b = 12/3 = 4$

Then, from Figure 7, $R/W = 0.235$,
and $R = 0.235 \cdot 8960 = 2106$ pounds.

If, however, the bottom is assumed to be wetted over the full 6-foot chine width at high speed the values become:

$$C_{Lb} = \frac{4 \cdot 2240}{(125)^2 \cdot (6)^2} = 0.016, \text{ and } l_{cp}/b = 12/6 = 2.$$

In this case Figure 7 shows that R/W will be equal to 0.42, which corresponds to a value of boat resistance of:

$R = 0.42 \cdot 8960 = 3763$ pounds.

This example obviously illustrates very vividly the vital importance in the case of a deep-Vee hull of producing a running condition at high speed in which the wetted width is much less than the width over the chines.

It is also instructive to consider that if a stepped hull having the same 12½ degree average deadrise angle is assumed, then the minimum R/W value of 0.121 shown in Figure 5 can be attained, and the hull resistance at 85 *mph* will be:

$R = 0.121 \cdot 8960 = 1085$ pounds.

대한조선학회논문집
Journal of the Society of Naval Architects of Korea
pISSN:1225-1143, Vol. 51, No. 5, pp. 349-355, October 2014
eISSN:2287-7355, http://dx.doi.org/10.3744/SNAK.2014.51.5.349

무인고속전차를 이용한 활주선 모형의 저항시험 기법 연구

이영길[1] · 하윤진[2,†] · 정광열[2] · 채순재[1]
인하대학교 조선해양공학과[1]
인하대학교 대학원 조선해양공학과[2]

A Study on the Resistance Test Method for Planning Hull Model using the High Speed Towing Carriage

Young-Gill Lee[1] · Yoon-Jin Ha[2,†] · Kwang-Leol Jeong[2] · Soon-Jae Chae[1]
Dept. of Naval Architects and Ocean Engineering, Inha University[1]
Dept. of Naval Architects and Ocean Engineering, Graduate School of Inha University[2]

The resistance test of a high speed craft such as planing ship is performed with a high speed towing carriage instead of ordinary towing carriage because of the speed limitation. In the resistance test using high speed towing carriage, the model ship is fixed to the carriage to restrain the running attitude for enough measuring time. Such method is called fixed model test method. In the fixed model test method, to get the appropriate running attitude, the model test is iteratively repeated until the trim moment and lift force are close to zero. In this research, trim free model test method is investigated to reduce the number of iteration. And, the limitation of towing speed range in the trim free model test method is investigated.

Keywords : High-speed towing carriage(고속전차), Trim free model test(자유 트림 시험기법), Fixed model test(완전 구속 시험기법) Planing hull(활주선형), Ship resistance(선박 저항)

1. 서 론

활주선형 등 고속으로 항주하는 선박에 대한 모형 시험은 기존 예인전차의 속도와 수조 길이의 한계 등으로 인하여 많은 어려움이 있다. 고속선의 모형 시험 시 예인전차를 이용할 경우 예인가능 속도의 제한으로 모형선이 작아져야 하나 모형선이 작아지게 되면 모형 시험 결과의 신뢰성에 한계가 있을 것이다. 따라서 무인 상태에서 고속으로 예인할 수 있는 경량화된 고속전차가 필요하다. 인하대학교에서는 고속모형선의 저항시험을 위하여 최대 20m/s까지 예인할 수 있는 무인고속전차를 제작하였다. 하지만 무인고속전차가 고속으로 주행 할 때, 정속구간에서 모형선의 항주자세가 정상상태에 이르러야 하지만 충분한 수조 길이가 확보되지 않으면, 모형선의 항주자세가 정상상태에 이르기 전에 모형시험이 끝나게 될 수도 있다. 따라서 무인고속전차를 이용한 고속선 모형 시험 시 기존의 모형 시험기법과는 다른 모형 시험기법이 요구된다. Kawahara, et al. (1993)의 연구에서는 모형선의 침하를 자유롭게 하여 트림만을 고정시키는 모형 시험기법(이하 : 자유 침하 시험기법)에 대하여 제안하였다. 하지만 이 시험기법의 경우 분력계를 이용하여 추진축 방향의 힘을 측정하여 항주시 모형선에 작용하는 부양력과 트림모멘트가 0에 근접 할 때까지 반복시험을 수행하는 것이다. 그리고 추진축 방향의 힘을 측정하여 별도의 수식에 의하여 저항이나 부양력, 트림모멘트를 추정해야한다. Ikeda (1990)는 Kawahara, et al. (1993)의 연구와는 다르게 모형선의 침하와 트림을 모두 구속하고 저항과 부양력, 트림모멘트를 3분력계를 이용하여 직접 계측하는 모형 시험기법(이하 : 완전 구속 시험기법, fixed)을 제안하였다. 이 연구에서는 직접 각 방향의 힘들을 계측함으로써 수식에 의한 힘들의 추정을 수행하지 않은 장점이 있지만, 모형선의 침하와 트림을 모두 구속하여 실험하기 때문에 예인 횟수가 증가하게 된다. 따라서 Lee, et al. (2008)은 이러한 단점들을 극복하고자 모형선의 트림을 자유롭게 하여 침하만을 구속하는 모형 시험기법(이하 : 자유 트림 시험기법, trim free)을 제안하였다. 이 연구에서는 완전 구속 시험기법에 비하여 예인 횟수가 줄었으며, 저항과 침하, 트림이 정성적, 정량적으로 완전 구속 시험기법과 근접한 결과를 보였다.

본 연구에서는 Lee, et al. (2008) 연구에서의 고속선 모형 속

접수일 : 2013년 4월 1일 | 1차 수정일 : 2014년 5월 9일 | 게재확정일 : 2014년 6월 10일
† Corresponding author : yj_ha0811@hanmail.net, 032-860-8840

도보다 고속으로 예인할 수 있는 고속선 모형으로 자유 트림 시험기법에 대한 모형 시험 결과의 신뢰성과 시험기법의 유용성을 파악하고 가능한 모형 시험 속도영역을 파악하여 보았다.

2. 무인고속전차

인하대학교에서는 고속선 모형 시험을 수행하기 위하여 최대 20m/s까지 예인할 수 있는 무인고속전차를 제작하였다.

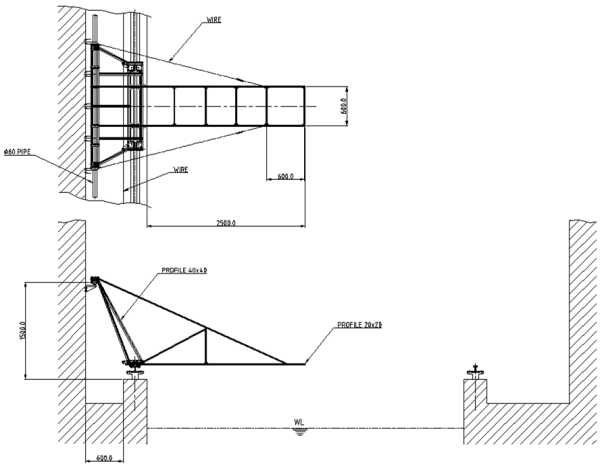

Fig. 1 Plan of the high speed towing carriage

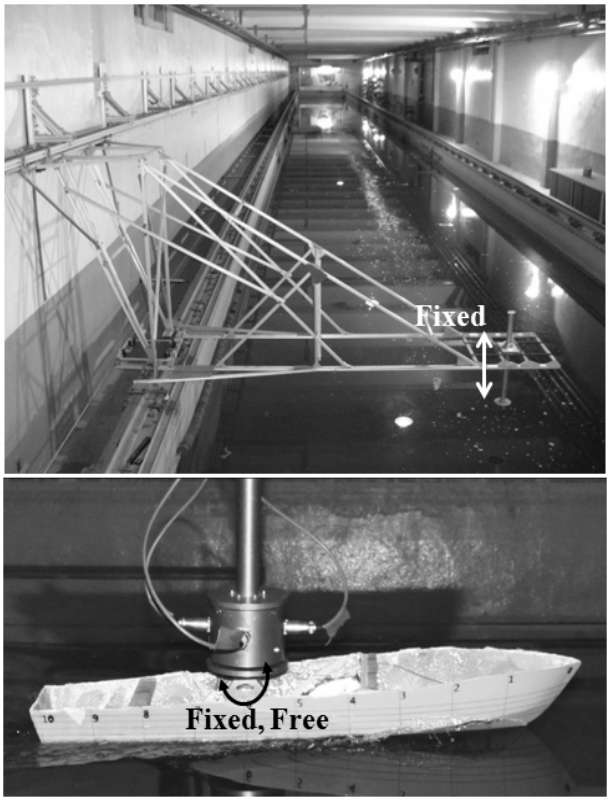

Fig. 2 Adjustment methods of sinkage and trim of a model ship

Fig. 1과 같이 truss구조로 제작되었으며, 외팔보의 형식이다. 모형시험 시 모형선의 침하, 트림 조정 방법은 Fig. 2와 같이 무인고속전차에 축을 두어 이를 고정하는 방식으로 모형선의 침하는 구속시킨다. 축 아래에는 3분력계가 설치되며, 3분력계와 모형사이에 포텐쇼메타가 설치되어있는 부분에 힌지로 트림을 자유롭게 하였으며, 힌지부분을 고정시키게 되면 트림을 구속시킬 수도 있다.

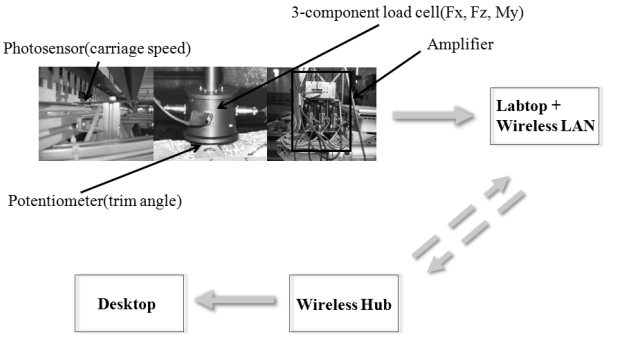

Fig. 3 Measuring system for the high speed towing carriage

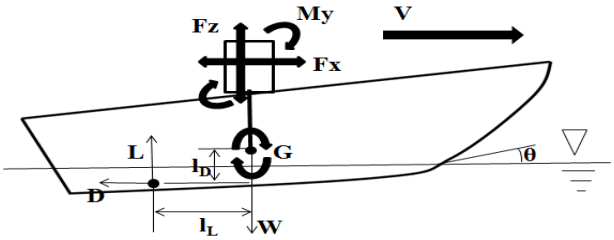

Fig. 4 Free body diagram of a towing model ship

Fig. 3은 모형 시험을 위한 계측시스템이다. 무인고속전차의 경우 모형 시험 시 무인으로 모형선을 예인하기 때문에 무선계측시스템을 구성하였다. 무인고속전차의 속도는 선형시험수조 측면에 펄스판을 설치하여 포토센서로 계측을 수행하며, 모형선의 힘들과 트림 각은 각각 3분력계, 포텐시오메타로 계측한다.

3. 완전 구속 시험기법과 자유 트림 시험기법 비교

3.1 모형 시험기법 비교

무인고속전차를 이용한 고속선 모형 시험은 수조 길이의 한계로 인하여 예인전차와는 다른 모형 시험기법이 요구된다. 따라서 Ikeda (1990)의 연구와 같이 완전 구속 시험 기법으로 모형 시험을 수행할 수 있다. 이 모형 시험기법은 Fig. 4와 같이 모형선의 침하와 트림을 구속하고 3분력계를 이용하여 항력과 부양력, 트림모멘트를 계측하는 것이다.

$$L - W = F_Z \quad (1)$$

$$L \cdot l_L + D \cdot l_D = M_Y \quad (2)$$

각 속도마다 식 (1)과 (2)에서 부양력과 트림모멘트가 0에 가까워질 때 항력(저항)을 얻어내는 것이다. 하지만 이 모형 시험기법의 경우 Fig. 4에서 부양력과 트림모멘트가 0에 근접해질 때까지 모형선의 침하와 트림을 반복적으로 조정해주어야 한다. 따라서 많은 예인 횟수가 필요할 것으로 예상된다. Lee, et al. (2008)의 연구에서 자유 트림 시험기법은 침하만을 조정하고 트림은 자유롭게 두어 부양력과 트림모멘트가 0에 근접해질 때까지 반복적으로 모형 시험을 수행하는 방법이다. 즉, 자유 트림 시험기법에서의 모형선 트림 각은 정상상태에서 완전 구속 시험기법의 트림 각과 근접해질 때, 부양력과 트림모멘트가 0에 근접해지는 것이다. 따라서 이 방법은 침하만을 조정하기 때문에 완전 구속 시험기법보다 예인 횟수가 줄어들 가능성이 있다.

3.2 모형 시험결과 비교

본 절에서는 Lee, et al. (2008)의 연구결과였던 완전 구속 시험기법과 자유 트림 시험기법을 이용한 모형 시험결과들을 재검토하였다. 이 연구에서는 고속경비정 M5008 선형(West Japan Fluid Engineering Laboratory Co., LTD, 2005)으로, Fn▽=0.78에서 Fn▽=3.73까지 모형 시험을 수행하였다. Fig. 5는 Fn▽=3.73에서 완전 구속 시험기법과 자유 트림 시험기법의 예인 횟수를 비교한 것이다. 완전 구속 시험기법의 경우 6번 정도 침하와 트림을 조정하여 예인하였을 때, 부양력과 트림 모멘트가 0에 근접해가는 것을 볼 수 있으며, 자유 트림 시험기법의 경우 3번 정도만 침하만 조정하여 예인하여도 부양력과 트림 모멘트의 힘들이 0에 근접해지는 것을 확인할 수 있다. 하지만 트림 각의 경우 두 모형 시험기법 모두 참고문헌 (West Japan Fluid Engineering Laboratory Co., LTD, 2005)에서의 모형 시험결과와 근접하지 않는 것을 볼 수 있다. 이는 참고문헌 (West Japan Fluid Engineering Laboratory Co., LTD, 2005)의 모형 시험결과의 경우 본 실험결과와 모형 시험조건이 다르기 때문에 오차를 보이는 것으로 예상되며, 추후 고찰이 필요할 것으로 생각된다. 하지만, 두 기법 모두 부양력과 트림모멘트의 힘들이 0에 근접해 졌을 때 트림 각의 정량적인 결과는 매우 근접한 것을 확인할 수 있다.

Fig. 6은 두 모형 시험기법을 이용하여 Fn▽=3.73에서 부양력과 트림모멘트가 0에 근접하였을 때, 계측결과들의 시간기록이다. 계측 결과들을 보면, 무인고속전차의 정속구간에서 약 7초 정도 유용한 결과가 얻어지는 것을 확인할 수 있다. 또한, 이 구간에서 두 모형 시험기법들의 항력과 트림 각이 정량적으로 근접한 것을 확인할 수 있으며, 자유 트림 시험기법의 경우 모형선의 트림 각이 무인고속전차의 정속구간에서 정상상태에 이른 것을 확인할 수 있다. 또한 Fig. 7은 전 속도구간에서의 모형 시험결과이다. 저속구간에서는 예인전차로 가능한 속도 구간까지 모형 시험을 수행하였으며, 두 속도영역에서 예인전차와 무인고속전차의 모형 시험결과를 비교하였다. 예인전차와 무인고속전차의 모형 시험결과를 비교하여 정량적으로 그 결과가 매우 근접한 것을 확인할 수 있다. 따라서 무인고속전차 모형 시험결과의 신뢰성을 파악할 수 있다.

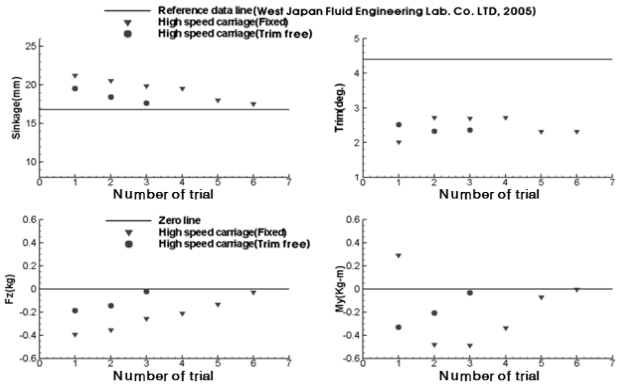

Fig. 5 Comparison of the fixed and the trim free model test methods (M5008, Fn▽ = 3.73, towing speed = 4.50m/s)

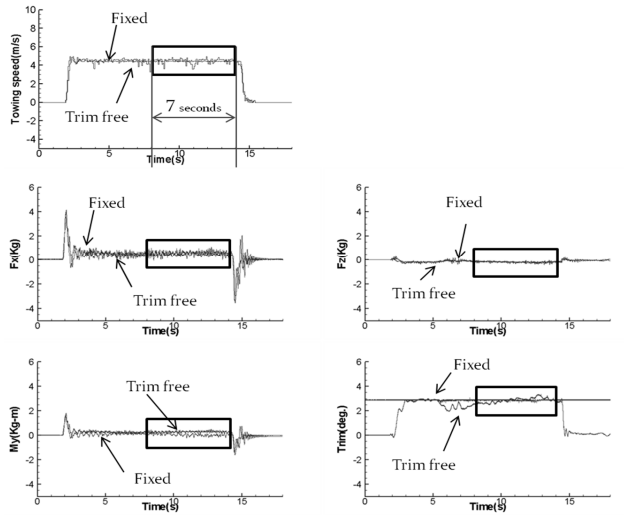

Fig. 6 Time histories of experimental results from the fixed and the trim free model test methods (M5008, Fn▽ = 3.73, towing speed = 4.50m/s)

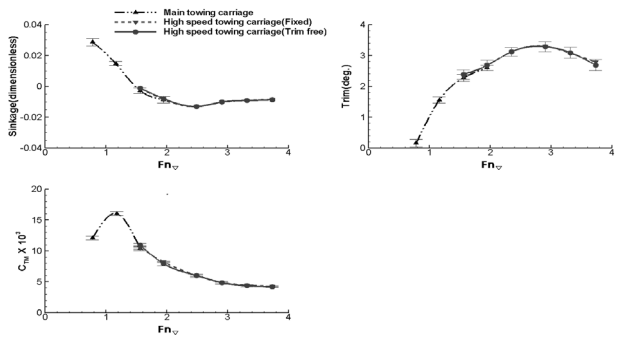

Fig. 7 Comparison of the total resistance coefficient, the sinkage and the trim angle of the model ship (M5008)

또한, 완전 구속 시험기법과 자유 트림 시험기법을 비교하면, 두 모형 시험기법 모두 정량적, 정성적으로 매우 근접한 것을 확인할 수 있다. 따라서 무인고속전차 모형 시험결과의 신뢰성과 자유 트림 시험기법의 유용성을 파악하였다.

4. 대상 모형

Lee, et al. (2008)에서의 선형보다 고속으로 예인할 수 있는 DTMB Series No. 62 Model 4667-1 선형 (Clement & Blount, 1963)을 이용하여 자유 트림 시험 기법에 대하여 모형 시험을 수행하였다(Fig. 8). 본 선형의 주요제원은 Table 1과 같으며, 최대 Fn▽=5.54(예인속도 : 6.38m/s)까지 예인시키기 때문에 모형선의 강도를 고려하여 FRP로 제작하였다. 또한 모형 크기결정은 무인고속전차가 외팔보이기 때문에 그 안정성을 고려하였다.

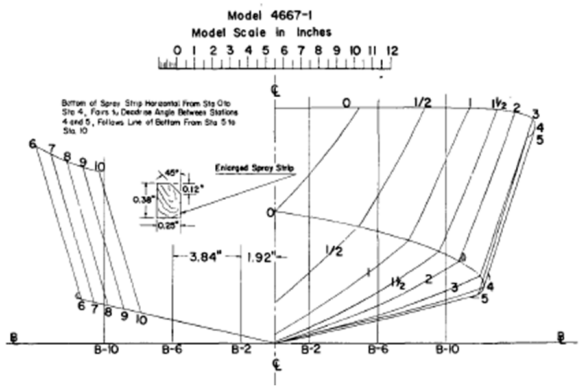

Fig. 8 Body plan of the DTMB Series No. 62 Model 4667-1

Table 1 Principal dimensions of the DTMB Series No. 62 Model 4667-1

	Reference model (Clement & Blount, 1963)	Model(IUTT)
Scale ratio	1/3.048	
LBP (m)	2.438	0.800
Breadth (m)	0.596	0.196
Draft, moulded F.P. (m)	0.103	0.034
Draft, moulded A.P. (m)	0.106	0.035
Displacement (Kg)	68.150	2.407
Range of Fn▽	0.26 ~ 5.54	

5. 모형 시험 기법 및 결과

본 연구에서는 Lee, et al. (2008)에서의 선형보다 고속으로 예인할 수 있는 DTMB Series No. 62 Model 4667-1 선형으로 자유 트림 시험 기법을 이용하여 모형 시험을 수행하였다. 침수표면적은 모형을 투명하게 제작하여 모형 시험 시 촬영을 통하여 계측을 수행하는 것이 관례이지만, 항주자세가 Clement and Blount (1963)의 모형 시험결과에 근접하기 때문에 Clement and Blount (1963)의 침수표면적 자료를 이용하였다.

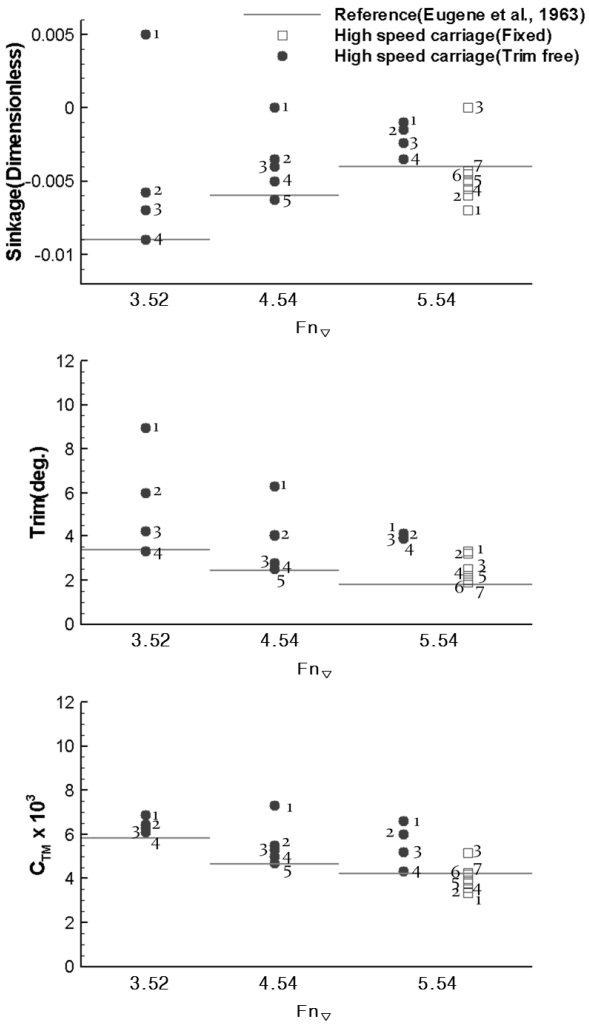

Fig. 9 Number of trials of the model tests (DTMB Series No. 62 Model 4667-1, Fn▽ = 3.73, 4.54, 5.54, towing speed = 4.05, 5.23, 6.38m/s)

Fig. 9는 모형 시험 시 Fn▽=3.52, 4.54, 5.54에서의 예인 횟수이다. Fn▽=3.52와 4.54에서는 각각 4, 5번 정도 예인하였을 때, Clement and Blount (1963)의 모형 시험결과와 근접한 것을 확인할 수 있다. 따라서 Lee, et al. (2008)의 연구(Fig. 5)와 본 연구의 결과를 비교하면, 자유 트림 시험기법은 3~5번 정도의 예인 횟수로 정량적인 결과를 얻을 수 있을 것으로 생각된다. 하지만 Fn▽=5.54에서는 4번 정도 예인하였을 때, 침하와 전저항계수의 경우 Clement and Blount (1963)의 결과와 근접하였지만, 트림 각의 경우 큰 오차를 보인다. 이를 확인하기 위하여 각

계측결과들의 시간기록을 확인하여 보았다. Fig. 10은 자유 트림 시험기법을 이용하여 Fn▽=4.54에서 부양력과 트림모멘트의 힘들이 0에 근접하였을 때, 계측결과들의 시간기록이다. 계측 결과들을 보면, 무인고속전차의 정속구간에서 약 4초 정도 유용한 결과가 얻어지는 것을 확인할 수 있다. 또한 모형선의 트림 각이 무인고속전차의 정속구간에서 정상상태에 이른 것을 확인할 수 있으며, Fig. 9에서와 같이 Clement and Blount (1963)의 모형 시험결과와 근접한 결과를 보인다. Fig. 11은 완전 구속 시험기법과 자유 트림 시험기법으로 Fn▽=5.54에서의 모형 시험결과이다.

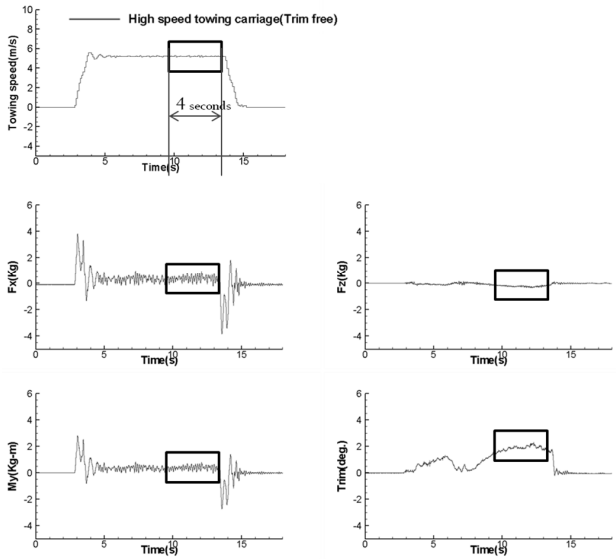

Fig. 10 Time histories of experimental results from the trim free model test method (DTMB Series No. 62 Model 4667-1, Fn▽ = 4.54, towing speed = 5.23m/s)

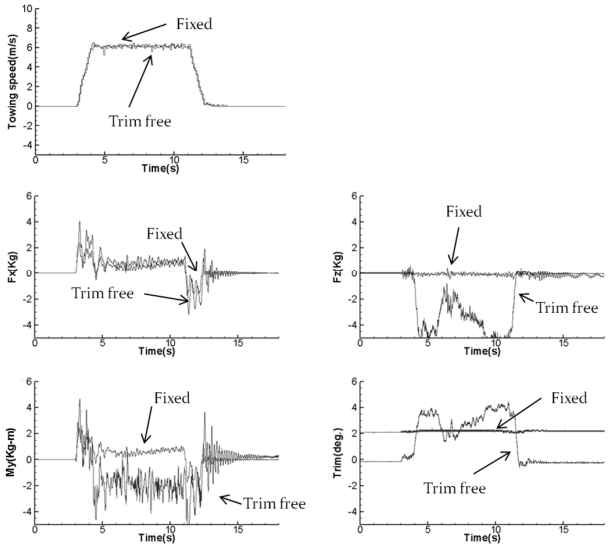

Fig. 11 Time histories of experimental results from the fixed and the trim free model test methods (DTMB Series No. 62 Model 4667-1, Fn▽ = 5.54, towing speed = 6.38m/s)

완전 구속 시험기법의 경우 부양력과 트림모멘트의 힘들이 0에 근접하였을 때의 결과이며, Fig. 9에서 확인할 수 있는 바와 같이 7번 정도 예인하여 Clement and Blount (1963)의 모형 시험결과와 정량적으로 근접하였다. 하지만 Fig. 11에서 자유 트림 시험기법의 경우 트림 각이 완전 구속 시험기법에 비하여 큰 결과를 보인다. 이는 무인고속전차의 정속구간에서 트림 각이 정상상태에 이르지만, Fig. 11에서 보이는 바와 같이 Fn▽=5.54에서 무인고속전차의 가속구간에서 모형선은 과도한 선미트림이 일어나고, Fig. 12를 보면, Fn▽=4.54에 비하여 Fn▽=5.54에서 선체에 스프레이 현상이 크게 일어나는 것을 확인할 수 있다. 무인고속전차의 가속구간에서 선체에 일어나는 큰 스프레이 현상으로 인하여 정속구간에서 트림 각이 작아지지 않는 것으로 생각된다. 또한 이러한 영향으로 인하여 3분력계로 계측된 결과들의 동요가 매우 큰 것으로 생각되며, Fn▽=5.54정도 이상의 속도영역에서는 자유 트림 시험기법을 이용한 모형 시험이 어려운 것으로 판단된다. Fig. 13은 전 속도구간에서의 모형 시험결과이다. Fig. 7과 마찬가지로 저속구간에서는 예인전차로 가능한 속도 구간까지 모형 시험을 수행하였다. Clement and Blount (1963)과 예인전차, 무인고속전차의 모형 시험결과들을 비교하였을 때, 정량적, 정성적으로 그 결과들이 매우 근접한 것을 확인할 수 있다. Fn▽=5.54를 제외하고 보다 고속영역에서 Clement and Blount (1963)과 무인고속전차 모형 시험결과를 비교하면, Fn▽=4.54까지는 매우 정량적, 정성적으로 근접한 것을 확인할 수 있으며, 약 4초 정도의 계측결과를 얻어낼 수 있다. 따라서 Fn▽=4.54까지는 자유 트림 시험기법이 무인고속전차를 이용한 모형 시험 시 매우 유용할 것으로 판단된다.

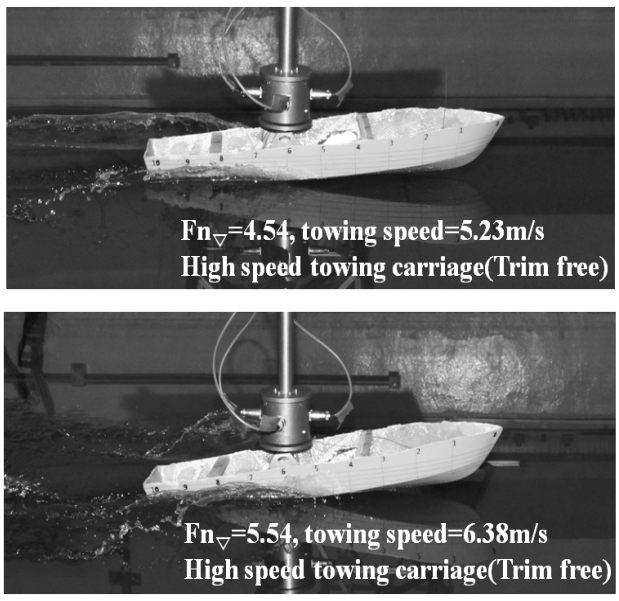

Fig. 12 Photographs of the model tests at Fn▽ = 4.54, 5.54 (DTMB Series No. 62 Model 4667-1, trim free, towing speed = 5.23, 6.38m/s)

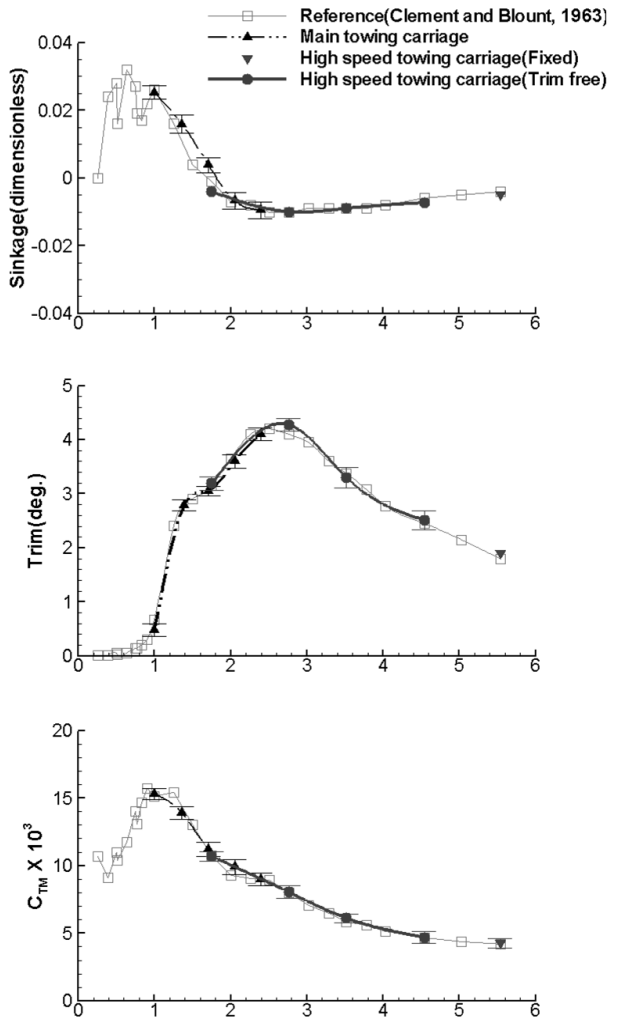

Fig. 13 Comparison of the total resistance coefficients, sinkages and trim angles of the model ship (DTMB Series No. 62 Model 4667-1)

하지만 본 연구 결과만을 확인하였을 때, Fn∇=5.54이상의 속도영역에서는 무인고속전차의 가속구간에서 모형선의 과도한 선미트림으로 인하여 자유 트림 시험기법을 이용한 모형 시험은 어려운 것으로 생각되며, 예인 횟수가 많아지지만 Fn∇=5.54이상의 완전 구속 시험기법을 이용하는 것이 적절할 것으로 판단된다.

6. 결 론

본 연구에서는 활주선형을 이용하여 자유 트림 시험기법의 유용성을 파악하고 모형 시험이 가능한 속도영역을 파악하여 보았다.

1) Lee, et al. (2008)의 연구에서는 완전 구속 시험기법과 자유 트림 시험기법을 비교하였을 때, 자유 트림 시험기법이 3번 정도로 예인 횟수를 줄였다. 또한 본 연구의 결과로 봤을 때, Fn∇= 5.54에서 완전 구속 시험기법으로는 예인 횟수 7번 정도가 필요하였으며, 자유 트림 시험기법을 이용하여서는 최대 5번 정도의 예인 횟수가 필요하다. 따라서 자유 트림 시험기법이 완전 구속 시험기법에 비하여 예인 횟수를 줄일 수 있다.

2) 본 연구 결과에서 Fn∇=5.54의 모형 시험결과는 무인고속전차의 가속구간에서 과도한 선미트림으로 인하여 큰 스프레이 현상이 발생하며, 이로 인하여 무인고속전차의 정속구간에서 트림 각이 감소하지 않았다. 완전 구속 시험기법을 이용하였을 때, 많은 예인 횟수가 요구되었지만, 정량적으로는 Clement and Blount (1963)과 근접한 결과를 보인다. 모형 시험 시 초기트림을 주거나, 무인고속전차의 가속구간이 길어 천천히 무인고속전차가 가속하게 되면, 초기에 모형선의 과도한 선미트림이 발생하지 않을 것으로 예상된다.

3) 본 연구 결과를 예인전차와 Clement and Blount (1963)의 모형 시험결과들과 비교하였을 때, 정량적, 정성적으로 매우 근접하며, Lee, et al. (2008)의 연구 결과에서도 정도 높은 모형 시험결과를 보인다. 따라서 무인고속전차를 이용하여도 정도 높은 모형 시험이 가능하며, 자유 트림 시험기법이 무인고속전차를 이용한 모형 시험에서 매우 유용한 모형 시험기법으로 판단된다.

4) 자유 트림 시험기법은 완전 구속 시험기법에 비하여 예인 횟수를 줄일 수 있지만, 본 연구 결과만을 보았을 때, Fn∇=4.54정도의 속도영역까지 모형 시험이 가능한 것으로 판단된다. 또한 자유 트림 시험기법을 이용할 때, Fn∇=4.54이하의 속도영역까지는 약 4초 이상의 계측된 데이터를 해석할 수 있다. Fn∇=5.54이상의 속도영역에서는 자유 트림 시험기법에 비하여 예인횟수가 많지만, 완전 구속 시험기법을 사용하는 것이 적절할 것으로 판단된다.

5) 본 연구에서는 Clement and Blount (1963)에서 계측된 침수표면적 결과가 있어 모형선의 침수표면적을 직접 계측하지 않았다. 새로운 고속선 모형 시험 시 모형선을 투명하게 제작하여, 촬영을 통하여 침수표면적을 계측할 것이며, 이를 저항 시험과 동시에 수행하므로 무인고속전차를 이용하였을 때 충분한 모형 시험이 가능할 것으로 생각된다.

후 기

이 논문은 인하대학교의 지원에 의하여 연구되었음.

References

Clement, E.P. & Blount, D.L., 1963. Resistance Tests of a Systematic Series of Planing Hull Forms. *Taransactions of The Society of Naval Architects and Marine Engineering*, 71.

Ikeda, Y., 1990. Measurement of hydrodynamic forces acting on a high-speed craft model fixed to a three-component load-cell on a carriage. *Proceeding of the 19th International Towing Tank Conference*, Madrid, Kingdom of Spain, 2, December 1990.

Kawahara, U. Suzuki, K. & Yabushita, K., 1993. Resistance Test Method for High-Speed Boats by Using a Trim Fixed Type of Dynamometer. *Jounal of Kansai Society Naval Architects*, Japan, 220, pp. 71-82.

Lee, Y.G. Ha, Y.J. Kim, K.S. & Chae, S.J., 2008, A Development on the method of resistance test using unmanned high-speed towing carriage. *Proceedings of the Society of Naval Architects of Korea*, Jeju, Republic of Korea, 30, May 2008, pp. 1243-1249.

West Japan Fluid Engineering Laboratory Co., LTD., 2005. *Tank Test of High speed planing hull, Nagasaki Pref. Japan, Report No. 11283-1*. Japan: West Japan Fluid Engineering Laboratory Co.

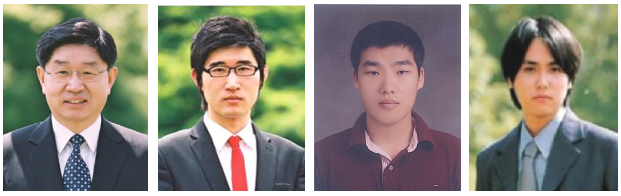

이 영 길 | 하 윤 진 | 정 광 열 | 채 순 재

SYMPOSIUM YACHT ARCHITECTURE '73

Third symposium on developments of interest to yacht architecture, under the auspices of the HISWA.
This symposium was held 21 - 22 March 1973, under the chairmanship of Prof. Ir. J. Gerritsma.

Under the auspices of: HISWA, 412 Keizersgracht, Amsterdam, Holland.
Publisher: Interdijk B.V., Schiphol-Oost, Holland

"THE INFLUENCE OF WEDGES ON THE PERFORMANCE OF PLANING HULLS"

BY

A.J. COLE AND A. MILLWARD

ABSTRACT

The paper describes a series of experiments which investigate the effects of fixed trailing edge wedges on the resistance characteristics of a planing hull. The hull design used was the DTMB Series 62 Revised Parent Model No. 4667-1. Two series of results are presented, the effect of a single wedge under varying hull loading conditions, and the effects of different wedges under one of these loading conditions.

Whether the wedges increased or decreased resistance was seen to be dependent on the loading conditions, the shape and size of the wedge itself, and the speed of the craft. It was found that a wedge became more effective in reducing the resistance as the displacement was increased, and also as the longitudinal centre of gravity of the craft moved aft. Under a given loading condition, there was an optimum for both the length and angle of the wedge, above and below which either its advantageous effect decreased, or its detrimental effect increased.

1. INTRODUCTION

It was Froude who first resolved the resistance of a ship into components as a basis for model testing. He divided the total into the frictional resistance, due to the shear forces at the hull surface, and the residual resistance, due to all the remaining forces acting on the craft. This division remains a useful basis from which to consider the minimisation of the resistance of a planing hull. Fig. 1 (taken from ref. 1) shows the total, frictional, and residual resistances for a planing craft at a fixed speed, with a varying angle of trim. It can be seen that to reduce the residual resistance, the craft should be run at the flattest angle that will afford the necessary lift. On the other hand, to reduce frictional resistance it should be run at the steepest angle that will leave sufficient surface for the lift. The most suitable compromise will therefore depend on the relative importance of the two resistance components, which will be a function of, among other things, the speed of the craft. This suggests that it may be advantageous to be able to alter the trim of a craft at its cruising speed from its normal attitude.

The first mention of any form of conscious trim control seems to appear in ref. 2. During the last war, German E-boats were fitted with twin auxiliary rudders, level with, and on either side of the propellers. As the boat gained speed, these were each turned outward at an angle of 10 or 15 degrees which had the effect of reducing the resistance appreciably. The author of ref. 2 suggests that their purpose was to delay squatting by the stern, thus reducing the wavemaking resistance. In the written discussion following ref. 3, Du Cane mentions a boat competing in the 1966 Rouen 24 hour race which had a moveable transom flap to adjust her trim. In the same discussion, Clement suggests a pair of independently adjustable transom flaps to correct both trim and undesirable heel angle.

Since these first stirrings, stern flaps have been optimised for individual boats, but no basic investigation of their properties appears to have been carried out. Both stern flaps and trailing edge wedges have been tested on planing craft in the towing tank at the University of Southampton, but this again on an individual optimisation basis for commercial use. The aim of the present work was to investigate the value of adding fixed wedges to a standard planing hull, under a systematic series of conditions.

Wedges were chosen rather than adjustable flaps as they are a simpler and more basic design feature. If a wedge can be found to improve the performance of a given hull, then once it is fitted no more control is necessary. With adjustable flaps another variable (i.e. the inclination of the flap) is introduced into the control of the boat, making operation more complex.

2. NOTATION

A_p = projected planing bottom area (m^2)

B_{pA} = mean breadth over chines A_p/L_p (m)

B_{pT} = breadth over chines at transom (m)

B_{px} = maximum breadth over chines (m)

F_∇ = Froude Number based on the cube root of the volume of water displaced at rest

$$(F_\nabla = \frac{V}{\sqrt{g(\nabla^{1/3})}})$$

L_p = projected chine length (m)

LCG = longitudinal centre of gravity

R = total resistance (kg)

R_e = Reynolds Number, based on arithmetic mean of wetted keel and chine lengths

S	=	wetted surface area, including area of sides wetted at low speeds but excluding area wetted by spray (m^2)
V	=	velocity of water in working section of channel (m/s)
W	=	displacement at rest (kg)
h	=	vertical displacement of centre of gravity from rest position (mm); positive values signify upward displacement
ℓ	=	length of wedge in direction parallel to keel (mm)
∇	=	volume of water displaced at rest (m^3)
α	=	trim angle (degrees)
β	=	angle between planing surface of wedge and planing surface of hull, measured in direction parallel to keel (degrees)
λ	=	length of wedge as a fraction of projected chine length ($\lambda = {}^{\ell}/L_p$)

3. THE MODEL

The DTMB Series 62 Revised Parent (ref. 4) design was chosen for the hull and a glass reinforced plastic (GRP) model was made one half* of the size of the original DTMB model, i.e. 1.22 m (4.00 ft.) projected chine length.** The body plan and form characteristics of the model are shown in Fig. 2. The reasons for choosing this particular design of hull were twofold. Firstly, it is the basic design for the most comprehensive set of resistance tests ever carried out on planing craft (ref. 4), and so the hull is becoming accepted as a standard form. Secondly, time limits the scope of the present work, both in the number of variables which can be considered, and in the range over which those chosen can be observed. Should it be possible to extend the tests sometime in the future, to investigate for instance the effect of changing the length/beam ratio of the hull on the usefulness of the wedges, the DTMB series would provide an ideal basis for such work.

For a given hull size and design, the two variable factors which affect the planing characteristics are the displacement (W) and the longitudinal position of the centre of gravity (LCG). In this paper these two variables are defined using the parameters described by Clement and Blount (ref. 4). The displacement is expressed as the dimensionless ratio $\frac{Ap}{\nabla^{2/3}}$ where Ap is the projected planing bottom area and ∇ the volume of water displaced at rest. The longitudinal centre of gravity position is defined as the distance of the LCG from the centroid of Ap, expressed as a percentage of the projected chine length Lp. Both these parameters were varied in the tests by moving ballast weights in the hull.

The larger wedges were made from wood and the smaller ones of GRP. They were attached to the hull using waterproof adhesive. As may be seen in Fig. 3, when the hull has deadrise there are actually two wedges, one on each planing surface, joining at the keel. The wedge may be adequately described using two parameters; its length, measured in a direction parallel to the keel of the hull and conveniently expressed as a fraction of the projected chine length (λ), and the angle (β) which the surface of the wedge makes with the bottom planing surface of the hull, again measured in a direction parallel to the keel. The leading edge of the wedge is perpendicular to the keel, and the trailing edge and sides made flush with the transom and upper hull surfaces respectively.

* This was the largest model which could be used in the channel before width effects became appreciable.

** The authors express their gratitude to Commander Dalla Mura of the U.S. Office of Naval Research for help in obtaining the lines of the model.

4. THE RECIRCULATING WATER CHANNEL

The test programme was carried out in the Recirculating Water Channel ("Flume") at the University of Liverpool, and since the use of such a facility as opposed to a towing tank is unusual in quantitative ship model testing, a brief description seems appropriate. A more detailed account of the design and operation of the flume is given by Preston (ref. 5).

The channel (Fig. 4) has a capacity of nearly 90,800 litres (20,000 gallons) of water, circulated by a 100 h.p. motor driving an axial flow impeller. On leaving the impeller, the water passes through a long, circular section diffuser, after which the cross-section of the channel becomes rectangular. Two sets of vanes and a honeycomb minimise the swirl, and the flow is accelerated through a contraction into the working section. This has a moveable false floor, which is adjustable in height and inclination to give a flat, level free surface at the required operating speed. After the working section, the topmost layer of water is separated from the flow by the first adjustable flap, or "splitter plate". This narrow layer, travelling at a super-critical speed, contains nearly all the air bubbles caused by the presence of a model in the working section. The water in the layer is slowed to sub-critical speed by a deepening after the splitter plate, and the slower movement of this portion of the flow allows the air time to escape to the surface before the water is re-introduced to the main flow at the second adjustable flap.

The flow velocity in the working section can be set and measured to an accuracy of ± 1%, the maximum speed being in the region of 6.1 m/s (20 ft./s). Due to the adjustable floor in the working section, any speed in this range can be maintained without the presence of either standing waves or a hydraulic jump. If the floor is left fixed at its lowest position the critical speed is in the region of 2.7 m/s (9 ft./s).

Early work on the flume showed that the wake at the free surface, caused by the boundary layer on the upper surface of the contraction, was appreciable, the velocity defect being large enough to render any work on shallow draft surface craft useless, so to correct this, a jet-bleed was introduced. Water is bled off from the lowest point of the system and pumped back into the main flow through a 1 mm wide slot, running the whole breadth of the channel, at the beginning of the working section (Fig. 5). By adjusting the pump speed, a velocity profile can be obtained which deviates less than ± ½% from stream velocity to within 1 cm of the free surface.

5. EXPERIMENTAL ARRANGEMENTS AND TEST PROGRAMME

The model was mounted over the flume on a balance which allowed it to pitch and heave, while measuring its resistance and vertical displacement from rest. An indicator mounted at the bow recorded the trim as well as providing a restraint against a sudden unstable yawing force (see Fig. 6). Scales along the keel, chine, and transom of the model allowed the respective wetted lengths and heights to be measured. Earlier work has shown that no turbulence stimulation is necessary when working with planing models in the flume at speeds upwards of 1.2 m/s (4 ft./s).

Preliminary tests showed that under most conditions the maximum possible water speed was in the region of 4.3 m/s (14 ft./s). Above this speed an excessive amount of water from the wake of the model was thrown clear of the working section into the laboratory. Apart from the more obvious disadvantages, this has the effect of reducing the total volume of water in the flume, thus disturbing the free surface. This maximum speed typifies a military-style planing craft travelling at about 21 m/s (35 knots), and while far from ideal, was considered an acceptable maximum. Moreover it was subsequently found that the pattern of behaviour produced by most wedges was adequately described by the time the model reached this maximum speed. Work is now in hand on modification of the flume to permit higher maximum speeds to be used on this type of work in the future.

The test programme was in two parts. Firstly, using a single small wedge, $\frac{Ap}{\nabla^{2/3}}$ and the LCG position were varied, to discover the broad limits of the effectiveness of wedges in general. Secondly, at fixed values of $\frac{Ap}{\nabla^{2/3}}$ and LCG position, the length and angle of the wedge was varied to see if an optimum wedge shape could be found. The wedges used were as follows:-

Wedge Length / Chine Length	Wedge Angle
λ	β^0
0.05	2, 5 and 10
0.10	2, 5 and 10
0.15	2, 5 and 10

The smallest wedge (i.e. $\lambda = 0.5$, $\beta = 2^0$) only was used in the first part of the test programme.

Accuracy

The quantities measured are believed to be accurate within the limits shown below. The first column indicates the division to which the measuring device may be read, and the second, the overall accuracy of the readings when fluctuations in the flow are considered.

Resistance (kg)	0.001	± 0.005
Trim (deg)	0.01	± 0.05
Height Change of C of G (mm)	0.2	± 0.5
Wetted Lengths of Keel and Chines (mm)	10	± 10
Wetted Height of Side at Transom (mm)	1	± 2

As mentioned before, the speed of the flow can be set to ±1%. The speed control mechanism is more sensitive than this, but the overall accuracy is limited by its pitot-tube calibration.

6. DISCUSSION OF RESULTS

The results presented apply directly to the model used, but the wetted surface area and Reynolds Number under each set of operating conditions have been calculated and included in the accompanying tables. Thus the figures may be scaled to any size of model or boat if required. The representative length used in calculating the Reynolds Number is the arithmetic mean of the wetted keel and wetted chine lenghts.

First under consideration is the effect of a single wedge on the planing characteristics of the model under varying loading conditions (Figs. 7 - 12). Fig. 7 shows the DTMB standard condition for planing craft (discussed in ref. 6). This is included mainly for incidental interest but does show that the wedge is ineffective under these loading conditions over the whole speed range.

The effect of the wedge on resistance, trim, and vertical displacement of the centre of gravity when $\frac{Ap}{\nabla^{2}/3}$ is held constant can be seen in Figs. 8 - 10. These show a heavy displacement condition. At the furthest forward LCG position (Fig. 8) the addition of the wedge actually increases the resistance, but as the LCG moves aft the wedge becomes more useful both increasing the amount of drag reduction and increasing the range over which it is effective. The amount which trim is reduced is very nearly constant for all LCG positions. The wedge appears to decrease the slope of the h/F_{∇} curve (once the initial period of negative h has been passed), an effect which becomes more noticeable as the LCG is moved forward. In general, the upwards vertical displacement, and therefore the dynamic lift, is decreased by the presence of the wedge.

With the LCG position held constant (Figs. 10 - 12), the wedge becomes more effective as displacement increases (i.e. as $Ap/\nabla^{2}/3$ diminishes). Again both the reduction in resistance and the speed range over which it takes place are improved. The change in trim seems independent of the displacement. The slope of the h/F_{∇} curve and the dynamic lift are once more both decreased

by the presence of the wedge, the effect becoming more marked as the displacement decreases. From Fig. 7 - 12 overall it seems that a wedge has a better chance of reducing the resistance of the hull if its presence has but a small effect on the dynamic lift.

It is interesting to note that the resistance curve of Fig. 10 with the wedge attached approaches closely that of Fig. 8 with no wedge present, suggesting that the wedge is cancelling the detrimental effect of moving the LCG rearwards. Similarly the resistance curve of Fig. 11 with the wedge attached approaches that of Fig. 12 with no wedge present, particularly in the upper half of the speed range, showing that in this case the wedge is neutralising the detrimental effect that increasing the displacement has on the resistance to displacement ratio.

The effect of using different wedges under a fixed loading condition can be seen in Fig. 13 - 15. Each figure presents wedges of the same length but different angles, Fig. 13 showing the shortest set of wedges and Fig. 15 the longest. In all cases wedge length is expressed as a fraction of the projected chine length. It will be seen that the curves showing the performance of the 10° wedges terminate before the maximum testing speed is reached. This is because these wedges thrust the bow of the hull so far into the water that an unacceptable amount of spray was produced. This was thrown both into the hull and out of the channel, making further increases in speed impracticable.

For all wedge lengths, the resistance curves for the 2° and 5° wedges are very close together, suggesting that there is an optimum wedge angle for these conditions, above and below which the wedge becomes less effective. For all lengths the 10° wedge greatly increased the resistance. Varying the angle of the wedge seems to have a far greater effect than varying its length, both on trim and lift. The only noticeable effect wedge length has on either of these quantities was that the shorter wedges decreased the lift rather more than the longer ones in the upper third of the speed range. Resistance is however, only reduced by the shortest wedges, suggesting that the optimum wedge length is in the region $0 < \lambda < 0.10$.

Overall, it can be seen that wedges do more than merely control the trim; the dynamic lift is also affected. It was more often reduced than increased, especially when the overall resistance was reduced, showing that for this hull at least the suggestion that the wedges help to reduce the drag by increasing the lift is unfounded. Previous work (as yet unpublished) on rectangular section hulls has however shown that this is not always the case. The overall effect of a wedge is undoubtedly complex.

7. CONCLUSIONS

It can be seen from the results that the addition of wedges to the hull proved the most useful when the loading conditions tended towards the abnormal. The DTMB series 62 models were particularly efficient hull forms, as observed by the authors of ref. 4, who also collected together data from several other designs - "At low speeds (below a F_∇ of 1.5) the hull forms of the series have slightly more drag than the other designs. At values of F_∇ of 2.0 and 2.5 the forms of the series have less drag than most of the other designs, and at values of F_∇ of 3.0 and above, the hull forms of the series have less drag than any of the other designs".

It would seem, therefore, that the addition of a wedge is unlikely to improve the performance of a well designed, correctly loaded hull. On the other hand, the performance of a craft which due to uncontrollable circumstances must be unfavourably loaded, or used in a speed range for which it was not designed, can be improved by a carefully chosen wedge. Such conditions may be brought about by abnormal power requirements, or the conversion of a craft from one use to a completely different one. Having decided that a wedge would be beneficial, it is then of more importance to select the optimum angle than the optimum length of wedge.

Even when limiting the work to one series of hull forms, it will be seen that the present tests have only scratched the surface of the investigation of the effects of trailing edge wedges on planing craft. The programme needs to be expanded in many directions before a true insight into the mechanics involved may be obtained. Two investigations which would be immediately useful are those of the effect of different sizes of wedge on loading conditions other than the one used for the present work, and the effect of the wedges on models of differing length/beam ratios. The latter could easily be carried out by using again the DTMB Series 62 hulls as the basic designs.

8. REFERENCES

1. Murray, A.B., "The hydrodynamics of planing hulls" SNAME Transactions, vol. 58 (1950).

2. Du Cane, P., "Small sea-going high speed craft" from "Shipbuilding and Ships", Worshipful Company of Shipwrights (1947).

3. Hadler, J.B., "The prediction of power performance on planing craft", SNAME Transactions, vol. 74 (1966).

4. Clement, E.P., and Blount, D.L., "Resistance tests on a systematic series of planing hull forms", SNAME Transactions, vol. 71 (1963).

5. Preston, J.H., "The design of high speed, free surface water channels", NATO Advanced Study Institute on "Surface Hydrodynamics", (1966).

6. Clement, E.P., "How to use the SNAME Small Craft Data Sheets for Design and for Resistance Prediction", SNAME Technical and Research Bulletin No. 1 - 23.

TEST CONDITIONS

Test no.	Model Weight (kg)	Ap $\nabla^{2/3}$	Static trim (deg)	LCG Fwd of station 10 (mm)	LCG aft of centroid of Ap, %Lp.	Water temp (deg C)	Wedge angle β (deg)	Wedge length Chine length λ
1	8.75	7.0	0.10	522	6	21.0	0	0
2	8.75	7.0	0.10	522	6	21.0	2	0.05
3	8.75	7.0	0.10	522	6	21.1	2	0.15
4	6.52	8.5	1.00	449	12	20.1	0	0
5	6.52	8.5	1.00	449	12	20.1	2	0.05
6	8.75	7.0	1.50	449	12	20.1	0	0
7	8.75	7.0	1.50	449	12	20.1	2	0.05
8	12.53	5.5	-0.32	546	4	20.4	0	0
9	12.53	5.5	-0.32	546	4	20.4	2	0.05
10	12.53	5.5	0.85	498	8	20.9	0	0
11	12.53	5.5	0.85	498	8	20.9	2	0.05
12	12.53	5.5	2.16	449	12	20.9	0	0
13	12.53	5.5	2.16	449	12	20.9	2	0.05
14	12.53	5.5	0.85	498	8	20.9	5	0.05
15	12.53	5.5	0.85	498	8	20.9	10	0.05
16	12.53	5.5	0.85	498	8	20.6	2	0.10
17	12.53	5.5	0.85	498	8	20.6	2	0.10
18	12.53	5.5	0.85	498	8	20.7	5	0.10
19	12.53	5.5	0.85	498	8	20.6	2	0.15
20	12.53	5.5	0.85	498	8	20.8	5	0.15
21	12.53	5.5	0.85	498	8	20.5	10	0.15

TEST No.1

V (m/s)	V (knots)	R (kg)	Wetted length of keel (cm)	Wetted length of chine (cm)	Rex 10^{-6}	S (m^2)	Trim (deg)	CG rise (mm)	F_V
0	0						0.10		0
1.13	2.20	0.31	120	110	1.318	0.320	0.02	-4	0.80
1.42	2.75	0.63	120	110	1.651	0.324	0.44	-3	1.00
1.70	3.30	0.85	118	105	1.925	0.320	1.93	-4	1.20
1.99	3.85	0.94	116	96	2.129	0.302	2.55	-5	1.40
2.27	4.40	1.06	115	95	2.406	0.299	2.72	-7	1.60
2.55	4.95	1.10	114	91	2.633	0.296	2.55	0	1.80
2.84	5.50	1.16	113	87	2.871	0.292	2.72	5	2.00
3.12	6.05	1.24	111	82	3.028	0.279	3.23	6	2.20
3.41	6.60	1.31	107	76	3.134	0.255	3.48	8	2.40
3.70	7.15	1.36	105	73	3.322	0.238	3.65	10	2.60
3.98	7.70	1.43	103	70	3.459	0.229	3.57	13	2.80
4.26	8.25	1.50	101	67	3.617	0.221	3.48	15	3.00
4.55	8.80	1.57	100	64	3.768	0.215	3.31	17	3.20

TEST No.2

V (m/s)	V (knots)	R (kg)	Wetted length of keel (cm)	Wetted length of chine (cm)	Re x 10^{-6}	S (m^2)	Trim (deg)	CG rise (mm)	F_V
	0						0.10		
1.13	2.20	0.33	120	110	1.318	0.319	-0.07	-3	0.80
1.42	2.75	0.64	120	110	1.651	0.324	0.27	-3	1.00
1.70	3.30	0.87	118	106	1.925	0.321	1.79	-3	1.20
1.99	3.85	0.98	116	100	2.169	0.307	2.55	-10	1.40
2.27	4.40	1.15	116	98	2.452	0.301	2.55	-7	1.60
2.55	4.95	1.20	116	96	2.736	0.304	2.72	-4	1.80
2.84	5.50	1.23	116	93	2.985	0.298	1.62	3	2.00
3.12	6.05	1.41	116	90	3.249	0.297	1.71	5	2.20
3.41	6.60	1.48	114	86	3.443	0.281	1.96	6	2.40
3.70	7.15	1.54	114	83	3.658	0.275	2.13	7	2.60
3.98	7.70	1.61	113	81	3.902	0.263	2.05	9	2.80
4.26	8.25	1.75	113	79	4.134	0.259	1.96	11	3.00

TEST No. 3

V (m/s)	V (knots)	R (kg)	Wetted length of keel (mm)	Wetted length of chine (mm)	Re x 10^{-6}	S (m^2)	Trim (deg)	CG rise (mm)	F_V
0							0.10		
1.13	2.20	0.34	120	110	1.321	0.320	0.02	-3	0.80
1.42	2.75	0.65	120	110	1.654	0.324	0.02	-3	1.00
1.70	3.30	0.86	118	105	1.912	0.319	1.87	-4	1.20
1.99	3.85	1.01	116	97	2.194	0.299	2.30	-3	1.40
2.27	4.40	1.13	115	95	2.412	0.298	2.64	-6	1.60
2.55	4.95	1.16	115	91	2.665	0.294	2.21	7	1.80
2.84	5.50	1.21	114	90	2.935	0.290	2.04	9	2.00
3.12	6.05	1.29	113	85	3.129	0.284	2.38	8	2.20
3.41	6.60	1.34	112	80	3.313	0.267	2.72	9	2.40
3.70	7.15	1.41	111	77	3.517	0.253	2.72	11	2.60
3.98	7.70	1.49	110	74	3.709	0.247	2.64	13	2.80
4.26	8.25	1.60	110	72	3.927	0.242	2.55	15	3.00

TEST No.4

V (m/s)	V (knots)	R (kg)	Wetted length of keel (mm)	Wetted length of chine (mm)	Re x 10^{-6}	S (m^2)	Trim (deg)	CG rise (mm)	F_V
0	0						1.00		
1.13	2.20	0.24	116	60	0.990	0.242	1.34	-3	0.84
1.42	2.75	0.47	116	85	1.410	0.286	2.01	-4	1.05
1.70	3.30	0.60	112	84	1.655	0.278	3.11	-4	1.26
1.99	3.85	0.68	110	81	1.874	0.258	3.37	-10	1.47
2.27	4.40	0.75	109	77	2.094	0.250	3.54	-5	1.68
2.55	4.95	0.81	106	74	2.282	0.241	3.54	0	1.89
2.84	5.50	0.87	102	69	2.397	0.223	3.62	6	2.10
3.12	6.05	0.93	95	65	2.479	0.209	3.79	8	2.31
3.41	6.60	0.99	93	61	2.605	0.200	3.88	9	2.52
3.70	7.15	1.04	92	59	2.751	0.195	3.71	12	2.73
3.98	7.70	1.10	90	57	2.885	0.188	3.54	14	2.94
4.26	8.25	1.16	90	55	3.046	0.185	3.54	14	3.15

TEST No. 5

V (m/s)	V (knots)	R (kg)	Wetted length of keel (mm)	Wetted length of chine (mm)	Re x 10^{-6}	S (m^2)	Trim (deg)	CG rise (mm)	F_V
0	0						1.00		
1.13	2.20	0.25	116	70	1.047	0.258	1.08	-2	0.84
1.42	2.75	0.49	116	90	1.452	0.295	1.68	-3	1.05
1.70	3.30	0.62	113	85	1.672	0.267	2.69	-2	1.26
1.99	3.85	0.70	112	83	1.914	0.264	2.69	-6	1.47
2.27	4.40	0.74	111	79	2.139	0.257	2.77	-3	1.68
2.55	4.95	0.78	111	76	2.358	0.252	2.44	3	1.89
2.84	5.50	0.84	110	74	2.595	0.247	2.44	5	2.10
3.12	6.05	0.93	110	71	2.789	0.242	2.27	7	2.31
3.41	6.60	1.03	110	69	3.011	0.238	2.10	9	2.52
3.70	7.15	1.11	110	68	3.264	0.236	2.01	10	2.73
3.98	7.70	1.24	110	67	3.478	0.235	1.85	11	2.94
4.26	8.25	1.38	111	65	3.723	0.230	1.68	11	3.15

TEST No.6

V (m/s)	V (knots)	R (kg)	Wetted length of keel (mm)	Wetted length of chine (mm)	Re x 10^{-6}	S (m^2)	Trim (deg)	CG rise (mm)	F_V
0	0						1.50		
1.13	2.20	0.37	118	78	1.103	0.281	1.67	-3	0.80
1.42	2.75	0.70	117	90	1.452	0.302	2.60	-3	1.00
1.70	3.30	0.92	110	85	1.638	0.284	4.29	-4	1.20
1.99	3.85	1.05	108	81	1.855	0.270	4.71	-10	1.40
2.27	4.40	1.14	104	77	2.026	0.264	4.88	-3	1.60
2.55	4.95	1.20	98	72	2.155	0.247	4.97	4	1.80
2.84	5.50	1.25	90	67	2.200	0.218	5.22	11	2.00
3.12	6.05	1.32	85	64	2.293	0.193	5.31	13	2.20
3.41	6.60	1.34	83	61	2.436	0.185	5.31	15	2.40
3.70	7.15	1.37	81	59	2.567	0.179	5.14	18	2.60
3.98	7.70	1.40	80	56	2.687	0.172	4.80	21	2.80
4.26	8.25	1.44	79	55	2.834	0.169	4.46	23	3.00

TEST No.7

V (m/s)	V (knots)	R (kg)	Wetted length of keel (mm)	Wetted length of chine (mm)	Re x 10^{-6}	S (m^2)	Trim (deg)	CG rise (mm)	F_∇
0	0						1.50		
1.13	2.20	0.37	117	80	1.103	0.285	1.67	-3	0.80
1.42	2.75	0.71	115	95	1.481	0.284	2.60	-3	1.00
1.70	3.30	0.97	112	87	1.672	0.290	3.70	-2	1.20
1.99	3.85	1.05	110	84	1.914	0.279	4.29	-10	1.40
2.27	4.40	1.10	109	82	2.139	0.275	4.12	-3	1.60
2.55	4.95	1.11	105	79	2.333	0.270	3.78	7	1.80
2.84	5.50	1.18	103	75	2.510	0.260	3.95	9	2.00
3.12	6.05	1.23	100	71	2.634	0.226	4.04	11	2.20
3.41	6.60	1.27	98	68	2.808	0.218	3.95	13	2.40
3.70	7.15	1.32	98	65	2.871	0.214	3.70	14	2.60
3.98	7.70	1.39	100	65	3.241	0.217	3.36	16	2.80
4.26	8.25	1.47	102	63	3.469	0.217	3.11	17	3.00

TEST No.8

V (m/s)	V (knots)	R (kg)	Wetted length of keel (mm)	Wetted length of chine (mm)	Re x 10^{-6}	S (m^2)	Trim (deg)	CG rise (mm)	F_∇
0	0						-0.32		
1.13	2.20	0.41	120	110	1.302	0.325	-0.66	-5	0.75
1.42	2.75	0.84	120	110	1.631	0.332	-0.40	-7	0.94
1.70	3.30	1.43	120	110	1.953	0.336	2.13	-3	1.13
1.99	3.85	1.78	119	110	2.263	0.334	3.06	-21	1.32
2.27	4.40	1.84	118	108	2.559	0.328	3.06	-10	1.51
2.55	4.95	1.85	117	105	2.831	0.326	2.64	0	1.70
2.84	5.50	1.93	116	101	3.064	0.322	2.73	6	1.89
3.12	6.05	1.98	114	94	3.242	0.319	3.49	7	2.08
3.41	6.60	1.96	109	85	3.301	0.286	4.50	10	2.27
3.70	7.15	2.00	105	81	3.431	0.250	4.58	15	2.45
3.98	7.70	2.04	103	77	3.578	0.241	4.58	19	2.64
4.26	8.25	2.09	101	74	3.702	0.233	4.50	22	2.83

TEST No.9

V (m/s)	V (knots)	R (kg)	Wetted length of keel (mm)	Wetted length of chine (mm)	Re x 10^{-6}	S (m^2)	Trim (deg)	CG rise (mm)	F_V
0	0						-0.32		
1.13	2.20	0.43	120	110	1.315	0.324	-0.74	-5	0.75
1.42	2.75	0.91	120	110	1.648	0.330	-0.57	-7	0.94
1.70	3.30	1.43	120	110	1.973	0.333	1.45	-5	1.13
1.99	3.85	1.79	119	110	2.285	0.332	2.55	-17	1.32
2.27	4.40	1.91	119	110	2.608	0.329	2.39	-9	1.51
2.55	4.95	1.97	119	110	2.938	0.329	1.79	1	1.70
2.84	5.50	2.16	118	109	3.238	0.329	1.71	6	1.89
3.12	6.05	2.42	118	108	3.558	0.334	1.88	4	2.08
3.41	6.60	2.35	115	97	3.644	0.321	2.64	6	2.27
3.70	7.15	2.22	113	90	3.764	0.275	3.15	10	2.45
3.98	7.70	2.24	112	86	3.976	0.267	3.57	9	2.64
4½26	8.25	2.32	111	83	4.170	0.263	3.15	15	2.83

TEST No.10

V (m/s)	V (knots)	R (kg)	Wetted length of keel (mm)	Wetted length of chine (mm)	Re x 10^{-6}	S (m^2)	Trim (deg	CG rise (mm)	F_V
0	0						0.85		
1.13	2.20	0.43	120	110	1.315	0.333	0.85	-6	0.75
1.42	2.75	0.84	120	105	1.648	0.332	1.32	-7	0.94
1.70	3.30	1.36	118	105	1.905	0.333	3.47	-9	1.13
1.99	3.85	1.65	115	101	2.165	0.319	4.57	-15	1.32
2.27	4.40	1.73	114	97	2.402	0.312	4.91	-10	1.51
2.55	4.95	1.70	112	92	2.628	0.308	4.57	1	1.70
2.84	5.50	1.83	108	87	2.780	0.301	4.99	6	1.89
3.12	6.05	1.93	103	81	2.897	0.275	5.42	10	2.08
3.41	6.60	2.00	101	76	3.025	0.236	6.35	14	2.27
3.70	7.15	2.04	93	72	3.056	0.217	6.35	17	2.45
3.98	7.70	2.06	91	69	3.213	0.209	6.10	21	2.64
4.26	8.25	2.07	89	66	3.310	0.202	6.01	23	2.83

TEST No.11

V (m/s)	V (knots)	R (kg)	Wetted length of keel (mm)	Wetted length of chine (mm)	Re x 10^{-6}	S (m^2)	Trim (deg)	CG rise (mm)	F_∇
0	0						0.85		
1.13	2.20	0.43	120	110	1.315	0.332	0.77	-5	0.75
1.42	2.75	0.88	120	110	1.648	0.338	1.19	-6	0.94
1.70	3.30	1.39	119	108	1.939	0.341	3.05	-6	1.13
1.99	3.85	1.69	116	105	2.205	0.326	4.23	-17	1.32
2.27	4.40	1.73	115	101	2.471	0.318	4.15	-9	1.51
2.55	4.95	1.71	114	97	2.706	0.314	3.72	2	1.70
2.84	5.50	1.78	113	93	2.952	0.311	3.81	7	1.89
3.12	6.05	1.86	111	88	3.117	0.308	4.15	9	2.08
3.41	6.60	1.90	108	83	3.266	0.278	4.57	11	2.27
3.70	7.15	1.93	106	80	3.466	0.250	4.39	15	2.45
3.98	7.70	1.98	105	78	3.655	0.245	4.23	18	2.64
4.26	8.25	2.04	105	76	3.869	0.242	4.06	20	2.83

TEST No.12

V (m/s)	V (knots)	R (kg)	Wetted length of keel (mm)	Wetted length of chine (mm)	Re x 10^{-6}	S (m^2)	Trim (deg)	CG rise (mm)	F_∇
0	0						2.16		
1.13	2.20	0.42	118	107	1.281	0.336	2.50	-4	0.75
1.42	2.75	0.85	117	104	1.576	0.337	3.60	-7	0.94
1.70	3.30	1.61	110	92	1.733	0.309	5.63	-6	1.13
1.99	3.85	1.84	105	87	1.925	0.290	6.47	-9	1.32
2.27	4.40	1.95	99	82	2.059	0.277	6.73	-1	1.51
2.55	4.95	2.07	93	77	2.190	0.263	6.98	8	1.70
2.84	5.50	2.20	85	72	2.235	0.241	7.40	14	1.89
3.12	6.05	2.26	80	66	2.299	0.188	8.16	18	2.08
3.41	6.60	2.23	77	63	2.406	0.179	7.82	22	2.27
3.70	7.15	2.18	76	61	2.534	0.175	7.40	26	2.45
3.98	7.70	2.16	75	57	2.651	0.166	7.07	28	2.64
4.26	8.25	2.12	74	56	2.794	0.163	6.64	31	2.83

TEST No. 13

V (m/s)	V (knots)	R (kg)	Wetted length of keel (mm)	Wetted length of chine (mm)	Rex10^{-6}	S (m^2)	Trim (deg)	CG rise (mm)	F_V
0	0						2.16		
1.13	2.20	0.42	118	107	1.281	0.336	2.41	-3	0.75
1.42	2.75	0.86	117	106	1.591	0.338	3.43	-5	0.94
1.70	3.30	1.61	112	99	1.802	0.321	5.46	-6	1.13
1.99	3.85	1.83	108	88	1.965	0.293	5.88	-7	1.32
2.27	4.40	1.89	105	84	2.151	0.286	5.96	-4	1.51
2.55	4.95	1.94	99	79	2.293	0.277	6.04	8	1.70
2.84	5.50	2.02	94	75	2.407	0.253	6.13	11	1.89
3.12	6.05	2.09	88	70	2.488	0.206	6.39	16	2.08
3.41	6.60	2.06	85	67	2.613	0.197	6.04	19	2.27
3.70	7.15	2.03	85	65	2.795	0.194	5.63	23	2.45
3.98	7.70	2.02	85	67	3.052	0.197	5.20	25	2.64
4.26	8.25	2.02	86	61	3.138	0.189	4.78	27	2.83

TEST No. 14

V (m/s)	V (knots)	R (kg)	Wetted length of keel (mm)	Wetted length of chine (mm)	Rex10^{-6}	S (m^2)	Trim (deg)	CG rise (mm)	F_V
0	0						0.85		
1.13	2.20	0.46	120	110	1.315	0.332	0.73	-5	0.75
1.42	2.75	0.88	120	110	1.648	0.338	1.10	-6	0.94
1.70	3.30	1.45	118	107	1.922	0.335	3.05	-4	1.13
1.99	3.85	1.70	116	101	2.165	0.320	3.89	-15	1.32
2.27	4.40	1.75	115	99	2.448	0.316	3.89	-6	1.51
2.55	4.95	1.70	114	94	2.680	0.309	3.30	6	1.70
2.84	5.50	1.77	113	91	2.923	0.310	3.30	9	1.89
3.12	6.05	1.85	112	88	3.149	0.305	3.55	11	2.08
3.41	6.60	1.89	109	83	3.300	0.280	3.81	12	2.27
3.70	7.15	1.93	108	80	3.503	0.253	3.72	14	2.45
3.98	7.70	1.98	109	78	3.735	0.252	3.39	17	2.64
4.26	8.25	2.07	110	77	3.998	0.252	3.13	19	2.83

TEST No.15

V (m/s)	V (knots)	R (kg)	Wetted length of keel (mm)	Wetted length of chine (mm)	Rex10^{-6}	S (m2)	Trim (deg)	CG rise (mm)	F_V
0	0						0.85		
1.13	2.20	0.48	120	110	1.315	0.332	0.60	-5	0.75
1.42	2.75	0.93	120	110	1.648	0.338	0.68	-5	0.94
1.70	3.30	1.52	118	109	1.939	0.337	2.62	-3	1.13
1.99	3.85	1.73	117	105	2.225	0.326	3.39	-16	1.32
2.27	4.40	1.79	116	103	2.494	0.324	3.05	-6	1.51
2.55	4.95	1.79	116	101	2.783	0.317	2.32	7	1.70
2.84	5.50	1.94	117	102	3.124	0.320	1.70	11	1.89
3.12	6.05	2.22	118	104	3.495	0.324	1.27	11	2.08
3.41	6.60	2.68	119	106	3.850	0.328	0.77	11	2.27

TEST No.16

V (m/s)	V (knots)	R (kg)	Wetted length of keel (mm)	Wetted length of chine (mm)	Re x 10^{-6}	S (m^2)	Trim (deg)	CG rise (mm)	F_V
0	0						0.85		
1.13	2.20	0.44	120	110	1.309	0.333	0.93	-5	0.75
1.42	2.75	0.89	120	110	1.638	0.338	1.27	-7	0.94
1.70	3.30	1.47	117	106	1.893	0.335	3.20	-3	1.13
1.99	3.85	1.71	115	100	2.132	0.318	4.40	-13	1.32
2.27	4.40	1.78	113	96	2.365	0.309	4.40	-6	1.51
2.55	4.95	1.75	112	92	2.612	0.308	4.23	2	1.70
2.84	5.50	1.84	109	87	2.791	0.303	4.31	9	1.89
3.12	6.05	1.98	104	82	2.910	0.283	4.90	10	2.08
3.41	6.60	1.99	99	77	3.007	0.235	5.16	14	2.27
3.70	7.15	2.02	98	74	3.185	0.228	4.90	17	2.45
3.98	7.70	2.04	97	71	3.353	0.221	4.65	20	2.64
4.26	8.25	2.07	97	70	3.546	0.220	4.31	22	2.83

TEST No. 17

V (m/s)	V (knots)	R (kg)	Wetted length of keel (mm)	Wetted length of chine (mm)	Rex10^{-6}	S (m^2)	Trim (deg)	CG rise (mm)	F_V
0	0						0.85		
1.13	2.20	0.46	120	110	1.310	0.332	0.77	-5	0.75
1.42	2.75	0.91	120	110	1.641	0.338	1.19	-4	0.94
1.70	3.30	1.51	118	107	1.914	0.335	3.05	-5	1.13
1.99	3.85	1.75	116	103	2.176	0.322	3.	-14	1.32
2.27	4.40	1.79	114	100	2.438	0.316	3.64	-5	1.51
2.55	4.95	1.76	114	96	2.694	0.313	3.22	4	1.70
2.84	5.50	1.85	114	94	2.968	0.312	3.39	4	1.89
3.12	6.05	1.93	113	90	3.167	0.311	3.22	10	2.08
3.41	6.60	1.98	112	87	3.389	0.292	3.22	12	2.27
3.70	7.15	2.05	111	85	3.637	0.283	3.13	15	2.45
3.98	7.70	2.13	112	83	3.879	0.264	2.88	16	2.64
4.26	8.25	2.27	113	83	4.195	0.266	2.46	18	2.83

TEST No.18

V (m/s)	V (knots)	R (kg)	Wetted length of keel (mm)	Wetted length of chine (mm)	Re x10^{-6}	S (m^2)	Trim (deg)	CG rise (mm)	F_V
0	0						0.85		
1.13	2.20	0.54	120	110	1.312	0.328	0.51	-2	0.75
1.42	2.75	1.04	120	110	1.644	0.335	0.85	-3	0.94
1.70	3.30	1.59	119	108	1.934	0.334	1.02	-5	1.13
1.99	3.85	1.90	118	106	2.240	0.325	2.88	-8	1.32
2.27	4.40	1.94	117	104	2.511	0.320	2.88	-3	1.51
2.55	4.95	1.99	117	104	2.828	0.320	1.78	7	1.70
2.84	5.50	2.19	118	106	3.202	0.324	1.10	12	1.89
3.12	6.05	2.79	120	110	3.613	0.327	0	13	2.08

TEST No. 21

V (m/s)	V (knots)	R (kg)	Wetted length of keel (cm)	Wetted length of chine (cm)	$Rex10^{-6}$	S (m^2)	Trim (deg)	CG rise (mm)	F_V
0	0						0.85		
1.13	2.20	0.59	120	110	1.305	0.326	0.51	-2	0.75
1.42	2.75	1.13	120	110	1.634	0.332	0.51	-3	0.94
1.70	3.30	1.82	119	109	1.940	0.333	2.46	-4	1.13
1.99	3.85	2.12	118	106	2.227	0.321	3.22	-14	1.32
2.27	4.40	2.16	117	103	2.496	0.313	2.96	-3	1.51
2.55	4.95	2.22	118	104	2.837	0.318	1.78	9	1.70

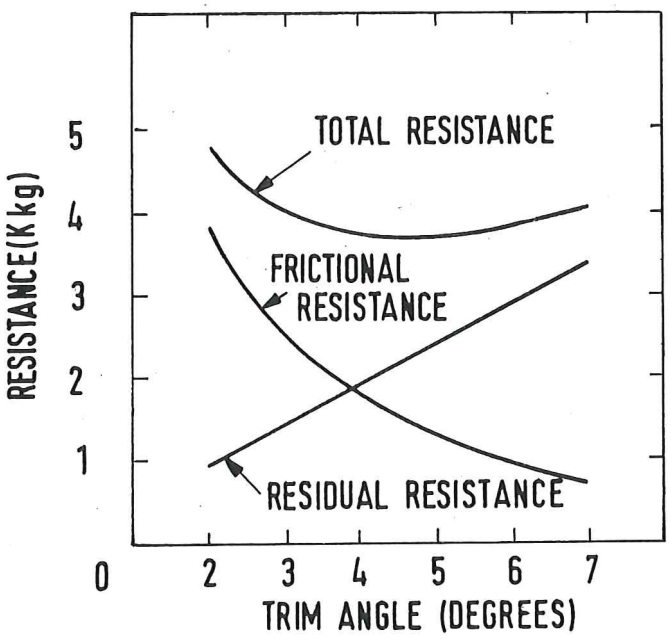

fig. 1 Resistance characteristics of a planing boat; 18.9 m. long weighing 27,200 kg., travelling at 40 knots (taken from ref. 1).

TEST No. 19

V (m/s)	V (knots)	R (kg)	Wetted length of keel (cm)	Wetted length of chine (cm)	$Rex10^{-6}$	S (m^2)	Trim (deg)	CG rise (mm)	F_V
0	0						0.85		
1.13	2.20	0.44	120	110	1.307	0.332	0.93	-5	0.75
1.42	2.75	0.87	120	110	1.638	0.338	1.27	-4	0.94
1.77	3.30	1.46	117	105	1.893	0.332	3.56	-3	1.13
1.99	3.85	1.75	115	98	2.112	0.315	4.57	-15	1.32
2.27	4.40	1.81	113	94	2.342	0.307	4.57	-6	1.51
2.55	4.95	1.79	112	90	2.586	0.305	4.40	3	1.70
2.84	5.50	1.86	108	85	2.734	0.299	4.57	10	1.89
3.12	6.05	1.99	102	79	2.816	0.269	5.24	12	2.08
3.41	6.60	2.03	102	75	3.007	0.236	5.33	16	2.27
3.70	7.15	2.05	100	72	3.185	0.227	5.16	19	2.45
3.98	7.70	2.07	93	70	3.233	0.214	4.90	21	2.64
4.26	8.25	2.08	93	67	3.418	0.209	4.57	24	2.83

TEST No. 20

V (m/s)	V (knots)	R (kg)	Wetted length of keel (cm)	Wetted length of chine (cm)	$Rex10^{-6}$	S (m^2)	Trim (deg)	CG rise (mm)	F_V
0	0						0.85		
1.13	2.20	0.45	120	110	1.313	0.330	0.68	-4	0.75
1.42	2.75	0.92	120	110	1.644	0.342	1.02	-4	0.94
1.77	3.30	1.60	117	108	1.918	0.334	3.22	-4	1.13
1.99	3.85	1.79	116	101	2.161	0.317	3.56	-5	1.32
2.27	4.40	1.87	115	100	2.443	0.315	3.89	-4	1.51
2.55	4.95	1.84	114	95	2.674	0.310	3.39	3	1.70
2.84	5.50	1.91	113	91	2.917	0.308	3.56	6	1.89
3.12	6.05	2.00	112	88	3.142	0.305	3.47	11	2.08
3.41	6.60	2.04	110	84	3.328	0.288	3.81	13	2.27
3.70	7.15	2.09	109	81	3.533	0.256	3.56	16	2.45
3.98	7.70	2.16	110	79	3.767	0.255	3.30	17	2.64
4.26	8.25	2.30	111	80	4.075	0.258	2.71	19	2.83

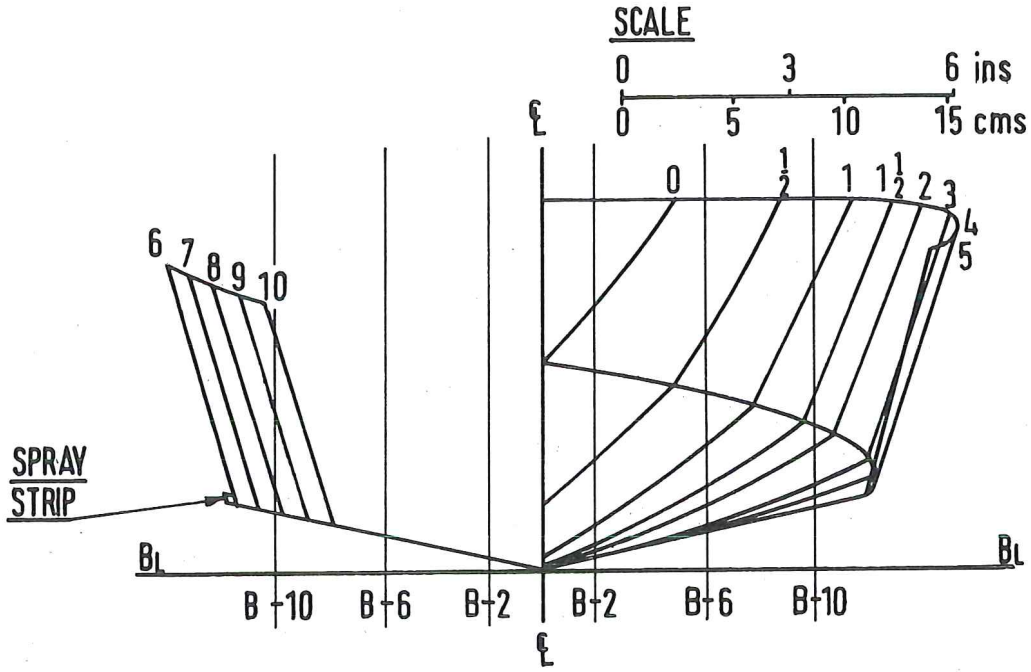

L_P	= 1·220 m (4·00 ft)	L_P / B_{PA}	= 5·00
A_P	= 0·297 m^2 (3·20 ft^2)	L_P / B_{PX}	= 4·09
B_{PA}	= 0·244 m (0·800 ft)	B_{PX} / B_{PA}	= 1·22
B_{PX}	= 0·298 m (0·978 ft)	B_{PT} / B_{PX}	= 0·64
B_{PT}	= 0·191 m (0·625 ft)	CENTROID A_P	= 0·595 m (1·95 ft FWD. OF TRAMSOM)

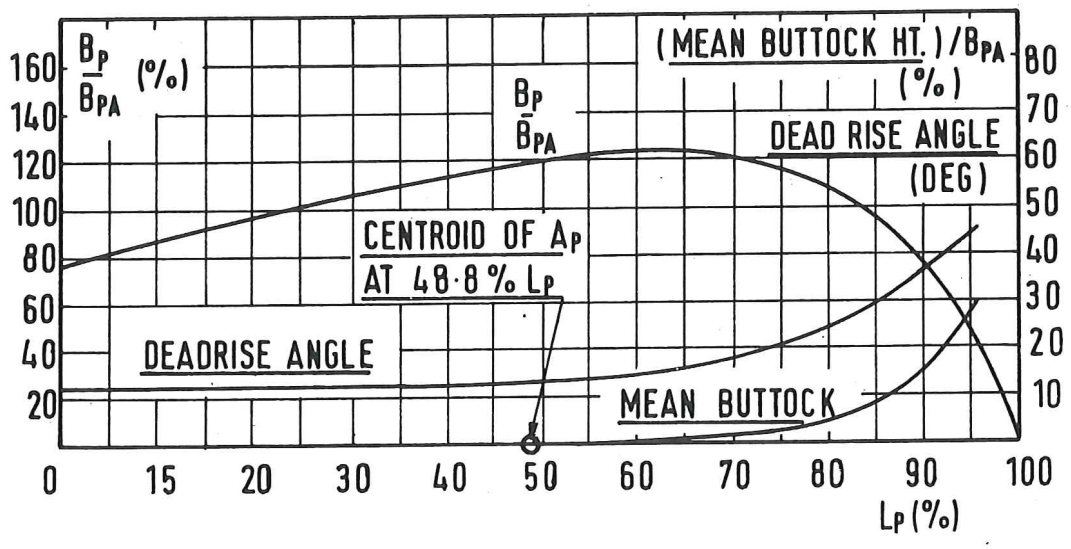

fig. 2 Body plan and form characteristics of DTMB Series 62 Parent Model No. 4667-1.

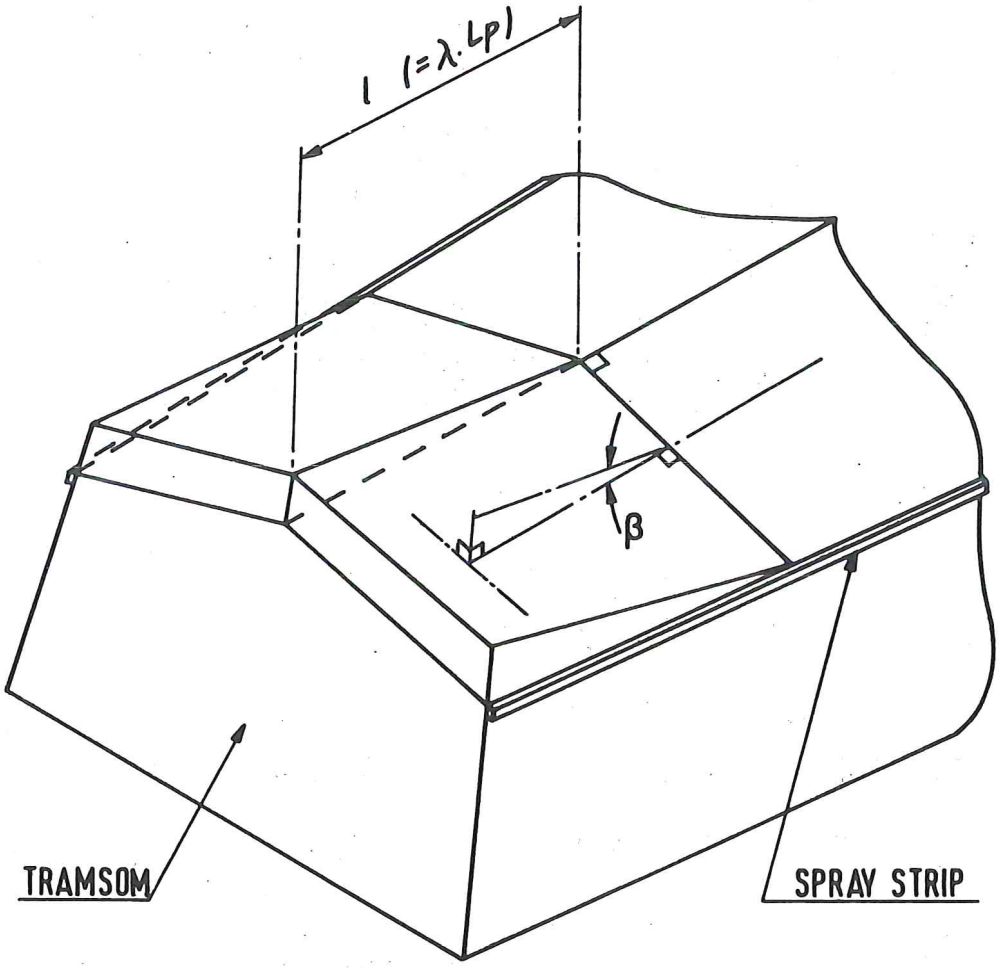

fig. 3 Wedge parameters.

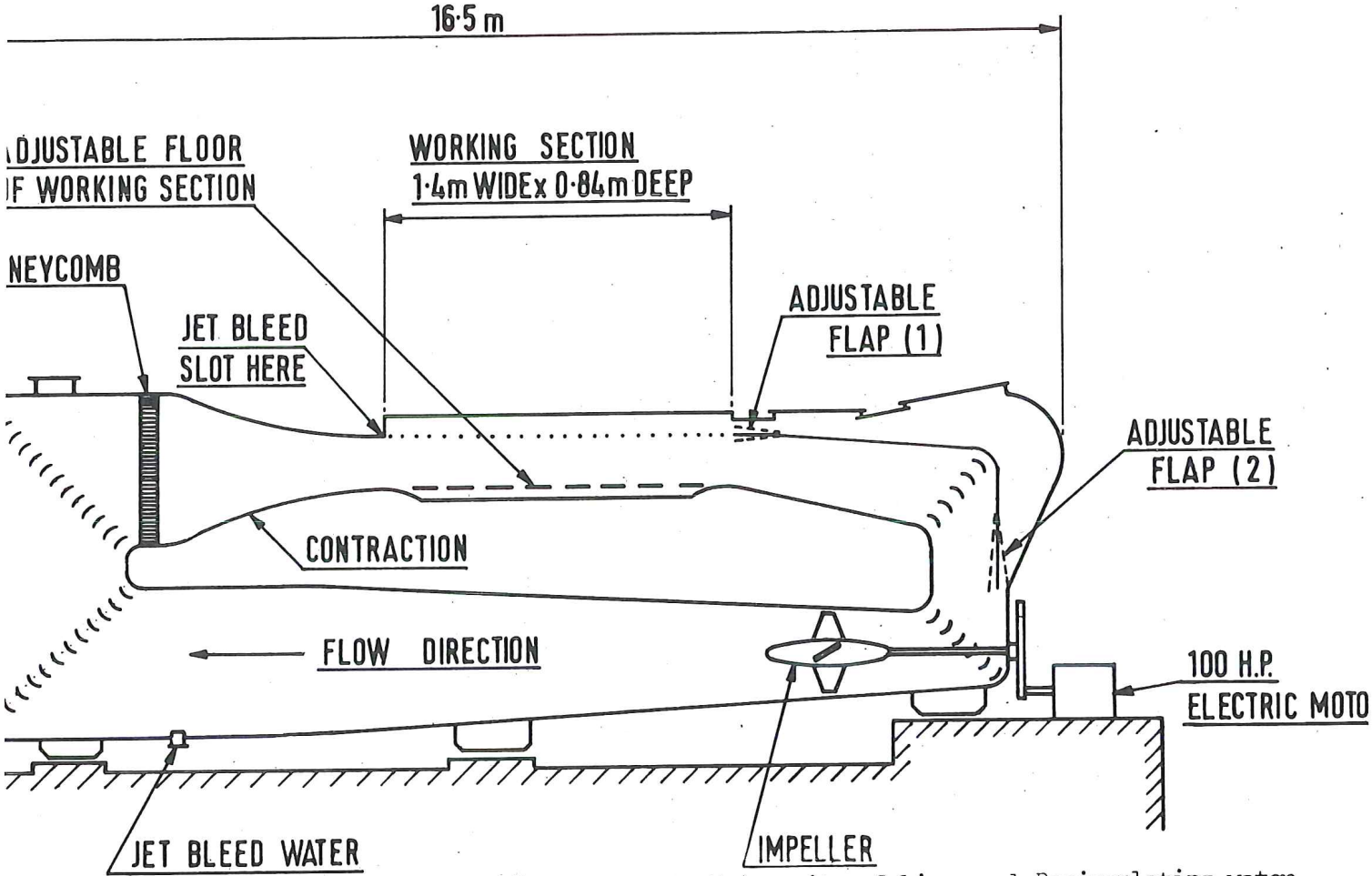

fig. 4 The University of Liverpool Recirculating water channel.

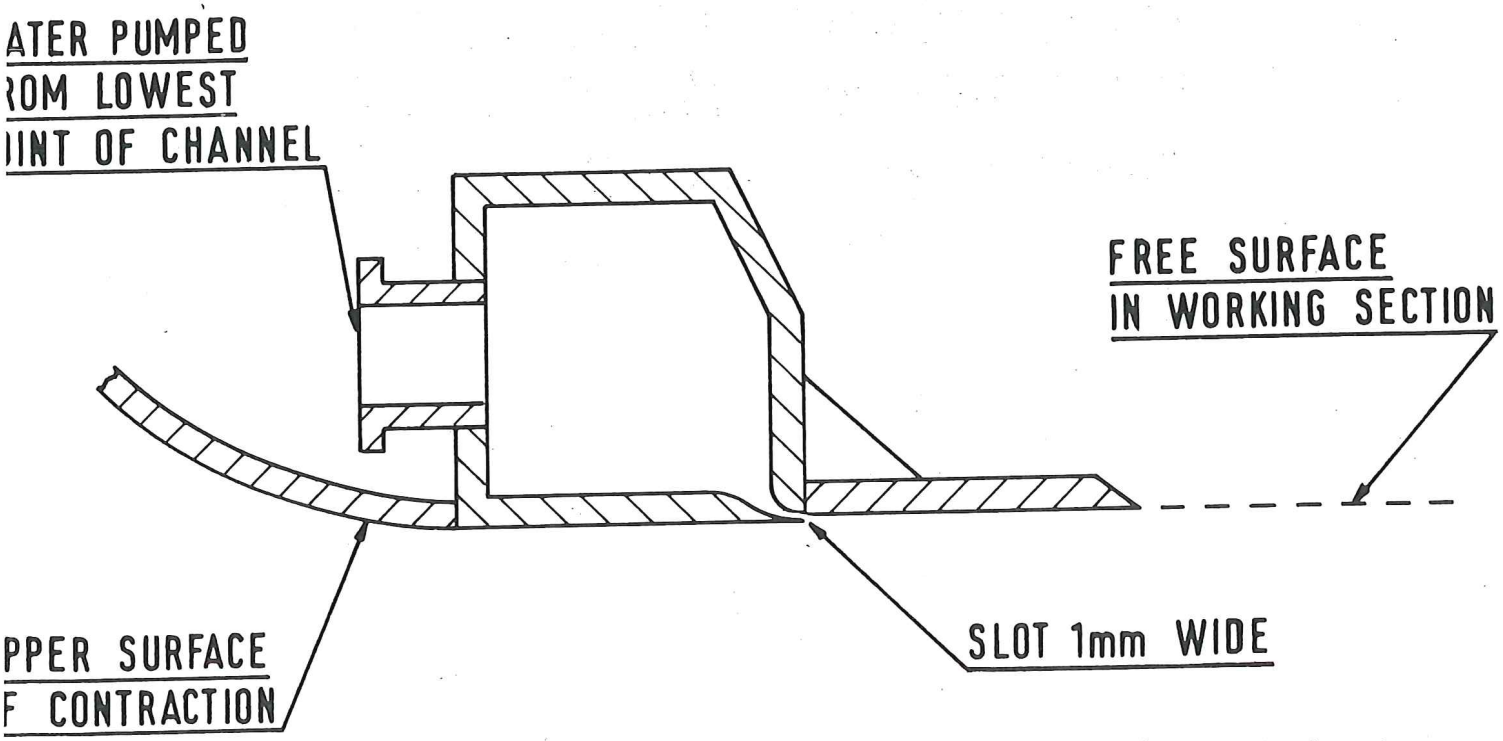

fig. 5. Section through the flume's jet-bleed system.

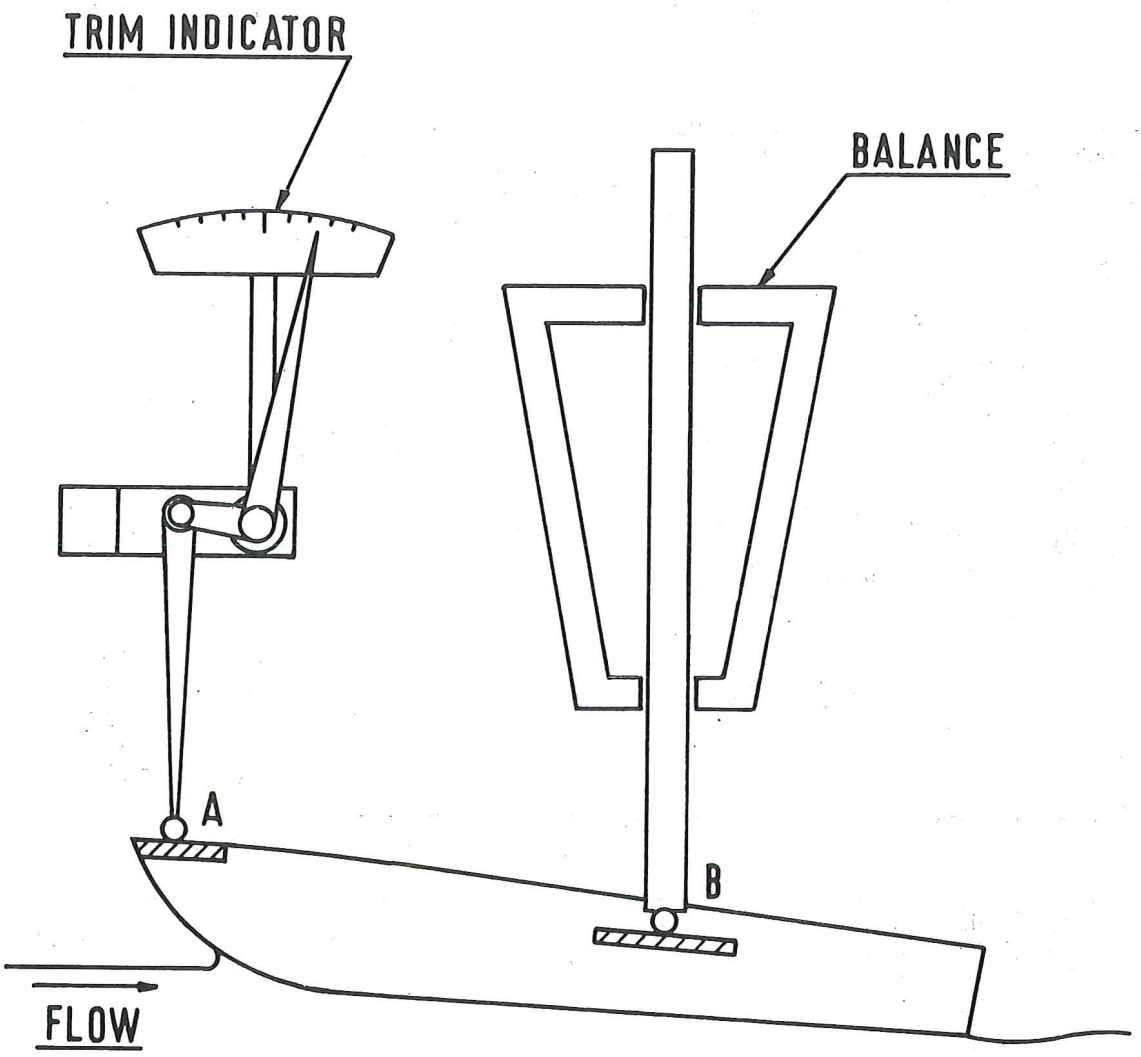

fig. 6 Arrangement of model over flume.

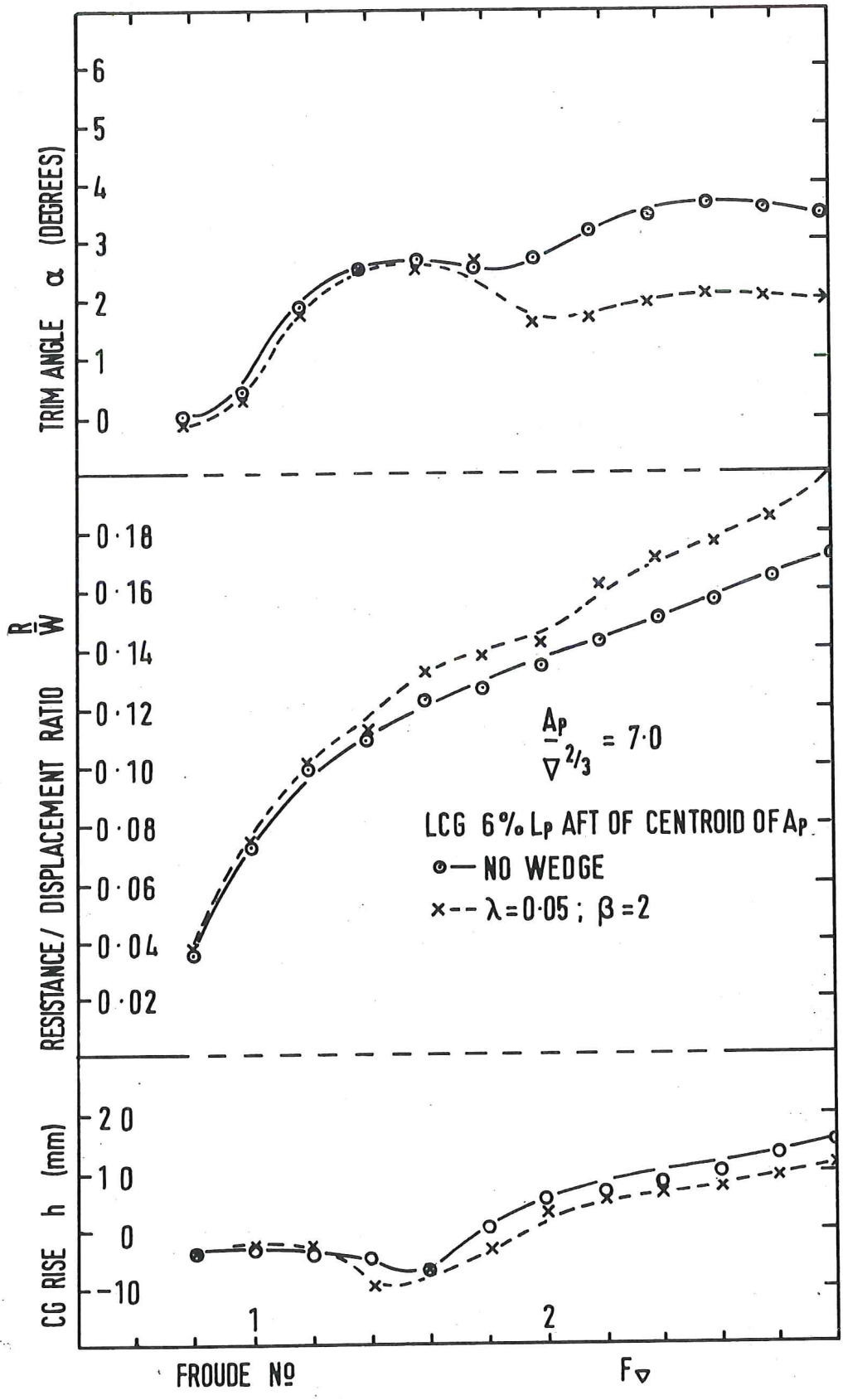

fig. 7-12 Effects of a single small wedge on the planing characteristics of the model under a range of loading conditions.

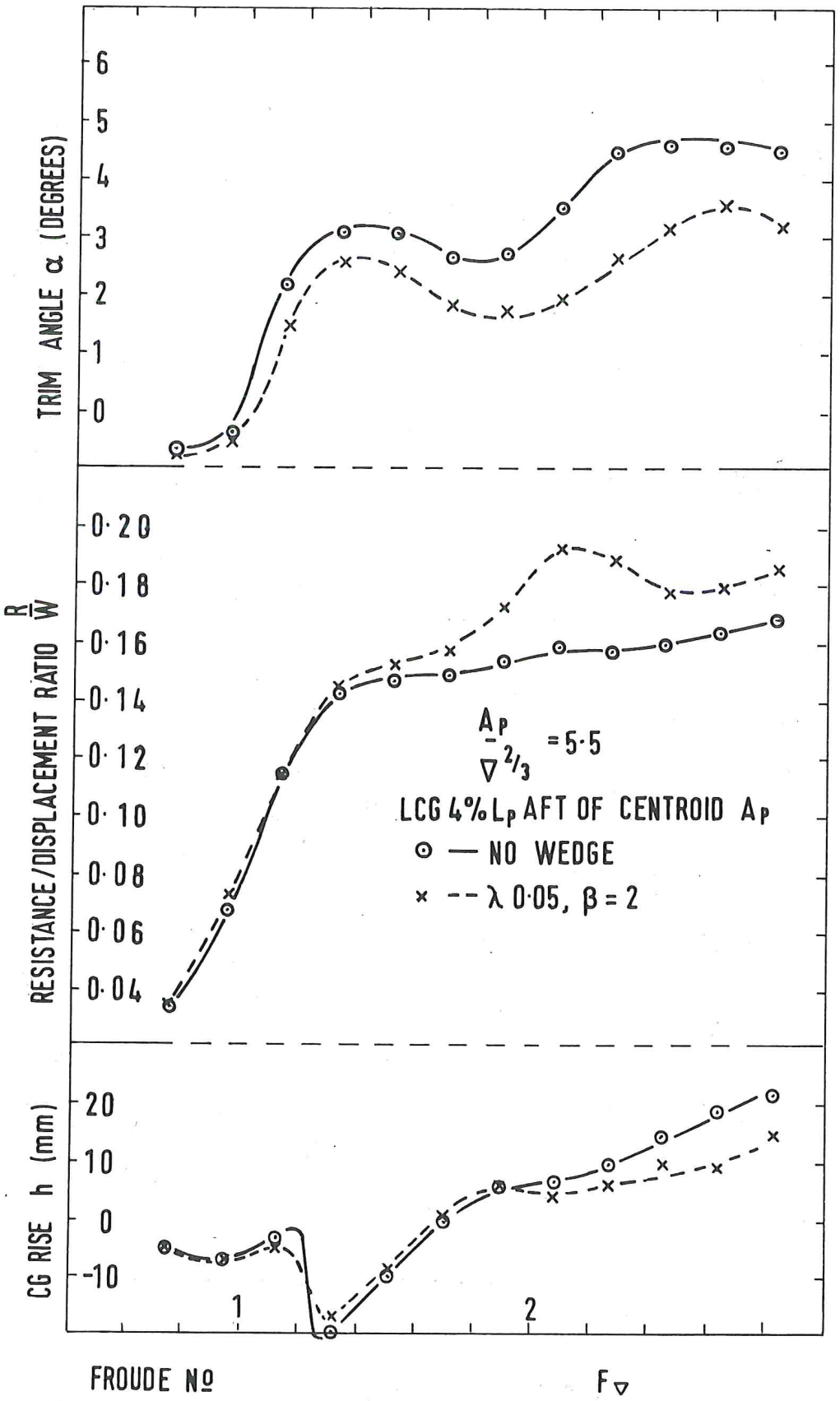
TRIM ANGLE α (DEGREES)
6
5
4
3
2
1
0
RESISTANCE/DISPLACEMENT RATIO R/W
0·20
0·18
0·16
0·14
0·12
0·10
0·08
0·06
0·04
A_P / ∇^2/3 = 5·5
LCG 4% L_P AFT OF CENTROID A_P
⊙ — NO WEDGE
× -- λ 0·05, β = 2
CG RISE h (mm)
20
10
0
-10
1
2
FROUDE Nº
F∇

FIG. 8

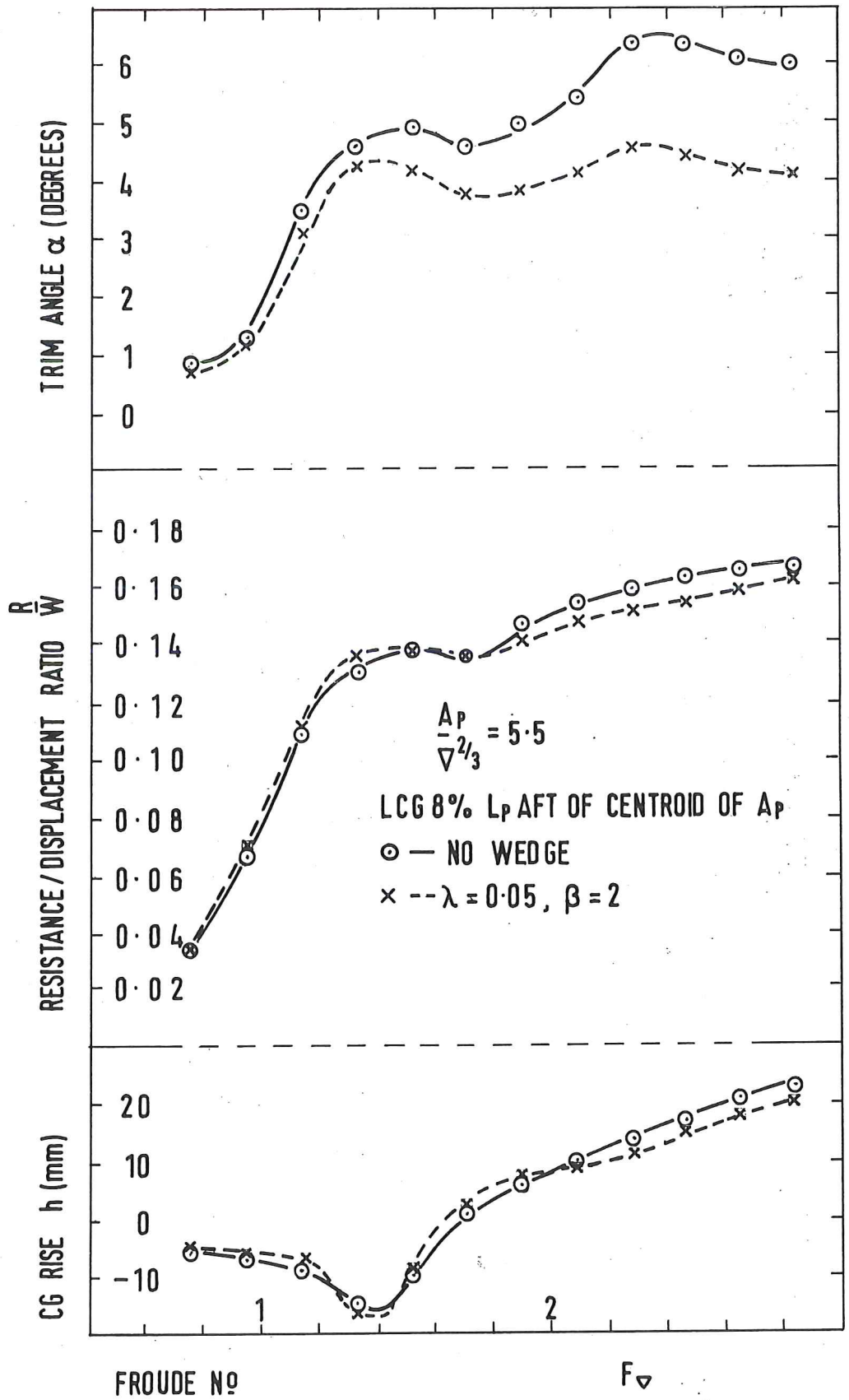
TRIM ANGLE α (DEGREES)
6
5
4
3
2
1
0
RESISTANCE/DISPLACEMENT RATIO R/W
0·18
0·16
0·14
0·12
0·10
0·08
0·06
0·04
0·02
A_P / ∇^2/3 = 5·5
LCG 8% L_P AFT OF CENTROID OF A_P
⊙ — NO WEDGE
× -- λ = 0·05, β = 2
CG RISE h (mm)
20
10
0
−10
1
2
FROUDE Nº
F∇

FIG. 9

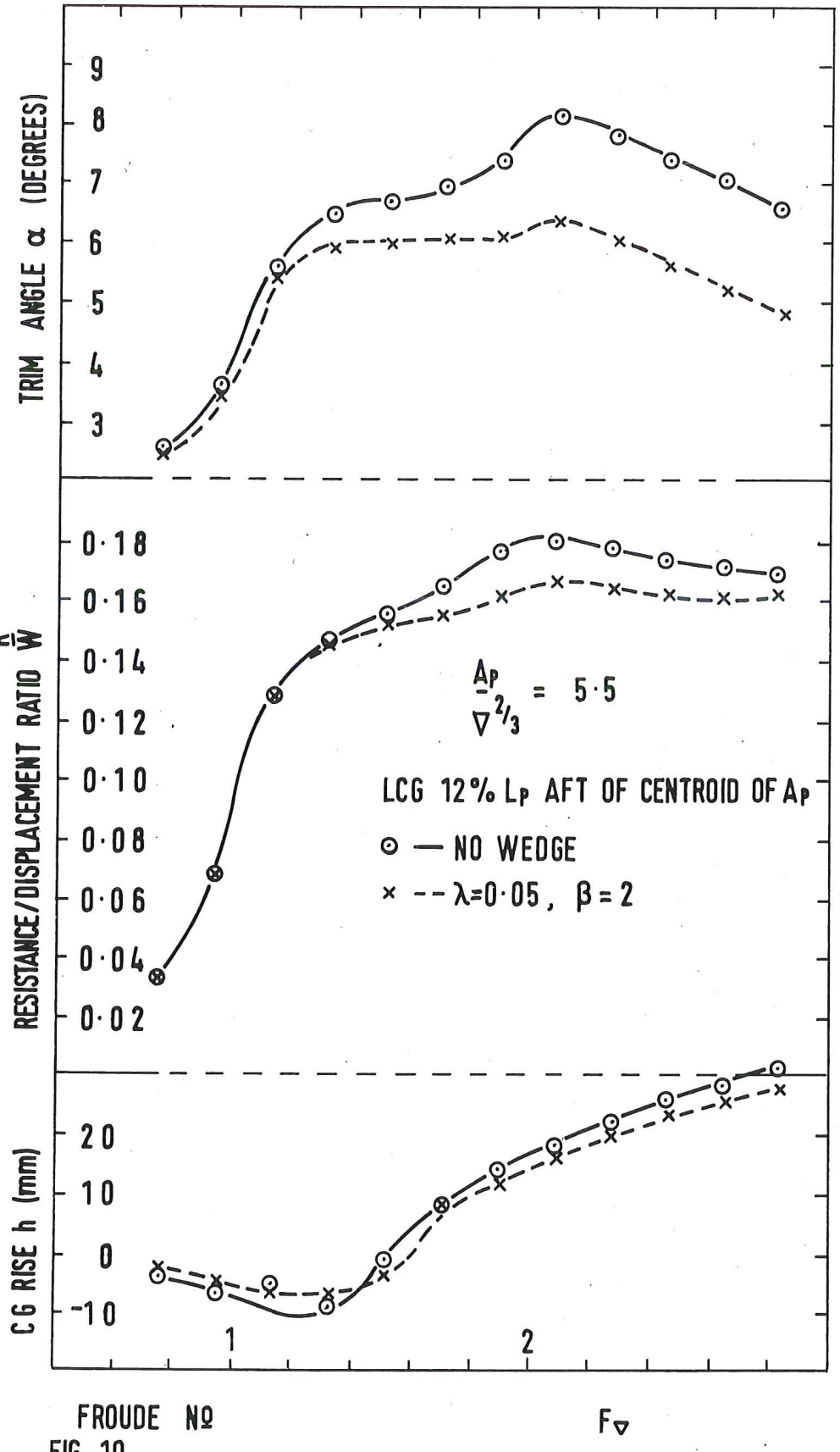
TRIM ANGLE α (DEGREES)
9
8
7
6
5
4
3
RESISTANCE/DISPLACEMENT RATIO R/W
0·18
0·16
0·14
0·12
0·10
0·08
0·06
0·04
0·02
Ap / ∇^2/3 = 5·5
LCG 12% Lp AFT OF CENTROID OF Ap
⊙ — NO WEDGE
× -- λ=0·05, β=2
C G RISE h (mm)
20
10
0
-10
1
2
FROUDE Nº
F∇

FIG. 10

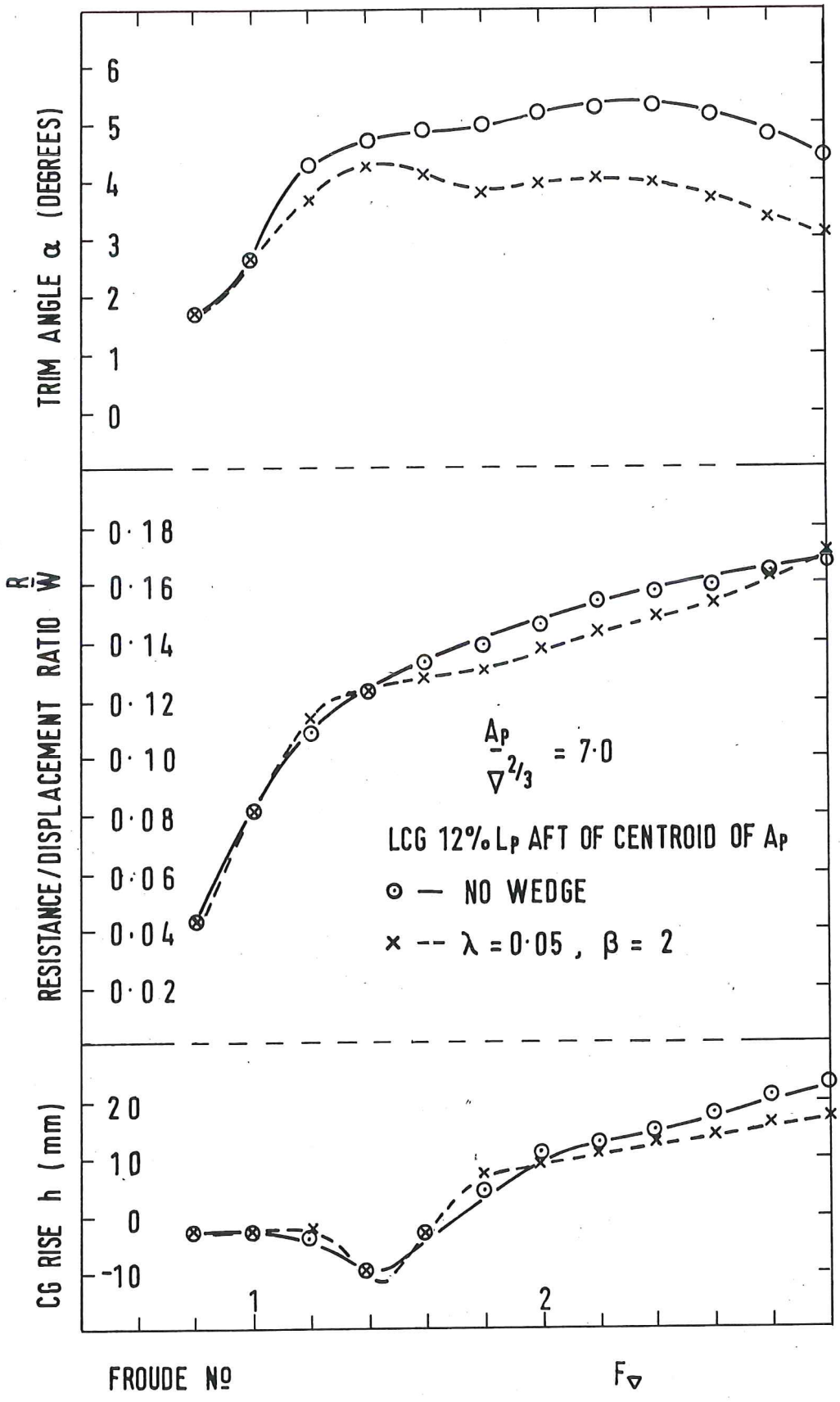
TRIM ANGLE α (DEGREES)
6
5
4
3
2
1
0
R/W RESISTANCE/DISPLACEMENT RATIO
0·18
0·16
0·14
0·12
0·10
0·08
0·06
0·04
0·02
$\frac{A_P}{\nabla^{2/3}} = 7{\cdot}0$
LCG 12% L_P AFT OF CENTROID OF A_P
⊙ — NO WEDGE
× -- λ = 0·05 , β = 2
CG RISE h (mm)
20
10
0
-10
1
2
FROUDE Nº
F_∇

FIG.11

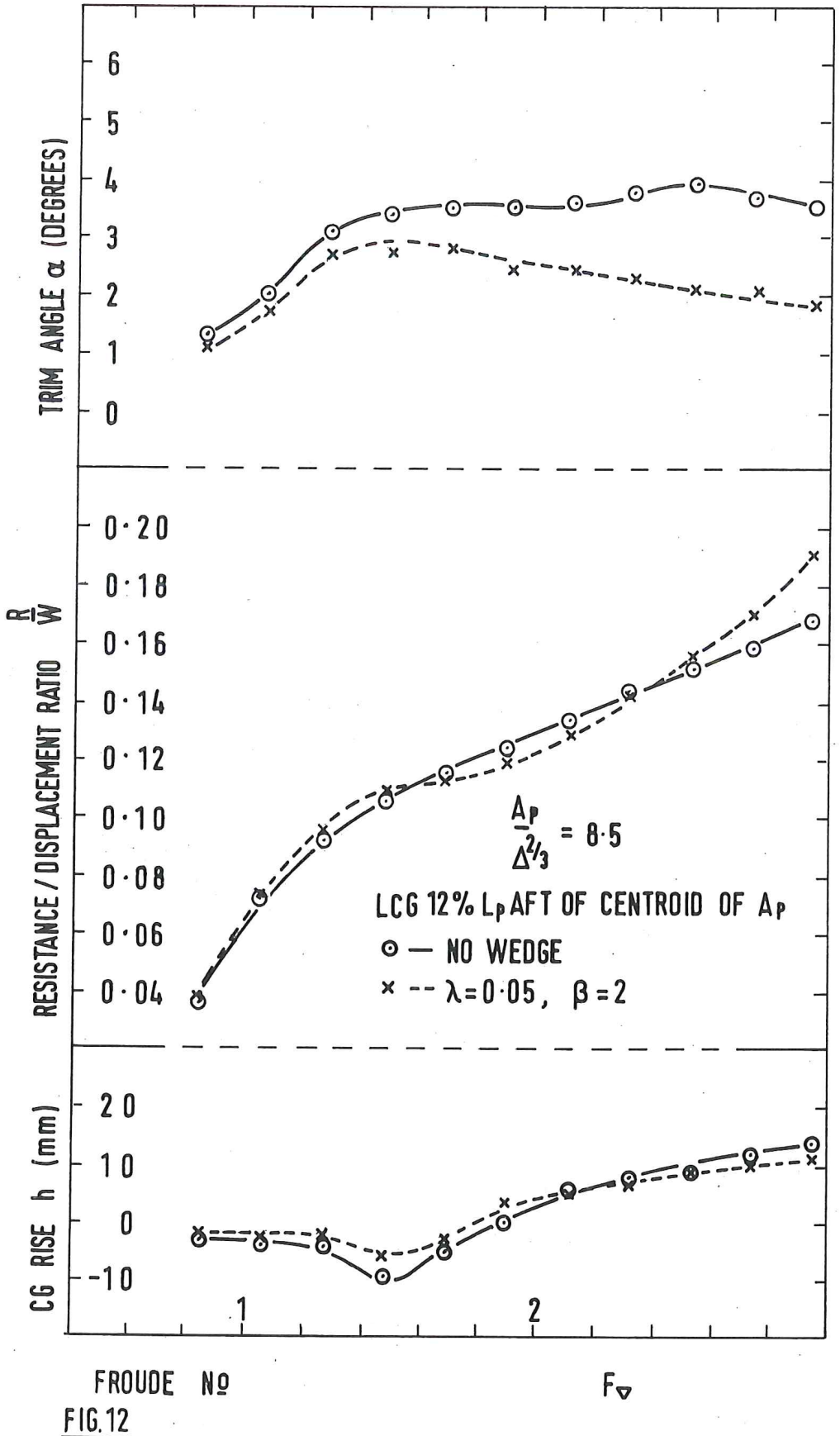
TRIM ANGLE α (DEGREES)
6
5
4
3
2
1
0
RESISTANCE / DISPLACEMENT RATIO R/W
0·20
0·18
0·16
0·14
0·12
0·10
0·08
0·06
0·04
A_P / Δ^2/3 = 8·5
LCG 12% L_P AFT OF CENTROID OF A_P
⊙ — NO WEDGE
× -- λ=0·05, β=2
CG RISE h (mm)
20
10
0
-10
1
2
FROUDE Nº
F∇

FIG.12

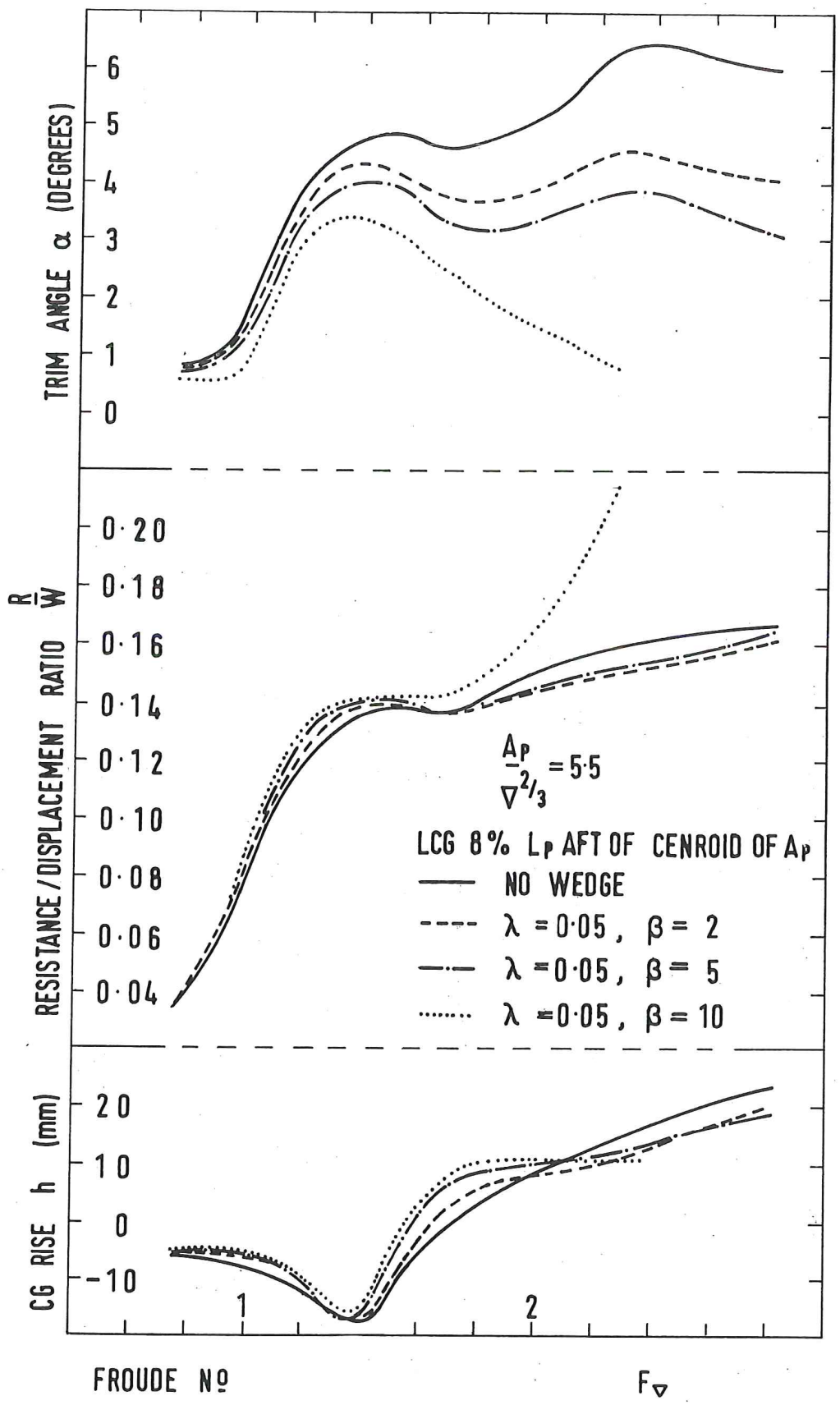

fig. (13-15) Effect of various wedge shapes on the planing characteristics of the model under constant loading conditions.

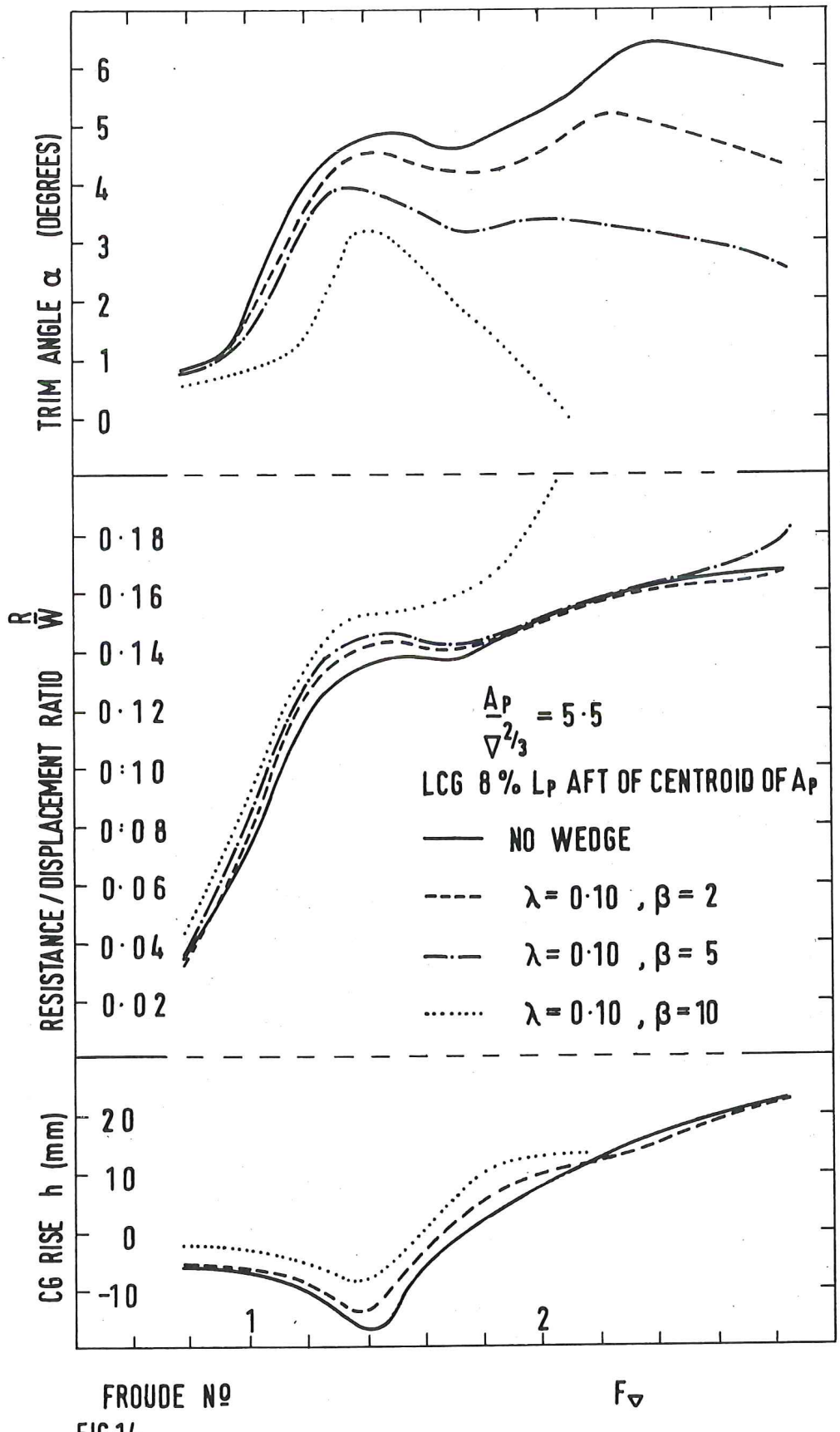
TRIM ANGLE α (DEGREES)
6
5
4
3
2
1
0
RESISTANCE/DISPLACEMENT RATIO R/W
0·18
0·16
0·14
0·12
0·10
0·08
0·06
0·04
0·02
Ap/∇2/3 = 5·5
LCG 8% Lp AFT OF CENTROID OF Ap
NO WEDGE
λ = 0·10 , β = 2
λ = 0·10 , β = 5
λ = 0·10 , β = 10
CG RISE h (mm)
20
10
0
-10
1
2
FROUDE Nº
F∇

FIG.14

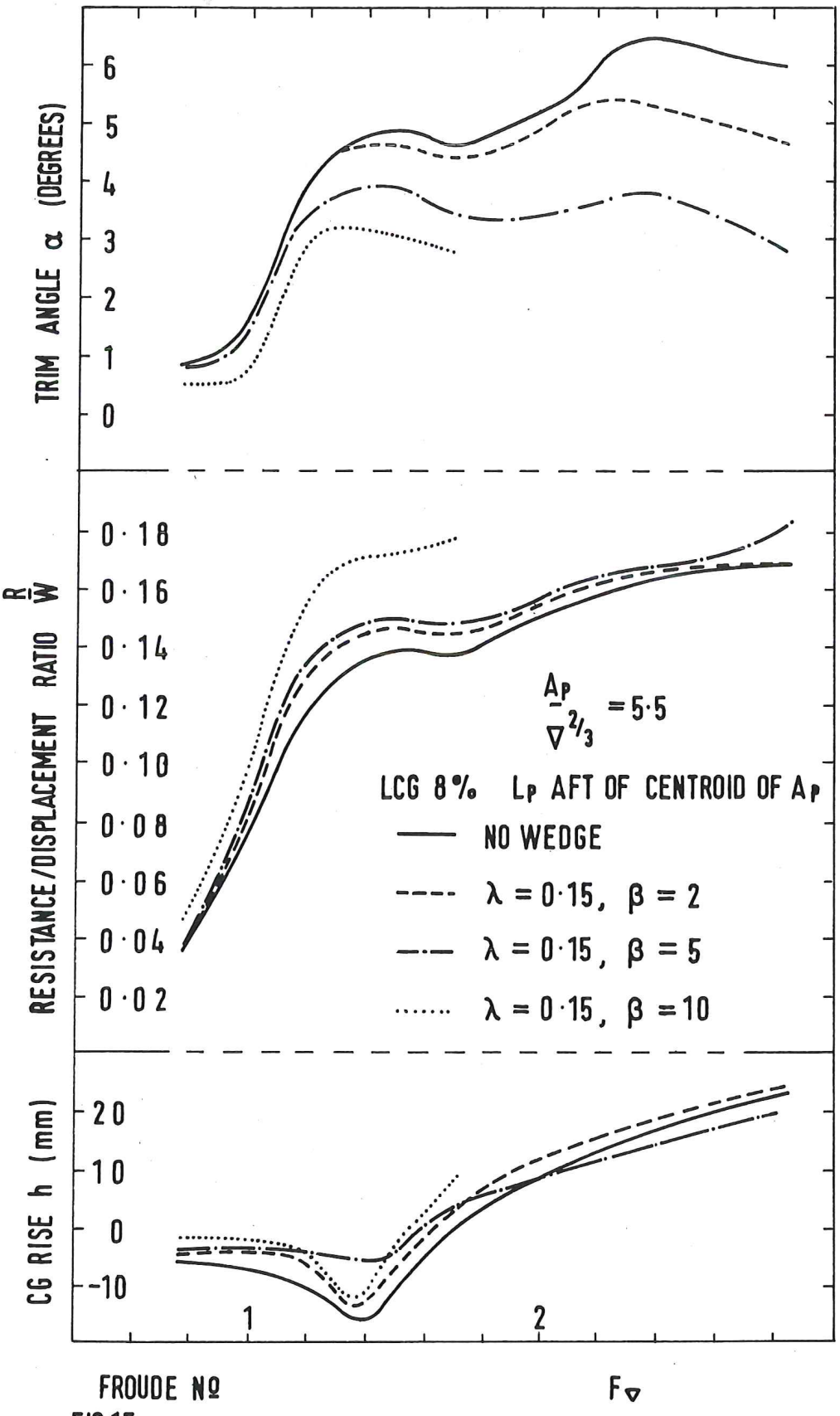
TRIM ANGLE α (DEGREES)
6
5
4
3
2
1
0
R/W
RESISTANCE/DISPLACEMENT RATIO
0·18
0·16
0·14
0·12
0·10
0·08
0·06
0·04
0·02
$\frac{A_P}{\nabla^{2/3}} = 5{\cdot}5$
LCG 8% L_P AFT OF CENTROID OF A_P
NO WEDGE
λ = 0·15, β = 2
λ = 0·15, β = 5
λ = 0·15, β = 10
CG RISE h (mm)
20
10
0
-10
1
2
FROUDE Nº
F_∇

FIG.15

Journal of Ship Research, Vol. 20, No. 4, Dec. 1976, pp. 224–232

Effect of Wedges on the Performance Characteristics of Two Planing Hulls

A. Millward[1]

An investigation has been made into the effect of adding wedges or trim tabs to two models of the DTMB Series 62 planing hulls over a range of longitudinal center of gravity positions and displacements to determine the optimum wedge configuration and the range of effectiveness of a wedge. Measurements were also made to confirm that a wedge has an effect on the dynamic lift on the hull and hence that there is a change in resistance other than that resulting from control of the trim angle.

Introduction

THE RESISTANCE of a planing hull depends on a number of variables, but for a given hull shape at a fixed displacement and center of gravity position this may be simplified to a dependence on trim angle. The resistance of a planing hull can be considered in the conventional manner as consisting of two largely independent components—the frictional resistance, due to the shear forces acting on the hull surface, and the residual resistance, due to all the remaining forces acting on the hull. This division of the total resistance into friction and residual resistances is illustrated in Fig. 1, based on data in [1],[2] for different trim angles at a fixed speed. It can be seen that to reduce the residual resistance the hull should be run at the lowest trim angle possible, whereas to reduce the friction resistance it should be run at the highest trim angle. Thus there is an optimum trim angle which will produce the minimum resistance at this speed. However, since this optimum condition depends on the relative importance of the two components of resistance, which are themselves a function of speed, it can be shown that the optimum trim also varies with speed of the craft even for a fixed displacement. If the total weight of the craft also changes then further variations in the optimum trim angle will occur.

In the process of designing a planing craft for specified conditions, the designer will probably have obtained information from either SNAME data sheets [2] or tank tests from which the optimum trim angles can be determined. In the case of a craft with a fixed displacement it is possible to arrange the position of the center of gravity so that the optimum trim angle is achieved at the cruising speed. In a more complex situation with a variety of loading conditions and cruise speeds, the optimum trim angle for each condition would require a changing center of gravity position. This can sometimes be obtained by such methods as appropriate distribution of payload or the redistribution of the fuel load into different tanks.

A different method of trim control which has been tried is the use of trim tabs attached to the stern or alternatively a fixed-angle wedge fastened underneath the hull at the stern. The earliest use of a form of auxiliary trim control appears to be that given by Du Cane [3] where during World War II the German E-boats were equipped with twin auxiliary rudders which were fitted level with and on either side of the propellers. As the boat speed was increased these rudders were turned outward about 10 to 15 deg to reduce the hull resistance. It has been suggested that the effect of these rudders in some way reduced squatting by the stern and hence affected the wavemaking part of the residual resistance. Trailing-edge wedges, illustrated in Fig. 2, have also been used as a method of trim control on hard chine and round bilge hulls. For example, Monk [4] has tested the effects of different wedges on an 11.3 m (37 ft) hull for speeds up to 9.2 m/s (17.8 knots) together with data from other craft from which he concluded that shorter wedges produced more effect. These conclusions, however, were largely based on experiments using two lengths of wedge on one arbitrary hull. Two other references to trim control are found in

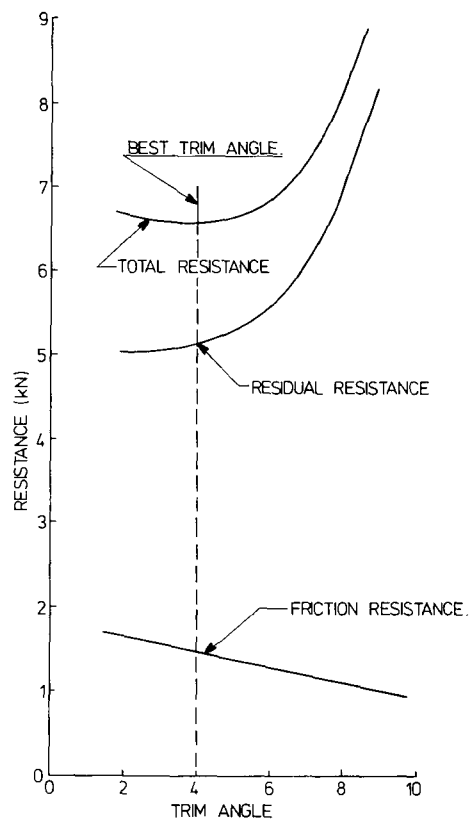

Fig. 1 Variation of components of resistance of a planing hull with trim angle

[1] Department of Mechanical Engineering, The University of Liverpool, Liverpool, England.

[2] Numbers in brackets designate References at end of paper.

Manuscript received at SNAME headquarters August 4, 1975; revised manuscript received May 3, 1976.

the discussion to [5]: Du Cane mentioned a boat in the 1966 Rouen 24-hr race with a movable transom flap and Clement suggested a pair of independently controlled transom flaps to correct both trim and also any undesirable heel angle in turning.

More recently the importance of trim control has been realized, and in powerboat racing, for example, trailing-edge wedges and transom flaps (or trim tabs) are widely used and can even be obtained as a 'bolt-on' accessory. A qualitative account of the use of wedges and trim tabs is given by West [6], although Maloney [7] queries the advisability of their use since they are sometimes required to operate at such large angles that they are likely to be inefficient. An example is also quoted by Du Cane [8] where the performance of a 33 m (110 ft) fast patrol boat was improved by wedge sections.

It can be seen therefore that in terms of practical experience the use of trim tabs or wedges as a method of trim control is widespread, with occasional attempts at some form of optimization for a particular hull. More recently Brown [9] has made a comprehensive series of tests on rectangular planing surfaces with flaps from which deductions can be made of the effectiveness of different flap configurations. Brown has also shown that in addition to trim control the flaps further alter the resistance by augmenting the dynamic lift on the hull. In the practical case this can be expected to reduce the effective displacement, although in Brown's work the wetted area was kept constant and the additional lift measured.

It was therefore decided in the present investigation to determine the value of adding fixed wedges to two models of a standard family of planing hulls (the DTMB Series 62) under a systematic series of conditions to find the optimum wedge configuration, the range of conditions over which a wedge was effective, and to confirm whether, for a real hull, a wedge had an effect on the resistance other than that resulting from control of the trim angle.

Wedges were chosen in preference to flaps since they can be regarded more as a change in hull shape while allowing the overall length and displacement to be kept the same as for the basic hull. It is appreciated however, that in practice it may be more convenient to fit transom flaps whose angle can be adjusted to suit the prevailing speed and loading conditions.

Experimental facilities and method

Model

The DTMB Series 62 hulls were used and models were made in glass-reinforced plastic (grp), one half the size of the original DTMB models, of the revised parent hull (Model 4667-1) and Model 4666. These were taken to represent hulls which would be appropriate to fast patrol boats and motor yachts, respectively. The body plans and other data of the two models are given in Figs. 3 and 4 and also in Table 1.

It can be seen in Fig. 2 that when the hull has deadrise as in these tests, there are actually two wedges, one on each planing surface, joining at the keel. The wedge has been defined in terms of its length expressed as a proportion of the projected chine length of the hull, and the wedge angle measured parallel to the keel and normal to the plane of the keel. The wedges were constructed of wood or grp and were glued onto the hull when in use.

Recirculating water channel

The tests were carried out in the Recirculating Water Channel (flume) at the University of Liverpool. A detailed account of the design and operation of the flume has been given by Preston [10], but since the use of such a facility is fairly unusual as compared to a conventional towing tank for ship model testing, a short description is included.

The channel, which is shown in Fig. 5, has a capacity of approximately 90,000 liters (20,000 gal) of water circulated by an impeller driven by a 100-hp electric motor. From the impeller

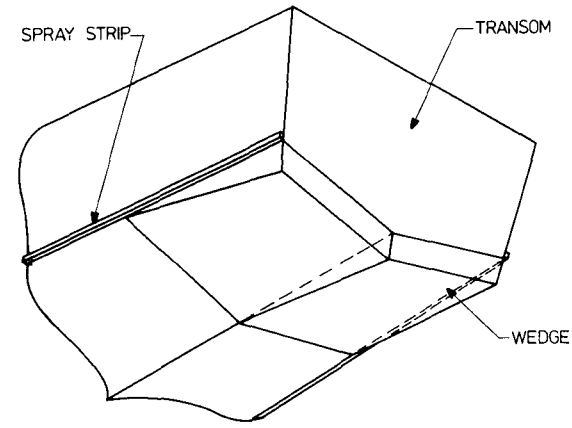

Fig. 2 Configuration of a wedge on a hull with deadrise

the water passes through a long circular-section diffuser after which the cross section becomes rectangular. The flow passes through two sets of guide vanes and a honeycomb to minimize swirl and is then accelerated through a contraction into the working section. This has a cross section 1.4 m wide, 0.84 m deep, 4.0 m long (4.5 ft × 2.75 ft × 13 ft) and has a movable false floor which can be adjusted both in height and inclination to give a flat, level water surface at the required operating speed. After the working section the top layer of water, which contains most of the air bubbles caused by the presence of the model in the channel, is separated by an adjustable flap or 'splitter plate.' This water is slowed by a deepening of the section and passed through several gauzes, allowing the air time to settle out before the water is reintroduced to the main circuit upstream of the impeller.

The flow velocity in the working section can be set within a range 0.03 to 6.1 m/s (0.1 to 20 fps). Due to the adjustable floor, any speed can be maintained without the presence of standing waves or a hydraulic jump; the critical speed with the floor in its lowest position would be in the region of 2.7 m/s (9 fps).

Early work [11] in the flume showed that there was an appreciable wake at the free surface caused by the boundary layer on the upper surface of the contraction. In order to correct this, a jet injection system was installed: water is bled off from the lowest part of the return circuit and pumped through a 1 mm wide slot running the full width of the channel at the upstream end of the working section. By adjusting the pump speed the velocity defect at the free surface can be corrected, with the beneficial side effect of further improving the flatness of the free surface.

Model arrangements and test program

The model was floated in the channel attached to a balance, which allowed the hull to trim and heave while measuring resistance and vertical displacement. An indicator mounted at the bow recorded trim while also providing an additional restraint against large yawing forces which might occur with forward center of gravity positions. Scales along the keel, chine, and transom of the model enabled the respective wetted lengths to be determined. Other work [12] has shown that for flat planing surface models in the channel there is no measurable change in resistance due to channel width provided the beam is less than 300 mm and, further, that no form of turbulence stimulation is necessary at speeds above 1.2 m/s (4 fps).

Measurements were made of the resistance, bow position and heave, and the keel, chine and transom wetted lengths for a range of speeds for each hull under a variety of displacements and center of gravity positions both for the bare hulls and with a range of wedges as given in Table 2. The tests were carried out in two se-

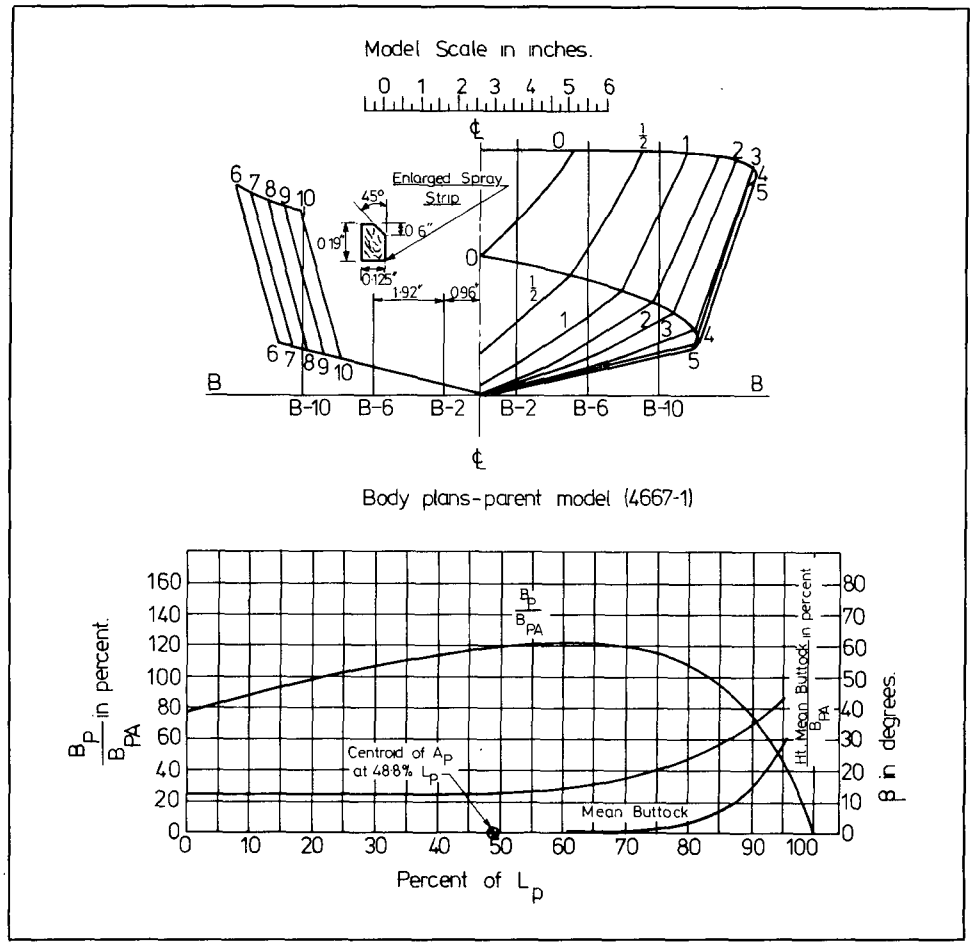

Fig. 3 Body plans and form characteristics curves for DTMB Series 62 revised parent model planing hull (4667-1)

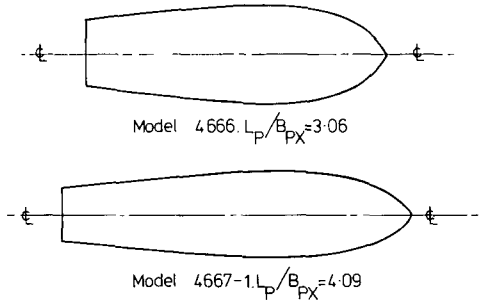

Fig. 4 Comparison of the chine lines in plan view of the two models

Table 1 Model dimensions

	Model 4666		Model 4667-1	
A_P	2.429 sq ft	0.2256 sq m	3.200 sq ft	0.2973 sq m
L_P	2.994 ft	0.9124 m	4.000 ft	1.2192 m
B_{PA}	0.812 ft	0.2475 m	0.800 ft	0.2438 m
B_{PX}	0.978 ft	0.2981 m	0.978 ft	0.2981 m
B_{PT}	0.693 ft	0.2112 m	0.625 ft	0.1905 m
L_P/B_{PA}			3.69	5.00
L_P/B_{PX}			3.06	4.09
B_{PX}/B_{PA}			1.21	1.22
B_{PT}/B_{PX}			0.71	0.64
Centroid of A_P, %L_P forward of transom			48.2	48.8
Angle of chine in plan view, deg			5.0	5.0
Half angle of waterline entrance, deg			49	46

ries; thus the earlier test, on the parent model (4667-1), was made by Cole [12] and reported briefly also in [13].

Presentation of results

For a given hull size and design, the variables which affect the planing characteristics are the displacement (W or ∇), the longitudinal position of the center of gravity (LCG), and the speed. In order for comparison to be made between different hulls and loading conditions, these variables have been expressed in terms of the parameters given by Clement and Blount [1] in the original tests on the DTMB Series 62 hulls. Thus

(*a*) the displacement was expressed as the dimensionless ratio $A_P/\nabla^{2/3}$ where A_P is the projected planing bottom area. It should be noted that a large numerical value of this ratio represents a light displacement condition and a small value correspondingly represents a heavy displacement.

(*b*) The longitudinal position of the center of gravity (LCG) was defined as the distance aft of the centroid of A_P expressed as

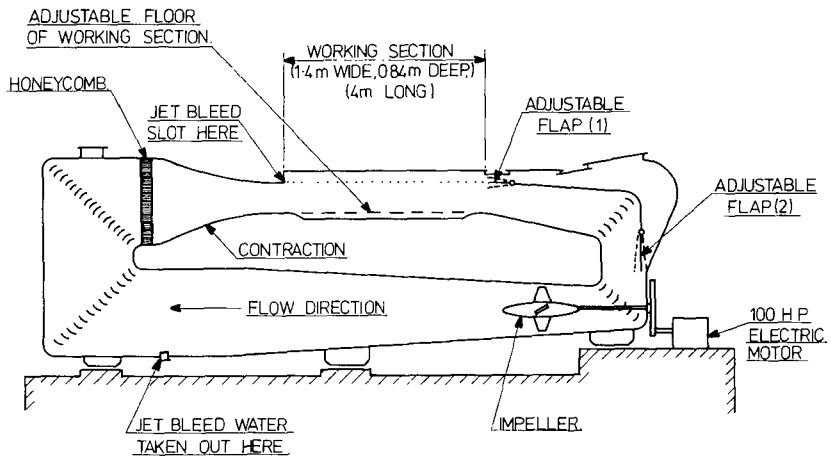

Fig. 5 Diagram of high-speed water channel at Liverpool University

a percentage of the projected chine length.

(*c*) The speed was expressed as a Froude number based on the cube root of the volume displacement as a representative length.

Measurements of the resistance, bow position, and heave at the point of attachment of the balance were converted and expressed as the ratio of resistance to displacement (R/W), trim angle (α), and vertical movement of the center of gravity (h).

Discussion of results

Validity of model tests

The general practice of using tests of models to predict the behavior of a full-size ship has been accepted for many years (see for example [14]). It is usual practice therefore to carry out tests on the model at the correct Froude number and made an appropriate allowance for the force dependent on Reynolds number using one of the existing friction correlation lines.

In the present investigation the model size was similar to that used in many smaller towing tanks with the added novelty that the model was held stationary in a flow of water. The use of a water channel is relatively unusual, though it can offer considerable advantages in certain areas, particularly, for example, with flow visualization, pressure measurements, and other techniques where it is simpler for the instrumentation to be stationary and to have an unlimited running time. It is important, however, to have a uniform velocity distribution in the working section and a horizontal water surface free from waves. This has been achieved in the water channel used in the present tests.

A preliminary investigation was carried out to compare the results obtained in the water channel with towing tank results on the two models 4667-1 and 4666. The results for the DTMB Standard condition for planing craft, that is, with the center of gravity 6 percent of the projected chine length aft of the centroid and at a displacement ratio ($A_P/\nabla^{2/3}$) of 7.0, and also the results for Model 4666 at two heavier displacements (5.5 and 4.0) have been compared with those given by Clement and Blount [1] and are reported in [15]. In general it was found that there was close agreement between results obtained in the channel and the towing tank, except at heavy displacements. In these later cases the drag was increased at the 'hump' speed by the effect of the restricted channel dimensions, suggesting that in this regime the results may not be quantitatively accurate although an order of merit may be assessed. It is thought that this effect may primarily be caused by the depth of the channel, and it is currently the subject of a further investigation.

Under most conditions, however, it would appear that the results

Table 2 Range of model displacements, center of gravity positions, and wedge configurations

Displacement, $A_P/\nabla^{2/3}$	LCG position aft of A_P, $\%L_P$	Wedge angle, $\beta°$	Wedge length, λ
Model 4667-1			
7.0	6	0, 2	0, 0.05, 0.15
8.5, 7.0, 5.5	12	0, 2	0, 0.05
5.5	4, 8	0, 2	0, 0.05
5.5	8	2, 5, 10	0.05, 0.10, 0.15
Model 4666			
5.5, 4.0	0, 4, 8, 12	0, 2, 5, 10	0, 0.05, 0.10, 0.15
7.0	6	0	0

Nomenclature

A_P = projected planing bottom area (excluding spray strips)
B_P = beam over chines (excluding spray strips)
B_{PA} = mean breadth over chines, A_P/L_P
B_{PT} = breadth over chines at transom (excluding spray strips)
B_{PX} = maximum breadth over chines (excluding spray strips)
F_∇ = Froude number based on volume displacement, $V\sqrt{g\nabla^{1/3}}$
L_P = projected chine length
LCG = longitudinal center of gravity
R = total resistance
V = water speed
W = displacement at rest (weight)
h = vertical displacement of center of gravity
α = trim angle
β = wedge angle
λ = length of wedge (related to projected chine length)
λ_B = length of wedge (related to chine beam)
∇ = displacement at rest (volume)
ΔR = difference between resistance with and without wedge ($R_{\text{no wedge}} - R_{\text{wedge}}$)

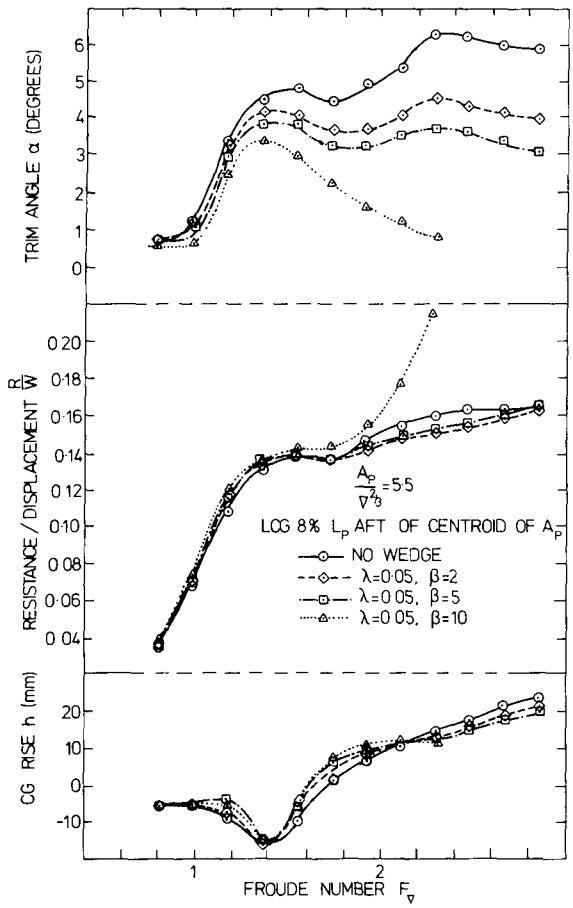

Fig. 6 Variation of resistance, trim, and center of gravity height with speed (Model 4667-1)—smallest wedge length

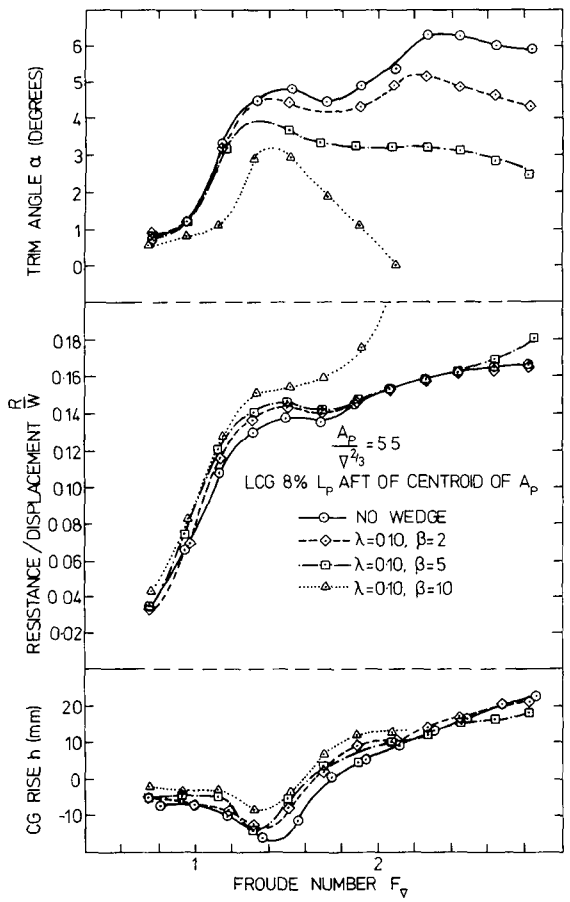

Fig. 7 Variation of resistance, trim, and center of gravity height with speed (Model 4667-1)—medium wedge length

obtained in the channel are comparable with those measured in the towing tank.

Effect of wedges

It has been suggested that trim tabs or wedges may have a dual effect—that in addition to the immediately apparent effect of altering the trim of the vessel, which in turn alters the resistance, the wedges may also change the dynamic lift. This in turn would alter the effective displacement and hence further change the resistance. Thus in analyzing the test results the answers to two separate questions were sought: first, to confirm that Brown's work on planing surfaces also applied to a real hull, that is, that the presence of the wedge would alter the dynamic lift on the hull, and second, the more practical problem that a designer would wish to know, the best combination of wedge length and angle for a given displacement, center of gravity position, and speed.

Dynamic lift. It has been suggested that trim tabs or wedges in addition to their effect on trim may also increase the dynamic lift on the hull. This in turn could be expected to reduce the effective displacement and further reduce the resistance. This effect, however, might be wholly or partially offset by the extra induced drag associated with the increased lift.

The general effects of a wedge on the resistance, trim and center of gravity height are shown in Figs. 6–9. It can be seen that over the range of speeds for which the resistance was reduced the center of gravity height was lower than for the bare hull, apparently suggesting a reduction in dynamic lift. The lift force, however, can be expected to be dependent on trim angle so that, since the wedge also changes the trim angle, such a direct comparison is misleading. However, Fig. 10 shows the curves of center of gravity height against speed for the same trim angle on the bare hull as with the wedge, and from that it can be seen that the center of gravity is raised by the wedge over the whole speed range, showing that the dynamic lift is indeed increased. A similar result was obtained for other configurations of displacement and LCG position. It can be expected that because of the increased lift there will be a corresponding increase in induced drag, but whether the total resistance is increased or decreased will depend on the effect of the change in displacement on other components of the resistance.

This result that a wedge can increase the dynamic lift is in agreement with that obtained by Brown [9] and also by Cole [12] in tests on planing surfaces. It seems likely that the effectiveness of a wedge in increasing the lift on the hull will be a function of the aspect ratio of the planing hull and in general would appear to explain the increased effectiveness of a wedge on the beamier (higher aspect ratio) hull mentioned in the section on trim control.

In the present tests no separate investigation was made of the effect of wedge aspect ratio per se, it being assumed that in practice a wedge would be fitted across the whole beam at the transom, resulting in the largest aspect ratio wedge for a given area.

In the practical application it would seem therefore that within the range of speeds ($1.0 < F_\nabla < 4.0$ approximately) over which a wedge has been shown to reduce the resistance it is preferable to use a wedge to control the trim angle rather than by, for example, a movement of weight longitudinally, since the increased dynamic lift can result in the resistance being lower than that obtained at

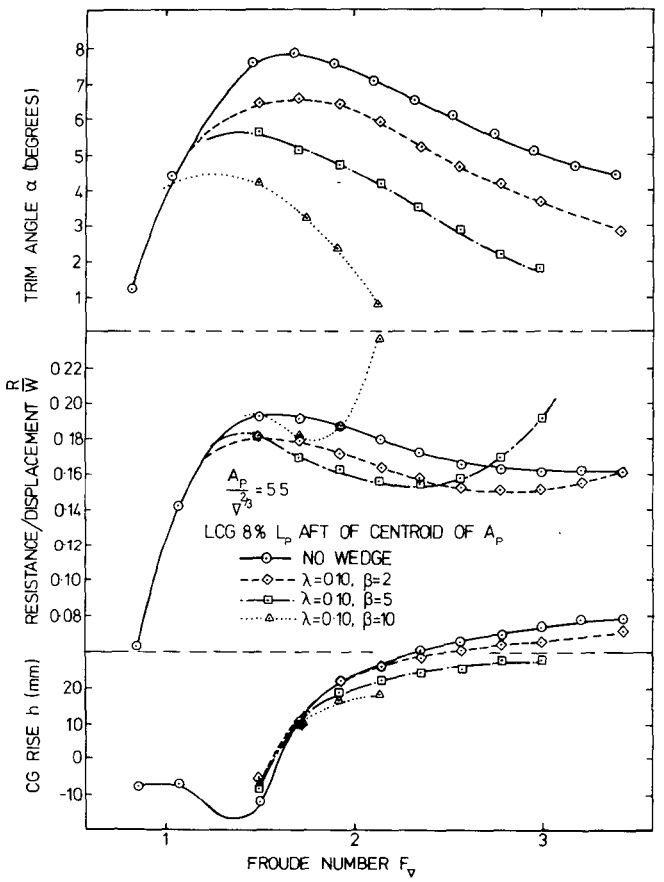

Fig. 8 Variation of resistance, trim, and center of gravity height with speed (Model 4666)—medium wedge length

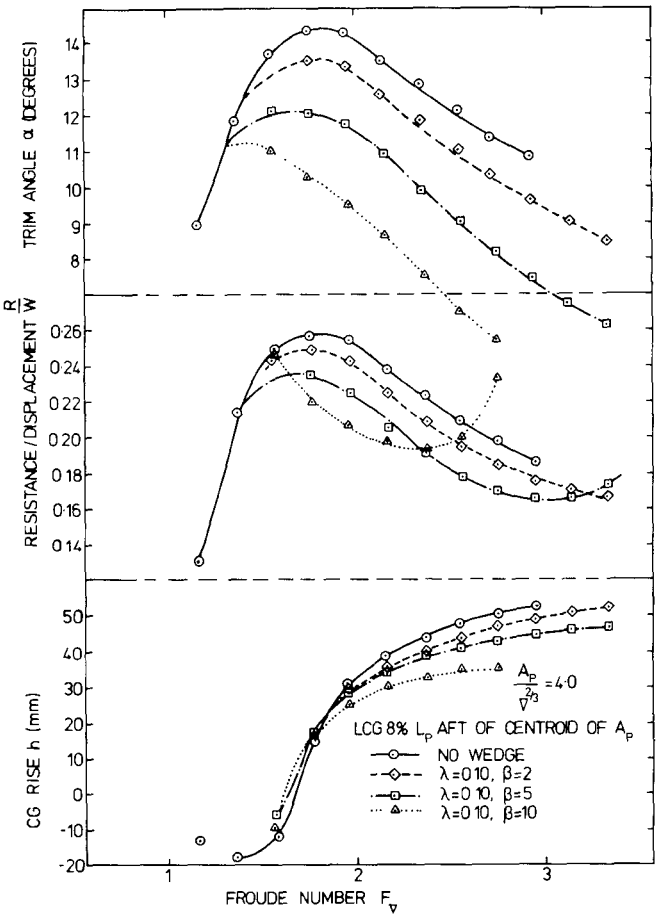

Fig. 9 Variation of resistance, trim, and center of gravity height with speed (Model 4666)—medium wedge length; heavier displacement

the optimum trim angle. This is shown in Fig. 11, where the minimum resistance for the bare hull is compared with the result obtained with a wedge at 4 percent LCG position.

Trim control. In considering the results from the tests with respect to the control of trim and any associated reduction in resistance, the effectiveness of a wedge is likely to be dependent on speed, wedge length (λ), and wedge angle (β) and may also vary with displacement and LCG position.

• General characteristics: Typical curves of the variation of resistance, trim angle, and center of gravity height with Froude number are shown in Figs. 6–9 for the two models both with and without wedges at different displacements and center of gravity positions. In each case the solid line represents the results obtained at the corresponding displacement and center of gravity position for the model without a wedge. The changes in resistance compared with the bare hull (that is, without a wedge) varied with wedge length and angle, speed, LCG position and displacement. The greatest resistance reductions obtained in the present tests were approximately 25 percent.

Figures 6 and 7 show the effect of changing the wedge angle at two wedge lengths (λ = 0.05 and 0.10) on the parent model (4667-1) at 5.5 displacement ratio and an LCG position 8 percent aft of the centroid of A_P. It can be seen that in all cases a wedge increased the resistance below a Froude number of 1.6, corresponding to the conditions when the hull was essentially in a displacement condition and including the 'hump' speed region where the transition between displacement and planing conditions is usually considered to occur. For the shorter wedge (λ = 0.05), shown in Fig. 6, it can be seen that between F_∇ = 1.6 and 3 the resistance was reduced a similar amount for the 2 deg and 5 deg wedges whereas the 10 deg wedge showed increased resistance over the whole speed range. For the longer wedge (λ = 0.10), shown in Fig. 7, only the 2 deg wedge reduced the resistance below that for the bare hull and then by a very much smaller amount and over a shorter range of speeds (from F_∇ = 2.0 to 2.8). Both Figs. 6 and 7 show, however, that in all cases a wedge reduced the trim angle, irrespective of whether there was a reduction in resistance.

Figures 8 and 9 show the same parameters (α, R/W, and h) plotted against Froude number for the beamier model (4666), also with an LCG position 8 percent aft of the centroid and for the middle wedge length (λ = 0.10). Figure 8 shows the results for the same displacement ratio (5.5) as the parent model (4667-1) while Fig. 9 is for a heavier displacement ratio (4.0).

A comparison of Figs. 7 and 8, which are for the same conditions on the two models, suggests immediately that a wedge was much more effective for the beamier model, producing a reduction in resistance for all three wedge angles (2, 5, and 10 deg) of greater magnitude and over a wider range of speeds. It would appear therefore that the wedge is more effective in reducing resistance for the beamier hull. It was noted however that a wedge produced a similar change in trim compared with the bare hull for each model, although this was difficult to determine accurately since the wedges were of different areas, aspect ratios, and distances from the center of pressure of the planing area.

• Wedge length: Curves of percentage drag reduction, relative to the bare hull, against Froude number for different wedge lengths (λ) at a fixed wedge angle are shown in Figs. 12 and 13 for

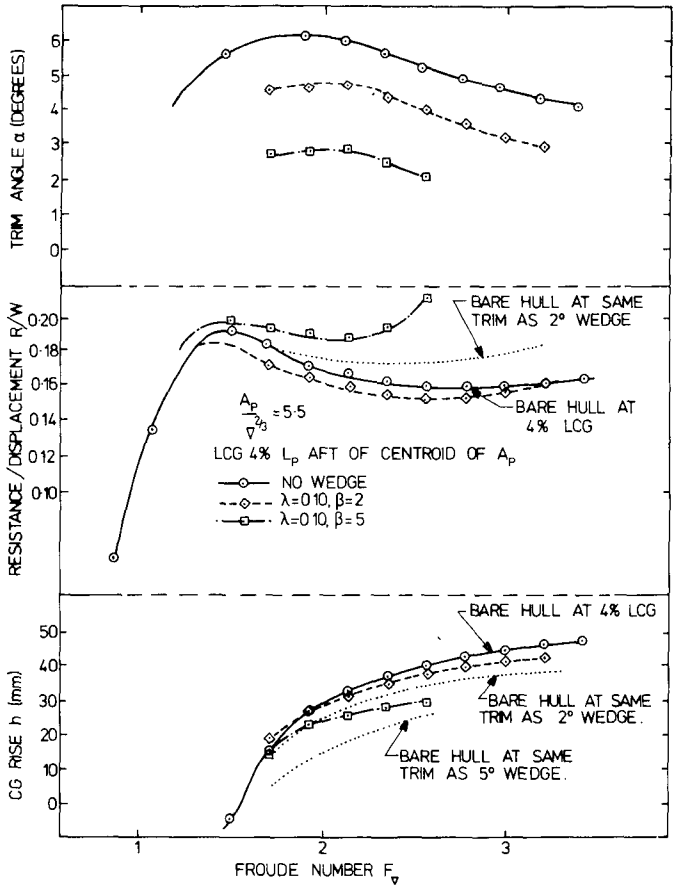

Fig. 10 Resistance and center of gravity height at same trim both with and without a wedge

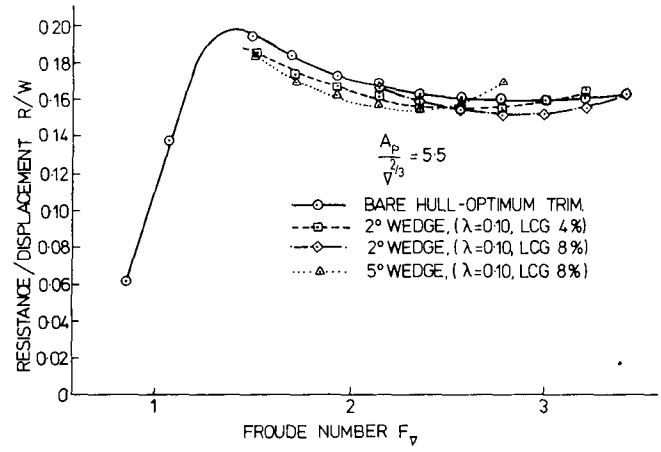

Fig. 11 Reduction of resistance by a wedge below optimum for bare hull

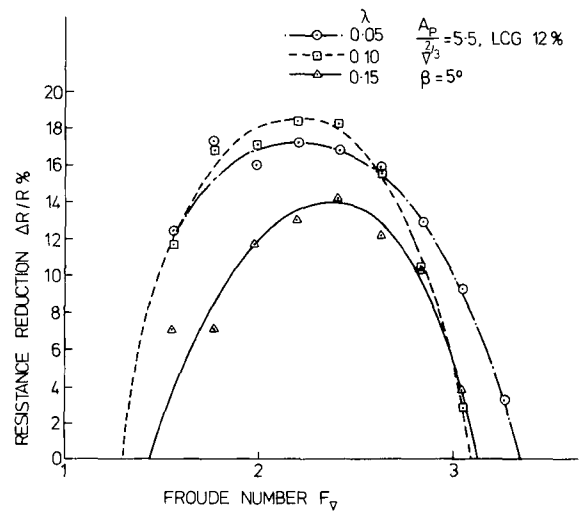

Fig. 12 Effect of wedge length on resistance (Model 4666)

different displacements and center of gravity conditions. In both cases it can be seen that the greatest resistance reduction was obtained with a wedge length of 0.10, but since the results for $\lambda = 0.05$ are only a little lower it seems likely that the optimum wedge length lies between 0.05 and 0.10, tending toward 0.05 for light displacements and forward center of gravity positions as shown in Fig. 14. The results for the parent model (4667-1) showed a similar trend but with the optimum wedge length close to $\lambda = 0.05$ for all conditions.

For comparison, the trim tabs as currently on the market have a maximum length of 0.05 for the shortest hulls (6 m), falling to $\lambda = 0.02$ for the larger hulls. The results of the present tests would suggest a longer wedge length in the range 0.05 to 0.10 for all hull lengths.

In Fig. 13 no experimental points are shown above a Froude number of 3.0, because the bare hull started to porpoise. It was noted, however, that porpoising did not occur on the hull when wedges were attached, and it would therefore appear that in addition to reducing the resistance a wedge can be employed to at least delay the onset of porpoising although the limits of this capability have not yet been determined.

• Wedge angle: Curves of the optimum wedge angle (that is, for maximum resistance reduction) against Froude number are shown in Figs. 15 to 17[3] for three LCG positions on Model 4666.

The curves show a similar trend for each LCG position and displacement with the required wedge angle rising sharply over a speed range corresponding approximately to the 'hump' speed region (see Figs. 8 and 9) but decreasing more gradually at higher Froude numbers. The limit of effectiveness of a wedge appeared to fall in the region $3 < F_\nabla < 4$, depending on displacement and LCG position. In general, the optimum wedge angle was a function of both displacement and LCG position, reaching a maximum of approximately 13 deg at the heaviest displacement and rearmost LCG position. It should be noted however that, as mentioned in an earlier section, the resistance of the model appears to have been increased by the effects of restricted channel dimensions over the lower part of the speed range and to be more sensitive to trim angle. It is likely therefore that the maximum wedge angles of 10 to 13 deg shown in Figs. 16 and 17 would be reduced in practice. In this context Maloney [7] has stated that the maximum angles of a wedge or tab should be 7½ to 10 deg, although it is not stated to what values of displacement etc. this referred, nor on what evidence the conclusion is based. It is clear however that Maloney did not appreciate that trim tabs can have a function other than simple trim control.

In considering the effect of wedge angle, the results showed that

[3] Solid symbols denote a value obtained by extrapolation above the speed at which porpoising occurred on the bare hull.

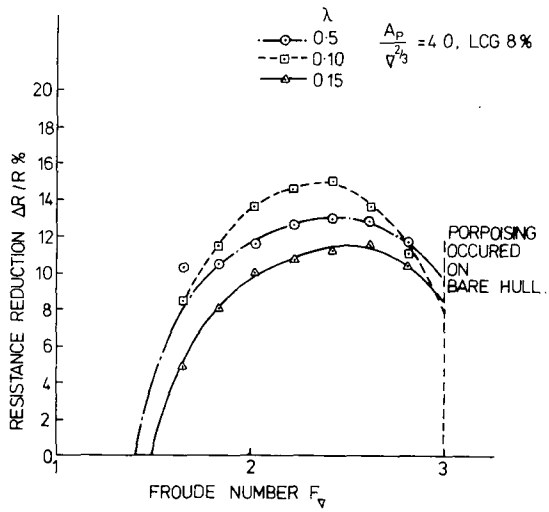

Fig. 13 Effect of wedge length on resistance (Model 4666)

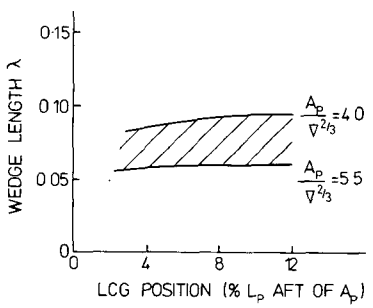

Fig. 14 Optimum wedge length for different LCG positions and displacements

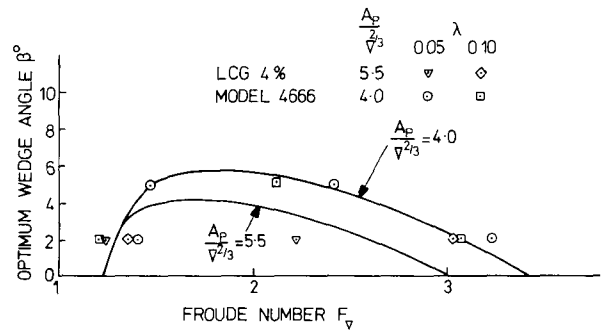

Fig. 15 Variation of optimum wedge angle with speed—4 percent LCG position

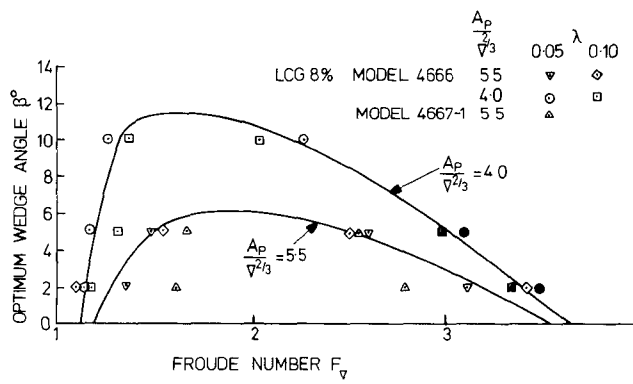

Fig. 16 Variation of optimum wedge angle with speed—8 percent LCG position

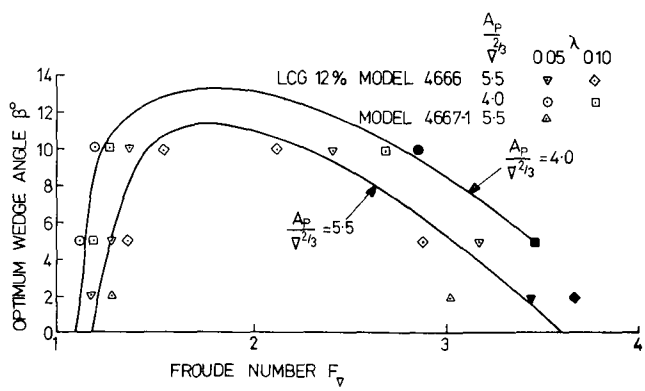

Fig. 17 Variation of optimum wedge angle with speed—12 percent LCG position

for minimum resistance at all speeds a variable angle wedge would be required with a maximum setting of approximately 10 deg, depending on the likely range of LCG positions and displacements. If it should be necessary to fit a fixed wedge, however, then the choice would depend on whether the boat was required to operate at a single speed or over a range of speeds since in general the greater the wedge angle the narrower the speed range over which it will be effective and the greater the resistance penalty outside that speed range.

• Comparison with planing surface data: The results of the present tests were compared with values calculated from the formulas given by Brown [9] derived from his tests on planing surfaces. The calculated values of resistance for the hull with a wedge or flap were in quite close agreement with the present tests although the calculated trim angles were somewhat higher.

It was found that similar trends were obtained for the smallest wedge lengths in the middle of the speed range for which wedges were effective. However, the agreement was less satisfactory at the limits of wedge effectiveness—the calculations predicting a resistance reduction for a wider range of speeds than was found in the present tests. The calculations were based, however, on formulas derived from work on planing surfaces where, as Brown pointed out, no attempt was made at that stage to allow for the effects of side wetting, which would be expected to occur at low speeds, or for the effects of bow shape. The results from the present tests showed that at the low end of the speed range (F_∇ = 1.5 approximately) side wetting did in fact occur on the real hull and at the higher speeds the trim angles were so small that the bow was becoming immersed; the calculated results at the higher speeds showed similar trim angles and wetted lengths. Thus the discrepancies on the range of effectiveness of the wedges appear to be largely caused by the limitations of planing surface formulas in being unable to allow for the effects of bow shape or side wetting.

For the larger wedge angles and wedge lengths, particularly λ = 0.15, there was little agreement since the calculations predicted resistance reductions which were not obtained in practice. A comparison is given below of the range of wedge sizes in the tests, from which Brown's formulas were obtained, with the present tests:

		Flap length	Flap angles
Brown		10%	1, 2, 4
		20%	0, 1, 2, 4, 10, 15

		Flap length	Flap angles
Millward	Model 4666	18%, 37%, 55%	0, 2, 5, 10
	Model 4667-1	25%, 50%, 75%	0, 2, 5, 10

where the flap length in the present tests has been expressed in terms of the mean hull beam to correspond with Brown's data.

It can be seen that the flap lengths investigated by Brown were very much smaller than the present tests, there being very little overlap, and it seems likely therefore that the two major results deduced from Brown's tests may not be valid for appreciably larger flap lengths. The deductions were:

(*a*) That the additional lift due to the wedge or flap was independent of trim angle of the hull.

(*b*) That the additional lift due to the wedge acted at a fixed geometric point on the hull so that the wedge pitching moment was independent of trim angle and wetted length.

Although these deductions are clearly valid for the range of parameters investigated by Brown ($\lambda_B \leq 20$ percent), it seems equally evident that they cannot be true for all values of wedge length and indeed are not supported by the results obtained by Cole [12] for large wedge lengths. This can be illustrated by considering the situation as the wedge length tends to the total wetted length; the implication would be that the lift of the hull is independent of trim angle, which seems unlikely. Fortunately, however, the deductions stated in the foregoing appear to be reasonably true for the lower end of the range of flap lengths which have been shown to be optimal in the present tests.

Thus the comparison with Brown's work [9] shows some agreement, but suggests equally that his results, which are basically more comprehensive, are limited in practical application by not being able to take into account the effects of side wetting, bow shape, and also large wedge or flap lengths. It is to be hoped that the present tests indicate the importance of extending Brown's valuable work.

Conclusions

The results of tests with a series of wedges on two models of the DTMB Series 62 planing hulls in the water channel have confirmed that a wedge or trim tab does increase the dynamic lift on the hull. Since the induced resistance is also increased, the wedge only reduces the total resistance if the change in effective displacement leads to a reduction in the other components of resistance.

In the cases where the total resistance is reduced it is an advantage to use a wedge as a method of reducing resistance and of trim control, as compared with longitudinal movement of weight, since the overall reduction in resistance is greater with a wedge.

It was found that reductions in resistance of up to 25 percent were obtained with the best wedge configuration, depending on displacement and LCG position, in the speed range $1 < F_\nabla < 4$. The optimum wedge length was found to fall in the range 0.05 to 0.10 of the projected chine length, tending to the lower value for lighter displacements and forward LCG positions.

The optimum wedge angle was also found to be a function of displacement, LCG position and speed, reaching a maximum of approximately 10 deg at the heaviest displacement ($A_P/\nabla^{2/3} = 4.0$). It was concluded therefore that for overall performance it was necessary to use a wedge or trim with an adjustable angle.

References

1 Clement, E. P. and Blount, D. L., "Resistance Tests of a Systematic Series of Planing Hull Forms," *Trans.* SNAME, Vol. 71, 1963, pp. 491–579.

2 Clement, E. P., "How to Use the SNAME Small Craft Data Sheets for Design and for Resistance Prediction," SNAME Technical and Research Bulletin No. 1-23, May 1963.

3 Du Cane, P., "Small Sea-Going High Speed Craft," *Shipbuilding and Ships*, Worshipful Company of Shipwrights, 1947.

4 Monk, E., "The Wedge. Experiments to Measure its Effectiveness in Lifting and Levelling Hulls," *Yachting*, Jan. 1958.

5 Hadler, J. B., "The Prediction of Power Performance on Planing Craft," *Trans.* SNAME, Vol. 74, 1966, pp. 563–610.

6 West, J., *Modern Powerboats*, Van Nostrand, 1970.

7 Maloney, W. H., "Offshore Racing Power Boat Design and Development," *Proceedings*, RINA Symposium on Small Craft, Southampton, England, Sept. 1971, pp. 1–13.

8 Du Cane, P., "Fast Patrol Boats." *Proceedings*, RINA Symposium on Small Craft, Southampton, England, Sept. 1971, pp. 93–104.

9 Brown, P. Ward, "An Experimental and Theoretical Study of Planing Surfaces with Trim Flaps," Stevens Institute of Technology, Davidson Laboratory Report SIT-DL-71-1463, 1971.

10 Preston, J. H., "The Design of High Speed, Free Surface Water Channels," NATO Advanced Study Institute on 'Surface Hydrodynamics,' 1966, pp. 14–82.

11 Nicholson, K., "Measurements of Hovercraft Wavemaking Drag in a Circulating Water Channel," Ph.D. Thesis, Liverpool University, 1972.

12 Cole, A. J., "The Influence of Wedges on the Performance of Planing Hulls," Ph.D. Thesis, Liverpool University, 1973.

13 Cole, A. J. and Millward, A., "The Influence of Wedges on the Performance of Planing Hulls," 3rd HISWA Symposium on Yacht Architecture. Amsterdam, March 1973, pp. 69–105.

14 *Principles of Naval Architecture*, J. P. Comstock, Ed., SNAME, 1967.

15 Millward, A., "The Use of a Water Channel for Model Tests on Planing Hulls," Liverpool University, Mechanical Engineering Department Report FM/A8/75, Jan. 1975.

Use of a Water Channel for Model Tests on Planing Hulls

Adrian Millward*
University of Liverpool, Liverpool, England

A comparison has been made of the resistance characteristics of two of the DTMB series 62 planing hulls obtained from measurements made in a high-speed recirculating water channel and a towing tank. The results showed good agreement at the DTMB standard displacement ratio, provided a correction was applied for shallow water effects due to the restricted working section depth. The results suggest that, with the present size models, resistance measurements can be made for a displacement ratio ($A_P/\nabla^{2/3}$) not less than 7.0. Further work is envisaged on the use of smaller models, in order to extend the range of displacement ratios that may be investigated.

Nomenclature

A_P = projected planing bottom area, excluding spray strips
B_P = beam over chines, excluding spray strips
B_{PA} = mean breadth over chines, A_P/L_P
B_{PT} = breadth over chines at transom, excluding spray strips
B_{PX} = maximum breadth over chines, excluding spray strips
F_∇ = Froude number based on volume displacement, $V/\sqrt{g\nabla^{1/3}}$
L_P = projected chine length
LCG = longitudinal center of gravity
R = total resistance
R_{Rd} = shallow water residual resistance
$R_{R\infty}$ = deep water residual resistance
V = water speed
W = displacement at rest (weight)
d = depth of water
h = vertical displacement of center of gravity
α = change in trim angle from at rest condition
β = deadrise angle
∇ = displacement at rest (volume)

Introduction

THE complicated nature of ship resistance has meant that considerable use has been made of model experiments to investigate basic hydrodynamic phenomena and to predict the performance of the full-size vessel. The most common technique used to determine the hydrodynamic forces on a model is to tow it through a tank of stationary water. This method is believed to date back as far as Leonardo da Vinci, although a more usual historical base line is the work of W. Froude, who established the first towing tank in 1872. An alternative technique is the converse idea of holding the model still in a controlled current of water. This method, analogous to the wind tunnel used by aerodynamicists, offers many apparent attractions, such as very long running times, easy flow observation, and stationary instrumentation, but the development of a successful water channel or flume has proved to be difficult. This is particularly so if any attempt is made to measure hydrodynamic forces as opposed to merely making observations of flow patterns. The results presented in this paper are of measurements made on two planing hulls using a high-speed recirculating water channel, which has been developed so that the flow in the working section is uniform with a flat and horizontal free surface. The purpose of the investigation was to compare the results obtained in the water channel with published towing tank data, in order to determine any limitations on the range of model displacements that might need to be imposed due to the restricted size of the channel's working section.

Received July 2, 1976; revision received Oct. 6, 1977.

Index categories: Research Facilities and Instrumentation; Marine Hydrodynamics, Vessel and Control Surface.

*Lecturer, Dept. of Mechanical Engineering (Fluid Mechanics).

Recirculating Water Channel

The model tests were carried out in the recirculating water channel (or flume) at the University of Liverpool. The channel, which is shown in Fig. 1, has a working section 1.4 m wide, 0.84 m deep, and 4.0 m long (4.5×2.75×13 ft) and a capacity of 90,000 liters (20,000 gal) circulated by an impeller driven by a 135 kW motor. From the impeller, the water passes through a long conical diffuser, after which the section becomes rectangular. The water flow passes through two sets of guide vanes and a honeycomb to minimize swirl and is then accelerated through the closed contraction into the working section. The top layer of water, which contains most of the larger entrained air bubbles, is separated at the downstream end of the working section by a splitter plate or adjustable flap. This water is slowed by a deepening of the local section, passing through several gauzes to allow time for the air to escape before it is reintroduced to the main circuit upstream of the impeller. A further advantage of the splitter plate is that, since the flow over the plate is supercritical at almost all speeds, wave disturbances are not transmitted upstream into the working section.

The flow velocity in the working section can be set within a range 0.03-6.1 m/s (0.1-20 fps). Due to the adjustable floor, any speed can be maintained without the presence of standing waves or a hydraulic jump – the critical speed with the floor in its lowest position would be in the region of 2.7 m/s (9 fps).

Early work in the flume[1] showed that there was an appreciable wake at the free surface caused by the boundary layer on the upper surface of the contraction. In order to correct this, a jet injection system was installed – water is bled off from the lowest part of the return circuit and pumped through a 1-mm wide slot running the full width of the channel at the upstream end of the working section. By adjusting the pump speed, the velocity defect at the free surface can be corrected with the beneficial side effect of further improving the flatness of the free surface.

A detailed account of the design of the channel has been given by Preston.[2]

Experimental Facilities and Method

The DTMB series 62 hulls were used and models were made in glass reinforced plastic (grp), one-half the size of the original DTMB models of the revised parent hull (model 4667-1) and model 4666. These were taken to represent hulls which would be appropriate to fast patrol boats and motor yachts

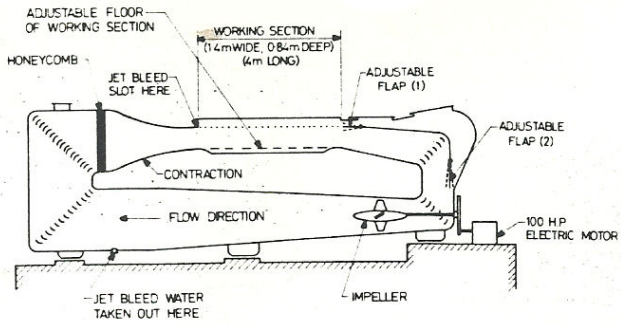

Fig. 1 Diagram of high-speed water channel.

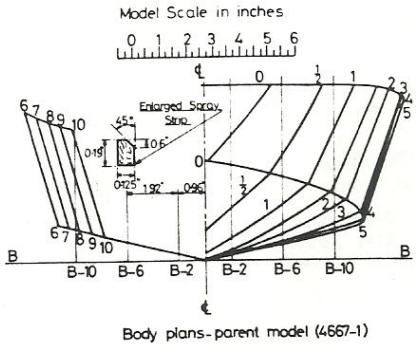

Body plans - parent model (4667-1)

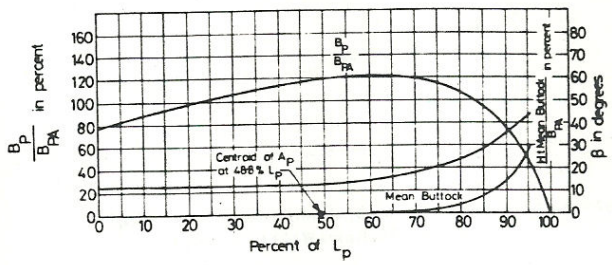

Form characteristics curves for parent model

Fig. 2 Body plan and form characteristics curve for DTMB series 62 revised parent model (4667-1).

respectively. The body plans of the two models are given in Figs. 2 and 3, and other data are given in Table 1 and Ref. 3.

The model was floated in the channel attached to a balance through a tow point on the shaft line, as in Ref. 3, which allowed the hull to trim and heave while measuring resistance and vertical displacement. An indicator mounted at the bow recorded trim, while also providing an additional restraint against large yawing forces which might occur with forward

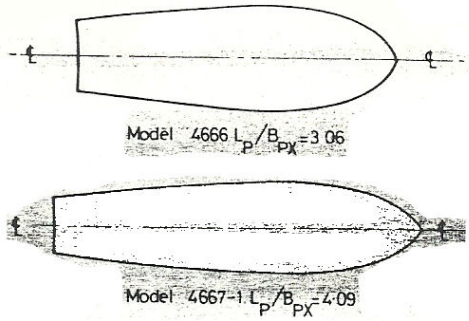

Fig. 3 Chine lines in plan view of the two models of the DTMB series 62 hulls.

center of gravity positions. Scales along the keel, chine, and transom of the model enabled the respective wetted lengths to be determined. Other work[4] has shown that for planing surfaces in the channel there is no measurable change in the resistance due to channel width, provided the beam is less than 300 mm and also that no form of turbulence stimulation is necessary at speeds above 1.2 m/s (4 fps).

Measurements were made of resistance, heave, bow height, and wetted area over a range of speeds on both models at the DTMB standard condition, i.e., with the center of gravity 6% aft of the centroid of the planing area and at a displacement ratio of 7.0. Subsequently, similar measurements were made on the beamier hull (model 4666) at two heavier displacements and at four positions of the center of gravity.

Presentation of Results

For a given hull size and design, the variables which affect the planing characteristics of the hull are the displacement (W or ∇), the longitudinal position of the center of gravity (LCG), and the speed; these were defined using the parameters given by Clement and Blount.[3] The displacement is expressed as the dimensionless ratio $A_P/\nabla^{2/3}$, where A_P is the projected planing bottom area and ∇ the volume of water displaced at rest. It should be noted that with this ratio a high numerical value implies a light displacement condition and a low value correspondingly a heavy displacement. The longitudinal position of the center of gravity was defined as the LCG position aft of the centroid of A_P expressed as a percentage of the projected chine length. The speed was given in terms of a Froude number F_∇, based on the cube root of the displacement as the representative length.

The results have been expressed in terms of the resistance as a ratio of the weight (R/W), the change in trim angle (α), and the change in vertical height of the center of gravity (h) against the Froude number F_∇.

Table 1 Model dimensions

	Model 4666		Model 4667-1	
A_P	2.429 ft^2	0.2256 m^2	3.200 ft^2	0.2973 m^2
l_p	2.994 ft	0.9124 m	4.000 ft	1.2192 m
B_{PA}	0.812 ft	0.2475 m	0.800 ft	0.2438 m
B_{PX}	0.978 ft	0.2981 m	0.978 ft	0.298 m
B_{PT}	0.693 ft	0.2112 m	0.625 ft	0.1905 m
L_P/B_{PA}	3.69		5.00	
L_P/B_{PX}	3.06		4.09	
B_{PX}/B_{PA}	1.21		1.22	
B_{PT}/B_{PX}	0.71		0.64	
Centroid of A_P, %L_P forward of transom	48.2		48.8	
Angle of chine in plan view, deg	5.0		5.0	
Half-angle of waterline entrance, deg	49		46	

The results obtained in the towing tank were taken from Ref. 3 and have been scaled to the model size of the present tests using the A.T.T.C. friction correlation line (Ref. 5) with zero roughness allowance.

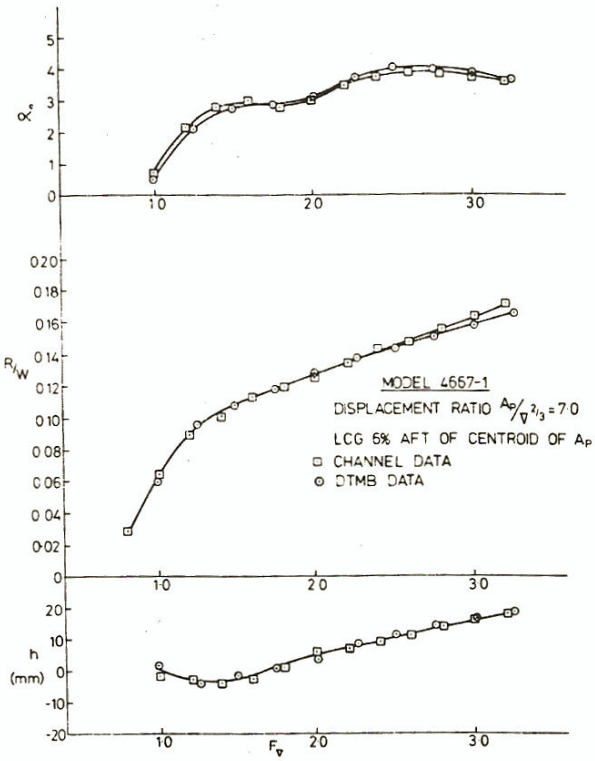

Fig. 4 Comparison of results obtained in the water channel and towing tank – model 4667-1, DTMB standard condition.

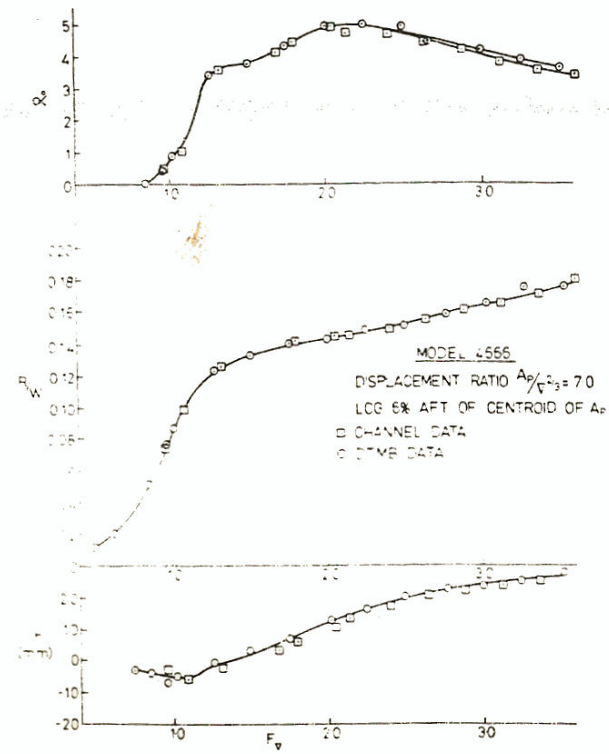

Fig. 5 Comparison of results obtained in the water channel and

Discussion of Results

In order to compare the results obtained from the model tests in the water channel with the towing tank results, the possible effects of the restricted channel had to be considered. Information on the effects of channel dimensions over the required speed regime appeared to be scanty, since most of the data available, such as Refs. 5 and 6, are confined to the Froude numbers appropriate to displacement vessels. However, Toro[7] has measured the effects of shallow water on one of the hulls used in the present tests (model 4666). A correction was therefore applied to the results obtained in the channel, using a linear interpolation technique based on Toro's data, to obtain the deep water resistance for comparison with the towing tank data.

The curves for resistance (expressed as R/W), trim change α, and center of gravity change h against Froude number F_∇ are shown in Fig. 4 for the parent model (4667-1) and in Fig. 5 for the beamier model (4666) in the water channel and in the towing tank. In both cases, the curves, particularly of resistance, are effectively identical, particularly when the various possibilities for differences are considered, such as minor variations in model dimensions built to the same drawings and assumptions made in the normal scaling method. It was noted that for the displacement corresponding to the DTMB standard condition, the corrections due to shallow water effects were generally small. The maximum correction was approximately 7% on the residual resistance, which was of the order of 85% of the total resistance at that condition and occurred over a limited range of Froude numbers in the region $1.4 < F_\Delta < 1.9$. Outside this range of Froude numbers, the corrections were numerically smaller. Above $F_\nabla = 2.1$, the corrections were negative, showing that the effect of shallow water is to reduce the resistance below that for deep water in the planing regime. These results show that the data obtained in the water channel are consistent with

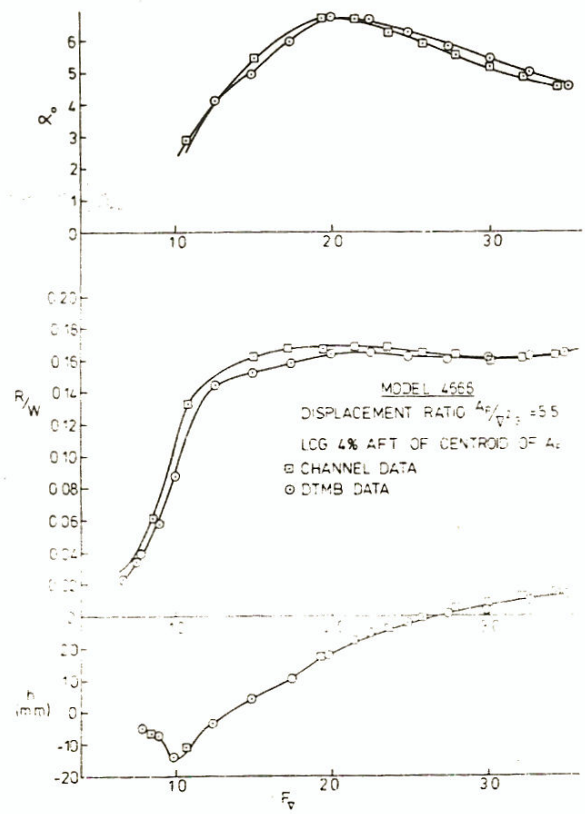

Fig. 6 Comparison of results obtained in the water channel and towing tank – model 4666 at a heavier displacement ($A_P/\nabla^{2/3} = 5.5$, LCG 4%).

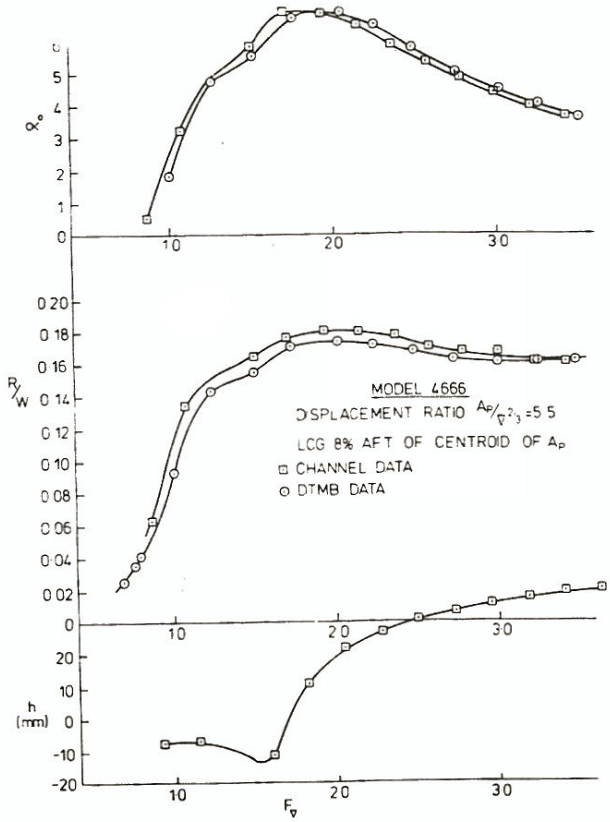

Fig. 7 Comparison of results obtained in the water channel and towing tank – model 4666 at a heavier displacement ($A_P/\nabla^{2/3} = 5.5$, LCG 8%).

data from the towing tank at the DTMB standard displacement ($A_P/\nabla^{2/3} = 7.0$), provided a correction is applied for shallow water effects.

At a heavier displacement ratio ($A_P/\nabla^{2/3} = 5.5$), the resistance measurements on model 4666 showed differences between the results from the water channel and the towing tank of 10-15% in the hump region. The results, after correction for shallow water effects using Toro's data, are shown in Figs. 6 and 7 for LCG positions 4% and 8% aft of the centroid of A_P. It can be seen that application of the shallow water correction has reduced the difference between the water channel and towing tank data by about half, resulting in differences of up to 6% in the region $1.1 < F_\nabla < 1.7$. Similar results were obtained at the two other LCG positions at this displacement. A comparison of the results for the heaviest displacement ratio ($A_P/\nabla^{2/3} = 4.0$) showed larger differences between the water channel and towing tank data, even after a shallow water correction had been applied.

It was, therefore, evident from these results, that with the existing model size ($L_P = 0.91$ m), the effect of channel dimensions increased with the larger displacement conditions and would not be satisfactorily accounted for by shallow water effects based on existing data for a displacement ratio

Table 2 Test conditions

Model	Displacement $A_P/\nabla^{2/3}$	LCG position % aft of centroid of A_P
4667-1	7.0	6
4666	7.0	6
	5.5	0, 4, 8, 12
	4.0	0, 4, 8, 12

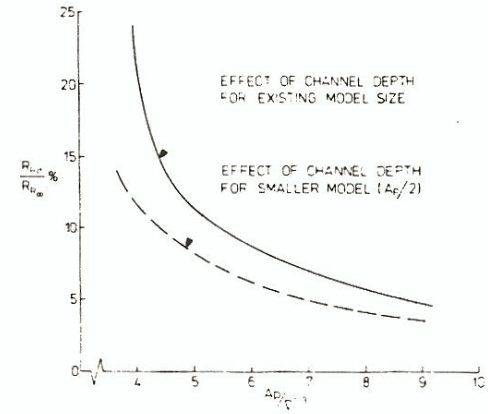

Fig. 8 The effect of displacement ratio on the shallow water correction.

less than the DTMB standard condition ($A_P/\nabla^{2/3} = 7.0$), i.e., for heavier models. The model size had been chosen with regard to towing tank experience, where it has been found difficult to obtain a turbulent boundary-layer flow on smaller models. However, subsequent experience has shown that in the water channel, a turbulent boundary can be more easily obtained at low Reynolds numbers. This has been attributed to the more uniform residual turbulence existing in the recirculating water channel. The predicted effect of shallow water corresponding to the channel depth for the present size of model is shown in Fig. 8. It can be seen that for the range of displacement ratios covered by the series 62 planing hull tests ($8.5 > A_P/\nabla^{2/3} > 4.0$), the correction ranges from 5% to 24%. The result of halving the planing area, giving a model length of 0.64 m, is also shown, and it can be seen that the shallow water effect is reduced to 10% at the lowest displacement ratio. It was also noted that the tests to determine the maximum permissible beam of model for the water channel (Ref. 4) were carried out with a light displacement model. It seems likely, therefore, that significant interference effects from the side of the channel may have been present with the two heavier displacement conditions of the present tests ($A_P/\nabla^{2/3} = 5.5$ and 4.0). Consequently, it is intended to investigate the possibility of using smaller models than in the present tests, in order to allow satisfactory measurements to be made at lower displacement ratios before restricted channel effects become significant.

It was also noted that Toro's data[1] was restricted to one hull model (model 4666) at a single displacement and three LCG positions. Toro has suggested that the effect of LCG position can be eliminated by expressing the results as a ratio of the shallow water to deep water residual resistance. It was found, however, that since Toro's measurements were carried out with the model free to trim the effects of trim, and hence LCG position, could not be entirely eliminated. Experience has also shown that in the hump speed regime it would be preferable to establish the shapes of the experimental curves more positively, in order to carry out an accurate interpolation technique. Thus it is intended to carry out a wider investigation into shallow water effects in order to produce data which can be applied generally to planing hulls. This will be carried out in the water channel, since the adjustable floor, used to obtain a flat water surface, can be moved vertically to allow the water depth in the working section to be progressively reduced from the maximum of 0.84 m down to 0.15 m depth.

Conclusions

A comparison of measurements made on two DTMB series 62 planing hulls (models 4667-1 and 4666) in the water channel, with results obtained in the towing tank, has shown satisfactory agreement for a displacement corresponding to

the DTMB standard condition ($4_P/\nabla^{2/3} = 7.0$), provided a correction is made for shallow water effects due to the restricted depth of the water channel.

At heavier displacements (lower displacement ratios), satisfactory agreement was not obtained. It is, therefore, intended to further investigate the possibility of using smaller models and also producing more comprehensive data on the effects of shallow water on planing hulls.

References

[1] Nicolson, K., "Measurements of Hovercraft Wavemaking Drag in a Circulating Water Channel," Ph.D. Thesis, Liverpool University, 1972.

[2] Preston, J. H., "The Design of High Speed, Free Surface Water Channels," NATO Advanced Study Institute on "Surface Hydrodynamics," 1966, pp. 14-82.

[3] Clement, E. P. and Blount, D. L., "Resistance Test of a Systematic Series of Planing Hull Forms," S.N.A.M.E. Transactions, Vol. 71, 1963, pp. 491-579.

[4] Cole, A. J., "The Influence of Wedges on the Performance of Planing Hulls," Ph.D. Thesis, Liverpool University, 1973.

[5] Comstock, J. P., "Principles of Naval Architecture," S.N.A.M.E., 1967.

[6] Saunders, H. E., "Hydrodynamics in Ship Design," Vol. 2, S.N.A.M.E., 1957.

[7] Toro, A.I., "Shallow Water Performance of a Planing Boat," University of Michigan Report 019, April 1969.

Engineering Notes

ENGINEERING NOTES are short manuscripts describing new developments or important results of a preliminary nature. These Notes cannot exceed 6 manuscript pages and 3 figures; a page of text may be substituted for a figure and vice versa. After informal review by the editors, they may be published within a few months of the date of receipt. Style requirements are the same as for regular contributions (see inside back cover).

Wedge Effect on Planing Hulls

Chun-Tsung Wang*
National Taiwan University, Taipei, Taiwan

Introduction

IN 1971 Brown[1] reported a series of test results on planing surfaces with trim flaps. For the full-span flap series tested, flap angle δ varied between 0 and 15 deg, but flap length L_F was kept at 20% of the beam b of the planing hull for most of the tests conducted. The effect of some flap parameters, as determined experimentally on planing hull performance, were reported, and these were later incorporated into the widely used Savitsky equations[2] to study the resistance D and running trim τ of a planing hull with trim flaps or wedges.[3] The relations developed were:

1) Flap lift coefficient:

$$\Delta C_{LF} = \frac{\Delta_F}{0.5\rho V^2 b_F{}^2} = 0.046\lambda_F \cdot \delta \tag{1}$$

2) Distance from transom to point of resultant force due to flap lift:

$$LOF = 0.6\, b_F \tag{2}$$

3) Added resistance coefficient:

$$\Delta C_D = \frac{\Delta D}{0.5\rho V^2 b_F{}^2} = 0.0052\Delta C_{LF}(\tau + \delta) \tag{3}$$

where b_F is the flap width, $\lambda_F = L_F/b_F$ the flap length-beam ratio, V the speed of the planing hull, ρ the fluid density, and Δ_F and ΔD the added lift and resistance due to flap, respectively.

For flap lengths beyond those tested by Brown, Millward[4] found that the experimentally determined parameters are not applicable. This might be attributed to the limited range of validity of the parameters determined from Brown's restricted range of flap length. This Note presents a method based on the use of Savitsky's equations in an effort to obtain more rational parameters which may give a better understanding of the effect of trim flaps or wedges on planing hulls.

Analysis

When a trim flap or wedge is attached to the rear end of a planing hull, the mean wetted length λb of a planing hull is generally much larger than the flap length under most planing conditions. The fluid under the planing hull flows parallel to the bottom of the planing hull before it reaches the trim flap. It is assumed that the added lift of a trim flap can be approximated by imagining the trim flap acts like another planing surface with a mean wetted length equal to the flap length at a trim angle δ. The effective mean wetted length-beam ratio of the trim flap is taken to be $\lambda_F + 0.3$, and it is further assumed that Savitsky equations[2] can be applied to evaluate the added lift due to the trim flap as provided by

$$\Delta C_{LF} = C_{LOF} - 0.0065\beta C_{LOF}^{\,0.6} \tag{4}$$

where β is the deadrise angle of the planing surface, and C_{LOF} is the flap lift coefficient at zero deadrise angle as given by

$$C_{LOF} = \delta^{1.1}(0.012(\lambda_F + 0.3)^{0.5} + 0.0055(\lambda_F + 0.3)^{2.5}/C_V^2) \tag{5}$$

where $C_v = V/(gb)^{0.5}$ is the speed coefficient, and g is the gravity acceleration. Figure 1 shows the relation between ΔC_{LF} and δ for different λ_F values computed from Eqs. (1) and (4). Also shown in the figure are the test data reported by Brown[1] for $\lambda_F = 0.2$ and 0.1, where C_v^2 varied between 10 and 50, and λ/λ_F varied between 11 and 21. The test data are comparable with results computed from both Eqs. (1) and (4) within the test range covered by Brown. But as the flap length increases, the difference between ΔC_{LF} values computed from Eqs. (1) and (4) becomes larger. It is observed from Fig. 1 that Eq. (1) tends to overestimate the added lift due to trim flap at larger flap lengths, and may not be applicable beyond the data range where it was derived.

When a trim flap is attached to the stern of a planing hull, and added drag is anticipated, the added drag due to the trim flap can be approximated by[5]

$$\Delta C_D = \lambda_F \tan\delta \cdot f(\delta) \tag{6}$$

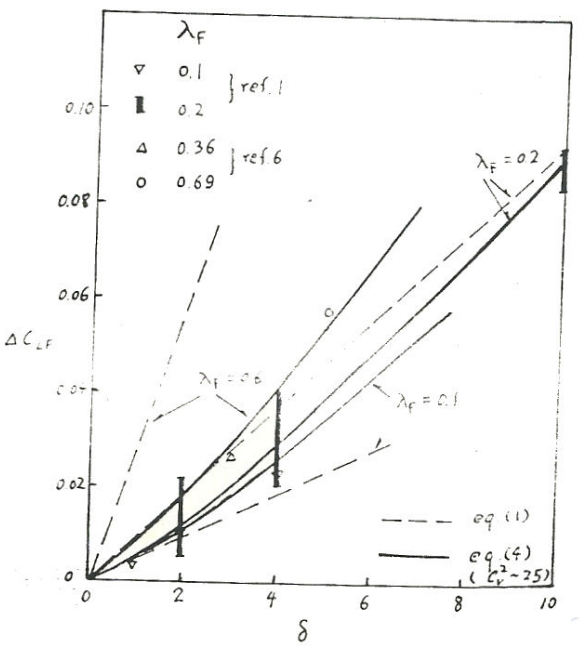

Fig. 1 Relation between ΔC_{LF} and δ.

Received Sept. 17, 1979; revision received May 19, 1980.

Index categories: Marine Hydrodynamics, Vessel and Control Surface; Marine Vessel Design (including Loads).

*Professor, Institute of Naval Architecture.

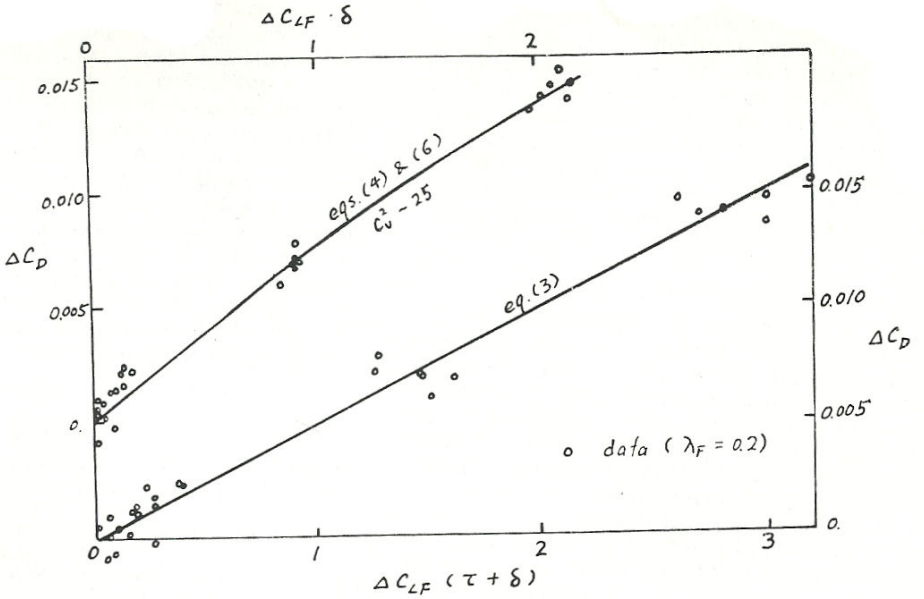

Fig. 2 Relation between ΔC_D and ΔC_{LF}.

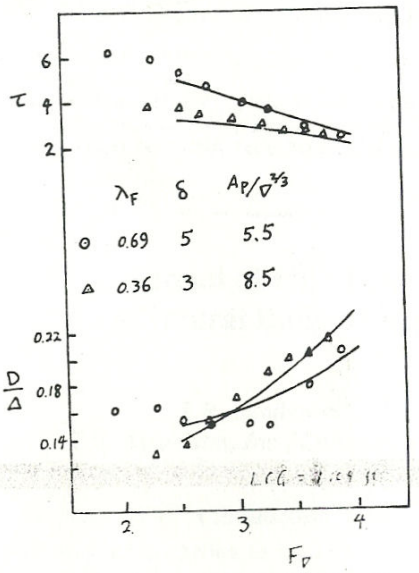

Fig. 3 Comparison with experimental results.

where

$$f(\delta) = 2\delta/90 \quad \text{for } \delta < 5 \text{ deg}$$
$$= 0.111 + 0.0169(\delta - 5) \quad 5 \text{ deg} \le \delta \le 15 \text{ deg}$$

Figure 2 shows two ways of replotting the data reported by Brown.[1] The lower curve corresponds to the relation represented by Eq. (3), and thus test data plotted have the same degree of scattering as that shown in Fig. 16 of Ref. 1. The upper curve corresponds to a relation between ΔC_D and $\Delta C_{LF} \cdot \delta$ computed from Eqs. (4) and (6) for the test condition conducted by Brown. It is apparent that better correlation between the theoretical curve and experimental data appears in the upper curve, suggesting that Eq. (6) may be a better representation than Eq. (4) to give the added drag due to a trim flap or wedge.

Millward[4] pointed out in his paper that it is difficult to [illegible] lift due to the flap acted at a fixed geometric point on the hull which does not change as the flap length increases. A re-examination of the data on added moment due to trim flap as shown in Fig. 17 of Brown's report tends to show that LOF is between 0.5 and 0.6 b_F, which is approximately equal to the effective flap mean wetted length 0.5 b_F corresponding to a flap length of 0.2 b_F used by Brown. Therefore, it seems reasonable to assume at this stage that the distance forward of the transom to the point of resultant force on the hull due to flap lift is approximately equal to the effective mean wetted length of the trim flap, i.e.,

$$LOF = (\lambda_F + 0.3) b_F \tag{7}$$

The drag and running trim of a planing hull with trim flap or wedge can now be evaluated by substituting Eqs. (4), (6), and (7) into the following governing equations.[3] They are:

1) The effective lift coefficient of the planing hull

$$C_{L\delta} = \frac{\Delta - \Delta_F}{0.5\rho V^2 b^2} = C_{L0} - 0.0065\beta C_{L0}^{0.6} \tag{8}$$

where Δ is the load of the planing hull.

2) The effective lift coefficient at zero deadrise angle

$$C_{L0} = \tau^{1.1}(0.012\lambda^{0.5} + 0.0055\lambda^{2.5}/C_\lambda^2) \tag{9}$$

where τ is the trim angle and λ the mean wetted length-beam ratio.

3) The equation relating the effective longitudinal center of gravity

$$\frac{\Delta LCG - \Delta_f LOF}{(\Delta - \Delta_f)\lambda b} = 0.75 - (5.21 C_\lambda^2/\lambda^2 + 2.39) \tag{10}$$

where LCG is the longitudinal distance of gravity from transom, and

4) The total horizontal hydrodynamic drag component

$$D = \Delta \tan\tau + \frac{c_f \lambda \rho V^2 b^2}{2\cos\tau\cos\beta} + \Delta D \tag{11}$$

where c_f is the friction drag coefficient.

Most of the test results of model length 3 to 4 ft reported by Millward[4] were in the preplaning range and were likely subject to tank (1.4 m wide × 0.84 m deep) wall effect when wedges were attached to the planing hulls. They are not suitable for the present analysis. Instead, models of Series 62 4667-1 planing hulls of 3 ft length with larger wedge lengths were tested at the Ship Model Basin (4 m wide × 2.5 m deep tank) of the National Taiwan University.[6] Figure 3 shows the test data as well as the analytical solutions obtained by solving Eqs. (8-11). In the planing range, comparisons between analytical and experimental results are reasonably good to suggest that Eqs. (4), (6), and (7) introduced in this Note could replace Eqs. (1-3) originally proposed by Brown[1] to study the effects of trim flaps or wedges on planing hulls, since Eqs. (4), (6), and (7) are applicable for both small and large flap or wedge lengths.

References

[1] Brown, P.W., "An Experimental and Theoretical Study of Planing Surfaces with Trim Flaps, Davidson Lab., SIT, Hoboken, N.J., SIT-DL-71-1463, April 1971.

[2] Savitsky, D., "Hydrodynamic Design of Planing Hulls," *Marine Technology*, Vol. 1, Oct. 1964, pp. 71-95.

[3] Savitsky, D. and Brown, P.W., "Procedures for Hydrodynamic Evaluation of Planing Hulls in Smooth and Rough Water," *Marine Technology*, Vol. 13, Oct. 1976, pp. 381-400.

[4] Millward, A., "Effect of Wedges on the Performance Characteristics of Two Planing Hulls," *Journal of Ship Research*, Vol. 20, Dec. 1976, pp. 224-232.

[5] Hoerner, S.F., "Fluid-Dynamic Drag," 148 Busteed Dr., Midland Park, N.J., 1965.

[6] Wang, C.T. and Hsu, C.J., "Studies on the Effect of Wedges on Planing Hulls," Institute of Naval Architecture, National Taiwan University, Taipei, NTU-INA-Tech. Rept. 79, June 1978.